VISCOUS FLOW IN MULTIPARTICLE SYSTEMS

AT

INTERMEDIATE REYNOLDS NUMBERS

VISCOUS FLOW IN MULTIPARTICLE SYSTEMS AT INTERMEDIATE REYNOLDS NUMBERS

BY

Brian Peter LeClair

A Thesis

Submitted to the Faculty of Graduate Studies

in Partial Fulfilment of the Requirements for

the Degree

Doctor of Philosophy

McMaster University

August 1970

DOCTOR OF PHILOSOPHY (1970)
(Chemical Engineering)

McMaster University
Hamilton, Ontario.

TITLE : Viscous Flow in Multiparticle Systems at Intermediate Reynolds Numbers

AUTHOR : Brian Peter LeClair

B.A.Sc. (University of British Columbia)
M.A.Sc. (University of British Columbia)

SUPERVISOR : Professor A.E. Hamielec

NUMBER OF PAGES : xix; 341

SCOPE AND CONTENTS :

This dissertation describes an extention of fluid mechanical data for flow around blunt objects in the intermediate Reynolds Number regime using the digital computer. The aim was to develop fluid mechanical models to predict the flow phenomena around a blunt object in an infinite fluid and a multiparticle system.

The dissertation is divided into two self- contained parts. Part I describes the flow around a blunt object in an infinite fluid media. The flow around a solid sphere in steady flow, a solid sphere in accelerating flow and a spherical liquid drop in steady flow are described. The study demonstrates that the actual drag becomes asymptotic with the Oseen drag relation as the Reynold Number approaches zero. Secondly, the study demonstrates that acceleration from rest of a sphere under the influence of gravity can be predicted precisely by solving the fluid mechanical equations. Finally the flow in and around a circulating spherical raindrop is presented.

Part II describes the extension of the cell model for multi-particle systems in the creeping flow regime to the intermediate Reynolds Number regime. Three cases were studied: beds of solid spheres, cylinder bundles in cross-flow and gas bubble swarms. Theoretical predictions of pressure drop through the assemblage and material or heat transport were obtained. Comparison of these predictions with experimental data has shown that the approach provides an excellent first approximation for predicting multiparticle phenomena.

I offer this work as the mathematical principles of philosophy, for the whole burden of philosophy seems to consist in this - from the phenomena of motions to investigate nature, and from these forces to demonstrate the phenomena. We are certainly not to relinquish the evidence of experiments for the sake of dreams and vain fictions of our own devising.

Sir Isaac Newton,

"Principia Mathematica"

ACKNOWLEDGEMENTS

The author wishes to express his gratitude to those who contributed to this work. He is particularly indebted to:

His research director, Dr. A.E. Hamielec, for his enthusiasm, interest, and guidance throughout the course of this study.

His Ph.D. Supervisory Committee members, Dr. A.I. Johnson and Dr. D. Kenworthy, for providing encouragement and control at the proper times.

Dr. H.R. Pruppacher, Dept. of Meteorology, UCLA for his useful comments and suggestions.

The Computation Centre, in particular Mr. P. O'Day, for their patience and forbearance during the course of this work.

The National Research Council of Canada for providing financial support in the form of an NRC Scholarship.

Mrs. Ora Orbach for her careful and conscientious work in typing this dissertation.

PART II Multiparticle Systems

TABLE INDEX

Part I Flow Around a Blunt Object in an Infinite Media

Part II Multiparticle Systems

FIGURE INDEX

Part I Flow Around a Blunt Object in an Infinite Media

Part II Multiparticle Systems

PART I

FLOW AROUND A BLUNT OBJECT IN AN INFINITE MEDIA

A. Introduction

A.1 Steady State Flow Around Solid Spheres

Viscous flow of fluids is governed by the well-known Navier Stokes equations. These are nonlinear second order partial differential equations for which exact solutions are generally unattainable. Early attempts at the analytical solution of these equations usually involved radical linearization procedures which severely limited the applicability of such solutions.

The subject of low Reynolds number flow was introduced by Stokes (1851) in his study of flow past a spherical body. Stokes assumed to the first approximation that inertial effects in the fluid motion could be neglected compared to friction effects. This assumption is equivalent to requiring that the Reynolds number be very small when compared to one.

Further investigations have been concerned with relaxing Stokes' initial assumptions. Oseen (1910) showed that Stokes' solution for the flow velocities was not uniformily valid far from the body and thus was poor for use in approximating the inertia terms. He showed that as every body moving steadily through a viscous fluid must experience some resistance, consideration of the momentum flux across a large surface surrounding the body shows that the magnitude of the disturbance to the uniform velocity of the stream cannot everywhere fall to zero more rapidly than the inverse square of the distance from the body. For the disturbance of a sphere moving through a fluid, the acceleration of the fluid at a great distance from the body cannot be negligible in comparison

to the local viscous force. For the former is almost entirely due to the convective effect of the stream which is a constant multiple of the first derivative of velocity, whereas the latter is a multiple of the second derivative of the velocity. Thus the viscous force can only be dominant if the decay of the disturbance is exponentially rapid. Stokes' theory is therefore not self-consistent at a great distance from the body.

Recently Maxworthy (1965) and Pruppacher and Steinberger (1968) showed that if the actual drag D on a sphere is non-dimensionalized by the Stokes drag D_s and the quantity $(D/D_s)-1$ is plotted as a function of Reynolds number, large differences between the various experimental and theoretical results are revealed. From experimental determinations of the drag Maxworthy and Pruppacher and Steinberger concluded that as N_{Re} approaches zero the drag approaches zero via the Oseen drag rather than via the Stokes drag. This finding may be interpreted to mean that the flow about a sphere is strictly speaking only symmetric with a plane perpendicular to the flow field at $N_{Re} = 0$ and asymmetric at all Reynolds numbers above zero. This concept has received considerable support from the experiments of Steinberger, Pruppacher and Neiburger (1968) who determined the velocities, accelerations and drag forces experienced by two equal spheres falling along their line of centers in a viscous fluid at Reynolds numbers between 0.216 and 0.060. These authors found that even at the lowest Reynolds number investigated both spheres continually accelerated as they fell, and the upper sphere fell faster than the lower one, a result which must be interpreted as being due entirely to non-Stokes behaviour of the fluid.

Utilizing the Oseen approach many researchers have tried to obtain better approximations to the flow field. Goldstein (1929) subsequently expanded Oseen's analysis to obtain higher Reynolds number corrections for the drag force. Proudman and Pearson (1957) showed that Oseen's equations should only be employed to compute the first order Reynolds number correction to the drag. Proudman and Pearson used an expansion technique which retains the ideas of both Stokes and Oseen. The procedure used an inner successive approximation expansion of the Stokes type to satisfy the boundary conditions at the body surface and an outer Oseen expansion to satisfy the free stream conditions. The series are made unique by requiring that the two series match identically near the obstacle. Details of the expansion procedures are summarized in Holt (1968). Recently Chester (1968) and Chester, Breach and Proudman (1969) extended the Proudman and Pearson theory to higher order terms in the hope of extending the range of applicability of this theory. However, Chester and Breach had to conclude that the additional terms in the expansion did not improve the agreement with experiment and in fact caused the disagreement to be even more pronounced. In the range of higher Reynolds numbers, computations of the drag on a sphere were carried out by Jenson (1959), Hamielec, Hoffman and Ross (1967), Rhodes (1967) and Rimon and Cheng (1969) who solved the Navier Stokes equations by numerical techniques.

A.2 Unsteady State Flow Around Solid Spheres

In spite of the considerable amount of study devoted to the steady fall of a sphere through a fluid medium, little has been accomplished to define the accelerated portion of fall. Many phenomena are complicated by relative acceleration between particle and fluid. Pulsations have been shown to enhance the stability of fluidized beds, decrease the viscosity of dispersed suspensions and increase heat and mass transfer rates by orders of magnitude. In fact, because of a lack of reliable experimental or theoretical data, it has been common practice to apply directly, easily obtainable steady state drag data to all drag resistance problems, steady state or not. This practice is not always justifiable as in many instances it does not correctly predict the motion of an accelerating particle.

Torobin and Gauvin (1959) have summarized the theoretical and experimental work prior to 1959. They found that the acceleration drag phenomena data were poor because of the difficulty in obtaining a time-distance record of sufficient precision to give accurate values of the second derivative of distance, the acceleration. The conclusion was that the best method of accounting for the altered drag due to acceleration was by expressing it in terms of a modified drag coefficient, C_{DA}, given by

$$\frac{4}{3}\pi a^3 \rho_s \frac{dV_p}{dt} = \frac{4}{3}\pi a^3(\rho_s-\rho)g - \frac{1}{2} C_{DA}\rho\pi a^2 V_p^2 \qquad (A.1)$$

There have been two major experimental studies. The first was that of Lunnon, who worked with rubber, wood, stone and steel spheres in air (1926) and bronze, lead and steel spheres in water (1928).

In addition to his original time-distance data, Lunnon evaluated steady flow drag coefficients and carried masses, b, for each sphere using the following equation:

$$C_{DA} = C_D + \frac{b}{\pi a^3 \rho}\left(\frac{2a}{v_p^2}\frac{dv_p}{dt}\right) \qquad (A.2)$$

The most extensive experimental study was carried out by Moorman (1955). He studied the terminal Reynolds number range between 1 and 2000 for ratios of the density of the solid to the density of the liquid between 1.2 and 9. Odar (1966) has shown that an error of a considerable fraction of the full time increment occurred in most of Moorman's runs, resulting in a shift of the data parallel to the time axis. Recalculation of most of Moormans data has been subsequently done by Odar (1965).

The first analytical representation of the accelerated portion of fall of a sphere was performed by Basset (1888, 1910). He described the motion by an integro-differential equation based upon the Navier Stokes equation for a viscous, incompressible fluid when the convective acceleration terms have been neglected. The resulting expression is

$$\frac{4}{3}\pi a^3 \rho_s \frac{dV_p}{dt} + \frac{2}{3}\pi a^3 \rho \frac{dV_p}{dt} = \frac{4}{3}\pi a^3(\rho_s - \rho)g - 6\pi a \mu V_p - 6a^2(\pi\mu\rho)^{\frac{1}{2}} \int_0^t \frac{\left(\frac{dV_p}{d\tau}\right)}{(t-\tau)^{\frac{1}{2}}}\, d\tau \qquad (A.3)$$

and has been the basis for most of the later work. In this relationship the first term is the particle mass times acceleration, and the second accounts for the acceleration of the added mass. The first term on the right is the buoyant force, and the second is the steady state drag at

the instantaneous velocity. The final term is the Basset history integral, which corrects the viscous drag for the transient condition.

The added mass, which is the same as that for potential flow arises naturally in the derivation from the Navier Stokes equation. In a physical sense it represents the increase in inertia of the sphere due to the resistance to acceleration of the fluid clinging to the sphere. The concept was first expressed by DuBuat (1776) and later given exact mathematical interpretation by Birkhoff (1960).

The first numerical evaluation of the velocity relations was carried out by Hughes and Gilliland (1952). They evaluated the complex error function by its infinite series representation. Velocity time curves calculated by Hughes and Gilliland are presented in Figure A.1.

Hjelmfelt and Mockros (1967) showed that the Basset equation exactly predicts experimental data in the creeping flow regime when all terms in the equation are retained. The significance of the added mass term and the history integral are clearly demonstrated in plots where equations with and without these terms and experimental data were compared. The differences due to neglect of the history and added mass terms are greatest for small density ratios ρ_s/ρ and decrease with increasing density ratio becoming negligible for density ratios greater than 1000.

The Basset formulation has been extended to include the intermediate Reynolds number regime by Brush, Ho and Yen (1964) and Odar (1966). The first authors replaced the laminar flow friction drag by the instantaneous Reynolds number and its corresponding experimental steady state drag. The coefficient of the integral term was assumed to be the

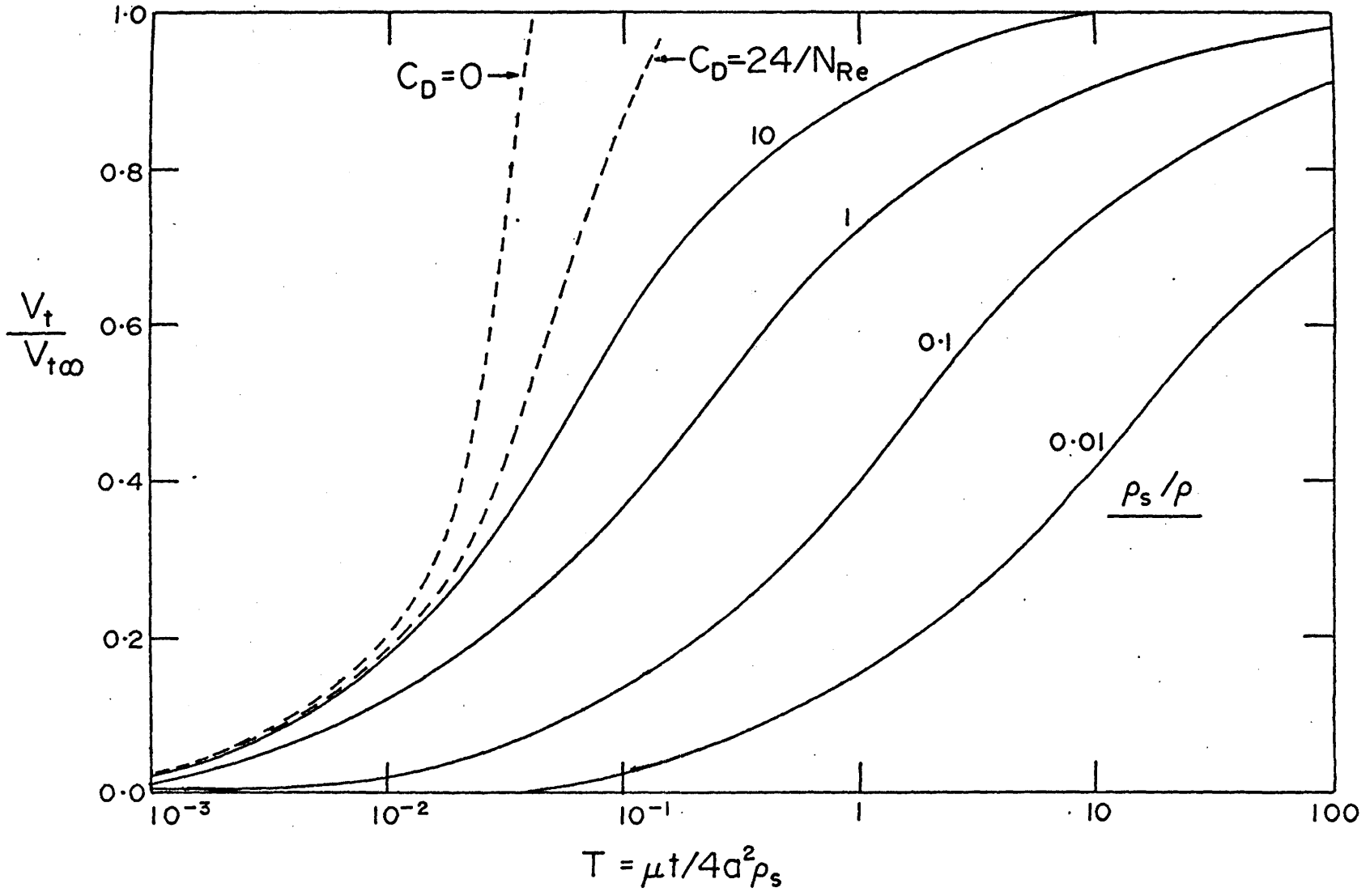

FIGURE A.1 HUGHES AND GILLILAND (1952) ACCELERATING SPHERE SOLUTIONS

same as that for laminar flow. The equation was then integrated numerically to obtain velocity-time data. Odar and Hamilton (1964) proposed that the fluid resistance force on a sphere in rectilinear acceleration could be described by a Basset relationship of the following form

$$-F = \frac{1}{2} C_D \pi a^2 \rho |v_p| v_p + C_V \frac{4}{3}\pi a^3 \rho \left(\frac{dv_p}{dt}\right) + C_H a^2 (\pi\mu\rho)^{\frac{1}{2}} \int_0^t \frac{(dv_p/d\tau)}{(t-\tau)^{\frac{1}{2}}} \qquad (A.4)$$

where C_V, the added mass coefficient and C_H, the history coefficient are functions of the local and convective acceleration. The coefficients, C_V and C_H were determined from experiment by best fit techniques and found to be

$$C_V = 1.05 - 0.066/(N_{Ac}^2 + 0.12) \qquad (A.5)$$

$$C_H = 2.88 + 3.2 \ /(N_{Ac} + 1)^2 \qquad (A.6)$$

where $N_{Ac} = V_p^2/a\left(\frac{dv_p}{dt}\right)$, and is the acceleration number. Odar (1966) used the Basset equation and these coefficients to determine velocity-time curves for spheres falling under the influence of gravity and obtained very good agreement with the experimental data of Moorman.

A.3 Steady State Flow Around a Fluid Sphere

Early theoretical studies on fluid spheres were confined to creeping motion in an infinite medium, by introducing modifications to Stokes' solution for rigid spheres. The dimensionless Navier-Stokes equation of motion in polar coordinates allowing for axial symmetry in terms of the stream function is

$$\frac{N_{Re}}{2}\left[\frac{\partial\psi}{\partial r}\cdot\frac{\partial}{\partial\theta}\left(\frac{E^2\psi}{r^2\sin^2\theta}\right)-\frac{\partial\psi}{\partial\theta}\frac{\partial}{\partial r}\left(\frac{E^2\psi}{r^2\sin^2\theta}\right)\right]\sin\theta+E^4\psi=0 \qquad (A.7)$$

where

$$E^2=\frac{\partial^2}{\partial r^2}+\frac{\sin\theta}{r^2}\frac{\partial}{\partial\theta}\left(\frac{1}{\sin\theta}\frac{\partial}{\partial\theta}\right) \qquad (A.8)$$

The creeping motion equation is obtained by neglecting the inertia terms in the flow field, which reduces equation (A.7) to

$$E^4(\psi)=0 \qquad (A.9)$$

Stokes found an exact solution of this equation to be:

$$\psi=\left(\frac{A}{r}+Br+Cr^2+Dr^4\right)\sin^2\theta \qquad (A.10)$$

Solutions by Hadamard (1911) and those done independently by Rybczynski (1911) using the Stokes solution have shown that the change in boundary conditions at the particle interface yields a significant change in the velocity of a falling particle. The boundary conditions in the Hadamard-Rybczynski model are:

(1) far from the drop the flow is undisturbed and parallel.

(2) the velocity components are finite at all points within the drop.

(3) the normal components of the inner and outer velocities are zero at the drop surface.

(4) tangential velocity components are continuous at the interface.

(5) the normal and tangential components of the viscous shear stress tensor are continuous at the interface.

(6) the drop is spherical

The solution for the external fluid is

$$\psi = \left(\frac{A}{r} + Br\right) \sin^2\theta \tag{A.11}$$

and for the interior fluid is

$$\psi = (Cr^2 + Dr^4) \sin^2\theta \tag{A.12}$$

They predict the terminal velocity and drag coefficient for the fluid sphere as

$$U = \frac{2(\rho_i - \rho_o)ga^2}{9\mu_o} \left(\frac{3\mu_i + 3\mu_o}{3\mu_i + 2\mu_o}\right) \tag{A.13}$$

and $$C_D = \frac{24}{N_{Re}} \left(\frac{3\mu_i + 2\mu_o}{3\mu_i + 3\mu_o}\right) \tag{A.14}$$

The solution predicts that all drops moving in the Stokes regime will have internal circulation. This has not been found experimentally, in particular there appears to be a critical size below which circulation does not exist.

Boussinesq (1913) put forth the hypothesis that a thin layer of high viscosity exists near the interface for a surface undergoing dilatation. The change was attributed to a combined effect of the surface tension and a "dynamic" increment to the normal surface tension, with the latter varying over the surface. The velocity of fall of the drop according to Boussinesq's theory is given by

$$U = \frac{2(\rho_o - \rho_i)ga^2}{3\mu_o} \left(\frac{\mu_o + \mu_i + \frac{2e}{3a}}{2\mu_o + 3\mu_i + \frac{2e}{a}}\right) \qquad (A.15)$$

where e is the surface viscosity coefficient which expresses the relation between surface tension and the rate at which the surface of the liquid changes. The coefficient can only be evaluated from experimental data, and is used to explain the drag curve intermediate between those of rigid and fully circulating fluid spheres.

Early experimental results indicated that the drag for small droplets was much closer to that given by Stokes for a rigid sphere than to the Hadamard-Rybczynski solution. Bond and Newton (1928) have shown that for small drop radii the rate of descent of a drop is very close to the value given by Stokes' law for rigid spheres. With increasing radii the rate of descent is in accord with Stokes formula until a critical radius is reached when the rate of descent changes comparatively rapidly and reaches Hadamard's value. From Bond and Newtons work came a criteria for circulation, the Bond number,

$$B = \frac{(\rho_o - \rho_i)ga^2}{\sigma} = \frac{\text{gravity force}}{\text{surface force}} \qquad (A.16)$$

which determines whether a drop will circulate. This result, which defines a sharp transition from Stokes to Hadamard's value, is in contradiction with the Boussinesq theory where the change is gradual.

Savic (1953) investigated experimentally drops falling in the stagnant to circulating transition region. He observed that with drops of small diameter, the center of the vortex ring appeared to be forward of the horizontal equator yielding a flow which was asymmetric. This

result is in agreement with a growing body of theoretical and experimental evidence.

A further observation was that a stagnant cap appeared to develop in the upper region of the drop with a fairly well defined edge at which the circumferential streaming came to an abrupt stop. With smaller drops the cap was larger, and for the smallest drops it enveloped the whole drop. These observations lead Savic to propose the circulation under a stagnant monolayer model for drop hydrodynamics. He postulated that a relatively incompressible surface layer is formed, which over a portion of the surface inhibits transmission of the viscous surface traction from the external medium into the liquid of the drop.

Scriven (1960) formulated the dynamics of a newtonian fluid interface which is characterized by an equilibrium surface tension and two coefficients of surface viscosity. With consideration of the intimate coupling between surface and substrate, the analysis yields the interfacial boundary conditions for two-phase flows. In spherical polar coordinates the analysis yields the following:

$$-J_{r\theta} + \hat{J}_{r\theta} = \frac{1}{a}\frac{\partial\sigma}{\partial\theta} + (K+\varepsilon)\frac{1}{a}\frac{\partial}{\partial\theta}\left\{\frac{1}{a\sin\theta}\left(\frac{\partial(v_\theta\sin\theta)}{\partial\theta} + \frac{\partial v_\phi}{\partial\phi}\right)\right\}$$

$$+ \varepsilon\left\{\frac{2v_\theta}{a^2} + \frac{1}{a\sin\theta}\frac{\partial}{\partial\phi}\left\{\frac{1}{a\sin\theta}\left(\frac{\partial v_\theta}{\partial\phi} - \frac{\partial(v_\theta\sin\theta)}{\partial\phi}\right)\right\}\right\} \qquad (A.17)$$

$$-J_{r\phi} + \hat{J}_{r\phi} = \frac{1}{a\sin\theta}\frac{\partial\sigma}{\partial\phi} + (K+\varepsilon)\frac{1}{a\sin\theta}\frac{\partial}{\partial\phi}\left\{\frac{1}{a\sin\theta}\left(\frac{\partial(v_\theta\sin\theta)}{\partial\theta} + \frac{\partial v_\phi}{\partial\phi}\right)\right\}$$

$$+ \varepsilon\left\{\frac{2v_\theta}{a^2} + \frac{1}{r}\frac{\partial}{\partial\theta}\left\{\frac{1}{a\sin\theta}\left(\frac{\partial(v_\theta\sin\theta)}{\partial\theta} - \frac{\partial v_\theta}{\partial\phi}\right)\right\}\right\} \qquad (A.18)$$

$$-J_{rr} + \hat{J}_{rr} = \frac{2\sigma}{a} - \frac{2K}{a}\left\{\frac{1}{a\sin\theta}\left(\frac{\partial(v_\theta \sin\theta)}{\partial\theta} + \frac{\partial v_\phi}{\partial\phi}\right)\right\} \qquad (A.19)$$

With the introduction of large and fast computers, much work has been done on the solution of the Navier Stokes equations. Hamielec and Johnson (1962) solved the complete Navier-Stokes equation for a circulating droplet using a numerical method after Kawaguti. The results show moderate agreement with experiment, however they do not reduce to the Hadamard-Rybczynski solution at low Reynolds numbers. An interesting result is the prediction of a secondary vortex within the droplet at large Reynolds numbers and viscosity ratios. Secondary vortices have been observed experimentally and their effect on a stagnant monolayer and indirectly on the stagnant monolayer theory will prove interesting. Complete solution of the Navier-Stokes equation for solid spheres and gas bubbles using finite difference techniques have been done by Hamielec, Hoffman and Ross (1967) and Hamielec, Johnson and Houghton (1967) respectively. These solutions should provide limiting solutions for fluid droplets.

Mo... ...s of continuity, momentum and energy are developed using a fixed reference frame (or coordinate system) with respect to which distances and velocities are measured. This frame of reference is normally referred to as the laboratory frame of reference. If a non-rotating reference frame moves at constant relative velocity with respect to the laboratory reference frame, a Galilean transformation yields a relationship between velocities in both reference frames (Whitaker, 1968).

Consider the reference frame moving with velocity $\bar{w}$, then the relative velocity is

$$\bar{v}_r = \bar{v} - \bar{w} \tag{B.1}$$

and the equation of motion takes the form:

$$\rho \left[\frac{\partial}{\partial t}(\bar{v}_r+\bar{w}) + (\bar{v}_r+\bar{w}).\nabla(\bar{v}_r+\bar{w})\right] = -\nabla_p + \rho\bar{g} + \mu\nabla^2(\bar{v}_r+\bar{w}) \tag{B.2}$$

if $\bar{w}$ is independent of time, $\bar{w}\neq\bar{w}(t)$, this reduces to

$$\rho \frac{\partial \bar{v}_r}{\partial t} + \rho\bar{w}.\nabla\bar{v}_r + \rho\bar{v}_r.\nabla\bar{v}_r = -\nabla_p + \mu\nabla^2\bar{v}_r + \rho\bar{g} \tag{B.3}$$

which reduces to

$$\rho \frac{d\bar{v}_r}{dt} + \rho\bar{v}_r.\nabla\bar{v}_r = -\nabla_p + \mu\nabla^2\bar{v}_r + \rho\bar{g} \tag{B.4}$$

and the equation of motion takes the same form for an observer moving with velocity, $\bar{w}$, as for a fixed observer. If $\bar{w}$ is a function of time $\bar{w} = \bar{w}(t)$, the equation reduces to

$$\rho \frac{\partial \bar{v}_r}{\partial t} + \rho \bar{w} \cdot \nabla \bar{v}_r + \rho \frac{d\bar{w}}{dt} + \rho \bar{v}_r \cdot \nabla \bar{v}_r = -\nabla_p + \mu \nabla^2 \bar{v}_r + \rho \bar{g} \qquad (B.5)$$

which reduces to

$$\rho \frac{d\bar{v}_r}{dt} + \rho \bar{v}_r \cdot \nabla \bar{v}_r + \rho \frac{d\bar{w}}{dt} = -\nabla_p + \mu \nabla^2 \bar{v}_r + \rho \bar{g} \qquad (B.6)$$

for an observer in the accelerating frame of reference (Batchelor, 1969; Bradbury, 1968). The term $\rho d\bar{w}/dt$ is a fictitious uniform body force and provides an additional contribution to the fluid pressure on a body when viewed in an accelerating frame of reference.

B.1.2 Mathematical Methods

Viscous flow of fluids is governed by the well-known Navier Stokes equations. These are nonlinear second-order partial differential equations. Although approximate methods of solution would be best for parametric understanding, it is well known that in many problems of hydrodynamics one cannot obtain valid solutions in closed form. The asymptotic behaviour of the solutions and even more generally their qualitative properties are barely obtainable through analytical work alone. This is even true of some problems which have already been made highly schematic by neglecting various physical parameters. For these reasons a great deal of effort has been spent on developing finite difference methods.

There are two main finite difference methods for obtaining steady-state solutions to transport phenomena problems, namely, the steady-state method and the unsteady-state method. The general numerical procedures are similar in each case except that the derivative with respect to time is dropped in the steady state method. A steady-state solution can only be obtained if the scheme used is stable and convergent,

assuming, of course, that such a solution exists for the system of differential equations and boundary conditions.

A differentiation between stability and convergence is appropriate at this point. Son (1968) has very adequately differentiated between these two frequently confused definitions. He points out that in the numerical solution of any partial differential equation, three solutions must be considered: the exact solution of the partial differential equation, the exact solution of the partial difference equation (obtained by replacing the derivatives in the partial differential equation by some type of finite difference representation) and the numerical solution of the partial difference equation. The difference between the first and second solution is due to truncation error of the finite difference representation of the derivatives, whereas, the difference between the second and third solution is caused by truncation of the numbers involved in the actual computation since only a certain number of digits can be retained. A scheme is said to be stable if the numerical solution of the partial difference equation approaches its exact solution. On the other hand, the scheme is convergent if the exact solution of the partial difference equation approaches the exact solution of partial differential equation. Stability does not necessarily imply convergence. Lax and Richtmeyer (1956) have shown that for a linear initial value problem, stability implies convergence if certain restrictions are satisfied. Similarly convergence has been proved for linear elliptic equations, however, mathematicians have been unable to prove convergence for non-linear equations. Interval size is also tied into accuracy and stability.

The interval size affects the discretization error and round-off error in the opposite sense. The first decreases as the interval decreases, while the round-off error generally increases. It is for this reason that one cannot generally assert that decreasing the mesh size always increases accuracy and stability (Ames, 1965).

One of the advantages of the unsteady state approach is that both transient and steady state solutions are obtained if the solution is started at the initial conditions or at some time when the solution is known. Another advantage is that a program so written could be used to obtain the steady state solution starting with an estimate of this solution just as in the steady state method. This reduces markedly the computer time required in parametric studies. However, there are stability problems associated with the unsteady state method which reduces the size of time step that can be used to advance the solution.

The disadvantage of the steady state approach is that it is difficult to obtain an estimate of the steady state solution in certain problems. This is particularly true in the present problems. Approximate solutions are not available at the Reynolds numbers of interest. Furthermore, it is not known whether a steady state solution exists at higher Reynolds numbers.

Because of their importance, viscous flow computations have received considerable attention in the literature. Based upon numerical method one may divide the papers into three groups: Fromm and Harlow method, Jensen method, and Pearson method.

Fromm and Harlow Method

Fromm (1963) and Fromm and Harlow (1963) at Los Alamos developed an explicit forward time difference method of solving the Navier Stokes equation. Their method has been used by Thoman and Szewczyk (1966) to determine time dependent two dimensional cross flow of a viscous incompressible fluid over stationary and rotating cylinders and by Rimon and Cheng (1969) to study uniform flow over a sphere. In the method vorticity and stream function are introduced into the equations of motion yielding the vorticity transport equation and the stream function equation. The basic steps involved in advancing the configuration through the cycle from time t to time t+dt are as follows:

1) at the beginning of the cycle all required quantities are available in the computer memory, either as initial data, or as results from the previous cycle.

2) for each vorticity point, a new value is found by an explicit forward difference approximation of the vorticity transport equation.

3) for each stream function point, a new value is found from a finite difference approximation of the defining equation for vorticity. The method of solution involves a succession of iterations. The most often used method is the extrapolated-Liebman method, or successive over-relaxation method.

4) the new components of velocity, surface pressure, surface vorticity are calculated.

Jenson Method

The Jenson method (1959) is a solution of the steady-state Navier Stokes equation. In the method, the stream function and vorticity are introduced into the equations of motion yielding the vorticity transport equation and the defining equation for vorticity as in Fromm and Harlow's method. The finite difference analogues of these equations are solved simultaneously using an iterative method, usually successive over relaxation. The method has been used by many authors, in particular, Hamielec, Hoffman and Ross (1967) used the method to study flow around a sphere with and without blowing, Hamielec and Raal (1969) to study flow around a circular cylinder in cross-flow and Epstein and Masliyah (1969) to study non-turbulent flow past oblate and prolate spheroids.

Pearson Method.

Pearson (1965) developed a time-dependent method for solving viscous flow problems which employs an implicit procedure. The method is a variation of the predictor-corrector methods for solving parabolic equations discussed by Ames (1965). The vorticity transport equation is approximated by an implicit Crank Nicholson method where the non-linear terms, the stream function and its derivatives, have been linearized over the time interval. The basic steps in the method for advancing from time t to time t+dt are as follows:

1) predict new values for each vorticity point using an implicit method where all stream function values used are at time t.

2) for each stream function point, a new value is found by successive over relaxation.

3) correct new values of vorticity using implicit method and a linearized stream function and its derivatives by averaging stream function values at time t and previously calculated value at t+dt.

4) determine steam function again by successive over relaxation.

5) repeat steps (3) and (4) until the change in vorticity at time t+dt is less than a specified tolerance between successive iterations. The method of solution of the Crank Nicholson approximation of the vorticity transport equation is the implicit alternating direction method devised by Peaceman and Rachford (1955). Son (1968) used the Pearson method to study flow around a cylinder.

B.2 Steady State Flow Around a Solid Sphere

B.2.1 Formulation

In the present formulation values for the drag on a sphere falling in a viscous fluid at its terminal velocity have been computed by solving the Navier Stokes equations numerically using a digital computer. For this purpose a finite difference technique described in detail by (Hamielec, Hoffman, and Ross, 1967) was employed. Using all quantities in their nondimensionalized form, which are defined as follows

$$v'_\theta = v_\theta/U_\infty, \quad v'_r = v_r/U_\infty, \quad r' = r/a$$

$$\psi' = \psi/a^2U_\infty, \quad \xi' = \xi a/U_\infty, \quad P' = (P-P_\infty)/\tfrac{1}{2}\rho U_\infty^2$$

$$N_{Re} = 2a\rho U_\infty/\mu$$

where, a, is the sphere radius, U_∞, the free stream velocity far from the sphere, and, P_∞, the fluid pressure far from the sphere; the complete, steady state Navier-Stokes equations for viscous incompressible, axisymmetric flow in terms of the stream function in spherical coordinates can be

written as

$$\frac{N_{Re}}{2}\left[\frac{\partial\psi}{\partial r}\cdot\frac{\partial}{\partial\theta}\left(\frac{E^2\psi}{r^2\sin^2\theta}\right)-\frac{\partial\psi}{\partial\theta}\frac{\partial}{\partial r}\left(\frac{E^2\psi}{r^2\sin^2\theta}\right)\right]\sin\theta = E^4\psi \qquad (B.7)$$

where

$$E^2 = \frac{\partial^2}{\partial r^2}+\frac{\sin\theta}{r^2}\frac{\partial}{\partial\theta}\left(\frac{1}{\sin\theta}\frac{\partial}{\partial\theta}\right) \qquad (B.8)$$

and where the primes have been suppressed for ease of writing.

The equation may be split into two simultaneous second order equations by introducing the vorticity in the form

$$E^2\psi = \xi r\sin\theta \qquad (B.9)$$

The equation then becomes

$$\frac{N_{Re}}{2}\left[\frac{\partial\psi}{\partial r}\frac{\partial}{\partial\theta}\left(\frac{\xi}{r\sin\theta}\right)-\frac{\partial}{\partial\theta}\frac{\partial}{\partial r}\left(\frac{\xi}{r\sin\theta}\right)\right]\sin\theta = E^2(\xi r\sin\theta) \qquad (B.10)$$

The velocity components are related to the stream function by the relations

$$v_\theta = \frac{1}{r\sin\theta}\frac{\partial\psi}{\partial r} \qquad v_r = \frac{-1}{r^2\sin\theta}\frac{\partial\psi}{\partial\theta}$$

The boundary conditions used for solving equations (B.9) and (B.10) are given as follows:

$$\theta = 0^\circ \text{ and } \theta = 180^\circ, \quad \psi = 0, \quad \xi = 0$$

on the sphere surface

$$r = 1, \quad \psi = 0, \quad \frac{\partial\psi}{\partial r} = 0$$

On the boundary remote from the surface of the sphere and concentric with the sphere there is undisturbed parallel flow

$$r = r_\infty, \quad \psi = \frac{1}{2}r_\infty^2\sin^2\theta, \quad \xi = 0$$

Following Jenson (1959), an exponential step size in the radial direction is used for the flow field. The substitution is $r = e^z$ and equal intervals are taken in z. The stream function and vorticity vary most rapidly near the particle surface and hence it is desirable to have a small step size at the surface. As the core storage of a digital computer is a limiting factor in problems where there are boundaries at infinity, the exponential step size plays an important role in reducing the number of mesh points. When written in terms of z the equations appear as

$$\frac{N_{Re}}{2}\left[\frac{\partial\psi}{\partial z}\frac{\partial}{\partial\theta}\left(\frac{\xi}{e^z\sin\theta}\right)-\frac{\partial\psi}{\partial\theta}\frac{\partial}{\partial z}\left(\frac{\xi}{e^z\sin\theta}\right)\right]e^z\sin\theta = e^{2z}E^2(\xi e^z\sin\theta) \qquad (B.11)$$

and

$$\xi e^{3z}\sin\theta = e^{2z}E^2\psi \qquad (B.12)$$

where

$$e^{2z}E^2 = \frac{\partial^2}{\partial z^2} - \frac{\partial}{\partial z} + \sin\theta\frac{\partial}{\partial\theta}\left(\frac{1}{\sin\theta}\frac{\partial}{\partial\theta}\right) \qquad (B.13)$$

The boundary conditions are transformed to:

along the axis of symmetry

$$\theta = 0^\circ \text{ and } \theta = 180^\circ,\ \psi = 0,\ \xi = 0$$

on the sphere surface

$$z = 0,\ \psi = 0,\quad \frac{\partial\psi}{\partial z} = 0$$

on the boundary remote from the sphere surface

$$z = z_\infty,\ \psi = \frac{1}{2}e^{2z_\infty}\sin^2\theta,\ \xi = 0$$

B.2.2 Surface Pressure Distribution and Drag Coefficients

The pressure at any point in the flow field may be determined by integrating the component forms of the Navier Stokes equations from point to point along the parametric lines making up the grid. The frontal stagnation pressure is obtained by integrating the r-component of the equation of motion along the parametric line $\theta = 0°$. The equation reduces to

$$P_o = 1 + \frac{4}{N_{Re}} \int_1^{r_\infty} \left(\frac{\partial \xi}{\partial \theta} + \xi \cot\theta\right) \frac{dr}{r} \qquad (B.14)$$

The term $\xi\cot\theta$ is indeterminate at $\theta = 0°$, however it may be resolved using ℓ'Hospital's rule. The final form of the equation is

$$P_o = 1 + \frac{8}{N_{Re}} \int_1^{z_\infty} \left(\frac{\partial \xi}{\partial \theta}\right) dz \qquad (B.15)$$

The surface pressure may be found by integrating the θ-component of the equation of motion from the frontal stagnation point over the surface along the parametric line $r = 1$ $(z=0)$. The equation reduces to

$$P_\theta = P_o + \frac{4}{N_{Re}} \int_o^{\theta} \left(\frac{\partial \xi}{\partial z} + \xi\right) d\theta \qquad (B.16)$$

These equations are in dimensionless form (primes supressed); where the pressure was made dimensionless by the following relation $P' = P/\frac{1}{2}\rho U_\infty^2$.

The dimensionless drag coefficients, defined as $C_D = F/(\pi a^2 \frac{1}{2}\rho U_\infty^2)$ may be obtained by integrating the viscous forces and the surface pressure over the sphere surface. The pressure drag relationship is as follows

$$C_{DP} = \int_o^{\pi} P \sin 2\theta d\theta \qquad (B.17)$$

The friction drag coefficient which is obtained by integrating the normal and tangential components of the viscous stress tensor, as mentioned above, reduces to

$$C_{DF} = \frac{8}{N_{Re}} \int_0^{\pi} \xi\Big/_{z=o} \sin^2\theta d\theta \qquad (B.18)$$

The total drag coefficient is the sum of the component coefficients.

$$C_D = C_{DF} + C_{DP} \qquad (B.19)$$

B.2.3 Method of Solution

The solution of the stream function and vorticity transport equations is obtained by modified form of the Extrapolated-Liebman method. (Fox, 1962; and Lapidus, 1962). The finite difference approximation to the stream function equation is

$$(\psi_{ij}^{m+1})^* = f(\psi_{i+1,j}^{m}, \psi_{i-1,j}^{m+1}, \psi_{i,j-1}^{m+1}, \psi_{i,j+1}^{m} \xi_{ij}^{m+1}) \qquad (B.20)$$

$$(\xi_{ij}^{m+1})^* = f(\xi_{i+1,j}^{m}, \xi_{i-1,j}^{m+1} \xi_{i,j-1}^{m+1}, \xi_{i,j+1}^{m},$$

$$\psi_{i+1,j}^{m}, \psi_{i-1,j}^{m+1}, \psi_{i,j-1}^{m+1}, \psi_{i,j+1}^{m}) \qquad (B.21)$$

where ψ_{ij}^{m} and ψ_{ij}^{m+1}, etc are approximations to the stream function and vorticity at the m^{th} and $(m+1)$th iterations respectively. In the iterative procedure, relaxation factors are used to stabilize the computations. These are introduced as follows:

$$\psi_{ij}^{m+1} = (1-w)\psi_{ij}^{m} + w(\psi_{ij}^{m+1})^* \qquad (B.22)$$

$$\xi_{ij}^{m+1} = (1-v)\xi_{ij}^{m} + v(\xi_{ij}^{m+1})^* \qquad (B.23)$$

The effective change per iteration is taken as a fraction of the actual change and is governed by the values selected for v and w. Suitable values of these relaxation parameters may be found by trial and error. In particular, excessively large values produced oscillating solutions which diverged, with very small values, however, computation times are excessive.

Briefly, the Extrapolated-Liebman method consists of applying the finite difference approximation equations at every interval grid point in regular succession. The points are scanned row by row and left to right starting from the row next to the solid boundary at the frontal stagnation point end. This completes one iteration. The procedure is repeated until values of the stream function and vorticity in two successive iterations satisfy the equations

$$|\psi_{i,j}^{m+1} - \psi_{i,j}^{m}| \leq 10^{-5}$$

$$|\xi_{i,j}^{m+1} - \xi_{i,j}^{m}| \leq 10^{-5}$$

at all grid points. The computations were carried out in the McMaster University IBM7040 and CDC6400 computers. A FORTRAN IV listing of the program is given in Appendix I-A.

B.3 Unsteady State Flow Around a Solid Sphere

B.3.1 Formulation

The determination of flow around a sphere is most easily handled by using spherical polar coordinates centered at the sphere center. In the case of a sphere accelerating under the influence of gravity, a rectilinear accelerating frame of reference is obtained. For an observer in the accelerating frame of reference there is another term in the equations of motion. The term is a fictitious uniform body force and provides an additional contribution to the fluid pressure on a body (Batchelor, 1969; Bradley, 1968).

The flow around a sphere, in the absence of vortex shedding ($N_{Re} \leq 300$), is axisymmetric and thus may be described in (r, θ) plane. If the curl of the momentum equation is taken, the vorticity transport equation is obtained. With axial symmetry the vorticity is always in the azimuthal direction. The time dependent transport equation in the two dimensions is as follows:

$$\frac{\partial}{\partial t}(\xi r\sin\theta) + \frac{1}{r^2\sin\theta}\left[\frac{\partial\psi}{\partial r}\frac{\partial}{\partial\theta}(\xi r\sin\theta) - \frac{\partial\psi}{\partial\theta}\frac{\partial}{\partial r}(\xi r\sin\theta)\right]$$

$$\frac{-2\xi}{r\sin\theta}\left[\frac{\partial\psi}{\partial r}\cos\theta - \frac{1}{r}\frac{\partial\psi}{\partial\theta}\sin\theta\right] = \upsilon\left[\frac{\partial^2}{\partial r^2}(\xi r\sin\theta) + \frac{1}{r^2}\frac{\partial^2}{\partial\theta^2}(\xi r\sin\theta)\right.$$

$$\left. - \frac{\cot\theta}{r^2}\frac{\partial}{\partial\theta}(\xi r\sin\theta)\right] \qquad \text{(B.24)}$$

where the stream function, ψ, has been introduced by

$$v_\theta = \frac{1}{r\sin\theta}\frac{\partial\psi}{\partial r} \quad , \quad v_r = -\frac{1}{r^2\sin\theta}\frac{\partial\psi}{\partial\theta}$$

and the vorticity, ξ, has been defined by the equation

$$r\sin\theta\xi = \frac{\partial^2\psi}{\partial r^2} + \frac{1}{r^2}\frac{\partial^2\psi}{\partial\theta^2} - \frac{\cot\theta}{r^2}\frac{\partial\psi}{\partial\theta} \tag{B.25}$$

and satisfies the continuity equation. This equation is commonly referred to as the stream function equation.

By introduction of dimensionless quantities defined by the equations

$$\psi' = \psi/U_p(t)a^2, \quad \xi' = \xi a/U_p(t), \quad r' = r/a$$

$$T = \mu t/4\rho_s a^2, \quad N_{Re} = 2a\rho U_p(t)/\mu$$

where a is the particle radius, $U_p(t)$ the instantaneous particle velocity, ρ_s the particle density, and μ and ρ the fluid viscosity and density respectively and replacing the dimensionless radial coordinate r' by z through the transformation $r' = e^z$ equations (B.24) and (B.25) after suppressing the primes become:

$$\xi = \frac{e^{-3z}}{\sin\theta}\left[\frac{\partial^2\psi}{\partial z^2} - \frac{\partial\psi}{\partial z} + \frac{\partial^2\psi}{\partial\theta^2} - \cot\theta\frac{\partial\psi}{\partial\theta}\right] \tag{B.26}$$

$$\frac{\partial\xi}{\partial T} = \frac{4\rho_s}{\rho}e^{-2z}\left[\frac{\partial^2\xi}{\partial z^2} + \frac{\partial\xi}{\partial z} + \frac{\partial^2\xi}{\partial\theta^2} + \cot\theta\frac{\partial\xi}{\partial\theta} - (1+\cot^2\theta)\xi\right] \tag{B.27}$$

$$- \frac{2\rho_s N_{Re} e^{-3z}}{\rho\sin\theta}\left[\frac{\partial\psi}{\partial z}\frac{\partial\xi}{\partial\theta} - \frac{\partial\psi}{\partial\theta}\frac{\partial\xi}{\partial z} + \xi\left(\frac{\partial\psi}{\partial\theta} - \cot\theta\frac{\partial\psi}{\partial z}\right)\right] - \frac{\xi}{N_{Re}}\frac{dN_{Re}}{dT}$$

The boundary conditions used in the solution of the transport equations are

along the axis of symmetry

$$\theta = 0° \text{ and } \theta = 180°, \quad \psi = 0, \quad \xi = 0$$

on the sphere surface

$$z = 0, \quad \psi = 0, \quad \frac{\partial \psi}{\partial z} = 0$$

far from the sphere there is undisturbed parallel flow

$$z = z_\infty, \quad \psi = \frac{1}{2} e^{2z_\infty} \sin^2\theta, \quad \xi = 0$$

The initial condition applied to the equations was

$$T = 0, \quad \psi = 0, \quad \xi = 0, \quad N_{Re} = 0$$

As the coordinate system is centered on the sphere, the equation of motion for the particle must be solved simultaneously with the transport equation. For a particle accelerating in the intermediate Reynolds number regime the drag forces are best expressed in terms of the instantaneous drag coefficient and the instantaneous particle velocity (Birkhoff, 1960). Thus

$$\frac{4}{3}\pi a^3(\rho_s + \frac{1}{2}\rho)\frac{dU_p(t)}{dt} = \frac{4}{3}\pi a^3(\rho_s - \rho)g - \frac{1}{2}\rho U_p^2(t)\pi a^2 C_D \qquad \text{(B.28)}$$

The equation is made dimensionless by using the same quantities as in the transport equation yielding

$$[1 + \frac{1}{2}(\frac{\rho}{\rho_s})]\frac{dN_{Re}}{dT} = \frac{8a^3}{\mu^2}\rho(\rho_s - \rho)g - \frac{3}{4}N_{Re}^2 C_D \qquad \text{(B.29)}$$

where $\frac{8a^3}{\mu^2}\rho(\rho_s - \rho)g = \frac{3}{4}N_{Re_f}^2 C_{D_f}$ and N_{Re_f} and C_{D_f} are the steady-state Reynolds number and drag coefficient respectively. The drag coefficient at any time may be calculated by integrating the surface forces around the sphere. The pressure distribution is determined from the θ-component of the equation of motion, thus:

$$\left(\frac{\partial P}{\partial \theta}\right)_{z=o} = \frac{4}{N_{Re}}\left(\xi + \frac{\partial \xi}{\partial z}\right) + \left(\frac{\rho}{\rho_s}\right)\frac{1}{N_{Re}^2}\frac{dN_{Re}}{dT}\sin\theta \qquad \text{(B.30)}$$

Equation (B.30) is then integrated to give the pressure drag coefficient:

$$C_{DP} = \int_0^{\pi} (P)_{z=0} \, 2\sin\theta\cos\theta d\theta \tag{B.31}$$

The friction drag coefficient is found by integrating the normal and tangential stresses over the surface; the relationship reduces to

$$C_{DF} = \frac{8}{N_{Re}} \int_0^{\pi} (\xi)_{z=0} \sin^2\theta d\theta \tag{B.32}$$

The total drag, C_D, is

$$C_D = C_{DF} + C_{DP} \tag{B.33}$$

B.3.2 Method of Solution

The solution is obtained by constructing a finite difference approximation to the vorticity transport equation and the stream function relationship on an expanding polar grid system. The particle equation is solved simultaneously using the Adam-Moulton method (Lapidus, 1962). In using the finite difference method, the object is to calculate the values of ψ and ξ at the intersections of the grid, for each time step.

An alternating-direction-implicit method developed by Peaceman and Rachford (1955) as modified by Pearson (1965) is used to calculate the values of the vorticity at the new time step. The method divides the time step, into two half-steps, and a finite-difference approximation is written for each half-step. The nonlinear terms, functions of ψ and N_{Re}, are linearized over the time steps. As these terms are not known at the new time a predictor-corrector type procedure is applied to the solution for each time step. The solution of the stream-function equation, equation (B.26), is obtained by successive overrelaxation at each time step.

To go from time nt to time $(n+1)t$ the procedure is as follows:

(a) Obtain a first approximation for ξ^{n+1} by solving the vorticity transport equation in the predictor form

(b) solve the stream function equation at time $(n+1)t$ using values of ξ^{n+1}, this gives values for ψ^{n+1}

(c) determine the boundary value of ξ^{n+1} on the sphere surface using the stream function equation with boundary conditions incorporated

(d) advance the particle equation one time step using vorticity and stream function values at $(n+1)t$

(e) obtain another approximation to $(\xi^{n+1})^m$ by solving the vorticity transport equation in the corrector form, incorporating previously calculated values of $(\psi^{n+1})^{m-1}$, $(N_{Re}{}^{n+1})^{m-1}$

(f) obtain another approximation to $(\psi^{n+1})^m$ using stream function equation

(g) determine boundary value of $(\xi^{n+1})^m$ on surface of sphere

(h) resolve the particle equation for $(N_{Re}{}^{n+1})^m$ using values of $(\xi^{n+1})^m$ and $(\psi^{n+1})^m$

(i) repeat steps, e, f, g, h iteratively m times until convergence has resulted. The time step is then complete. The above procedure is repeated for successive time steps until a steady state solution is obtained.

The calculations were carried out on the Master University CDC6400 computer. The dimensionless time step was varied from 0.00002 to 0.05 as the run progressed. It was increased at such a rate that the surface vorticity changed by less than one percent of its value per step. A FORTRAN IV listing of the program is given in Appendix I-A.

B.4 Steady State Flow Around a Fluid Sphere

B.4.1 Formulation

The Navier-Stokes equation for viscous, incompressible, axisymmetric flow for the stream function, ψ, in spherical polar coordinates may be written as

$$\frac{N_{Re}}{2}\left[\frac{\partial\psi}{\partial r}\frac{\partial}{\partial\theta}\left(\frac{E^2\psi}{r^2\sin^2\theta}\right) - \frac{\partial\psi}{\partial\theta}\frac{\partial}{\partial r}\left(\frac{E^2\psi}{r^2\sin^2\theta}\right)\right]\sin\theta = E^4\psi \qquad (B.34)$$

The equation may be split into two simultaneous second-order equations by introducing the vorticity, ξ, as follows

$$E^2\psi = \xi r\sin\theta \qquad (B.35)$$

$$\frac{N_{Re}}{2}\left[\frac{\partial\psi}{\partial r}\frac{\partial}{\partial\theta}\left(\frac{\xi}{r\sin\theta}\right) - \frac{\partial\psi}{\partial\theta}\frac{\partial}{\partial r}\left(\frac{\xi}{r\sin\theta}\right)\right]\sin\theta = E^2(\xi r\sin\theta) \qquad (B.36)$$

where $$E^2 = \frac{\partial^2}{\partial r^2} + \frac{\sin\theta}{r^2}\frac{\partial}{\partial\theta}\left(\frac{1}{\sin\theta}\frac{\partial}{\partial\theta}\right)$$

The equations can be made dimensionless by using the following dimensionless variables:

$$v'_\theta = v_\theta/U_\infty\ ,\quad v'_r = v_r/U_\infty,\quad r' = r/a$$

$$\psi' = \psi/U_\infty a^2,\quad \xi' = \xi a/U_\infty,\quad N_{Re} = \frac{2aU_\infty\rho_o}{\mu_o}$$

where, a, is the drop radius, U_∞, is the main stream velocity far from the drop, and ρ_o and μ_o are the viscosity and density of the continuous phase fluid.

In the case of fluid drops, these equations apply separately inside and outside of the drop. That is, we have two boundary value problems, each consisting of a set of second-order partial differential

equations and coupled by a common boundary. As the boundary conditions of the common boundary exist as derivatives a matching of solutions at the common boundary is necessary.

In the solution of problems of this nature, a numerical solution is necessary as valid solutions cannot be obtained in closed form. Following Jenson (1959), an exponential step size in the radial direction is used in the flow field outside the drop, by employing the substitution $r = e^z$ and taking equal intervals in z. As the stream function and vorticity vary most rapidly near the drop surface it is desirable to have a small step size near the surface. Also, because core storage in a digital computer is a limiting factor in solution of problems where there is a boundary at infinity, the exponential step size plays an important role in reducing the number of mesh points. Within the drop, equal intervals in r are used. The dimensionless equations after removing the primes become:

outside the drop (continuous phase)

$$\frac{N_{Re}}{2}\left[\frac{\partial\psi_o}{\partial z}\frac{\partial}{\partial\theta}\left(\frac{\xi_o}{e^z\sin\theta}\right) - \frac{\partial\psi_o}{\partial\theta}\frac{\partial}{\partial z}\left(\frac{\xi_o}{e^z\sin\theta}\right)\right]e^z\sin\theta = e^{2z}\underline{E}^2(\xi_o e^z\sin\theta) \quad (B.37)$$

$$\xi_o\, e^{3z}\sin\theta = e^{2z}\underline{E}^2\psi_o \quad (B.38)$$

where $$e^{2z}\underline{E}^2 = \frac{\partial^2}{\partial z^2} - \frac{\partial}{\partial z} + \sin\theta\,\frac{\partial}{\partial\theta}\left(\frac{1}{\sin\theta}\frac{\partial}{\partial\theta}\right)$$

inside the drop (dispersed phase)

$$\left(\frac{\mu_o}{\mu_i}\right)\left(\frac{\rho_i}{\rho_o}\right)\frac{N_{Re}}{2}\left[\frac{\partial\psi_i}{\partial r}\frac{\partial}{\partial\theta}\left(\frac{\xi_i}{r\sin\theta}\right) - \frac{\partial\psi_i}{\partial\theta}\frac{\partial}{\partial r}\left(\frac{\xi_i}{r\sin\theta}\right)\right]\sin\theta = E^2(\xi_i r\sin\theta) \quad (B.39)$$

$$\xi_i r\sin\theta = E^2\psi_i \tag{B.40}$$

To solve these equations for the flow fields inside and outside the drop, boundary conditions are required which completely enclose each flow field. The boundary conditions are given below in point form and in Figure B.1 descriptively:

(1) far from the drop undisturbed parallel flow is assumed

$$\psi_o = \frac{1}{2} e^{2z_\infty} \sin^2\theta \quad , \quad \xi_o = 0$$

(2) along the axis of symmetry

$$\theta = 0 \qquad \psi_o = 0, \quad \xi_o = 0, \quad \psi_i = 0, \quad \xi_i = 0$$

$$\theta = \pi \qquad \psi_o = 0, \quad \xi_o = 0, \quad \psi_i = 0, \quad \xi_i = 0$$

(3) at the fluid-fluid interface

i) no material transfer across the interface

$$r = 1, \quad z = 0; \qquad \psi_o = \psi_i = 0$$

ii) continuity of angular velocity across the interface

$$r = 1, \quad z = 0; \qquad \frac{\partial\psi_i}{\partial r} = \frac{\partial\psi_o}{\partial z}$$

iii) continuity of shear stress across the interface

$$r = 1, \quad z = 0; \qquad J_{r\theta_o} = J_{r\theta_i}$$

$$\left(\frac{\partial^2\psi_o}{\partial z^2} - \frac{3\partial\psi_o}{\partial z}\right) = \frac{\mu_i}{\mu_o}\left(\frac{\partial^2\psi_i}{\partial r^2} - \frac{2\partial\psi_i}{\partial r}\right)$$

B.4.2 Method of Solution

The solution of the stream function and vorticity transport equations in both flow fields is obtained numerically by a modified form of the Extrapolated-Liebman method (Fox, 1962; and Lapidus, 1962). The finite difference approximations are of the form

$$(\psi_{ij}^{m+1})^* = f(\psi_{i+1,j}^{m}, \psi_{i-1,j}^{m+1}, \psi_{i,j-1}^{m+1}, \psi_{i,j+1}^{m}, \xi_{ij}^{m+1}) \tag{B.41}$$

$$(\xi_{ij}^{m+1})^* = f(\xi_{i+1,j}^{m}, \xi_{i-1,j}^{m+1}, \xi_{i,j+1}^{m}, \xi_{i,j-1}^{m+1}, \psi_{i+1,j}^{m}, \psi_{i-1,j}^{m+1}, \psi_{i,j-1}^{m+1}, \psi_{i,j+1}^{m}) \tag{B.42}$$

where ψ_{ij}^{m} and ψ_{ij}^{m+1}, etc are approximations to the stream function and vorticity at the m^{th} and $(m+1)$th iterations respectively. In the iterative procedure, relaxation factors are used to stabilize the computations. The factors are introduced as follows:

$$\psi_{ij}^{m+1} = (1-w)\psi_{ij}^{m} + w(\psi_{ij}^{m+1})^* \tag{B.43}$$

$$\xi_{ij}^{m+1} = (1-v)\xi_{ij}^{m} + v(\xi_{ij}^{m+1})^* \tag{B.44}$$

The effective change per iteration is taken as a fraction of the actual change and is governed by the values selected for v and w. Suitable values of these relaxation factors may be found by trial and error. In particular, excessively large values could produce oscillating or divergent solutions, while small values although yielding stable solutions could be very time consuming.

Briefly, the Extrapolated-Liebman method consists of applying the finite difference approximation equations at every grid point in regular succession. The points are scanned row by row, from frontal stagnation line to rear stagnation line beginning with the row next to the interface and moving outward in the continuous fluid region and inward in the dispersed fluid region. The procedure is repeated until values of the stream function and vorticity in two successive iterations satisfy the equations

$$|\psi_{i,j}^{m+1} - \psi_{i,j}^{m}| \leq 10^{-5}$$

$$|\xi_{i,j}^{m+1} - \xi_{i,j}^{m}| \leq 10^{-5}$$

at all grid points.

The interface boundary between the two regions and the coupling equations (continuity of angular velocity and shear stress) are handled in the following manner. Assume that near the boundary the stream function may be approximated by the following equations (Jenson, 1959; Goodbody and Rhodes, 1969):

$$\psi_o = az + (Kb + \frac{3a}{2}) z^2 + cz^3 \qquad (B.45)$$

$$\psi_i = -a\alpha + (b+a)\,\alpha^2 + d\alpha^3 \qquad (B.46)$$

where $\alpha = 1-r$ and $K = \mu_i/\mu_o$

The interface conditions are automatically satisfied by these equations. The coefficients a, b, c, d can be found by fitting the polynomials to four points, two on each side of the boundary. Denoting values of ψ at these points by ψ_1, ψ_2 (outer fluid) and ψ_{-1}, ψ_{-2} (inner fluid) the coefficients are

$$a = \frac{\Delta\alpha^2(8\psi_1 - \psi_2) - K\Delta z^2(8\psi_{-1} - \psi_{-2})}{6\Delta\alpha\Delta z^2 K - 4\Delta\alpha^2\Delta z^2 K + 6\Delta z\Delta\alpha^2 + 6\Delta z^2\Delta\alpha^2} \tag{B.47}$$

$$b = \frac{(8\psi_1 - \psi_2)(4\Delta\alpha^2 - 6\Delta\alpha) - (8\psi_{-1} - \psi_{-2})(6\Delta z + 6\Delta z^2)}{4K\Delta z^2(4\Delta\alpha^2 - 6\Delta\alpha) - 4\Delta\alpha^2(6\Delta z + 6\Delta z^2)} \tag{B.48}$$

The coefficients may then be used in equations to determine the boundary value of vorticity in both regions of flow. The equations are:

$$\xi_o = \frac{2}{\sin\theta}(a + Kb), \quad \xi_i = \frac{2}{\sin\theta}(b + a)$$

Using these equations, the boundary surface vorticity values are updated at the end of each Extrapolated-Liebman iteration.

B.4.3 Surface Pressure Distribution and Drag Coefficients

The pressure at any point in the flow field may be determined by integrating the component forms of the Navier Stokes equations from point to point along parametric lines making up the grid. The frontal stagnation pressure is obtained by integrating the r-component of the equation of motion along the parametric line $\theta = 0°$. The equation reduces to

$$P_o = 1 + \frac{8}{N_{Re}} \int_1^\infty \left(\frac{\partial\xi}{\partial\theta}\right)_{\theta=o} \frac{dr}{r} \tag{B.49}$$

The surface pressure may be found by integrating the θ-component of the equation of motion from the frontal stagnation point over the surface along the parametric line r=1(z=0). The equation reduces to

$$P = P_o + \frac{4}{N_{Re}} \int_o^\theta \left(\frac{\partial\xi}{\partial r} + \xi\right) d\theta - v_\theta^2 \tag{B.50}$$

These equations are in dimensionless form (primes suppressed), where the pressure has been made dimensionless by the following relation

$$P' = P/\frac{1}{2}\rho_o U_\infty^2 \tag{B.51}$$

The dimensionless drag coefficients, defined as $C_D = F/(\pi a^2 \frac{1}{2}\rho_o U_\infty^2)$ may be obtained by integrating the viscous forces and the surface pressure over the sphere surface. The pressure drag relationship is as follows

$$C_{DP} = \int_o^\pi P \sin 2\theta d\theta \tag{B.52}$$

The friction drag coefficient, which is obtained by integrating the normal and tangential components of the viscous stress tensor, as mentioned above, reduces to

$$C_{DF} = \frac{8}{N_{Re}} \int_o^\pi \left(\frac{\partial v_\theta}{\partial r} \sin\theta - \frac{v_\theta}{r} \sin\theta - \frac{2\partial v_r}{\partial r} \sin\theta\right) \sin\theta d\theta \tag{B.53}$$

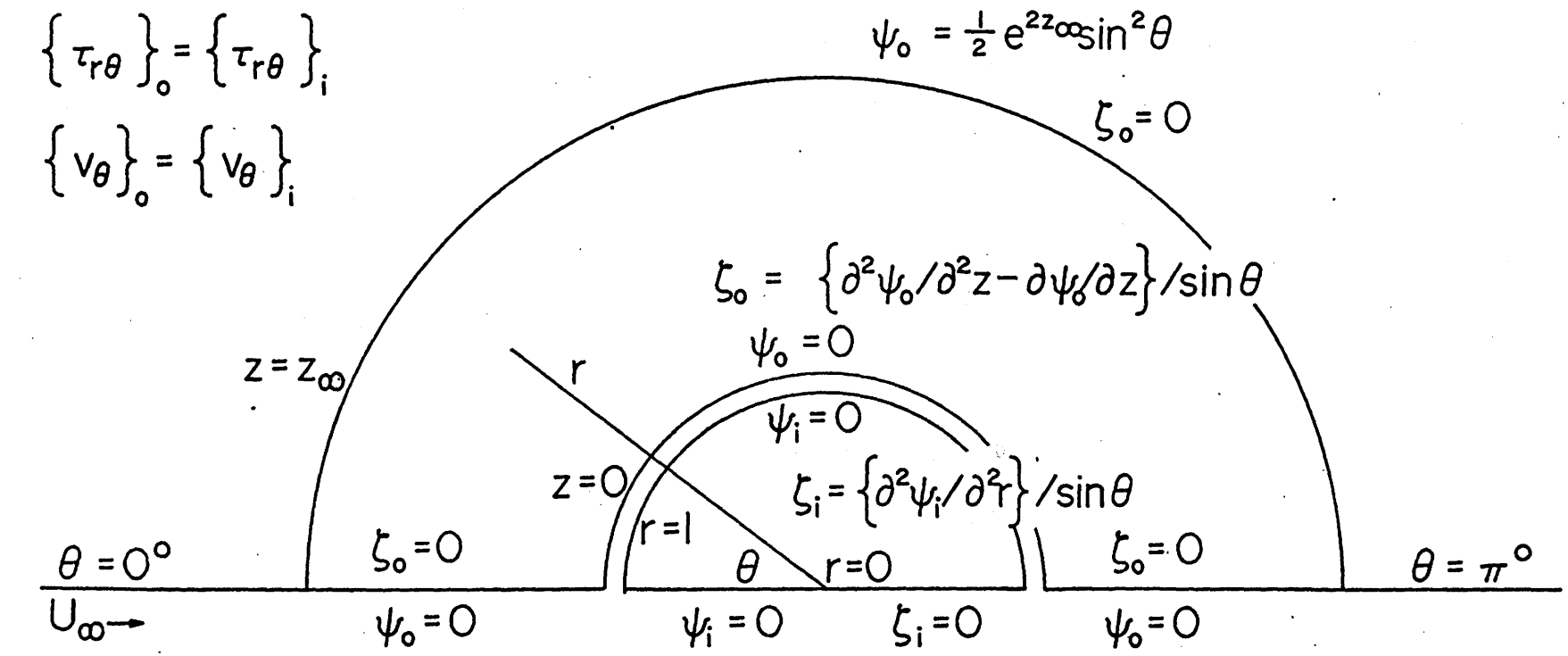

FIGURE B.1 BOUNDARY CONDITIONS FOR CIRCULATING DROPLET MODEL

C. Results and Discussion

C.1 Steady State Flow Around Solid Spheres

C.1.1 Drag Phenomena

The step sizes and the position of the outer boundary $r = r_\infty$ were varied in order to test the accuracy of the solutions. The results of these tests are presented in Table C.1. In simulating an unbounded fluid the position of the outer boundary was limited to about 1000 sphere radii by requirements for core storage and particularly computation time. The errors resulting from the position of the outer boundary and those resulting from finite step size were estimated from a comparison using the analytical solution of the Navier-Stokes equation in the form developed by Hamielec, Hoffman, and Ross (1967) and the numerical solution of the Navier-Stokes equations with the non-linear terms removed. For Stokes flow the Navier Stokes equation of motion reduces to the linear form

$$E^4 \psi = 0 \qquad (C.1)$$

This equation, to-gether with the same boundary conditions as those for the non-linear equation, was solved numerically. Alternatively, the equation can be solved analytically. The stream function can be expressed as

$$\psi = (A'/r + B'r + C'r^2 + D'r^4) \sin^2\theta \qquad (C.2)$$

The constants A', B', C' and D' in the equation were found by satisfying the same boundary conditions as those for the numerical solution and are given as a function of r_∞ by the relations

$$B' = \frac{(15/2)r_\infty^2}{2-10r_\infty^3 + 18r_\infty^5 - 10r_\infty^6} \tag{C.3}$$

$$C' = \frac{-(5/2)r_\infty^3 - 5r_\infty^6}{2-10r_\infty^3 + 18r_\infty^5 - 10r_\infty^6} \tag{C.4}$$

$$D' = \frac{(3/2)r_\infty^3}{2-10r_\infty^3 + 18r_\infty^5 - 10r_\infty^6} \tag{C.5}$$

The total drag coefficient is given by

$$C_D = -32\ B'/N_{Re} \tag{C.6}$$

The results of these computations are listed as a function of Reynolds number in Table C.2. The step size error was estimated from a comparison between the analytical solution and the numerical solution of the Stokes equation assuming that the inertial forces do not significantly change this error. The analysis showed that the step size error was less than 0.1% at low Reynolds numbers. At higher Reynolds numbers that step size was reduced until the change in the value for C_D was less than 0.5%. The effect of the position of the outer boundary on the value of C_D was estimated from a comparison between C_D computed from the analytical solution of the Stokes equation for a bounded fluid and C_D given by the Stokes solution for an unbounded fluid

$$C_D = 24/N_{Re} \tag{C.7}$$

The total correction which was applied to the values of C_D obtained from the numerical solution of the non-linear equation of motion could, therefore, be found from a comparison between equation C.7 and the numerical solution of equation C.1. It was found that the wall correction varied

with Reynolds number. In particular, at $N_{Re} < 1$ the wall effect for a given distance to the outer boundary increased strongly with decreasing N_{Re}. A similar result was found experimentally by Fidleris and Whitmore (1961). It was found furthermore that at $N_{Re} \leq 1$ the inertial terms influenced the boundary effect stronger the farther the boundary and the smaller the Reynolds number. This is seen from Figure C.1 where the difference between C_D obtained from the numerical solution of the non-linear and the linear equation of motion is plotted as a function of $1/r_\infty$. An extrapolation of the curve for $N_{Re} = 0.01$ to $(\frac{1}{r_\infty}) = 0$ suggests that at $(\frac{1}{r_\infty}) = 0$ $C_D \cong C_{DO}$, where

$$C_{DO} = \frac{24}{N_{Re}} (1 + \frac{3}{16} N_{Re}) = C_{DS} + 4.5 \qquad (C.8)$$

for an unbounded fluid. In a similar fashion the value of C_D corrected for an unbounded fluid was determined for $N_{Re} = 0.1$ and $N_{Re} = 1.0$ from Figure C.1 by graphical extrapolation.

The drag and surface phenomena results are displayed in Tables C.3 - C.7 and Figure C.2. In Table C.3 the computed values for C_D and $(D/D_s)-1$ corrected for wall effect and step size error are listed for Reynolds numbers between 0.01 and 400. In Table C.5 the corrected values for $(D/D_s)-1$ are compared with those computed from other available theoretical expressions listed in Table C.4. In Table C.6 the values computed for surface pressure and in Table C.7 those for the surface vorticity are given as a function of the angle from the frontal stagnation point on the sphere. Graphical comparison between the various theoretical and experimental values for $(D/D_s)-1$ is made in Figure C.2. It can be concluded from Figure C.2 that at all Reynolds numbers between 0.01 and

and 400 the drag on a sphere calculated by the present numerical method is in close agreement with the drag obtained experimentally by Pruppacher and Steinberger (1968). The variation of the computed values for the drag with Reynolds number suggests that as the Reynolds number approaches zero the drag indeed approaches zero via the Oseen drag as suggested experimentally by Maxworthy (1965) and Pruppacher and Steinberger (1968). Figure C.2 suggests further that the theories of Oseen (1927), Goldstein (1929) and Proudman and Pearson (1957) are only applicable at Reynolds numbers below about 0.1. At larger Reynolds numbers these theories progressively overestimate the drag. The recent results of Chester and Breach (1969), who extended the Proudman and Pearson theory to higher order terms, do not give a better fit to the experimental drag. Proudman tried to remedy this problem by pointing out that the poor convergence of the Proudman and Pearson expansion is, at least in part, due to the lack of suitability of the function D for expansion in terms of N_{Re}. Based on semi-empirical arguments, Proudman suggested a new functional relationship between N_{Re} and D/D_s which is numerically evaluated for various values of the parameter m in his relationship. The results for the case that m=5 which seems to give the best fit to the experimental results is plotted in Figure C.2. It is seen that the agreement between Proudman's proposed relationship and the actual drag is rather poor. The agreement quoted by Proudman between his relationship for m=4 and Maxworthy's experimental results which have been shown to suffer from some inaccuracy (Pruppacher and Steinberger, 1968) must be merely incidental. On the other hand, it is seen from Figure C.2 that the values derived for the drag from a semi-empirical

modification of Oseen flow proposed by Carrier (1953) provide a reasonably good fit to the true drag at least for $2 \leq N_{Re} \leq 20$. At Reynolds numbers larger than about 20 calculations must rely on flow fields numerically determined by methods such as the present one.

TABLE C.1 EFFECT OF COMPUTATIONAL PARAMETERS ON DRAG COEFFICIENT AND STAGNATION PRESSURE

N_{Re}	A	B (deg.)	r_∞	V	W	$C_{DP}(r_\infty)$	$C_{DF}(r_\infty)$	$C_D(r_\infty)$	P_0	P_π
0.01	0.05	3	90	1.0	1.0	811.096	1635.598	2446.695	617.933	-599.700
0.01	0.05	3	365	1.0	1.0	799.993	1613.206	2413.199	609.693	-591.307
0.01	0.05	3	1000	1.0	1.0	798.483	1610.186	2408.669	608.583	-590.151
0.1	0.05	3	90	1.0	1.0	81.652	164.572	246.224	63.041	- 59.541
0.1	0.05	3	365	1.0	1.0	81.025	163.382	244.407	62.640	- 59.000
0.1	0.05	3	1000	1.0	1.0	81.056	163.445	244.501	62.664	- 59.023
1.0	0.05	3	150	1.0	0.5	9.114	18.281	27.394	7.797	- 5.898
1.0	0.1	6	221	0.5	0.5	8.975	18.456	27.432	7.995	- 5.528
1.0	0.05	3	1000	1.0	0.1	9.086	18.289	27.375	7.810	- 5.843
5.0	0.05	3	90	1.0	0.25	2.444	4.677	7.121	2.601	- 1.163
10.0	0.05	3	90	1.0	0.1	1.536	2.801	4.337	1.869	- 0.606
20.0	0.05	3	90	1.0	0.1	1.017	1.719	2.736	1.469	- 0.326
30.0	0.05	3	90	1.0	0.05	0.818	1.307	2.126	1.326	- 0.237
100.0	0.025	3	12	1.0	0.1	0.507	0.590	1.096	1.106	- 0.163
200.0	0.025	3	12	1.0	0.1	0.400	0.372	0.772	1.055	- 0.143
300.0	0.025	3	12	1.0	0.07	0.350	0.283	0.632	1.037	- 0.123
400.0	0.025	3	12	1.0	0.02	0.320	0.323	0.552	1.028	- 0.117

* A is the radial step size, B is the angular step size, V is the stream function relaxation factor, W is the vorticity relaxation factor, and P_π is the rear stagnation point surface pressure.

TABLE C.2 EFFECT OF BOUNDARY ON THE COMPUTATION OF C_D

N_{Re}	r_∞	C_D from analytical solution. Equ.(C.6)	C_D from numerical solution. Equ.(C.1)	C_D from numerical solution. Equ. (B.11) & (B.12)	C_D corrected for unbounded fluid
0.01	90	2448.980	2446.510	2446.695	2400.185
	365	2411.890	2412.302	2413.199	2400.897
	1000	2404.328	2406.795	2408.669	2401.874
0.1	90	244.898	244.651	246.224	241.573
	365	241.189	241.230	244.407	243.177
	1000	240.433	240.680	244.501	243.821
1.0	150	24.292	24.273	27.394	27.121
	220	24.198	24.204	27.432	27.230
	1000	24.043	24.068	27.375	27.307

TABLE C.3 COMPUTED VALUES FOR C_D AND $(D/D_s)-1$

CORRECTED FOR WALL EFFECT AND STEP SIZE ERROR

N_{Re}	C_D corrected	$(D/D_s)-1$ corrected
0.01	2404.5*	1.875×10^{-3}*
0.1	244.07*	1.695×10^{-2}*
1.0	27.315	0.1378
5.0	7.029	0.4644
10.0	4.288	0.7867
20.0	2.711	1.2592
30.0	2.110	1.6375
40.0	1.86**	2.10**
100.0	1.12**	3.67**
100.0	1.096	3.567
200.0	0.772	5.433
300.0	0.632	6.900
400.0	0.552	8.200

* extrapolated values (Figure C.1)

** adapted from Hamielec, Hoffman and Ross (1967).

TABLE C.4 EMPIRICAL AND THEORETICAL RELATIONS FOR $D/D_s - 1$

Stokes	$(D/D_s)-1 = 0$	
Oseen	$(D/D_s)-1 = (3/16)\ N_{Re}$	
Goldstein	$(D/D_s)-1 = (3/16)\ N_{Re} - (19/1280)\ N_{Re}^2 + (71/20,480)\ N_{Re}^3$ $- (30,179/34,406,400)\ N_{Re}^4 + (122,519/560,742,400)\ N_{Re}^5$	
Proudman and Pearson	$(D/D_s)-1 = (3/16)\ N_{Re} + (9/160)\ N_{Re}^2\ \ell n\ (N_{Re}/2)$	
Chester	$(D/D_s)-1 = (3/16)\ N_{Re} + (9/160)\ N_{Re}^2\ [\ell n\ (N_{Re}/2) + \gamma + (5/3)\ \ell n 2 - (323/360)]$ $+ (27/640)\ N_{Re}^3\ \ell n\ (N_{Re}/2)$	
	γ = Euler's constant = 0.57722	
Carrier	$(D/D_s)-1 = k_c\ (3/16)\ N_{Re}$	
	$k_c = 0.43$	
Pruppacher, et.al.	$(D/D_s)-1 = 0.102\ N_{Re}^{0.955}$	$0.01 \leq N_{Re} \leq 1.5$ (for minimum values)
	$(D/D_s)-1 = 0.115\ N_{Re}^{0.802}$	$3 \leq N_{Re} \leq 18$
	$(D/D_s)-1 = 0.189\ N_{Re}^{0.632}$	$24 \leq N_{Re} \leq 300$

TABLE C.5 COMPARISON OF EXPERIMENTAL AND THEORETICALLY COMPUTED VALUES FOR $(D/D_s)-1$

N_{Re}	0.01	0.1	1.0	5.0	10	20	30	100	200	300	400
Present analysis (corrected values)	* 1.875×10^{-3}	* 1.695×10^{-2}	0.1378	0.464	0.787	1.259	1.637	3.567	5.433	6.900	8.200
Pruppacher & Steinberger max.	1.87×10^{-3}	1.63×10^{-2}	0.115	0.418	0.729	1.271	1.622	3.471	5.379	---	---
Pruppacher & Steinberger min.	1.27×10^{-3}	1.14×10^{-2}	0.102								
Carrier	0.806×10^{-3}	0.806×10^{-2}	0.0806	0.401	0.806	1.612	---	---	---	---	---
Oseen	1.875×10^{-3}	1.875×10^{-2}	0.1875	0.937	1.875	---	---	---	---	---	---
Goldstein	1.874×10^{-3}	1.861×10^{-2}	0.1752	0.759	1.375	---	---	---	---	---	---
Proudman & Pearson	1.845×10^{-3}	1.706×10^{-2}	0.1485	---	---	---	---	---	---	---	---

* extrapolated values (see Figure C.1)

Θ degrees / N_{Re}	0 96	12 108	24 120	36 132	48 144	60 156	72 168	84 180
0.01	608.583 - 55.093	595.390 -177.481	556.437 -291.481	493.453 -392.694	409.253 -476.194	307.556 -538.562	192.848 -577.105	70.174 -590.151
0.1	62.664 - 6.188	61.259 - 18.485	57.122 - 29.845	50.459 - 39.805	41.602 - 47.972	30.983 - 54.034	19.108 - 57.764	6.529 - 59.023
1.0	7.810 - 1.241	7.593 - 2.505	6.963 - 3.571	5.971 - 4.423	4.699 - 5.064	3.242 - 5.504	1.704 - 5.760	0.182 - 5.843
10.0	2.601 - 0.752	2.498 - 1.006	2.204 - 1.154	1.757 - 1.217	1.214 - 1.222	0.638 - 1.199	0.090 - 1.174	0.383 - 1.163
20.0	1.469 - 0.642	1.385 - 0.666	1.148 - 0.626	0.801 - 0.552	0.402 - 0.468	0.016 - 0.394	- 0.305 - 0.344	- 0.527 - 0.326
30.0	1.326 - 0.629	1.242 - 0.615	1.006 - 0.548	0.663 - 0.460	0.277 - 0.374	- 0.088 - 0.302	- 0.375 - 0.254	- 0.556 - 0.237
100.0	1.106 - 0.590	1.021 - 0.503	0.782 - 0.401	0.440 - 0.317	0.063 - 0.259	- 0.273 - 0.215	- 0.506 - 0.179	- 0.607 - 0.163
200.0	1.055 - 0.538	0.966 - 0.424	0.717 - 0.327	0.362 - 0.268	- 0.020 - 0.243	- 0.348 - 0.217	- 0.552 - 0.170	- 0.605 - 0.143
300.0	1.037 - 0.499	0.944 - 0.377	0.686 - 0.293	0.320 - 0.254	- 0.069 - 0.248	- 0.391 - 0.226	- 0.575 - 0.163	- 0.596 - 0.123
400.0	1.029 - 0.474	0.931 - 0.352	0.663 - 0.281	0.287 - 0.255	- 0.109 - 0.261	- 0.428 - 0.242	- 0.596 - 0.166	- 0.591 - 0.117

TABLE C.7 COMPUTED SURFACE VORTICITY DISTRIBUTIONS

θ degrees	0	12	24	36	48	60	72	84
N_{Re}	96	108	120	132	144	156	168	180
0.01	0.0	0.3151	0.6158	0.8894	1.1239	1.3090	1.4367	1.5015
	1.5007	1.4344	1.3057	1.1201	0.8858	0.6130	0.3135	0.0
0.1	0.0	0.3266	0.6375	0.9187	1.1574	1.3432	1.4681	1.5276
	1.5199	1.4462	1.3109	1.1203	0.8832	0.6098	0.3114	0.0
1.0	0.0	0.4229	0.8182	1.1623	1.4358	1.6259	1.7268	1.7397
	1.672	1.5352	1.3435	1.1114	0.8518	0.5754	0.2897	0.0
5.0	0.0	0.7064	1.3489	1.8738	2.2418	2.4330	2.4487	2.3101
	2.0534	1.7229	1.3634	1.0130	0.6978	0.4289	0.2020	0.0
10.0	0.0	0.9676	1.8373	2.5276	2.9800	3.168	3.1005	2.8191
	2.3894	1.8871	1.3842	0.9363	0.5766	0.3139	0.1332	0.0
20.0	0.0	1.3710	2.5904	3.5316	4.1045	4.2711	4.0524	3.5265
	2.8121	2.0422	1.3327	0.7604	0.3581	0.1227	0.0224	0.0
30.0	0.0	1.7012	3.2063	4.3514	5.0189	5.1596	4.8043	4.0629
	3.1042	2.1145	1.2482	0.5938	0.1737	-0.0316	-0.0658	0.0
100.0	0.0	3.2065	6.0259	8.1233	9.2405	9.2415	8.1625	6.2604
	4.0104	1.9723	0.5340	-0.2569	-0.6192	-0.7443	-0.5479	0.0
200.0	0.0	4.6589	8.7359	11.7232	13.2173	12.9818	11.0355	7.7948
	4.1712	1.2851	-0.2794	-0.7631	-0.9827	-1.5876	-1.4593	0.0
300.0	0.0	5.8176	10.8874	14.5566	16.3027	15.8046	13.0588	8.6295
	3.9009	0.5710	-0.7932	-0.8289	-1.2406	-2.7085	-2.5656	0.0
400.0	0.0	6.8352	12.7666	17.0087	18.9346	18.1513	14.6377	9.1099
	3.4658	-0.0438	-1.0929	-0.6858	-1.5462	-3.8480	-3.6228	0.0

FIGURE C.1 VARIATION OF NUMERICALLY COMPUTED VALUES FOR $C_D - C_{Ds}$ AS A FUNCTION OF DISTANCE TO OUTER BOUNDARY

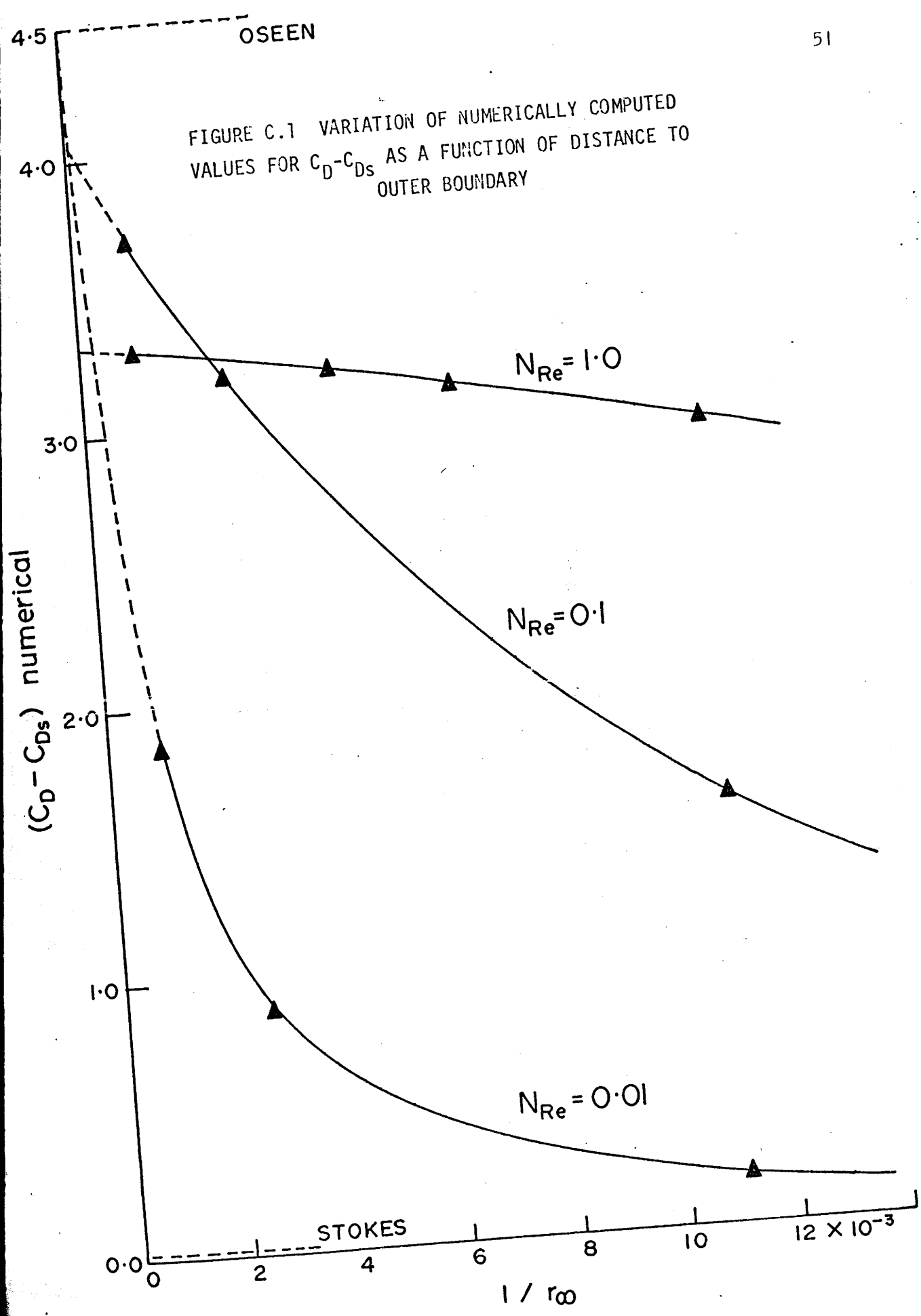

FIGURE C.2 VARIATION OF THE QUANTITY $(D/D_S)-1$ WITH REYNOLDS NUMBER
(COMPARISON OF THEORY AND EXPERIMENT)

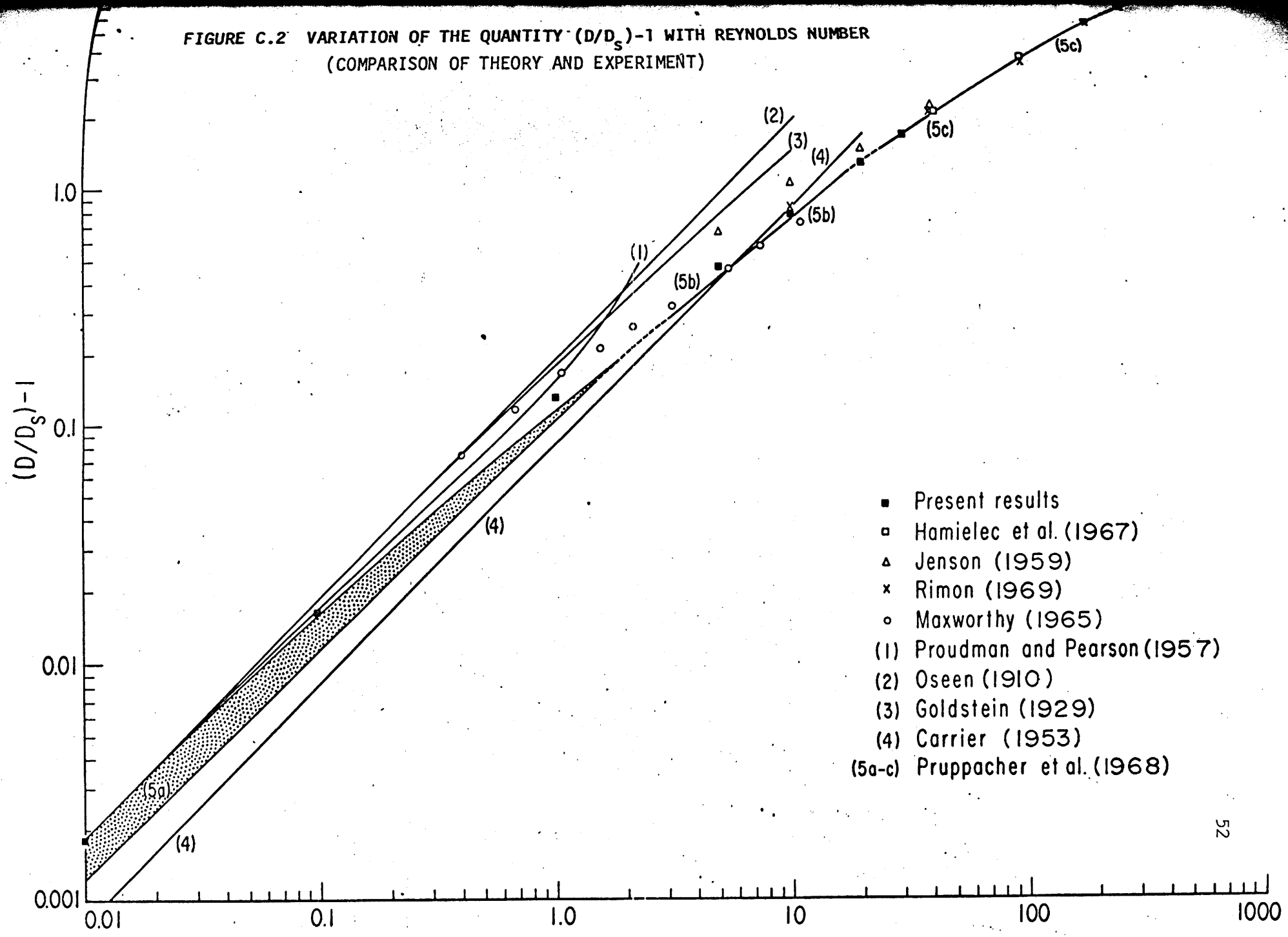

C.1.2 Flow Field Phenomena

Figure C.2 shows that there are two pronounced breaks in the drag curve; one at N_{Re} = 20 and one at N_{Re} = 400. In order to test whether these breaks which separate 3 drag "regimes" are in any way related to the regimes in the flow field past a sphere, the variation with Reynolds numbers of the length of the standing eddy behind the sphere and the corresponding angle of flow separation were investigated. Both of these quantities are thought to be characteristic of the flow field past a sphere. The eddy length and angle of flow separation were calculated from the numerical solution of the Navier-Stokes equations of motion. The results for the variation of the vortex length L/d as a function of N_{Re} are presented in Figure C.3 and the results for the variation of the angle of flow separation θ_s as a function of log N_{Re} are presented in Figure C.4 where they are compared with the theoretical results of Jenson (1959), Hamielec, Hoffman and Ross (1967), Rimon and Cheng (1969), Rhodes (1967), and Proudman and Pearson (1957), and with the experimental results of Taneda (1956), Garner and Grafton (1954), and Nisi and Porter (1923). It is seen from these figures that L/d varies approximately linearly with N_{Re} over the Reynolds number range plotted while θ_s varies with log N_{Re} for $N_{Re} \gtrsim 40$. The agreement between experiment and theory is good except at low Reynolds numbers where Taneda somewhat underestimates the vortex length. This is understandable considering the extreme difficulties in visualizing the flow with tracer particles of finite size and finite fall velocities relative to the fluid motion. The experimental results of Nisi and Porter were probably biased

by their method of sphere support. The value for L/d obtained theoretically by Rimon and Cheng for N_{Re} = 10 is biased by the downstream boundary conditions and the position of the outer boundary they assumed in their numerical model. The numerical computations of this work, displayed in Figures C.3 and C.4 indicate that the onset of the development of a standing eddy in the back of the sphere takes place at N_{Re} = 20. By varying the step size and distance to the outer boundary, this work made sure that the computed values for L/d and θ_s were not biased by these parameters. The effect of step size and wall proximity on θ_s for N_{Re} = 20 is shown in Table C.8. This table suggests that indeed θ_s = 0 for N_{Re} = 20, The values for L/d and θ_s are further compared with those determined by Proudman and Pearson from a stream function based on two terms of the Stokes expansion. These relations predict an onset of a recirculatory wake at N_{Re} = 16 and a growth of the eddy which is in astonishingly good agreement with the numerical and experimental results as far as its length is concerned but is in quite poor agreement with those as far as its angular extent is concerned. In cases where the next higher order term in the Stokes expansion of Proudman and Pearson is taken into account, no eddy at all is predicted (Van Dyke, 1964). This result is very surprising but consistent with the findings of Chester and Breach (1969) regarding the drag discussed above. Unfortunately, available theoretical models and numerical techniques have up to the present not allowed predicting the Reynolds number for onset of shedding of vortices from the rear of a sphere. Experiments by Mollier (1938), Taneda (1956) and Goldburg and Florshein (1966) indicate that shedding of vortices

TABLE C.8 EFFECT OF STEP SIZE ON THE COMPUTATION OF ANGLE OF FLOW SEPARATION AT N_{Re} = 20 FOR THE CASE OF A SPHERE

	Δz	$\Delta\theta$	r_∞	θ_s
Jenson (1959)	0.1	12°	6.05	9°
Rhodes (1967)	0.05	6°	6.05	2.5°
Hamielec, Hoffman & Ross (1967)	0.05	3°	7.02	0°
Present Results	0.05	3°	90	0°
	0.0167	3°	90	0°

* Δz is the radial step size, $\Delta\theta$ is the angular step size and $r_\infty = r'_\infty/a$ is the nondimensional distance to the boundary.

begin at Reynolds numbers between 300 and 450.

A comparison between drag and flow field reveals that the Reynolds number marking the transition from one flow field regime to another coincide well with the Reynolds numbers which mark the transition between the observed drag "regimes". This suggests that the observed drag "regimes" are manifestations of the flow field regimes: one regime at $N_{Re} = 0$, the Stokes flow regime, characterized by flow past a sphere which is symmetric with respect to a plane perpendicular to the direction of fluid flow (Figures C.5 and C.6); one regime $0 < N_{Re} < 20$ characterized by flow which is asymmetric with respect to the flow fore and aft and becomes increasingly so with increasing Reynolds number, but is not separated at the sphere yet (Figures C.7 and C.8); one regime $20 < N_{Re} < 400$ characterized by flow which is separated at the sphere and has a standing recirculatory wake at the downstream end of the sphere (Figures C.9, C.10 C.11 and C.12); one regime $N_{Re} > 400$ characterized by flow containing eddies shed from the downstream end of the sphere into the main stream.

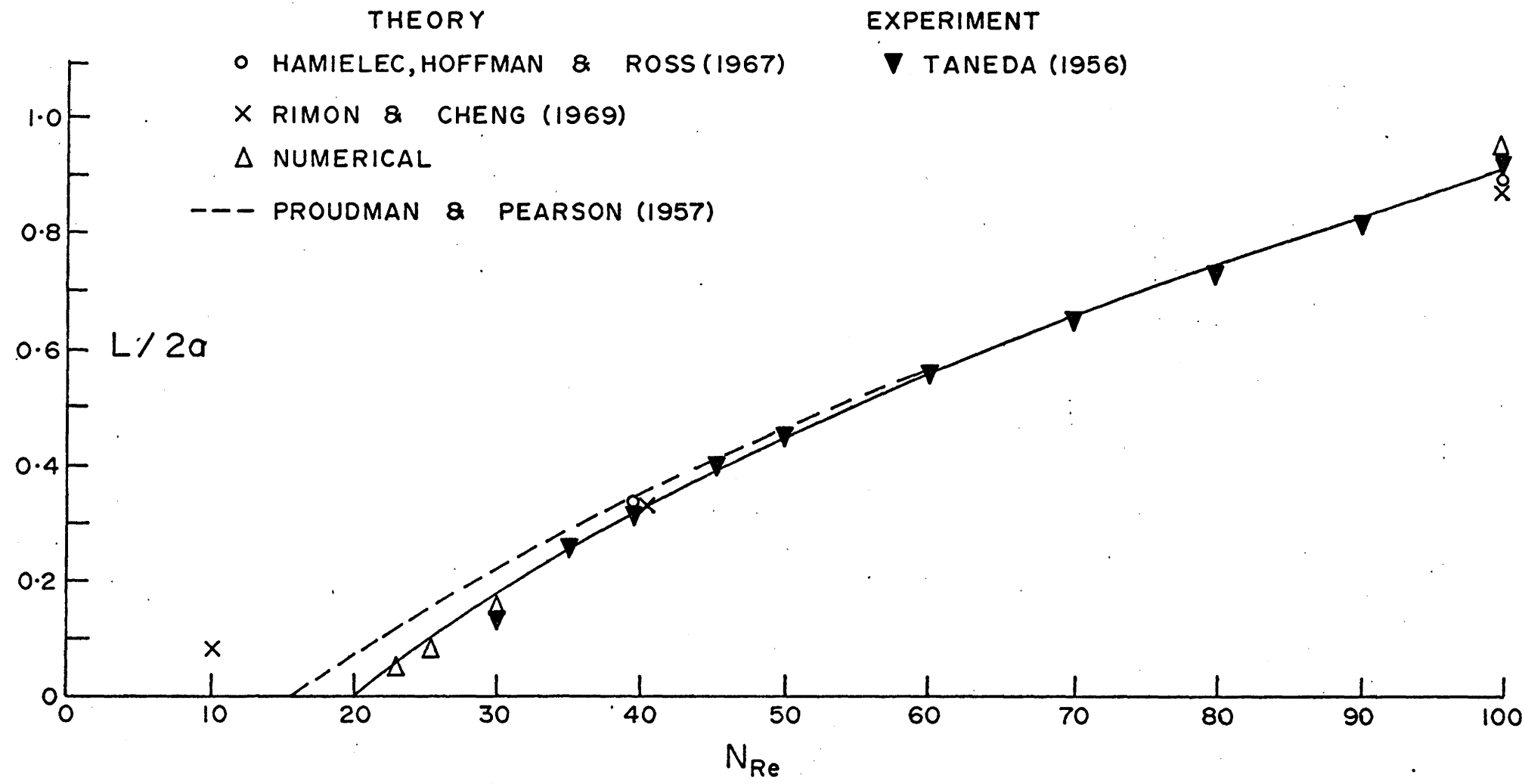

FIGURE C.3 VARIATION OF EDDY LENGTH WITH REYNOLDS NUMBER FOR A SPHERE

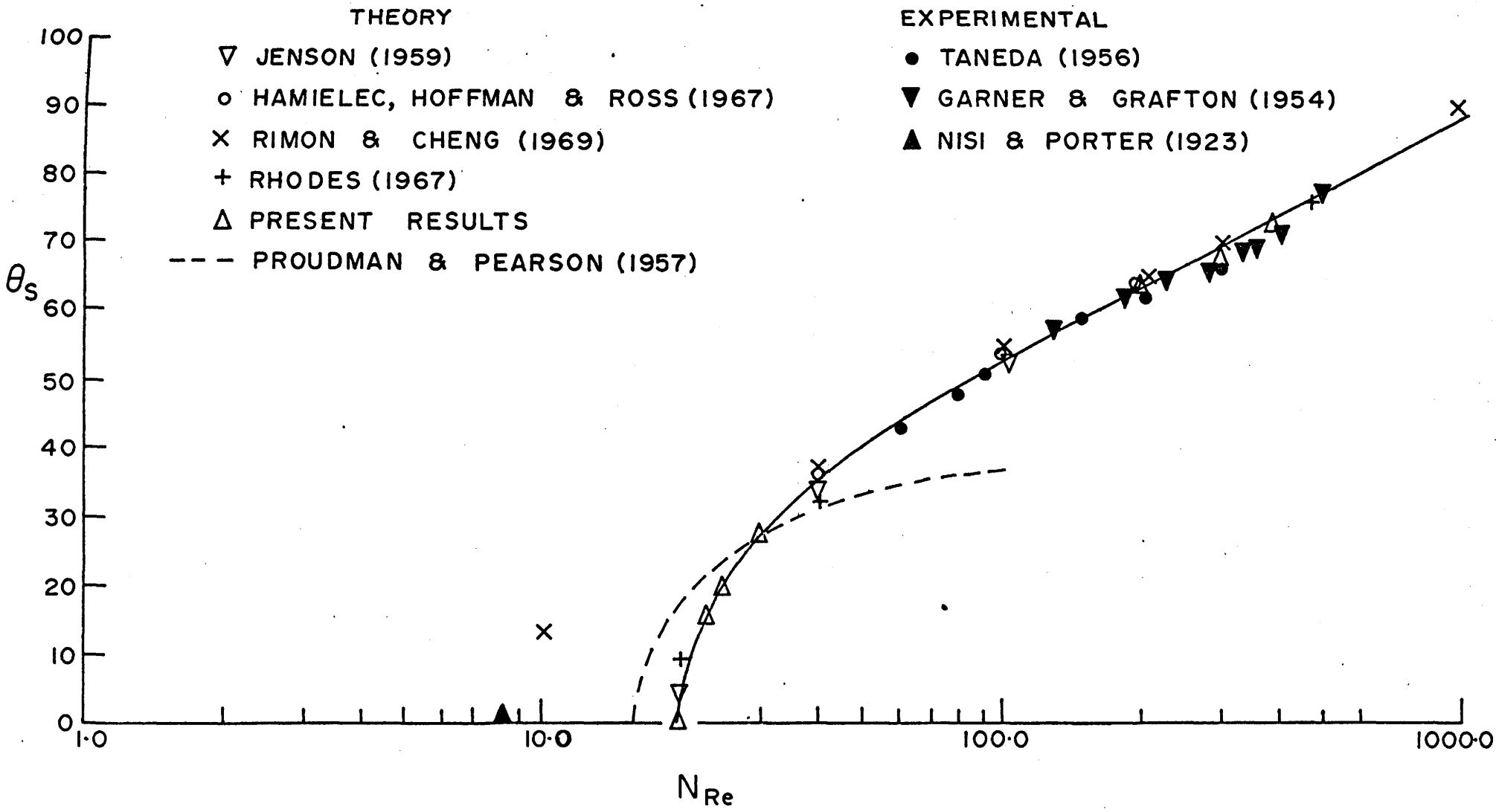

FIGURE C.4 VARIATION OF THE ANGLE OF FLOW SEPARATION WITH REYNOLDS NUMBER FOR A SPHERE

Key for FIGURES C.5 to C.12

N_{Re}	0.01		10.0		30.0		300.0	
Fig. Sym.	C.5	C.6	C.7	C.8	C.9	C.10	C.11	C.12
A	0.01	0.001	0.01	0.001	0.0	0.001	-0.05	-0.8
B	0.1	0.01	0.1	0.01	0.01	0.01	-0.035	-0.6
C	0.5	0.03	0.5	0.03	0.1	0.03	-0.02	-0.4
D	1.0	0.05	1.0	0.05	0.5	0.05	-0.005	-0.2
E	2.0	0.1	2.0	0.1	1.0	0.1	0.0	0.0
F	3.0	0.2	3.0	0.2	2.0	0.2	0.002	0.01
G	4.5	0.3	4.5	0.3	3.0	0.3	0.01	0.1
H	6.0	0.5	6.0	0.5	4.5	0.5	0.05	0.5
I	10.0	0.8	10.0	0.8	6.0	0.8	0.1	1.0
J	15.0	1.5	15.0	1.5	10.0	1.5	0.5	2.0
K			20.0	2.0	15.0	2.0	1.0	3.0
L			-	2.5	20.0	2.5	-	5.0
M			-		-	3.0	-	8.0
N	-		-		-	3.5	-	11.0

FIGURE C.5 STREAM FUNCTION CONTOURS FOR $N_{Re} = 0.01$

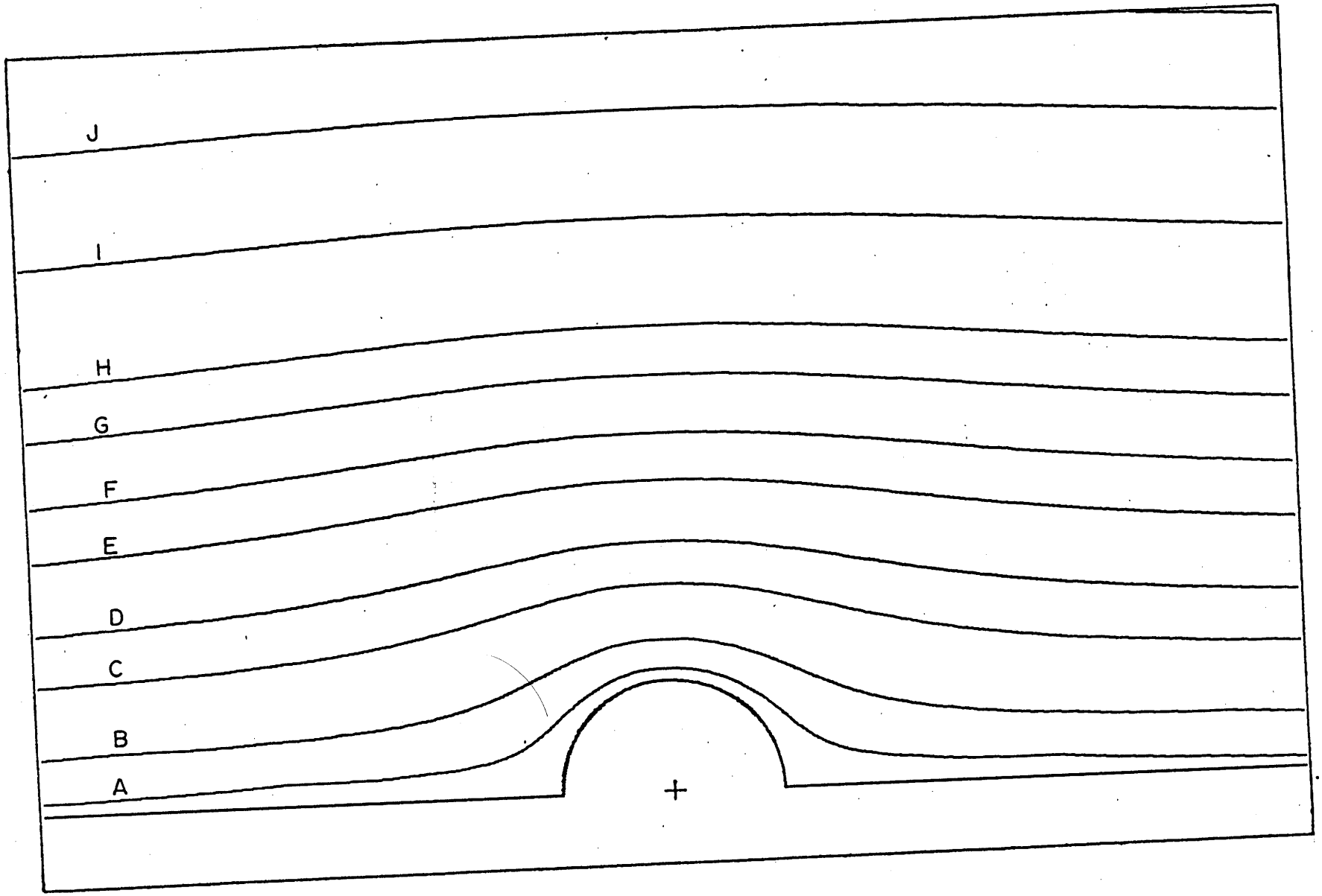

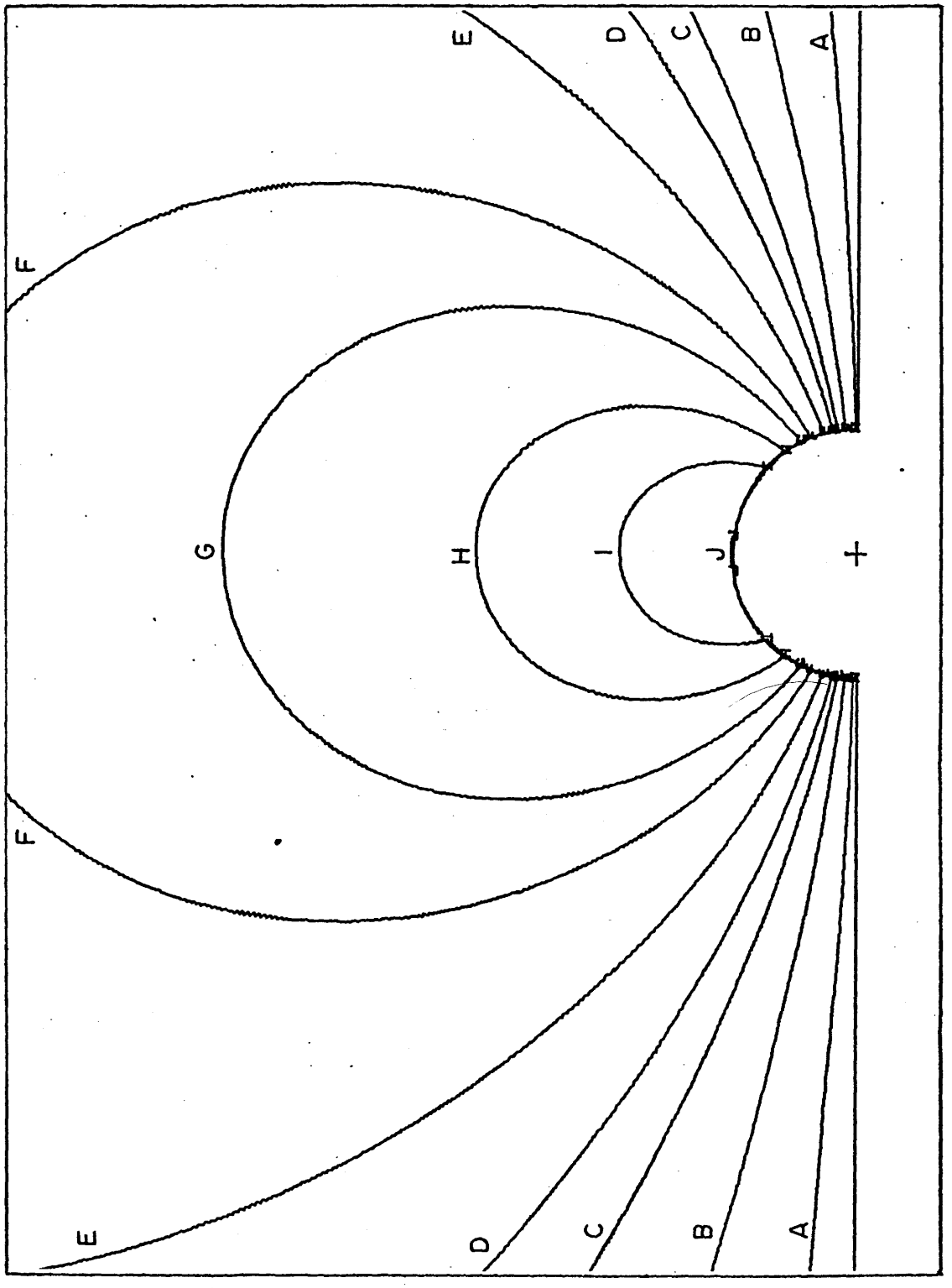

FIGURE C.6 VORTICITY CONTOURS FOR $N_{Re} = 0.01$

FIGURE C.7 STREAM FUNCTION CONTOURS FOR N_{Re} = 10.0

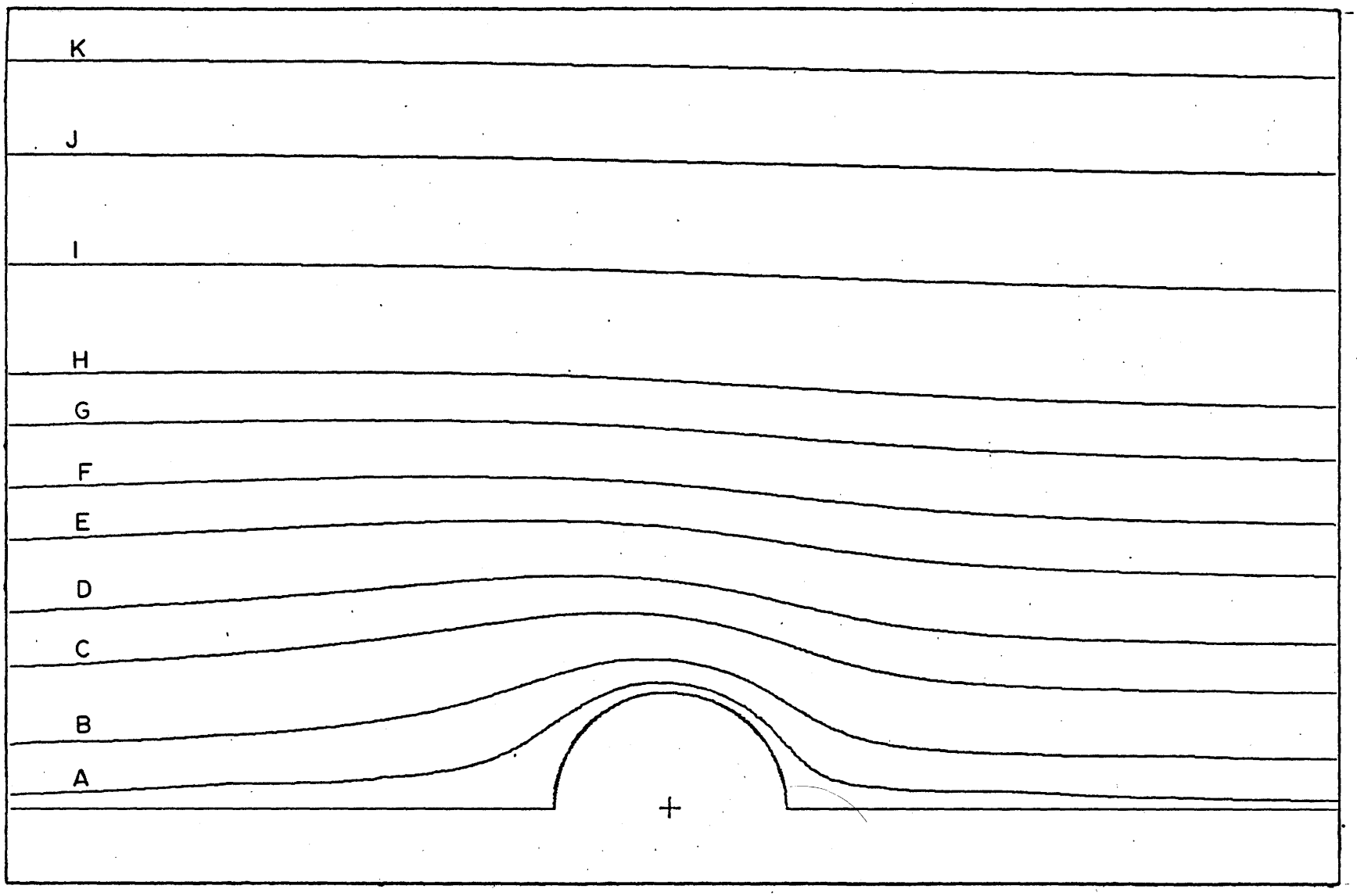

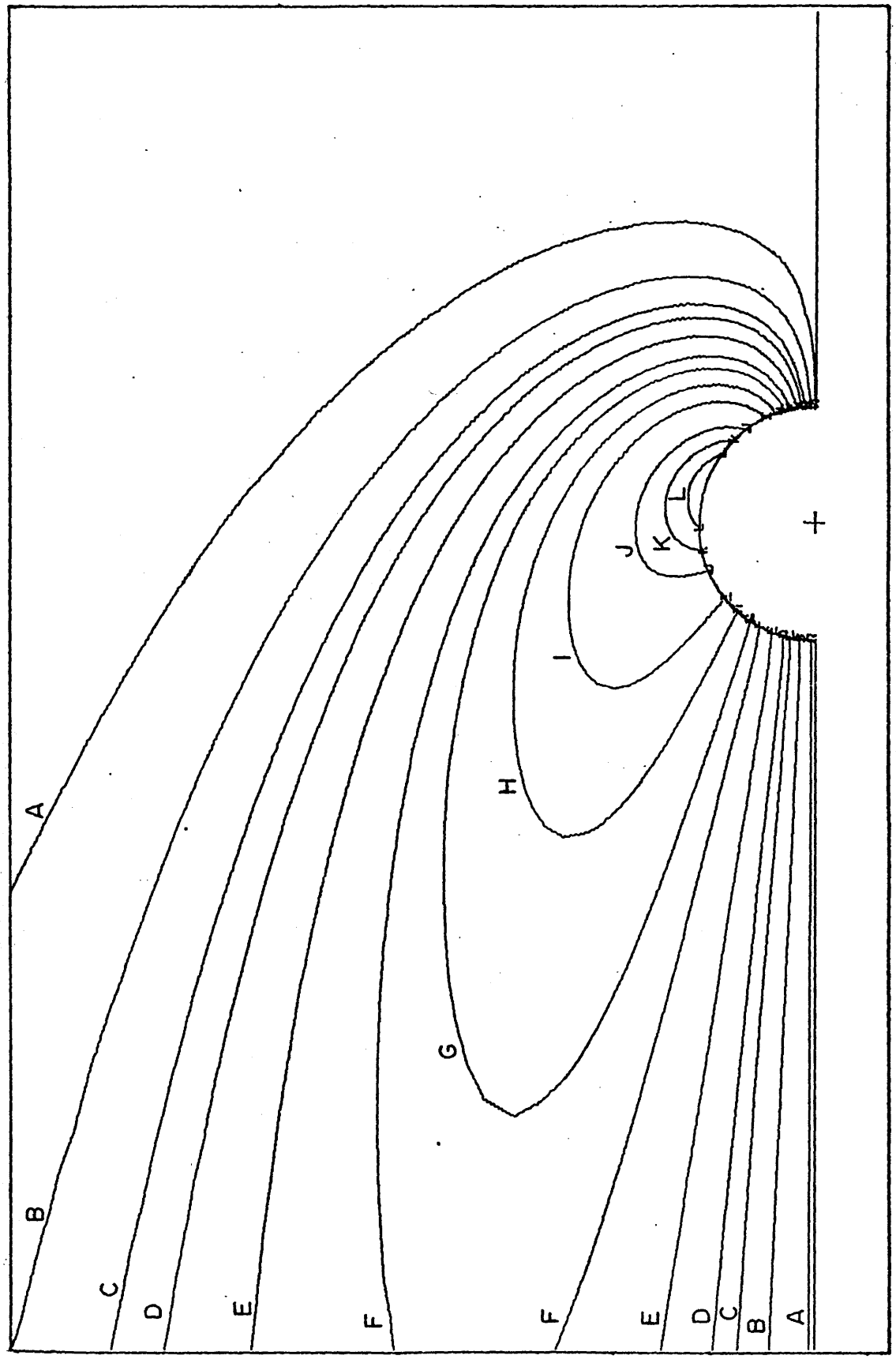

FIGURE C.8 VORTICITY CONTOURS FOR N_{Re} = 10.0

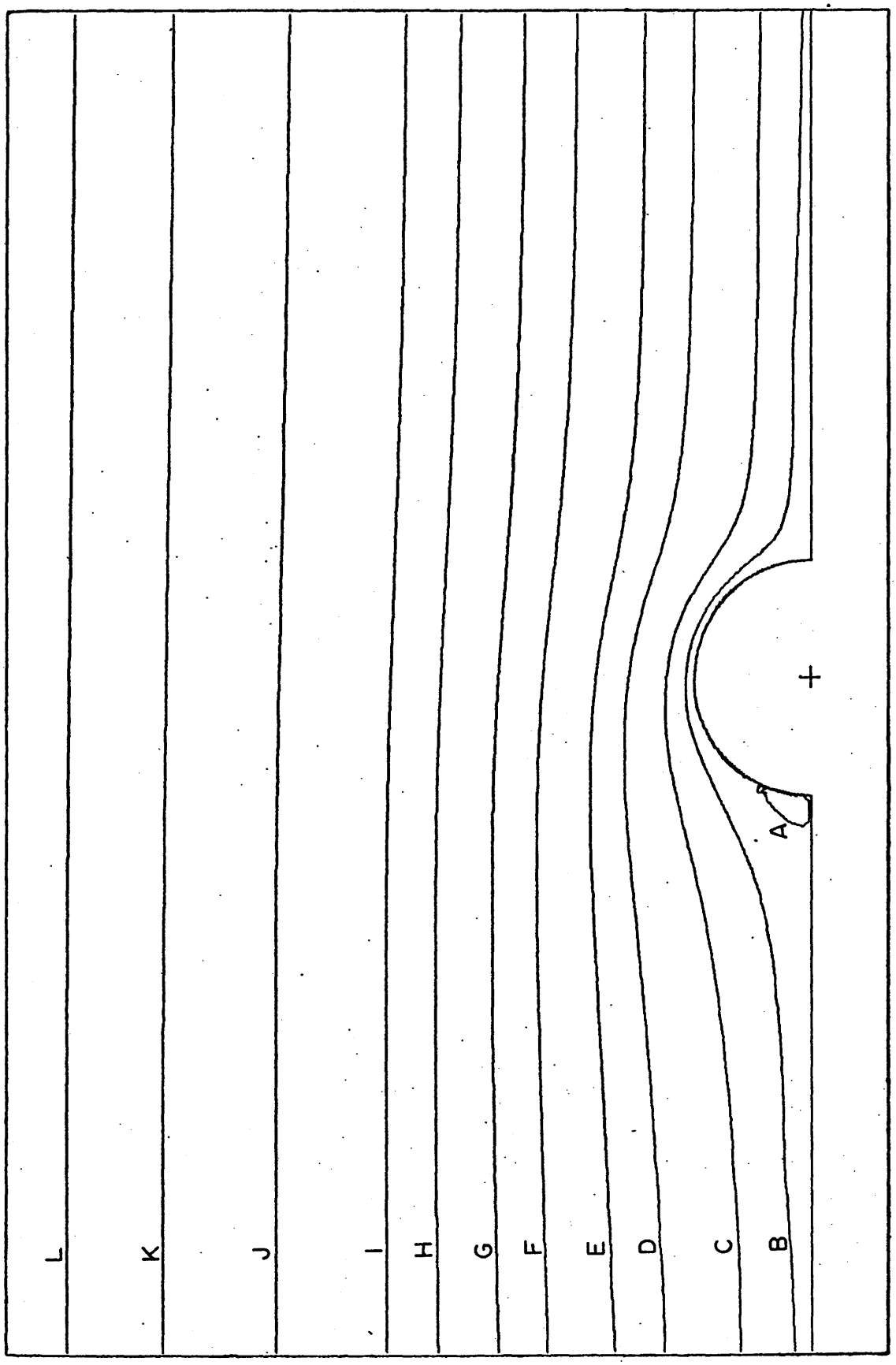

FIGURE C.9 STREAM FUNCTION CONTOURS FOR N_{Re} = 30.0

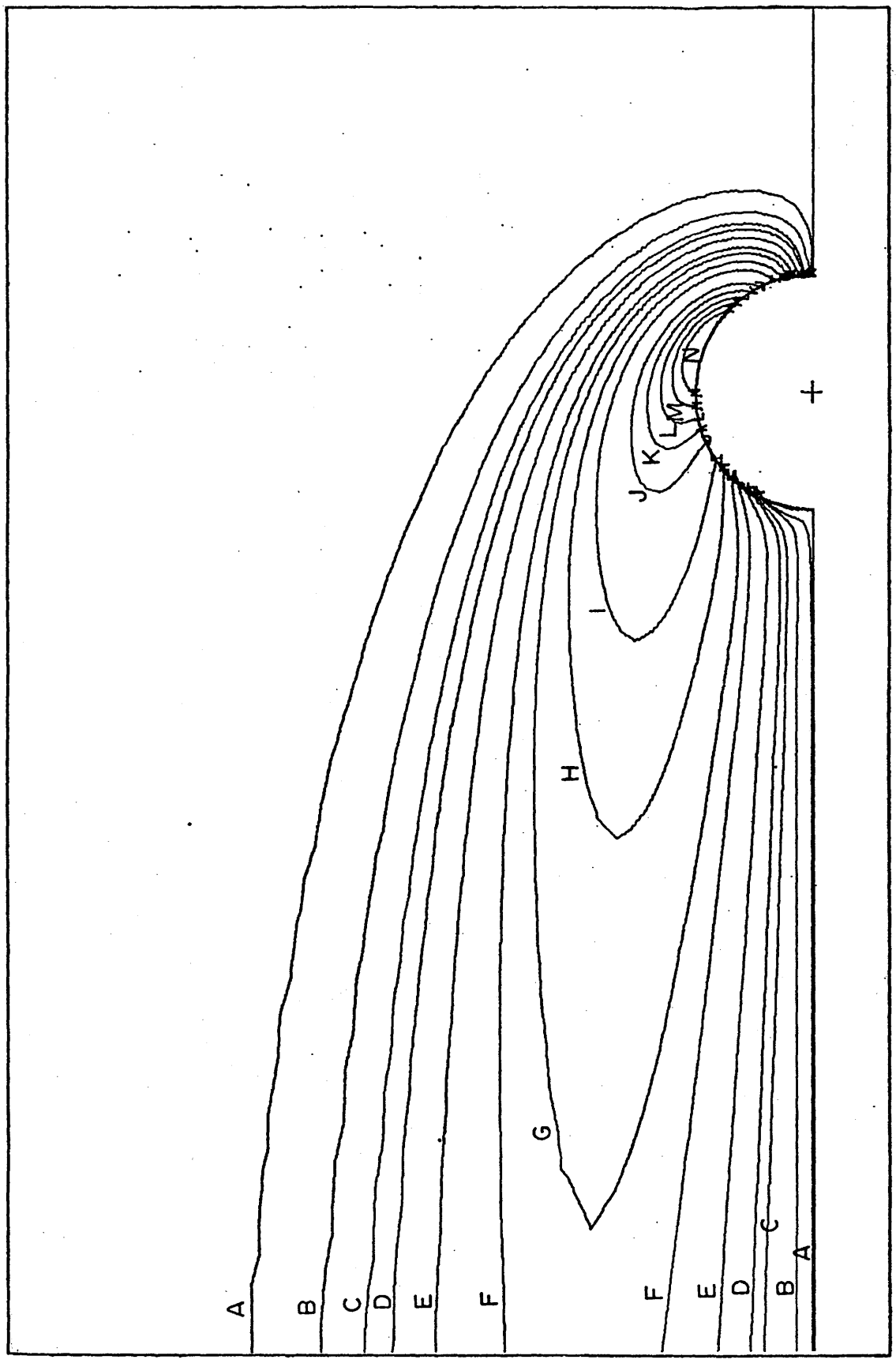

FIGURE C.10 VORTICITY CONTOURS FOR N_{Re} = 30.0

FIGURE C.11 STREAM FUNCTION CONTOURS FOR N_{Re} = 300.0

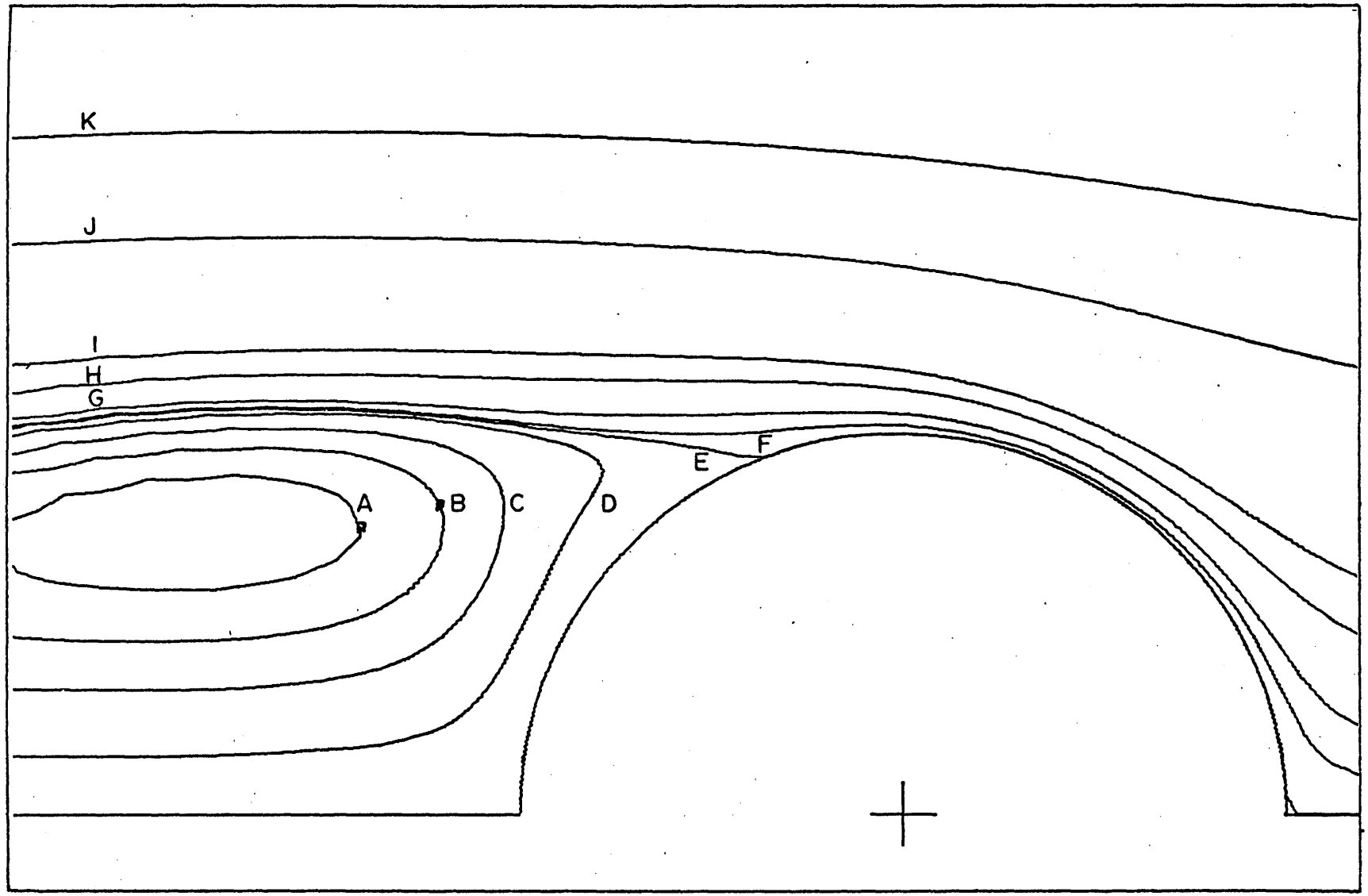

FIGURE C.12 VORTICITY CONTOURS FOR N_{Re} = 300.0

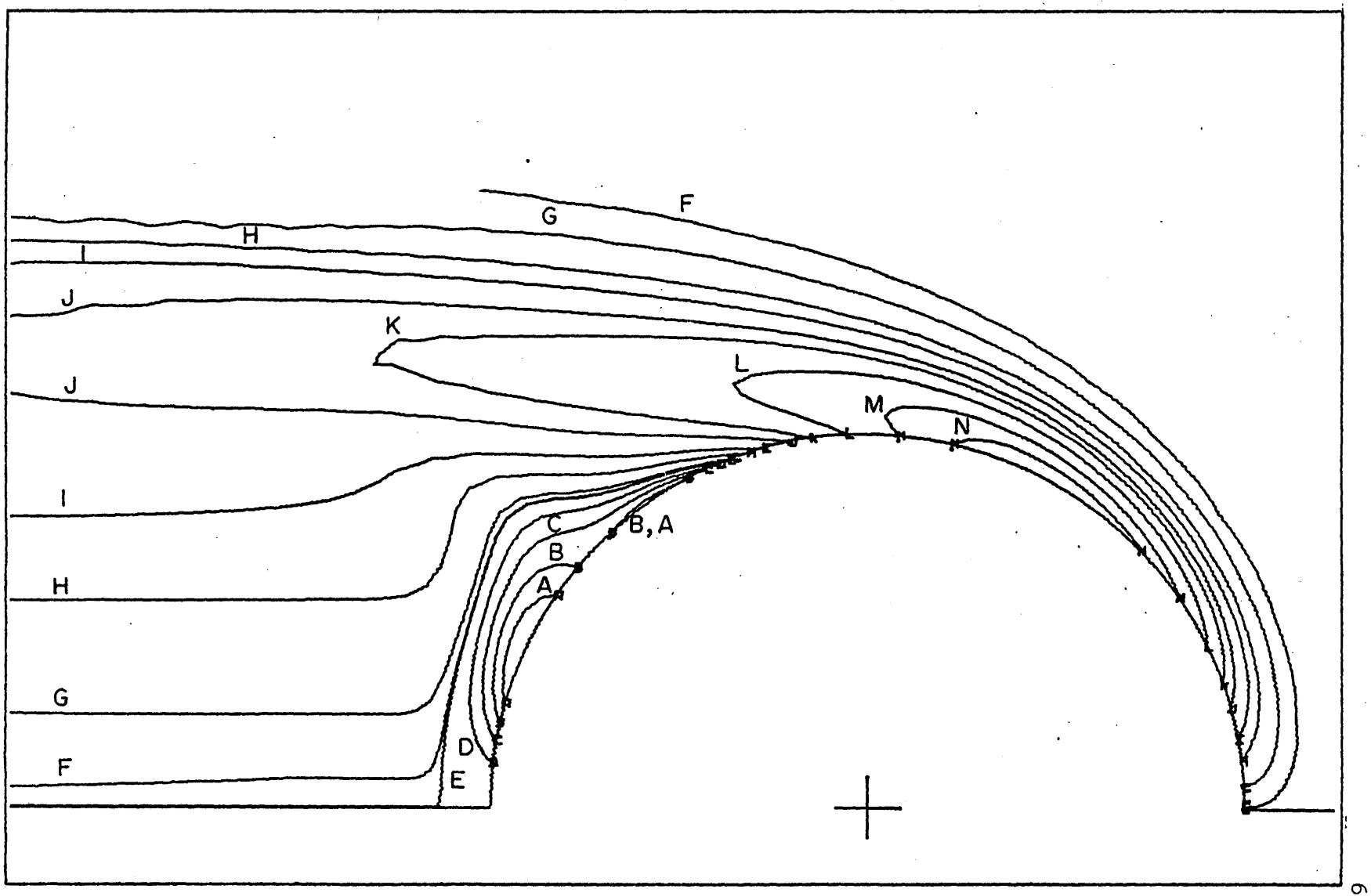

C.2 Unsteady State Flow Around a Solid Sphere

C.2.1 Drag Phenomena

The significant effect of acceleration on drag is clearly shown in Figures C.13, C.14 and C.15. In these figures are plotted C_{Dt}/C_{Dt_∞} the ratio of the actual drag coefficient to that for steady motion at the same Reynolds number, as a function of $N_{Ret}/N_{Re\infty}$. Figure C.13 contains data for the case of a final steady-state Reynolds number of 0.01 and a sphere to fluid density ratio of 2.65. Figure C.14 contains data for the case of a final steady-state Reynolds number of 9 and a sphere to fluid density of 9.15. Figure C.15 contains data for the case of a final steady-state Reynolds number of 145 and a sphere to fluid density of 1.74. From these figures it is apparent that as the density ratio ρ_s/ρ increases, the effect of acceleration on drag decreases. The C_{Dt}/C_{Dt_∞} curve of Figure C.14 is to the left and below that of Figure C.15 which has a density ratio of 1.74. This effect of acceleration on drag was first calculated by Hughes and Gilliland (1952), who obtained solutions for Basset's equation for the acceleration of a sphere in the creeping flow regime. As the density ratio approached infinity, they found that the actual drag approached the steady-state drag for all velocity ratios. Also shown in these figures is the ratio of the actual drag force to the drag force at steady state, $F_{Dt}/F_{D\infty}$. These plots clearly show that the actual drag increases monotonicly with time and exhibits no maxima nor minima.

C.2.2 Flow Visualization

The nature of the flow around a sphere is presented in the next series of figures. Figure C.16(1) and C.16(2) show the stream function and vorticity development for the case of a final steady-state Reynolds number of 0.01. The time sequence in these figures is from the top to the bottom of the page. The pertinent data relating to these figures is given in Table C.9.

TABLE C.9 DATA FOR $N_{Re_\infty} = 0.01$

TIME (T)	N_{Re_t}	$N_{R_{et}}/N_{Re_\infty}$	C_{DF}	C_{DP}	C_{Dt}
0.0001	0.000019	0.0019	1.0530×10^{7}	6.0889×10^{6}	1.6619×10^{7}
0.0046	0.000506	0.0506	1.8614×10^{5}	1.7993×10^{5}	3.6606×10^{5}
0.01585	0.0014	0.14	4.0078×10^{4}	2.7836×10^{4}	6.7914×10^{4}
0.04585	0.002988	0.2988	1.2819×10^{4}	7.3491×10^{3}	2.0168×10^{4}
0.08585	0.004262	0.4262	7360.48	3924.89	1.1285×10^{4}
0.13585	0.005256	0.5256	5275.06	2972.18	8247.25

The values of the contours in these figures, beginning with those closest to the sphere surface and moving outwards are as follows: stream function (0.0, 0.01, 0.1, 1.0, 2.0, 3.0, 6.0, 10.0, 20.0) and vorticity (2.5, 2.0, 1.5, 0.8, 0.5, 0.3, 0.1, 0.05, 0.03, 0.01, 0.001).

In the next sequence of figures, results are presented for the case of a final steady-state Reynolds number of 9.0 and a density ratio of 9.15. The relevant data pertaining to this series of figures is presented in Table C.10.

TABLE C.10 DATA FOR $N_{Re_\infty} = 9.0$

TIME (T)	N_{Re_t}	N_{Re_t}/N_{Re_∞}	C_{DF}	C_{DP}	C_{Dt}
0.00244	0.523361	0.0582	145.314	125.934	271.248
0.00964	1.79854	0.1999	25.215	16.028	41.243
0.01860	3.067684	0.3409	11.959	6.943	18.902
0.04836	5.851485	0.6502	4.983	2.695	7.679
0.07716	7.253121	0.8059	3.826	2.049	5.875
0.11316	8.100051	0.9000	3.397	1.811	5.173

Figures C.18 and C.19 show the change in the surface vorticity and surface pressure distributions respectively with time. The pressure term appearing in the ordinate in Figure C.19 is relative to the pressure at the rear stagnation point. In Figures C.17(1) and C.17(2), the time sequence development of the stream function and vorticity contours are presented. The time sequence is down the left side of the figure and then down the right side. Values of the contours, beginning with those closest to the sphere surface and moving outwards are as follows: stream function (0.0, 0.01, 0.1, 1.0, 2.0, 3.0, 6.0, 10.0, 20.0) and vorticity (2.0, 1.0, 0.5, 0.3, 0.1, 0.05, 0.03, 0.01, 0.001).

In the next sequence of figures, results are presented for the case of a final steady state Reynolds number of 145.0 and a density ratio of 1.72. The relevant data pertaining to the figures is given in Table C.11.

TABLE C.11 DATA FOR N_{Re_∞} = 145.0

TIME(T)	N_{Re_t}	N_{Re_t}/N_{Re_∞}	C_{DF}	C_{DP}	C_{Dt}
0.00074	6.631825	0.045	39.9958	95.2068	135.2026
0.00186	15.654622	0.108	10.9750	17.7120	28.6869
0.00346	27.546777	0.190	4.6929	5.9280	10.6209
0.00570	42.783836	0.295	2.4285	2.5985	5.0270
0.00837	59.217976	0.408	1.5074	1.4555	2.9629
0.01112	74.213654	0.512	1.0982	1.0059	2.1041
0.01387	87.191687	0.601	0.8874	0.8052	1.6926
0.01687	99.125406	0.684	0.7555	0.6893	1.4449
0.01987	108.95769	0.751	0.6734	0.6124	1.2859
0.02387	119.31243	0.823	0.6044	0.5496	1.1540
0.02787	127.11963	0.877	0.5607	0.5174	1.0781
0.03487	136.45404	0.941	0.5151	0.4874	1.0026

Figures C.21 and C.22 show the change in the surface vorticity and surface pressure distributions respectively with time. The pressure term appearing in the ordinate in Figure C.22 is relative to the pressure at the rear stagnation point. In Figures C.20(1), C.20(2) and C.20(3), the time sequence development of the stream function and vorticity contours are presented. The time sequence is down the page from top to bottom. Values of the contours, beginning with those closest to the sphere surface and moving outwards are as follows: stream function (0.0, 0.01, 0.1, 1.0, 2.0, 3.0, 6.0, 10.0, 20.0) and vorticity (9.0, 7.0, 5.0, 3.0, 2.0, 1.0, 0.5, 0.1, 0.01, 0.001, 0.0001). Figure C.23 shows the development of the vortex

ring behind the sphere with time. The pertinent details are presented in Table C.12, where the variables have been defined as follows: θ_s, separation angle measured from rear stagnation point; L, length of the vortex ring measured from the rear stagnation point along the line $\theta = \pi$. Values of the contours used in Figure C.23 are as follows: Stream function (-0.02, -0.01, -0.007, -0.003, -0.001, -0.0005, 0.0, 0.001, 0.01, 0.05, 0.1, 0.2, 0.7) and vorticity (-0.6, -0.4, -0.2, 0.0, 0.01, 0.1, 0.5, 1.0, 2.0, 3.0, 5.0).

TABLE C.12 DATA OF VORTEX RING DIMENSIONS FOR N_{Re_∞} = 145.0

TIME (T)	N_{Re_t}	N_{Re_t}/N_{Re_∞}	C_{Dt}	θ_s	L
0.01787	102.62	0.708	1.3815	30.0	0.19
0.02187	114.50	0.790	1.2092	42.0	0.48
0.02387	119.31	0.823	1.1540	45.5	0.61
0.02687	125.37	0.865	1.1035	49.0	0.82
0.02912	129.14	0.891	1.0677	52.0	1.00
0.03487	136.45	0.941	1.0026	55.0	1.31

C.2.3 Velocity-Time Phenomena

Velocity-time results have been obtained by numerous authors for spheres in the accelerated portion of fall (Hjelmfelt and Mockros, 1967; Odar, 1965). In Figure C.24, results are plotted for N_{Re_∞} = 0.01 and a density ratio of 2.65. Also plotted in the figure are the exact analytical solution of Basset's equation, the solution when the history term is neglected, and the solution when the history term and the added mass are neglected done by Hjelmfelt and Mockros (1967). The numerical solution

falls on top of the exact analytical solution, indicating that the numerical formulation and procedure are correct. The effect of neglecting the history term and the added mass term is clearly indicated. It should be noted that the exact solution of Hjelmfelt and Mockros (1967) gives excellent predictions of the velocity-time data of experimental work in the creeping flow regime.

In Figures C.25 and C.26, the numerical solutions are compared with the experimental data of Moorman (1955). The agreement is reasonable. The importance of the added mass term is evident when Figure C.27 is considered. In this case the problem was solved with the added mass term removed from the particle equation. The particle acceleration is much too great, indicating the reality of the added mass effect.

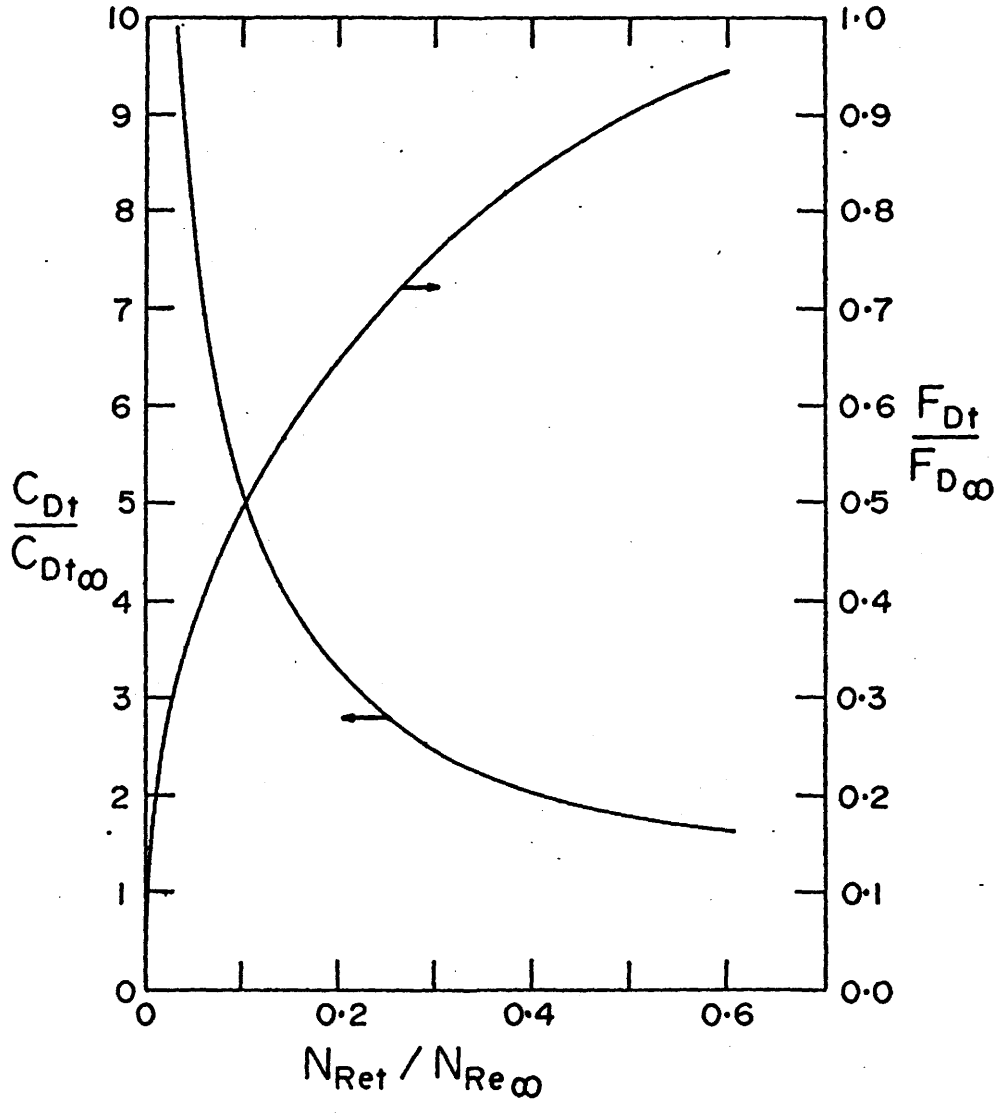

FIGURE C.13 THE EFFECT OF ACCELERATION ON DRAG $N_{Re_\infty} = 0.01$

FIGURE C.14 THE EFFECT OF ACCELERATION ON DRAG $N_{Re_\infty} = 9.0$

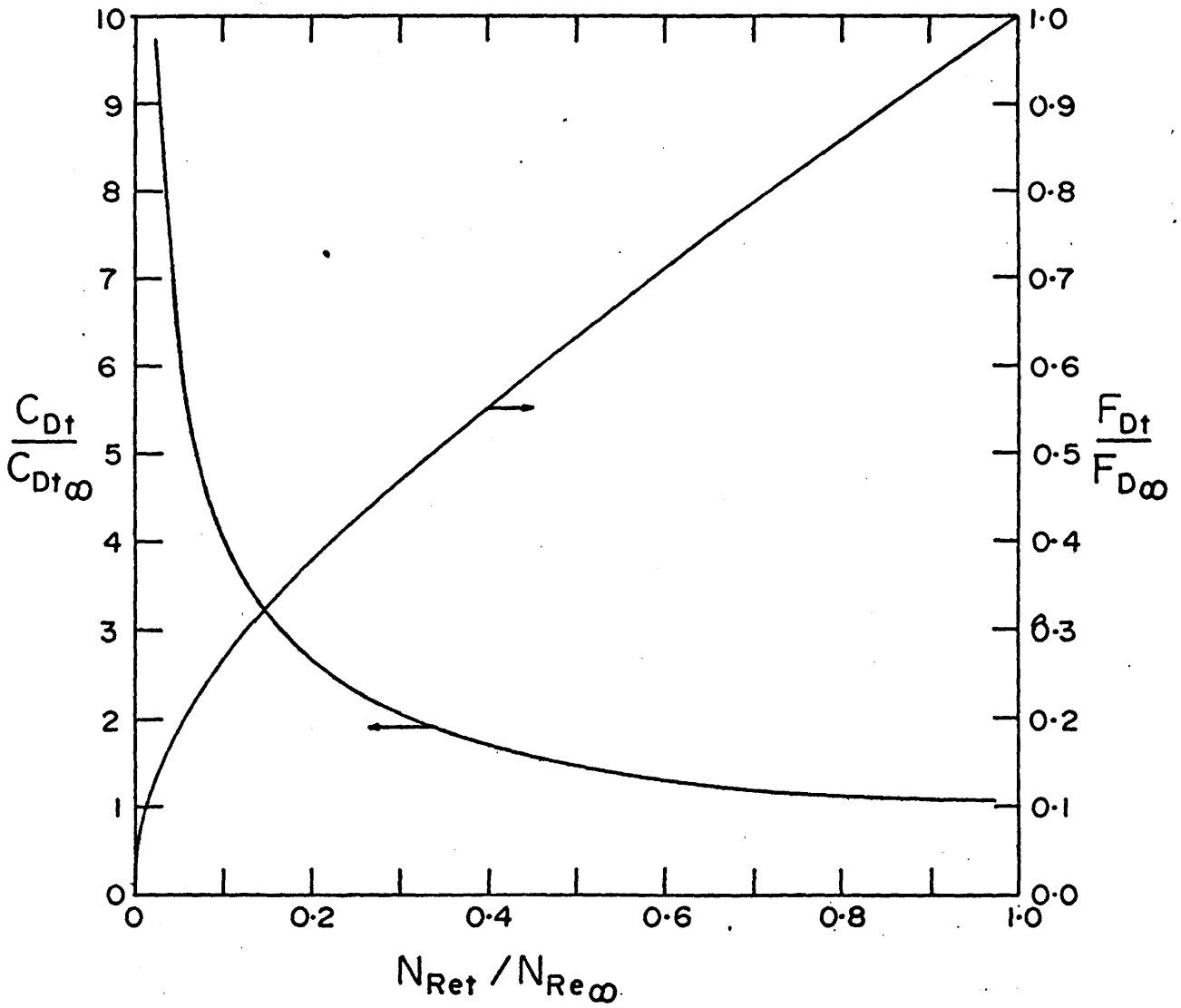

FIGURE C.15 THE EFFECT OF ACCELERATION ON DRAG N_{Re_∞} = 145.0

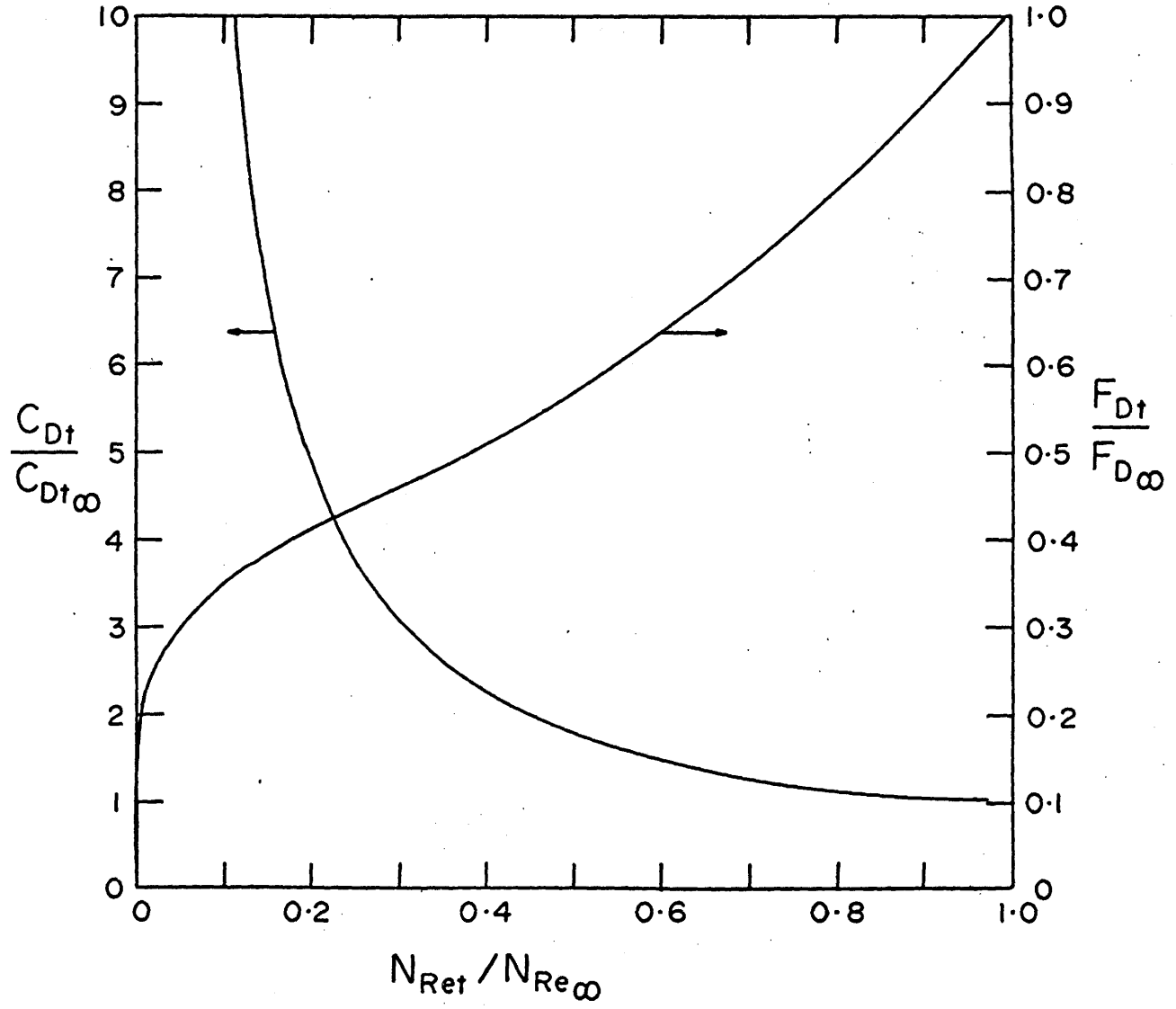

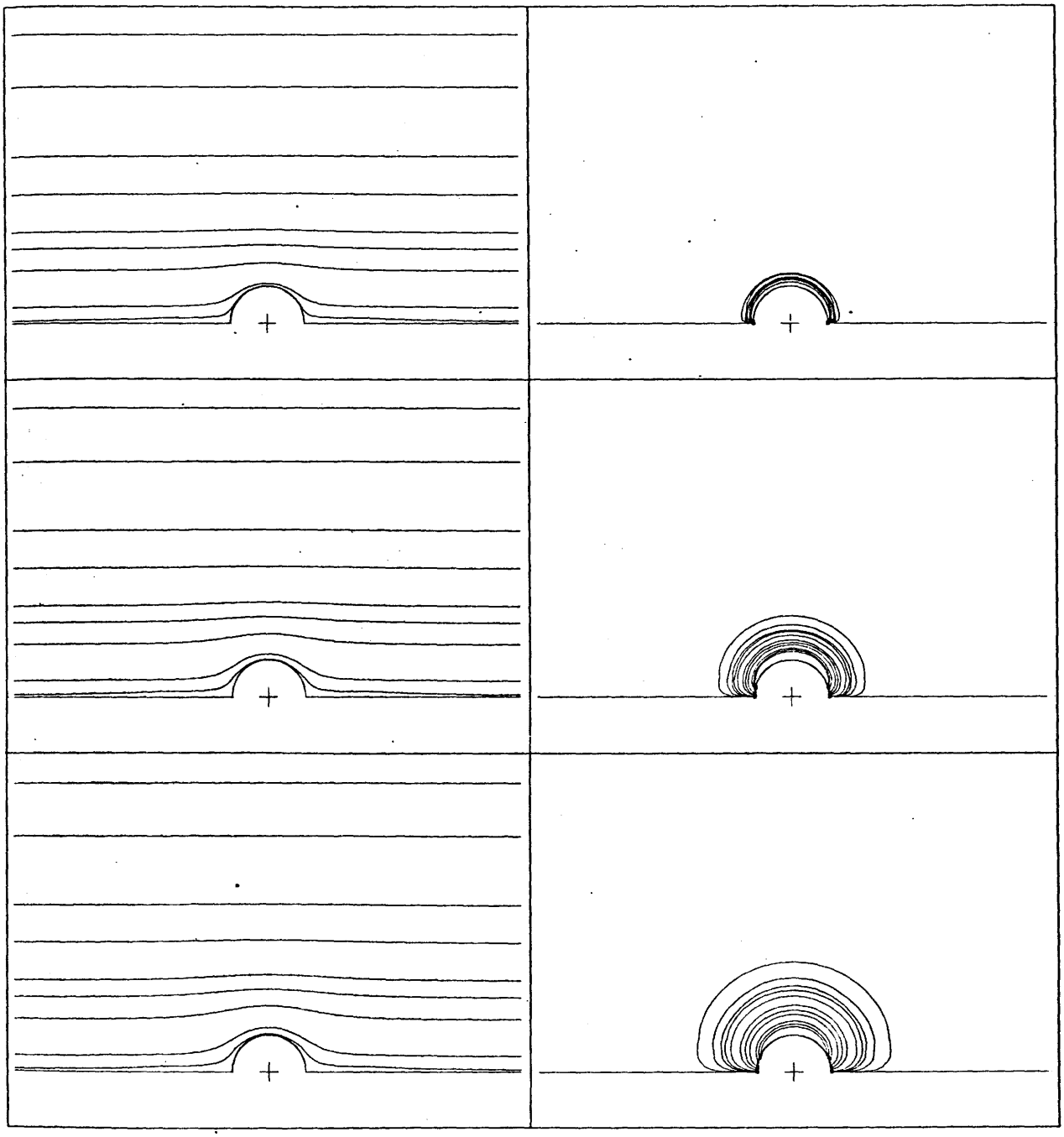

FIGURE C.16(1) VORTICITY AND STREAM FUNCTION CONTOUR PLOTS FOR N_{Re_∞} = 0.01

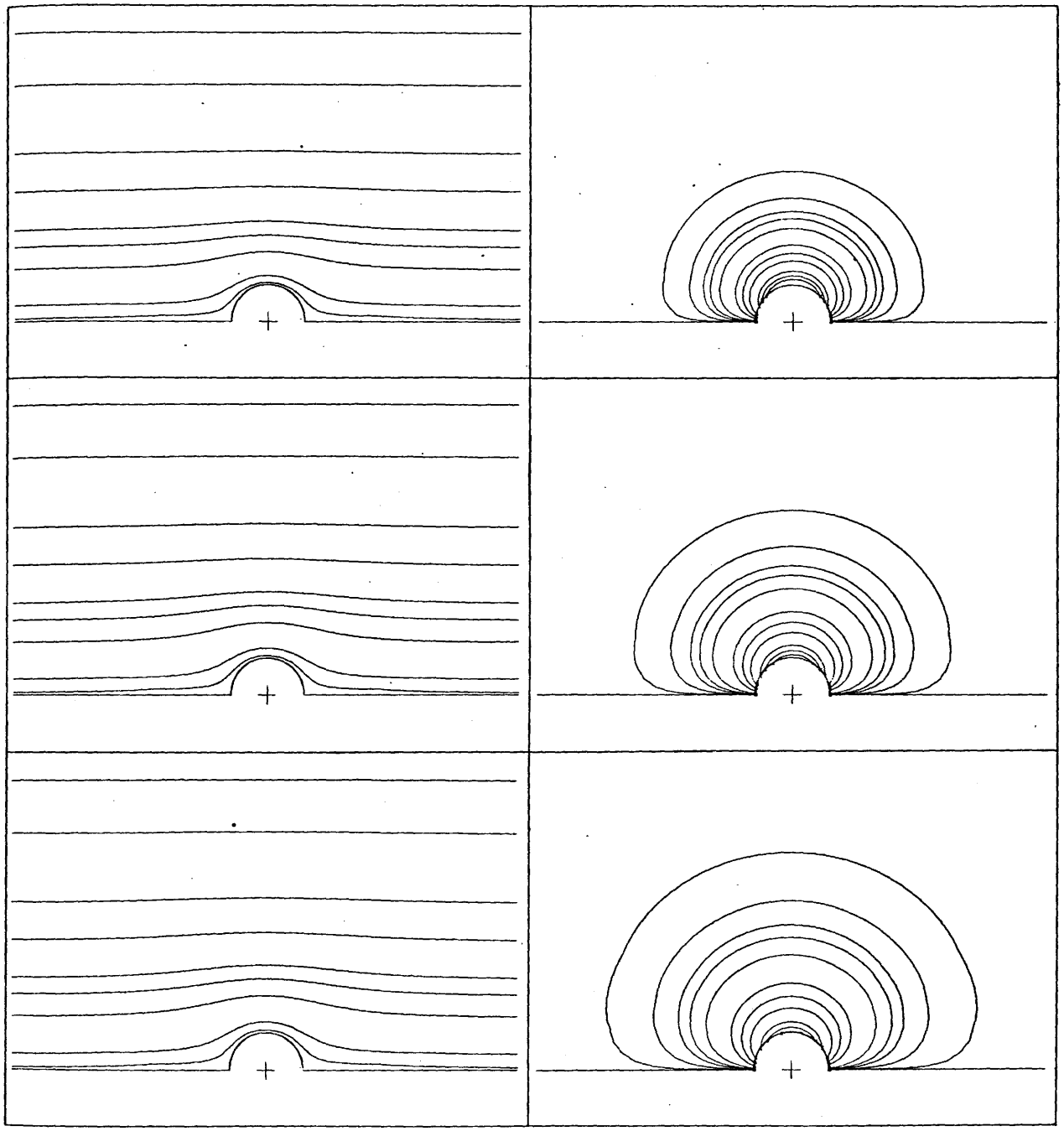

FIGURE C.16(2) VORTICITY AND STREAM FUNCTION CONTOUR PLOTS FOR $N_{Re_\infty} = 0.01$

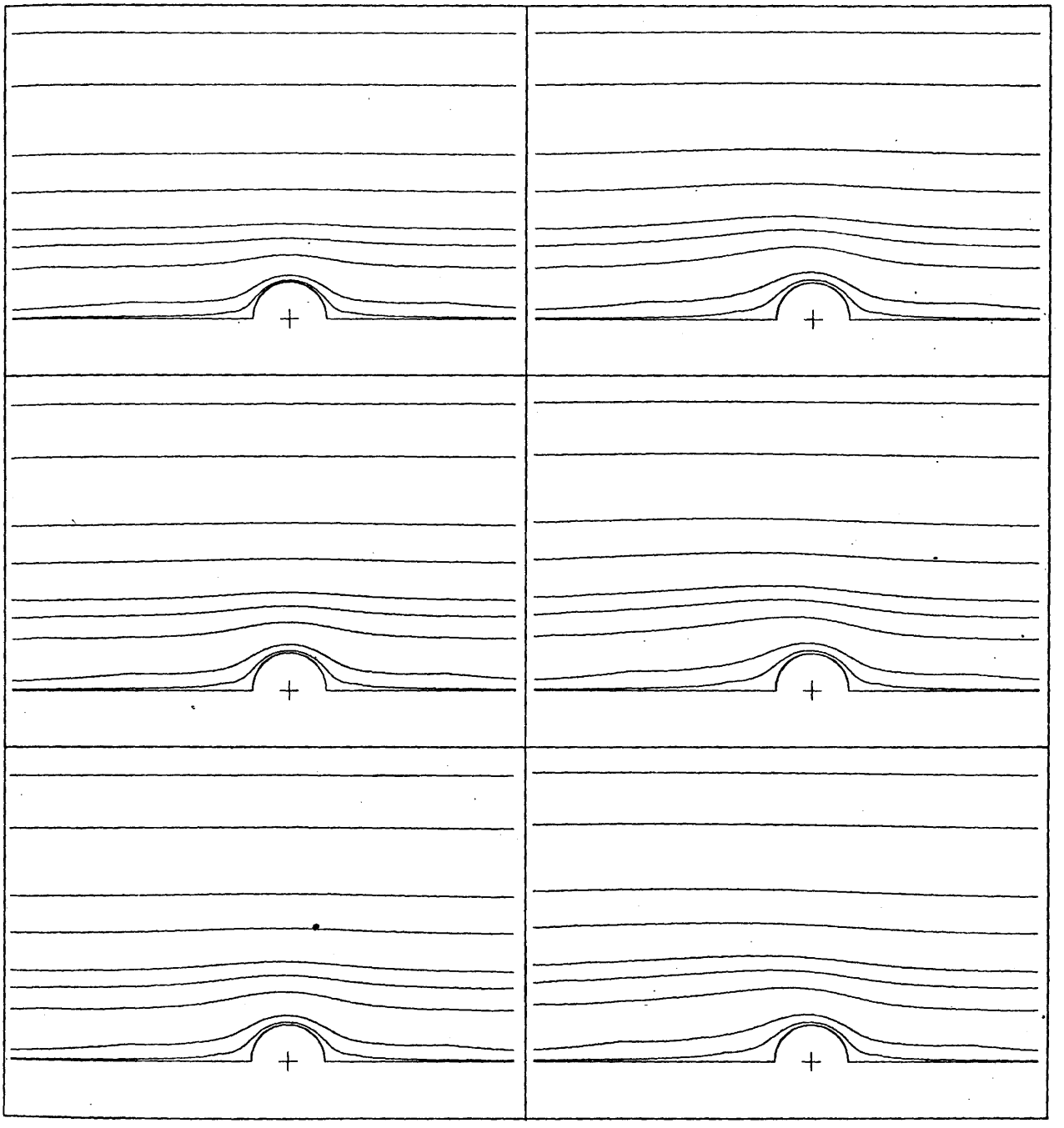

FIGURE C.17(1) VORTICITY AND STREAM FUNCTION CONTOUR PLOTS FOR N_{Re_∞} = 9.0

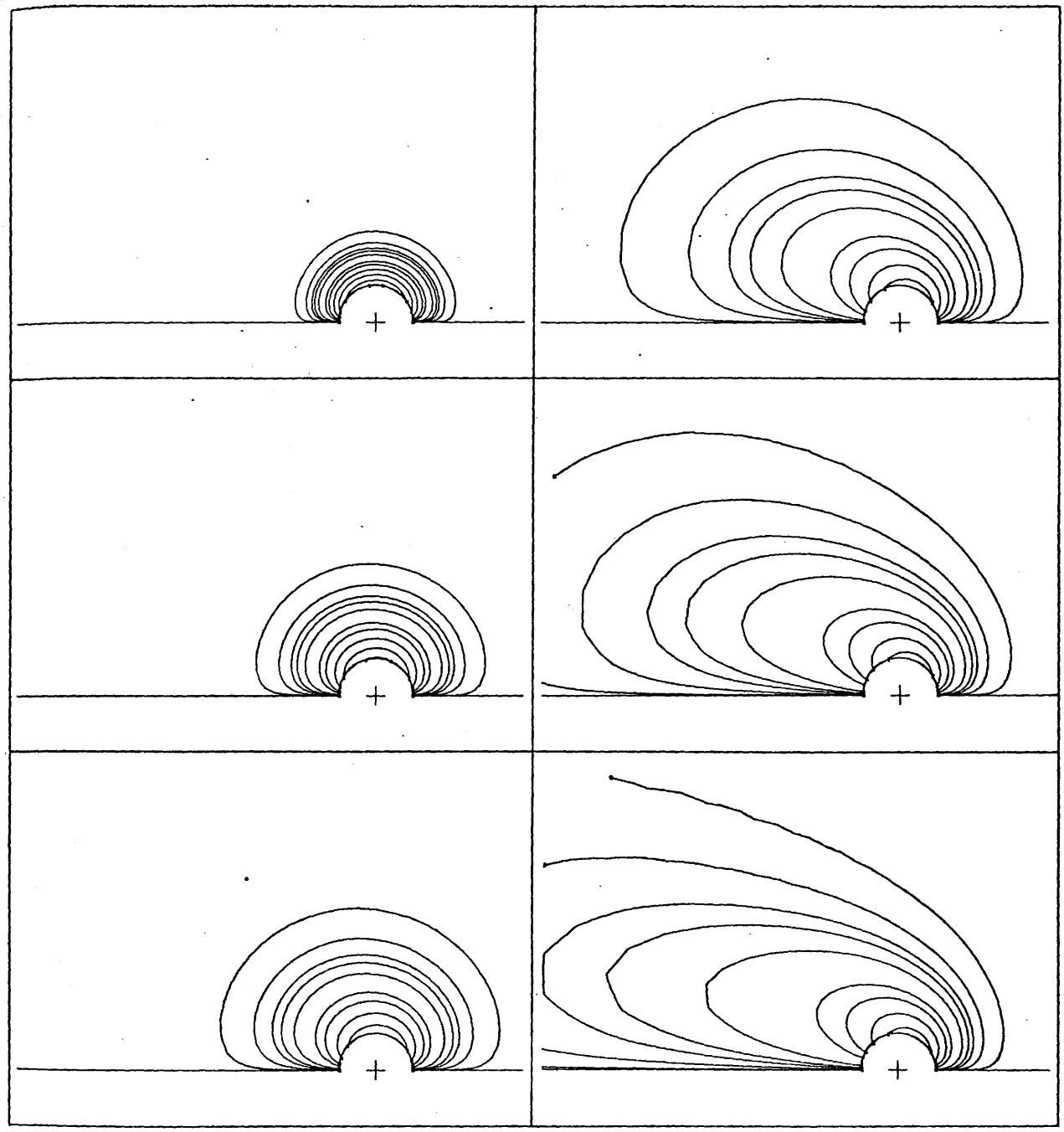

FIGURE C.17(2) VORTICITY AND STREAM FUNCTION CONTOUR PLOTS FOR N_{Re_∞} = 9.0

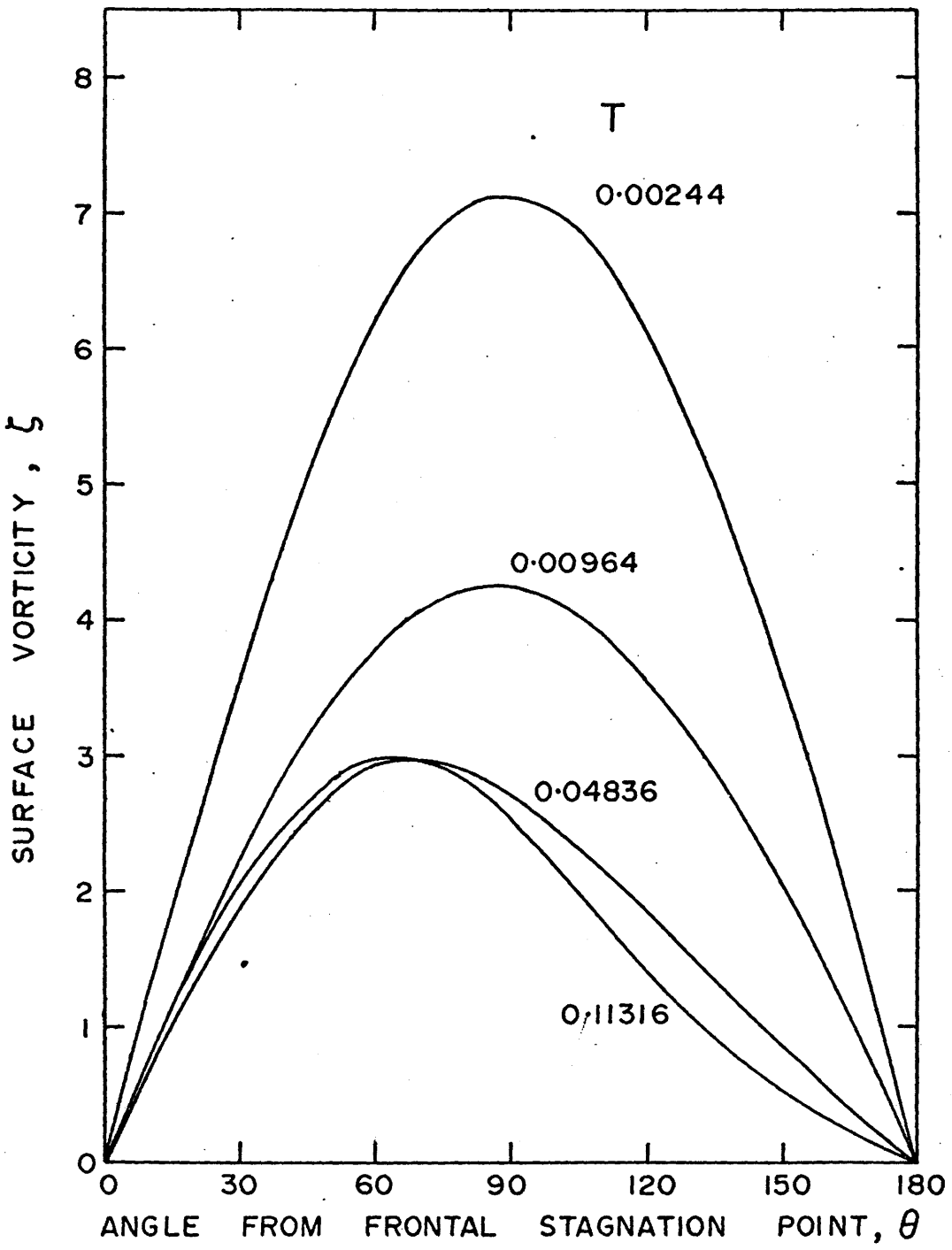

FIGURE C.18 SURFACE VORTICITY DISTRIBUTIONS FOR N_{Re_∞} = 9.0

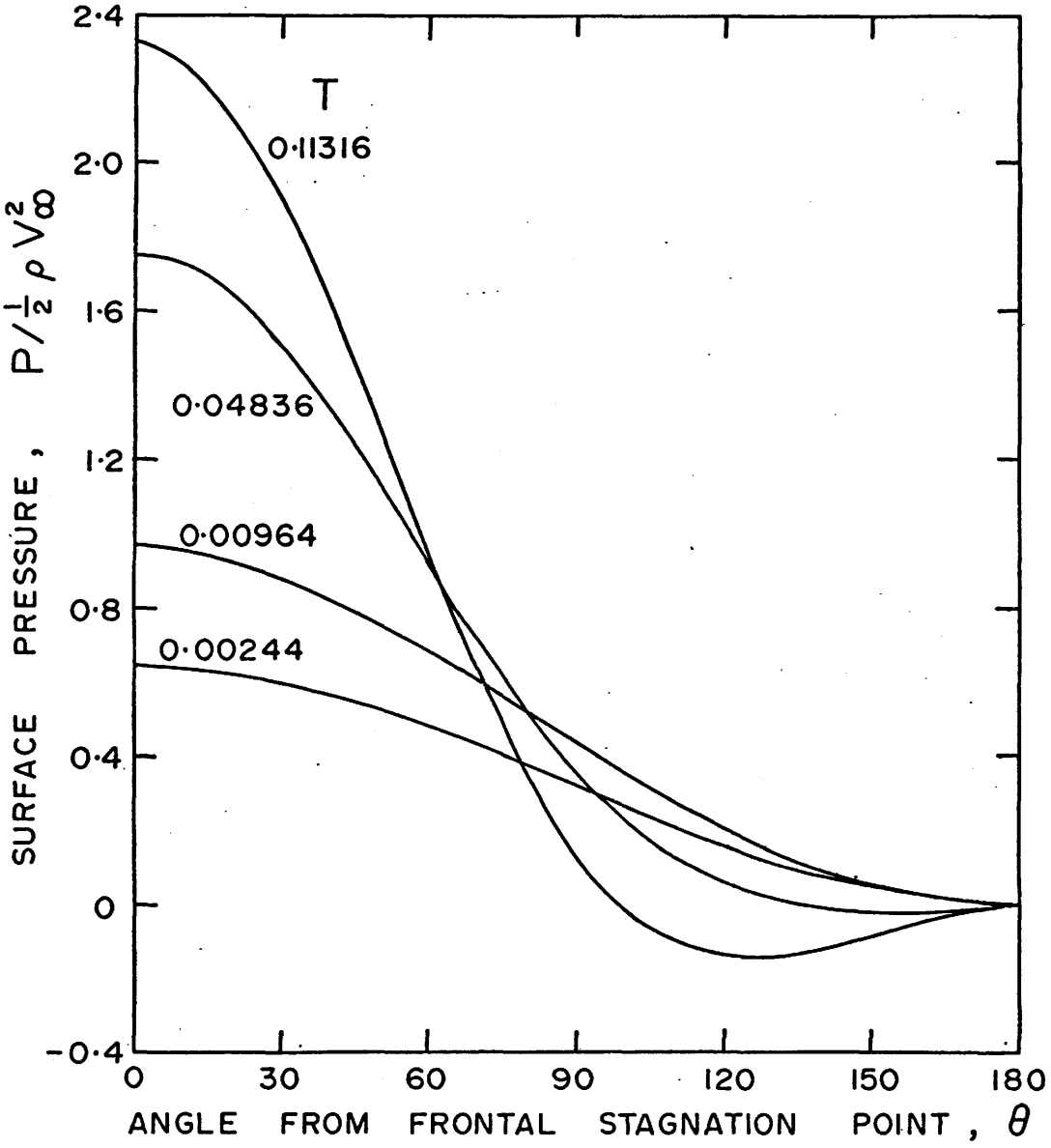

FIGURE C.19 SURFACE PRESSURE DISTRIBUTIONS FOR N_{Re_∞} = 9.0

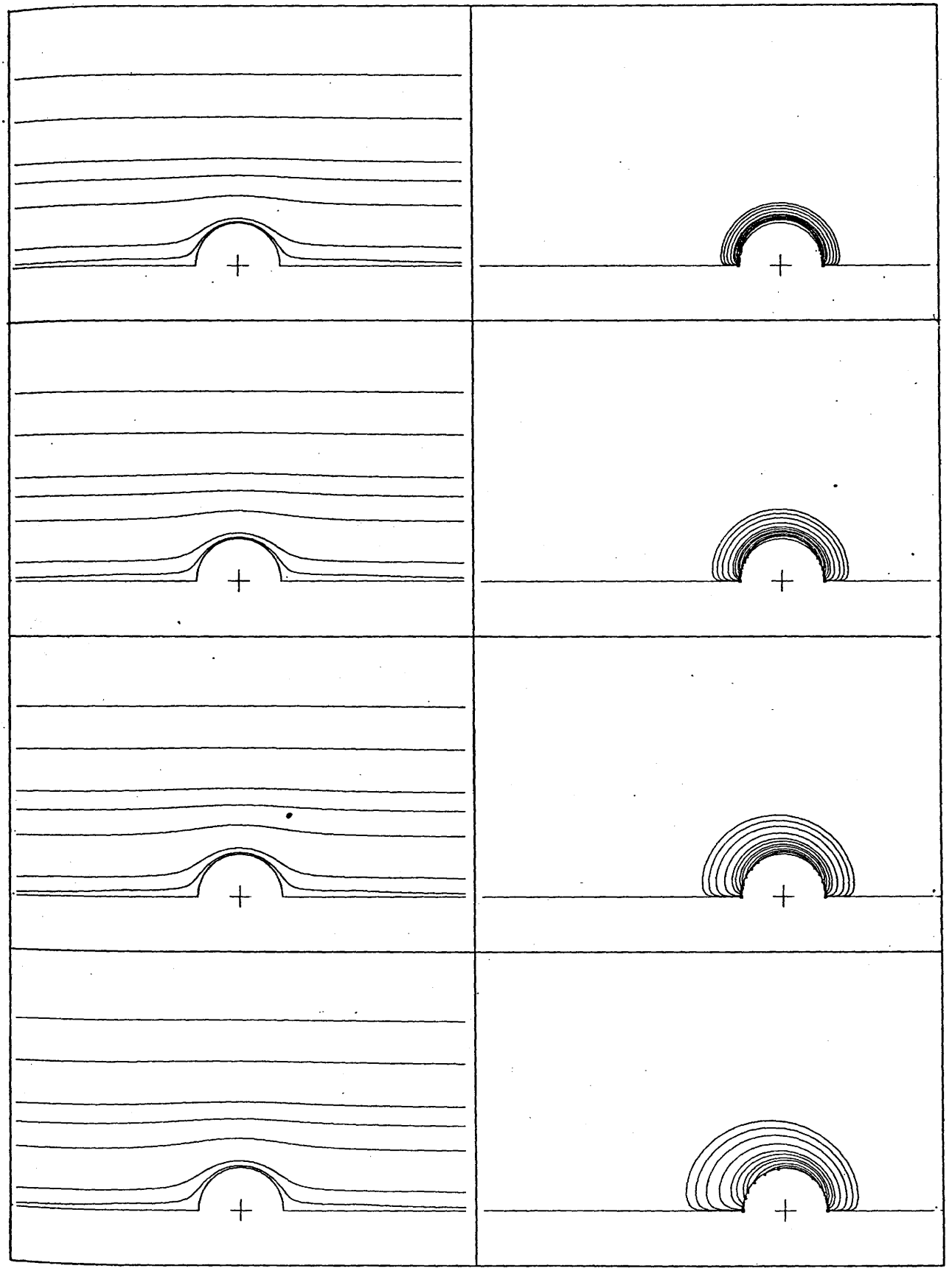

FIGURE C.20(1) VORTICITY AND STREAM FUNCTION CONTOUR PLOTS FOR N_{Re_∞} = 145.0

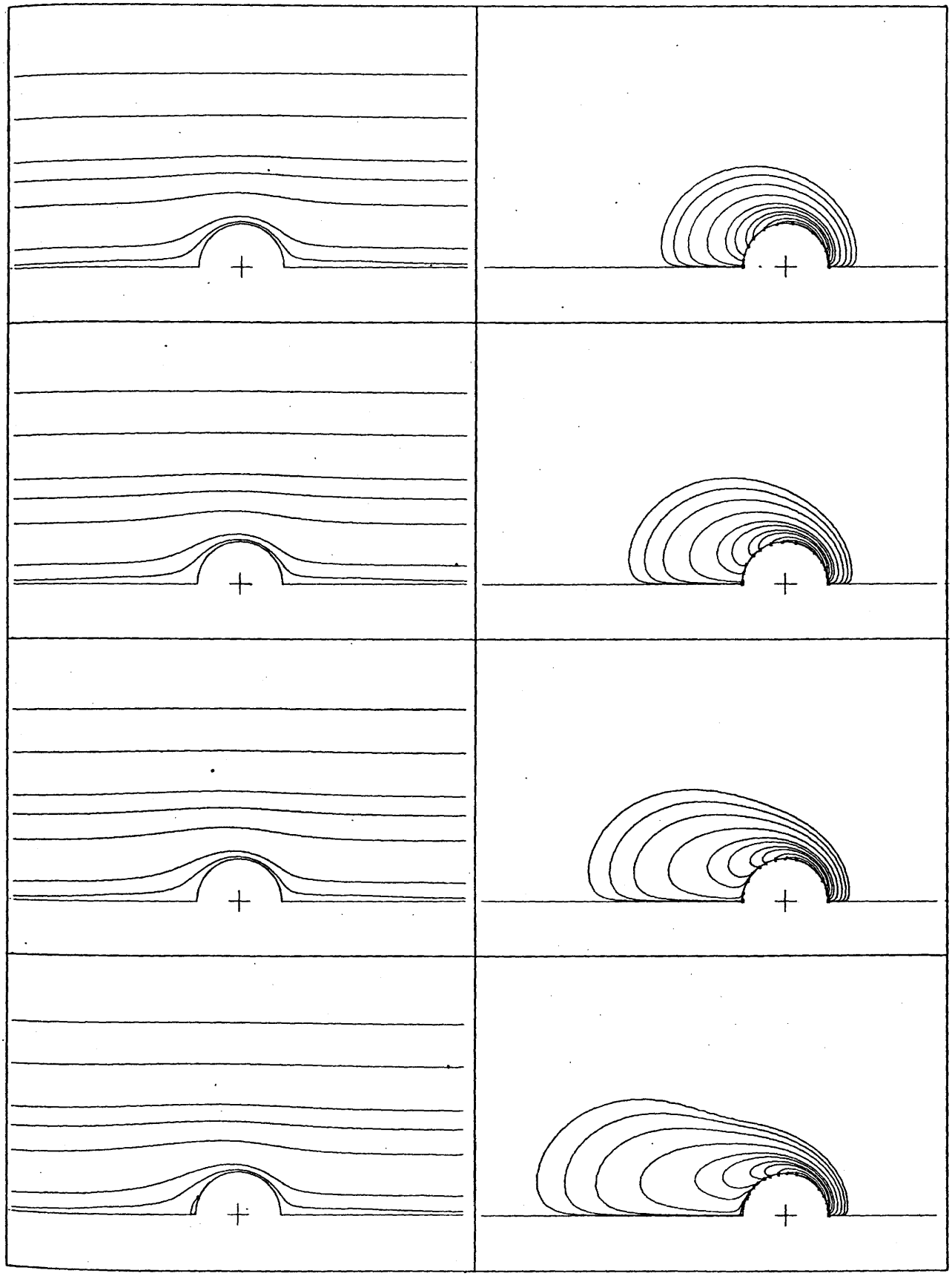

FIGURE C.20(2) VORTICITY AND STREAM FUNCTION CONTOUR PLOTS FOR N_{Re_∞} = 145.0

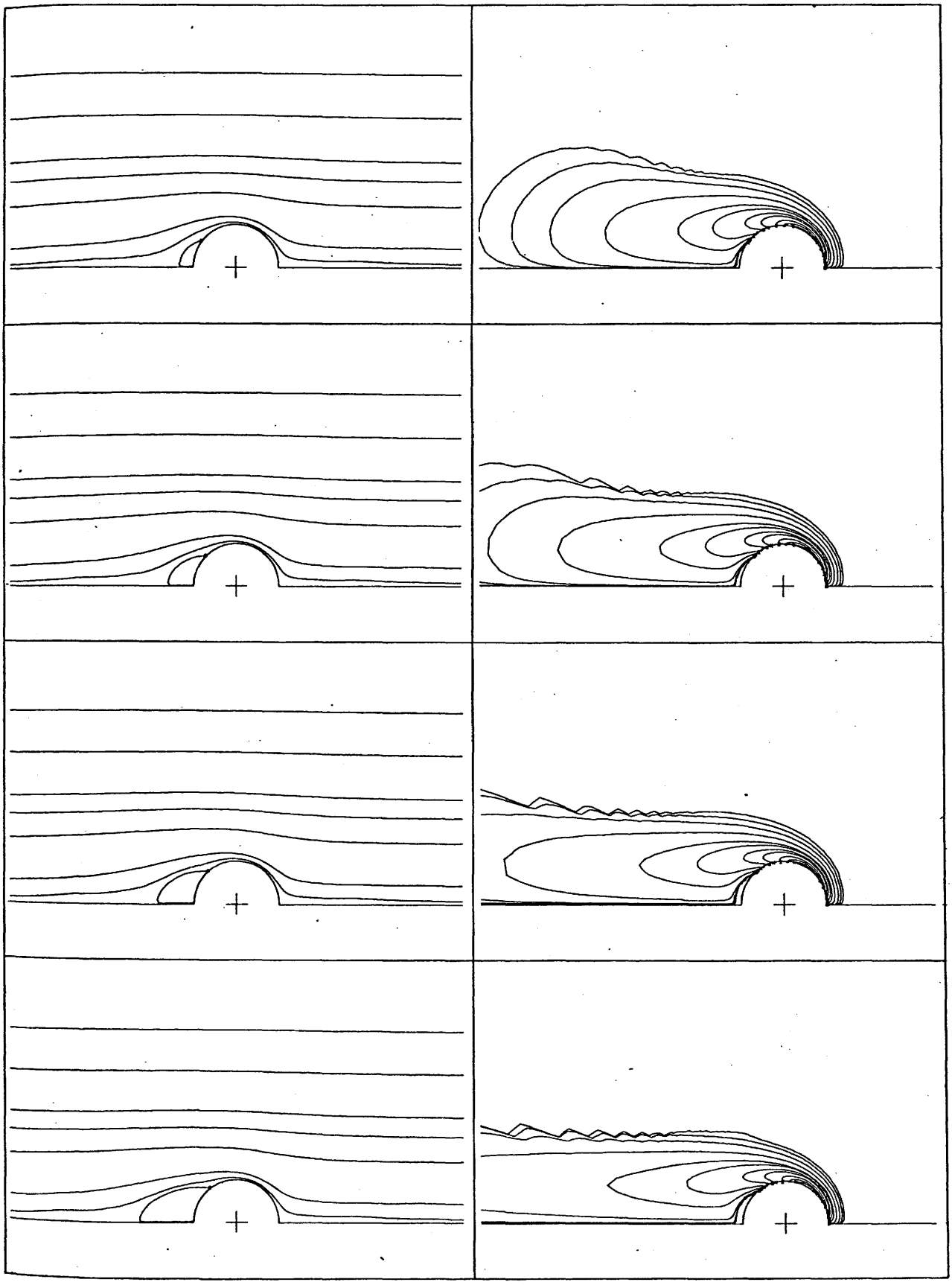

FIGURE C.20(3) VORTICITY AND STREAM FUNCTION CONTOUR PLOTS FOR N_{Re_∞} = 145.0

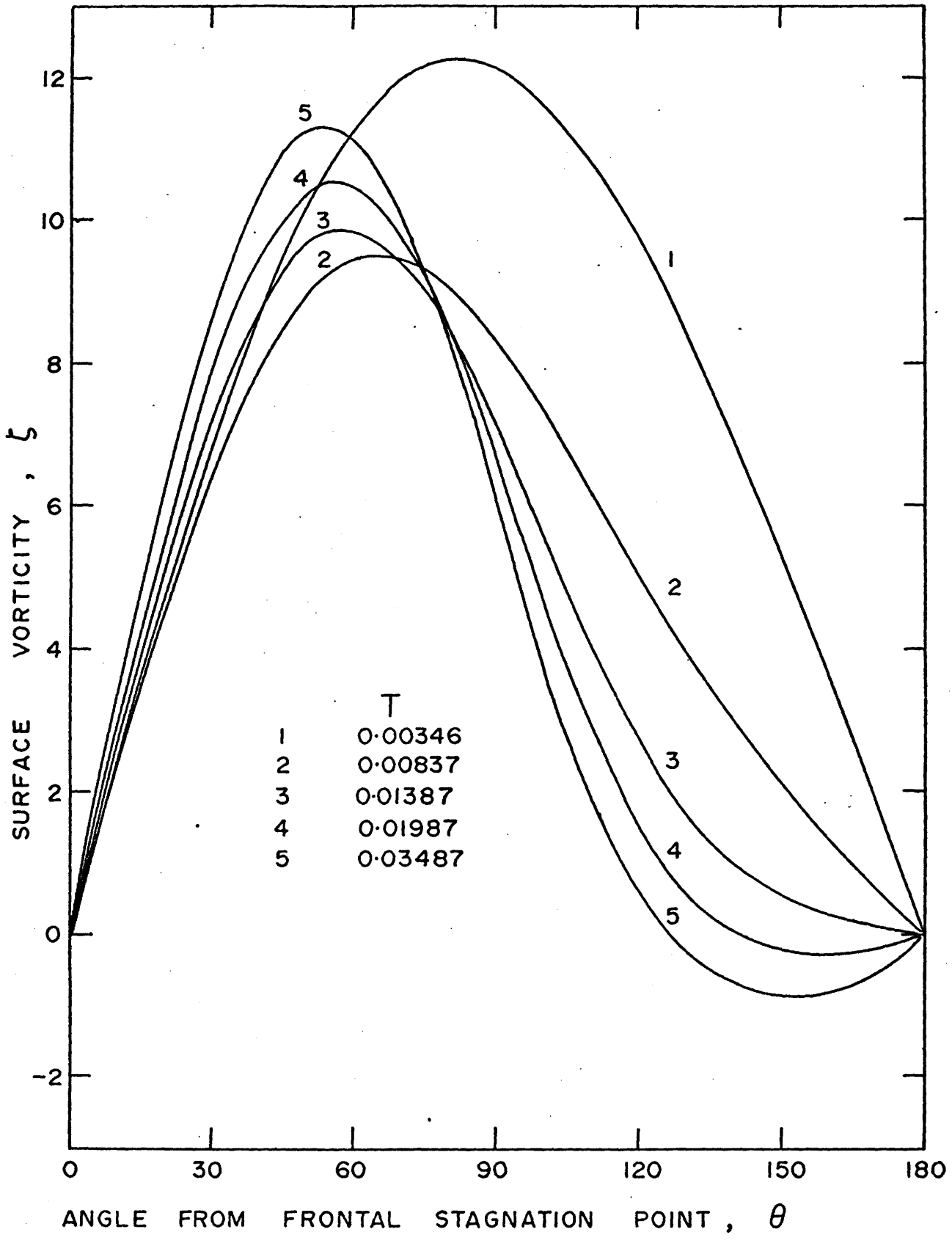

FIGURE C.21 SURFACE VORTICITY DISTRIBUTIONS FOR N_{Re_∞} = 145.0

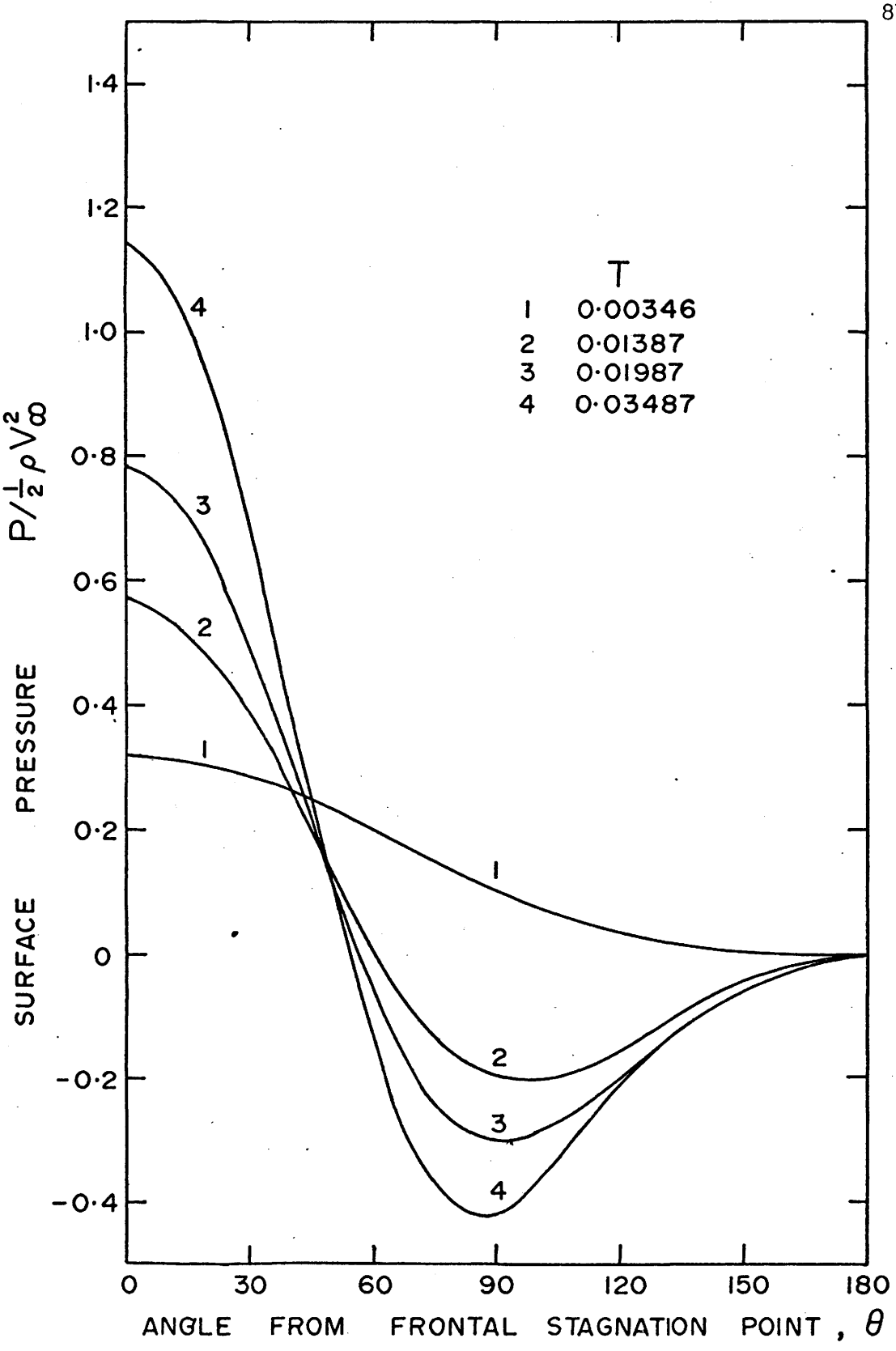

FIGURE C.22 SURFACE PRESSURE DISTRIBUTIONS FOR N_{Re_∞} = 145.0

FIGURE C.23 VORTEX RING DEVELOPMENT FOR N_{Re_∞} = 145.0

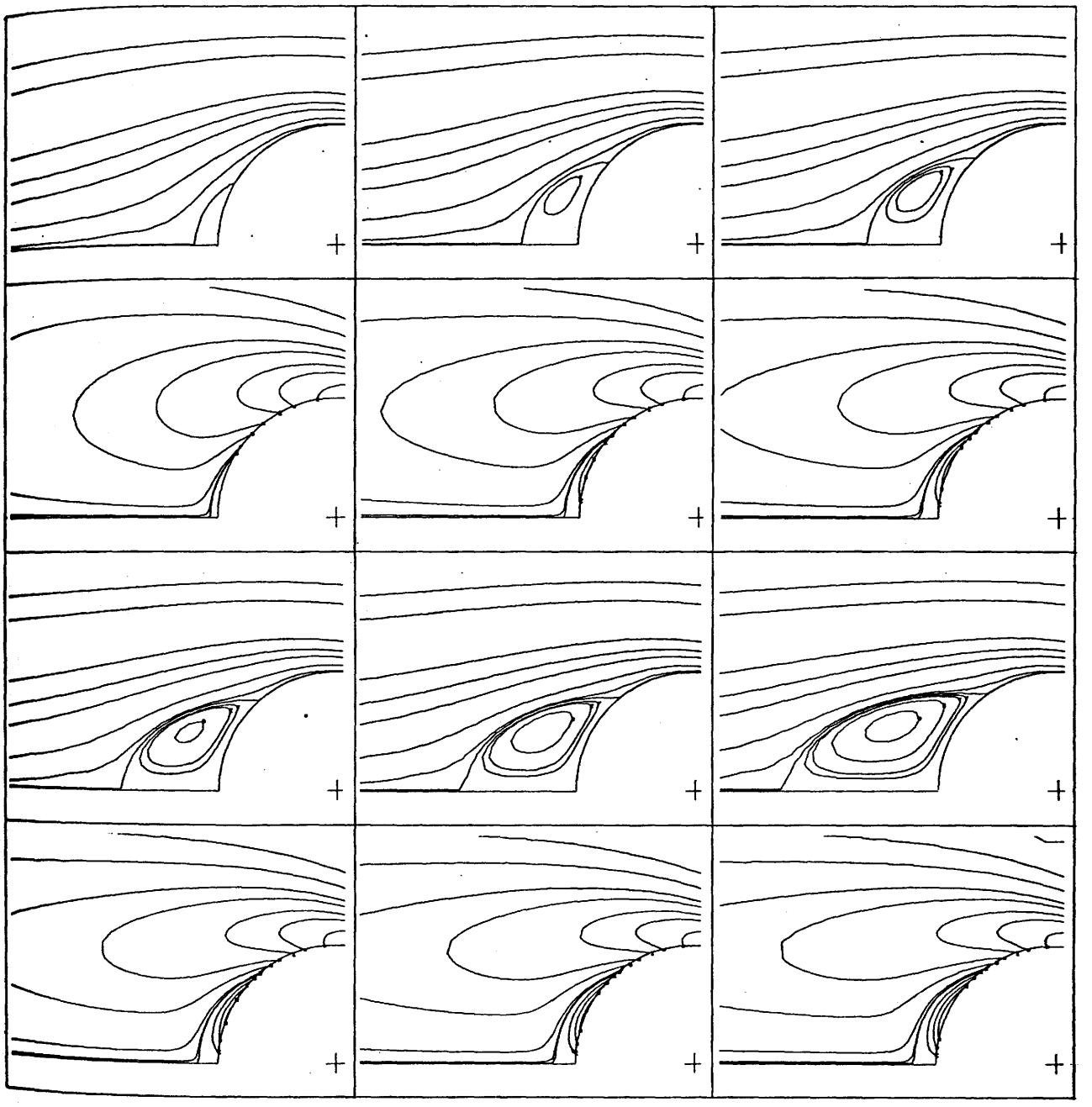

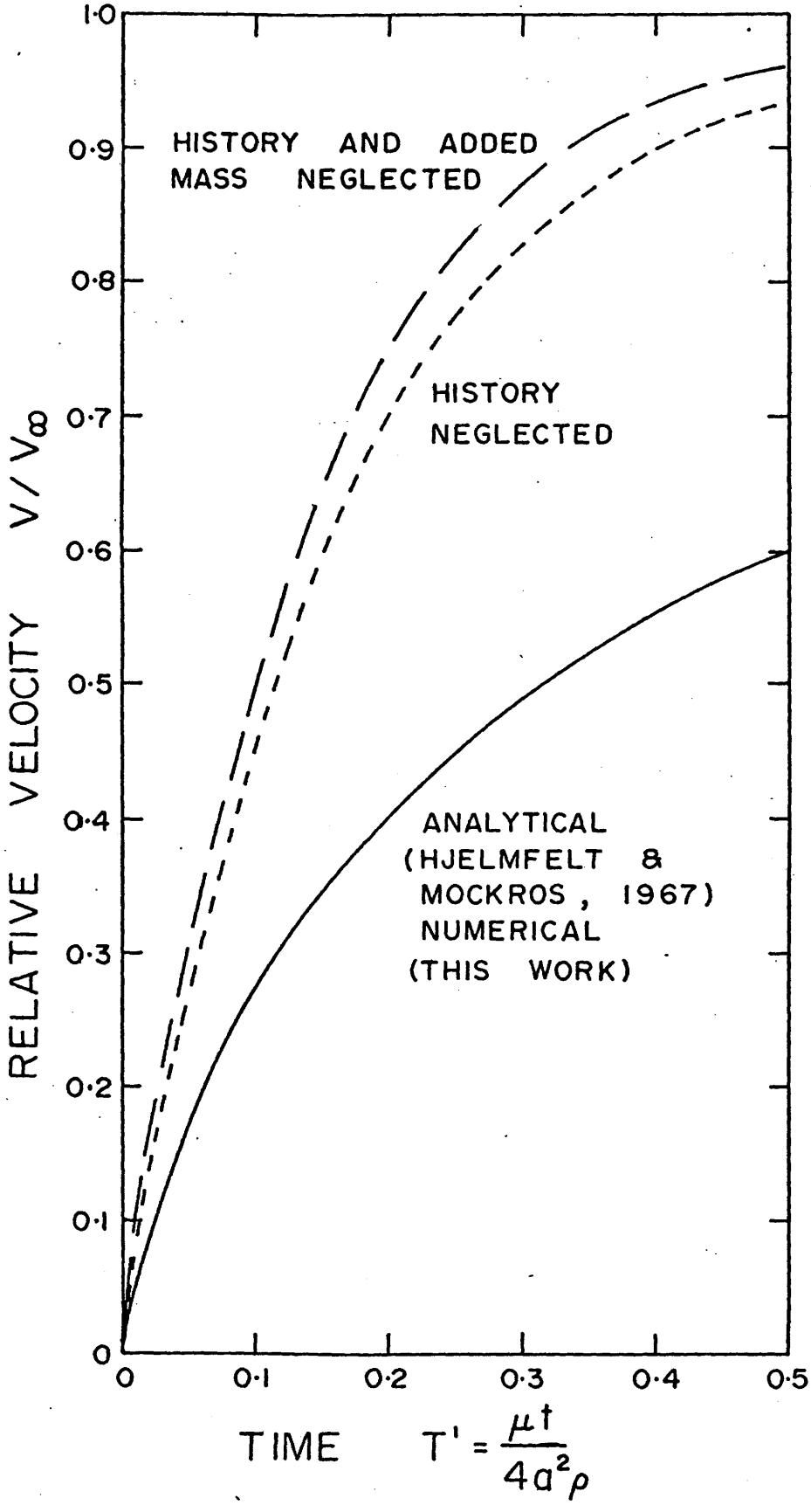

FIGURE C.24 COMPARISON OF EXPERIMENTAL AND NUMERICAL SOLUTIONS FOR $N_{Re_\infty} = 0.01$

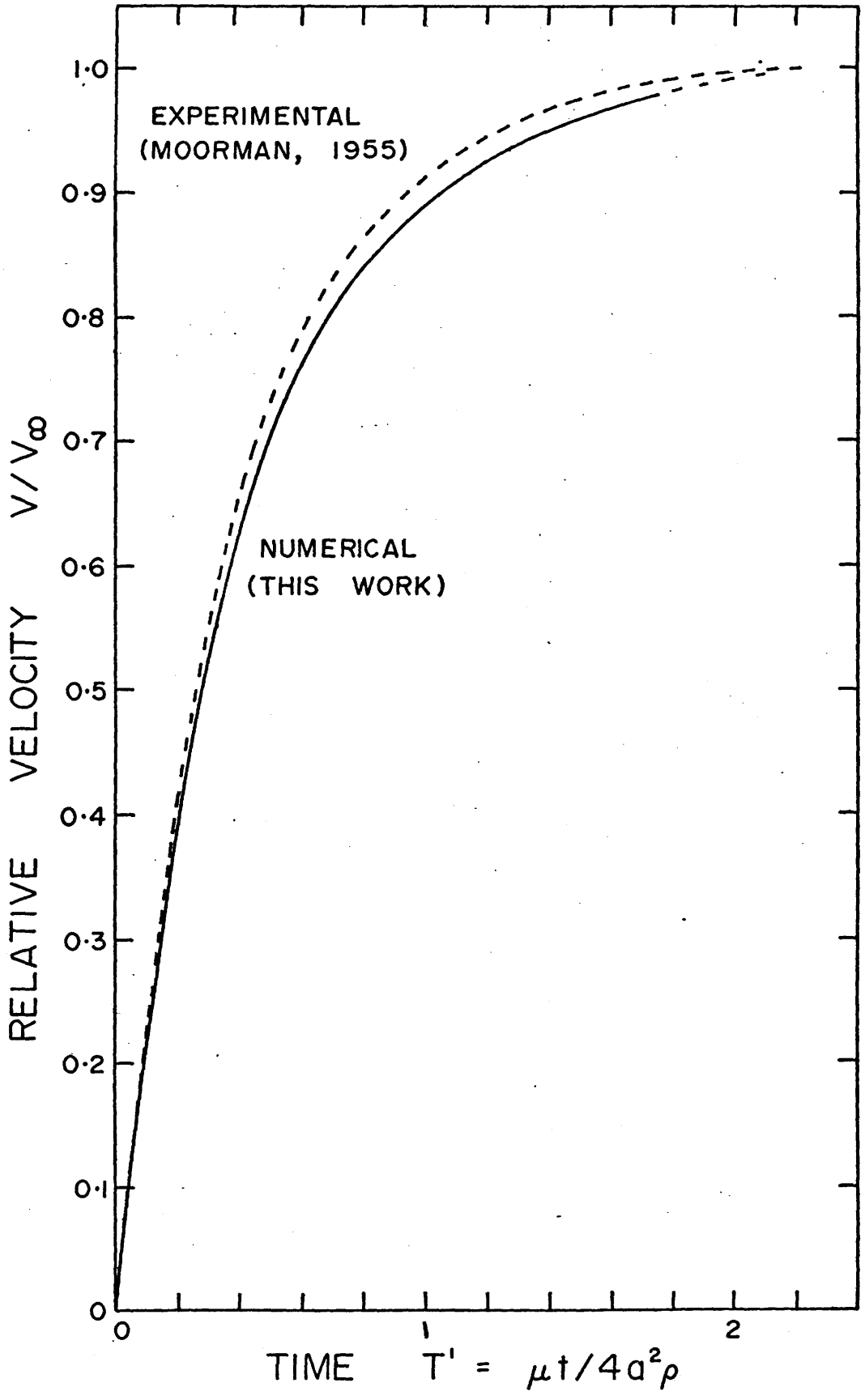

FIGURE C.25 COMPARISON OF EXPERIMENTAL AND NUMERICAL SOLUTIONS FOR $N_{Re_\infty} = 9.0$

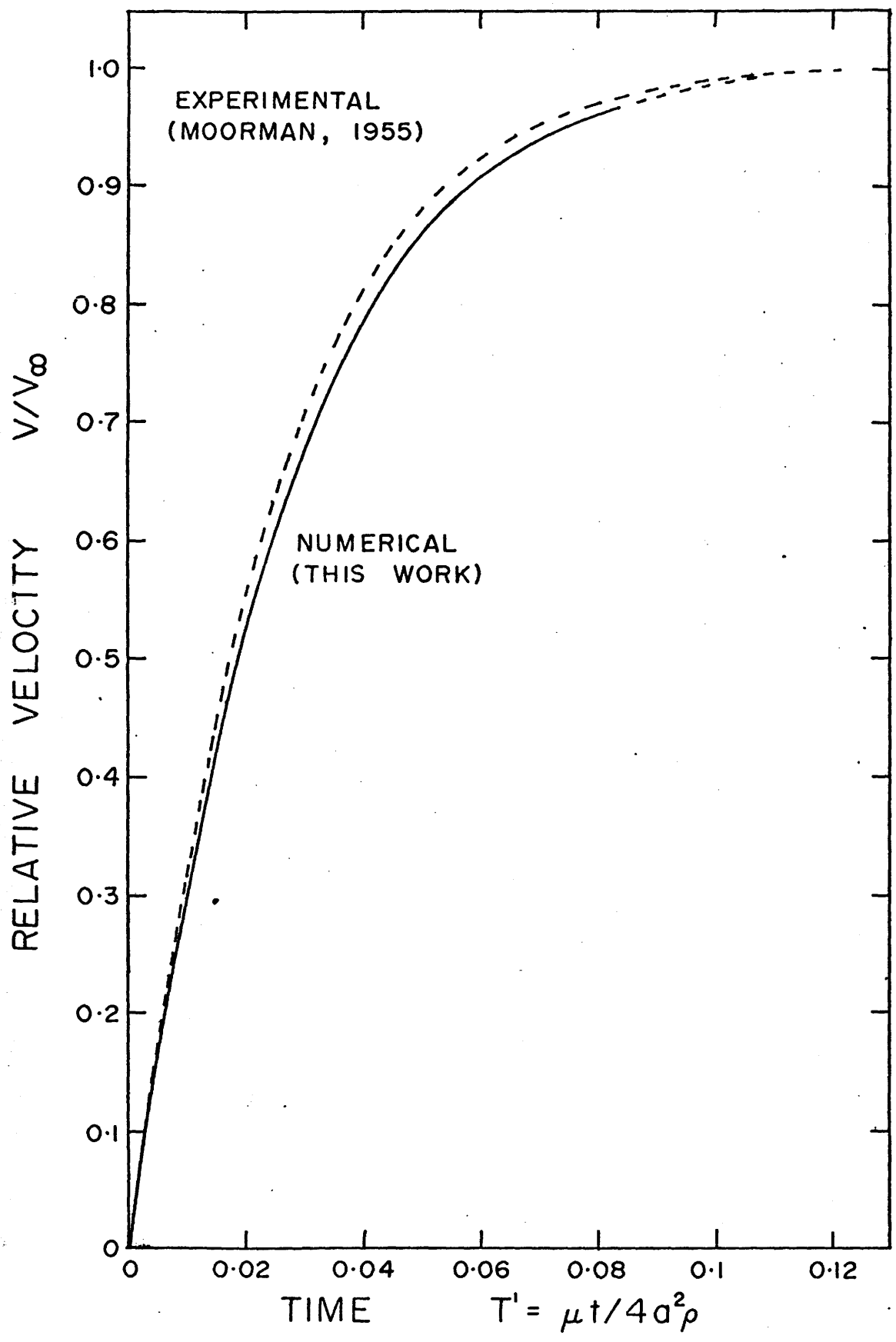

FIGURE C.26 COMPARISON OF EXPERIMENTAL AND NUMERICAL SOLUTIONS FOR N_{Re_∞} = 145.0

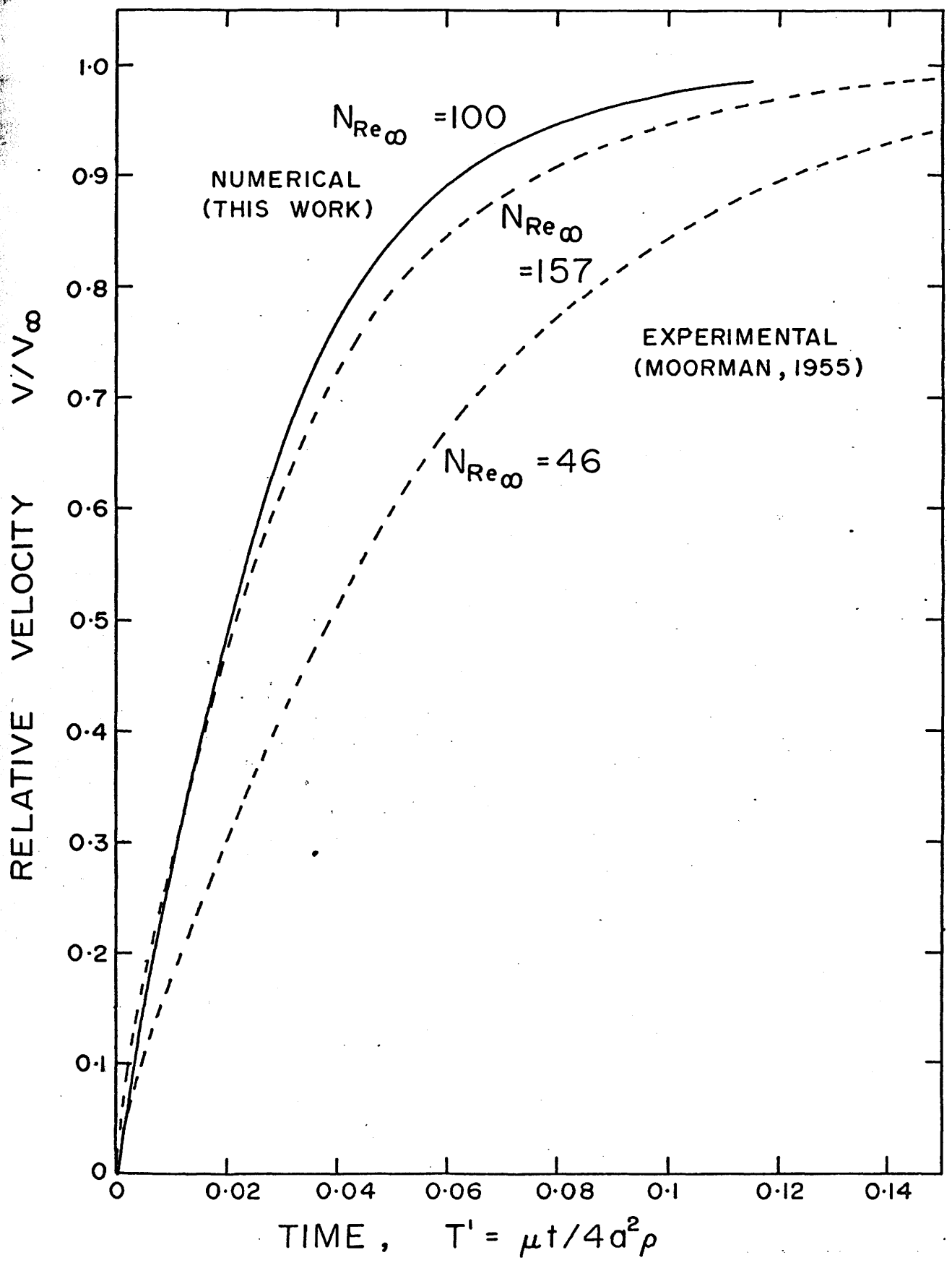

FIGURE C.27 COMPARISON OF EXPERIMENTAL AND NUMERICAL SOLUTIONS (WITH ADDED MASS NEGLECTED)

C.2.4 Discussion

With the use of the added mass concept and the application of an accelerating frame of reference it has been possible to predict with precision the trajectory of an accelerating sphere. Good agreement with experimental data over a wide density ratio range has confirmed this fact. Previous work involved solving Basset's equation or modification of it for particle trajectory or solving the Navier Stokes equations for creeping accelerating flow (Sy, Taunton, and Lightfoot, 1970). None of the previous works have predicted local velocity distributions of accelerating flows at intermediate Reynolds numbers. This additional information will permit the calculation of heat and mass transfer rates for accelerating spheres. Secondly, the numerical solutions can be used to extend experimental fluid mechanical data with great precision.

The concept of added mass is a familiar one. However, although the concept has been rigorously proved for irrotational flows, it has only enjoyed varying degrees of popularity for viscous flows. In fact, it has been described as completely inadequate by several workers (Torobin and Gauvin, 1959). The argument against added mass is related to the constancy of the coefficient of virtual mass, the increase in inertia of an object as a fraction of the mass of fluid displaced by the object. Correlation of experimental data using the equations of motion yields values of the added mass between 0.5 and 9.0 (Feinman, 1964; Lunnon, 1948). The question, however is, whether the added mass concept is correct or the approximate equations of motion used to describe the flow are adequate. In this work, the complete Navier-Stokes equations and the added mass concept were used

to predict particle trajectories. Excellent agreement was found with experimental data. These results suggest that the added mass concept is also exact and constant for viscous flows as well as irrotational flows.

The effect of acceleration on drag was also studied for a sphere accelerating under the influence of gravity. Qualitatively the results show that the effect of acceleration on drag is large when the acceleration is large and the density ratio, solid over fluid density is small. These results refute most of the work done on two and three particle systems in the creeping flow regime. In most of the formulations of mathematical models, the pseudo-steady state approximation is made (Stimson and Jeffrey, 1926). That is, the acceleration term is assumed negligible with respect to the viscous term. This is only true where the particles are far apart or the system forces are almost balanced, and is undoubtedly the reason why these models predict results which are not in agreement with experiment (Pruppacher, Steinberger and Neiburger, 1968).

C.3 Steady State Flow Around Fluid Spheres

C.3.1 Drag Phenomena

The step size and the position of the outer boundary $r = r_\infty$ used in the numerical studies are equal to those used for solid spheres. As the disturbance which results from spherical circulating drops is less than solid spheres, the accuracy of the solutions are as good as those for solid spheres. Thus step size and outer boundary position parametric studies were not carried out.

Although many combinations of the three parameters, viscosity ratio, density ratio and Reynolds number, which affect the flow phenomena could be studied only two combinations of the physical property parameters were investigated. As this work was undertaken (1) to demonstrate the feasibility of the present numerical method for circulating droplets at intermediate Reynolds numbers and (2) to provide local velocity data which could be used in theoretical models for mass transfer and mass transfer with chemical reaction of circulating droplets at intermediate Reynolds numbers only a small number of numerical cases were solved. The physical systems which correspond to these parameter combinations are (1) cyclohexanol in water at 25°C (Tyroler, Johnson and Hamielec, 1969) and (2) liquid water drops in air at 20°C and 100% humidity (Beard and Pruppacher, 1969). Results for the friction, pressure and total drag, and the frontal stagnation pressure are given in Table C.13. The total drag coefficient obtained experimentally by Beard and Pruppacher is shown in brackets under the numerically calculated value. The agreement is excellent. Values at the droplet surface of the pressure, shear stress, vorticity and angular

velocity for the four cases are given in Tables C.14 to C.17.

C.3.2 Flow Field Phenomena

The flow phenomena outside and inside the circulating spherical liquid droplets is very interesting. Contour plots of the stream function and vorticity for all cases considered are presented in Figures C.28 to C.43. The form and character of the stream function and vorticity contour plots for the exterior flow region are almost identical with those of solid spheres (See Figures C.9 to C.12). Features to note in the regions inside and outside the drop are the following: shape of the vortex ring outside the drop, relative sizes of regions of negative vorticity and negative stream function inside drop - secondary vortex, the high vorticity regions in the drop which bulge inward towards the center and rear of the drop, position of the center of the primary vortex in the drop. The features indicate that the nonlinear nature of the phenomena is important as results are not as generally expected. It was expected that the center of the primary vortex inside the drop would move towards the front of the drop as the maximum surface vorticity moved towards the front of the drop and the trailing vortex behind the drop grows. In reality the forward movement of the primary vortex center is restricted by two phenomena, the rearward penetration of the high vorticity into the drop and the reduction of the vortex ring separation angle. The rearward motion of the drop surface moves the trailing vortex back and away from the drop surface. The effect is similar to that obtained for blowing (Hamielec, Hoffman, and Ross, 1967). The rearward movement of the high vorticity region and surface movement are also responsible for reducing the size of the secondary vortex inside the drop.

TABLE C.13 DRAG COEFFICIENT RESULTS FOR CIRCULATING DROPLETS

N_{Re}	μ_i/μ_o	ρ_i/ρ_o	N_{Re_i}	C_{DF}	C_{DP}	C_D	P_o
2.56	0.06565	1.04590	40.7845	5.0930	2.6255	7.7185	2.5434
30.0	54.9450	836.056	456.487	1.2913	0.8137	2.1150 (2.095)	1.3186
100.0	54.9450	836.056	1521.623	0.5906	0.4917	1.0823 (1.073)	1.1035
300.0	54.9450	836.056	4564.870	0.2938	0.3429	0.6367 (0.638)	1.0364

TABLE C.14 SURFACE VALUES OF PARAMETERS FOR N_{Re} = 2.45

ANGLE	v_θ	$J_{r\theta}$	ξ	P_θ
0	0.0	0.0	0.0	2.5434
6	0.0698	0.0141	0.1558	2.5190
12	0.1383	0.0277	0.3089	2.4468
18	0.2048	0.0407	0.4569	2.3293
24	0.2681	0.0528	0.5978	2.1701
30	0.3274	0.0636	0.7292	1.9745
36	0.3818	0.0730	0.8494	1.7486
42	0.4305	0.0808	0.9566	1.4990
48	0.4730	0.0870	1.0495	1.2331
54	0.5087	0.0915	1.1271	0.9579
60	0.5372	0.0945	1.1885	0.6806
66	0.5584	0.0959	1.2334	0.4077
72	0.5721	0.0958	1.2612	0.1448
78	0.5784	0.0944	1.2735	-0.1033
84	0.5774	0.0919	1.2695	-0.3327
90	0.5696	0.0884	1.2504	-0.5408
96	0.5553	0.0841	1.2173	-0.7259
102	0.5352	0.0791	1.1714	-0.8874
108	0.5096	0.0736	1.1141	-1.0256
114	0.4794	0.0677	1.0467	-1.1415
120	0.4452	0.0615	0.9707	-1.2367
126	0.4076	0.0552	0.8877	-1.3131
132	0.3672	0.0488	0.7989	-1.3731
138	0.3247	0.0425	0.7057	-1.4191
144	0.2805	0.0361	0.6091	-1.4533
150	0.2351	0.0299	0.5101	-1.4780
156	0.1889	0.0238	0.4095	-1.4952
162	0.1420	0.0177	0.3079	-1.5067
168	0.0949	0.0118	0.2056	-1.5139
174	0.0475	0.0059	0.1029	-1.5178
180	0.0	0.0	0.0	-1.5190

TABLE C.15 SURFACE VALUES OF PARAMETERS FOR N_{Re} = 30.0

ANGLE	v_θ	$J_{r\theta}$	ξ	P_θ
0	0.0	0.0	0.0	1.3186
6	0.0028	0.8619	0.8504	1.2973
12	0.0056	1.6966	1.6745	1.2349
18	0.0083	2.4817	2.4505	1.1343
24	0.0108	3.1949	3.1569	1.0005
30	0.0130	3.8163	3.7741	0.8398
36	0.0150	4.3289	4.2860	0.6599
42	0.0167	4.7197	4.6796	0.4691
48	0.0181	4.9800	4.9464	0.2758
54	0.0191	5.1061	5.0824	0.0883
60	0.0197	5.0996	5.0888	-0.0859
66	0.0200	4.9676	4.9718	-0.2406
72	0.0199	4.7225	4.7426	-0.3711
78	0.0194	4.3815	4.4171	-0.4746
84	0.0185	3.9655	4.0149	-0.5500
90	0.0174	3.4983	3.5585	-0.5980
96	0.0161	3.0041	3.0714	-0.6212
102	0.0146	2.5067	2.5767	-0.6228
108	0.0130	2.0268	2.0956	-0.6072
114	0.0113	1.5814	1.6457	-0.5787
120	0.0096	1.1829	1.2401	-0.5417
126	0.0081	0.8388	0.8876	-0.4998
132	0.0066	0.5524	0.5923	-0.4563
138	0.0053	0.3238	0.3549	-0.4133
144	0.0041	0.1509	0.1741	-0.3726
150	0.0031	0.0303	0.0466	-0.3356
156	0.0023	-0.0425	-0.0318	-0.3032
162	0.0016	-0.0734	-0.0670	-0.2765
168	0.0010	-0.0700	-0.0666	-0.2565
174	0.0005	-0.0418	-0.0404	-0.2440
180	0.0	0.0	0.0	-0.2398

TABLE C.16 SURFACE VALUES OF PARAMETERS FOR N_{Re} = 100.0

ANGLE	v_θ	$J_{r\theta}$	ξ	P_θ
0	0.0	0.0	0.0	1.1035
6	0.0048	1.6231	1.6099	1.0816
12	0.0096	3.1939	3.1681	1.0170
18	0.0142	4.6685	4.6313	0.9133
24	0.0186	6.0030	5.9560	0.7757
30	0.0228	7.1568	7.1022	0.6116
36	0.0265	8.0943	8.0349	0.4292
42	0.0299	8.7858	8.7251	0.2382
48	0.0327	9.2093	9.1513	0.0484
54	0.0349	9.3516	9.3005	-0.1308
60	0.0363	9.2103	9.1705	-0.2905
66	0.0370	8.7952	8.7708	-0.4234
72	0.0368	8.1304	8.1242	-0.5244
78	0.0357	7.2549	7.2686	-0.5910
84	0.0338	6.2229	6.2561	-0.6235
90	0.0311	5.1014	5.1510	-0.6251
96	0.0279	3.9640	4.0250	-0.6015
102	0.0242	2.8829	2.9490	-0.5599
108	0.0204	1.9189	1.9837	-0.5080
114	0.0167	1.1125	1.1711	-0.4529
120	0.0133	0.4805	0.5303	-0.3999
126	0.0102	0.0164	0.0568	-0.3527
132	0.0077	-0.3055	-0.2733	-0.3130
138	0.0055	-0.5235	-0.4979	-0.2807
144	0.0037	-0.6763	-0.6568	-0.2545
150	0.0023	-0.7833	-0.7703	-0.2319
156	0.0012	-0.8324	-0.8262	-0.2105
162	0.0005	-0.7904	-0.7897	-0.1896
168	0.0001	-0.6293	-0.6314	-0.1708
174	-0.0000	-0.3527	-0.3547	-0.1574
180	0.0000	0.0	0.0	-0.1525

TABLE C.17 SURFACE VALUES OF PARAMETERS FOR N_{Re} = 300.0

ANGLE	v_θ	$J_{r\theta}$	ξ	P_θ
0	0	0	0	1.0363
6	0.0048	2.9424	2.9104	1.0124
12	0.0096	5.7906	5.7221	0.9419
18	0.0142	8.4644	8.3511	0.8290
24	0.0186	10.8824	10.7138	0.6801
30	0.0227	12.9672	12.7328	0.5037
36	0.0265	14.6577	14.3392	0.3098
42	0.0300	15.8607	15.4743	0.1097
48	0.0331	16.5525	16.0918	-0.0852
54	0.0359	16.6821	16.1594	-0.2634
60	0.0383	16.2246	15.6626	-0.4147
66	0.0403	15.1775	14.6099	-0.5306
72	0.0418	13.5712	13.0408	-0.6055
78	0.0428	11.4831	11.0373	-0.6375
84	0.0431	9.0537	8.7351	-0.6295
90	0.0423	6.4946	6.3259	-0.5892
96	0.0403	4.0686	4.0397	-0.5284
102	0.0370	2.0287	2.0969	-0.4603
108	0.0324	0.5351	0.6445	-0.3963
114	0.0271	-0.3952	-0.2882	-0.3435
120	0.0217	-0.8638	-0.7794	-0.3039
126	0.0167	-1.0011	-0.9425	-0.2763
132	0.0126	-0.9225	-0.8742	-0.2593
138	0.0092	-0.8627	-0.8099	-0.2519
144	0.0060	-1.1146	-1.0690	-0.2494
150	0.0030	-1.6912	-1.6603	-0.2446
156	0.0004	-2.3021	-2.2816	-0.2314
162	-0.0012	-2.5621	-2.5515	-0.2079
168	-0.0018	-2.2235	-2.2232	-0.1789
174	-0.0012	-1.2971	-1.3009	-0.1546
180	0	0	0	-0.1450

KEY FOR FIGURES C.28 to C.43

N_{Re}	2.56				30.0				100.0				300.0			
Fig. Sym.	C.28	C.29	C.30	C.31	C.32	C.33	C.34	C.35	C.36	C.37	C.38	C.39	C.40	C.41	C.42	C.43
A	0.01	0.001	0.0001	0.0001	0.0	0.001	0.0001	0.0001	-0.008	-0.2	0.0001	-0.003	-0.035	-0.8	0.0	-0.015
B	0.1	0.01	0.0003	0.001	0.01	0.01	0.00025	0.0003	-0.005	-0.1	0.0003	-0.001	-0.02	-0.6	0.0001	-0.01
C	0.5	0.03	0.0007	0.01	0.1	0.03	0.0004	0.0005	-0.001	0.0	0.0007	-0.0002	-0.005	-0.4	0.0002	-0.005
D	1.0	0.05	0.001	0.05	0.5	0.05	0.00055	0.0007	0.0	0.01	0.001	0.0001	0.0	-0.2	0.0005	-0.001
E	2.0	0.1	0.005	0.1	1.0	0.1	0.0007	0.001	0.001	0.1	0.003	0.0006	0.002	0.0	0.001	-0.0001
F	3.0	0.2	0.01	0.3	2.0	0.2	0.00085	0.003	0.01	0.25	0.007	0.001	0.01	0.01	0.0015	0.0001
G	4.5	0.3	0.02	0.6	3.0	0.3	0.001	0.005	0.1	0.5	0.01	0.002	0.05	0.1	0.002	0.001
H	6.0	0.5	0.03	0.9	4.5	0.5	0.00115	0.007	0.5	1.0	0.013	0.006	0.1	0.5	0.0025	0.01
I	10.0	0.8	0.04	1.2	6.0	0.8	0.0013	0.01	1.0	2.0	0.017	0.01	0.5	1.0	0.003	0.05
J	15.0	1.5	0.05	1.5	10.0	1.5	0.00145	0.02	1.5	3.0	0.02	0.04	1.0	2.0	0.0035	0.1
K	-	-	0.06	1.8	15.0	2.0	0.0016	0.04	2.0	4.0	0.025	0.08	2.0	3.0	0.004	0.15
L	-	-	0.065	2.1	20.0	2.5	0.00175	0.06	2.5	5.0	0.030	0.12	-	5.0	0.0045	0.2
M	-	-	0.07	2.4	-	3.0	0.0019	0.08	3.0	6.0	0.035	0.16	-	8.0	0.0049	0.25
N	-	-	-	2.7	-	3.5	0.0020	0.1	-	7.0	0.038	0.20	-	11.0	-	0.3

FIGURE C.28 STREAM FUNCTION CONTOURS OUTSIDE DROP AT N_{Re} = 2.56

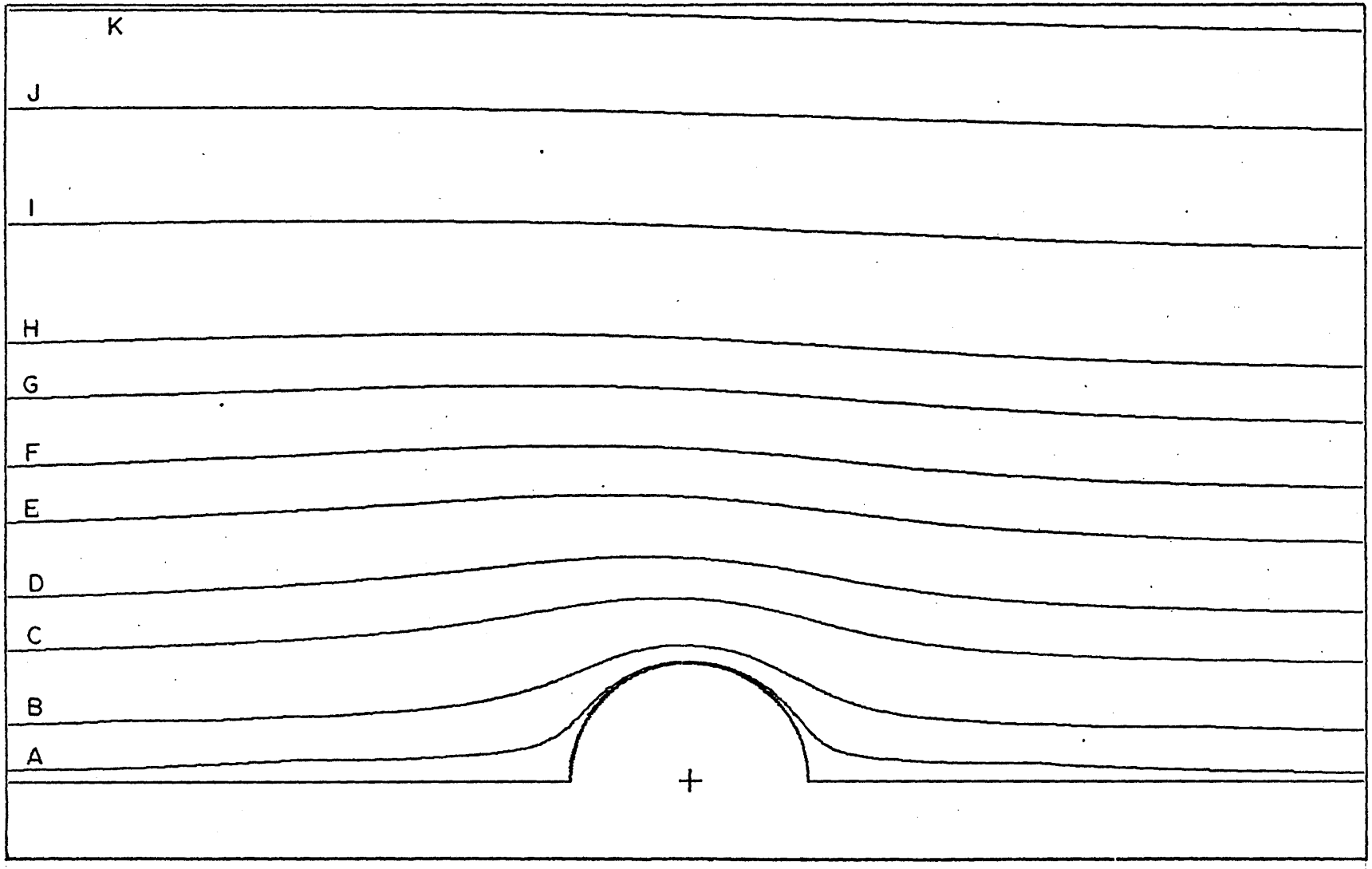

FIGURE C.29 VORTICITY CONTOURS OUTSIDE DROP AT N_{Re} = 2.56

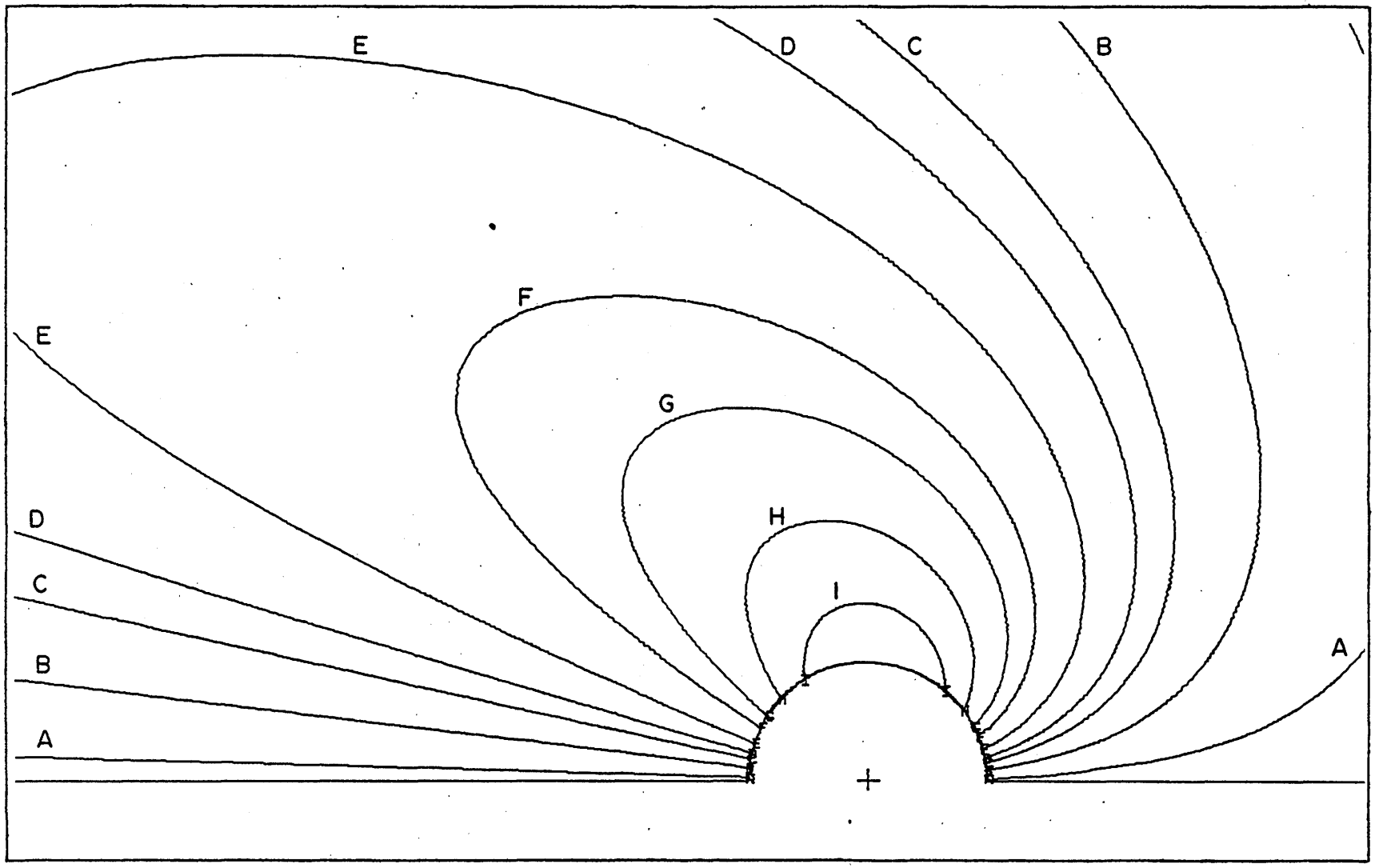

FIGURE C.30 STREAM FUNCTION CONTOURS INSIDE DROP AT $N_{Re} = 2.56$

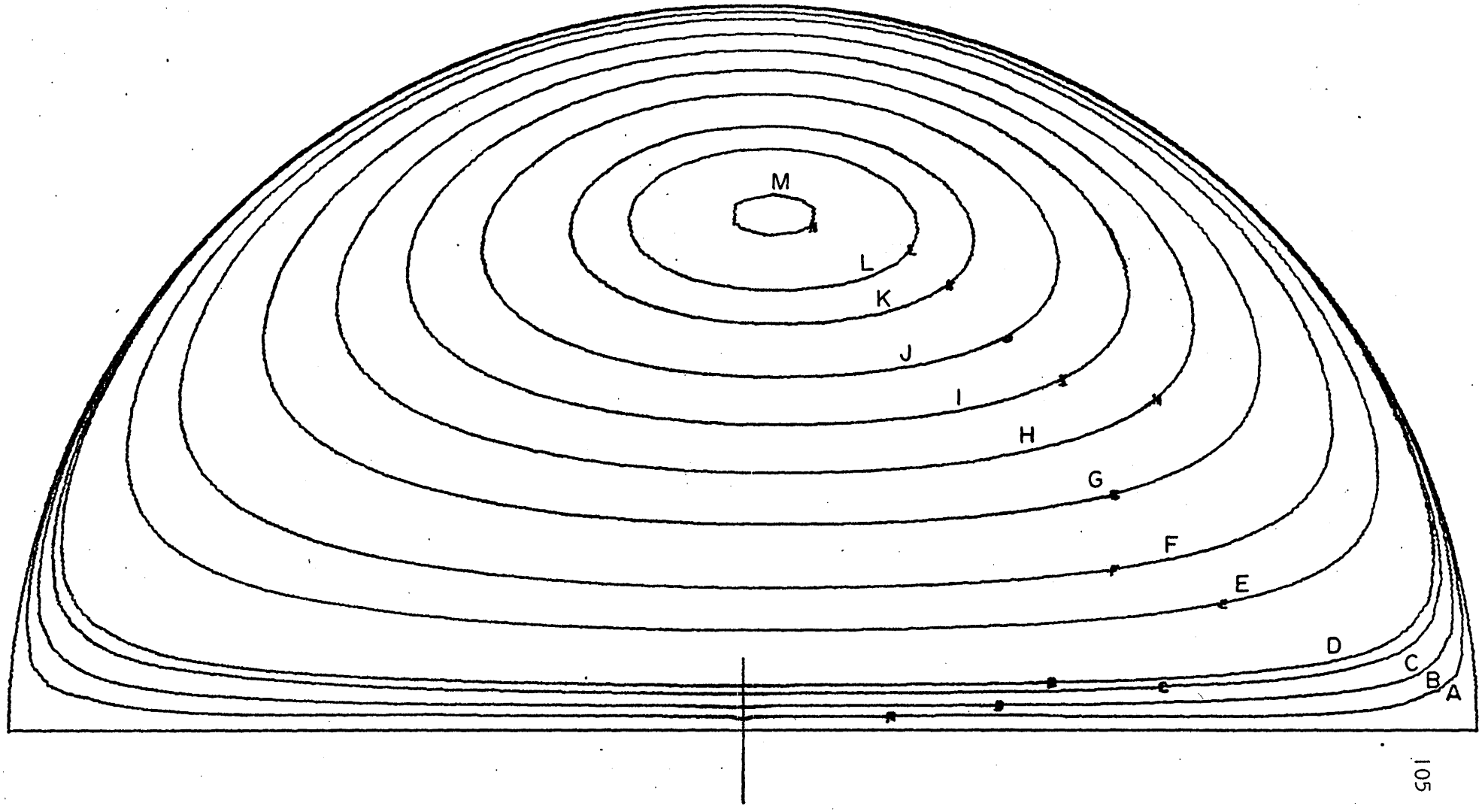

FIGURE C.31 VORTICITY CONTOURS INSIDE DROP AT N_{Re} = 2.56

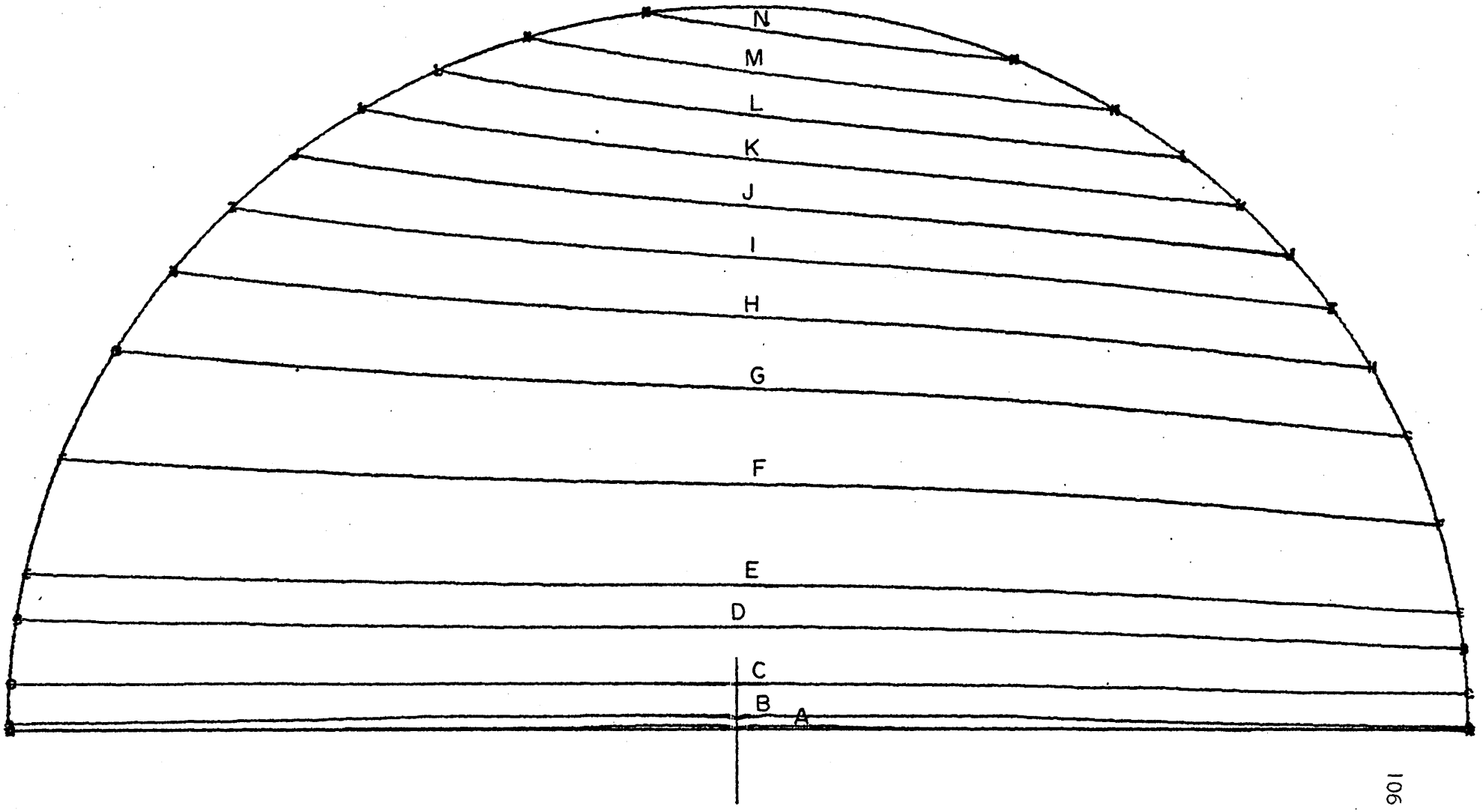

FIGURE C.32 STREAM FUNCTION CONTOURS OUTSIDE RAINDROP AT N_{Re} = 30

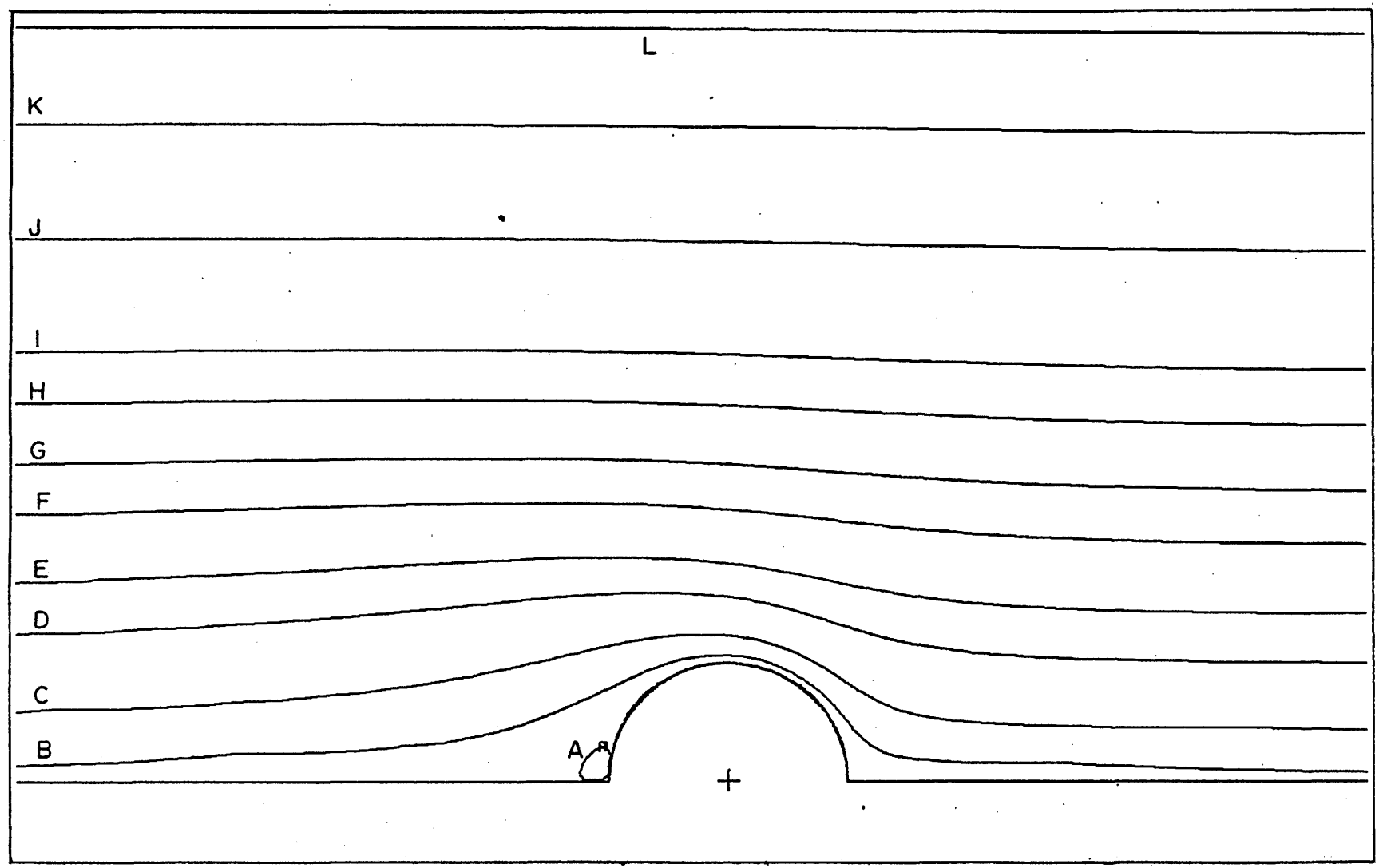

FIGURE C.33 VORTICITY CONTOURS OUTSIDE RAINDROP AT N_{Re} = 30

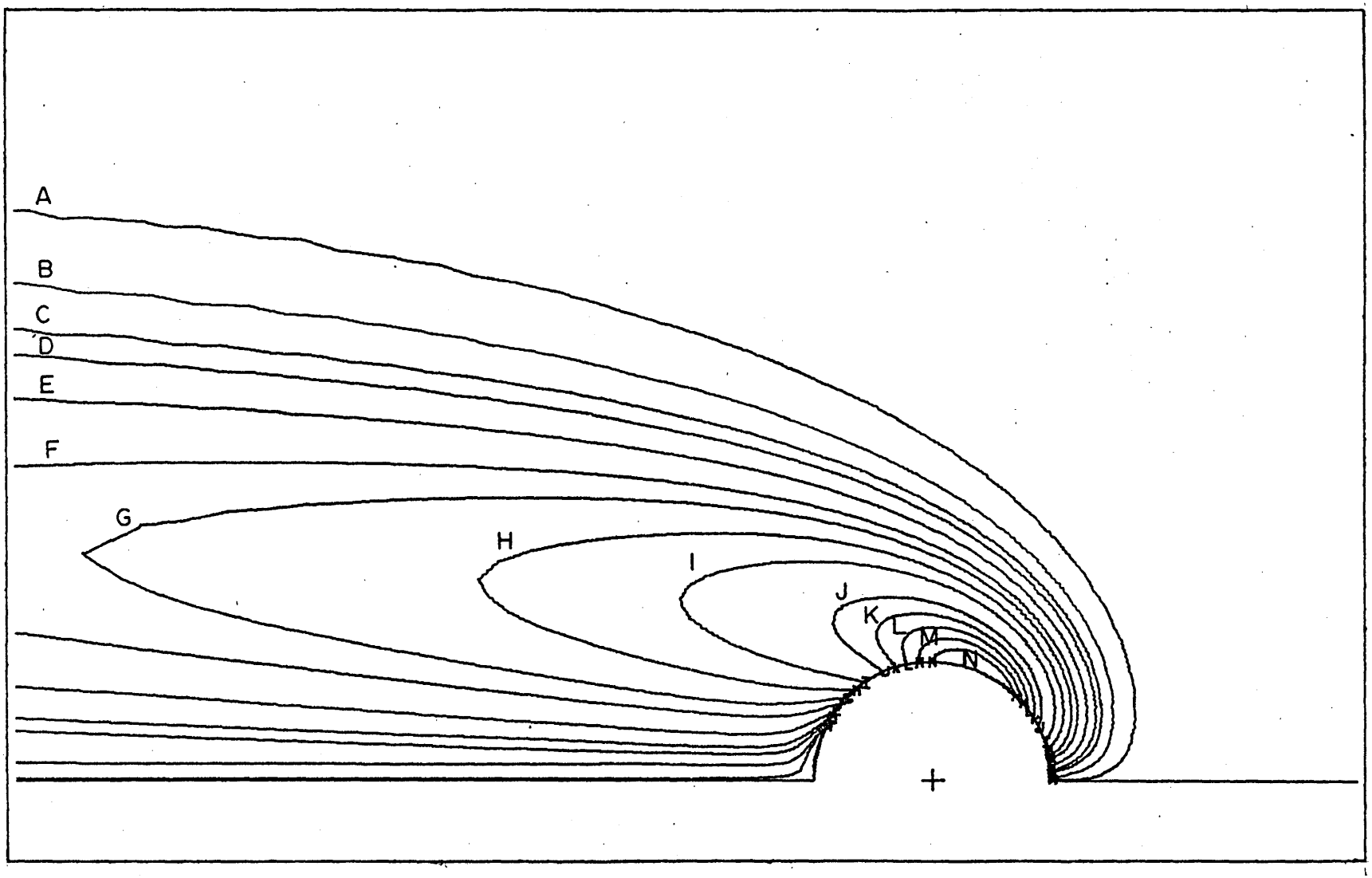

FIGURE C.34 STREAM FUNCTION CONTOURS INSIDE RAINDROP AT N_{Re} = 30

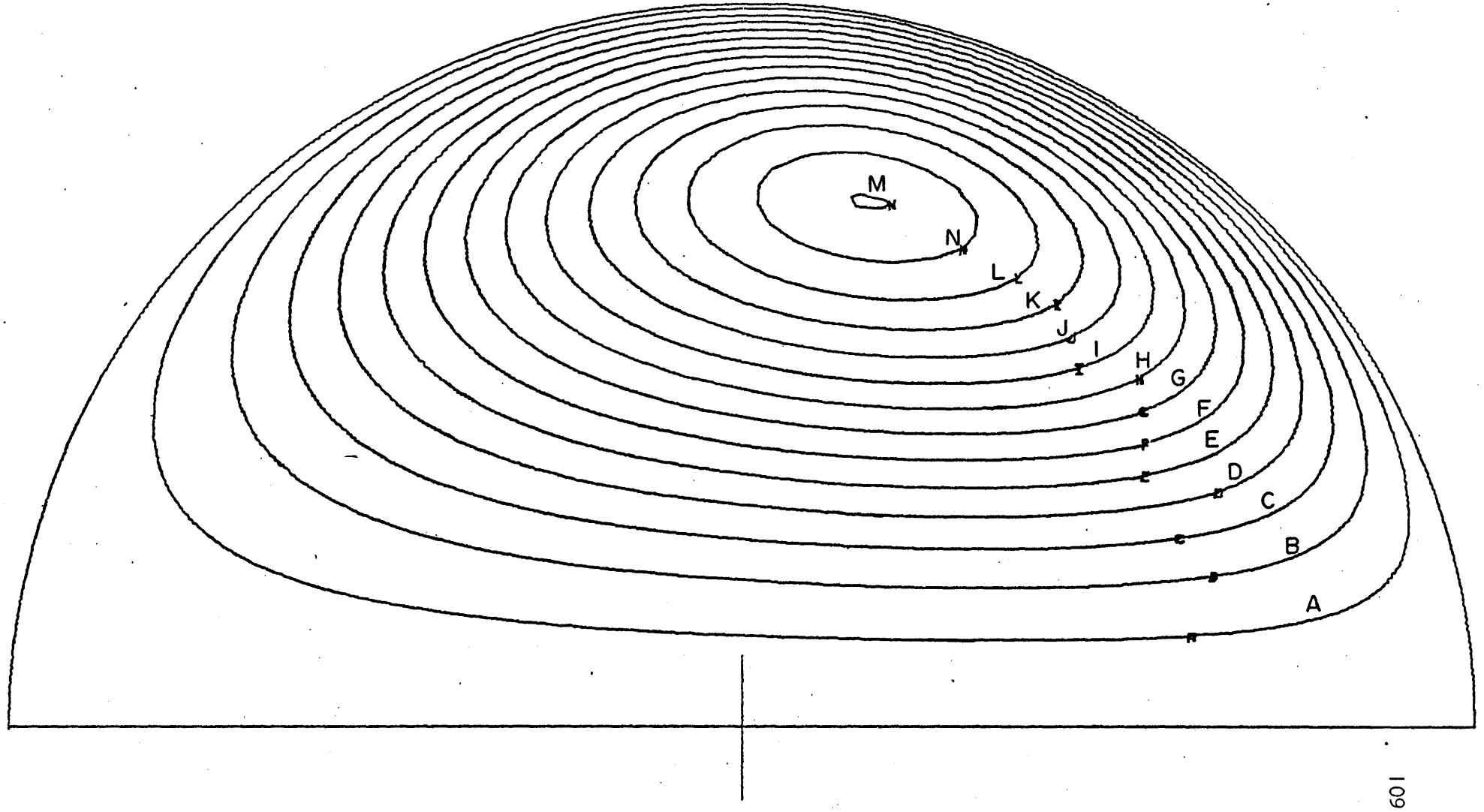

FIGURE C.35 VORTICITY CONTOURS INSIDE RAINDROP AT $N_{Re} = 30$

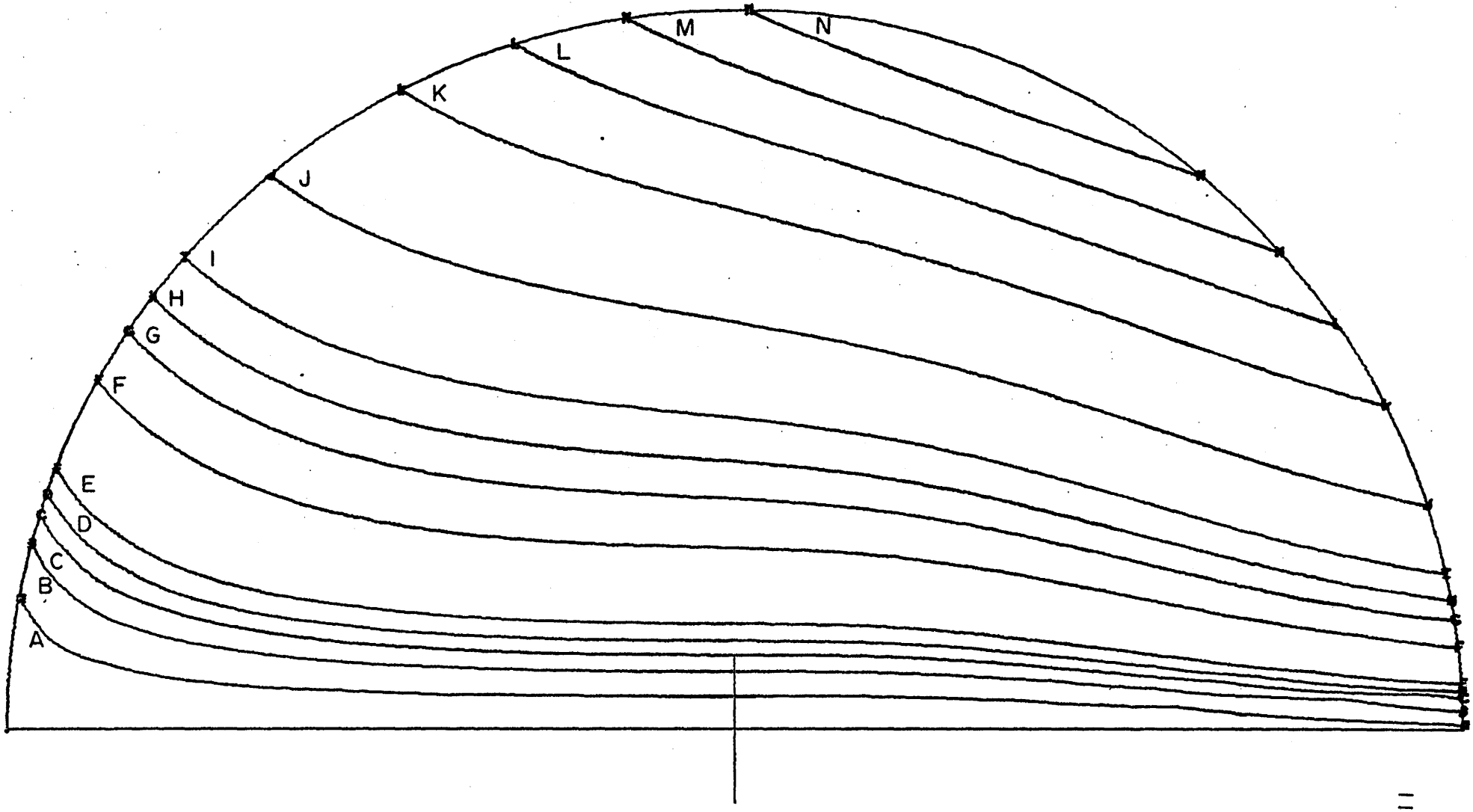

FIGURE C.36 STREAM FUNCTION CONTOURS OUTSIDE RAINDROP AT N_{Re} = 100

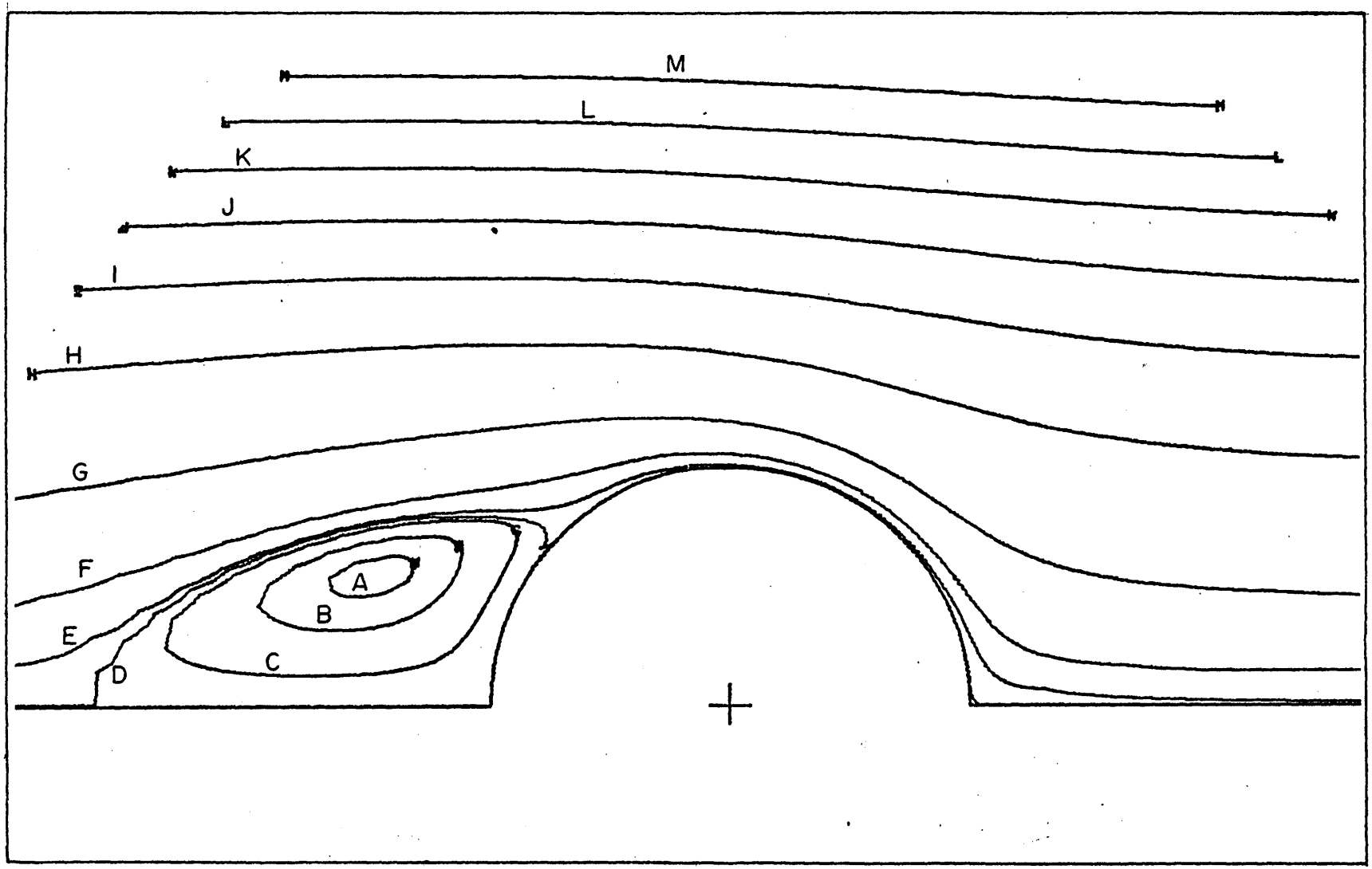

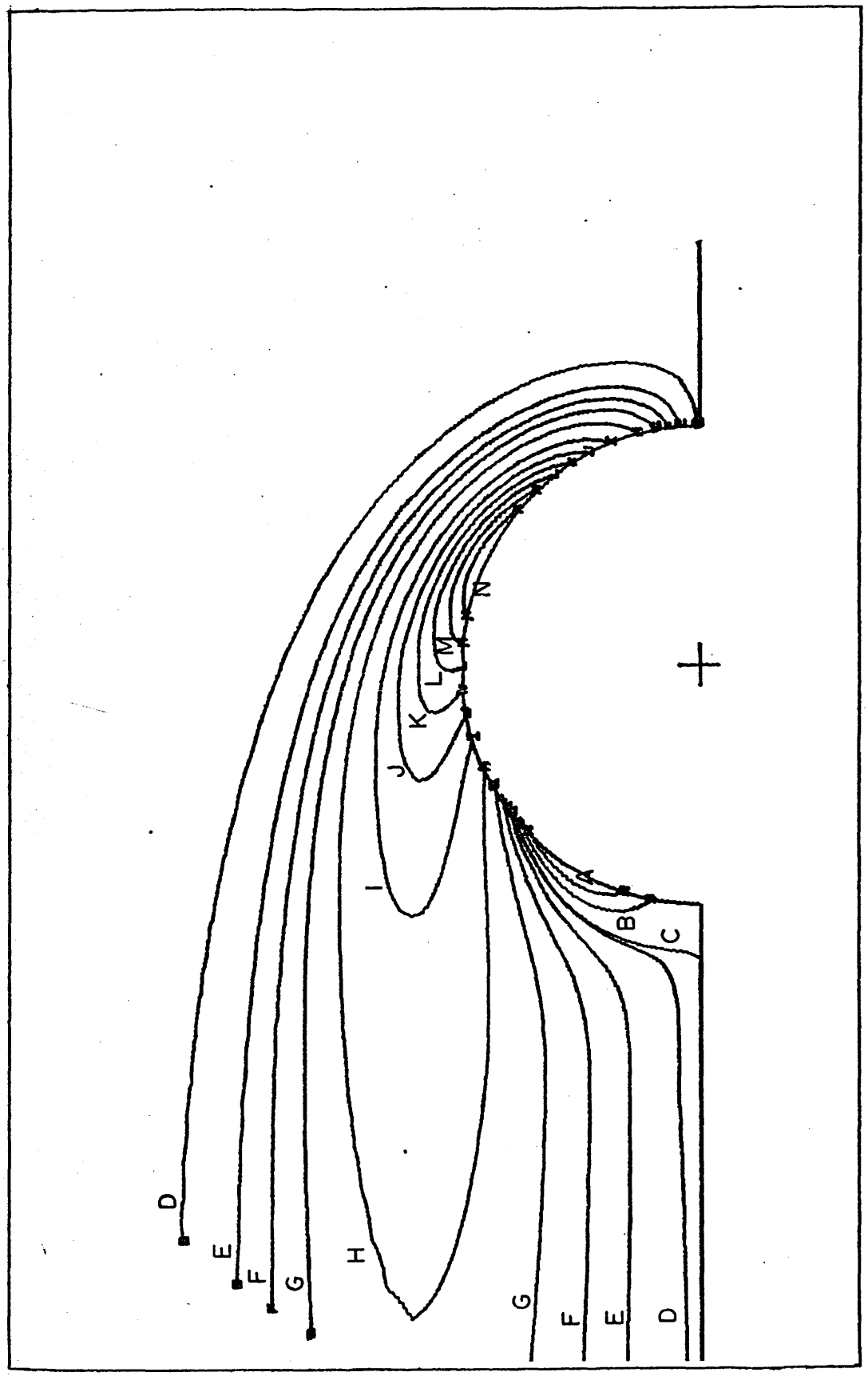

FIGURE C.37 VORTICITY CONTOURS OUTSIDE RAINDROP AT N_{Re} = 100

FIGURE C.38 STREAM FUNCTION CONTOURS INSIDE RAINDROP AT N_{Re} = 100

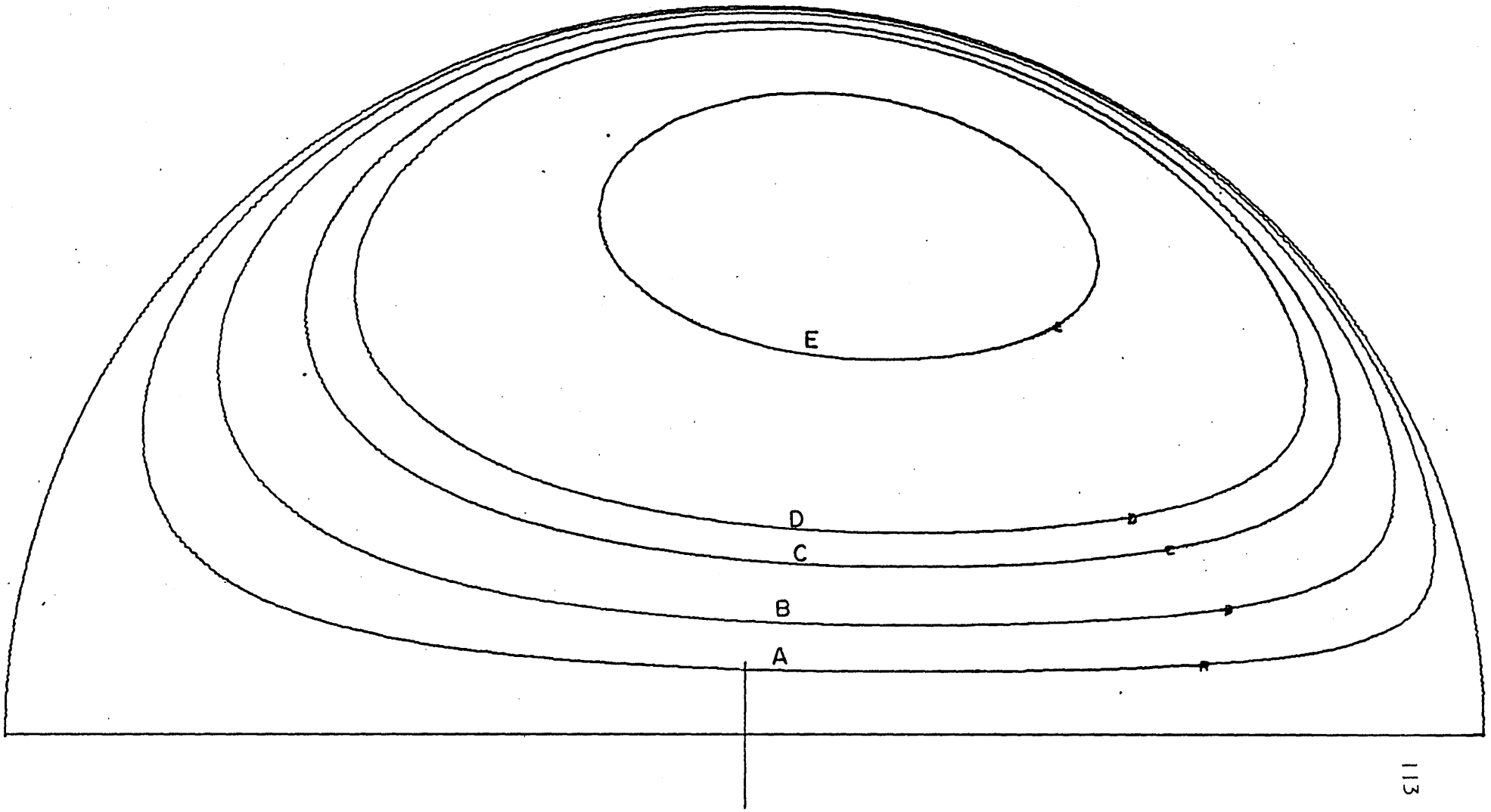

FIGURE C.39 VORTICITY CONTOURS INSIDE RAINDROP AT N_{Re} = 100

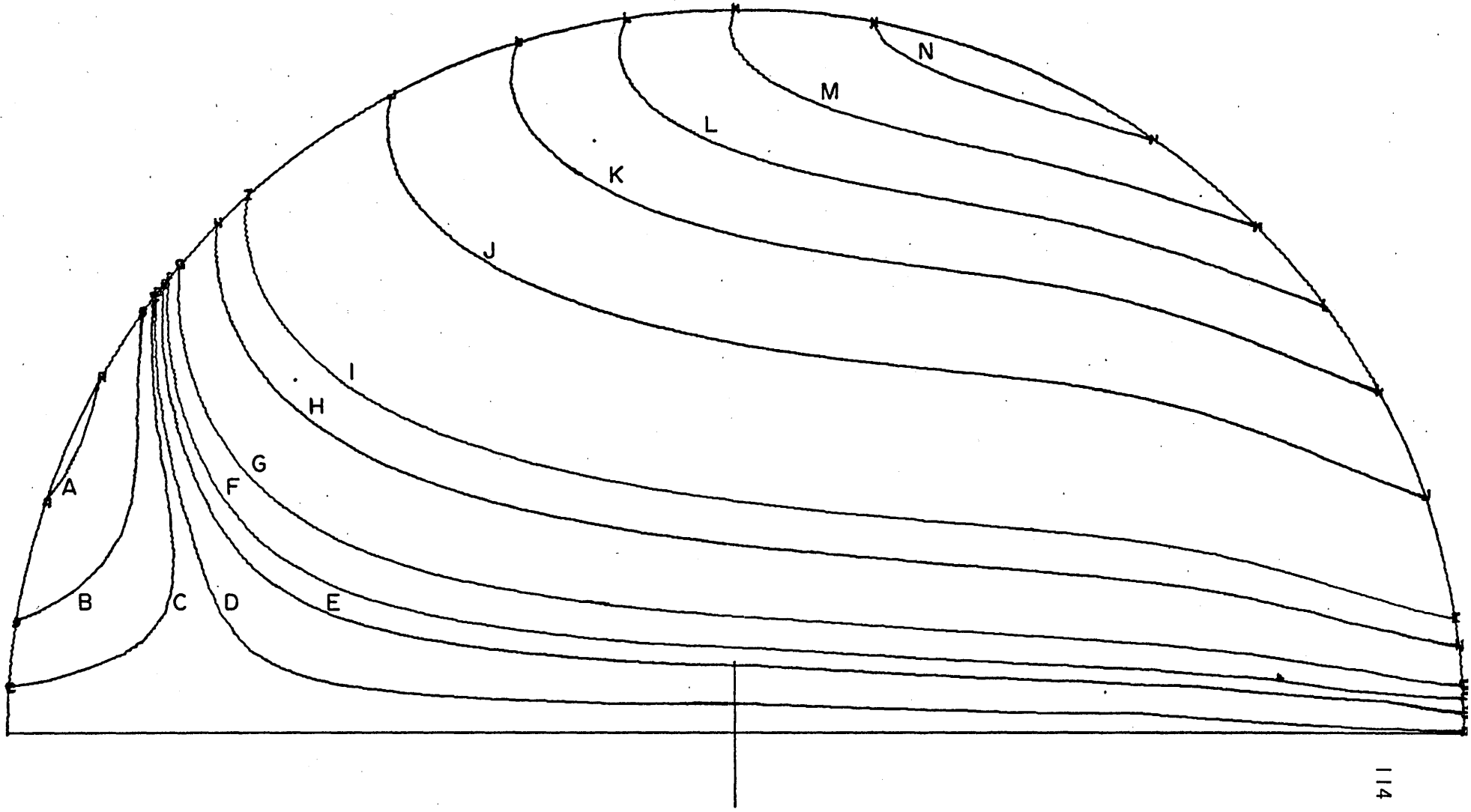

FIGURE C.40 STREAM FUNCTION CONTOURS OUTSIDE RAINDROP AT N_{Re} = 300

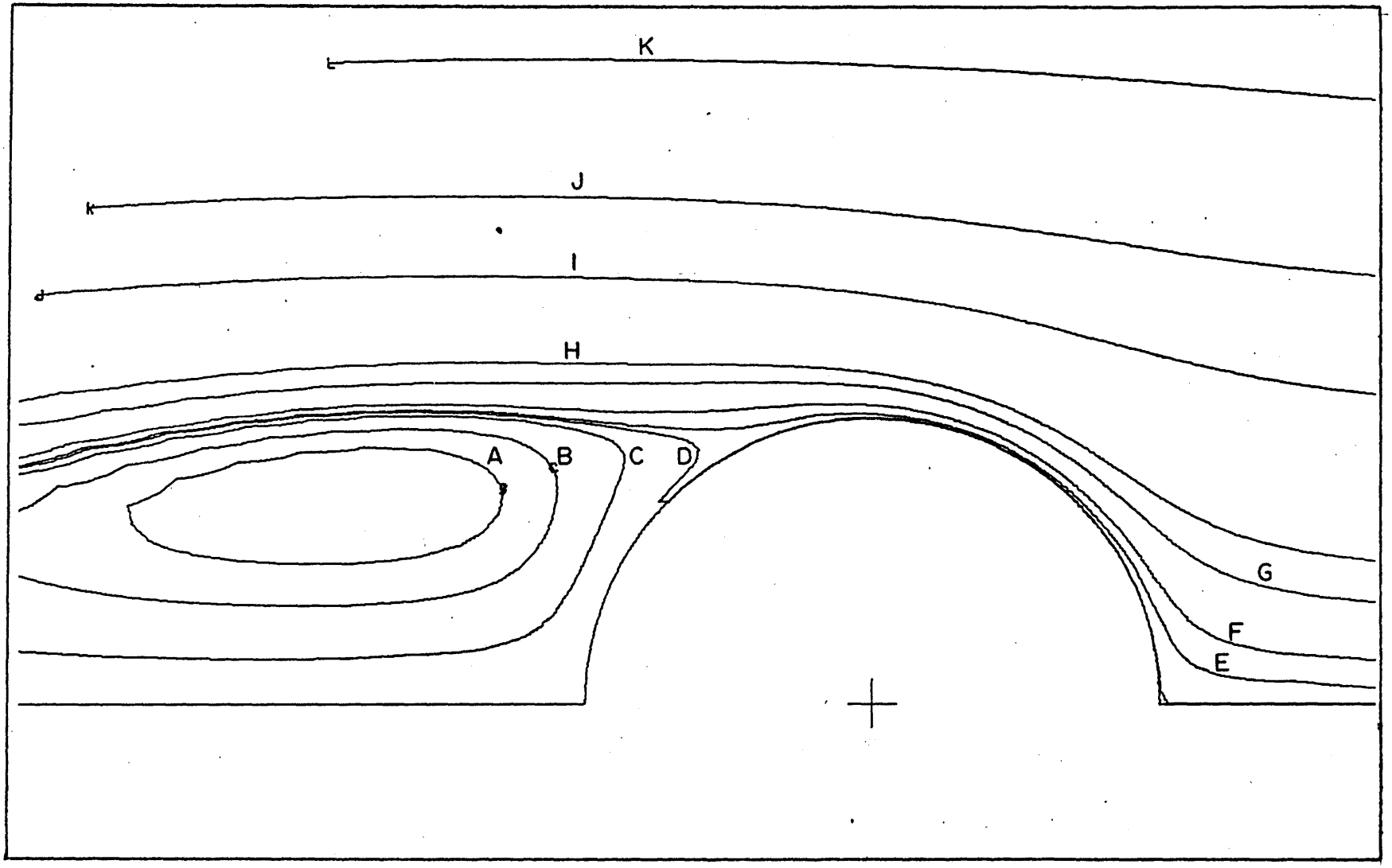

FIGURE C.41 VORTICITY CONTOURS OUTSIDE RAINDROP AT N_{Re} = 300

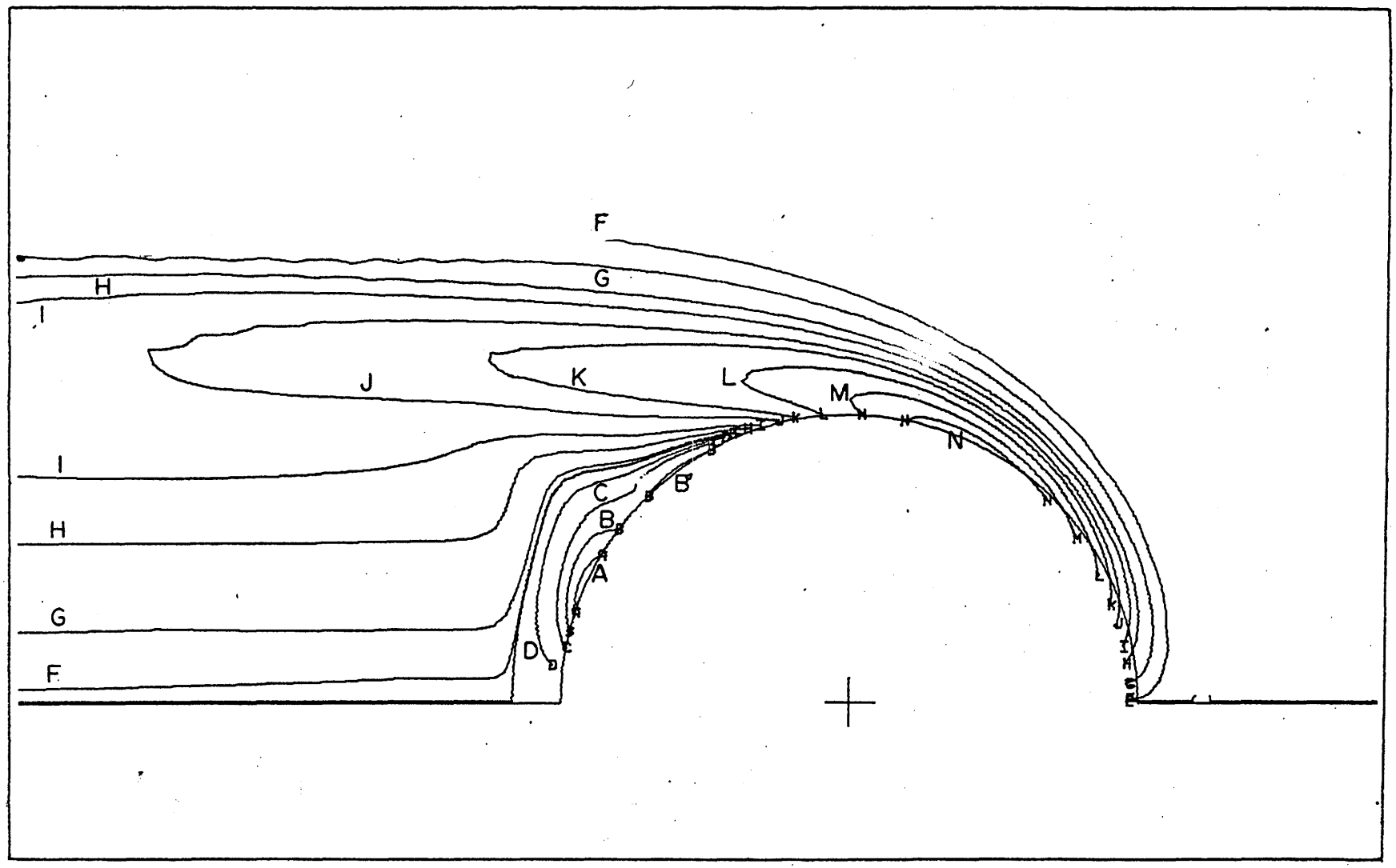

FIGURE C.42 STREAM FUNCTION CONTOURS INSIDE RAINDROP AT N_{Re} = 300

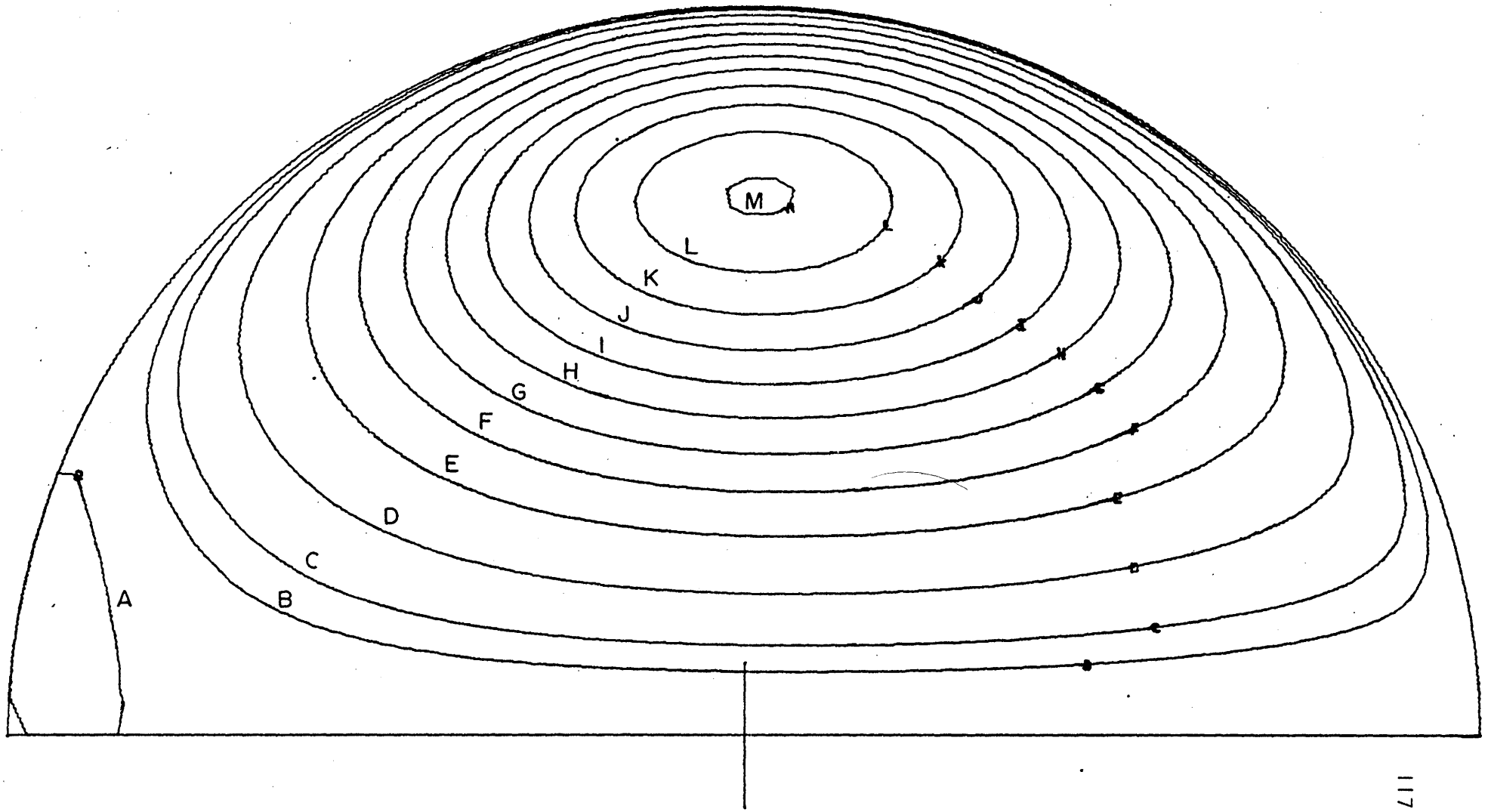

FIGURE C.43 VORTICITY CONTOURS INSIDE RAINDROP AT N_{Re} = 300

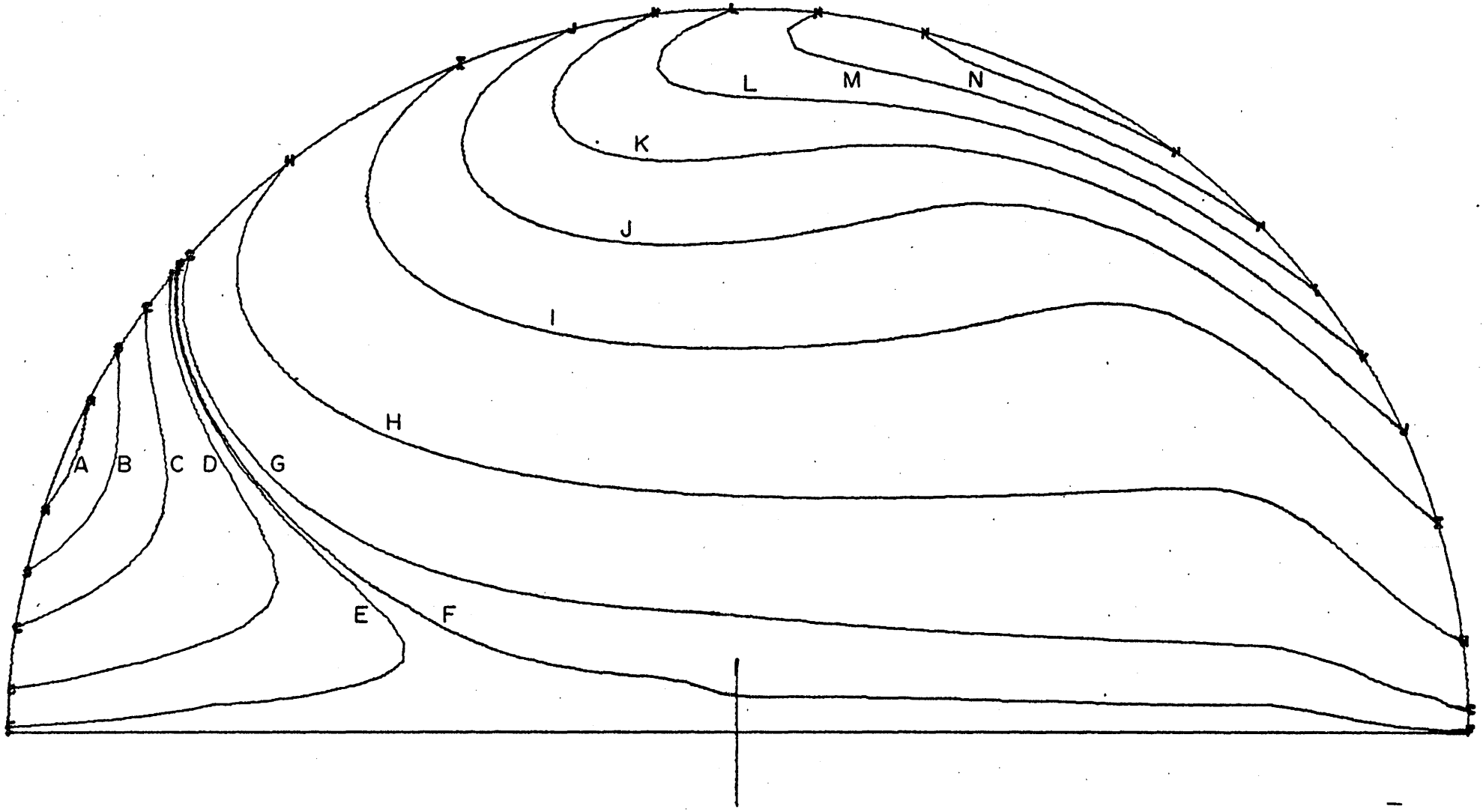

D. Summary and Conclusions

This work has dealt with several fluid mechanical phenomena in intermediate Reynolds number flow. The single most important result of the work has been the realization that most phenomena of fluid motion may be determined more accurately and easily by numerical solution of the theoretical equations than by experiment. In fact, it may be said that all phenomena in the Newtonian laminar flow regime are theoretically predictable and thus there is no need for experimental work. However, the same may not be said for multiparticle phenomena. In this area one still has difficulty in formulation of the equations and extreme difficulty in solving the systems of equations which have been formulated.

The work was concerned with three areas, steady state intermediate Reynolds number flow around spheres, flow around an accelerating sphere in intermediate Reynolds number flow and flow in and around spherical circulating droplets at high intermediate Reynolds numbers. The results confirm the ability to predict numerically fluid mechanical phenomena.

E. Recommendations for Further Work

In the area of transient flows, knowledge is required about the acceleration from rest under gravity of gas bubbles and liquid drops. The study of gas bubble transient flow is the most important as it yields a situation where the added mass effect is very pronounced. A knowledge of transient flow from rest is also important for liquid drops. Simultaneous solution with the convection equation will provide information about the fraction of the total mass transfer which occurs during drop acceleration. With this information, one will be able to make a better estimate of the mass transfer occurring during drop formation. Another important area of concern in transient single particle flows are those situations where the bulk fluid also accelerates, for example, levitation of solid particles in oscillating or pulsed flows.

The most important area for further studies is multiparticle systems. Probably the most important problem is the two sphere problem. Although many papers have appeared on the two-sphere interaction problem, they are of little practical value because the inertia and transient terms have been dropped from the equations of motion. In fact, these solutions have led to theories for multiparticle systems which are fundamentally wrong and contradicted by experimental evidence. A case in point , is the situation of two equal spheres falling along their line of centers. Limiting solutions, using the Stokes stream function, predict the velocity of fall will be the same for both particles. A result which has been shown to be wrong by experiment.

Other important problems require the solution of the equations of motion in three dimensions as well as time. These will have to wait until larger and faster computers and improved numerical techniques are available.

In the field of deformable circulating droplets there is need for further study. The effect of two interacting phenomena, deformation and surface active material accumulation, on circulation must be studied. These phenomena in their affect on the hydrodynamics will have a pronounced effect on mass transfer and mass transfer with chemical reaction to and from liquid drops.

F. Contributions to Knowledge

In this dissertation several contributions to knowledge are claimed. The first is concerned with the drag on a sphere at low Reynolds numbers. Numerical solutions have shown that the drag on a solid sphere is asymptotic with the Oseen drag formulation as the Reynolds number approaches zero. For Reynolds numbers of 0.01 and less the Oseen drag is exact, while Stokes' drag is only exact at a Reynolds number of zero.

The second contribution was the formulation and solution of the flow around a sphere accelerating from rest under the influence of gravity. The work provides the first solutions of the complete Navier Stokes equations for accelerating spheres in the intermediate Reynolds number range.

The final contribution was the formulation and solution of the flow in and around a fluid sphere in the intermediate Reynolds number range. The special case of spherical raindrops was studied. Several learned papers written on this work are listed below:

LeClair, B.P., Hamielec, A.E., and Pruppacher, H.R.,
"A Numerical Study of the Drag on a Sphere at Low and Intermediate Reynolds Numbers",
J. Atmos. Sci., 27, 308 (1970).

Pruppacher, H.R., LeClair, B.P., and Hamielec, A.E.,
"Some Relations Between Drag and Flow Pattern of Viscous Flow Past a Sphere and a Cylinder at Low and Intermediate Reynolds Numbers", in press Journal of Fluid Mechanics.

LeClair, B.P., and Hamielec, A.E.,
"Flow Behaviour Around a Sphere Accelerating in a Viscous Fluid", accepted for the Fluid Dynamics Symposium, McMaster University, August 1970.

LeClair, B.P., Hamielec, A.E., and Pruppacher, H.R.,
"Flow In and Around Spherical Raindrops in the Intermediate Reynolds Number Regime".

G. Nomenclature

$A, B, C, D, A', B', C', D'$ - coefficients in Stokes' stream function

a - sphere radius

b - carried mass (Lunnon, 1926)

B - Bond Number

C_D - total drag coefficient

C_{DA} - modified drag coefficient (Torobin and Gauvin, 1959)

C_{Df} - final steady state drag coefficient

C_H - history coefficient (Odar and Hamilton, 1964)

C_V - added mass coefficient (Odar and Hamilton, 1964)

D - drag on a sphere

D_s - Stokes drag on a sphere

e - surface viscosity coefficient

F - force on sphere

g - acceleration of gravity

K - viscosity ratio, μ_i/μ_o

N_{Ac} - acceleration number

N_{Re} - Reynolds number

N_{Re_f} - final steady state Reynolds number

P - pressure

P_o - frontal stagnation pressure

P_∞ - pressure at infinity

r - radial position vector

r_∞ - radial position approximating infinity

T - dimensionless time, $\mu t/4\rho_s a^2$

t - time

U, V, v - velocity

U_∞, V_∞ - velocity at infinity

V_p, v_p - particle velocity

z - dimensionless radial position vector

ε - coefficient of surface shear viscosity

ξ - vorticity

θ - angular position vector

k - coefficient of surface dilational viscosity

μ, μ_i, μ_o - dispersed and continuous phase viscosities

$\rho, \rho_s, \rho_i, \rho_o$ - solid, dispersed and continuous phase viscosities

σ - surface tension

τ - fluid shear stress

ϕ - angular position vector

ψ - stream function

H. References

Ames, W.F.,
Nonlinear Partial Differential Equations in Engineering,
Academic Press, 1965.

Basset, A.B.,
Phil. Trans. (London), 17, 43 (1888).

Basset, A.B.,
Quart. J. Math., 41, 369 (1910).

Batchelor, G.K.,
An Introduction to Fluid Mechanics,
Cambridge University Press, 1969.

Beard, K.V., and Pruppacher, H.R.,
J. Atmos. Sci., 26, 1066 (1969).

Birkhoff, G.,
Hydrodynamics A Study in Logic, Fact and Similitude,
Princeton University Press, 1960.

Bond, W.N., and Newton, D.A.,
Phil. Mag., 5, 794 (1928).

Boussinesq, J.,
Compt. Rend. Acad. Sci., 156, 1124 (1913).

Bradbury, T.C.,
Theoretical Mechanics,
John Wiley & Sons, 1968.

Brush, L.M., Ho, H.W., and Yen, B.C.,
J. Hydraulics Div. ASCE, 90, 149 (1964).

Carrier, G.F.,
Office of Naval Research, rept. N-our-653-00/1, 1953.

Chester, W.,
Office of Naval Research, rept. As-68-8, N-our-222(79), 1968.

Chester, W., and Breach, D.R.,
J. Fluid Mech., 37, 751 (1969).

DuBuat,
Principles d'Hydraulique, p.221, Paris (1776).

Feinman, J.,
PhD Dissertation, University of Pittsburgh, 1964.

Fidleris, V., and Whitmore, R.L.,
Brit. J. Appl. Phys., 12, 490 (1961).

Fox, L.,
Numerical Solution of Ordinary and Partial Differential Equations,
Addison-Wesley, 1962.

Fromm, J.E.,
Los Alamos Scientific Laboratory, LA-2910 (1963).

Fromm, J.E., and Harlow, F.H.,
Phys. Fluids, 6, 975 (1963).

Garner, F.H., and Grafton, R.W.,
Proc. Roy. Soc., A224, 70 (1954).

Goldburg, A., and Florsheim, B.H.,
Phys. Fluids, 9, 45 (1966).

Goldstein, S.,
Proc. Roy. Soc., A213, 216 (1929).

Goodbody, A.M., and Rhodes, P.C.,
Research Paper 79, University of Calgary, 1969.

Hadamard, J.S.,
Compt. Rend. Acad. Sci., 152, 1735 (1911).

Hamielec, A.E., and Johnson, A.I.,
Can. J. Chem. Eng., 40, 41 (1962).

Hamielec, A.E., Hoffman, T.W., and Ross, L.L.,
AIChEJ, 13, 212 (1967).

Hamielec, A.E., Johnson, A.I., and Houghton, W.T.,
AIChEJ, 13, 220 (1967).

Hamielec, A.E., and Raal, J.D.,
Phys. Fluids, 12, 11 (1969).

Hjelmfelt, A.T., and Mockros, L.F.,
J. Eng. Mech. Div. ASCE, 93, 87 (1967).

Holt, H.,
Basic Developments in Fluid Mechanics,
Academic Press, 1968.

Hughes, R.R., and Gilliland, E.R.,
Chem. Eng. Progr., 48, 497 (1952).

Jenson, V.G.,
Proc. Roy. Soc., 249A, 346 (1959).

Lax, P.D., and Richtmeyer, R.D.,
Comm. Pure Appl. Math., 9, 267 (1956).

Lunnon, R.G.,
Proc. Roy. Soc., 110A, 302 (1926).

Lunnon, R.G.,
Proc. Roy. Soc., 118A, 680 (1928).

Masliyah, J.H.,
PhD Thesis, University of British Columbia, Vancouver, 1970.

Maxworthy, T.,
J. Fluid Mech., 23, 369 (1965).

Mollier, W.,
Phys. Z., 39, 57 (1938).

Moorman, R.B.,
PhD Dissertation, State University of Iowa, Iowa, 1955.

Nisi, H., and Porter, A.W.,
Phil. Mag, ser. B, 754 (1923).

Odar, F., and Hamilton, W.S.,
J. Fluid Mech., 18, 302 (1964).

Odar, F.,
USA Cold Regions Research and Engineering Laboratory Report 190, 1965.

Odar, F.,
J. Fluid Mech., 25, 591 (1966).

Oseen, C.W.,
Arkiv. Mat. Astron. Fys., 6, 1 (1910).

Oseen, C.W.,
Hydrodynamik, Akad. Verlagsgesellschaft, Leipzig, 1927.

Peaceman, D.W., and Rachford, H.H.,
J. SIAM, 3, 28 (1955).

Pearson, C.E.,
J. Fluid Mech., 21, 611 (1965).

Perry, J.,
Chem. Eng. Handbook, 3rd. Ed., McGraw-Hill, N.Y., 1950.

Proudman, I., and Pearson, J.R.A.,
J. Fluid Mech., 2, 237 (1957).

Pruppacher, H.R., and Beard, K.V.,
Quart. J. Roy. Meteorol. Soc., 96, 247 (1970).

Pruppacher, H.R., and Steinberger, E.H.,
J. Appl. Phys., 39, 4129 (1968).

Pruppacher, H.R., Steinberger, E.H., Neiburger, M.,
J. Fluid Mech., 34, 809 (1968).

Rhodes, J.M.,
PhD Thesis, University of Tennessee, 1967.

Rimon, Y., and Cheng, S.I.,
Phys. Fluids, 12, 949 (1969).

Rybczinski, W.,
Bull. Acad. Sci., Cracovie, ser. A, 40 (1911).

Savic, P.,
National Research Council of Canada, rept. MT-22, 1953.

Scriven, L.E.,
Chem. Eng. Sci., 12, 98 (1960).

Son, J.S.,
PhD Thesis, University of Illinois, Urbana, 1968.

Steinberger, E.H., Pruppacher, H.R., and Neiburger, M.,
J. Fluid Mech., 36, 809 (1968).

Stimson, M., and Jeffery, G.B.,
Proc. Roy. Soc., A111, 110 (1926).

Stokes, G.G.,
Trans. Cambridge Phil. Soc., 9, 8 (1851).

Sy, F., Taunton, J.W., and Lightfoot, E.N.,
AIChEJ, 16, 386 (1970)

Taneda, S.,
Repts. Res. Inst. f. Appl. Math., 6, No. 16, 99 (1956).

Thoman, D.C., and Szewczyk, A.A.,
University of Notre Dame Report 66-14 (1966).

Torobin, L.B., and Gauvin, W.H.,
Can. J. Chem. Eng., 37, 224 (1959).

Tyroler, G.P., Johnson, A.I., and Hamielec, A.E.,
19th Chem. Eng. Conf., Edmonton, Alberta, October 1969.

Van Dyke, M.,
Perturbation Methods in Fluid Mechanics,
Academic Press, 1964.

Whitaker, S.,
Introduction to Fluid Mechanics,
Prentice-Hall, 1968.

APPENDIX I-A

COMPUTATIONAL DETAILS

COMPUTER PROGRAM FOR CALCULATING THE FLOW AROUND A SOLID SPHERE

```
      PROGRAM SPHERE(INPUT,OUTPUT,PUNCHB,TAPE5=INPUT,TAPE6=OUTPUT,
     1TAPE7=PUNCHB,TAPE8,TAPE1)
      DIMENSION Z(272),EZ1(272),EZ2(272),EZ3(272),EZ4(272),EZ5(272)
      DIMENSION EZ6(272),THETA(62),SI(62),CO(62),COT(62),ANGLE(62)
      DIMENSION PSI(62,272),G(62,272)
      DIMENSION P(62),SVORT(62)
      DIMENSION VR(272)
      READ (5,10) RE,A1,B1
      READ (5,11) WS,WV
      READ (5,13) EPSS,EPSV
      READ (5,12) M,N
      READ (5,14) RSSIZE
      READ(5,12) NLOOPS
      READ(5,12) NSTART
      READ(5,12) NLOOP1
      WRITE (6,19)
      WRITE (6,20) RE
      WRITE (6,21) M,N,RSSIZE
      WRITE (6,23) WS,WV
      MP1=M+1
      NM1=N-1
      A=RSSIZE
      B=3.1416/(FLOAT(M))
      Z(1)=0.0
      THETA(1)=0.0
      THETA(2)=B
      DO 100 I=2,M
      THETA(I+1)=THETA(I)+B
      CO(I)=COS(THETA(I))
      SI(I)=SIN(THETA(I))
  100 COT(I)=CO(I)/SI(I)
      DO 110 J=1,N
      Z(J+1)=Z(J)+A
      EZ1(J)=EXP(Z(J))
      EZ2(J)=EZ1(J)**2
      EZ3(J)=EZ1(J)**3
      EZ4(J)=EZ1(J)**4
      EZ5(J)=EZ1(J)**5
  110 EZ6(J)=EZ1(J)**6
      DO 120 I=1,MP1
      THETA(I+1)=THETA(I)+B
  120 ANGLE(I)=THETA(I)*180.0/3.1416
      DUM1=(2.0-A)/2.0*B*B
      DUM2=(2.0+A)/2.0*B*B
      DUM5=A*A*B*B
      DUM6=1.0/(2.0*(A*A+B*B))
      SI(1)=0.0
      SI(MP1)=0.0
      CO(1)=1.0
      CO(MP1)=-1.0
      IF(NSTART.EQ.1) GO TO 1000
      A2=-(120.+75.*A1)/29.
      A3=(153.+63.*A1)/29.
      A4=-(47.5+17.*A1)/29.
      B2=-69.*B1/27.
      B3=57.*B1/27.
      B4=-15.*B1/27.
      DO 300 I=2,M
      DO 300 J=1,NM1
```

```
      PSI(I,J)=SI(I)*SI(I)*(0.5*EZ2(J)+A1/EZ1(J)+A2/EZ2(J)+A3/EZ3(J)+A4      0600
     1/EZ4(J)-CO(I)*(B1/EZ1(J)+B2/EZ2(J)+B3/EZ3(J)+B4/EZ4(J)))               0610
      G(I,J)=SI(I)*SI(I)*((4.*A2/EZ4(J)+10.*A3/EZ5(J)+18.*A4/EZ6(J))         0620
  900 1+CO(I)*(4.*B1/EZ3(J)-6.*B3/EZ5(J)-14.*B4/EZ6(J)))                     0630
      DO 400 I=1,MP1                                                        0640
      PSI(I,1)=0.0                                                          0650
      G(I,N)=0.0                                                            0660
  400 PSI(I,N)=0.5*EZ2(N)*(SI(I)*SI(I))                                     0670
      DO 410 J=1,N                                                          0680
      PSI(1,J)=0.0                                                          0690
      PSI(MP1,J)=0.0                                                        0700
      G(1,J)=0.0                                                            0710
  410 G(MP1,J)=0.0                                                          0720
      GO TO 1010                                                            0730
 1000 REWIND 8                                                              0740
      READ (8) ((PSI(I,J),I=1,MP1),J=1,N)                                   0750
      IF(EOF,8) 152,150                                                     0760
   50 READ(8)((G(I,J),I=1,MP1),J=1,N)                                       0770
      IF(EOF,8) 152,151                                                     0780
   51 REWIND 8                                                              0790
 1010 JJ=0                                                                  0800
      JJ1=0                                                                 0810
 1100 II=0                                                                  0820
      JJ=JJ+1                                                               0830
      JJ1=JJ1+1                                                             0840
      DO 500 I=2,M                                                          0850
 2100 IP1=I+1                                                               0860
      IM1=I-1                                                               0870
      DUM3 =(2.0-B*COT(I) )*A*A/2.0                                         0880
      DUM4 =(2.0+B*COT(I))*A*A/2.0                                          0890
      G(I,1)=(8.0*PSI(I,2)-PSI(I,3)-7.0*PSI(I,1))/(2.0*A*A)                 0900
      DO 500 J=2,NM1                                                        0910
      JP1=J+1                                                               0920
      JM1=J-1                                                               0930
      DMPSII=(PSI(IP1,J)-PSI(IM1,J))/B                                      0940
      DMPSIJ=(PSI(I,JP1)-PSI(I,JM1))/A                                      0950
      DUMA=G(I,JP1)/(EZ2(JP1)*SI(I)*SI(I))                                  0960
      DUMC=G(I,JM1)/(EZ2(JM1)*SI(I)*SI(I))                                  0970
      IF(I.EQ.2) GO TO 501                                                  0980
      DUMD=G(IM1,J)/(EZ2(J)*SI(IM1)*SI(IM1))                                0990
      GO TO 502                                                             1000
  501 DUMD=G(2,J)/(EZ2(J)*SI(2)*B)                                          1010
  502 IF(I.EQ.M) GO TO 503                                                  1020
      DUMB=G(IP1,J)/(EZ2(J)*SI(IP1)*SI(IP1))                                1030
      GO TO 504                                                             1040
  503 DUMB=G(M,J)/(EZ2(J)*SI(M)*B)                                          1050
  504 STRMF=DUM6*(PSI(I,JP1)*DUM1+PSI(I,JM1)*DUM2+PSI(IP1,J)*DUM3           1060
     1+PSI(IM1,J)*DUM4-DUM5*G(I,J)*EZ2(J))                                  1070
      STRMF=PSI(I,J)+WS*(STRMF-PSI(I,J))                                    1080
      IF(ABS(STRMF-PSI(I,J)).GT.EPSS) II=1                                  1090
      PSI(I,J)=STRMF                                                        1100
      DPSI=DMPSIJ/2.0*(DUMB-DUMD)/B-DMPSII/2.0*(DUMA-DUMC)/A                1110
      VORT=DUM6*(G(I,JP1)*DUM1+G(I,JM1)*DUM2+G(IP1,J)*DUM3+G(IM1,J)*        1120
     1DUM4-RE*(SI(I)*EZ1(J)*DPSI*DUM5/4.0))                                 1130
      VORT=G(I,J)+WV*(VORT-G(I,J))                                          1140
      IF(ABS(VORT-G(I,J)).GT.EPSV) II=1                                     1150
      G(I,J)=VORT                                                           1160
  500 CONTINUE                                                              1170
```

```
      IF(JJ.EQ.NLOOPS) GO TO 2000                                       118
      IF(II.NE.1) GO TO 2000                                            119
      IF(JJ1.LT.NLOOP1) GO TO 1100                                      120
      JJ1=0                                                             121
      REWIND 8                                                          122
      WRITE(8)((PSI(I,J),I=1,MP1),J=1,N)                                123
      WRITE(8)((G(I,J),I=1,MP1),J=1,N)                                  124
      REWIND 8                                                          125
      REWIND 1                                                          126
      WRITE(1)((PSI(I,J),I=1,MP1),J=1,N)                                127
      WRITE(1)((G(I,J),I=1,MP1),J=1,N)                                  128
      REWIND 1                                                          129
      IF(II.EQ.1) GO TO 1100                                            130
      GO TO 2100                                                        131
 000  REWIND 8                                                          132
      WRITE (8) ((PSI(I,J),I=1,MP1),J=1,N)                              133
      WRITE (8) ((G(I,J),I=1,MP1),J=1,N)                                134
      END FILE 8                                                        135
      REWIND 8                                                          136
      REWIND 1                                                          137
      WRITE(1)((PSI(I,J),I=1,MP1),J=1,N)                                138
      WRITE(1)((G(I,J),I=1,MP1),J=1,N)                                  139
      ENDFILE 1                                                         140
      REWIND 1                                                          141
      WRITE (7) ((PSI(I,J),I=1,MP1),J=1,N)                              142
      WRITE (7) ((G(I,J),I=1,MP1),J=1,N)                                143
 2100 WRITE (6,22) JJ                                                   144
      LL1=1                                                             145
   10 DO 8000 LLLL=1,10                                                 146
   11 LL2=LL1+14                                                        147
   12 IF(LL2.GE.MP1) LL2=MP1                                            148
   13 WRITE(6,997)                                                      149
   14 WRITE(6,999)(ANGLE(I),I=LL1,LL2)                                  150
   20 WRITE(6,997)                                                      151
   21 WRITE(6,995)(EZ1(J),(PSI(I,J),I=LL1,LL2),J=1,N)                   152
   22 WRITE(6,997)                                                      153
   23 WRITE(6,995)(EZ1(J),(G(I,J),I=LL1,LL2),J=1,N)                     154
   30 IF(LL2.EQ.MP1) GO TO 8001                                         155
 000  LL1=LL1+15                                                       156
 001  CONTINUE                                                         157
   36 SVORT(1)=0.0                                                     158
   37 SVORT(MP1)=0.0                                                   159
      DO 660 I=2,M                                                     160
   60 SVORT(I)=G(I,1)/SI(I)                                            161
      WRITE (6,39)                                                     162
      WRITE(6,2050)(SVORT(I),I=1,MP1)                                  163
      DMGF=0.0                                                         164
      DO 620 J=2,NM1                                                   165
  620 DMGF=DMGF+(4.0*G(2,J)/SI(2)-G(3,J)/SI(3))/EZ1(J)                 166
      FSPRES=1.0+(DMGF+0.5*((4.0*G(2,1)/SI(2)-G(3,1)/SI(3))/EZ1(1)     167
     1+(4.0*G(2,N)/SI(2)-G(3,N)/SI(3))/EZ1(N)))*4.0*A/(RE*B)           168
      P(1)=FSPRES                                                      169
      DO 630 K=2,M                                                     170
      DUMG=0.0                                                         171
      DO 631 I=2,K                                                     172
  631 DUMG=DUMG+(4.0*G(I,2)/EZ1(2)-G(I,3)/EZ1(3)-3.0*G(I,1))           173
     1/(2.0*A*SI(I))+G(I,1)/SI(I)                                      174
  630 P(K)   =P(1)   +4.0/RE*B*(DUMG-0.5*((4.0*G(K,2)/EZ1(2)-G(K,3)/EZ1(3)  175
```

```
     1-3.0*G(K,1))/(2.0*A*SI(K))+G(K,1)/SI(K)))                          1760
      P(MP1)  =P(M)  +4.0/RE*B*(0.5*((4.0*G(M,2)/EZ1(2)-G(M,3)/EZ1(3)    1770
     1-3.0*G(M,1))/(2.0*A*SI(M))+G(M,1)/SI(M)))                          1780
      WRITE (6,36)                                                       1790
      WRITE (6,2030) (P(I,1),I=1,MP1)                                    1800
      DUMP=0.0                                                           1810
      DO 640 I=2,M                                                       1820
  640 DUMP=DUMP+P(I,1)*SI(I)*CO(I)*2.0                                   1830
      CDP=DUMP*B                                                         1840
      WRITE (6,37)                                                       1850
      WRITE (6,2020) CDP                                                 1860
      DUMPSI=0.0                                                         1870
      DO 650 I=2,M                                                       1880
  650 DUMPSI=DUMPSI+G(I,1)*SI(I)                                         1890
      CDF=8.0*DUMPSI*B/RE                                                1900
      WRITE (6,35)                                                       1910
      WRITE (6,2020) CDF                                                 1920
      CTOTAL=CDF+CDP                                                     1930
      WRITE (6,38)                                                       1940
      WRITE (6,2020) CTOTAL                                              1950
      DO 555 J=1,N                                                       1960
      VR(J)=(8.*PSI(M,J)-PSI(M-1,J))/(2.*B*B*EZ2(J))                     1970
  555 CONTINUE                                                           1980
      WRITE (6,55)                                                       1990
      WRITE (6, 2070) (EZ1(J),VR(J),J=1,N)                               2000
   53 STOP                                                               2010
   55 FORMAT (1H0,15HRADIAL VELOCITY/)                                   2020
 2070 FORMAT (1H ,20X,F10.4,F20.6)                                       2030
   10 FORMAT (3F10.6)                                                    2040
   11 FORMAT (2F10.6)                                                    2050
   12 FORMAT (2I5)                                                       2060
   13 FORMAT (2F10.6)                                                    2070
   14 FORMAT (F10.6)                                                     2080
   20 FORMAT (1H0,10X,F10.6)                                             2090
   21 FORMAT (1H0,10X,2I10,F10.6)                                        2100
   22 FORMAT (I5)                                                        2110
   23 FORMAT (1H0,10X,2F10.6)                                            2120
   30 FORMAT (1H0,15HSTREAM FUNCTION/)                                   2130
   31 FORMAT (1H0,9HVORTICITY/)                                          2140
   35 FORMAT (1H0,20HFRICTION DRAG COEFF./)                              2150
   36 FORMAT (1H0,27HSURFACE PRESS. DISTRIBUTION/)                       2160
   37 FORMAT (1H0,16HFORM DRAG COEFF./)                                  2170
   38 FORMAT (1H0,17HTOTAL DRAG COEFF./)                                 2180
   39 FORMAT (1H0,30HSURFACE VORTICITY DISTRIBUTION/)                    2190
  154 FORMAT(10X 25H END OF FILE ENCOUNTERED )                           2200
  995 FORMAT(1X,F9.3,15F8.4)                                             2210
  997 FORMAT(//)                                                         2220
  999 FORMAT(1H0,9X,15F8.2)                                              2230
 2010 FORMAT (1H ,F6.3,16F8.4)                                           2240
 2020 FORMAT (1H ,10X,F20.6)                                             2250
 2030 FORMAT (1H ,6X,8F16.6)                                             2260
 2040 FORMAT (1H0,6X,16F8.2/)                                            2270
 2050 FORMAT (1H ,6X,16F8.4)                                             2280
   19 FORMAT (1H0,10X,*FLOW ARROUND A SOLID SPHERE*/)                    2290
 2080 FORMAT (1H ,F6.3,13F8.4)                                           2300
 2090 FORMAT (1H0,6X,13F8.2/)                                            2310
      END                                                                2320
```

COMPUTER PROGRAM FOR CALCULATING THE FLOW AROUND A SOLID SPHERE ACCELERATING FROM REST UNDER THE INFLUENCE OF GRAVITY

```
      PROGRAM ACCEL1(INPUT,OUTPUT,PUNCHB,TAPE5=INPUT,TAPE6=OUTPUT,TAPE7=     0010
     1PUNCHB,TAPE9,TAPE10)                                                   0020
C     SOLUTION OF THE FLOW FIELD AROUND A SPHERE ACCELERATING UNDER THE      0021
C     INFLUENCE OF GRAVITY. THE SOLUTION IS OBTAINED IN AN ACCELERATING      0022
C     COORDINATE FRAME OF REFERENCE.                                         0023
C     N NUMBER OF MESH POINTS IN THE RADIAL DIRECTION                        0024
C     M--NUMBER OF MESH POINTS IN THE ANGULAR DIRECTION                      0025
C     REF--STEADY STATE REYNOLDS NUMBER                                      0025
C     A--RADIAL STEP SIZE                                                    0027
C     C--TIME STEP SIZE                                                      0028
C     DRAGF--STEADY STATE DRAGF COEFFICIENT                                  0029
C     DENS--RATIO OF SOLID SPHERE DENSITY TO LIQUID DENSITY                  0030
C     EPS--ERROR TOLERANCE                                                   0031
C     WW--STREAM FUNCTION CONVERGENCE PROMOTER                               0032
C     W--VORTICITY RELAXATION FACTOR                                         0033
C     CONST--DIMENSIONLESS GROUPING OF PHYSICAL PROPERTY PARAMETERS          0034
C     RE--REYNOLDS NUMBER                                                    0035
C     CD--DRAG COEFFICIENT                                                   0036
C     DREDT--DERIVATIVE OF REYNOLDS NUMBER DIVIDED BY REYNOLDS NUMBER        0037
C     OK--FRONTAL STAGNATION PRESSURE                                        0038
C     JPT--TIME ITERATIONS PER PRINTOUT                                      0039
C     NPT--ITERATIONS ALLOWED PER TIME STEP                                  0040
C     NNPT--TIME ITERATIONS ALLOWED PER RUN                                  0041
      COMMON N,M,NM1,MM1,PSI(62,76,2),G(62,76,2)                             0050
      COMMON RE,RE2,DREDT,DREDT2,DUMA,DUMB,DUMC,DUMD,DUME                    0060
      COMMON SI(62),COT(62),SII(62),COTT(62),X2(101),X4(101),X5(101)         0070
      COMMON/BLK2/DUM1,DUM2,DUM3,DUM4,DUM5,DUM6,DUM7,TVV(101),DUM9,DUM8      0080
      COMMON/BLK3/NEXIT,WW,NPT,EPS,DUDCOT(62),W,JJ,J2J,NCOUNT                0090
      COMMON/BLK5/SURVT(62),OMIKO(62),SCDPM,SCDFM,CDX,CD,CONST1,CONST2,       0100
     1 BOTWO,CO(62),C,DENS,NCONT                                             0110
      DIMENSION Z(101),X1(101),X3(101),ANGLE(62),DVORT(101)                  0120
      INTEGER CHECK                                                          0130
      READ(5,100) CHECK                                                      0140
      IF(CHECK) 20,20,21                                                     0150
   20 READ(5,100) N,M,REF,A,C,EPS,WW,DRAGF,DENS                              0160
      READ(5,1017)RE,CD,DREDT,W,BETIM,CONST                                  0170
      GO TO 22                                                               0180
   21 CALL UPDATE(CHECK,REF,A,CONST,DRAGF,BETIM,OK)                          0190
      CHECK=CHECK+1                                                          0200
   22 READ(5,101) JRD,JPT,NPT,NNPT,NPUTB                                     0210
      READ(5,1017) C,W                                                       0220
      WRITE(6,102) N,M,REF,EPS,WW,A,C,CONST                                  0230
      WRITE(6,103) JRD,JPT,NPT,NNPT                                          0240
      NM1=N-1                                                                0250
      MM1=M-1                                                                0260
      B=3.1416/FLOAT(MM1)                                                    0270
      DUMA=1./(A*A)                                                          0280
      DUMB=1./(B*B)                                                          0290
      DUMC=1./(2.*A)                                                         0300
      DUMD=1./(2.*B)                                                         0310
      DUME=1./(2.*(DUMA+DUMB))                                               0320
      DUM1=4.*DUMA/DENS                                                      0330
      DUM2=4.*DUMB/DENS                                                      0340
      DUM3=4.*DUMC/DENS                                                      0350
      DUM4=4.*DUMD/DENS                                                      0360
      DUM5=2./C                                                              0370
      DUM6=2.*DUMD/DENS                                                      0380
      DUM7=2.*DUMC/DENS                                                      0390
      DUM8=4./DENS                                                           0400
```

```
UM9=2./DENS                                                          0410
ONST1=CONST/(1.+0.5*DENS)                                            0420
ONST2=0.75/(1.+0.5*DENS)                                             0430
OTWO=A/2.                                                            0440
OTWO=0.5*B                                                           0450
(1)=0.                                                               0460
NGLE(1)=0.                                                           0470
NGLE(M)=180.                                                         0480
HETA=B                                                               0490
HTC=180./3.1416                                                      0500
O 90 I=2,MM1                                                         0510
I(I)=SIN(THETA)                                                      0520
O(I)=COS(THETA)                                                      0530
II(I)=1./SI(I)                                                       0540
OT(I)=CO(I)/SI(I)                                                    0550
OTT(I)=COT(I)*COT(I)+1.                                              0560
UDCOT(I)=DUMD*COT(I)                                                 0570
NGLE(I)=THETA*THTC                                                   0580
HETA=THETA+B                                                         0590
O 89 I=1,M,MM1                                                       0600
I(I)=0.0                                                             0610
II(I)=0.0                                                            0620
O(I)=0.0                                                             0630
OT(I)=0.0                                                            0640
OTT(I)=0.0                                                           0650
UDCOT(I)=0.0                                                         0660
O 91 J=1,NM1                                                         0670
(J+1)=Z(J)+A                                                         0680
1(J)=1./EXP(Z(J))                                                    0690
2(J)=X1(J)*X1(J)                                                     0700
3(J)=1./X1(J)                                                        0710
5(J)=EXP(3.*Z(J))                                                    0720
4(J)=1./X5(J)                                                        0730
1(N)=1./EXP(Z(N))                                                    0740
2(N)=X1(N)*X1(N)                                                     0750
3(N)=1./X1(N)                                                        0760
5(N)=EXP(3.*Z(N))                                                    0770
4(N)=1./X5(N)                                                        0780
IJ=0                                                                 0790
JJ=0                                                                 0800
SJ=0                                                                 0810
VJ=0                                                                 0820
EXIT=0                                                               0830
F(CHECK.EQ.1) GO TO 9                                                0840
O 1007 I=1,M                                                         0850
O 1007 J=1,N                                                         0860
SI(I,J,1)=PSI(I,J,2)                                                 0870
O 1008 I=1,M                                                         0880
(I,N,1)=0.0                                                          0890
O 1009 J=1,N                                                         0900
(1,J,1)=0.0                                                          0910
(M,J,1)=0.0                                                          0920
O TO 26                                                              0930
ALL POFLOW                                                           0940
SJ=JSJ+JJ                                                            0950
=2                                                                   0960
RITE(6,964) JSJ                                                      0970
F(NEXIT.EQ.1) GO TO 111                                              0980
```

```
      K=2                                                                0990
      KP=1                                                               1000
1000  KM=KP                                                              1010
      KP=K                                                               1020
      K=KM                                                               1030
      NCOUNT=1                                                           1033
      NCONT=1                                                            1036
      CALL VORT1(KP,K)                                                   1040
      CALL VORT2(KP,K)                                                   1050
      CALL STREAM(K)                                                     1060
      JSJ=JSJ+JJ                                                        1070
      WRITE(6,964) JSJ                                                   1080
      IF(NEXIT.EQ.1) GO TO 111                                           1090
      DO 300 I=2,MM1                                                     1100
      BG=0.5*(8.*PSI(I,2,K)-PSI(I,3,K))*DUMA*SII(I)                      1110
      G(I,1,K)=G(I,1,KP)+W*(BG-G(I,1,KP))                                1120
00    TVV(I)=G(I,1,K)                                                    1130
      CALL REDRAG(K)                                                     1140
      J2J=1                                                              1150
00    CALL VORT3(KP,K)                                                   1160
      CALL VORT4(KP,K)                                                   1170
      CALL STREAM(K)                                                     1180
      JSJ=JSJ+JJ                                                        1190
      IF(NEXIT.EQ.1) GO TO 111                                           1200
      CALL VORTBD(K)                                                     1210
      DO 305 I=2,MM1                                                     1220
05    TVV(I)=G(I,1,K)                                                    1230
      CALL REDRAG(K)                                                     1240
      J2J=J2J+1                                                          1250
      IF(J2J.EQ.NPT) GO TO 111                                           1260
      IF(NEXIT.EQ.2) GO TO 400                                           1270
      CD=CDX                                                             1280
      RE=RE2                                                             1290
      DREDT=DREDT2                                                       1300
      JVJ=JVJ+J2J                                                        1310
      WRITE(6,964) JSJ                                                   1320
      WRITE(6,963) JVJ                                                   1330
      JJJ=JJJ+1                                                          1340
      JIJ=JIJ+1                                                          1350
      IF(JJJ.EQ.NNPT) GO TO 70                                           1360
      IF(JIJ.EQ.JPT) GO TO 70                                            1370
      GO TO 1000                                                         1380
      JIJ=0                                                              1390
      DUM33=DUMB*DENS/(C*RE)                                             1400
      DUM34=DREDT*DENS*DUMB/RE                                           1410
      DUM35=8./(RE*6.*B)                                                 1420
      DO 31 J=1,N                                                        1430
      DVORT(J)=(18.*G(2,J,K)-9.*G(3,J,K)+2.*G(4,J,K))*DUM35-X1(J)*(4.*(  1440
     1PSI(3,J,K)-PSI(3,J,KP))-5.*(PSI(2,J,K)-PSI(2,J,KP))-PSI(4,J,K)+    1450
     2PSI(4,J,KP))*DUM33-X1(J)*(4.*PSI(3,J,K)-5.*PSI(2,J,K)-PSI(4,J,K))  1460
     3*DUM34                                                             1470
      CONTINUE                                                           1480
      OK=0.0                                                             1490
      DO 32 J=2,N                                                        1500
      OK=AOTWO*(DVORT(J-1)+DVORT(J))+OK                                  1510
      CONTINUE                                                           1520
      OK=OK+1.0              +DENS*DREDT*(X3(N)-1.)/RE                   1530
      DO 33 I=1,M                                                        1540
```

```
)MIKO(I)=OMIKO(I)+OK                                                    1550
:ONTINUE                                                                1560
'IME=C*FLOAT(JJJ)+BETIM                                                 1570
/RITE(6,983)                                                            1580
/RITE(6,984) REF,DRAGF,TIME,RE,DENS                                     1590
/RITE(6,1013) SCDFM,SCDPM,CD,OK,DREDT                                   1600
/RITE(6,983)                                                            1610
WRITE(6,101) CHECK                                                      1620
WRITE(6,997)                                                            1630
WRITE(6,1010)                                                           1640
WRITE(6,996) (OMIKO(I),I=1,M)                                           1650
WRITE(6,997)                                                            1660
WRITE(6,1016)                                                           1670
WRITE(6,996) (SURVT(I),I=1,M)                                           1680
WRITE(6,997)                                                            1690
WRITE(10) CHECK                                                         1700
WRITE(10) N,M,REF,EPS,WW,A,C,CONST                                      1710
WRITE(10) DRAGF,TIME,RE,DENS,W                                          1720
WRITE(10) SCDFM,SCDPM,CD,OK,DREDT                                       1730
WRITE(10)((PSI(I,J,K),I=1,M),J=1,N)                                     1740
WRITE(10)((G(I,J,K),I=1,M),J=1,N)                                       1750
CHECK=CHECK+1                                                           1760
IF(JJJ.EQ.NNPT) GO TO 112                                               1770
GO TO 1000                                                              1780
WRITE(6,997)                                                            1790
WRITE(6,981)                                                            1800
TIME=C*FLOAT(JJJ)+BETIM                                                 1810
WRITE(6,997)                                                            1820
WRITE(6,984) REF,DRAGF,TIME,RE,DENS                                     1830
IF(NPUTB.EQ.0) GO TO 43333                                              1840
WRITE(7)((PSI(I,J,K ),I=1,M),J=1,N)                                     1850
WRITE(7)((G(I,J,K ),I=1,M),J=1,N)                                       1860
CONTINUE                                                                1870
ENDFILE 10                                                              1880
REWIND 10                                                               1890
LL1=1                                                                   1900
DO 8000 LLLL=1,10                                                       1910
LL2=LL1+14                                                              1920
IF(LL2.GE.M) LL2=M                                                      1930
WRITE(6,997)                                                            1940
WRITE(6,999) (ANGLE(I),I=LL1,LL2)                                       1950
WRITE(6,997)                                                            1960
WRITE(6,995)(Z(J),(PSI(I,J,K ),I=LL1,LL2),J=1,N)                        1970
WRITE(6,997)                                                            1980
WRITE(6,995)(Z(J),(G(I,J,K ),I=LL1,LL2),J=1,N)                          1990
IF(LL2.EQ.M) GO TO 8001                                                 2000
LL1=LL1+15                                                              2010
CONTINUE                                                                2020
STOP                                                                    2030
FORMAT(2I5,7F10.0)                                                      2040
FORMAT(2F10.0,E10.2,3F10.0)                                             2050
FORMAT(5I5)                                                             2060
FORMAT(10X 5H N = ,I5,10X 5H M = ,I5,10X 7H REO = ,F10.4,10X 6HEPS      2070
1 = ,F10.4,10X 6H WW = ,F10.4/10X 20H RADIAL STEP SIZE = ,F10.4,        2080
210X  18H TIME STEP SIZE = ,F10.6,10X 9H CONST = ,F10.4)                2090
FORMAT(10X 7H JRD = ,I5,10X 7H JPT = ,I5, 10X 7H NPT = ,I5,             2100
1  10X 8H NNPT = ,I5)                                                   2110
FORMAT(10X 7H JVJ = ,I10)                                               2120
```

```
 FORMAT(10X 7H JSJ = ,I10)                                                      2130
 FORMAT(F10.0)                                                                  2140
 FORMAT(10X 72H DID NOT CONVERGE STREAM FUNCTION - CEASING CALCULAT             2150
1IONS AT THIS POINT     )                                                       2160
 FORMAT(1X,131(1H*))                                                            2170
 FORMAT(30X 19H LOOPS COMPLETED = ,I5)                                          2180
 FORMAT(1X,F9.3,15F8.4)                                                         2190
 FORMAT(1X,10F12.4)                                                             2200
 FORMAT(//)                                                                     2210
 FORMAT(1H0,9X,15F8.2)                                                          2220
 FORMAT(1X,30H SURFACE PRESSURE DISTRIBUTION  )                                 2230
 FORMAT(1X, 19H SURFACE VORTICITY  )                                            2240
 FORMAT(  5X 19H STEADY STATE RE = ,F10.2, 5X 9H DRAGF = ,F10.4,                2250
1 5X 13H DIM. TIME = ,F10.6, 5X 6H RE = ,F12.6,5X 8H DENS = ,F7.2/              2260
2)                                                                              2270
 FORMAT(  2X 8H SCDF = ,F16.4, 2X 8H SCDP = ,F16.4,  2X 6H CD = ,               2280
1 F16.4, 2X 16H STAG. PRESS. = ,F16.4,3X 5HDREDT,F13.4)                         2290
 END                                                                            2300
 SUBROUTINE UPDATE(CHECK,REF,A,CONST,DRAGF,BETIM,OK)                            2310
 COMMON N,M,NM1,MM1,PSI(62,76,2),G(62,76,2)                                     2320
 COMMON RE,RE2,DREDT,DREDT2,DUMA,DUMB,DUMC,DUMD,DUME                            2330
 COMMON SI(62),COT(62),SII(62),COTT(62),X2(101),X4(101),X5(101)                 2340
 COMMON/BLK2/DUM1,DUM2,DUM3,DUM4,DUM5,DUM6,DUM7,TVV(101),DUM9,DUM8              2350
 COMMON/BLK3/NEXIT,WW,NPT,EPS,DUDCOT(62),W,JJ,J2J,NCOUNT                        2360
 COMMON/BLK5/SURVT(62),OMIKO(62),SCDPM,SCDFM,CDX,CD,CONST1,CONST2,               2370
1 BOTWO,CO(62),C,DENS,NCONT                                                     2380
 INTEGER CHECK,CHECK1                                                           2390
 REWIND 9                                                                       2400
 REWIND 10                                                                      2410
 READ(9) CHECK1                                                                 2420
 IF(EOF,9) 2,3                                                                  2430
 CHECK=CHECK1                                                                   2440
 READ(9) N,M,REF,EPS,WW,A,C,CONST                                               2450
 READ(9) DRAGF,BETIM,RE,DENS,W                                                  2460
 READ(9) SCDFM,SCDPM,CD,OK,DREDT                                                2470
 READ(9)((PSI(I,J,2),I=1,M),J=1,N)                                              2480
 READ(9)((G(I,J,2),I=1,M),J=1,N)                                                2490
 WRITE(10) CHECK                                                                2500
 WRITE(10) N,M,REF,EPS,WW,A,C,CONST                                             2510
 WRITE(10) DRAGF,BETIM,RE,DENS,W                                                2520
 WRITE(10) SCDFM,SCDPM,CD,OK,DREDT                                              2530
 WRITE(10)((PSI(I,J,2),I=1,M),J=1,N)                                            2540
 WRITE(10)((G(I,J,2),I=1,M),J=1,N)                                              2550
 GO TO 1                                                                        2560
 REWIND 9                                                                       2570
 WRITE(6,100) CHECK                                                             2580
 RETURN                                                                         2590
 FORMAT(I10)                                                                    2600
 END                                                                            2610
 SUBROUTINE VORT1(KP,K)                                                         2620
 COMMON N,M,NM1,MM1,PSI(62,76,2),G(62,76,2)                                     2630
 COMMON RE,RE2,DREDT,DREDT2,DUMA,DUMB,DUMC,DUMD,DUME                            2640
 COMMON SI(62),COT(62),SII(62),COTT(62),X2(101),X4(101),X5(101)                 2650
 COMMON/BLK2/DUM1,DUM2,DUM3,DUM4,DUM5,DUM6,DUM7,TVV(101),DUM9,DUM8              2660
 COMMON/BLK4/F(101),T(101),D(101),GG(101),TV(101)                               2670
 DO 100 I=2,MM1                                                                 2680
 TV(I)=G(I,1,KP)                                                                2690
 DUM66=DUM6*RE                                                                  2700
```

```
 7=DUM7*RE                                                                2710
 9=DUM9*RE                                                                2720
300 J=2,NM1                                                               2730
J+1                                                                       2740
J-1                                                                       2750
1=DUM1*X2(J)                                                              2760
I=DUM2*X2(J)                                                              2770
J=DUM4*X2(J)                                                              2780
K=DUM66*X4(J)                                                             2790
L=2.*DUMI                                                                 2800
M=2.*DUMH                                                                 2810
N=DUM3*X2(J)                                                              2820
O=DUM77*X4(J)                                                             2830
P=DUM8*X2(J)                                                              2840
Q=DUM99*X4(J)                                                             2850
H1=DUMH-DUMN                                                              2860
MH2=DUMH+DUMN                                                             2870
ML1=DUM5+DUML                                                             2880
MM1=DUM5-DUMM                                                             2890
 400 I=2,MM1                                                              2900
=I+1                                                                      2910
I=I-1                                                                     2920
SI1=(PSI(I,JP,KP)-PSI(I,JM,KP))*DUMC                                      2930
SI2=(PSI(IP,J,KP)-PSI(IM,J,KP))*DUMD                                      2930
SII1=COT(I)*PSI1                                                          2950
JMQ1=DUMQ*SII(I)                                                          2960
UMO1=DUMO*SII(I)*PSI2                                                     2970
UMP1=DUMP*COTT(I)                                                         2980
(I)=-DUMI+DUMJ*COT(I)-DUMK*SII(I)*PSI1                                    2990
(I)=DUML1+0.5*((PSI2-PSI11)*DUMQ1+DREDT+DUMP1)                            3000
(I)=-F(I)-DUML                                                            3010
G(I)=G(I,JM,KP)*(DUMH1-DUMO1)+G(I,J,KP)*(DUMM1+0.5*((PSI11-PSI2)*         3020
DUMQ1-DREDT-DUMP1))+G(I,JP,KP)*(DUMH2+DUMO1)                              3030
(I,JM,K)=TV(I)                                                            3040
ALL BANSOL(MM1)                                                           3050
ONTINUE                                                                   3060
O 500 I=2,MM1                                                             3070
(I,NM1,K)=TV(I)                                                           3080
ETURN                                                                     3090
ND                                                                        3100
UBROUTINE BANSOL(K1)                                                      3110
OMMON N,M,NM1,MM1,PSI(62,76,2),G(62,76,2)                                 3120
OMMON RE,RE2,DREDT,DREDT2,DUMA,DUMB,DUMC,DUMD,DUME                        3130
OMMON SI(62),COT(62),SII(62),COTT(62),X2(101),X4(101),X5(101)             3140
OMMON/BLK4/F(101),T(101),D(101),GG(101),TV(101)                           3150
IMENSION WR(101),VR(101),RR(101)                                          3160
R(2)=D(2)/T(2)                                                            3170
R(2)=GG(2)/T(2)                                                           3180
O 100 K=3,K1                                                              3190
R(K)=T(K)-F(K)*WR(K-1)                                                    3200
R(K)=D(K)/RR(K)                                                           3210
O 200 K=3,K1                                                              3220
R(K)=(GG(K)-F(K)*VR(K-1))/RR(K)                                           3230
=K1                                                                       3240
V(L)=VR(L)                                                                3250
2=K1-2                                                                    3260
O 300 K=1,K2                                                              3270
=K1-K                                                                     3280
```

```
      TV(L)=VR(L)-WR(L)*TV(L+1)                                          3290
      RETURN                                                             3300
      END                                                                3310
      SUBROUTINE STREAM(K5)                                              3320
      COMMON N,M,NM1,MM1,PSI(62,76,2),G(62,76,2)                         3330
      COMMON RE,RE2,DREDT,DREDT2,DUMA,DUMB,DUMC,DUMD,DUME                3340
      COMMON SI(62),COT(62),SII(62),COTT(62),X2(101),X4(101),X5(101)     3350
      COMMON/BLK3/NEXIT,WW,NPT,EPS,DUDCOT(62),W,JJ,J2J,NCOUNT            3360
      NEXIT=0                                                            3370
      JJ=1                                                               3380
      II=0                                                               3390
      DO 335 I=2,MM1                                                     3400
      IP=I+1                                                             3410
      IM=I-1                                                             3420
      XIX=M-I                                                            3430
      XIX=1./(XIX**2)                                                    3440
      DO 335 J=2,NM1                                                     3450
      JP=J+1                                                             3460
      JM=J-1                                                             3470
      XJX=J                                                              3480
      XJX=1./(XJX**2)                                                    3490
      DUMN=PSI(I,JP,K5)-PSI(I,JM,K5)                                     3500
      DUMM=PSI(IP,J,K5)-PSI(IM,J,K5)                                     3510
      DUMO=PSI(I,JP,K5)+PSI(I,JM,K5)                                     3520
      DUMP=PSI(IP,J,K5)+PSI(IM,J,K5)                                     3530
      STRMF=DUME*(-SI(I)*X5(J)*G(I,J,K5)+DUMO*DUMA+DUMP*DUMB-DUMN*DUMC   3540
     1 -DUMM*DUDCOT(I))                                                  3550
      WW=2./(1.+2.22*SQRT(XIX+XJX))                                      3560
      STRMF=PSI(I,J,K5)+WW*(STRMF-PSI(I,J,K5))                           3570
      IF(ABS(STRMF-PSI(I,J,K5)).GT.EPS) II=1                             3580
      PSI(I,J,K5)=STRMF                                                  3590
      CONTINUE                                                           3600
      IF(II.EQ.1) GO TO 65                                               3610
      RETURN                                                             3620
      JJ=JJ+1                                                            3630
      IF(JJ.EQ.NPT) GO TO 75                                             3640
      GO TO 100                                                          3650
      NEXIT=1                                                            3660
      RETURN                                                             3670
      END                                                                3680
      SUBROUTINE VORT3(KP,K)                                             3690
      COMMON N,M,NM1,MM1,PSI(62,76,2),G(62,76,2)                         3700
      COMMON RE,RE2,DREDT,DREDT2,DUMA,DUMB,DUMC,DUMD,DUME                3710
      COMMON SI(62),COT(62),SII(62),COTT(62),X2(101),X4(101),X5(101)     3720
      COMMON/BLK2/DUM1,DUM2,DUM3,DUM4,DUM5,DUM6,DUM7,TVV(101),DUM9,DUM8  3730
      COMMON/BLK4/F(101),T(101),D(101),GG(101),TV(101)                   3740
      DUMC1=0.75*DUMC                                                    3750
      DUMC2=0.25*DUMC                                                    3760
      DUMD1=0.75*DUMD                                                    3770
      DUMD2=0.25*DUMD                                                    3780
      R3=0.75*RE+0.25*RE2                                                3790
      DRED3=0.75*DREDT+0.25*DREDT2                                       3800
      DO 100 I=2,MM1                                                     3810
      TV(I)=G(I,1,KP)                                                    3820
      DUM66=DUM6*R3                                                      3830
      DUM77=DUM7*R3                                                      3840
      DUM99=DUM9*R3                                                      3850
      DO 300 J=2,NM1                                                     3860
```

```
  =J+1                                                                  3870
  =J-1                                                                  3880
  MH=DUM1*X2(J)                                                         3890
  MI=DUM2*X2(J)                                                         3900
  MJ=DUM4*X2(J)                                                         3910
  MK=DUM66*X4(J)                                                        3920
  ML=2.*DUMI                                                            3930
  MM=2.*DUMH                                                            3940
  MN=DUM3*X2(J)                                                         3950
  MO=DUM77*X4(J)                                                        3960
  MP=DUM8*X2(J)                                                         3970
  MQ=DUM99*X4(J)                                                        3980
  MH1=DUMH-DUMN                                                         3990
  MH2=DUMH+DUMN                                                         4000
  ML1=DUM5+DUML                                                         4010
  MM1=DUM5-DUMM                                                         4020
  0 400 I=2,MM1                                                         4030
  P=I+1                                                                 4040
  M=I-1                                                                 4050
 SI1=(PSI(I,JP,KP)-PSI(I,JM,KP))*DUMC1+(PSI(I,JP,K)-PSI(I,JM,K))*       4060
 )UMC2                                                                  4070
 SI2=(PSI(IP,J,KP)-PSI(IM,J,KP))*DUMD1+(PSI(IP,J,K)-PSI(IM,J,K))*       4080
 )UMD2                                                                  4090
 SI11=COT(I)*PSI1                                                       4100
 )UMQ1=DUMQ*SII(I)                                                      4100
 )UMO1=DUMO*SII(I)*PSI2                                                 4120
 DUMP1=DUMP*COTT(I)                                                     4130
 F(I)=-DUMI+DUMJ*COT(I)-DUMK*SII(I)*PSI1                                4140
 T(I)=DUML1+0.5*((PSI2-PSI11)*DUMQ1+DRED3+DUMP1)                        4150
 D(I)=-F(I)-DUML                                                        4160
 GG(I)=G(I,JM,KP)*(DUMH1-DUMO1)+G(I,J,KP)*(DUMM1+0.5*((PSI11-PSI2)*     4170
  DUMQ1-DRED3-DUMP1))+G(I,JP,KP)*(DUMH2+DUMO1)                          4180
 G(I,JM,K)=TV(I)                                                        4190
 CALL BANSOL(MM1)                                                       4200
 CONTINUE                                                               4210
 DO 500 I=2,MM1                                                         4220
 G(I,NM1,K)=TV(I)                                                       4230
 RETURN                                                                 4240
 END                                                                    4250
 SUBROUTINE VORT2(KP,K)                                                 4260
 COMMON N,M,NM1,MM1,PSI(62,76,2),G(62,76,2)                             4270
 COMMON RE,RE2,DREDT,DREDT2,DUMA,DUMB,DUMC,DUMD,DUME                    4280
 COMMON SI(62),COT(62),SII(62),COTT(62),X2(101),X4(101),X5(101)         4290
 COMMON/BLK2/DUM1,DUM2,DUM3,DUM4,DUM5,DUM6,DUM7,TVV(101),DUM9,DUM8      4300
 COMMON/BLK4/F(101),T(101),D(101),GG(101),TV(101)                       4310
 DO 100  J=2,NM1                                                       4320
 TV(J)=G(1,J,K)                                                         4330
 DUM11=DUM3-DUM1                                                        4340
 DUM77=DUM7*RE                                                          4350
 DUM21=2.*DUM1                                                          4360
 DUM99=DUM9*RE                                                          4370
 DUM66=DUM6*RE                                                          4380
 DUM22=2.*DUM2                                                          4390
 DO 300 I=2,MM1                                                         4400
 IP=I+1                                                                 4410
 IM=I-1                                                                 4420
 DUMH=DUM77*SII(I)                                                      4430
 DUMI=DUM99*SII(I)                                                      4440
```

```
      DUMJ=DUM8*COTT(I)                                                  4450
      DUMK=DUM66*SII(I)                                                  4460
      DUML=DUM2-DUM4*COT(I)                                              4470
      DUMM=DUM2+DUM4*COT(I)                                              4480
      DUMN=DUM99*SII(I)                                                  4490
      DO 400 J=2,NM1                                                     4500
      JP=J+1                                                             4510
      JM=J-1                                                             4520
      PSI1=(PSI(IP,J,KP)-PSI(IM,J,KP))*DUMD                              4530
      PSI2=(PSI(I,JP,KP)-PSI(I,JM,KP))*DUMC                              4540
      DUM212=DUM21*X2(J)                                                 4550
      DUMN1=DUMN*X4(J)                                                   4560
      DUMJ1=DUMJ*X2(J)                                                   4570
      DUMK1=DUMK*X4(J)*PSI2                                              4580
      PSI21=COT(I)*PSI2                                                  4590
      F(J)=DUM11*X2(J)+DUMH*X4(J)*PSI1                                   4600
      T(J)=DUM5+DUM212+0.5*((PSI1-PSI21)*DUMN1+DREDT+DUMJ1)              4610
      D(J)=-F(J)-DUM212                                                  4620
      GG(J)=G(IM,J,K)*(DUML*X2(J)+DUMK1)+G(I,J,K)*(DUM5-DUM22*X2(J)+     4630
     10.5*((PSI21-PSI1)*DUMN1-DREDT-DUMJ1))+G(IP,J,K)*(DUMM*X2(J)-DUMK1) 4640
      G(IM,J,K)=TV(J)                                                    4650
      GG(2)=GG(2)-F(2)*G(I,1,KP)                                         4660
      CALL BANSOL(NM1)                                                   4670
      CONTINUE                                                           4680
      DO 500 J=2,NM1                                                     4690
      G(MM1,J,K)=TV(J)                                                   4700
      RETURN                                                             4710
      END                                                                4720
      SUBROUTINE VORT4(KP,K)                                             4730
      COMMON N,M,NM1,MM1,PSI(62,76,2),G(62,76,2)                         4740
      COMMON RE,RE2,DREDT,DREDT2,DUMA,DUMB,DUMC,DUMD,DUME                4750
      COMMON SI(62),COT(62),SII(62),COTT(62),X2(101),X4(101),X5(101)     4760
      COMMON/BLK2/DUM1,DUM2,DUM3,DUM4,DUM5,DUM6,DUM7,TVV(101),DUM9,DUM8  4770
      COMMON/BLK4/F(101),T(101),D(101),GG(101),TV(101)                   4780
      DUMC1=0.75*DUMC                                                    4790
      DUMC2=0.25*DUMC                                                    4800
      DUMD1=0.75*DUMD                                                    4810
      DUMD2=0.25*DUMD                                                    4820
      R3=0.75*RE2+0.25*RE                                                4830
      DRED3=0.75*DREDT2+0.25*DREDT                                       4840
      DO 100  J=2,NM1                                                    4850
      TV(J)=G(1,J,K)                                                     4860
      DUM11=DUM3-DUM1                                                    4870
      DUM77=DUM7*R3                                                      4880
      DUM21=2.*DUM1                                                      4890
      DUM99=DUM9*R3                                                      4900
      DUM66=DUM6*R3                                                      4910
      DUM22=2.*DUM2                                                      4920
      DO 300 I=2,MM1                                                     4930
      IP=I+1                                                             4940
      IM=I-1                                                             4950
      DUMH=DUM77*SII(I)                                                  4960
      DUMI=DUM99*SII(I)                                                  4970
      DUMJ=DUM8*COTT(I)                                                  4980
      DUMK=DUM66*SII(I)                                                  4990
      DUML=DUM2-DUM4*COT(I)                                              5000
      DUMM=DUM2+DUM4*COT(I)                                              5010
      DUMN=DUM99*SII(I)                                                  5020
```

```
 400 J=2,NM1                                                          5030
 J+1                                                                  5040
 J-1                                                                  5050
 1=(PSI(IP,J,KP)-PSI(IM,J,KP))*DUMD2+(PSI(IP,J,K)-PSI(IM,J,K))*       5060
MD1                                                                   5060
 2=(PSI(I,JP,KP)-PSI(I,JM,KP))*DUMC2+(PSI(I,JP,K)-PSI(I,JM,K))*      5080
MC1                                                                   5090
 4212=DUM21*X2(J)                                                     5100
 MN1=DUMN*X4(J)                                                       5110
 MJ1=DUMJ*X2(J)                                                       5120
 MK1=DUMK*X4(J)*PSI2                                                  5130
 I21=COT(I)*PSI2                                                      5140
 J)=DUM11*X2(J)+DUMH*X4(J)*PSI1                                       5150
 J)=DUM5+DUM212+0.5*((PSI1-PSI21)*DUMN1+DRED3+DUMJ1)                  5160
 J)=-F(J)-DUM212                                                      5170
 (J)=G(IM,J,K)*(DUML*X2(J)+DUMK1)+G(I,J,K)*(DUM5-DUM22*X2(J)+         5180
 5*((PSI21-PSI1)*DUMN1-DRED3-DUMJ1))+G(IP,J,K)*(DUMM*X2(J)-DUMK1)     5190
 IM,J,K)=TV(J)                                                        5200
 G(2)=GG(2)-F(2)*TVV(I)                                               5210
ALL BANSOL(NM1)                                                       5220
ONTINUE                                                               5230
O 500 J=2,NM1                                                         5240
 (MM1,J,K)=TV(J)                                                      5250
ETURN                                                                 5260
ND                                                                    5270
UBROUTINE POFLOW                                                      5280
OMMON N,M,NM1,MM1,PSI(62,76,2),G(62,76,2)                             5290
OMMON RE,RE2,DREDT,DREDT2,DUMA,DUMB,DUMC,DUMD,DUME                    5300
OMMON SI(62),COT(62),SII(62),COTT(62),X2(101),X4(101),X5(101)         5310
O 92 K=1,2                                                            5320
O 92 J=1,N                                                            5330
G(1,J,K)=0.                                                           5340
PSI(1,J,K)=0.                                                         5350
G(M,J,K)=0.                                                           5360
PSI(M,J,K)=0.                                                         5370
O 93 K=1,2                                                            5380
O 93 I=1,M                                                            5390
PSI(I,1,K)=0.                                                         5400
O 94 K=1,2                                                            5410
O 94 I=1,M                                                            5420
G(I,N,K)=0.                                                           5430
O 95 K=1,2                                                            5440
O 95 I=2,MM1                                                          5450
O 95 J=2,NM1                                                          5460
G(I,J,K)=0.                                                           5470
O 96 I=2,MM1                                                          5480
O 96 J=2,NM1                                                          5490
PSI(I,J,2)=0.5*SI(I)*SI(I)*(1.-X4(J))/X2(J)                           5500
O 88 K=1,2                                                            5510
O 88 I=2,MM1                                                          5520
PSI(I,N,K)=0.5*SI(I)**2/X2(N)                                         5530
ALL STREAM(2)                                                         5540
O 99 I=2,MM1                                                          5550
O 99 J=2,NM1                                                          5560
PSI(I,J,1)=PSI(I,J,2)                                                 5570
O 3355 I=2,MM1                                                        5580
G(I,1,2)=0.5*(8.*PSI(I,2,2)-PSI(I,3,2))*SII(I)*DUMA                   5590
ETURN                                                                 5600
```

```
      END                                                                5610
      SUBROUTINE REDRAG(K5)                                              5620
      COMMON N,M,NM1,MM1,PSI(62,76,2),G(62,76,2)                         5630
      COMMON RE,RE2,DREDT,DREDT2,DUMA,DUMB,DUMC,DUMD,DUME                5640
      COMMON SI(62),COT(62),SII(62),COTT(62),X2(101),X4(101),X5(101)     5650
      COMMON/BLK5/SURVT(62),OMIKO(62),SCDPM,SCDFM,CDX,CD,CONST1,CONST2,  5660
     1 BOTWO,CO(62),C,DENS,NCONT                                         5670
      DIMENSION DK(62),CDP(62),SCDP(62),CDF(62),SCDF(62),DSRVT(62)       5680
      IF(NCONT.LE.10) GO TO 2003                                         5685
      DO 71 I=2,MM1                                                      5690
      SURVT(I)=G(I,1,K5)                                                 5700
      SURVT(1)=0.0                                                       5710
      SURVT(M)=0.0                                                       5720
      CDO=CD                                                             5730
      REO=RE                                                             5740
      DREDT1=CONST1-CONST2*REO**2*CDO                                    5750
      REX=REO+C*DREDT1                                                   5760
      DREDTY=DREDT1                                                      5770
1     DREDTX=DREDTY/REX                                                  5780
      DK(1)=0.0                                                          5790
      DK(M)=0.0                                                          5800
      OMIKO(1)=0.0                                                       5810
      CDP(1)=0.0                                                         5820
      SCDP(1)=0.0                                                        5830
      CDF(1)=0.0                                                         5840
      CDF(M)=0.0                                                         5850
      SCDF(1)=0.0                                                        5860
      DO 73 I=2,M                                                        5870
      DSRVT(I)=(4.*G(I,2,K5)-G(I,3,K5)-3.*G(I,1,K5))*DUMC                5880
      DK(I)=4.*(DSRVT(I)+SURVT(I))/REX+DENS*DREDTX*SI(I)/REX             5890
      OMIKO(I)=BOTWO*(DK(I-1)+DK(I))+OMIKO(I-1)                          5900
      CDP(I)=OMIKO(I)*2.*SI(I)*CO(I)                                     5910
      SCDP(I)=BOTWO*(CDP(I-1)+CDP(I))+SCDP(I-1)                          5920
      CDF(I)=8.*SURVT(I)*SI(I)*SI(I)/REX                                 5930
      SCDF(I)=BOTWO*(CDF(I-1)+CDF(I))+SCDF(I-1)                          5940
      CDX=SCDP(M)+SCDF(M)                                                5950
      DREDTZ=CONST1-CONST2*REX**2*CDX                                    5960
      REZ=REO+0.5*C*(DREDTZ+DREDT1)                                      5970
      XLIM=0.0005*REZ                                                    5985
      IF(ABS(REZ-REX).LT.XLIM) GO TO 2002                                5990
      REX=REZ                                                            6000
      DREDTY=DREDTZ                                                      6010
      JJS=JJS+1                                                          6020
      GO TO 4321                                                         6030
      RE2=REZ                                                            6040
      DREDT2=DREDTZ/RE2                                                  6050
      SCDFM=SCDF(M)                                                      6060
      SCDPM=SCDP(M)                                                      6070
      GO TO 2005                                                         6073
      NCONT=NCONT+1                                                      6076
      RE2=RE+0.95*C*(CONST1-CONST2*RE**2*CD)                             6079
      DREDT2=0.92*DREDT                                                  6082
      RETURN                                                             6085
      END                                                                6090
      SUBROUTINE VORTBD(K)                                               6100
      COMMON N,M,NM1,MM1,PSI(62,76,2),G(62,76,2)                         6110
      COMMON RE,RE2,DREDT,DREDT2,DUMA,DUMB,DUMC,DUMD,DUME                6120
      COMMON SI(62),COT(62),SII(62),COTT(62),X2(101),X4(101),X5(101)     6130
```

```
MON/BLK2/DUM1,DUM2,DUM3,DUM4,DUM5,DUM6,DUM7,TVV(101),DUM9,DUM8          6140
MON/BLK3/NEXIT,WW,NPT,EPS,DUDCOT(62),W,JJ,J2J,NCOUNT                    6150
                                                                        6152
ENSION SWX(10)                                                          6154
A SWX/0.3,0.3,0.32,0.32,0.34,0.34,0.4,0.5,0.6,0.7/                      6156
SWX(NCOUNT)                                                             6158
UNT=NCOUNT+1                                                            6159
NCOUNT.EQ.11)   NCOUNT=1                                                6160
IT=0                                                                    6170
100 I=2,MM1                                                             6180
0.5*(8.*PSI(I,2,K)-PSI(I,3,K))*DUMA*SII(I)                              6190
TVV(I)+SW*(BG-TVV(I))                                                   6200
ABS(BG-TVV(I)).GT.EPS) NEXIT=2                                          6210
,1,K)=BG                                                                6220
URN                                                                     6230
)
```

COMPUTER PROGRAM FOR CALCULATING THE FLOW IN AND AROUND A CIRCULATING SPHERICAL LIQUID DROPLET

```
      PROGRAM DROP2(INPUT,OUTPUT,PUNCHB,TAPE5=INPUT,TAPE6=OUTPUT,TAPE7=     0010
     1PUNCHB,TAPE8,TAPE9)                                                   0020
      SOLUTION OF THE NAVIER STOKES EQUATIONS FOR SPHERICAL DROPS           0030
      THIS PROGRAM IS THE SOLUTION OF TWO SECOND ORDER SIMULTANEOUS         0040
      PARTIAL  DIFFERENTIAL EQUATIONS FOR FLOW OUTSIDE A DROP COUPLED TO    0050
      THE SOLUTION OF THE TWO PDE'S WHICH REPRESENT THE FLOW INSIDE THE     0060
      DROP ---                                                              0070
                                                                            0080
      THIS PROGRAM IS CONTROLLED BY THE FOLLOWING PARAMETERS----            0090
      JRD---CONTROL FOR BEGINNING A NEW CALCULATION OR CONTINUING OLD       0100
      CALCULATION                                                           0110
            JRD=1  NEW CALCULATION---STOKES                                 0120
            JRD=2  OLD CALCULATION--READ DATA FROM CARDS                    0130
            JRD=3  OLD CALCULATION---READ DATA FROM TAPE ON TC1             0140
            JRD=4  NEW CALCULATION --KAWAGUTI                               0150
      JPT---CARD OR TAPE OUTPUT                                             0160
            JPT=1 TAPE OUTPUT ON TC1                                        0170
            JPT=2 CARD OUTOUT                                               0180
      NPT---MAXIMUM NUMBER OF LOOPS ALLOWED FOR ANY CASE                    0190
      JRRT---MAXIMUM NUMBER OF SEARCHES ALLOWED IN ANY CASE                 0200
      WWI,WWO--- CONVERGENCE RELAXATION FACTOR                              0210
      NEXIT--- ENTRY AND EXIT CONTROL AND INDICATOR                         0220
            0--NORMAL                                                       0230
            2--ENTRY AND EXIT OUTER SOLUTION                                0240
            4--ENTRY AND EXIT INNER SOLUTION                                0250
      PARAMETERS IN SOLUTION                                                0260
      N---NUMBER OF RADIAL MESH POINTS                                      0270
      M---NUMBER OF ANGULAR MESH POINTS                                     0280
      RE---REYNOLDS MUNBER                                                  0290
      A---RADIAL STEP SIZE                                                  0300
      W---VORTICITY RELAXATION FACTOR                                       0310
      WW---STREAM FUNCTION RELAXATION FACTOR                                0320
      EPS---TOLERANCE                                                       0330
      XVISC---VISCOSITY RATIO (INSIDE/OUTSIDE)                              0340
      XDENS---DENSITY RATIO (INSIDE/OUTSIDE)                                0350
      NINS---NUMBER OF RADIAL MESH POINTS INSIDE                            0360
      AINS---RADIAL STEP SIZE INSIDE                                        0370
      WINS---VORTICITY RELAXATION FACTOR INSIDE                             0380
      WWINS---STREAM FUNCTION RELAXATION FACTOR INSIDE                      0390
                                                                            0400
      COMMON N,M,RE,A,W,WW,EPS,JRD,JPT,NPT,NINS,XVISC,XDENS,WINS,WWINS      0410
      COMMON NN,NNINS,NNNINS,NM3,MM,B,AINS,A1,B1,C1,KM                      0420
      COMMON PSI(31,80),G(31,80),GI(31,40),PSII(31,40),SURVT(31),           0430
     1 OMIKO(31),BETA(31),ALPHA(31),DVORT(2),SCDP(2),DK(2),CDP(2),          0440
     2 CDF(2),THETA(31),COT(31),CO(31),SI(31),SII(31),ANGLE(31),            0450
     3 DUM3(80),DUM4(80),DUM27(80),DUM28(80),Z(80),XX(80),X2(80),           0460
     4 XXX2(80),ZI(40),XI2(40),XXXI2(40),SCDF(2),DKK(2),DUM26(80),          0470
     5 DUM25(80),DUM24(80),DUM23(80),DUM13(80)                              0480
      COMMON DUM1,DUM2,DUM5,DUM6,DUM7,DUM8,DUM9,DUM10,DUM11,DUM12,          0490
     1 DUM14,DUM15,DUM16,DUM17,DUM18,DUM19,DUM20,DUM21,DUM22,DUM29,         0500
     2 DUM30,DUM31,DUM32,DUM33,DUM34,DUM35,DUM36,DUM37,DUM38,DUM39,         0510
     3 DUM40,DUM41,DUM42                                                    0520
      COMMON /BLK1/ DVTHO(31),DVTHI(31),TRTHO(31),TRTHI(31),GNEWO(31),      0530
     1GNEWI(31)                                                             0540
      READ(5,1001)N,M,RE,A,W,WW,EPS                                         0550
      READ(5,1002)JRD,JPT,NPT,NEXIT                                         0560
      READ(5,1018)NINS,XVISC,XDENS,WINS,WWINS                               0570
      READ(5,1018) KM,A1,B1,C1                                              0580
      READ(5,1001)JRT,JRRT,WWO,WWI                                          0590
```

```
      NNINS=NINS-1                                                      0600
      NNNINS=NINS-2                                                     0610
      NM3=NINS-3                                                        0620
      AINS=1./FLOAT(NNINS)                                              0630
      NN=N-1                                                            0640
      MM=M+1                                                            0650
      B=3.1416/(FLOAT(M))                                               0660
      DVTHI(1)=0.0                                                      0670
      DVTHI(MM)=0.0                                                     0680
      DVTHO(1)=0.0                                                      0690
      DVTHO(MM)=0.0                                                     0700
      TRTHI(1)=0.0                                                      0710
      TRTHI(MM)=0.0                                                     0720
      TRTHO(1)=0.0                                                      0730
      TRTHO(MM)=0.0                                                     0740
      GNEWO(1)=0.                                                       0750
      GNEWI(1)=0.0                                                      0760
      GNEWO(MM)=0.0                                                     0770
      GNEWI(MM)=0.0                                                     0780
      CALL OUTPUT(1,NEXIT)                                              0790
      CALL VARIBLE                                                      0800
      CALL CONSTNT                                                      0810
      CALL BOUNDRY                                                      0820
      IOEXIT=0                                                          0830
      CALL INITIAL(IOEXIT)                                              0840
      IF(IOEXIT) 305,305,310                                            0850
      CALL OUTPUT(5,NEXIT)                                              0860
      JJ=0                                                              0870
      IF(NEXIT.EQ.2) GO TO 150                                          0880
      IF(NEXIT.EQ.4) GO TO 120                                          0890
      NEXIT=0                                                           0900
      DO 100 I=2,M                                                      0910
      DVTHO(I)=DUM42*(18.*PSI(I,2)-9.*PSI(I,3)+2.*PSI(I,4))/SI(I)       0920
      TRTHO(I)=(4.*PSI(I,3)-5.*PSI(I,2)-PSI(I,4))/(A*A*SI(I))-3.*DVTHO(I 0930
     1)                                                                 0940
      DVTHI(I)=DUM41*(9.*PSII(I,NNNINS)-18.*PSII(I,NNINS)-2.*PSII(I,NM3) 0950
     1)/SI(I)                                                           0960
      TRTHI(I)=(4.*PSII(I,NNNINS)-5.*PSII(I,NNINS)-PSII(I,NM3))*DUM30/  0970
     1SI(I)-2.*DVTHI(I)                                                 0980
      GNEWO(I)=(4.*PSI(I,3)-5.*PSI(I,2)-PSI(I,4))/(A*A)-DVTHO(I)*SI(I)  0990
      GNEWI(I)=(4.*PSII(I,NNNINS)-5.*PSII(I,NNINS)-PSII(I,NM3))*DUM30   1000
      CONTINUE                                                          1010
      CALL OUTPUT(2,NEXIT)                                              1020
      CALL AVERAGE                                                      1030
      CALL OUTPUT(6,NEXIT)                                              1040
      IF(JRT.EQ.JRRT) GO TO 200                                         1050
      CALL SOLVEOS(NEXIT,JJ)                                            1070
      IF(NEXIT.EQ.2) GO TO 200                                          1080
      CALL OUTPUT(3,NEXIT)                                              1090
      DO 110 I=2,M                                                      1100
      DVTHI(I)=DUM41*(9.*PSII(I,NNNINS)-18.*PSII(I,NNINS)-2.*PSII(I,NM3) 1110
     1)/SI(I)                                                           1120
      DVTHO(I)=DUM42*(18.*PSI(I,2)-9.*PSI(I,3)+2.*PSI(I,4))/SI(I)       1130
      TRTHO(I)=(4.*PSI(I,3)-5.*PSI(I,2)-PSI(I,4))/(A*A*SI(I))-3.*DVTHO(I 1140
     1)                                                                 1150
      GNEWO(I)=(4.*PSI(I,3)-5.*PSI(I,2)-PSI(I,4))/(A*A)-DVTHO(I)*SI(I)  1160
      GNEWI(I)=(4.*PSII(I,NNNINS)-5.*PSII(I,NNINS)-PSII(I,NM3))*DUM30   1170
      TRTHI(I)=(4.*PSII(I,NNNINS)-5.*PSII(I,NNINS)-PSII(I,NM3))*DUM30/  1180
```

```
)-2.*DVTHI(I)                                                          1190
. OUTPUT(2,NEXIT)                                                      1200
. AVERAGE                                                              1210
. OUTPUT(6,NEXIT)                                                      1220
JRT.GE.JRRT) GO TO 200                                                 1230
=JRT+1                                                                 1240
L SOLVEIS(NEXIT,JJ)                                                    1260
NEXIT.EQ.4) GO TO 200                                                  1270
L OUTPUT(3,NEXIT)                                                      1280
TO 270                                                                 1290
TINUE                                                                  1300
L OUTPUT(3,NEXIT)                                                      1310
L OUTPUT(5,NEXIT)                                                      1320
P                                                                      1330
MAT(2I5,5F10.0)                                                        1340
MAT(4I5)                                                               1350
MAT(I5,4F10.0)                                                         1360
)                                                                      1370
BROUTINE AVERAGE                                                       1380
MMON N,M,RE,A,W,WW,EPS,JRD,JPT,NPT,NINS,XVISC,XDENS,WINS,WWINS         1390
MMON NN,NNINS,NNNINS,NM3,MM,B,AINS,A1,B1,C1,KM                         1400
MMON PSI(31,80),G(31,80),GI(31,40),PSII(31,40),SURVT(31),              1410
MIKO(31),BETA(31),ALPHA(31),DVORT(2),SCDP(2),DK(2),CDP(2),             1420
DF(2),THETA(31),COT(31),CO(31),SI(31),SII(31),ANGLE(31),               1430
UM3(80),DUM4(80),DUM27(80),DUM28(80),Z(80),XX(80),X2(80),              1440
XX2(80),ZI(40),XI2(40),XXXI2(40),SCDF(2),DKK(2),DUM26(80),             1450
UM25(80),DUM24(80),DUM23(80),DUM13(80)                                 1460
MMON DUM1,DUM2,DUM5,DUM6,DUM7,DUM8,DUM9,DUM10,DUM11,DUM12,             1470
UM14,DUM15,DUM16,DUM17,DUM18,DUM19,DUM20,DUM21,DUM22,DUM29,            1480
UM30,DUM31,DUM32,DUM33,DUM34,DUM35,DUM36,DUM37,DUM38,DUM39,            1490
UM40,DUM41,DUM42                                                       1500
 71 I=2,M                                                              1510
RVT(I)=G(I,1)/SI(I)                                                    1520
RVT(1)=0.0                                                             1530
RVT(MM)=0.0                                                            1540
(1)=0.0                                                                1550
IKO(1)=0.0                                                             1560
P(1)=0.0                                                               1570
K(1)=0.0                                                               1580
DP(1)=0.0                                                              1590
F(1)=0.0                                                               1600
DF(1)=0.0                                                              1610
 73 I=2,MM                                                             1620
(I.EQ.MM) GO TO 72                                                     1630
RVT=DUM9*(4.*G(I,2)/XX(2)-G(I,3)/XX(3)-3.*G(I,1))/SI(I)                1640
VEL=DUM9*(4.*PSI(I,2)-PSI(I,3))/SI(I)                                  1650
VEL=DSVEL*DSVEL                                                        1660
(2)=DUM15*(DSRVT+SURVT(I))                                             1670
 TO 733                                                                1680
(2)=0.0                                                                1690
VEL=0.0                                                                1700
K(2)=DUM17*(DK(1)+DK(2))+DKK(1)                                        1710
IKO(I)=DKK(2)-SRVEL                                                    1720
P(2)=OMIKO(I)*2.*SI(I)*CO(I)                                           1730
DP(2)=DUM17*(CDP(1)+CDP(2))+SCDP(1)                                    1740
(I.EQ.MM) GO TO 734                                                    1750
F(2)=SI(I)*((4.*PSI(I,3)-5.*PSI(I,2)-PSI(I,4))*DUM36-(18.*PSI(I,       1760
-9.*PSI(I,3)+2.*PSI(I,4))*DUM38)+CO(I)*DUM37*(18.*(PSI(I+1,2)-         1770
```

```
PSI(I-1,2))-9.*(PSI(I+1,3)-PSI(I-1,3))+2.*(PSI(I+1,4)-PSI(I-1,4))
O TO 735
DF(2)=0.0
CDF(2)=DUM40*(CDF(1)+CDF(2))+SCDF(1)
K(1)=DK(2)
KK(1)=DKK(2)
DP(1)=CDP(2)
CDP(1)=SCDP(2)
DF(1)=CDF(2)
SCDF(1)=SCDF(2)
O 74 I=1,MM
ALPHA(I)=0.5*G(I,1)
BETA(I)=DUM18*(3.*PSI(I,1)-4.*PSI(I,2)+PSI(I,3))
OK=0.
DVORT(1)=DUM21*G(2,1)/XX(1)-DUM22*G(3,1)/XX(1)
O 32 J=2,N
DVORT(2)=DUM21*G(2,J)/XX(J)-DUM22*G(3,J)/XX(J)
OK=DUM19*(DVORT(1)+DVORT(2))+OK
DVORT(1)=DVORT(2)
OK=1.+8.*OK/RE
O 33 I=1,MM
OMIKO(I)=OMIKO(I)+OK
RETURN
END
SUBROUTINE CONSTNT
COMMON N,M,RE,A,W,WW,EPS,JRD,JPT,NPT,NINS,XVISC,XDENS,WINS,WWINS
COMMON NN,NNINS,NNNINS,NM3,MM,B,AINS,A1,B1,C1,KM
COMMON PSI(31,80),G(31,80),GI(31,40),PSII(31,40),SURVT(31),
1 OMIKO(31),BETA(31),ALPHA(31),DVORT(2),SCDP(2),DK(2),CDP(2),
2 CDF(2),THETA(31),COT(31),CO(31),SI(31),SII(31),ANGLE(31),
3 DUM3(80),DUM4(80),DUM27(80),DUM28(80),Z(80),XX(80),X2(80),
4 XXX2(80),ZI(40),XI2(40),XXXI2(40),SCDF(2),DKK(2),DUM26(80),
5 DUM25(80),DUM24(80),DUM23(80),DUM13(80)
COMMON DUM1,DUM2,DUM5,DUM6,DUM7,DUM8,DUM9,DUM10,DUM11,DUM12,
1 DUM14,DUM15,DUM16,DUM17,DUM18,DUM19,DUM20,DUM21,DUM22,DUM29,
2 DUM30,DUM31,DUM32,DUM33,DUM34,DUM35,DUM36,DUM37,DUM38,DUM39,
3 DUM40,DUM41,DUM42
DUM1=B*B*((2.-A)/2.)
DUM2=B*B*((2.+A)/2.)
DUM5=A*A*B*B
DUM6=1./(2.*(A*A+B*B))
DUM7=1./A
DUM8=RE*DUM5/4.
DUM9=1./(2.*A)
DUM10=1./(2.*B)
DUM11=A*A/2.
DUM12=DUM9/B
DUM14=0.5*DUM10
DUM15=4.0/RE
DUM17=B/2.0
DUM18=1./(4.*A**3)
DUM19=A/2.
DUM20=8./RE
DUM21=2./(B*SI(2))
DUM22=1./(2.*B*SI(3))
DUM142=DUM8*DUM12
DO 41 I=2,M
```

```
 13(I)=DUM142*SI(I)                                                      2360
 3(I)=DUM11*(2.-B*COT(I))                                                2370
 4(I)=DUM11*(2.+B*COT(I))                                                2380
 141=RE*XDENS/(8.*AINS*B*XVISC)                                          2390
 230 J=2,NNINS                                                           2400
 140=2.*(B*B*XI2(J)+AINS*AINS)                                           2410
 123(J)=B*B*XI2(J)/DUM140                                                2420
 124(J)=AINS*AINS/DUM140                                                 2430
 125(J)=AINS*AINS*DUM23(J)                                               2440
 128(J)=DUM25(J)*DUM141                                                  2450
 231 I=2,M                                                               2460
 426(I)=1.+B*COT(I)/2.                                                   2470
 427(I)=1.-B*COT(I)/2.                                                   2480
 429=1./(2.*AINS)                                                        2490
 M30=1./(AINS*AINS)                                                      2500
 M31=1./(6.*A)                                                           2810
 M32=2.*(1.-1./XVISC)                                                    2520
 M33=1./XVISC                                                            2530
 M34=(1.-XVISC)/(3.*A)                                                   2540
 M35=XVISC/(AINS*AINS)                                                   2550
 M36=DUM7*DUM7                                                           2560
 M37=2./(12.*A*B)                                                        2570
 M38=3./(6.*A)                                                           2580
 M40=DUM17*8./RE                                                         2590
 M41=1./(6.*AINS)                                                        2600
 M42=1./(6.*A)                                                           2610
ETURN                                                                    2620
ND                                                                       2630
UBROUTINE SOLVEOS(NEXIT,JJ)                                              2640
OMMON N,M,RE,A,W,WW,EPS,JRD,JPT,NPT,NINS,XVISC,XDENS,WINS,WWINS          2650
OMMON NN,NNINS,NNNINS,NM3,MM,B,AINS,A1,B1,C1,KM                          2960
OMMON PSI(31,80),G(31,80),GI(31,40),PSII(31,40),SURVT(31),               2670
OMIKO(31),BETA(31),ALPHA(31),DVORT(2),SCDP(2),DK(2),CDP(2),              2680
CDF(2),THETA(31),COT(31),CO(31),SI(31),SII(31),ANGLE(31),                2690
DUM3(80),DUM4(80),DUM27(80),DUM28(80),Z(80),XX(80),X2(80),               2700
XXX2(80),ZI(40),XI2(40),XXXI2(40),SCDF(2),DKK(2),DUM26(80),              2710
DUM25(80),DUM24(80),DUM23(80),DUM13(80)                                  2720
OMMON DUM1,DUM2,DUM5,DUM6,DUM7,DUM8,DUM9,DUM10,DUM11,DUM12,              2730
DUM14,DUM15,DUM16,DUM17,DUM18,DUM19,DUM20,DUM21,DUM22,DUM29,             2740
DUM30,DUM31,DUM32,DUM33,DUM34,DUM35,DUM36,DUM37,DUM38,DUM39,             2750
DUM40,DUM41,DUM42                                                        2760
EXIT=1                                                                   2770
I=0                                                                      2780
O 35 I=2,M                                                               2790
O 35 J=2,NN                                                              2800
UMA=G(I,J+1)*SII(I)*XXX2(J+1)                                            2810
UMC=G(I,J-1)*SII(I)*XXX2(J-1)                                            2820
F(I.EQ.2) GO TO 45                                                       2830
UMD=G(I-1,J)*SII(I-1)*XXX2(J)                                            2840
O TO 50                                                                  2850
UMD=G(2,J)/(X2(J)*B*SI(2))                                               2860
F(I.EQ.M) GO TO 55                                                       2870
UMB=G(I+1,J)*SII(I+1)*XXX2(J)                                            2880
O TO 60                                                                  2890
UMB=G(M,J)/(X2(J)*B*SI(M))                                               2900
TRMF=DUM6*(PSI(I,J+1)*DUM1+PSI(I,J-1)*DUM2+PSI(I+1,J)*DUM3(I)            2910
 +PSI(I-1,J)*DUM4(I)-DUM5*G(I,J)*X2(J))                                  2920
TRMF=PSI(I,J)+WW*(STRMF-PSI(I,J))                                        2930
```

```
PSI=(PSI(I,J+1)-PSI(I,J-1))*(DUMB-DUMD)-(PSI(I+1,J)-PSI(I-1,J))*(      2940
UMA-DUMC)                                                              2950
ORT=DUM6*(G(I,J+1)*DUM1+G(I,J-1)*DUM2+G(I+1,J)*DUM3(I)+                2960
 G(I-1,J)*DUM4(I)-DUM13(I)*XX(J)*DPSI)                                 2970
ORT=G(I,J)+W*(VORT-G(I,J))                                             2980
F (ABS(STRMF-PSI(I,J)).GT.EPS)  II=1                                   2990
SI(I,J)=STRMF                                                          3000
F(ABS(VORT-G(I,J)).GT.EPS) II=1                                        3010
(I,J)=VORT                                                             3020
ONTINUE                                                                3030
F(II.NE.1) GO TO 877                                                   3040
IJ=JJ+1                                                                3050
F(JJ.LE.NPT) GO TO 100                                                 3060
IEXIT=2                                                                3070
RETURN                                                                 3080
END                                                                    3090
SUBROUTINE BOUNDRY                                                     3100
COMMON N,M,RE,A,W,WW,EPS,JRD,JPT,NPT,NINS,XVISC,XDENS,WINS,WWINS       3110
COMMON NN,NNINS,NNNINS,NM3,MM,B,AINS,A1,B1,C1,KM                       3120
COMMON PSI(31,80),G(31,80),GI(31,40),PSII(31,40),SURVT(31),            3130
 OMIKO(31),BETA(31),ALPHA(31),DVORT(2),SCDP(2),DK(2),CDP(2),           3140
 CDF(2),THETA(31),COT(31),CO(31),SI(31),SII(31),ANGLE(31),             3150
 DUM3(80),DUM4(80),DUM27(80),DUM28(80),Z(80),XX(80),X2(80),            3160
 XXX2(80),ZI(40),XI2(40),XXXI2(40),SCDF(2),DKK(2),DUM26(80),           3170
 DUM25(80),DUM24(80),DUM23(80),DUM13(80)                               3180
COMMON DUM1,DUM2,DUM5,DUM6,DUM7,DUM8,DUM9,DUM10,DUM11,DUM12,           3190
 DUM14,DUM15,DUM16,DUM17,DUM18,DUM19,DUM20,DUM21,DUM22,DUM29,          3200
 DUM30,DUM31,DUM32,DUM33,DUM34,DUM35,DUM36,DUM37,DUM38,DUM39,          3210
 DUM40,DUM41,DUM42                                                     3220
DO 10 I=1,MM                                                           3250
PSI(I,1)=0.0                                                           3260
DO 15 J=1,N                                                            3280
G(1,J)=0.0                                                             3290
PSI(1,J)=0.0                                                           3300
G(MM,J)=0.0                                                            3310
PSI(MM,J)=0.0                                                          3320
DO 20 I=1,MM                                                           3340
PSI(I,N)=0.5*(SI(I)**2*X2(N))                                          3350
G(I,N)=0.0                                                             3360
DO 200 I=1,MM                                                          3390
PSII(I,NINS)=0.0                                                       3400
DO 201 J=1,NINS                                                        3420
GI(1,J)=0.0                                                            3430
PSII(1,J)=0.0                                                          3440
GI(MM,J)=0.0                                                           3450
PSII(MM,J)=0.0                                                         3460
DO 202 I=1,MM                                                          3480
PSII(I,1)=0.0                                                          3490
GI(I,1)=0.0                                                            3500
RETURN                                                                 3510
END                                                                    3520
SUBROUTINE INITIAL(IOEXIT)                                             3530
COMMON N,M,RE,A,W,WW,EPS,JRD,JPT,NPT,NINS,XVISC,XDENS,WINS,WWINS       3540
COMMON NN,NNINS,NNNINS,NM3,MM,B,AINS,A1,B1,C1,KM                       3550
COMMON PSI(31,80),G(31,80),GI(31,40),PSII(31,40),SURVT(31),            3560
 OMIKO(31),BETA(31),ALPHA(31),DVORT(2),SCDP(2),DK(2),CDP(2),           3570
 CDF(2),THETA(31),COT(31),CO(31),SI(31),SII(31),ANGLE(31),             3580
 DUM3(80),DUM4(80),DUM27(80),DUM28(80),Z(80),XX(80),X2(80),            3590
```

```
(XX2(80),ZI(40),XI2(40),XXXI2(40),SCDF(2),DKK(2),DUM26(80),          3600
)UM25(80),DUM24(80),DUM23(80),DUM13(80)                              3610
OMMON DUM1,DUM2,DUM5,DUM6,DUM7,DUM8,DUM9,DUM10,DUM11,DUM12,          3620
DUM14,DUM15,DUM16,DUM17,DUM18,DUM19,DUM20,DUM21,DUM22,DUM29,         3630
DUM30,DUM31,DUM32,DUM33,DUM34,DUM35,DUM36,DUM37,DUM38,DUM39,         3640
DUM40,DUM41,DUM42                                                    3650
)O.TO (9,417,93,84),JRD                                              3660
(EAD(5) ((PSI(I,J),I=1,MM),J=1,N)                                    3670
(EAD (5) ((G(I,J),I=1,MM),J=1,N)                                     3680
(EAD(5)((PSII(I,J),I=1,MM),J=1,NINS)                                 3690
(EAD(5)((GI(I,J),I=1,MM),J=1,NINS)                                   3700
GO TO 26                                                             3710
IOEXIT=1                                                             3720
REWIND 9                                                             3730
READ(9) ((PSI(I,J),I=1,MM),J=1,N)                                    3740
IF(EOF,9)94,95                                                       3750
IOEXIT=2                                                             3760
READ (9) ((G(I,J),I=1,MM),J=1,N)                                     3770
IF(EOF,9)94,96                                                       3780
IOEXIT=3                                                             0790
READ(9)((PSII(I,J),I=1,MM),J=1,NINS)                                 3800
IF(EOF,9)94,97                                                       3810
IOEXIT=4                                                             3820
READ(9)((GI(I,J),I=1,MM),J=1,NINS)                                   3830
IF(EOF,9)94,98                                                       3840
IOEXIT=0                                                             3850
REWIND 9                                                             3860
GO TO 26                                                             3870
WRITE(6,99)IOEXIT                                                    3880
FORMAT(10X 12H END OF FILE ,I5)                                      3890
GO TO 26                                                             3900
XVISC1=-0.25/(1.+XVISC)                                              3910
XVISC2=2.5/(1.+XVISC)                                                3920
XVISC3=0.5*(3.*XVISC+2.)/(1.+XVISC)                                  3930
XVISC4=0.25*(3.*XVISC+2.)/(1.+XVISC)                                 3940
XVISC5=0.25*XVISC/(1.+XVISC)                                         3950
A1=XVISC3                                                            3960
B1=0.0                                                               3970
C1=0.0                                                               3980
DO 30 I=2,M                                                          3990
SIIJ2=SI(I)**2                                                       4000
G(I,1)=XVISC3*SIIJ2                                                  4010
DO 30 J=2,NN                                                         4020
PSI(I,J)=SIIJ2*(0.5*X2(J)-XVISC4*XX(J)+XVISC5/XX(J))                 4300
G(I,J)=XVISC3*SIIJ2/XX(J)                                            4040
DO 210 I=2,M                                                         4050
SIIJ3=SI(I)**2                                                       4060
GI(I,NINS)=XVISC2*SIIJ3                                              4070
DO 210 J=2,NNINS                                                     4080
PSII(I,J)=XVISC1*SIIJ3*XI2(J)*(1.-XI2(J))                            4090
GI(I,J)=XVISC2*SIIJ3*XI2(J)                                          4100
GO TO 26                                                             4110
DUM100=8.+3.*XVISC                                                   4120
DUM101=6.+3.*XVISC                                                   4130
DUM102=14.+6.*XVISC                                                  4140
A2=-(10.+7.5*XVISC)/DUM100-DUM102/DUM100*A1                          4150
A3=(6.+6.*XVISC)/DUM100+DUM101/DUM100*A1                             4160
A4=2.*A1                                                             4170
```

```
      A5=6.*A2                                                          4180
      A6=12.*A3                                                         4190
      B2=-DUM102/DUM100*B1                                              4200
      B3=DUM101/DUM100*B1                                               4210
      B4=2.*B1                                                          4220
      B5=6.*B2                                                          4230
      B6=12.*B3                                                         4240
      C11=-5./DUM100-A1/DUM100                                          4250
      C31=-C11                                                          4260
      D11=-B1/DUM100                                                    4270
      D31=-D11                                                          4280
      C12=2.*C11                                                        4290
      C32=12.*C31                                                       4300
      D12=2.*D11                                                        4310
      D32=12.*D31                                                       4320
      DO 300 I=2,M                                                      4330
      SIN2=SI(I)**2                                                     4340
      SIN2CO=SIN2*CO(I)                                                 4350
      DO 100 J=1,NN                                                     4360
      XOX=1./XX(J)                                                      4370
      XOX3=XOX**3                                                       4380
      PSI(I,J)=(0.5*XX(J)+XOX*(A1+XOX*(A2+XOX*A3)))*SIN2+XOX*(B1+XOX*(B2 4390
     1 +XOX*B3))*SIN2CO                                                 4400
      G(I,J)=(1.+XOX3*(A4+XOX*(A5+XOX*A6)))*SIN2+XOX3*(B4+XOX*(B5+XOX*B6 4410
     1 ))*SIN2CO                                                        4420
      DO 200 J=2,NINS                                                   4430
      XIX=ZI(J)**2                                                      4440
      PSII(I,J)=XIX*(C11+XIX*C31)*SIN2+XIX*(D11+XIX*D31)*SIN2CO         4450
      GI(I,J)=(C12+C32*XIX)*SIN2+(D12+D32*XIX)*SIN2CO                   4460
      PSII(I,NINS)=0.0                                                  4470
      PSI(I,1)=0.0                                                      4480
      IF(KM.EQ.0) GO TO 27                                              4490
      READ(5,28)(G(I,1),I=1,MM)                                         4500
      READ(5,28)(GI(I,NINS),I=1,MM)                                     4510
      DO 25 I=2,M                                                       4520
      GI(I,NINS)=GI(I,NINS)*SI(I)                                       4530
      G(I,1)=G(I,1)*SI(I)                                               4540
      RETURN                                                            4550
      FORMAT(8F10.0)                                                    4560
      END                                                               4570
      SUBROUTINE VARIBLE                                                4580
      COMMON N,M,RE,A,W,WW,EPS,JRD,JPT,NPT,NINS,XVISC,XDENS,WINS,WWINS  4590
      COMMON NN,NNINS,NNNINS,NM3,MM,B,AINS,A1,B1,C1,KM                  4600
      COMMON PSI(31,80),G(31,80),GI(31,40),PSII(31,40),SURVT(31),       4610
     1 OMIKO(31),BETA(31),ALPHA(31),DVORT(2),SCDP(2),DK(2),CDP(2),      4620
     2 CDF(2),THETA(31),COT(31),CO(31),SI(31),SII(31),ANGLE(31),        4630
     3 DUM3(80),DUM4(80),DUM27(80),DUM28(80),Z(80),XX(80),X2(80),       4640
     4 XXX2(80),ZI(40),XI2(40),XXXI2(40),SCDF(2),DKK(2),DUM26(80),      4650
     5 DUM25(80),DUM24(80),DUM23(80),DUM13(80)                          4660
      COMMON DUM1,DUM2,DUM5,DUM6,DUM7,DUM8,DUM9,DUM10,DUM11,DUM12,      4670
     1 DUM14,DUM15,DUM16,DUM17,DUM18,DUM19,DUM20,DUM21,DUM22,DUM29,     4680
     2 DUM30,DUM31,DUM32,DUM33,DUM34,DUM35,DUM36,DUM37,DUM38,DUM39,     4690
     3 DUM40,DUM41,DUM42                                                4700
      Z(1)=0.0                                                          4710
      ZI(1)=0.0                                                         4720
      THETA(1)=0.0                                                      4730
      THETA(2)=B                                                        4740
      DO 90 I=2,M                                                       4750
```

```
      THETA(I+1)=THETA(I)+B                                              4760
      CO(I)=COS(THETA(I))                                                4770
      SI(I)=SIN(THETA(I))                                                4780
      SII(I)=1./(SI(I)**2)                                               4790
      COT(I)=CO(I)/SI(I)                                                 4800
      THTC=57.2956                                                       4810
      DO 27 I=1,MM                                                       4820
      ANGLE(I)=THETA(I)*THTC                                             4830
      SI(1)=0.0                                                          4840
      CO(1)=1.0                                                          4850
      SI(MM)=0.0                                                         4860
      CO(MM)=-1.0                                                        4870
      COT(1)=0.0                                                         4880
      COT(MM)=0.0                                                        4890
      DO 91 J=1,NN                                                       4900
      Z(J+1)=Z(J)+A                                                      4910
      XX(J)=EXP(Z(J))                                                    4920
      X2(J)=XX(J)**2                                                     4930
      XXX2(J)=1./X2(J)                                                   4940
      XX(N)=EXP(Z(N))                                                    4950
      X2(N)=XX(N)**2                                                     4960
      XXX2(N)=1./X2(N)                                                   4970
      ZI(2)=AINS                                                         4980
      DO 203 J=2,NNINS                                                   4990
      ZI(J+1)=ZI(J)+AINS                                                 5000
      XI2(J)=ZI(J)**2                                                    5010
      XXXI2(J)=1./XI2(J)                                                 5020
      XI2(NINS)=ZI(NINS)**2                                              5030
      XXXI2(NINS)=1./XI2(NINS)                                           5040
      XI2(1)=0.0                                                         5050
      XXXI2(1)=0.0                                                       5060
      RETURN                                                             5070
      END                                                                5080
      SUBROUTINE OUTPUT(NOUT,NEXIT)                                      5090
      COMMON N,M,RE,A,W,WW,EPS,JRD,JPT,NPT,NINS,XVISC,XDENS,WINS,WWINS   5100
      COMMON NN,NNINS,NNNINS,NM3,MM,B,AINS,A1,B1,C1,KM                   5110
      COMMON PSI(31,80),G(31,80),GI(31,40),PSII(31,40),SURVT(31),        5120
     1 OMIKO(31),BETA(31),ALPHA(31),DVORT(2),SCDP(2),DK(2),CDP(2),       5130
     2 CDF(2),THETA(31),COT(31),CO(31),SI(31),SII(31),ANGLE(31),         5140
     3 DUM3(80),DUM4(80),DUM27(80),DUM28(80),Z(80),XX(80),X2(80),        5150
     4 XXX2(80),ZI(40),XI2(40),XXXI2(40),SCDF(2),DKK(2),DUM26(80),       5160
     5 DUM25(80),DUM24(80),DUM23(80),DUM13(80)                          5170
      COMMON DUM1,DUM2,DUM5,DUM6,DUM7,DUM8,DUM9,DUM10,DUM11,DUM12,       5180
     1 DUM14,DUM15,DUM16,DUM17,DUM18,DUM19,DUM20,DUM21,DUM22,DUM29,      5190
     2 DUM30,DUM31,DUM32,DUM33,DUM34,DUM35,DUM36,DUM37,DUM38,DUM39,      5200
     3 DUM40,DUM41,DUM42                                                5210
      COMMON /BLK1/ DVTHO(31),DVTHI(31),TRTHO(31),TRTHI(31),GNEWO(31),   5220
     1GNEWI(31)                                                          5230
      DIMENSION SURNT(31)                                                5240
      GO TO (10,20,30,40,50,60),NOUT                                     5250
      WRITE(6,1003)                                                      5260
      WRITE(6,1019)RE,A,W,WW,EPS                                         5270
      WRITE(6,1019)AINS,XVISC,XDENS,WINS,WWINS                           5280
      WRITE(6,1006)N,M,NINS,JRD,JPT,NPT                                  5290
      WRITE(6,1019) A1,B1,C1                                             5300
      WRITE(6,1006) KM                                                   5310
      GO TO 100                                                          5320
      WRITE(6,2003)                                                      5330
```

```
WRITE(6,996)(DVTHI(I),I=1,MM)                                          5340
WRITE(6,2004)                                                          5350
WRITE(6,996)(DVTHO(I),I=1,MM)                                          5360
WRITE(6,2007)                                                          5370
WRITE(6,996)(TRTHI(I),I=1,MM)                                          5380
WRITE(6,2006)                                                          5390
WRITE(6,996)(TRTHO(I),I=1,MM)                                          5400
WRITE(6,2009)                                                          5410
WRITE(6,996) (GNEWO(I),I=1,MM)                                         5420
WRITE(6,2010)                                                          5430
WRITE(6,996) (G(I,1),I=1,MM)                                           5440
WRITE(6,2011)                                                          5450
WRITE(6,996) (GNEWI(I),I=1,MM)                                         5460
WRITE(6,2012)                                                          5470
WRITE(6,996)(GI(I,NINS),I=1,MM)                                        5480
SURNT(1)=0.0                                                           5490
SURNT(MM)=0.0                                                          5500
DO 21 I=2,M                                                            5510
SURNT(I)=GI(I,NINS)/SI(I)                                              5520
CONTINUE                                                               5530
WRITE(6,2008)                                                          5540
WRITE(6,996)(SURNT(I),I=1,MM)                                          5550
GO TO 100                                                              5560
GO TO (97,877),JPT                                                     5570
WRITE(7)((PSI(I,J),I=1,MM),J=1,N)                                      5580
WRITE(7) ((G(I,J),I=1,MM),J=1,N)                                       5590
WRITE(7)((PSII(I,J),I=1,MM),J=1,NINS)                                  5600
WRITE(7)((GI(I,J),I=1,MM),J=1,NINS)                                    5610
GO TO 100                                                              5620
REWIND 8                                                               5630
WRITE(8) ((PSI(I,J),I=1,MM),J=1,N)                                     5640
WRITE(8) ((G(I,J),I=1,MM),J=1,N)                                       5650
WRITE(8)((PSII(I,J),I=1,MM),J=1,NINS)                                  5660
WRITE(8)((GI(I,J),I=1,MM),J=1,NINS)                                    5670
ENDFILE 8                                                              5680
REWIND 8                                                               5690
GO TO 100                                                              5700
WRITE (6,994) I,J                                                      5710
WRITE(6,997)                                                           5720
WRITE(6,1017) NEXIT                                                    5730
WRITE(6,1020)                                                          5740
LL1=1                                                                  5750
DO 8000 LLLL=1,5                                                       5760
LL2=LL1+14                                                             5770
IF(LL2.GE.MM) LL2=MM                                                   5780
WRITE(6,997)                                                           5790
WRITE(6,999)(ANGLE(I),I=LL1,LL2)                                       5800
WRITE(6,997)                                                           5810
WRITE(6,998)(Z(J),(PSI(I,J),I=LL1,LL2),J=1,N)                          5820
WRITE(6,997)                                                           5830
WRITE(6,998)(Z(J),(G(I,J),I=LL1,LL2),J=1,N)                            5840
IF(LL2.EQ.MM) GO TO 8001                                               5850
LL1=LL1+15                                                             5860
WRITE(6,997)                                                           5870
WRITE(6,1021)                                                          5880
LL1=1                                                                  5890
DO 8002 LLLL=1,5                                                       5900
LL2=LL1+14                                                             5910
```

```
      IF(LL2.GE.MM) LL2=MM                                                    5920
      WRITE(6,997)                                                            5930
      WRITE(6,999)(ANGLE(I),I=LL1,LL2)                                        5940
      WRITE(6,997)                                                            5950
      WRITE(6,998)(ZI(J),(PSII(I,J),I=LL1,LL2),J=1,NINS)                      5960
      WRITE(6,997)                                                            5970
      WRITE(6,998)(ZI(J),(GI(I,J),I=LL1,LL2),J=1,NINS)                        5980
      IF(LL2.EQ.MM) GO TO 8003                                                5990
   02 LL1=LL1+15                                                              6000
   03 GO TO 100                                                               6010
      WRITE (6,1009)                                                          6020
      WRITE (6,996) (SURVT(I),I=1,MM)                                         6030
      WRITE(6,1010)                                                           6040
      WRITE(6,996)(OMIKO(I),I=1,MM)                                           6050
      WRITE(6,1011)                                                           6060
      WRITE(6,996)(ALPHA(I),I=1,MM)                                           6070
      WRITE(6,1012)                                                           6080
      WRITE(6,996)(BETA(I),I=1,MM)                                            6090
      WRITE(6,1014)SCDF(1)                                                    6100
      WRITE(6,1013)SCDP(1)                                                    6110
      WRITE(6,997)                                                            6120
      WRITE(6,1004) OMIKO(1)                                                  6130
      WRITE(6,1017) NEXIT                                                     6140
   00 RETURN                                                                  6150
  992 FORMAT(3X,2F20.6)                                                       6160
  993 FORMAT(3X,2I5,F20.6,2I5,F20.6)                                          6170
  994 FORMAT (1H0,24HDIVERGING AT MESH POINT  ,2I4)                           6180
  996 FORMAT(1X,10F12.4)                                                      6190
  997 FORMAT(//)                                                              6200
  998 FORMAT(1X,F9.3,15F8.4)                                                  6210
  999 FORMAT (1H0,9X,15F8.2)                                                  6220
  003 FORMAT(1H1)                                                             6230
  004 FORMAT(F10.5)                                                           6240
  006 FORMAT(6(10X,I5))                                                       6250
 1009 FORMAT(1H0,1X,19HSURFACE VORTICITIES)                                   6260
 1010 FORMAT(1H0,1X,29HSURFACE PRESSURE DISTRIBUTION)                         6270
 1011 FORMAT(1H0,1X,18HALPHA*DISTRIBUTION)                                    6280
 1012 FORMAT(1H0,1X,17HBETA DISTRIBUTION)                                     6290
 1013 FORMAT(1H0,22H  THE PRESSURE DRAG IS,E12.6)                             6300
 1014 FORMAT(1H0,22H  THE FRICTION DRAG IS,E12.6)                             6310
  017 FORMAT(10X,I5)                                                          6320
  019 FORMAT(5(10X,F10.5))                                                    6330
  020 FORMAT(10X 43H STREAM FUNCTION AND VORTICITY OUTSIDE DROP )             6340
  021 FORMAT(10X 42H STREAM FUNCTION AND VORTICITY INSIDE DROP )              6350
  003 FORMAT( 10X 25H ANGULAR VELOCITY INSIDE  )                              6360
  004 FORMAT( 10X 26H ANGULAR VELOCITY OUTSIDE  )                             6370
  005 FORMAT(10X 27H OUTSIDE SURFACE VORTICITY  )                             6380
  006 FORMAT(10X 22H SHEAR STRESS OUTSIDE )                                   6390
  007 FORMAT(10X 21H SHEAR STRESS INSIDE )                                    6400
  008 FORMAT(10X 26H SURFACE VORTICITY INSIDE )                               6410
  009 FORMAT( 10X 35H SURFACE VALUE OUTSIDE FROM STREAM )                     6420
  010 FORMAT( 10X 23H SURFACE VALUE OUTSIDE )                                 6430
  011 FORMAT( 10X 34H SURFACE VALUE INSIDE FROM STREAM )                      6440
  012 FORMAT( 10X 22H SURFACE VALUE INSIDE )                                  6450
      END                                                                     6460
      SUBROUTINE SOLVEIS(NEXIT,JJ)                                            6470
      COMMON N,M,RE,A,W,WW,EPS,JRD,JPT,NPT,NINS,XVISC,XDENS,WINS,WWINS        6480
      COMMON NN,NNINS,NNNINS,NM3,MM,B,AINS,A1,B1,C1,KM                        6490
```

```
 COMMON PSI(31,80),G(31,80),GI(31,40),PSII(31,40),SURVT(31),
1 OMIKO(31),BETA(31),ALPHA(31),DVORT(2),SCDP(2),DK(2),CDP(2),
2 CDF(2),THETA(31),COT(31),CO(31),SI(31),SII(31),ANGLE(31),
3 DUM3(80),DUM4(80),DUM27(80),DUM28(80),Z(80),XX(80),X2(80),
4 XXX2(80),ZI(40),XI2(40),XXXI2(40),SCDF(2),DKK(2),DUM26(80),
5 DUM25(80),DUM24(80),DUM23(80),DUM13(80)
 COMMON DUM1,DUM2,DUM5,DUM6,DUM7,DUM8,DUM9,DUM10,DUM11,DUM12,
1 DUM14,DUM15,DUM16,DUM17,DUM18,DUM19,DUM20,DUM21,DUM22,DUM29,
2 DUM30,DUM31,DUM32,DUM33,DUM34,DUM35,DUM36,DUM37,DUM38,DUM39,
3 DUM40,DUM41,DUM42
 NEXIT=3
 II=0
 DO 235 I=2,M
 DO 235 J=2,NNINS
 DUMAI=GI(I,J+1)*SII(I)*XXXI2(J+1)
 IF(J.EQ.2) GO TO 261
 DUMCI=GI(I,J-1)*SII(I)*XXXI2(J-1)
 GO TO 262
 DUMCI=(4.*GI(I,2)/ZI(2)- GI(I,3)/ZI(3))*DUM29*SII(I)
 IF(I.EQ.2) GO TO 245
 DUMDI=GI(I-1,J)*SII(I-1)*XXXI2(J)
 GO TO 250
 DUMDI=GI(2,J)/(XI2(J)*B*SI(2))
 IF(I.EQ.M) GO TO 255
 DUMBI=GI(I+1,J)*SII(I+1)*XXXI2(J)
 GO TO 260
 DUMBI=GI(M,J)/(XI2(J)*B*SI(M))
 STRMFI=DUM23(J)*(PSII(I,J-1)+PSII(I,J+1))+DUM24(J)*(DUM26(I)*PSII(
1I-1,J)+DUM27(I)*PSII(I+1,J))-DUM25(J)*GI(I,J)
 STRMFI=PSII(I,J)+WWINS*(STRMFI-PSII(I,J))
 DPSII=(PSII(I,J+1)-PSII(I,J-1))*(DUMBI-DUMDI)-(PSII(I+1,J)-
1 PSII(I-1,J))*(DUMAI-DUMCI)
 VORTI=DUM23(J)*(GI(I,J+1)+GI(I,J-1))+DUM24(J)*(DUM26(I)*GI(I-1,J)+
1 DUM27(I)*GI(I+1,J))-DUM28(J)*SI(I)*DPSII
 VORTI=GI(I,J)+WINS*(VORTI-GI(I,J))
 IF(ABS(STRMFI-PSII(I,J)).GT.EPS) II=1
 PSII(I,J)=STRMFI
 IF(ABS(VORTI-GI(I,J)).GT.EPS) II=1
 GI(I,J)=VORTI
 CONTINUE
 IF(II.NE.1) GO TO 877
 JJ=JJ+1
 IF(JJ.LE.NPT) GO TO 100
 NEXIT=4
 RETURN
 END
```

PART II

MULTIPARTICLE SYSTEMS

A. Introduction

A.1 Assemblages of Spheres

In many fields of science and technology an extremely wide range of problems are concerned with fluid flow relative to assemblages of particles. Any hydrodynamic treatment therefore involves a considerable idealization with respect to the nature of the fluid, the nature of the solid medium, the proportion of fluid to solid and the relative motion of solids and fluids. However, theoretical transport equations do furnish a useful basis for achieving a uniform treatment and a better understanding of the principles underlying these phenomena.

The relative motion of solids and fluids can be divided into three areas, sedimentation, packed beds and fluidization or hindered settling. In sedimentation, particles settle under the influence of gravity and the fluid experiences no net motion. In packed beds, the particles are held immobile by contact with each other and the fluid passes through them. The solids concentration is normally very high in this situation. Intermediate situations between sedimentation and packed beds, where both particles and fluid may move are termed fluidization or hindered settling. In these three areas there are a great number of experimental correlations and semi-theoretical models in the literature. The papers have been collected together in several excellent monographs (Leva, 1959; Zenz and Othmer, 1960; and Happel and Brenner, 1965; Orr, 1966).

There is, however, a need for precise information on local velocity distributions about particles in such assemblages. For example, local velocity distributions could be used with the equations of continuity and energy to predict heat, mass, and chemical reaction rates. This information would allow chemical reaction rate data obtained in packed or fluidized beds to be properly interpreted. Local velocity data can only come from theoretical models as any experiment will give integrated results and local values with great difficulty.

The development of a theoretical model generally has followed either the continuum or cell (molecular) approach. In the continuum model approach the hydrodynamic forces and torques exerted on the particles by the fluid are generated taking into account all particle-particle and particle-fluid interactions, then solving this complicated problem in the bounded region. The cell model approach divides the assemblage into a number of identical cells, one particle occupying each cell. The boundary problem is thus reduced to the behaviour of a single particle and its bounding envelope.

The continuum approach is concerned with hydrodynamic forces and torques exerted by the fluid on the particles. When these are known, the inverse problem of determining the state of motion of the particles from known gravitational body forces and torques acting on them may be solved. The only exact solution of a multiparticle problem (creeping flow regime) where particle interaction has been accounted for in this way is that of Stimson and Jeffery (1928). They solved the problem of the slow motion of two spheres parallel to their line of centres making use of a system

of bipolar coordinates, which permits the simultaneous satisfaction of the boundary conditions on the two spheres. As the method has made use of bipolar coordinates, it cannot be extended to more than two particles. The essential features of the motion of two particles have also been predicted by Smoluchowski (1911). He found that spheres of the same size falling under gravity, fall together with constant separation. However, they only fall vertically when the line of centers is horizontal or vertical. Otherwise they tend to slide downwards along the line of centers. Experimental results of Hall (1936) agree qualitatively with these calculations for large particle separations.

Kynch (1959) derived expressions for the velocity of two spheres moving slowly under the external forces through a viscous fluid, as a function of their separation and radii. He then extended his treatment to three or more spheres. The expressions are so complicated that generalizations are possible for only a few cases. Brenner (1964) also has developed general relationships for multiparticle systems. Hasimoto (1959) obtained spatially periodic fundamental solutions of the Stokes equations of motion for viscous flow past a periodic array of spheres by use of Fourier Series. Three types of lattice were examined (simple cubic, face centered cubic and body centered cubic) with the solutions being expressed in terms of the drag on one of the spheres. However, although it has been possible to formulate continuum models of multiparticle systems and in some cases obtain solutions as in Hasimoto's case, generally solutions are too complicated to be useful or are impossible to obtain.

Cell models have received extensive use, however, because of the relative ease of obtaining significant results. Normally it is assumed that a three dimensional assemblage may be considered to consist of a number of identical unit cells, each of which contains a particle surrounded by a fluid envelope. The volume of the fluid envelope is sufficient to make the fractional void volume in the cell identical to that of the entire assemblage. The two most extensively used models are the Happel free surface model (1958) and the Kawabura zero vorticity model (1959).

The Kawabura model consists of an imaginary sphere of radius, b, enclosing the given sphere of radius, a. On the imaginary sphere, the vorticity and the normal component of velocity are assumed to be zero; while on the solid sphere the velocity is equal to the negative of the mean flow velocity (Figure A.1.A). Consider the situation of a two-dimensional mean flow from left to right (Figure A.2.A). The concept of zero vorticity on the outer imaginary boundary is plausible. For on the upper side of the sphere the vorticity will be positive and on the lower side negative. Therefore between the spheres there must be lines of zero vorticity (broken lines in Figure A.2.A). The streamlines must also be closed in the neighbourhood of the sphere in a reference system moving at the mean flow velocity (Figure A.2.B), otherwise the flow pattern would consist of a series of strips of fluid with alternating flow located side by side.

Happel's model consists of two concentric spheres, the inner one of radius a, is solid, and the outer one of radius b, is frictionless (no tangential shear stress on the outer envelope). Happel is of the

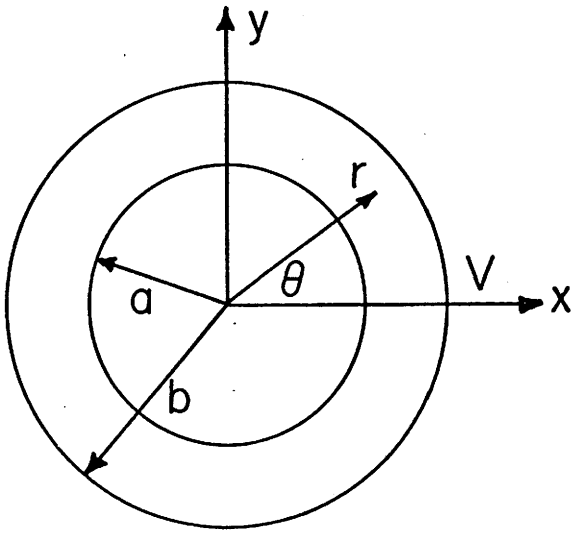

Boundary conditions

$r = a$

$U_x = V$

$v_y = v_z = 0$

$r = b$

$v_r = 0$

$$\mu\left(\frac{\partial v_\theta}{\partial r} - \frac{v_\theta}{r} + \frac{1}{r}\frac{\partial v_r}{\partial \theta}\right) = 0$$

$$1-\varepsilon = \phi = (a/b)^3$$

FIGURE A.1.A KAWABURA ZERO VORTICITY MODEL FOR SPHERES

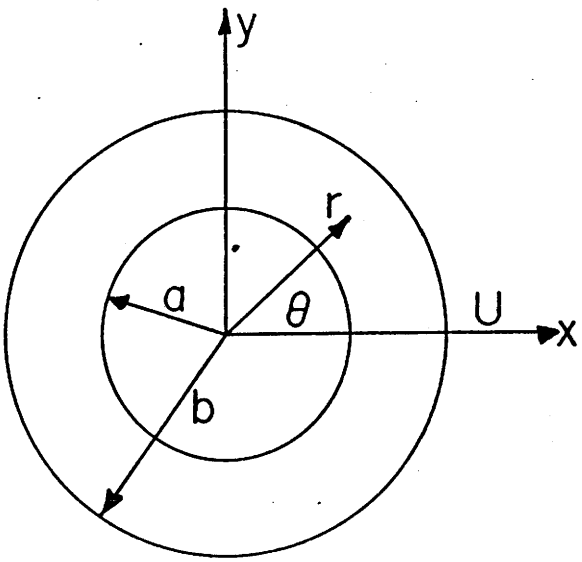

Boundary conditions

$r = a$

$v_r = v_\theta = 0$

$r = b$

$v_r = U\cos\theta$

$$\left(\frac{\partial v_\theta}{\partial r} + \frac{v_\theta}{r} - \frac{1}{r}\frac{\partial v_r}{\partial \theta}\right) = 0$$

$$1-\varepsilon = \phi = (a/b)^3$$

FIGURE A.1.B HAPPEL FREE SURFACE MODEL FOR SPHERES

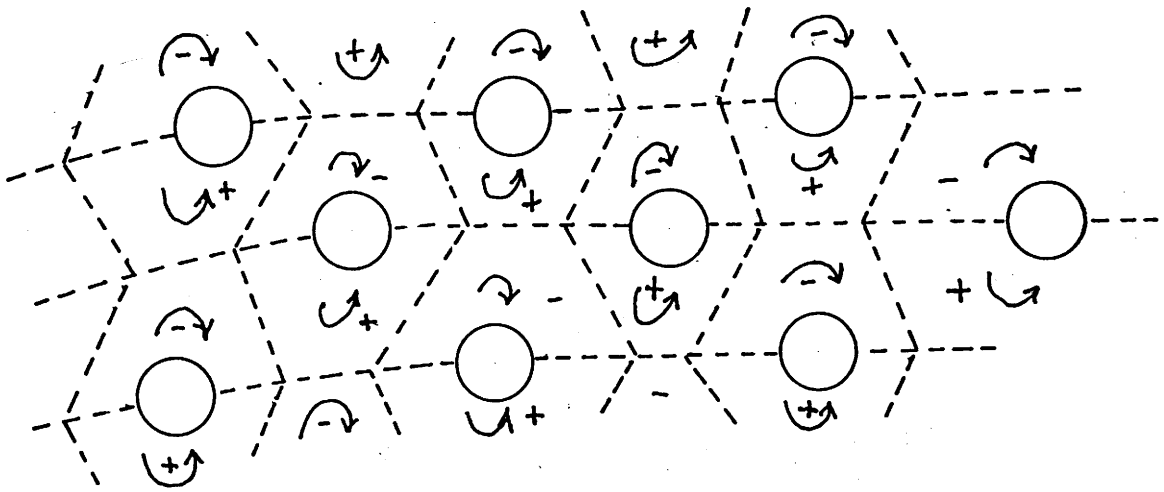

FIGURE A.2.A VORTICITY AROUND PARTICLES IN AN ASSEMBLAGE

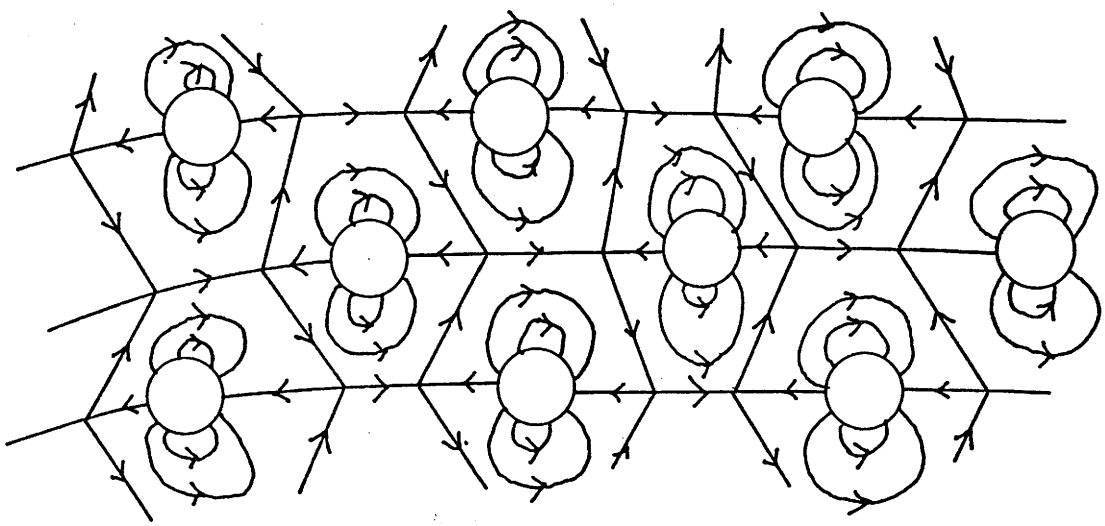

FIGURE A.2.B STREAM FUNCTION AROUND PARTICLES IN AN ASSEMBLAGE

opinion that a cell model should not require energy exchange with its surroundings or the assemblage cannot properly be considered as decomposed into independent cells. The entire disturbance due to each particle must be confined to the cell of fluid to which it is associated. Within the bounded region, the Navier Stokes equations omitting the inertia terms are taken to describe the fluid motion. The general solution after Lamb (1932) is applied to the boundary conditions using solid harmonics and the relative drag is found in terms of the liquid velocity and porosity of the bed.

Richardson and Zaki (1954) developed a semi-theoretical cell model for sedimenting spherical particles. The particles in the suspension model were arrayed in a hexagonal-type pattern in horizontal planes. Two models were proposed. In the first the vertical layers had the same spacing as the spacing between particles in the horizontal plane (Configuration I) and in the second, the vertical spacing was such that adjacent horizontal layers of spheres were in contact (Configuration II). In order to simplify the boundary conditions, it was assumed that each particle was surrounded by a cylinder of fluid with the same cross-sectional area as the hexagonal prism. The appropriate boundary conditions for symmetric flow with respect to adjacent particles and zero velocity at the particle surface were placed on the system and solutions obtained. In the development, the theoretical treatment was not rigourous and many assumptions were made. Satisfactory results are predicted for high concentrations of solids, howeverat low concentrations a decrease in drag is predicted as the calculated drag tends to zero as the particle

concentration approaches zero.

Gunn and Malik (1966) proposed a model for fluidized beds and sedimenting systems based upon arrays of particles where periodic conditions are established throughout the flow field. The model and boundary conditions are presented in Figure A.3. In the model the boundary conditions are such that the enclosing boundary is frictionless, therefore the total pressure drop across the cell can be equated to particle drag. As the mathematical difficulty of solving the equations subject to the boundary conditions was formidable; Gunn and Malik only presented some general properties of the solution in conjunction with experimental results.

Drag coefficients were determined for 30 distinct arrangements. The experimental results showed that geometric parameters distinctly affect the drag of the assemblage. For small Reynolds numbers, particles tend to form beds that offer a low resistance to flow and with increasing flow, perturbations, diminish the short range order of the particles.

The predicted results of the models are presented in Table A.1. In this table is tabulated the ratio of the drag in an assemblage to the drag in an infinite fluid as a function of solids concentration. Also included in this table are the results of the models of Happel and Ast (1960), Kawaguti (1958) and Wakiya (1953) which will be discussed in a later section. It should be noted that all these models apply only in the creeping flow regime. For comparison with experimental data the Richardson and Zaki (1954) correlation of experimental data in the creeping flow regime has been included.

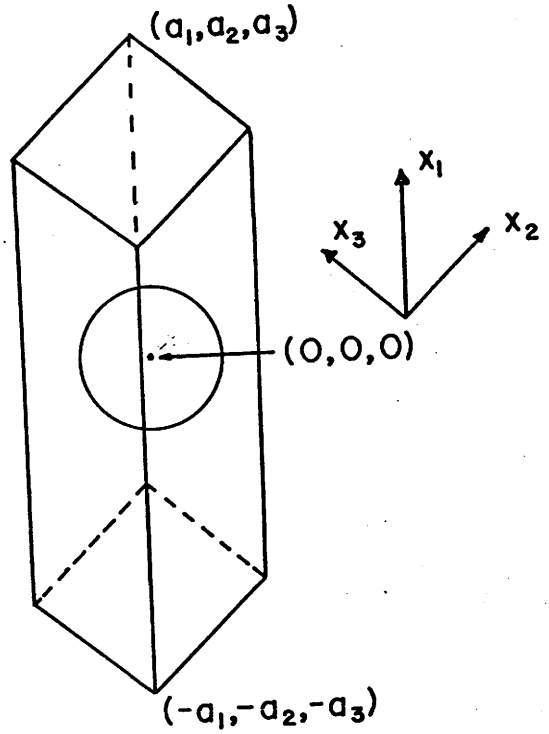

FIGURE A.3 GUNN AND MALIK MODEL

1) $u_1=u_2=u_3=0$ when $(x_1^2 + x_2^2 + x_3^2)^{\frac{1}{2}} = a$

2) $x_2 = \pm a_2$ } $\frac{\partial u_1}{\partial x_2} = 0$, $u_2 = 0$, $\frac{\partial u_3}{\partial x_2} = 0$
$x_2 = 0$

3) $x_3 = \pm a_3$ } $\frac{\partial u_1}{\partial x_3} = 0$, $u_3 = 0$, $\frac{\partial u_2}{\partial x_3} = 0$
$x_3 = 0$

4) distributions of velocity and velocity derivatives over face $x_1 = +a_1$. $x_1 = -a_1$ are identical to the distributions over face

TABLE A.1 INCREASE IN PARTICLE DRAG IN ASSEMBLAGES

$\lambda = a/b$	0.05	0.1	0.2	0.3	0.4	0.5	0.6	0.7
CONCENTRATION	0.0025	0.001	0.008	0.027	0.064	0.125	0.216	0.343
Wakiya	-	1.25	1.63	2.23	3.18	4.8	-	-
Kawaguti (S.C.)	-	1.219	1.548	2.063	2.920	4.430	7.106	10.652
Kawaguti (B.S.C.)	-	1.167	1.395	1.716	2.182	2.885	3.986	5.746
Happel & Ast	-	1.201	1.495	1.935	2.665	3.991	6.965	18.269
Happel	-	1.177	1.429	1.811	2.450	3.632	6.188	13.280
Kuwabara	-	1.198	1.515	2.016	2.768	3.836	5.286	7.186
Hasimoto (S.C.)	1.096	1.212	1.525	2.009	2.83	4.5	12.0	-
Hasimoto (B.S.C.)	1.098	1.217	1.539	2.044	2.89	4.47	8.0	20.0
Hasimoto (F.S.C.)	1.098	1.217	1.539	2.044	2.89	4.47	7.9	19.0
Richardson & Zaki (I)	-	0.40	0.59	0.87	1.27	1.95	3.06	5.15
Richardson & Zaki (II)	-	0.56	0.68	0.85	1.30	2.45	4.13	5.96
Richardson & Zaki (Experimental)	-	-	-	1.14	1.36	1.86	3.11	7.05

A.2 Cylinder Bundles

The cell technique has been employed to derive theoretical solutions for flows through arrays of cylinders in much the same way as for flow through assemblages of spheres. Happel (1959) extended his free surface model to flow perpendicular to cylinder bundles. The model consists of two concentric cylinders. The inner cylinder being one of the rods in the assemblage and the outer a fluid envelope with a free surface. The model and its boundary conditions are shown in Figure A.4.A. The relative volume of fluid to solid in the cell model is the same as that in the assemblage of cylinders. Within the bounded region the Stokes equations of motion have been solved.

Kuwabara (1959) also applied his zero vorticity model to flow perpendicular to cylinder bundles. The model and its boundary conditions are presented in Figure A.4.B. Cylinder drag within the assemblage has been determined by integrating the energy dissipation over the bounded region. As in Happel's model the Stokes equations of motion were solved within the bounded region.

Hasimoto (1959) also developed a continuum model for periodic arrays of cylinders. He obtained spatially periodic fundamental solutions of the Stokes equations of motion for a viscous fluid. Three types of lattices were examined, simple cubic, body centered cubic, and face centered cubic. The solutions have been expressed in terms of the drag on one of the cylinders.

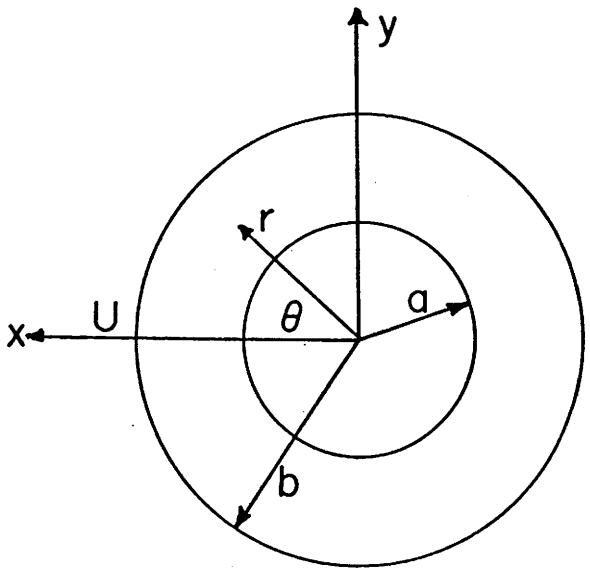

Boundary conditions

$r = a$

$v_x = U$

$v_r = U\cos\theta$

$v_\theta = -U\sin\theta$

$r = b$

$v_r = 0$

$$\frac{\partial v_\theta}{\partial r} + \frac{1}{r}\frac{\partial v_r}{\partial \theta} - \frac{v_\theta}{r} = 0$$

$$1-\varepsilon = (a/b)^2$$

FIGURE A.4.A HAPPEL FREE SURFACE MODEL FOR CYLINDERS

Boundary conditions

$r = a$

$v_r = v_\theta = 0$

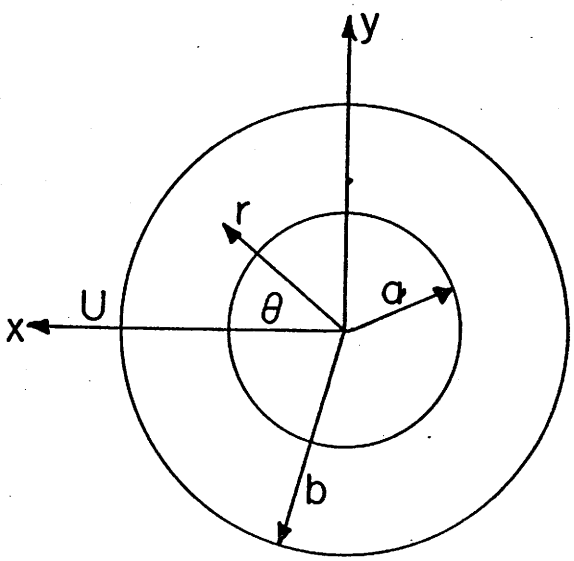

$r = b$

$v_r = U\cos\theta$

$$\frac{\partial v_\theta}{\partial r} - \frac{1}{r}\frac{\partial v_r}{\partial \theta} + \frac{v_\theta}{r} = 0$$

$$1-\varepsilon = (a/b)^2$$

FIGURE A.4.B KAWABURA ZERO VORTICITY MODEL FOR CYLINDERS

The aforementioned models have been derived for the creeping flow regime. Analytical models of flow in tube bundles in the inviscid potential region of flow (Reynolds number $\geq$ 3000) have also been developed by several workers (Grosh and Cess, 1958; and Hsu, 1964). The models were developed to predict heat transfer rates from tube bundles to liquid metals. The models are based upon the following assumptions: (a) constant property, non-dissipative flow, (b) steady two-dimensional temperature and velocity fields, (c) incompressible, non-viscous and irrotational flow, (d) negligible eddy transport of heat compared to molecular conduction, (e) no contact resistance at the solid liquid interface, (f) the hydrodynamic potential distribution on the surface of a cylinder located in a rod bundle is linear with respect to the distance along the diameter of the cylinder measured from the forward stagnation point, (g) the interaction of the thermal boundary layers of the cylinders in the rod bundle is negligible. In order to determine heat transfer rates the distribution of hydrodynamic potential around the rod in the bundle must be determined. The distribution is obtained by solving Laplace's equation for the specified rod bundle under suitable boundary conditions. For flow normal to a bundle, the distribution of stream and potential lines is approximated by those for flow across double infinite rows of cylinders with the same geometrical configuration. For this case Howland and McMullen (1936) have proposed a certain periodic function solution. This solution of the momentum transport is then combined with the energy equation to predict heat transfer rates. Excellent agreement with experiment data has been obtained.

Models developed for the creeping flow regime are compared in Table A.2. The Hasimoto model and Happel model (2) are only applicable to very low rod concentrations as they are based on treating the other interacting cylinders as point sources. This concept is only a good approximation for cylinders when b >> a. It should also be noted that the Kawabura model predicts a stronger dependence upon rod concentration than Happel's free surface model. This effect is the reverse of that for sphere assemblages (Table A.1). The model equations are also presented in this table.

TABLE A.2 CALCULATED VALUES OF $N_{Re}\ C_D$

a/b	CONC.	HASIMOTO	KUWABARA	HAPPEL (1)	HAPPEL (2)
0.1	0.01	16.065	16.084	13.942	13.930
0.2	0.04	28.845	27.956	22.621	22.605
0.3	0.09	54.072	46.379	35.343	35.634
0.4	0.16	141.116	78.588	56.964	60.640
0.5	0.25	neg	141.513	99.772	128.55
0.6	0.36	neg	284.301	199.942	1876.97
0.7	0.49	neg	685.376	498.665	neg

HAPPEL (1) $N_{Re}\ C_D = \pi/(\ell n(b/a) - \frac{1}{2}(b^4 - a^4)/(b^4 + a^4))$

HAPPEL (2) $N_{Re}\ C_D = 8\pi/(\ell n(\sqrt{\pi}b/a) - 1.07)$

KUWABARA $N_{Re}\ C_D = 8\pi/(-\frac{1}{2}\ell n(a/b)^2 - 3/4 + (\frac{a}{b})^2 - (a/b)^4/4)$

HASIMOTO $N_{Re}\ C_D = 8\pi/(\ell n(\sqrt{\pi}b/a) - 1.3107)$

A.3 Gas Bubble Swarms

The rise velocity of a swarm of bubbles has also been investigated using cell models. Marrucci (1965) derived an expression for the rise velocity using Happel's free surface model. Within the bounded region the equations for irrotational flow were solved after the method of Lamb (1945). The energy dissipation per unit time was found to be

$$12\pi\mu U^2 a(1-\varepsilon^{5/3})/(1-\varepsilon)^2 \qquad (A.1)$$

where U is the superficial liquid velocity (velocity of the bubble with respect to the liquid above and below the swarm). The drag can be found by dividing by U giving

$$D_s = 12\pi\mu Ua(1-\varepsilon^{5/3})/(1-\varepsilon)^2 \qquad (A.2)$$

Marrucci considered that the drag on a single bubble was $D = 12\pi\mu Ua$ after Levich (1949) producing a swarm correction factor of

$$K = \frac{D_s}{D} = \frac{(1-\varepsilon^{5/3})}{(1-\varepsilon)^2} \qquad (A.3)$$

Thus Marrucci's model is restricted to the range of high Reynolds numbers ($100 \leq N_{Re} \leq 1000$).

Bhatia (1969) recently derived an expression for predicting the rise velocity of swarms by combining Mendelson's wave-interfacial disturbance analogy (1967) and the porosity concept of the cell model technique proposed by Happel and Ast (1960). Mendelson's derivation for the rise velocity of a single bubble in an infinite media is

$$V_\infty = \left(\frac{\rho}{r_e \rho} + g r_e\right)^{\frac{1}{2}} \qquad (A.4)$$

and applies in flow region where surface forces and gravity forces are important and the bubbles have a prolate or spherical cap shape. Mendelson and Maneri (1968) demonstrated that the rise velocity of a bubble in a tube can be approximated by

$$U/U_{\infty} = \tanh[0.25\ r/r_e])^{\frac{1}{2}} \qquad (A.\ )$$

when the Eotvos number is very large (bubble diameter to column diameter ratio very small). Bhatia substituted the Happel and Ast model porosity definition

$$1-\varepsilon = (r_e/r)^3 \qquad (A.6)$$

in the above equation and thus obtained an expression for the rise velocity of a bubble swarm.

Although the porosity definition is from the Happel and Ast model, the Mendelson and Maneri equation physically is the cell model proposed where a frictional outer boundary is assumed rather than a frictionless boundary as proposed by Happel and Ast.

The Happel and Ast model is a sphere in cylinder model developed to represent the process of sedimentation. The model and its boundary conditions are shown in Figure A.6; the key concept is the postulate of zero shear at the cylinder walls. Within the bounded region, the Stokes equations for viscous flow have been solved using the method of Haberman to obtain the drag on the particle. The porosity has been determined rather arbitarily. The concept is similar to that of Richardson and Zaki (1954) in that the area perpendicular to the flow which is available for flow has been considered as the important parameter, yielding the porosity

relationship

$$1 - \varepsilon = (a/b)^3 \qquad (A.7)$$

Kawaguti (1958) proposed an identical model to Happel and Ast, however he used Faxen's method to solve the resulting boundary value problem. He considered two possible cases for determining the porosity, depending on whether the particle configuration could be classified as face centered cubic or simple cubic. The expressions are, respectively,

$$1 - \varepsilon = M^{-3} \left(\frac{a}{b}\right)^3 \qquad (A.8)$$

$M = 0.9095$ for simple cubic

$M = 1.1458$ for body centered cubic.

One should also consider Wakiya's model (1953), which is another sphere in cylinder model. The Stokes equations of flow are solved in the bounded region using Faxen's method. The boundary conditions used are given in Figure A.5.

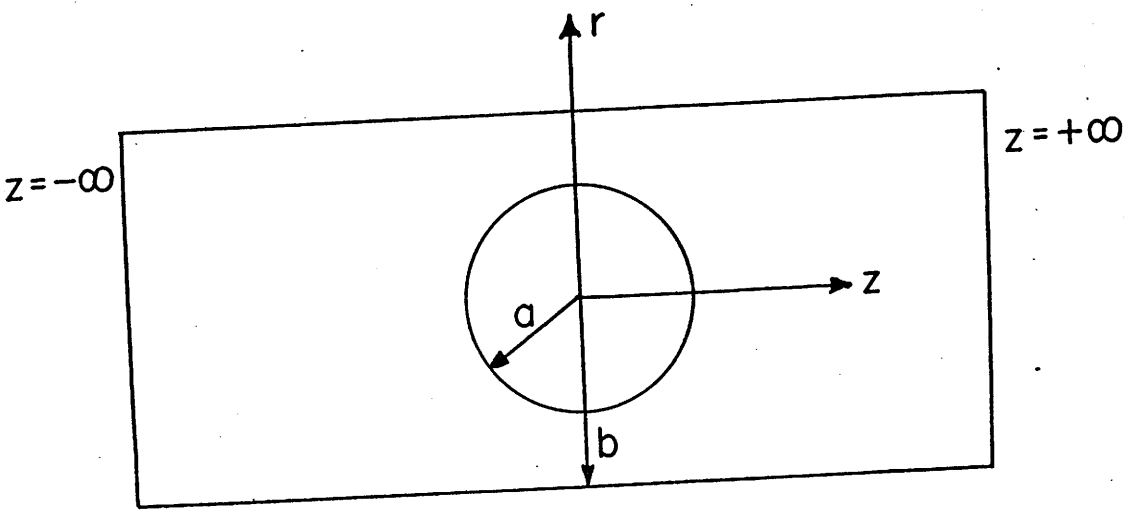

FIGURE A.5 WAKIYA MODEL FOR SPHERES

The boundary conditions are:

$$Z = \pm \infty$$

$$v_r = 0$$

$$v_z = U_p(1-r^2/b^2)$$

$$r = \pm b$$

$$v_r = v_z = 0$$

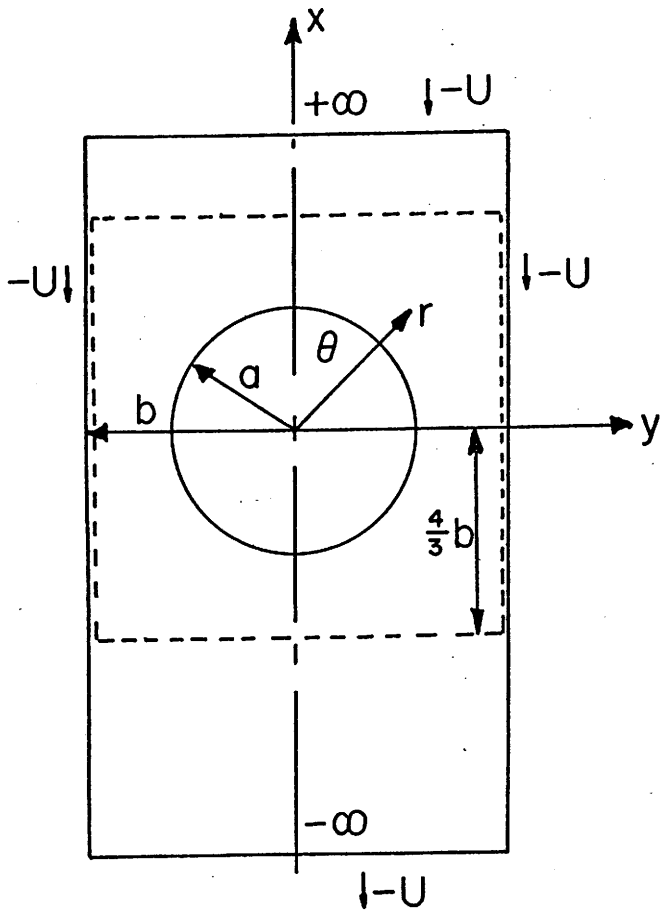

FIGURE A.6 AST AND HAPPEL MODEL FOR SPHERES

The boundary conditions are:

on the surface of the sphere (r=a)

$$v_r = 0 \quad , \quad v_\theta = 0$$

on infinity ($x = \pm \infty$)

$$v_x = -U \quad , \quad v_y = 0$$

at cylinder walls

$$\frac{\partial v_x}{\partial y} = 0 \quad , \quad v_y = 0$$

(symmetry about longitudinal axis of cylinder)

$$\phi = 1 - \varepsilon = (a/b)^3$$

A.4 Transport of Heat or Mass

Theoretical studies of heat and mass transport processes in multiparticle systems in the intermediate Reynolds Number range are difficult because of the complex geometry of any system. This fact has motivated many experimental investigations into the problem producing a large number of empirical correlations for transfer coefficient. The correlations also extend to single particle work. Most of these studies have been reviewed and analyzed in the literature (Calderbank, 1967; Wilson and Geankoplis, 1966; Redfield and Houghton, 1965; and Rowe, Claxton and Lewis, 1965) and therefore will not be re-evaluated here. The data contained in these papers will be used to test the accuracy of the theoretical predictions of heat or mass transfer in multiparticle systems developed in this work.

In the creeping flow regime, it is possible to obtain analytic solutions describing heat or mass transfer for forced convection flow around spheres and cylinders. Acrivos and Taylor (1962) developed the most accurate solution for the low Peclet number range using perturbation techniques and provided an excellent review of all solutions prior to 1962.

Solutions for the entire Peclet number range have been obtained by Friedlander (1957) and Yuge (1960). In Friedlander's approach, rates of mass or heat transfer to single spheres or cylinders at low Reynolds numbers were predicted by a boundary layer approach. The velocity distributions derived by Tomotika and Aoi (1950) were used, thus solutions are restricted to $N_{Re} \leq 5$. In the case of a sphere the method permits the evaluation of the N_{Nu} over the entire Peclet number range in contrast

with perturbation methods which are useful only for small Peclet numbers. For the cylinder case, a simplified stream function correct only near the cylinder surface was used limiting the results to large Peclet numbers.

Yuge's method is rather novel. It involves successive applications of approximate solutions, which are even power series expansions of the spherical angle with coefficients that are functions of radius only, until a solution of the desired accuracy is obtained. The method has been extended by Johnson and Akehata (1965) to include mass transfer with first order chemical reaction from solid spheres and gas bubbles. These authors also investigated other methods of solution including finite difference techniques.

Analytic solutions have been obtained for the high Peclet number region. Levich (1962) and Friedlander (1961) obtained identical relationships after assuming that concentration changes could be confined within a thin boundary layer. For thin concentration boundary layers it is necessary to take into account only the first term in an expansion of the velocity near the wall when the equation of convective diffusion is solved. Baird and Hamielec (1962) used the approach to obtain analytic solutions for transfer from both circulating and solid spheres. Transfer rates in the recirculating vortex region were obtained using a unique approach. These authors assumed that "fresh fluid" entered the vortex region continuously along a line through the rear stagnation point. As a result they were able to obtain local transfer rates in this region. The values obtained are high as the vortex region contains little "fresh fluid", but rather may be saturated with the material being transferred.

The inability of most theories to predict satisfactorily the transfer rates in the vortex region is a severe limitation when considering transfer from solid spheres or cylinders. The wake area usually accounts for 40% of the total surface area for Reynolds numbers greater than 100. Thus accurate prediction of overall transfer rates is very difficult without a knowledge of the wake transfer rates.

There are very few mathematical models for mass transfer in disperse systems. Pfeffer and Happel (1964) used Happel's free surface model for dispersed systems and Yuge's method to predict transfer rates. Analytical solutions were obtained for particle to fluid heat and mass transfer rates in the creeping flow regime for Peclet numbers between 0.1 and 100. Theoretical solutions were also obtained for the case of surface chemical reaction. Pfeffer (1964) combined Happel's free surface model and the Levich "thin boundary layer solution" of the diffusion equation to predict transport rates in multiparticle systems in the high Peclet range. Chen and Pfeffer (1970) combined the Happel free surface model and a numerical solution of the convection equation to predict mass transfer rates when a homogeneous first order chemical reaction was occurring around the particles in a multiparticle system.

A theoretical model for transport in multiparticle systems in agitated vessels has been developed by Gal-Or and Resnick (1964). The simplified model proposed permits the prediction of total mass transfer rates for sparingly soluble gases in agitated mixers. The model is based upon the average residence time of the dispersed phase in the continuous phase, and permits the estimation of the rate of diffusion per unit

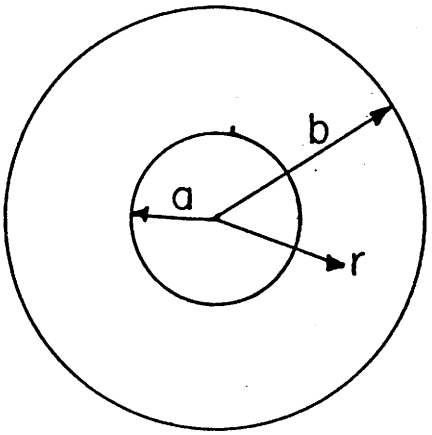

$t = 0,\ C = C_o$ for $a < r \leq b$

$r = a,\ C = C_i$ for $t \geq 0$

$r = b,\ C = C_o \exp(-kt)$ for $t \geq 0$

FIGURE A.7.A GAL-OR AND RESNICK MODEL FOR MASS TRANSFER

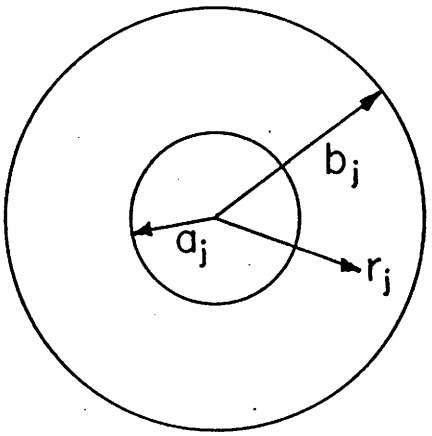

at $t = 0,\ C = C_o$ for $aj < r \leq b_j$

$r = a_j,\ C = C_i$ for $t \geq 0$

$r = b_j,\ \frac{\partial C}{\partial r} = 0$ for $t \geq 0$

FIGURE A.7.B GAL-OR AND HOELSCHER MODEL FOR MASS TRANSFER

volume as well as the total area for diffusion. A knowledge of the bubble diameter, reaction rate constant, gas diffusivity and contactor operating conditions is necessary to arrive at a numerical solution of the equations.

The model is based on the following assumptions (1) the dispersed phase is evenly distributed throughout the continuous phase (2) equilibrium is assumed at the interface and (3) agitation is such that no gross variations occur in the concentration throughout the continuous phase. The total volume of the continuous phase is subdivided into a number of equal volume elements, each containing a dispersed phase particle surrounded by a spherical shell of continuous phase fluid. Each bubble is introduced into its element and remains for the average residence time. Within the cell there is no relative flow between continuous phase and dispersed phase, the two phases move together. The model, presented in Figure A.7.A., is thus diffusion and reaction in a stagnant medium.

Gal-Or and Hoelscher (1966) modified the original model by including particle size distribution. They also changed the boundary conditions at the outer surface, Figure A.7.B. Gal-Or and Waslo (1968) introduced a new model incorporating hydrodynamic effects of surfactants and neighbour particles on the terminal velocity of an ensemble of drops and bubbles. A free surface cell model was used to solve the equations of viscous fluid motion and continuity simultaneously with a conservation equation governing diffusing surfactants. A general stream function for ensembles of particles was formulated and used to describe the flow patterns in the continuous and dispersed phase. When velocity profiles developed in the model are

coupled to the theory for coupled energy and multicomponent mass transport in dispersions and suspensions (Gal-Or, 1968; Gal-Or and Padmanabhan, 1968; and Gal-Or and Tavlarides, 1969) any problem in heat, mass and chemical reaction in drop and bubble ensembles in creeping flow may be solved.

B. Formulation

B.1 Assemblages of Solid Spheres

Exact mathematical modeling of a multiparticle fluidized or packed bed system is impossible. Any model which is proposed must contain generalizations; the present surface-interaction model has been developed on the following idealization. The fluid-particle system is represented as an assemblage of uniform spheres fixed in space, and assumed to be equally spaced in the radial and longitudinal directions with respect to the enclosing container. Each sphere, with a surrounding spherical envelope of fluid, is uncoupled from the system and considered separately. The bed porosity and particle interaction are imposed on the cell by the position of the outer spherical boundary with respect to the sphere diameter and the mathematical boundary conditions placed on this surface. Wall effect and entry and exit effects to the bed are neglected. Thus one model is used for all particles. Within the cell the fluid is Newtonian and incompressible.

The mathematical model considers an imaginary sphere of radius r_∞ enclosing and concentric with the given solid sphere of radius, a. On the imaginary sphere the vorticity is assumed to be zero and the flow undisturbed uniform parallel flow, while on the solid sphere the two components of velocity vanish. The volume $\frac{4}{3}\pi r_\infty^3$ of the imaginary sphere is taken to be the free volume corresponding to each sphere. The radius of the imaginary sphere is chosen so that the porosity in the cell is

equivalent to the average porosity of the fluidized bed.

The Navier-Stokes equations for incompressible, Newtonian, axi-symmetric flow for the stream function, ψ, and vorticity ξ, in spherical polar coordinates may be written as

$$\frac{N_{Re}}{2}\left[\frac{\partial\psi}{\partial r}\frac{\partial}{\partial\theta}\left(\frac{\xi}{r\sin\theta}\right) - \frac{\partial\psi}{\partial\theta}\frac{\partial}{\partial r}\left(\frac{\xi}{r\sin\theta}\right)\right]\sin\theta = E^2(\xi r\sin\theta) \qquad (B.1)$$

$$E^2\psi = \xi r\sin\theta \qquad (B.2)$$

where $$E^2 = \frac{\partial^2}{\partial r^2} + \frac{\sin\theta}{r^2}\frac{\partial}{\partial\theta}\left(\frac{1}{\sin\theta}\frac{\partial}{\partial\theta}\right)$$

The velocity components may be expressed as

$$v_\theta = \frac{1}{r\sin\theta}\frac{\partial\psi}{\partial r} \qquad v_r = \frac{-1}{r^2\sin\theta}\frac{\partial\psi}{\partial\theta}$$

where all quantities have been made dimensionless by putting

$$r = r'/a,\ \psi = \psi'/U_\infty a^2,\ \xi = \xi' a/U_\infty,\ v_r = v_r'/U_\infty,\ v_\theta = v_\theta'/U_\infty$$

The boundary conditions on the model become along the axis of symmetry

$$\theta = 0^\circ \text{ and } \theta = 180^\circ,\ \psi = \xi = 0$$

on the sphere surface

$$r = 1,\ \psi = \frac{\partial\psi}{\partial r} = 0, \text{ and } \xi = E^2\psi/\sin\theta$$

outer spherical boundary

$$r = r_\infty,\ \psi = \frac{1}{2}r_\infty^2\sin^2\theta, \text{ and } \xi = 0$$

The porosity of the sphere assemblage is

$$\varepsilon = 1 - r_\infty^{-3}$$

The porosity of the assemblage is varied by changing the value of r_∞. As $r_\infty \to \infty$, $\varepsilon \to 1$ and one has a sphere in an infinite fluid.

The frontal stagnation pressure may be determined by integrating the r-component of the equation of motion along the line $\theta = 0°$ from the outer boundary to the sphere surface. In dimensionless terms the equation becomes,

$$P_o = 1 + \frac{8}{N_{Re}} \int_1^\infty \left(\frac{\partial \xi}{\partial \theta}\right)_{\theta=0°} \frac{dr}{r} \tag{B.3}$$

The pressure distribution over the surface of the sphere is obtained by integrating the θ-component of motion over the surface. The equation reduces to,

$$P - P_o = \frac{4}{N_{Re}} \int_o^\theta \left(\frac{\partial \xi}{\partial r} + \xi\right)_{r=1} d\theta \tag{B.4}$$

The drag coefficient formulas used were

$$C_{DF} = \frac{8}{N_{Re}} \int_o^\pi \xi_{r=1} \sin^2\theta d\theta \tag{B.5}$$

$$C_{DP} = \int_o^\pi P_{r=1} \sin 2\theta d\theta \tag{B.6}$$

An analytical solution (Hamielec, Hoffman and Ross, 1967) of this boundary value problem at low Reynolds numbers can be found using the Stokes stream function, which is

$$\psi = (A/r + Br + Cr^2 + Dr^4) \sin^2\theta \tag{B.7}$$

The constants are found by satisfying the boundary conditions

$$r = 1, \quad \psi = 0, \quad \frac{\partial \psi}{\partial r} = 0$$

$$r = r_\infty, \quad \psi = \frac{1}{2} r_\infty^2 \sin^2\theta, \quad \xi = 0$$

which are identical to the boundary conditions which are used in the higher Reynolds number cases. The constants are related to r_∞ as follows:

$$B' = \frac{(15/2)r_\infty^2}{(2-10r_\infty^3 + 18r_\infty^5 - 10r_\infty^6)} \tag{B.8}$$

$$C' = \frac{-(5/2)r_\infty^3 + 5r_\infty^6}{(2-10r_\infty^3 + 18r_\infty^5 - 10r_\infty^6)} \tag{B.9}$$

$$D' = \frac{(3/2)r_\infty^3}{(2-10r_\infty^3 + 18r_\infty^5 - 10r_\infty^6)} \tag{B.10}$$

The total drag coefficient is given by

$$C_D = \frac{-32B'}{N_{Re}} \tag{B.11}$$

B.2 Cylinder Bundles and Bubble Swarms

B.2.1 Cylinder Bundles

The tube bank or fiber bundle is represented as an assemblage of uniform circular cylinders fixed in space. The cylinders are assumed to be equally spaced in the plane which is perpendicular to the long axis of the cylinders. Each cylinder, with a surrounding cylindrical envelope of fluid is uncoupled from the system and considered separately. The spacing in the bundle and cylinder interaction are imposed on the cell by the position of the outer imaginary coaxial cylindrical boundary with respect to the cylinder diameter, and the mathematical boundary

conditions placed on this surface. The boundary conditions used on the outer imaginary cylindrical surface were undisturbed uniform parallel flow and no rotation of the fluid elements. Within the cell the fluid is incompressible and Newtonian.

The Navier-Stokes equation for incompressible, Newtonian, two dimensional flow in terms of the stream function, ψ, and vorticity, ξ, in cylindrical coordinates may be written as

$$\frac{N_{Re}}{2r} \frac{\partial(\psi, \xi)}{\partial(r, \theta)} = \nabla^2 \xi \tag{B.12}$$

$$\xi = \nabla^2 \psi \tag{B.13}$$

where $$\nabla^2 = \frac{\partial^2}{\partial r^2} + \frac{1}{r} \frac{\partial}{\partial r} + \frac{1}{r^2} \frac{\partial^2}{\partial \theta^2}$$

The velocity components are expressed as

$$v_r = - \frac{1}{r} \frac{\partial \psi}{\partial \theta}, \quad v_\theta = \frac{\partial \psi}{\partial r}$$

where all quantities have been made dimensionless by putting

$$r = r'/a, \ \psi = \psi'/U_\infty a, \quad = a\xi'/U_\infty$$

where the primed quantities are dimensional. The Reynolds number is $N_{Re} = 2aU_\infty \rho/\mu$.

The boundary conditions on the model are

along the axis of symmetry

$$\theta = 0° \text{ and } 180°, \ \psi = \xi = 0$$

on the cylinder surface

$$r = 1, \ \psi = 0, \ \frac{\partial \psi}{\partial r} = 0, \text{ and } \xi = \nabla^2 \psi$$

on the concentric imaginary boundary

$$r = r_\infty, \quad \psi = r_\infty \sin\theta, \quad \xi = 0$$

The porosity of the cylinder bundle assemblage is

$$\varepsilon = 1 - r_\infty^{-2} \tag{B.14}$$

In the limit as $N_{Re} \to 0$, the Navier-Stokes equations reduce to the linear asymptotic form

$$\nabla^4 \psi = 0 \tag{B.15}$$

The Stokes solution may be expressed as

$$\psi = (C' r^3 + D' r \ln r + E' r + F'/r) \sin\theta \tag{B.16}$$

The constants can be found by satisfying the boundary conditions

$$r = 1, \ \psi = 0 \text{ and } \partial\psi/\partial r = 0$$

$$r = r_\infty, \ \psi = r_\infty \sin\theta \text{ and } \xi = 0$$

These boundary conditions are identical to those satisfied in the finite difference method. The constants are related to r_∞ as follows

$$C' = \frac{r_\infty}{-4r_\infty^3 \ln r_\infty + 3r_\infty^3 - 4r_\infty + 1/r_\infty} \tag{B.17}$$

$$D' = \frac{-4r_\infty^3}{-4r_\infty^3 \ln r_\infty + 3r_\infty^3 - 4r_\infty + 1/r_\infty} \tag{B.18}$$

$$E' = \frac{2(r_\infty^3 - r_\infty)}{-4r_\infty^3 \ln r_\infty + 3r_\infty^3 - 4r_\infty + 1/r_\infty} \tag{B.19}$$

$$F' = \frac{-2r_\infty^3 + r_\infty}{-4r_\infty^3 \ln r_\infty + 3r_\infty^3 - 4r_\infty + 1/r_\infty} \tag{B.20}$$

When the surface forces are used to calculate the drag coefficient, it is

given by

$$C_D = \frac{4\pi D'}{N_{Re}} \tag{B.21}$$

The surface pressure and drag equations used are given in Table B.2.

B.2.2 Bubble Swarms

The rise of a swarm of bubbles in a column is represented as a uniform assemblage of spherical bubbles fixed in space. The bubbles are assumed to equally spaced in the radial and longitudinal direction with respect to the enclosing container. Each bubble with a surrounding spherical envelope of fluid, is uncoupled from the system and considered separately. The swarm porosity and bubble interaction are imposed on the cell by the position of the outer imaginary spherical boundary with respect to the bubble radius and the mathematical boundary conditions placed on this surface. Within the cell the fluids are Newtonian and incompressible.

The mathematical model considers an imaginary sphere of radius r_∞ enclosing and concentric with the given gas bubble of radius a. On the imaginary outer sphere the vorticity is assumed zero and the flow is assumed to be uniform undisturbed parallel flow. The volume $\frac{4}{3}\pi r_\infty^3$ of the imaginary sphere is taken to be the free volume corresponding to each sphere. The radius, r_∞, is chosen so that the porosity of the cell is equal to the porosity in the bubble swarm. At the bubble surface the tangential shear stress is assumed to vanish and no transfer is allowed across the interface.

The Navier-Stokes equations for incompressible, Newtonian, axisymmetric flow for the stream function, ψ, and vorticity, ξ, in spherical coordinates is given in Table B.1. The boundary conditions on the model become

along the axis of symmetry

$$\theta = 0° \text{ and } \theta = 180°, \ \psi = \xi = 0$$

on the bubble surface

$$r = 1, \ \psi = 0, \ (J_{r\theta} = 0) \ \xi = \frac{2}{\sin\theta} \frac{\partial \psi}{\partial r}$$

outer spherical boundary

$$r = r_\infty, \ \psi = \frac{1}{2} r_\infty^2 \sin^2\theta, \ \xi = 0$$

The porosity of the bubble swarm is given by

$$\varepsilon = 1 - r_\infty^{-3}$$

The drag coefficient and pressure distribution formulas used in the calculations are given in Table B.2.

An analytical solution has been found (Hamielec, Johnson and Houghton, 1967) for creeping flow whose boundary conditions are identical to those used in the finite difference method. The solution is

$$\psi = (A'/r + B'r + C'r^2 + D'r^4)\sin^2\theta \qquad (B.22)$$

The constants are found by satisfying the boundary conditions

$$r = 1, \ \psi = 0, \ J_{r\theta} = 0$$

$$r = r_\infty, \ \psi = \frac{1}{2} r_\infty^2 \sin^2\theta, \ \xi = 0$$

The constants are given by the relationships

$$B' = -C' = \frac{(5/2)r_\infty^6}{(-5r_\infty^6 + 6r_\infty^5 - 1)} \tag{B.23}$$

$$D' = -A' = \frac{(1/2)r_\infty^3}{(-5r_\infty^6 + 6r_\infty^5 - 1)} \tag{B.24}$$

The total drag is given by

$$C_D = -32\ B'/N_{Re} \tag{B.25}$$

TABLE B.I FUNDAMENTAL FLUID MECHANICAL EQUATIONS

	SPHERE	GAS BUBBLE	CYLINDER
Vorticity transport equation	$\frac{1}{r^2\sin\theta}\frac{\partial(\psi,r\xi\sin\theta)}{\partial(r,\theta)} - \frac{2\xi}{r\sin\theta}\left[\frac{\partial\psi}{\partial r}\cos\theta - \frac{1}{r}\frac{\partial\psi}{\partial\theta}\sin\theta\right]$	$= \frac{2}{N_{Re}}E^2(r\xi\sin\theta)$	$\frac{N_{Re}}{2r}\frac{\partial(\psi,\xi)}{\partial(r,\theta)} = +\nabla^2 w$
	$\xi = E^2\psi/r\sin\theta$		$\xi = \nabla^2\psi$
	where: $E^2 = \frac{\partial^2}{\partial r^2} + \frac{\sin\theta}{r^2}\frac{\partial}{\partial\theta}\left(\frac{1}{\sin\theta}\frac{\partial}{\partial\theta}\right)$		where: $\nabla^2 = \frac{\partial^2}{\partial r^2} + \frac{1}{r}\frac{\partial}{\partial r} + \frac{1}{r^2}\frac{\partial^2}{\partial\theta^2}$
Velocity components	$v_r = -\frac{1}{r^2\sin\theta}\frac{\partial\psi}{\partial\theta}$, $v_\theta = \frac{1}{r\sin\theta}\frac{\partial\psi}{\partial r}$		$v_r = -\frac{1}{r}\frac{\partial\psi}{\partial\theta}$, $v_\theta = \frac{\partial\psi}{\partial r}$
Boundary conditions			
1) along axis of symmetry			
$\theta = 0°$ and $\theta = 180°$	$\psi = 0,\ \xi = 0$	$\psi = 0,\ \xi = 0$	$\psi = 0,\ \xi = 0$
2) on particle surface			
$r = 1$	$\frac{\partial\psi}{\partial r} = \psi = 0,\ \xi = E^2\psi/\sin\theta$	$\psi = 0,\ \xi = \frac{2}{\sin\theta}\frac{\partial\psi}{\partial r}$	$\frac{\partial\psi}{\partial r} = \psi = 0,\ \xi = \nabla^2\psi$
3) on concentric circular boundary remote from surface	$\psi = \frac{r_\infty^2}{2}\sin^2\theta,\ \xi = 0$	$\psi = \frac{r_\infty^2}{2}\sin^2\theta,\ \xi = 0$	$\psi = r_\infty\sin\theta,\ \xi = 0$
$r = r_\infty$			

TABLE B.2 INTEGRAL EXPRESSIONS FOR MODELS

	SPHERE	GAS BUBBLE	CYLINDER
Stagnation Pressure	$P_o = 1 + \frac{8}{N_{Re}} \int_1^\infty (\frac{\partial \xi}{\partial \theta}) \frac{dr}{r}$		$P_o = 1 + \frac{4}{N_{Re}} \int_1^\infty (\frac{\partial \xi}{\partial \theta}) \frac{dr}{r}$
Surface Pressure	$P-P_o = \frac{4}{N_{Re}} \int_o^\theta (\frac{\partial \xi}{\partial r} + \xi)\, d\theta$	$P-P_o = \frac{4}{N_{Re}} \int_o^\theta (\frac{\partial \xi}{\partial r} + \xi) d\theta - v_\theta^2$	$P-P_o = \frac{4}{N_{Re}} \int_o^\theta (\frac{\partial \xi}{\partial r})\, d\theta$
Friction drag coefficient	$C_{DF} = \frac{8}{N_{Re}} \int_o^\pi \xi \sin^2\theta d\theta$	$C_{DF} = \frac{4}{N_{Re}} \int_o^\pi (\frac{\partial \xi}{\partial \theta} + \xi \cot\theta)\sin 2\theta d\theta$	$C_{DF} = \frac{4}{N_{Re}} \int_o^\pi \xi \sin\theta d\theta$
Pressure drag coefficient	$C_{DP} = \int_o^\pi P \sin 2\theta d\theta$		$C_{DP} = \int_o^\pi P \cos\theta d\theta$
Porosity	$\varepsilon = 1 - r_\infty^{-3}$		$\varepsilon = 1 - r_\infty^{-2}$

B.3 Transport of Heat or Mass

The transport of heat or mass from a particle to a flowing fluid in spherical polar coordinates for axisymmetric flow is given by

$$v_r \frac{\partial C}{\partial r} + \frac{v_\theta}{r} \frac{\partial C}{\partial \theta} = D\left(\frac{1}{r^2} \frac{\partial}{\partial r} \left(\frac{r^2 \partial C}{\partial r}\right) + \frac{1}{r^2 \sin\theta} \frac{\partial}{\partial \theta} \left(\sin\theta \frac{\partial C}{\partial \theta}\right)\right) \qquad (B.26)$$

For Peclet numbers much greater than one, the change in concentration occurs in a thin boundary layer, in spite of the fact that the liquid velocity varies gradually. The angular diffusion terms may be neglected since the derivatives along the surface are small compared to the radial derivatives. Also for thin concentration boundary layers $\frac{\partial^2 C}{\partial r^2} >> \frac{1}{r} \frac{\partial C}{\partial r}$, thus it is necessary to take into account only the first term in an expansion of the velocity in the region near the wall when the equation of convection is solved. For the region close to the surface of the sphere the diffusion equation when made dimensionless can be written as

$$v_r \frac{\partial C}{\partial r} + \frac{v_\theta}{r} \frac{\partial C}{\partial \theta} = \frac{2}{N_{Pe}} \frac{\partial^2 C}{\partial r^2} \qquad (B.27)$$

where $N_{Pe} = \frac{2aU_\infty}{D}$.

As the concentration boundary layer is much thinner than the hydrodynamic boundary layer, the tangential velocity v_θ can be written as

$$v_\theta = \dot{U}(r-a) = \dot{U}y \qquad (B.28)$$

where the velocity gradient $\dot{U}$ is some function of the polar angle θ and the Reynolds number. The velocity components defined in terms of the stream function are

$$v_\theta = \frac{1}{r\sin\theta} \frac{\partial \psi}{\partial r}, \quad v_r = -\frac{1}{r^2 \sin\theta} \frac{\partial \psi}{\partial \theta}$$

thus $\psi = \frac{1}{2}\dot{U}y^2 a\sin\theta$, $v_r = -\frac{y^2}{2a}\dot{U}' - \frac{\dot{U}y}{2a}\cot\theta$.

If a transformation of variables is made from $(r, \theta) \rightarrow (y, \theta)$ where $Y = \psi^{\frac{1}{2}}$ we obtain

$$\left(\frac{8}{\dot{U}a^5\sin^3\theta}\right)^{\frac{1}{2}} Y \frac{\partial C}{\partial \theta} = D\frac{\partial^2 C}{\partial y^2} \qquad (B.29)$$

Let

$$\frac{d\phi}{d\theta} = \left(\frac{\dot{U}a^5\sin^3\theta}{8}\right)^{\frac{1}{2}} \qquad (B.30)$$

and the equation reduces to

$$Y\frac{\partial C}{\partial \phi} = D\frac{\partial^2 C}{\partial y^2} \qquad (B.31)$$

The boundary conditions for this equation are

sphere surface (r=a) θ, $\phi \geq 0$ $Y = 0$, $C = C_s$

frontal stagnation point θ, $\phi = 0$ $Y > 0$, $C_o = 0$

bulk fluid θ, $\phi \geq 0$ $Y = \infty$, $C_o = 0$

The Leveque (1928) solution of this equation with the above boundary conditions is

$$\frac{C - C_o}{C_s - C_o} = 1 - \frac{1}{0.893}\int_o^z e^{-z^3}\,dz \qquad (B.32)$$

where $z = y(9\phi D)^{-1/3}$; $\phi = \int_o^\theta \left(\frac{\dot{U}a^5\sin^3\theta}{8}\right)^{\frac{1}{2}} d\theta$

At the sphere surface the velocity gradient, $\dot{U}$, is equal to the surface vorticity,

$$\xi = \frac{\partial v_\theta}{\partial r} + \cancel{\frac{v_\theta}{r}}^{\,o} - \frac{1}{r}\cancel{\frac{\partial v_r}{\partial \theta}}^{\,o} = \dot{U} \qquad (B.33)$$

Thus

$$\phi = \int_o^\theta \left(\frac{\xi a^5\sin^3\theta}{8}\right)^{\frac{1}{2}} d\theta$$

These equations may be used to obtain the local mass transfer coefficient, which is given by

$$k = 0.382D^{2/3}\left[\int_0^{\theta}\left(\frac{\xi a^5 \sin^3\theta}{8}\right)^{1/2} d\theta\right]^{-1/3}(\xi a \sin\theta)^{1/2} \qquad (B.34)$$

The local Sherwood Number is given by

$$N_{Sh} = 0.856\, N_{Pe}^{1/3}\left[\int_0^{\theta}(\bar{\xi}\sin^3\theta)^{1/2} d\theta\right]^{-1/3}(\bar{\xi}\sin\theta)^{1/2} \qquad (B.35)$$

where $\bar{\xi}$ is the dimensionless surface vorticity and is given by $\bar{\xi} = \frac{\xi a}{U_\infty}$. The average Sherwood Number is obtained by integrating over the sphere

$$\bar{N}_{Sh} = 0.641\, N_{Pe}^{1/3}\left[\int_0^{\pi}(\bar{\xi}\sin^3\theta)^{1/2}\, d\theta\right]^{2/3} \qquad (B.36)$$

The procedure presented above can be found in expanded form in several research papers (Baird and Hamielec, 1962; Levich, Physicochemical Hydrodynamics, p.81; and Lighthill, 1950).

This method is used to determine mass transfer rates from spheres in assemblages. In the region of reverse flow the Baird and Hamielec (1962) fresh fluid concept is used. In the vortex region it is assumed that "fresh" liquid ($C = C_o$) impinges on the sphere at the rear stagnation point, and θ is measured from this point.

The thin concentration boundary concept has also been applied to cylinder bundles in cross flow and bubble swarms. The equations derived for these cases are presented in Table B.3. A complete derivation for the gas bubble case appears in several research papers (Baird and Hamielec, 1962; and Levich, Physicochemical Hydrodynamics, p.405) and for cross flow to cylinders (Natanson, 1957).

TABLE B.3 MASS TRANSFER EQUATIONS

SPHERE

tangential velocity near surface $v_\theta \simeq (r-a) \frac{\partial v_\theta}{\partial r}$

where: $\frac{\partial v_\theta}{\partial r} = \xi \Big|$ surface vorticity

local Sherwood number

$$N_{Sh} = 0.856\, N_{Pe}^{1/3} \left[\int_0^\theta (\bar{\xi} \sin^3\theta)^{\frac{1}{2}} d\theta \right]^{-1/3} (\bar{\xi} \sin\theta)^{\frac{1}{2}}$$

mean Sherwood number

$$N_{Sh} = 0.641\, N_{Pe}^{1/3} \left[\int_0^\pi (\bar{\xi} \sin^3\theta)^{\frac{1}{2}} d\theta \right]^{2/3}$$

CYLINDER

tangential velocity near surface $v_\theta \simeq (r-a) \frac{\partial v_\theta}{\partial r}$

where: $\frac{\partial v_\theta}{\partial r} = \xi \Big|$ surface vorticity

local Sherwood number

$$N_{Sh} = 0.856\, N_{Pe}^{1/3} \left[\int_0^\theta \xi^{\frac{1}{2}}\, d\theta \right]^{-1/3} \xi^{\frac{1}{2}}$$

mean Sherwood number

$$\bar{N}_{Sh} = 0.641\, N_{Pe}^{1/3} \left[\int_0^\pi \xi^{\frac{1}{2}}\, d\theta \right]^{2/3}$$

GAS BUBBLE

local Sherwood number

$$N_{Sh} = \sqrt{\frac{6}{\pi}}\, N_{Pe}^{\frac{1}{2}} \left(\frac{v_\theta \sin^3\theta}{2 - 3\cos\theta + \cos 3\theta} \right)^{\frac{1}{2}}$$

TABLE B.3 (Continued)

where: $v_\theta = v_\theta\big/_{\text{surface}} = \dfrac{1}{r \sin\theta} \dfrac{\partial\psi}{\partial r}\Big/_{\text{surface}}$

mean Sherwood number

$$\bar{N}_{Sh} = \sqrt{12}\, N_{Pe}^{\frac{1}{2}} \int_0^{\pi} \left(\frac{v_\theta \sin^3\theta}{2-3\cos\theta+\cos 3\theta}\right) \cos\theta \, d\theta$$

B.4 Numerical Procedures

The same numerical procedure was used in the solution of the boundary value problems for the solid sphere, infinite circular cylinder in cross flow and gas bubble. The solution of the stream function and vorticity transport equations in the bounded region in each case were obtained using a modified form of the Extrapolated-Liebman method. The finite difference approximations to the stream function and vorticity equations may be written as follows:

$$(\psi_{ij}^{m+1})^* = f(\psi_{i+1,j}^{m}, \psi_{i-1,j}^{m+1}, \psi_{i,j-1}^{m+1}, \psi_{i,j+1}^{m}, \xi_{ij}^{m+1}) \tag{B.37}$$

$$(\xi_{ij}^{m+1})^* = f(\xi_{i+1,j}^{m}, \xi_{i-1,j}^{m+1}, \xi_{i,j-1}^{m+1}, \xi_{i,j+1}^{m}, \psi_{i+1,j}^{m}, \psi_{i-1,j}^{m+1}, \psi_{i,j-1}^{m+1}, \psi_{i,j+1}^{m}) \tag{B.38}$$

where ψ_{ij}^{m} and ψ_{ij}^{m+1}, etc are approximations to the stream function and vorticity at the m^{th} and $(m+1)^{th}$ iterations respectively. In the iterative procedure, relaxation factors are used to stabilize the computations. They were introduced as follows:

$$\psi_{ij}^{m+1} = (1-w)\ \psi_{ij}^{m} + w(\psi_{ij}^{m+1})^* \tag{B.39}$$

$$\xi_{ij}^{m+1} = (1-v)\ \xi_{ij} + v(\xi_{ij}^{m+1})^* \tag{B.40}$$

The effective change per iteration is taken as a fraction of the actual change and is governed by the values selected for v and w. Suitable values of these relaxation parameters were found by trial and error.

Briefly, the Extrapolated-Liebman method consists of applying the finite difference approximation equations at every interval grid point in regular succession. The points are scanned row by row and from left to right starting with the row next to the solid boundary at the frontal stagnation point end. The procedure is repeated until values of the stream function and vorticity on two successive iterations satisfy the equations

$$|\psi_{i,j}^{m+1} - \psi_{i,j}^{m}| \leq 10^{-4}$$

$$|\xi_{i,j}^{m+1} - \xi_{i,j}^{m}| \leq 10^{-4}$$

at all grid points. The computations were carried out in the McMaster University IBM7040 computer. A FORTRAN IV listing of the program for the sphere assemblage is given in Appendix I-A. The program listings for the cylinder bundle and bubble swarm cases are given in Appendix II-B.

C. Results and Discussion of Results

C.1 Sphere Assemblages

C.1.1 Accuracy of Solutions

The accuracy of the solutions was examined by varying both the radial and angular step sizes by factors of 2 until the resulting solutions of two successive trials varied by less than 1%.

Solutions were assumed to have converged when values of the vorticity and stream function at all mesh points changed by less than 0.0001 per iteration.

C.1.2 Surface Vorticity Distributions

The surface vorticity distributions for one Reynolds number (N_{Re}=500) and a range of porosities (ε = 0.4 to 1.0) are plotted in Figure C.1.A. These vorticity distributions are typical and similar results have been predicted for Reynolds numbers of 0.1, 1, 10, 20, 50, 100, 500 and 1000. They appear in Appendix II-A.

At the point of flow separation the surface vorticity changes sign, and this fact may be used to estimate the flow separation angle. The flow separation angle (measured from the rear stagnation point) and the size of the standing vortex ring decrease with decreasing porosity. The magnitude of the vorticity increases significantly as the porosity decreases, resulting in a rather large increase in friction drag.

C.1.3 Surface Pressure Distributions

The surface pressure distributions for N_{Re}=500 and for a range of porosities (ε = 0.4 to 1.0) are plotted in Figure C.1.B. Again these distributions are typical and similar results have been predicted for Reynolds numbers of 0.1, 1, 10, 20, 50, 100, 500 and 1000. They are presented in Appendix II-A.

The pressure at the rear stagnation point is strongly dependent on porosity. This suggests that for experimental verification, pressure distributions should be measured as a function of porosity (perhaps with a test sphere in a packed bed).

The frontal stagnation pressure is virtually independent of porosity at N_{Re}=500. At lower Reynolds numbers, however, the dependence is clearly evident, the stagnation pressure increasing as the porosity decreases. The effect of porosity on frontal stagnation pressure is shown in Figure C.2.A, for a range of Reynolds numbers and porosities.

C.1.4 Pressure, Friction, and Total Drag Coefficients

Pressure (form), friction and total drag coefficients for a range of porosities (ε = 0.4 to 1.0) and a range of Reynolds numbers are plotted in Figures C.2.B, C.2.C, and C.2.D and given in tabular form in Table C.1. The values for ε = 1.0 were estimated by extrapolation. First of all, the ratio of the predicted pressure drag coefficient to prediced friction drag coefficient was extrapolated to ε = 1.0. This ratio was then used with experimental total drag coefficient data (Lapple, 1951) to estimate the pressure and friction drag coefficients individually. They are shown by as broken lines in Figures C.2.B, and C.2.C. Total drag coefficients

(experimental) (Lapple, 1951) are shown as a broken line in Figure C.2.D. The extrapolation procedure used involved the assumption that at $\varepsilon = 1$, the first derivative of the extrapolated quantity (in this case C_{DP}/C_{DF}) with respect to ε was zero. Two points $\varepsilon = 0.909$ and $\varepsilon = 0.835$ were used to evaluate the constants in the polynomial

$$C_{DP}/C_{DF} = A_o + A_2(1-\varepsilon)^2 \qquad (C.1)$$

where A_o is the ratio of C_{DP}/C_{DF} at $\varepsilon = 1$.

Figures C.2.B, C.2.C, and C.2.D clearly indicate the very strong dependence of flow behaviour on porosity.

A general fluidization correlation more useful for design and analysis (Zenz, 1957) can be prepared by replotting the drag coefficient vs Reynolds number and porosity data as $(C_D N_{Re}^2)^{1/3}$ against $(N_{Re}/C_D)^{1/3}$ with porosity as parameter. Such a plot has been prepared and is presented as Figure C.2.E. The plot is useful as it results essentially in a plot of particle velocity against particle diameter with physical properties as parameters, that is:

$$(C_D N_{Re}^2)^{1/3} = 2a\left(\frac{4\rho(\rho_p - \rho)g}{3\mu^2}\right)^{1/3} \qquad (C.2)$$

$$(N_{Re}/C_D)^{1/3} = v_p\left(\frac{3\rho^2}{4\mu(\rho_p - \rho)g}\right)^{1/3} \qquad (C.3)$$

The relative velocity ratio against porosity relationship can be obtained simply by drawing a line parallel to the $(N_{Re}/C_D)^{1/3}$ axis through the particular particle diameter or free-settling Reynolds number desired.

C.1.5 Dimensions of Standing Vortex Ring

Lines of equivorticity and streamlines within the standing vortex ring have been plotted in Figure C.3.A and C.3.B, for one Reynolds number (N_{Re}=500) and two porosities (ε = 0.909 and ε = 0.741). The effect of reduction in porosity is to reduce the dimensions of the vortex ring-viz., the flow separation angle and the length of the vortex ring as measured along the axis $\theta = \pi$ become smaller. The critical Reynolds number for flow separation is increased as the porosity is reduced - viz., at N_{Re}=500, and ε = 1 there exists a large vortex ring - however, at N_{Re}=500, and ε = 0.645 the vortex ring does not exist.

The lines of equivorticity are swept downstream, but this convection appears to be abnormally interrupted by the position of the outer spherical boundary (where the vorticity has been fixed equal to zero). The blunt rather than streamlined shape of these lines emphasizes this fact. In reality, the vorticity would be greater than zero on the outer boundary downstream from the sphere.

C.1.6 Boundary Layer Development

Figure C.4 shows the angular velocity at the equatorial plane plotted against distance normal to the sphere surface for two Reynolds numbers (N_{Re}=20 and 500) and a range of porosities (ε = 0.4 to 0.9). At low Reynolds numbers the boundary-layer thickness decreases with decreasing porosity, but is almost independent of porosity at the high Reynolds number. This suggests that boundary layer assumptions might be valid at lower Reynolds numbers than one would expect, if the porosity is sufficiently small, and that one could expect higher mass and heat transfer rates by forced convection as the porosity is reduced.

TABLE C.I STAGNATION PRESSURE AND DRAG COEFFICIENTS

N_{Re}	ε	P_o	C_{DP}	C_{DF}	C_D
0.1	0.408	396.26	16469.	6190.7	22660.
	0.528	293.26	5973.8	3257.3	9231.1
	0.650	224.33	2361.5	1820.8	4182.3
	0.741	185.91	1225.7	1206.6	2432.3
	0.835	151.97	612.17	775.83	1388.0
	0.909	126.04	334.10	519.0	853.1
	1.0	114.70	88.0	152.0	240.0
1.0	0.408	40.47	1647.0	619.08	2266.0
	0.528	30.16	597.43	325.73	923.1
	0.650	23.27	236.2	182.09	418.2
	0.741	19.43	122.61	120.68	243.2
	0.835	16.03	61.27	77.61	138.9
	0.909	13.44	33.46	51.94	84.4
	1.0	12.31	9.80	16.70	26.5
10.0	0.408	4.89	165.25	61.98	227.22
	0.528	3.86	60.22	32.66	92.86
	0.650	3.17	24.06	18.33	42.37
	0.741	2.79	12.69	12.22	24.90
	0.835	2.45	6.57	7.98	14.54
	0.909	2.21	3.81	5.52	9.42
	1.0	2.10	1.59	2.51	4.10
20.0	0.408	2.92	83.46	31.09	114.55
	0.528	2.40	30.82	16.46	47.27
	0.650	2.06	12.66	9.33	21.98
	0.741	1.87	6.93	6.32	13.23
	0.835	1.71	3.81	4.25	8.05
	0.909	1.61	2.35	3.07	5.41
	1.0	1.57	0.94	1.31	2.55
50.0	0.408	1.74	35.62	12.71	48.32
	0.528	1.53	14.07	6.89	20.96
	0.650	1.40	6.43	4.08	10.51
	0.741	1.33	3.84	2.88	6.72
	0.835	1.29	2.26	2.05	4.31
	0.909	1.25	1.45	1.54	2.98
	1.0	1.21	0.70	0.80	1.50

TABLE C.1 (Continued)

N_{Re}	ε	P_o	C_{DP}	C_{DF}	C_D
100.0	0.417	1.34	19.71	6.43	26.13
	0.535	1.25	8.79	3.70	12.49
	0.645	1.20	4.65	2.39	7.04
	0.741	1.16	2.63	1.64	4.26
	0.835	1.14	1.69	1.24	2.91
	0.909	1.13	1.11	0.95	2.04
	1.0	1.12	0.56	0.51	1.07
500.0	0.417	1.06	9.31	1.87	11.17
	0.535	1.05	4.52	1.14	5.66
	0.645	1.04	2.57	0.77	3.34
	0.752	1.03	1.57	0.55	2.11
	0.835	1.03	1.08	0.44	1.51
	0.909	1.03	0.75	0.35	1.10
	1.0	1.03	0.37	0.18	0.55
1000.0	0.417	1.03	7.33	1.16	8.49
	0.535	1.02	3.87	0.74	4.61
	0.645	1.02	2.38	0.52	2.90
	0.752	1.02	1.40	0.36	1.76
	0.835	1.02	1.12	0.30	1.42
	0.909	1.02	0.78	0.24	1.02

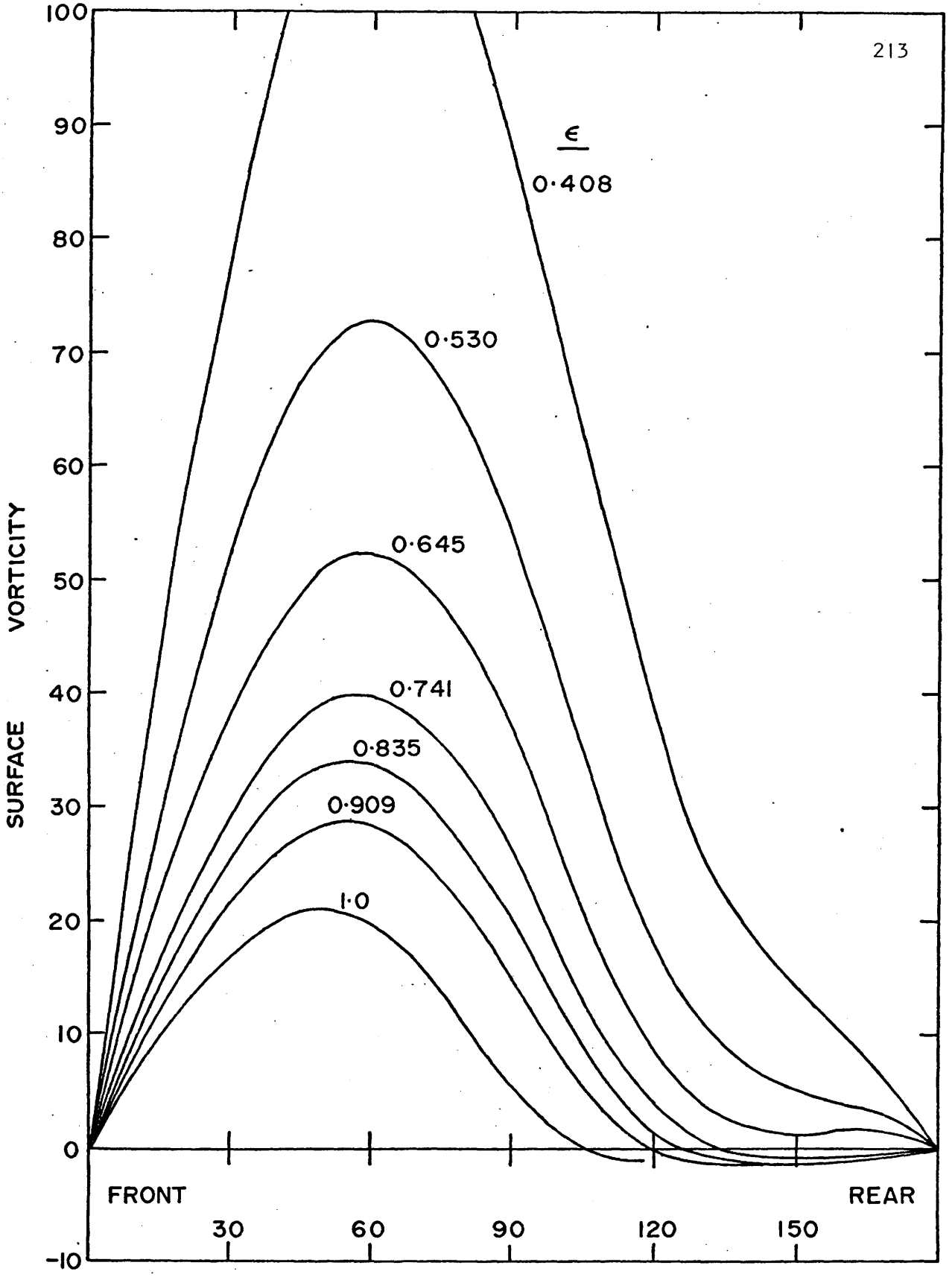

FIGURE C.1.A SURFACE VORTICITY DISTRIBUTION ABOUT A SPHERE AT N_{Re} = 500

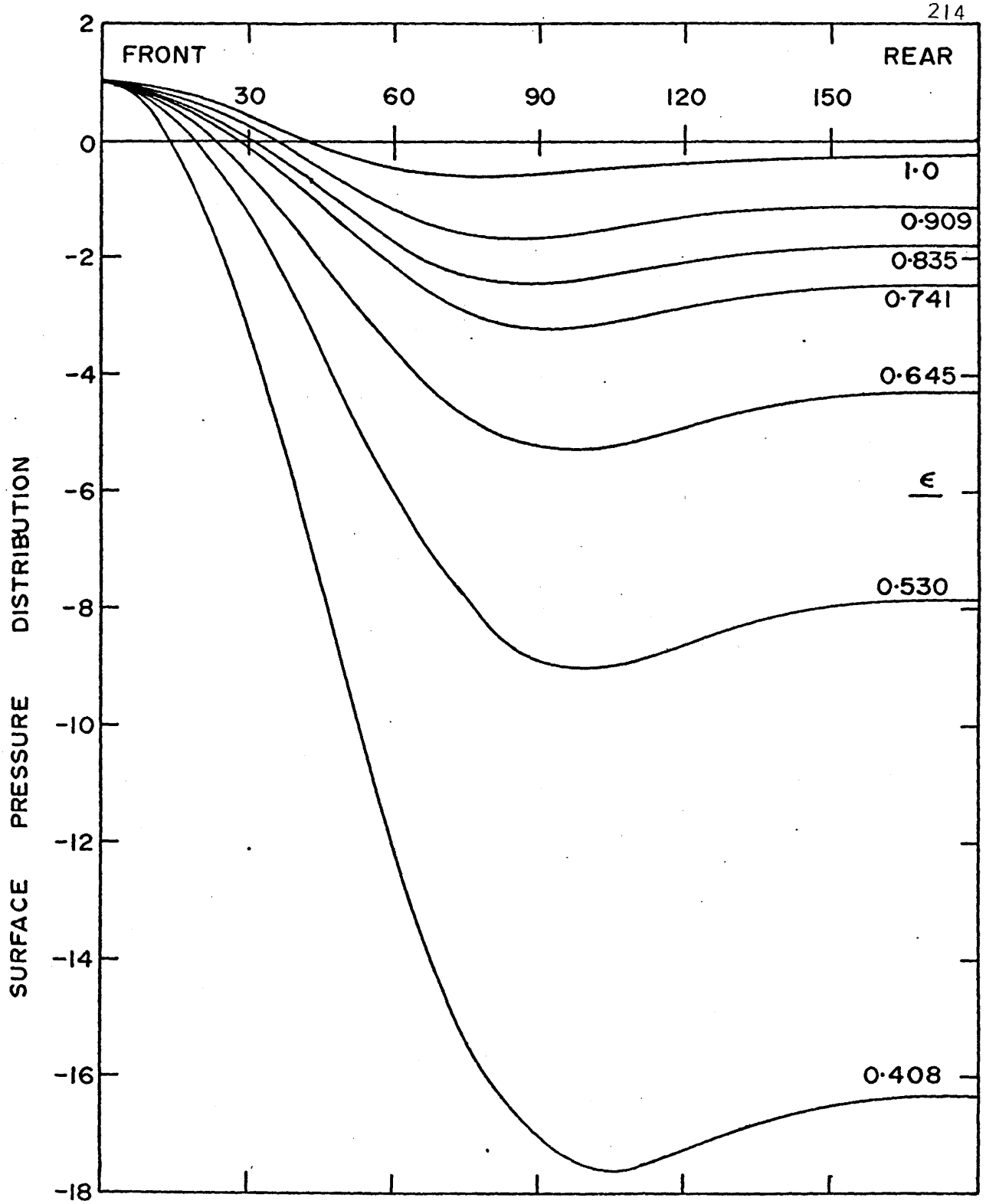

FIGURE C.1.B SURFACE PRESSURE DISTRIBUTION ABOUT A SPHERE AT N_{Re} = 500

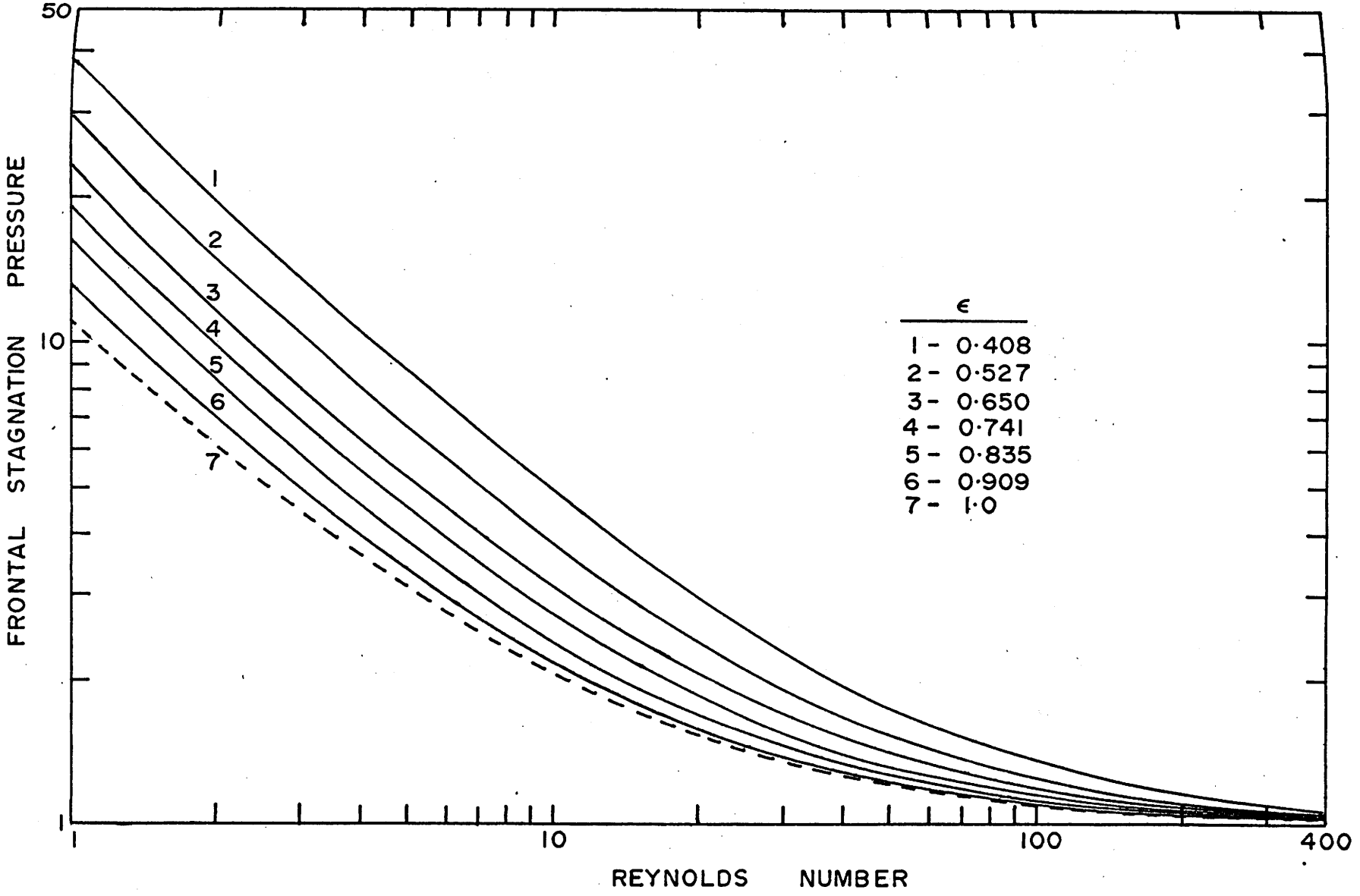

FIGURE C.2.A FRONTAL STAGNATION POINT PRESSURE VARIATION WITH REYNOLDS NUMBER AND POROSITY

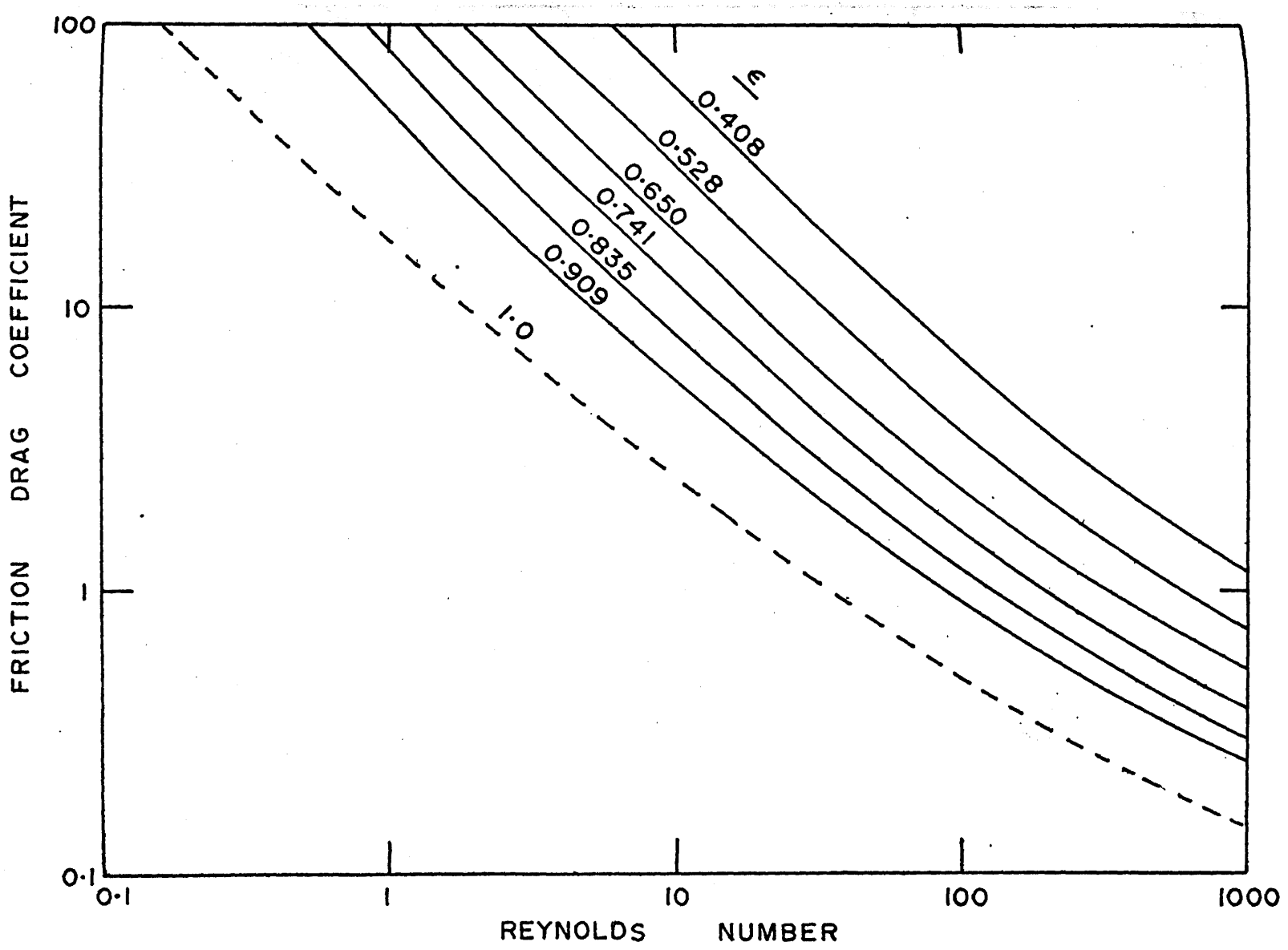

FIGURE C.2.B FRICTION DRAG COEFFICIENT VARIATION WITH REYNOLDS NUMBER AND POROSITY

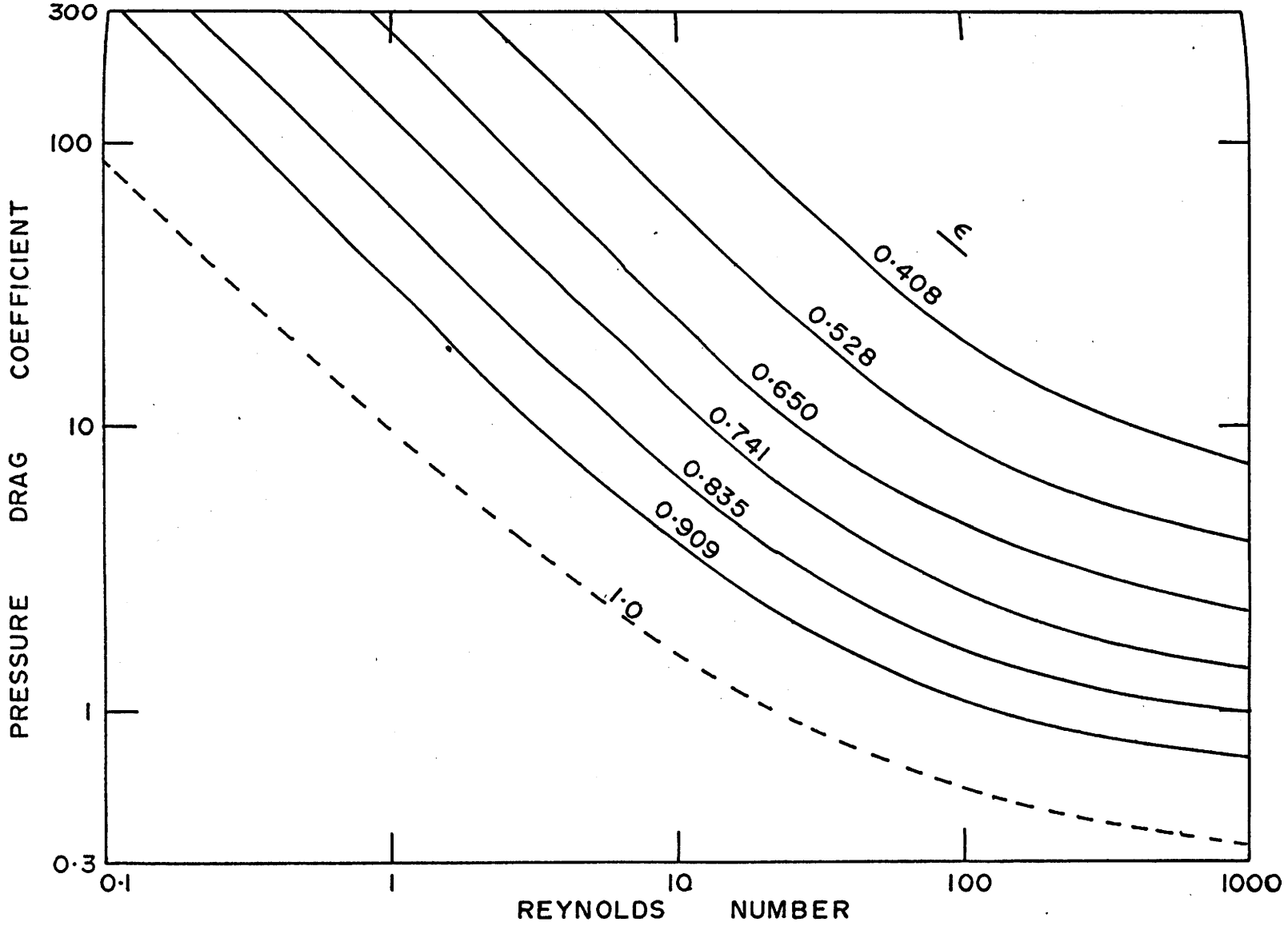

FIGURE C.2.C PRESSURE DRAG COEFFICIENT VARIATION WITH REYNOLDS NUMBER AND POROSITY

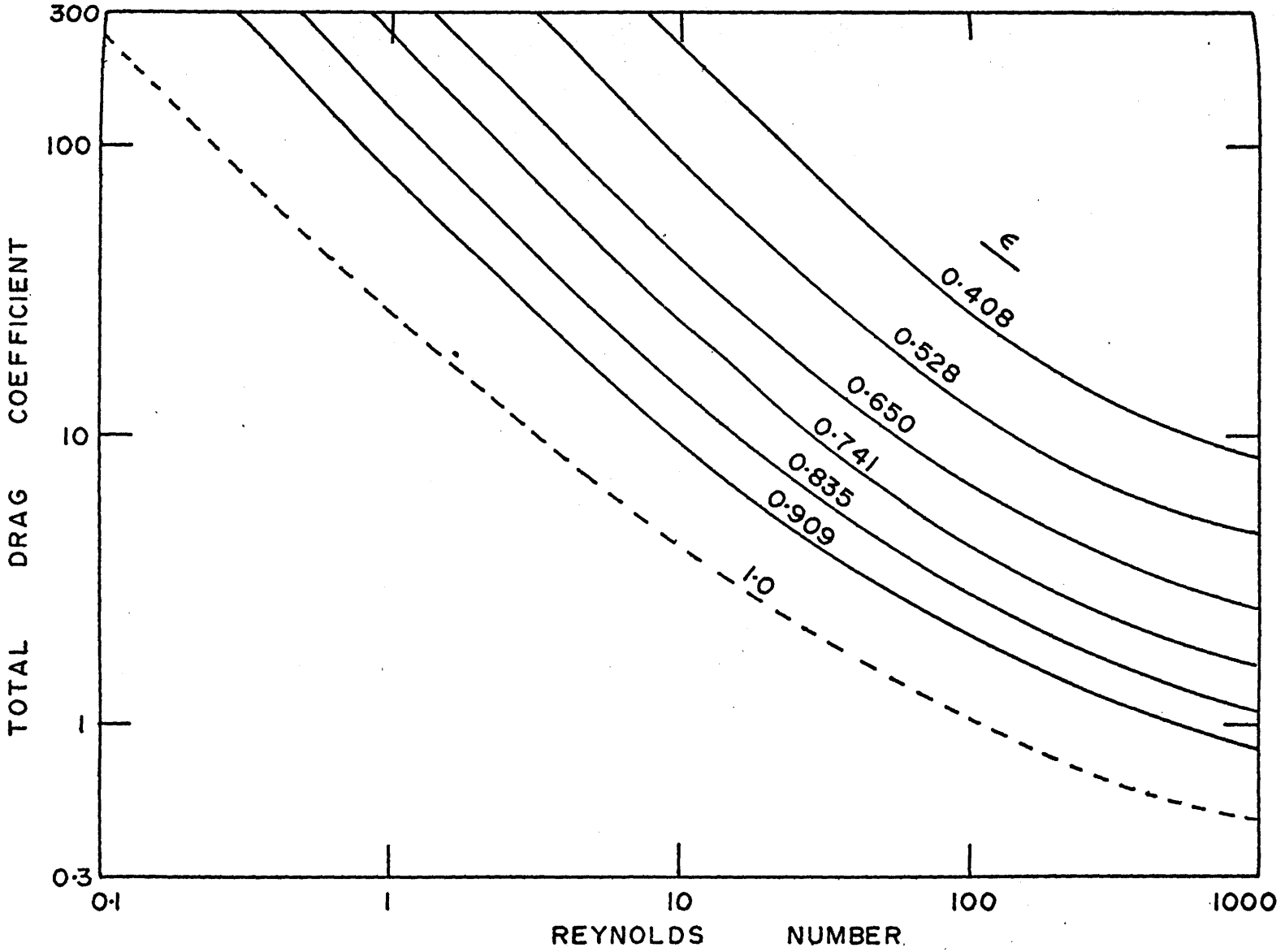

FIGURE C.2.D TOTAL DRAG COEFFICIENT VARIATION WITH REYNOLDS NUMBER AND POROSITY

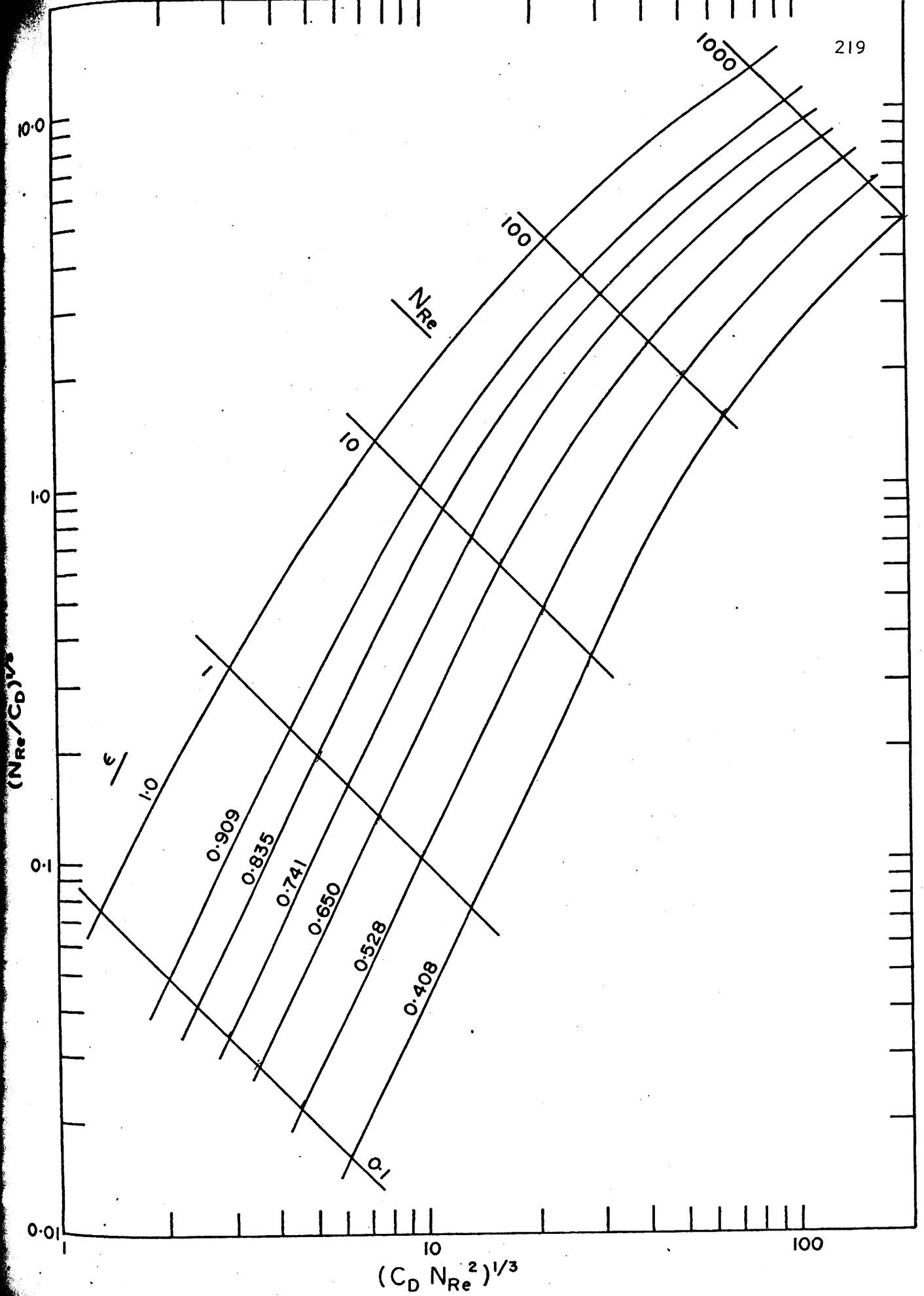

FIGURE C.2.E ZENZ CORRELATION FOR FLUIDIZATION

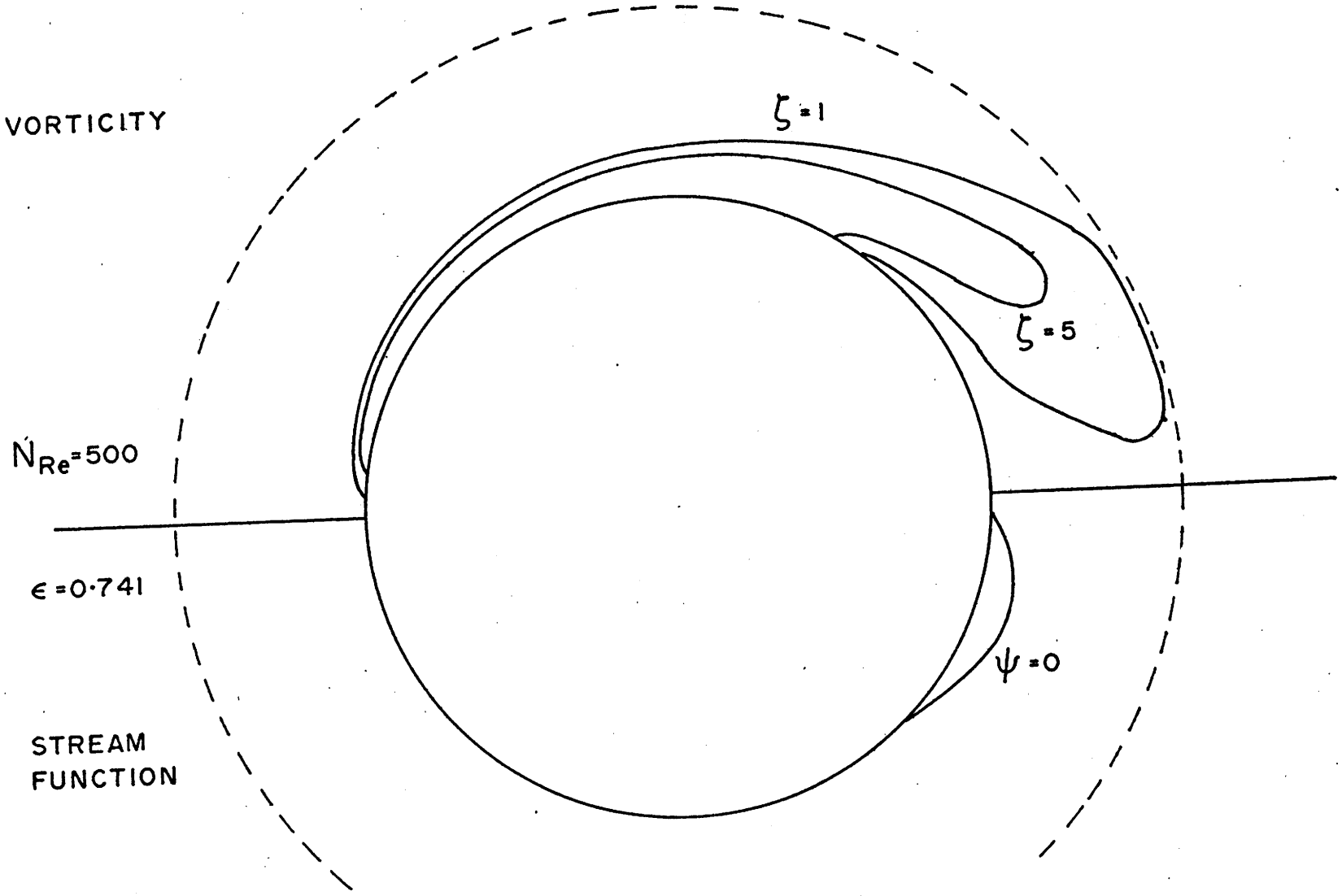

FIGURE C.3.A STREAM FUNCTION AND VORTICITY CONTOURS AT N_{Re} = 500 AND ε = 0.741

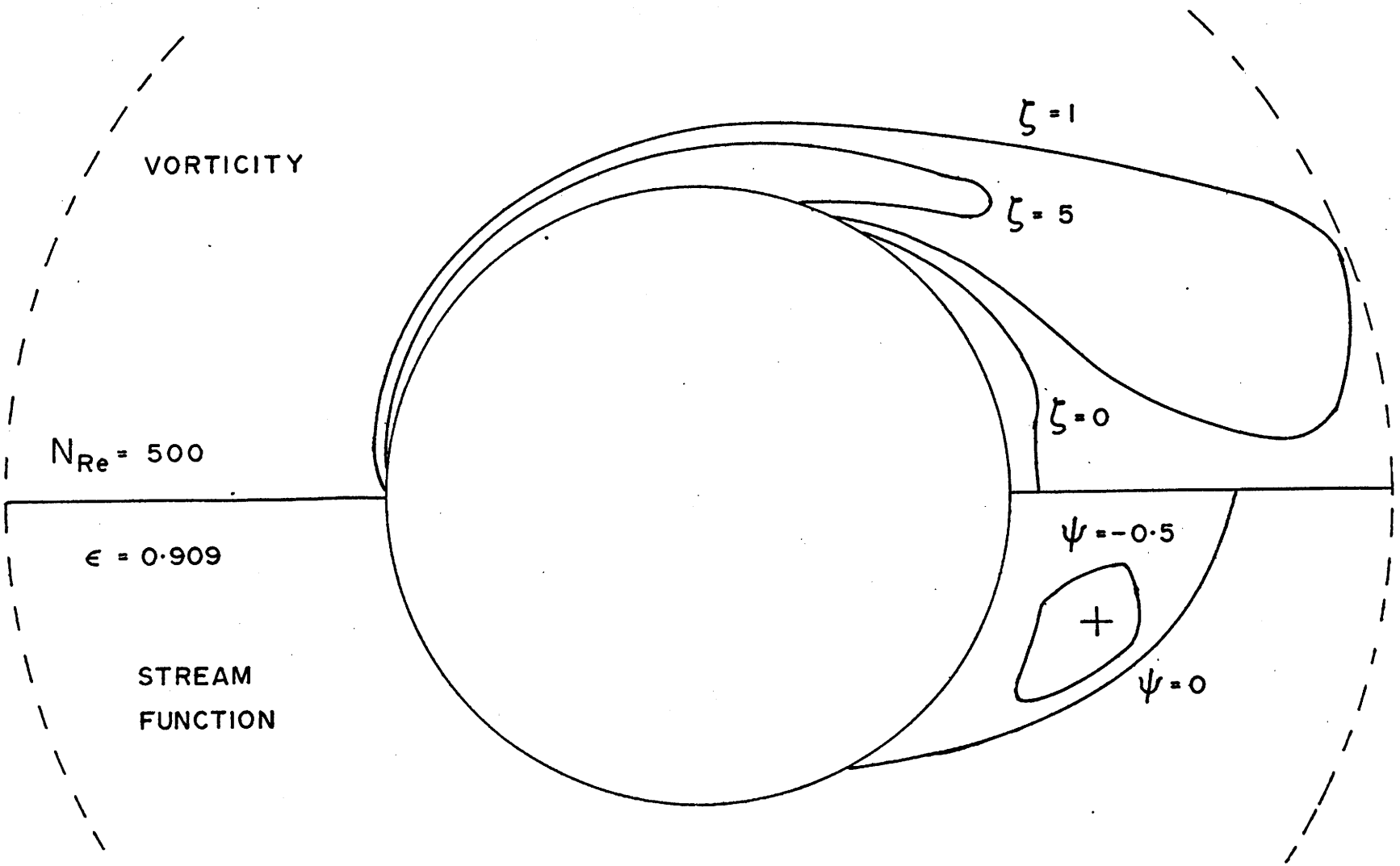

FIGURE C.3.B STREAM FUNCTION AND VORTICITY CONTOURS AT N_{Re} = 500 AND ϵ = 0.909

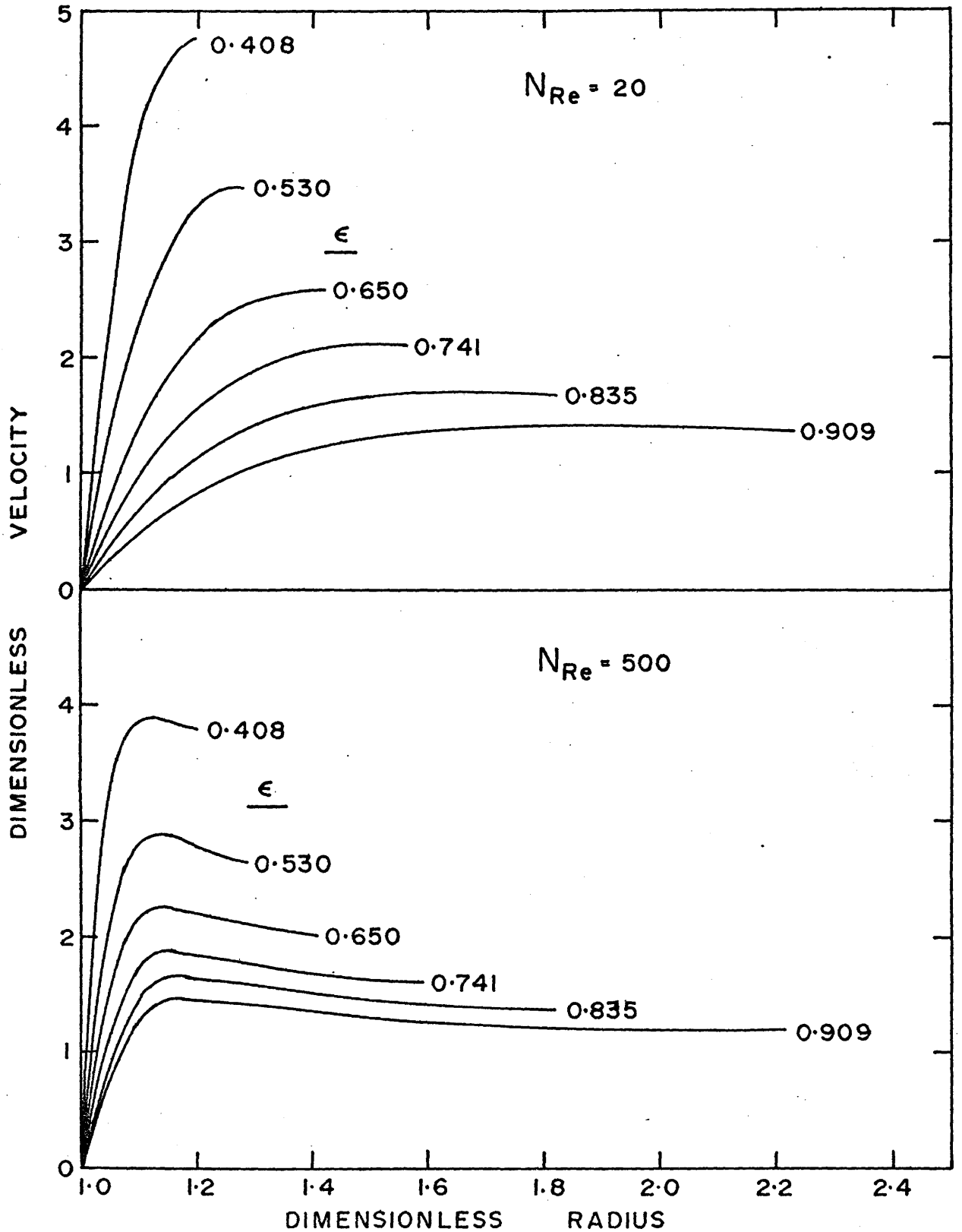

FIGURE C.4 DIMENSIONLESS ANGULAR VELOCITY VARIATION WITH RADIAL POSITION AT N_{Re} = 20 AND 500

C.1.7 Comparison of Predicted Results with Experimental Data for Packed Beds

Experimental drag data for low Reynolds number flow through packed beds of spheres may be represented by the Carman-Kozeny equation plotted in Figure C.5.A. Also shown is the theoretical line after Happel (1958) (derived for creeping flow using a free surface model) and the semitheoretical line after Hawksley and Vand (1951). The present results for low Reynolds ($N_{Re} < 1$) are almost identical to those of Happel. The small difference is due to the fact that the boundary conditions on the outer spherical boundary are not equivalent. Present results for two other Reynolds numbers and three porosities are also shown in this figure. The predicted effect of porosity appears reasonable; however a Reynolds number effect is suggested.

The Ergun equation (1952) is generally used to predict pressure drop data for packed beds in the intermediate Reynolds number range. Predicted theoretical drag data are compared with those from the Ergun equation for a bed porosity of 0.4 in Table C.2. The agreement is within $\pm$ 15% over the Reynolds number range $1 < N_{Re} < 30$. An explanation of the discrepancy at higher Reynolds will be dealt with in a latter section. Specific reference will be made to the surface-interaction model and the mechanism by which it accounts for changes in porosity.

C.1.8 Data for Fluidized Beds

The present predictions are shown for Reynolds numbers 1, 10, 100, and 500 over a porosity range of 0.4 to 1.0. Also shown in Figures C.5.B, C.5.C, C.5.D, and C.5.E are the theoretical line after Happel (1958) and the semi-theoretical lines after Hawksley and Vand (1951) and Oliver (1961). Experimental data are indicated by the dashed lines. Although the present theoretical lines account for a Reynolds number effect, where the others do not, the predicted velocities are always lower than the experimental data. The agreement is considerably improved over that observed for packed beds, but is not entirely satisfactory. For fluidized beds the agreement improves at higher Reynolds numbers.

TABLE C.2 THEORETICAL AND EXPERIMENTAL DRAG COEFFICIENTS

N_{Re}	C_D exptl. (Ergun, 1952)	C_D pred. present $\varepsilon=0.4$	Error %
1	1960	2260	+ 15.5
10	218	227	+ 4.1
20	131	114	- 13
50	75	48	- 36
100	56	26	- 54
500	37	12	- 69

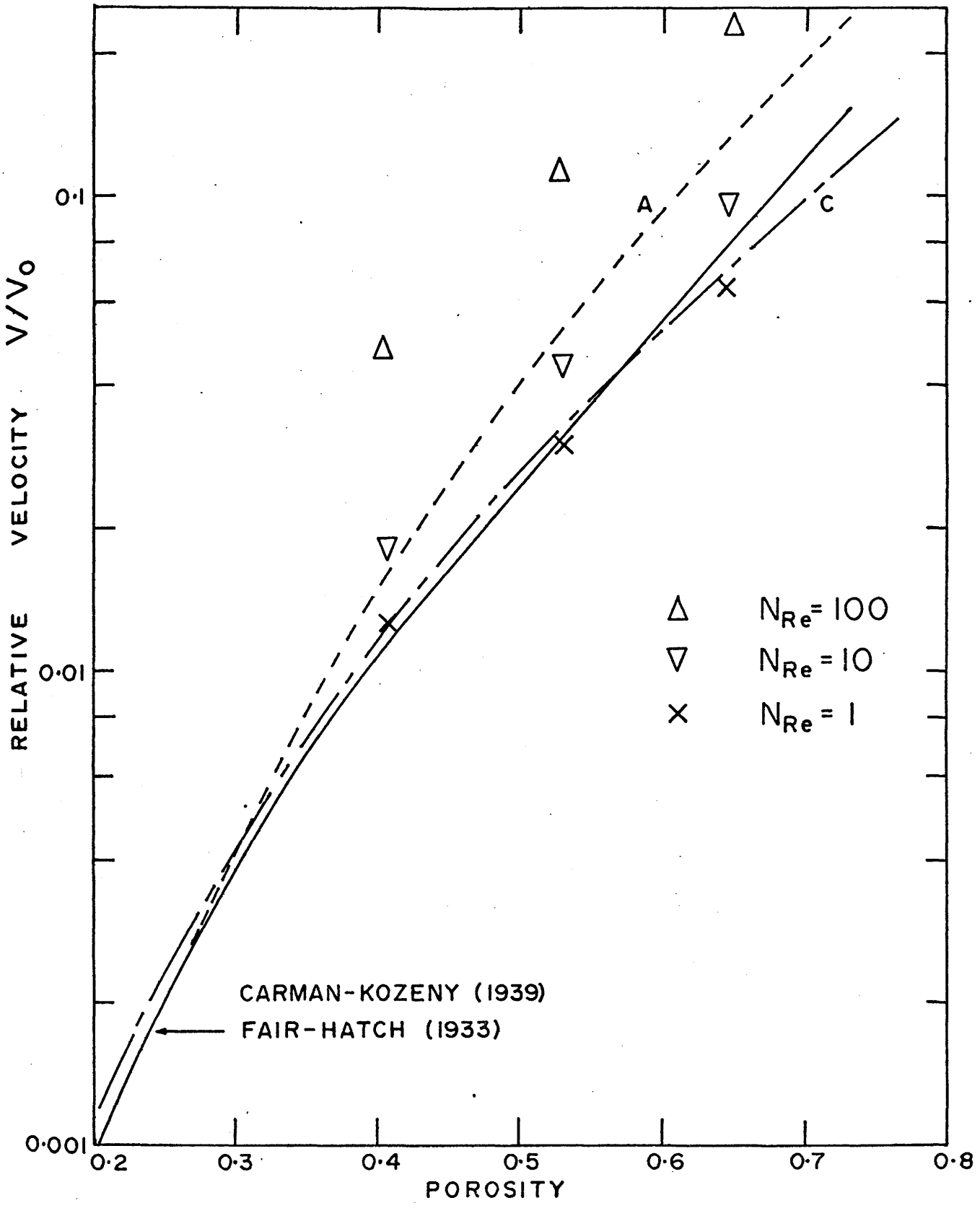

FIGURE C.5.A COMPARISON OF THEORETICAL RELATIONSHIP WITH DATA FOR FLOW THROUGH BEDS - PACKED BEDS

FIGURE C.5.B COMPARISON OF THEORETICAL RELATIONSHIP WITH DATA FOR FLOW THROUGH BEDS - FLUIDIZED BEDS AT $N_{Re_o} < 1$

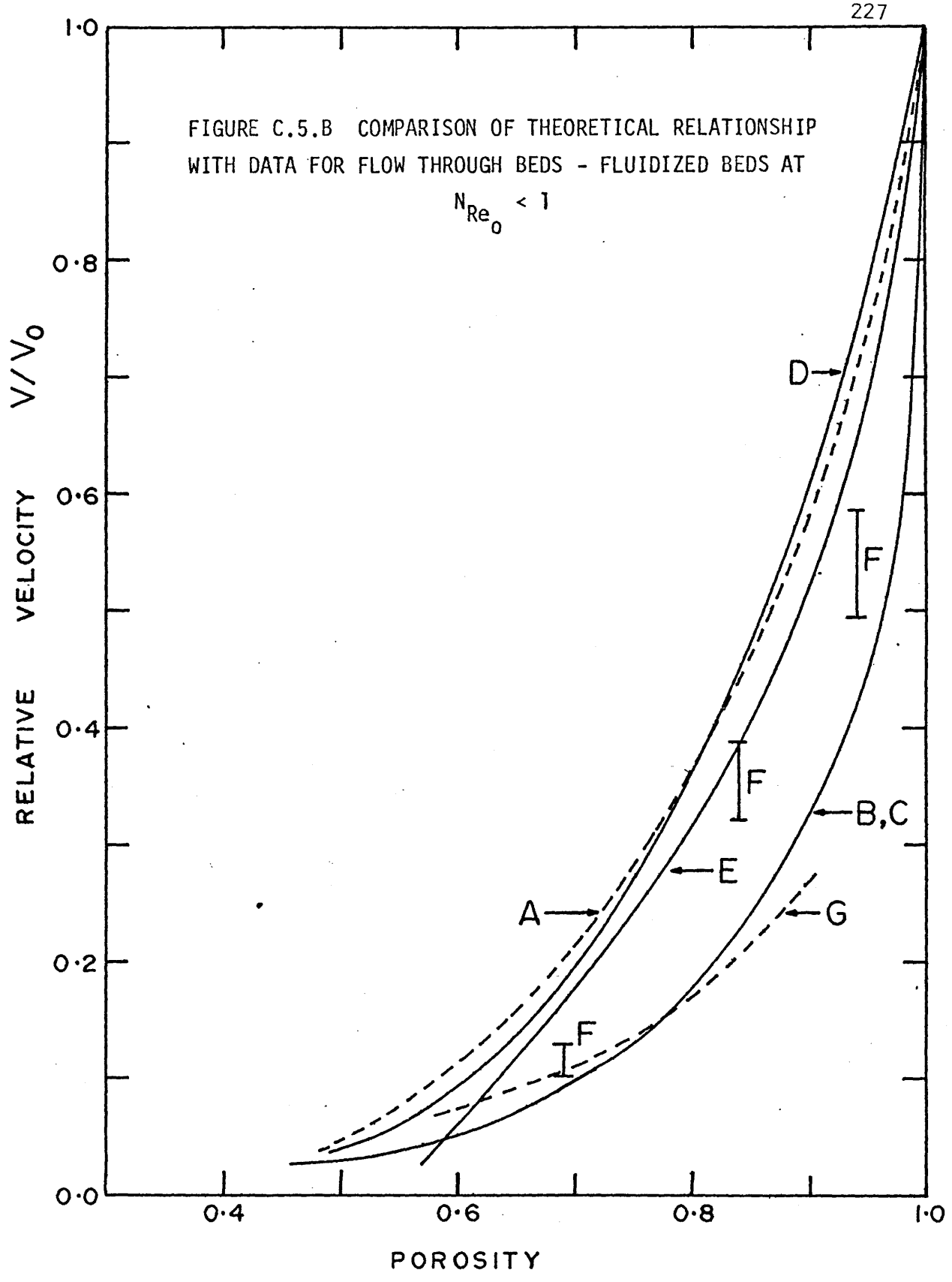

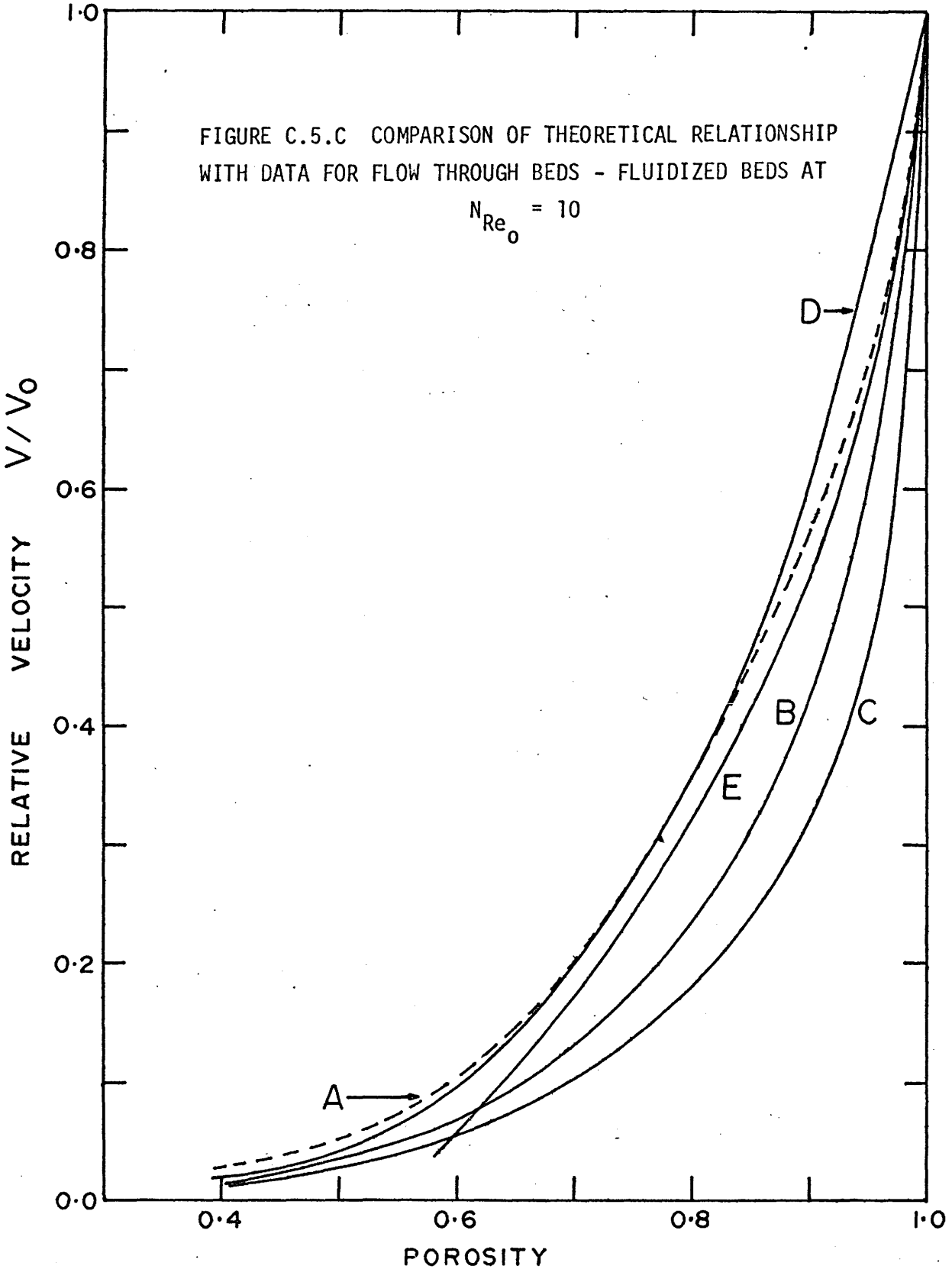

FIGURE C.5.C COMPARISON OF THEORETICAL RELATIONSHIP WITH DATA FOR FLOW THROUGH BEDS - FLUIDIZED BEDS AT $N_{Re_o} = 10$

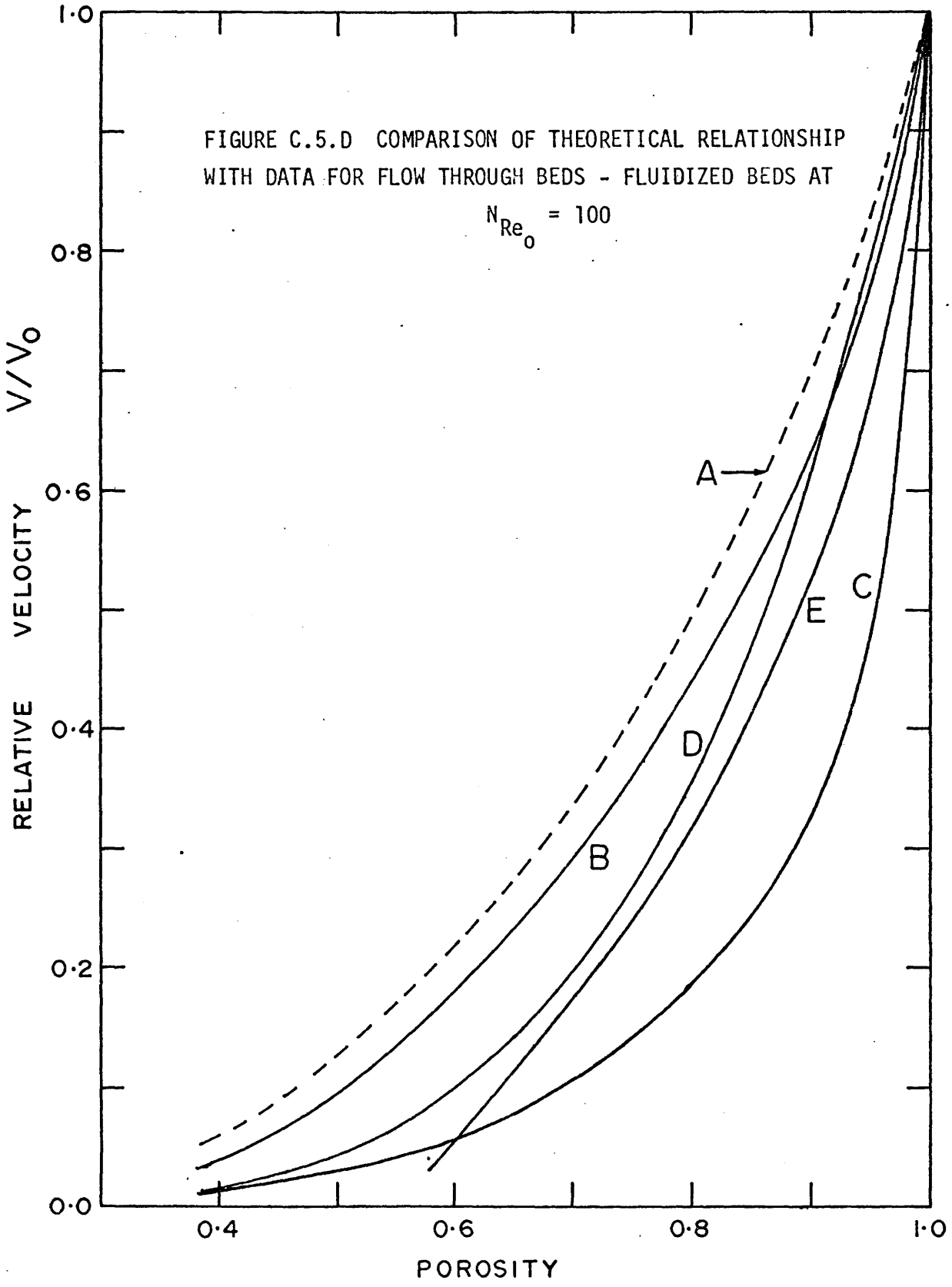

FIGURE C.5.D COMPARISON OF THEORETICAL RELATIONSHIP WITH DATA FOR FLOW THROUGH BEDS - FLUIDIZED BEDS AT $N_{Re_o} = 100$

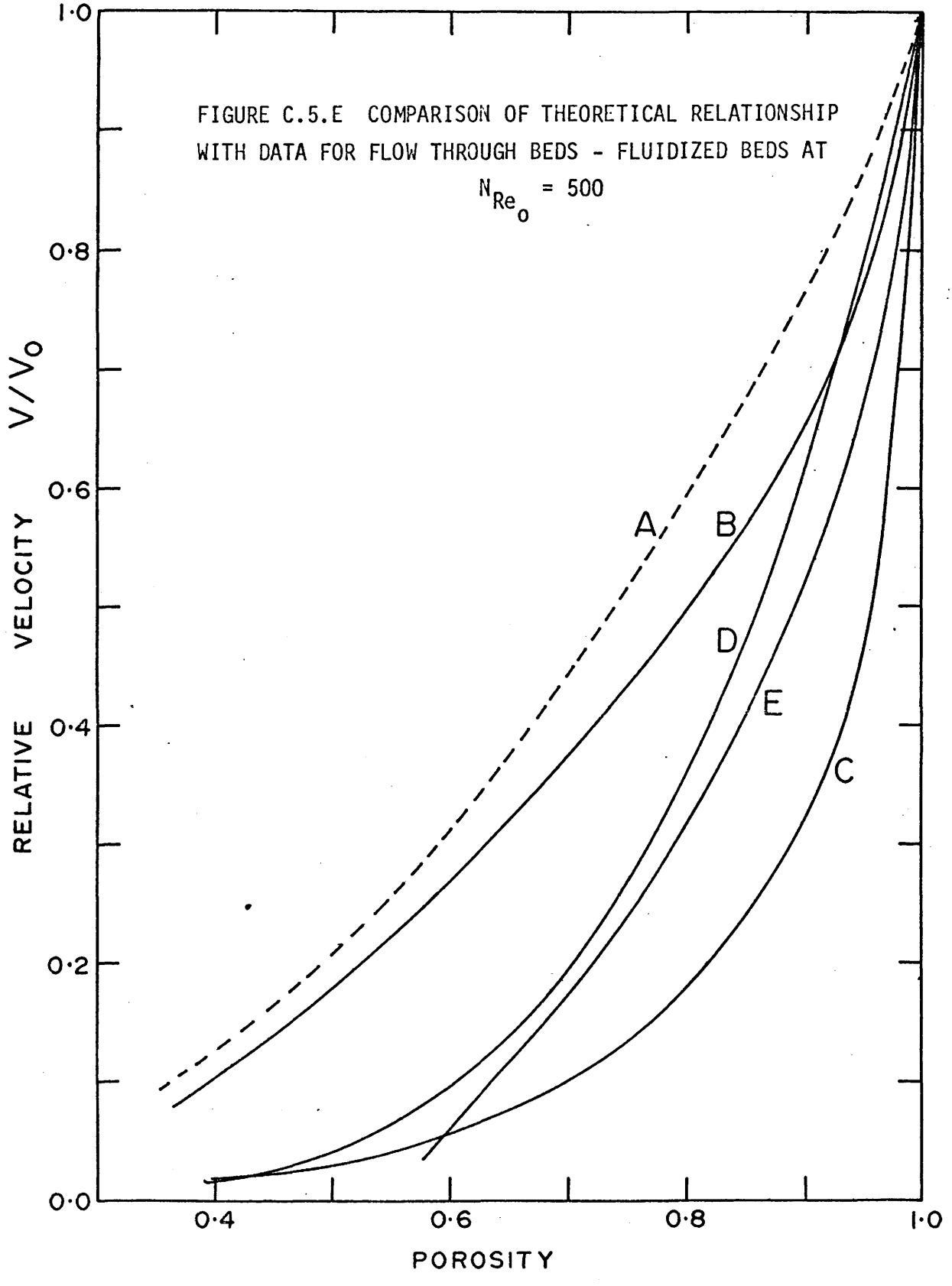

FIGURE C.5.E COMPARISON OF THEORETICAL RELATIONSHIP WITH DATA FOR FLOW THROUGH BEDS - FLUIDIZED BEDS AT $N_{Re_o} = 500$

C.1.9 Discussion of Cell Models

The cell model has permitted the prediction of the drag acting on sphere assemblages as a function of Reynolds number and particle interaction or porosity. No other solution of the Navier Stokes equations for sphere assemblages for intermediate Reynolds numbers exists in the literature. The solutions are at best a first attempt to define the flow behaviour at Reynolds numbers where the creeping flow equations no longer apply. It is realized that the cell models used by Happel (free-surface) and by the present authors do not truly represent the local flow behaviour in a multiparticle system; however, they are easy to apply.

The cell model applied in this study accounts for particle interaction by the relative position of the zero vorticity and parallel flow condition with respect to the particle surface. For low porosity or high particle interaction the boundary is close to the surface and for high porosity or low particle interaction it is far from the surface. The imposed boundary is a spherical shell around the particle.

The theoretical model predicts relative velocity ratios lower than experimental data for all Reynolds numbers. The deviation is most pronounced at low Reynolds numbers ($N_{Re} \simeq 1$). Velocity profiles at the equator (Figure C.4) suggest that the thick boundary layer at low Reynolds numbers is producing large peripheral velocities and thus much greater drag than would be expected. To obtain reduced drag and therefore an increased relative velocity ratio, the flow restriction must be decreased. An oblate spheroid having an equivalent volume and hence the

same porosity as the spherical shell should produce the desired effect. This observation is substantiated by the models developed by Richardson and Zaki (1954). Particle configuration (II) predicts a higher relative velocity than configuration (I).

At higher Reynolds numbers the boundary layer is thin (Figure C.4); therefore flow restriction should not be important. However, the model predicts a drag greater than that found experimentally. This undoubtedly results from too great a suppression of dounstream vorticity by the boundary condition on the outer spherical boundary. A prolate spheroid outer boundary would reduce the vortex ring suppression and, hence, increase the relative velocity ratio, producing results closer to experiment.

Table C.2 shows that a spherical outer boundary is satisfactory for Reynolds number about 13. This suggests an outer boundary shape which is a function of Reynolds number and changes from oblate at low Reynolds numbers through spherical to prolate at high Reynolds numbers. Support of this hypothesis would come from studies of local porosity variations in the radial and longitudinal directions. Happel and Epstein (1954) presented data on flow through cubical assemblages of uniform spheres. This is equivalent to a spherical outer boundary. Their results agree favourably with the data of Mertes and Rhodes (1955) for N_{Re} = 16, but in the low Reynolds number range their relative velocity results are lower than experiment. Further confirmation that direction porosity variations could account for the deviations between theoretical results and experiment.

Gunn and Malik (1966) performed an extensive study of extended beds (particle assemblages fixed in space) over the Reynolds number range 0.1 to 1000. Three regular arrays of spheres were investigated, simple cubic, body-centered cubic and face-centered cubic. Gunn and Malik presented their results as a series of figures of drag coefficient against porosity with inter-sphere spacing (distance between spheres in a plane perpendicular to the flow) and inter-planar spacing (distance between spheres in direction of flow) as parameters for several Reynolds numbers. These results are extremely interesting and are presented here as Figures C.6A, C.6.B, C.6.C and C.6.D. Included in the figures as well, are the results obtained in this investigation. These figures clearly show a non-symmetric distribution of particles is necessary to obtain the experimental drag results. At low Reynolds numbers (N_{Re} = 0.1 and 10), inter-sphere spacing must be greater than inter-planar spacing. Thus at low Reynolds numbers where the boundary layer is thick; particle blockage is the controlling resistance. Whereas at high Reynolds numbers, where a thin boundary layer is present, the trailing vortex and subsequent pressure reduction are controlling. Fluidized bed expansion is thus lateral expansion at low Reynolds numbers and longitudinal expansion at high Reynolds numbers.

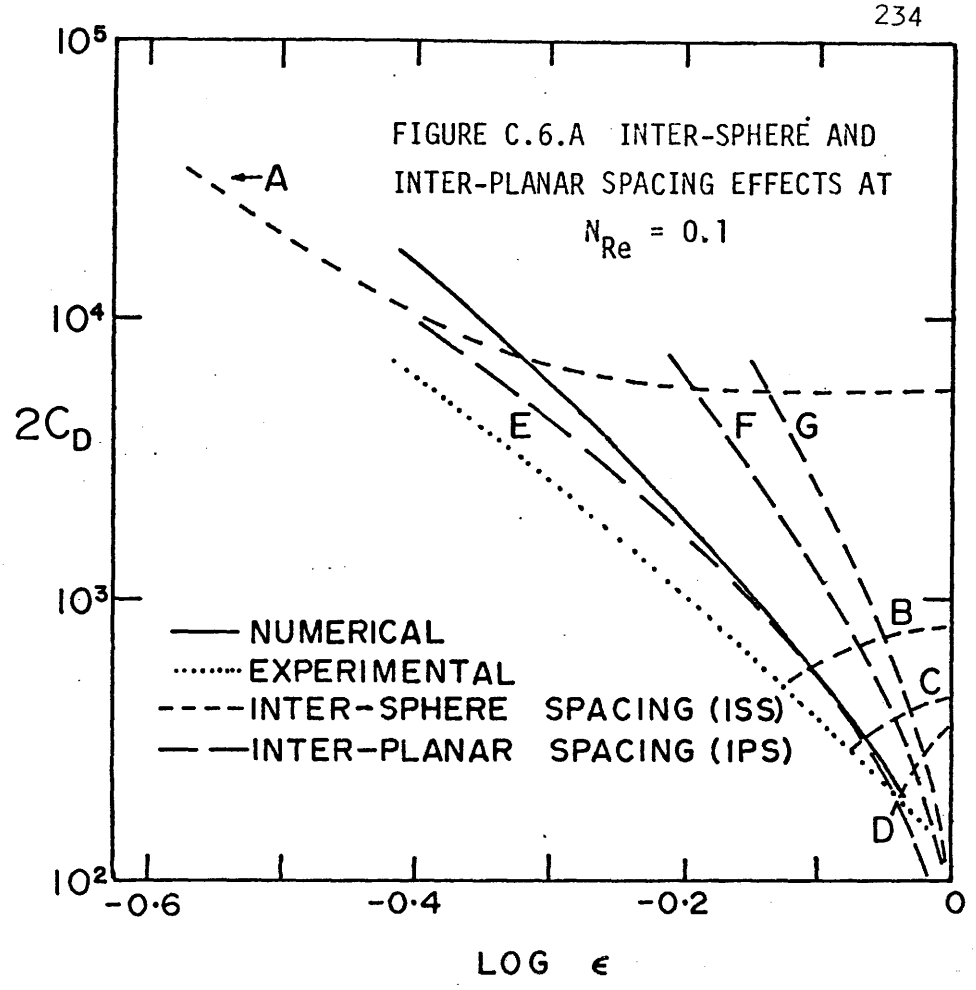
FIGURE C.6.A INTER-SPHERE AND INTER-PLANAR SPACING EFFECTS AT N_{Re} = 0.1
10^5
10^4
10^3
10^2
$2C_D$
A
E
F
G
B
C
D
NUMERICAL
EXPERIMENTAL
INTER-SPHERE SPACING (ISS)
INTER-PLANAR SPACING (IPS)
-0·6
-0·4
-0·2
0
LOG ϵ

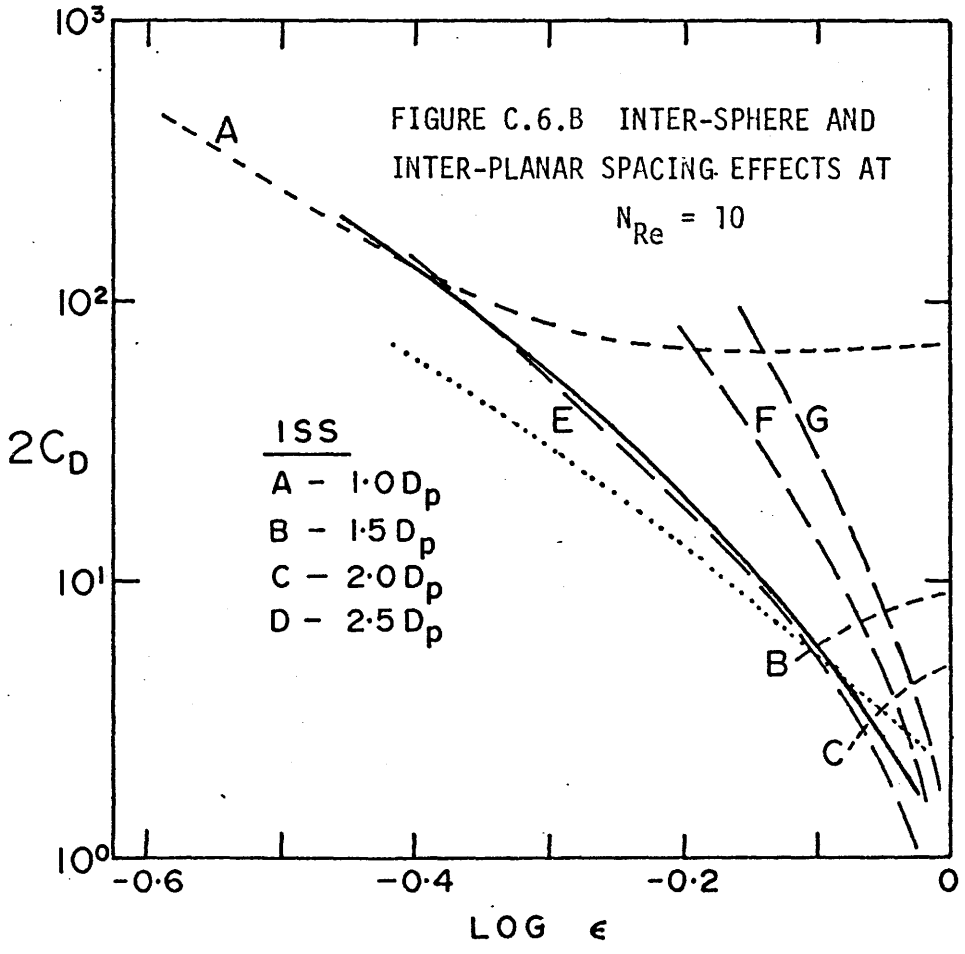
FIGURE C.6.B INTER-SPHERE AND INTER-PLANAR SPACING EFFECTS AT N_{Re} = 10
10^3
10^2
10^1
10^0
$2C_D$
A
E
F
G
B
C
ISS
A - 1·0 D_p
B - 1·5 D_p
C - 2·0 D_p
D - 2·5 D_p
-0·6
-0·4
-0·2
0
LOG ϵ

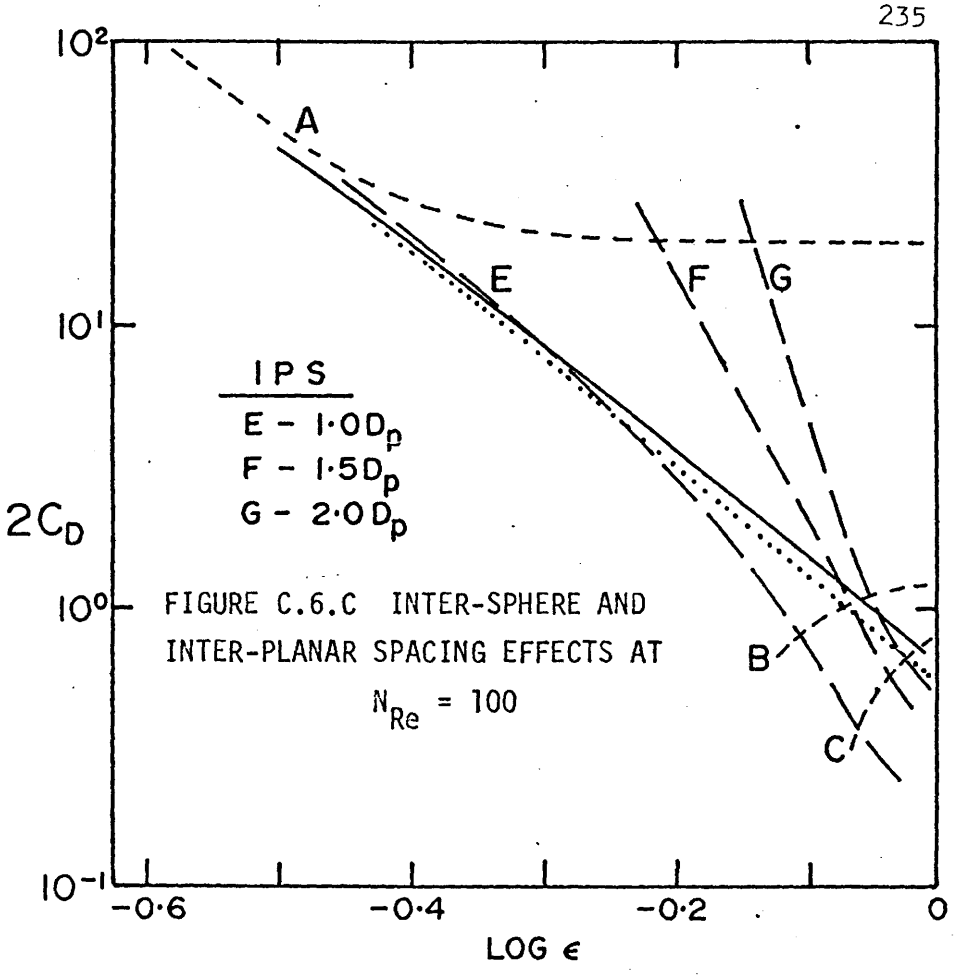

FIGURE C.6.C INTER-SPHERE AND INTER-PLANAR SPACING EFFECTS AT N_{Re} = 100

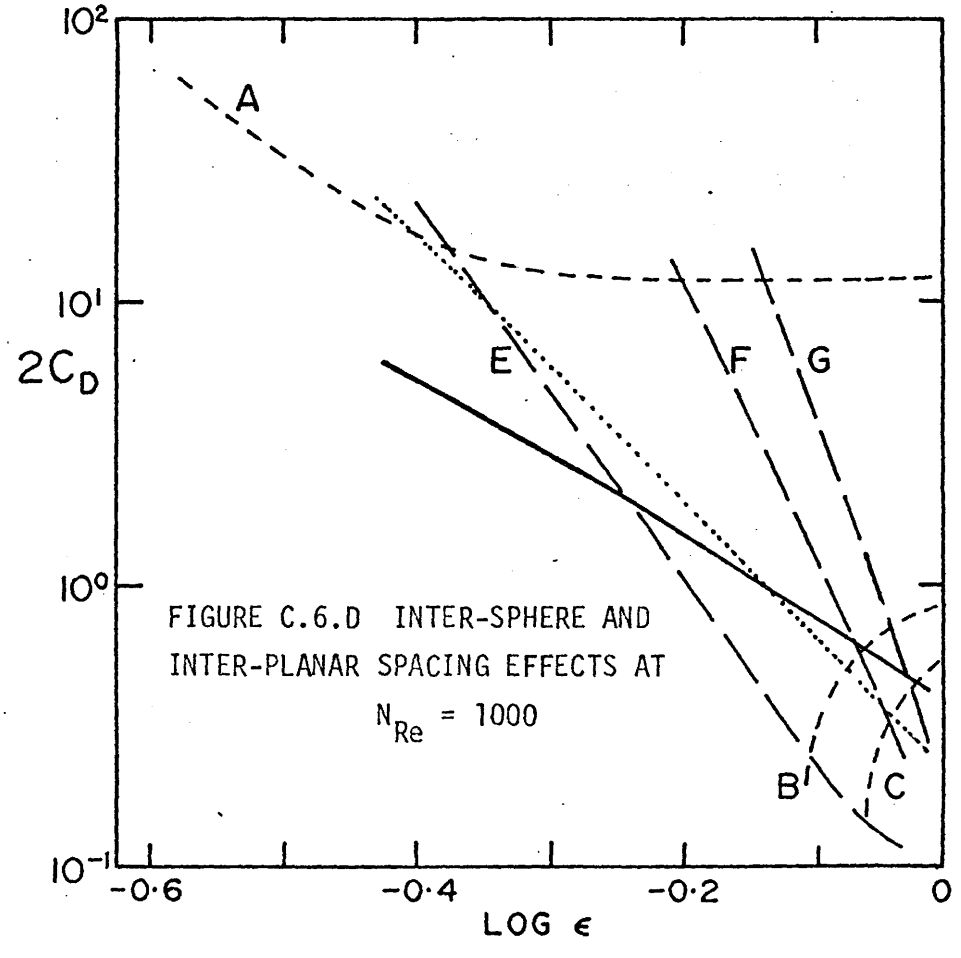

FIGURE C.6.D INTER-SPHERE AND INTER-PLANAR SPACING EFFECTS AT N_{Re} = 1000

C.2 Cylinder Bundles

C.2.1 Accuracy of Solutions

The accuracy of the solutions was examined by reducing both the radial and angular step sizes by a factor of two until the change between two successive solutions was less than two percent. The solutions were assumed to have converged when values of the vorticity and stream function at all mesh points changed by less than 0.0001 per iteration.

C.2.2 Surface Vorticity Distributions

The surface vorticity distributions for one Reynolds number (N_{Re} = 100) and for a range of porosities (ε = 0.4 to 1.0) are shown in Figure C.7.A. These vorticity distributions are typical and similar results have been obtained for Reynolds numbers of 0.1, 1, 10, 20, 50, 100 and 500. The results for all these cases are presented in Appendix II-A.

At the point of flow separation the surface vorticity changes sign and this fact may be used to estimate the flow separation angle. The flow separation angle (measured from the rear stagnation point) and the size of the vortex ring decrease with decreasing porosity. The magnitude of the vorticity increases significantly as the porosity decreases resulting in a rather large increase in friction drag.

C.2.3 Surface Pressure Distribution

The surface pressure distributions for one Reynolds number (N_{Re} = 100) and a range of porosities (ε = 0.4 to 1.0) are presented in Figure C.7.B. These distributions are typical and similar results have been predicted for Reynolds numbers of 0.1, 1, 10, 20, 100, and 500 and

may be found in Appendix II-A.

Frontal stagnation pressure is only slightly dependent on porosity at N_{Re} = 100. At lower Reynolds numbers, however, the dependence is clearly evident with the stagnation pressure increasing as the porosity decreases. The effect of porosity on frontal stagnation pressure is shown in Figure C.8.A for a range of Reynolds numbers and porosities.

C.2.4 Pressure, Friction, and Total Drag Coefficients

Pressure drag coefficients for a range of porosities (ε = 0.4 to 1.0) and for a range of Reynolds numbers are shown in Figure C.8.B. The values for a porosity of one were obtained from the literature (Hamielec and Raal, 1969). Similar results have been obtained for friction and total drag coefficients and are presented in Figures C.8.C and C.8.D. They also appear in Table C.3.

C.2.5 Dimensions of the Standing Vortex

The stagnation stream line of the standing vortex rings have been plotted in Figure C.9 for three Reynolds numbers (N_{Re} = 20, 50 and 100) and two porosities (ε = 0.5 and ε = 0.9). The effect of a reduction in porosity is to reduce the dimensions of the vortex ring-viz., the flow separation angle becomes smaller and the length of the vortex ring as measured along the axis $\theta = \pi$ is reduced. A reduction in size of the standing vortex ring has been observed experimentally in flow visualization experiments (Hiby, 1962). For a porosity of 0.5, no vortex ring is observed at N_{Re} = 20 and the ring is very much reduced at N_{Re} = 70. The theoretical calculations show that the vortex ring does not appear until $\varepsilon \geq 0.8$ at

TABLE C.3 STAGNATION PRESSURE AND DRAG COEFFICIENTS

N_{Re}	ε	P_o	C_{DP}	C_{DF}	C_D
1.0	0.4	27.844	1383.974	339.303	1723.277
	0.5	20.898	536.439	180.717	717.156
	0.6	17.023	270.196	114.141	384.337
	0.7	13.590	127.112	68.301	195.413
	0.8	10.958	62.444	41.509	103.953
	0.9	8.445	27.833	22.779	50.612
	1.0		5.583	5.470	11.053
10.0	0.4	3.610	140.675	34.056	174.731
	0.5	2.911	55.812	18.300	74.112
	0.6	2.526	28.987	11.685	40.672
	0.7	2.194	14.529	7.170	21.699
	0.8	1.953	7.954	4.585	12.539
	0.9	1.752	4.317	2.839	7.156
	1.0		1.533	1.232	2.765
20.0	0.4	2.257	74.142	17.323	91.465
	0.5	1.927	30.833	9.455	40.288
	0.6	1.740	16.944	6.174	23.118
	0.7	1.584	9.203	3.936	13.139
	0.8	1.477	5.434	2.637	8.071
	0.9	1.389	3.131	1.718	4.849
50.0	0.4	1.475	37.614	7.492	45.106
	0.5	1.349	17.688	4.307	21.995
	0.6	1.283	10.596	2.937	13.533
	0.7	1.234	6.198	1.970	8.168
	0.8	1.195	3.864	1.375	5.239
	0.9	1.164	2.337	0.933	3.270
	1.0		1.014	0.493	1.507
100.0	0.4	1.222	25.879	4.144	30.023
	0.5	1.171	13.892	2.601	16.493
	0.6	1.136	7.912	1.699	0.611
	0.7	1.115	5.101	1.220	6.321
	0.8	1.098	3.296	0.870	4.166
	0.9	1.086	2.047	0.606	2.653
	1.0		0.954	0.336	1.290

TABLE C.3 (Continued)

N_{Re}	ε	P_o	C_{DP}	C_{DF}	C_D
500.0	0.4	1.044	16.799	1.346	18.145
	0.5	1.034	9.797	0.888	10.685
	0.6	1.027	6.030	0.030	6.637
	0.7	1.024	4.205	0.454	4.659
	0.8	1.021	2.821	0.333	3.154
	0.9	1.021	2.127	0.242	2.369

TABLE C.4 VORTEX RING DIMENSIONS FOR CYLINDERS

N_{Re}	ϵ	0.4	0.5	0.6	0.7	0.8	0.9
20	θ_s	-	-	-	-	15.7	28.7
	L	-	-	-	-	0.078	0.317
50	θ_s	-	13.8	20.3	28.2	36.6	45.4
	L	-	0.041	0.176	0.317	0.544	1.065
100	θ_s	19.3	25.7	33.7	41.0	48.3	55.6
	L	0.127	0.215	0.336	0.499	0.786	1.450
500	θ_s	46.9	52.6	57.8	62.5	67.5	74.4
	L	0.228	0.333	0.484	0.669	0.943	1.770

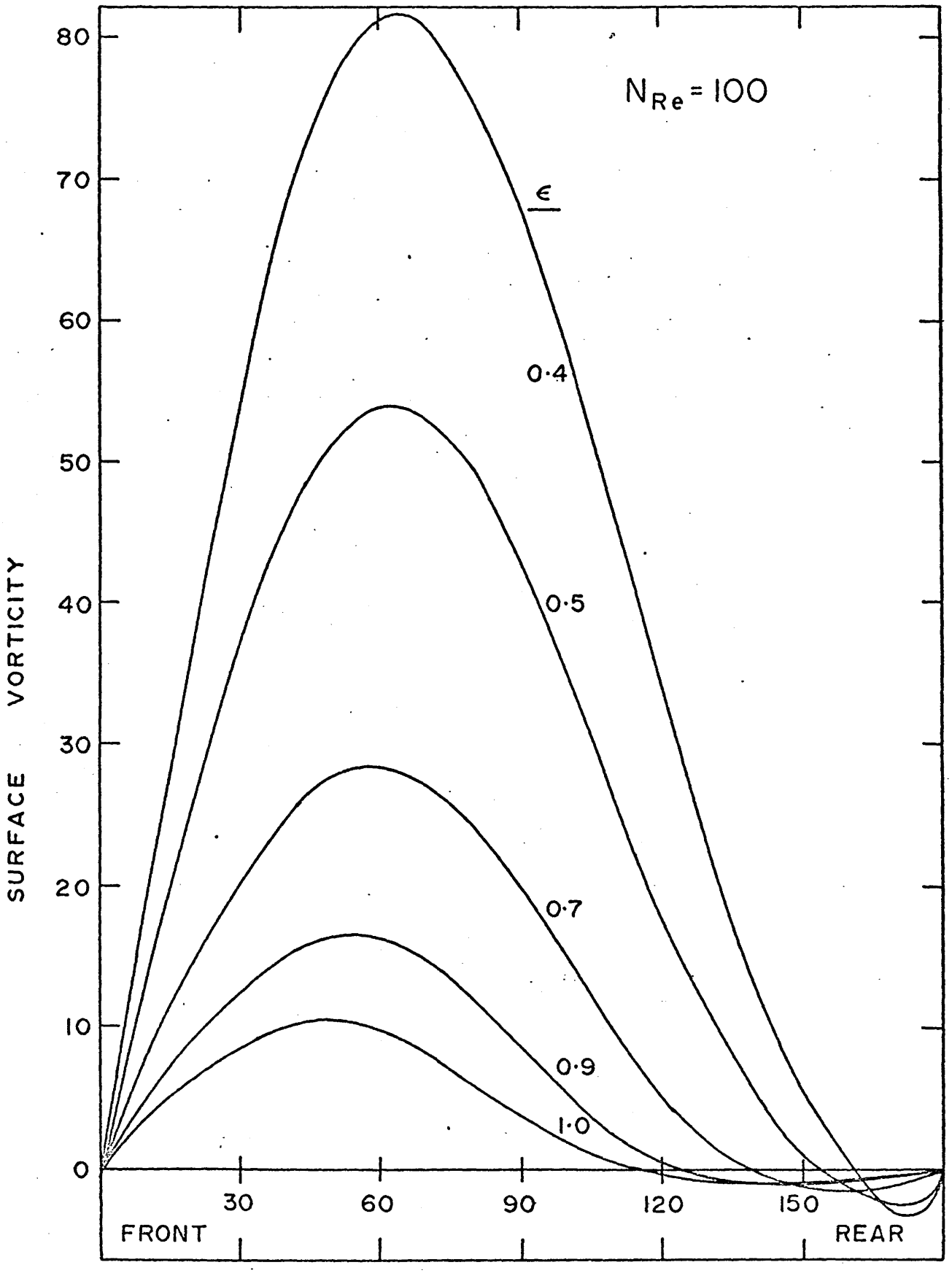

FIGURE C.7.A SURFACE VORTICITY DISTRIBUTIONS ABOUT A CYLINDER AT N_{Re} = 100

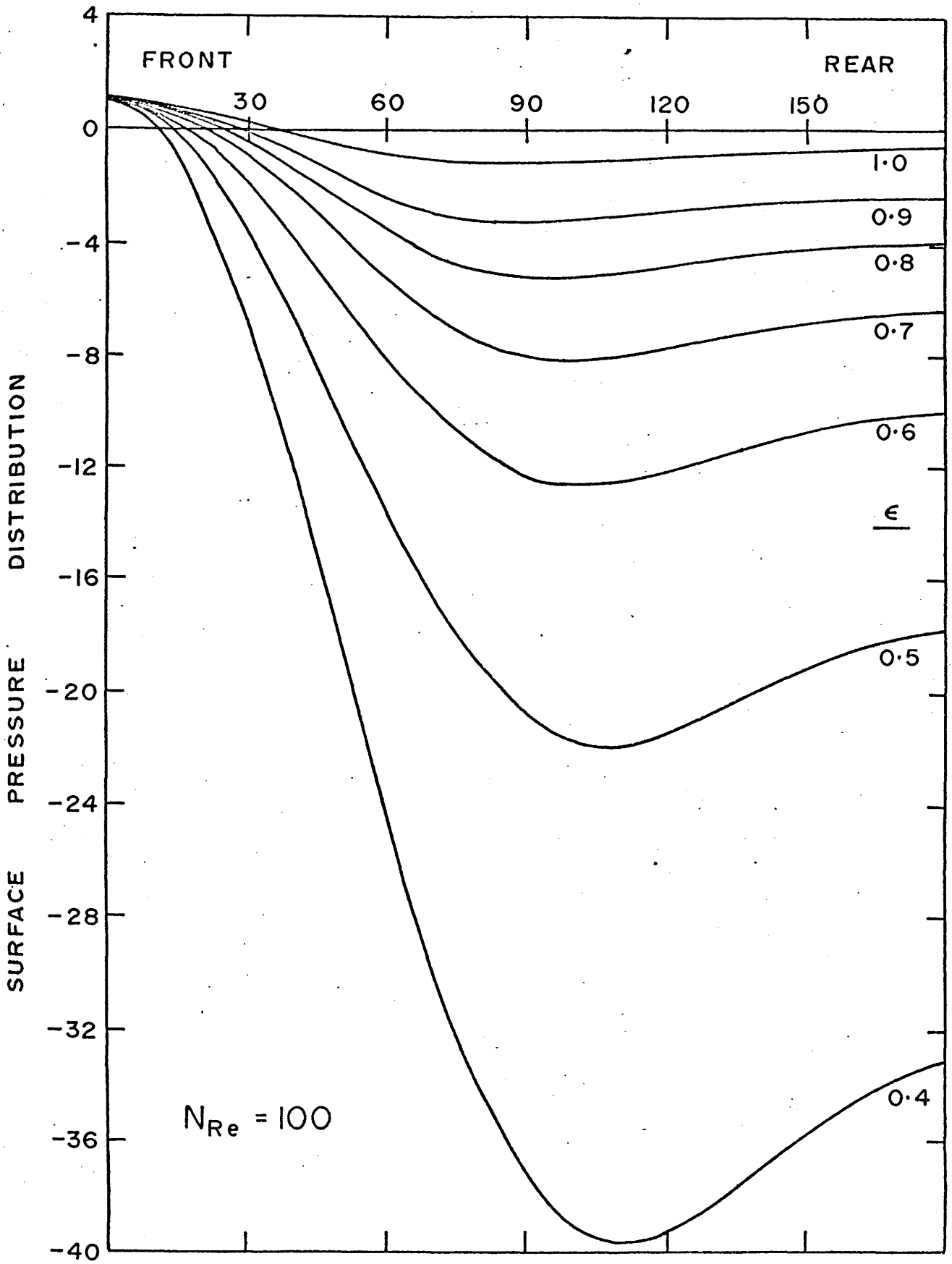

FIGURE C.7.B SURFACE PRESSURE DISTRIBUTIONS ABOUT A CYLINDER AT N_{Re} = 100

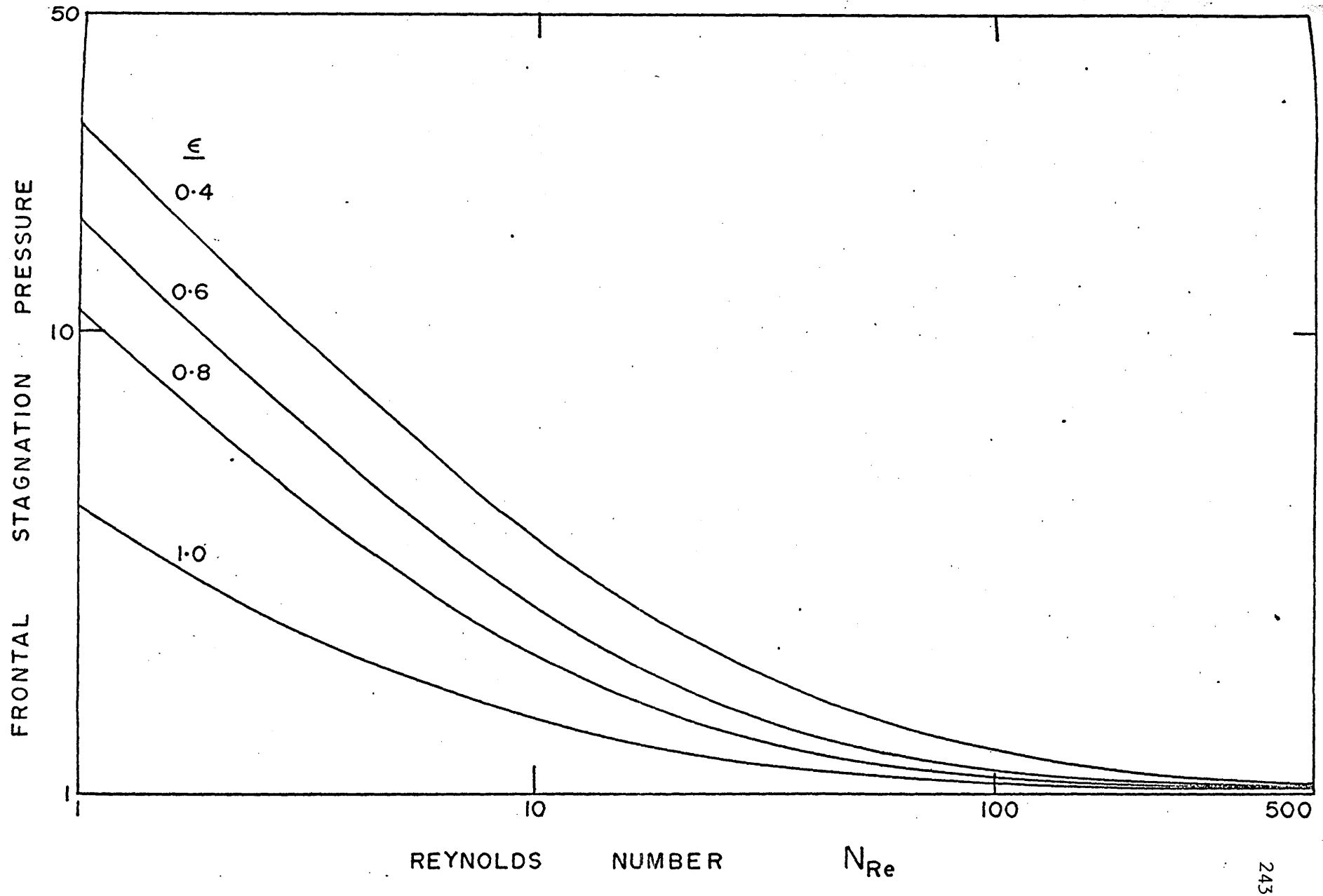

FIGURE C.8.A FRONTAL STAGNATION PRESSURE VARIATION WITH REYNOLDS NUMBER AND POROSITY

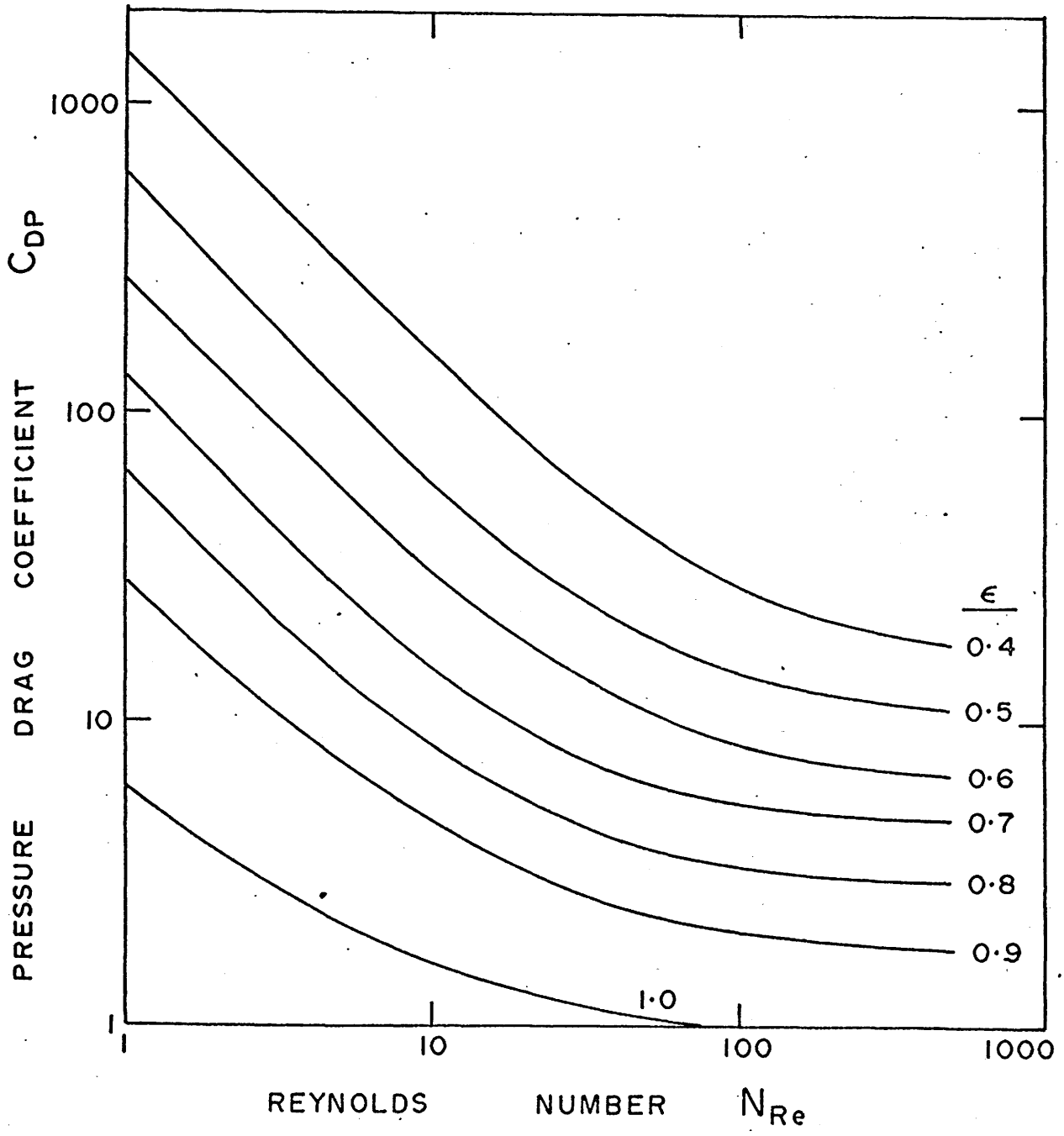

FIGURE C.8.B FRICTION DRAG COEFFICIENT VARIATION WITH REYNOLDS NUMBER AND POROSITY

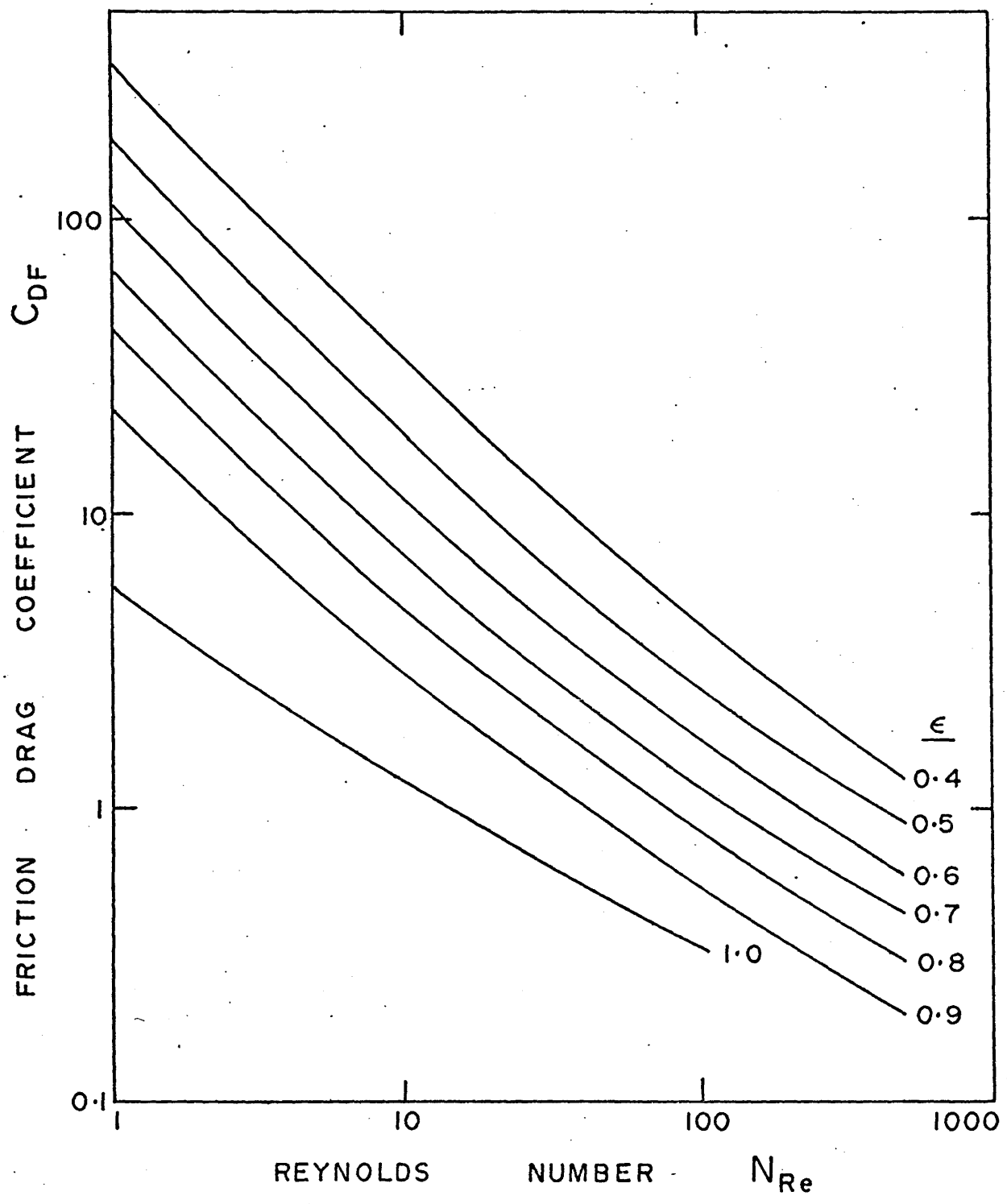

FIGURE C.8.C PRESSURE DRAG COEFFICIENT VARIATION WITH REYNOLDS NUMBER AND POROSITY

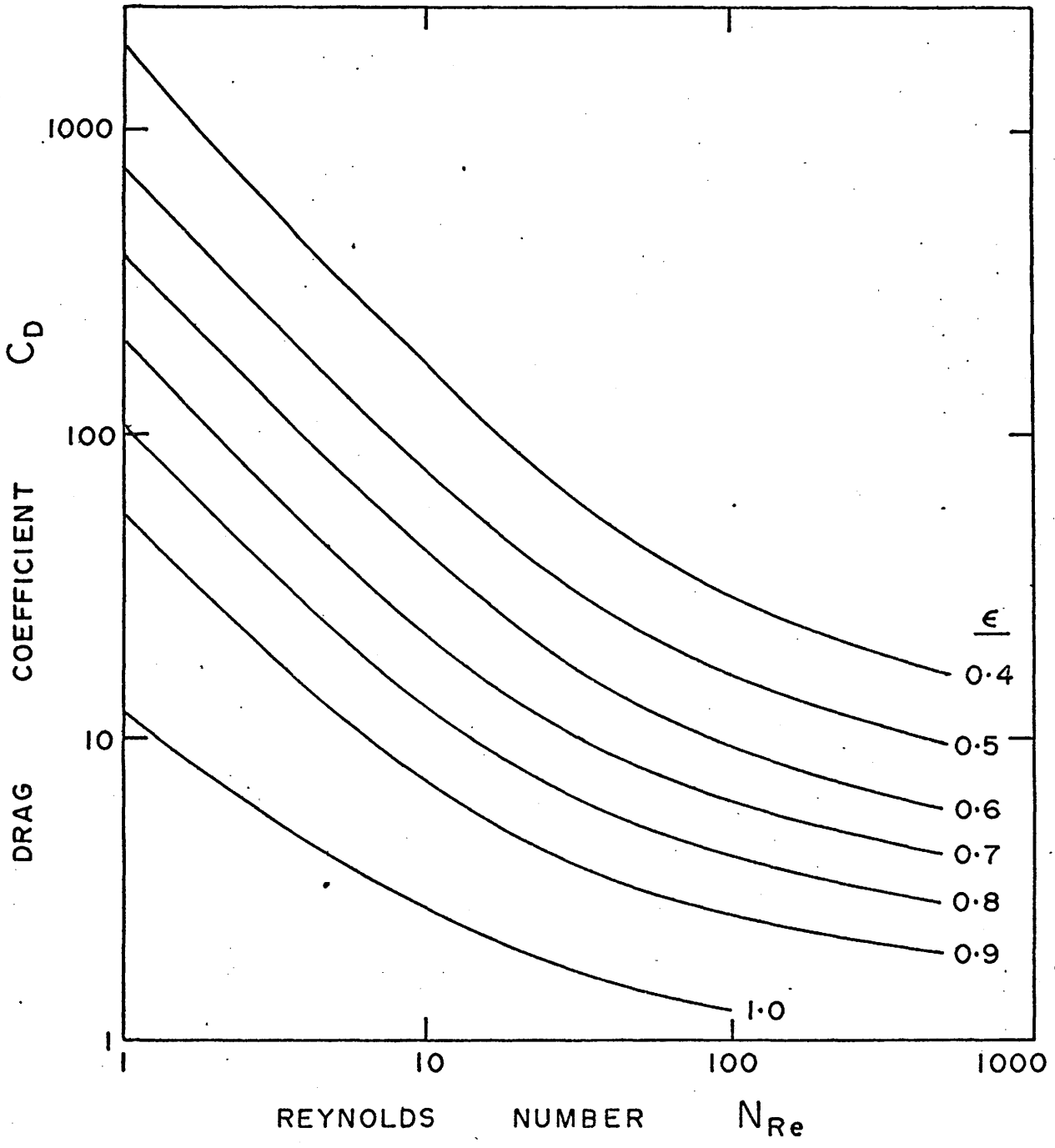

FIGURE C.8.D TOTAL DRAG COEFFICIENT VARIATION WITH REYNOLDS NUMBER AND POROSITY

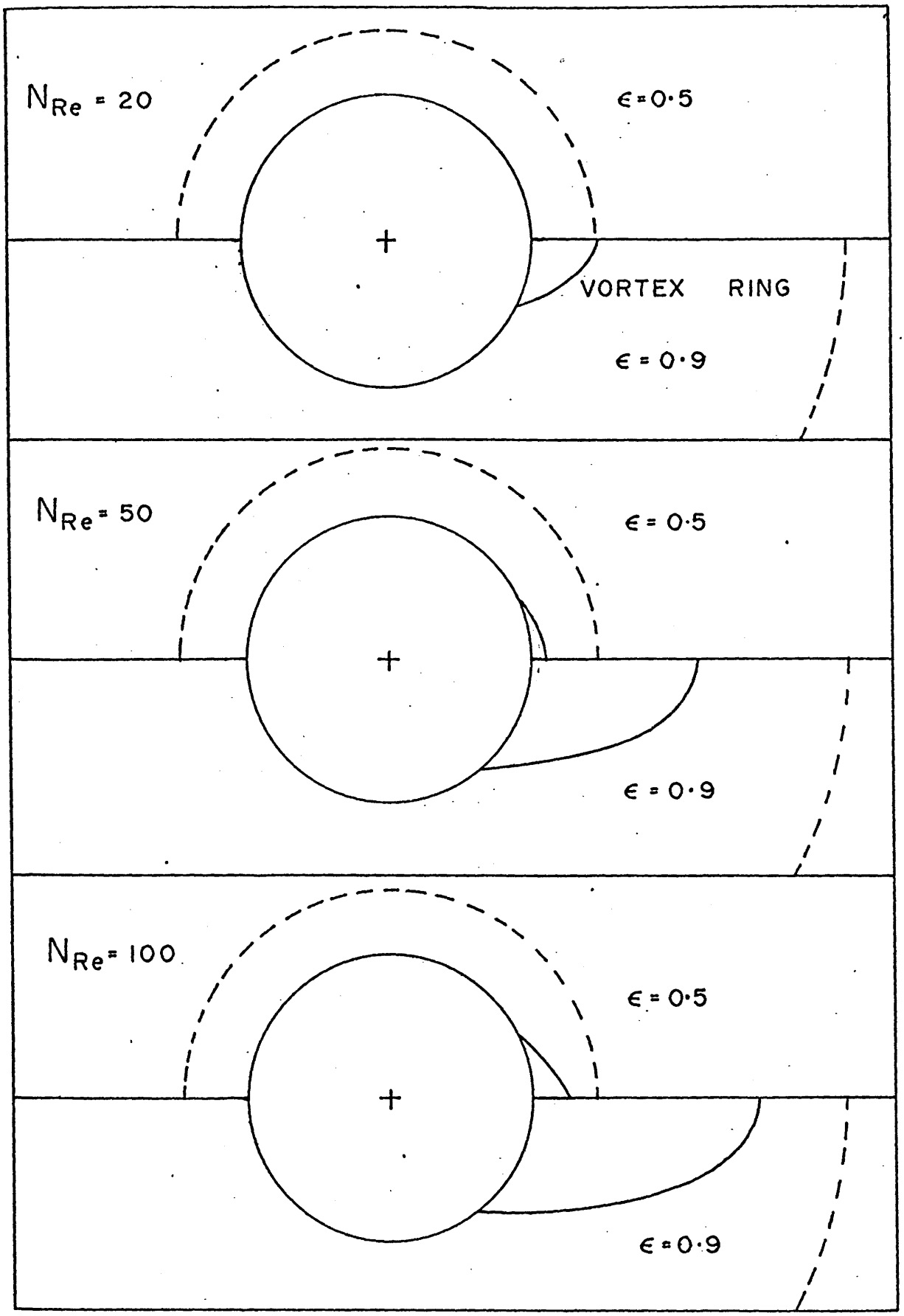

FIGURE C.9 VORTEX RING CONTOURS AT N_{Re} = 20, 50 AND 100

N_{Re} = 20 and until $\varepsilon \geq 0.5$ at N_{Re} = 50. Dimensions of the vortex ring at various Reynolds numbers and porosities are presented in Table C.4.

The lines of equivorticity are swept downstream but this convection is abnormally interrupted by the position of the outer spherical boundary (where the vorticity has been fixed equal to zero). The blunt rather than stream lined shape of these lines emphasizes this fact. In reality, the vorticity would be greater than zero on the outer boundary downstream from the cylinder.

C.2.6 Boundary Layer Development

At low Reynolds numbers the boundary layer thickness decreases with decreasing porosity, but is almost independent of porosity at the higher Reynolds numbers. This suggests that boundary layer assumptions might be valid at lower Reynolds numbers than one would expect if the porosity were sufficiently small. These results also suggest that one could expect higher mass or heat transfer rates by forced convection as the porosity is reduced.

C.2.7 Comparison of Predicted Results with Experiments

Although there exists a wide range of heat exchangers of the shell and tube type, there is very little information on heat transfer coefficients and pressure drops on the shell side. The available data are either the results for flow across single banks of tubes over a very narrow Reynolds number range or spot results on complete heat exchangers where physical information about the geometry is lacking. The only systematic studies done in the intermediate Reynolds number

regime have been those of Seider and Scott (1932), Gunter and Shaw (1945), Bergelin, Omohundro and Colburn (1949), and Bergelin, Brown and Doberstein (1952). Systematic studies with liquid metals have been carried out by numerous authors (Kalish and Dwyer, 1964; Hoe, Dropkin and Dwyer, 1957; Rickard, Dwyer and Dropkin, 1958; and Borishansky, Andreevsky, and Zhinka, 1962); however the Reynolds number range is of order 20,000. Thus liquid metal results can only be used in a qualitative way.

Experimental data has been correlated using a variety of correlations and variable groups. To compare results, relationships between theoretical model parameters and parameters used by experimentalists are established in the following section. In the experimental regime, one normally correlates data on the basis of interstitial Reynolds number, N_{Re_v}, volumetric hydraulic diameter, D_v and friction factor, f/2. The relationships are as follows:

$$D_v = \frac{4 \times \text{free volume}}{\text{exposed area of tubes}} = \frac{2a\,\varepsilon}{1-\varepsilon} \tag{C.4}$$

$$N_{Rev} \quad \frac{D_v G_{max}}{\mu} = N_{Re} \left[\frac{\varepsilon}{(1-\varepsilon)\left[1-(1-\varepsilon)^{\frac{1}{2}}\right]}\right] \tag{C.5}$$

$$N'_{Re} = \frac{D\,G_{max}}{\mu} = N_{Re} \left[\frac{1}{1-(1-\varepsilon)^{\frac{1}{2}}}\right] \tag{C.6}$$

$$\frac{f}{2} = \frac{2}{\pi} C_D\, \varepsilon\left[1-(1-\varepsilon)^{\frac{1}{2}}\right]^2 \tag{C.7}$$

$$f_{Ct} = C_D \left[(1-\varepsilon)^3 - 2(1-\varepsilon)^2 + (1-\varepsilon)\right] \tag{C.8}$$

These relationships can be derived as follows

$$\frac{f}{2} = \frac{2}{\pi} \varepsilon C_D [1-(1-\varepsilon)^{\frac{1}{2}}]^2 \qquad (C.18)$$

Another friction factor used in experimental work is

$$f_{ct} = \frac{2\Delta p \; g_c \; \rho}{4 \; G_{max}^2 \; N} \qquad (C.19)$$

$$= \frac{1}{2} \; \frac{\Delta p \; g_c \rho \; D_v}{L \; G_{max}^2} \; (\frac{SL}{D_v})$$

$$= \frac{1}{2} [\frac{f}{2}] \frac{S_L}{D_v} \qquad (C.20)$$

$$\frac{S_L}{D_v} = \frac{b}{a} (\frac{1-\varepsilon}{\varepsilon}) = \frac{(1-\varepsilon)^{\frac{1}{2}}}{\varepsilon} \qquad (C.21)$$

where S_L is the distance between transverse rows

Thus

$$f_{ct} = \frac{1}{2} [\frac{2}{\pi} C_D \; \varepsilon(1-(1-\varepsilon)^{\frac{1}{2}})^2] \; \frac{(1-\varepsilon)^{\frac{1}{2}}}{\varepsilon}$$

$$= \frac{C_D}{\pi} [(1-\varepsilon)^{3/2} - 2(1-\varepsilon) + (1-\varepsilon)^{\frac{1}{2}}] \qquad (C.22)$$

In Figure C.10.A the results for $\varepsilon = 0.4$ and $\varepsilon = 0.6$ are compared with the experimental data of Seider and Scott (1932) and the empirical correlation of Gunter and Shaw (1945). For the viscous range the Gunter and Shaw equation is

$$\frac{f}{2} = 90(N_{Re_v})^{-1} \qquad (C.23)$$

and for the turbulent range

$$\frac{f}{2} = 0.96(N_{Re_v})^{-0.145} \qquad (C.24)$$

The data of Seider and Scott were obtained in a tube bundle with equilateral triangular tube spacing and a porosity of 0.42. In Figure C.10.B the calculated results are compared with the data of Bergelin, Brown and Doberstein (1952). Model 1 and 3 have equilateral triangular tube spacing and porosities of 0.37 and 0.55 respectively. It is to be expected that the disagreement will be much greater for tube arrangements, such as square array, as channeling will occur.

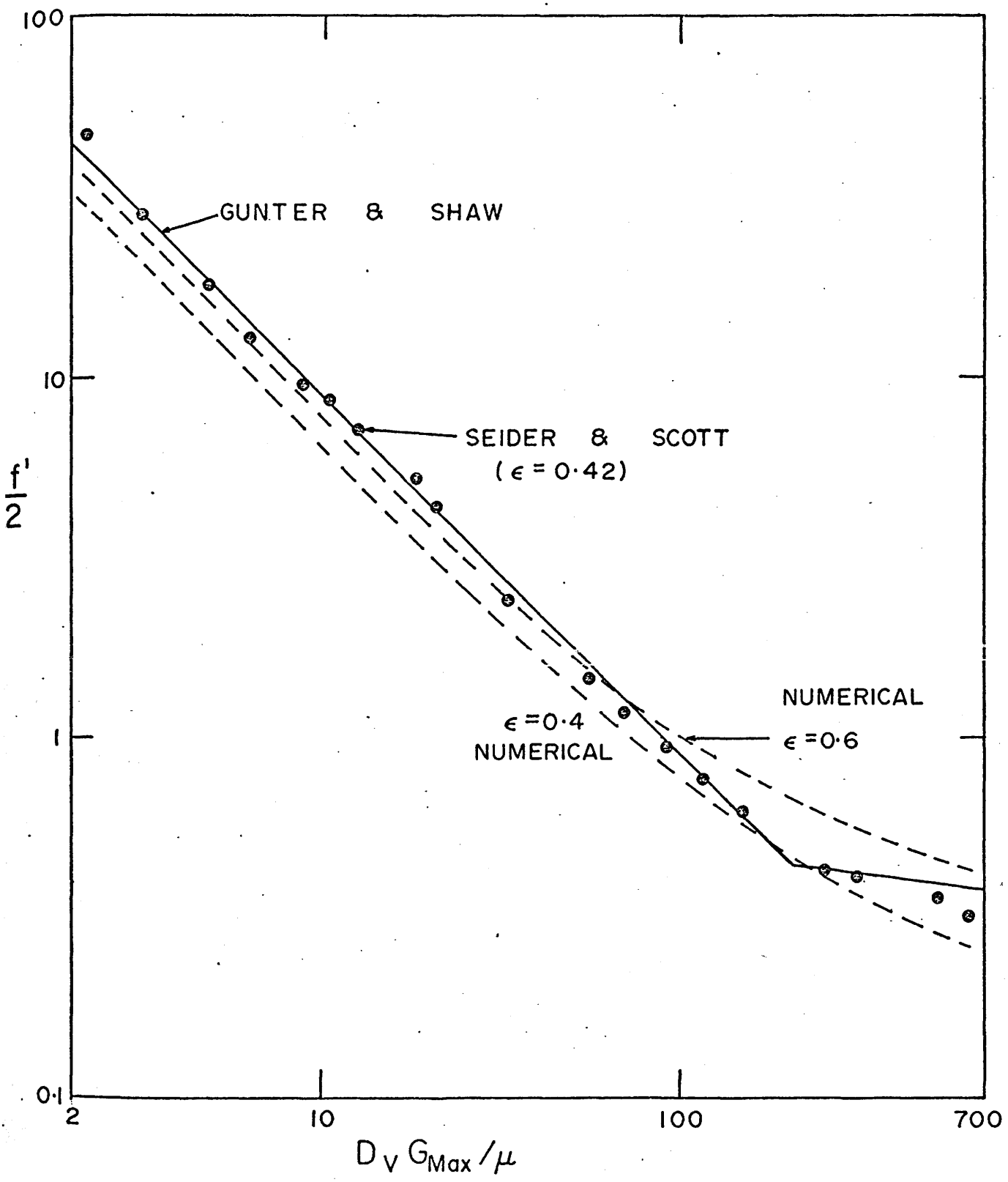

FIGURE C.10.A FRICTION FACTOR VS REYNOLDS NUMBER FOR FLOW IN TUBE BUNDLES

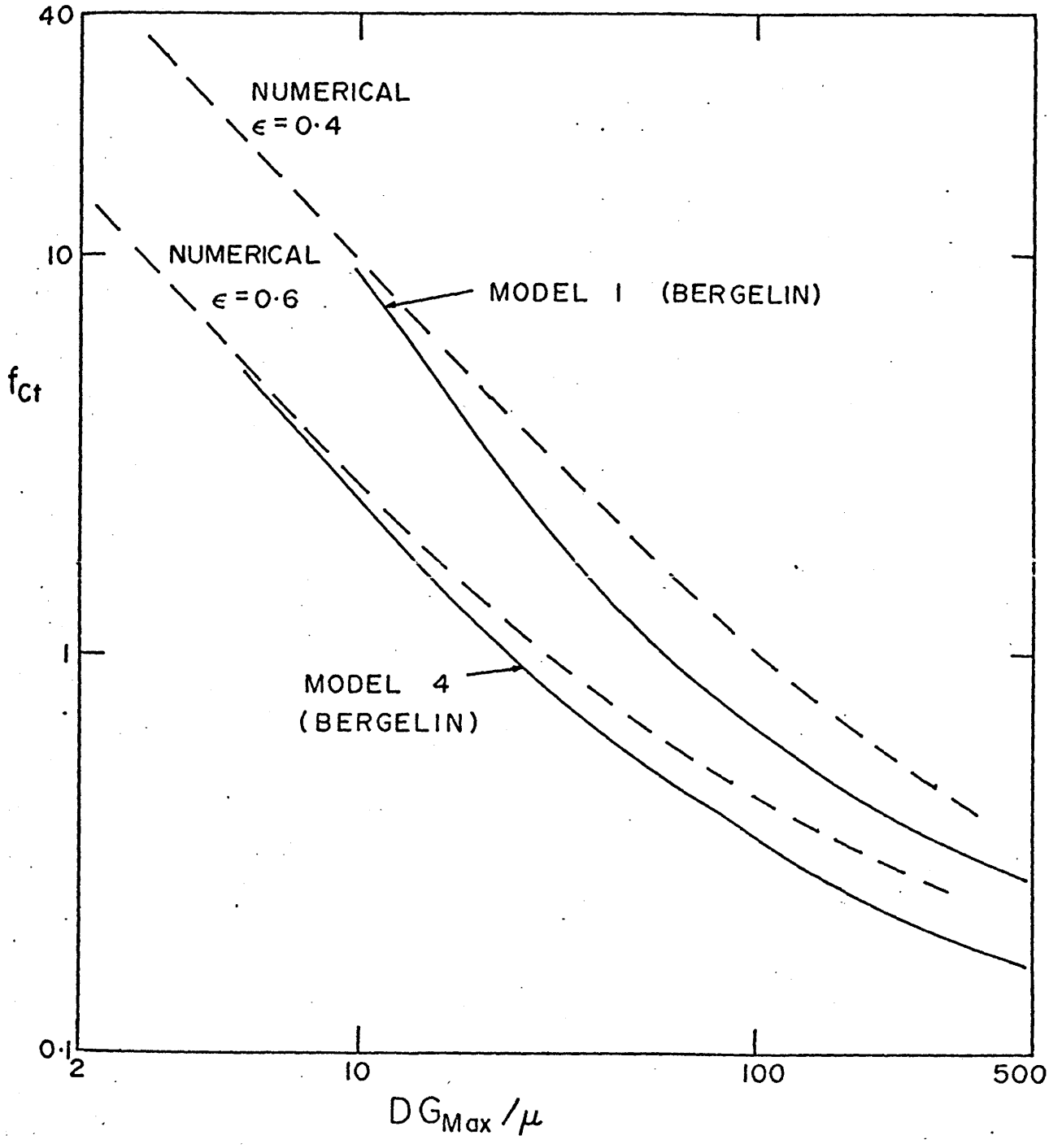

FIGURE C.10.B FRICTION FACTOR VS REYNOLDS NUMBER FOR FLOW IN TUBE BUNDLES

C.3 Bubble Swarms

C.3.1 Accuracy of Solutions

The accuracy of the solutions was examined by reducing both the radial and angular step sizes by a factor of two until the change between two successive solutions was less than one percent. The solutions were assumed to have converged when values of the vorticity and stream function at all mesh points changed by less than 0.0001 per iteration.

C.3.2 Surface Vorticity Distributions

The surface vorticity distribution for one Reynolds number (N_{Re} = 500) and for a range of porosities (ε = 0.4 to 1.0) are shown in Figure C.11.A. These vorticity distributions are typical and similar results have been obtained for Reynolds numbers of 0.1, 1, 10, 100, and 1000. The results for these cases are presented in Appendix II-A.

C.3.3 Surface Pressure Distributions

The surface pressure distributions for one Reynolds number (N_{Re} = 500) and a range of porosities (ε = 0.4 to 1.0) are presented in Figure C.11.B. These distributions are typical and similar results have been predicted for Reynolds numbers of 0.1, 1, 10, 100 and 1000 and may be found in Appendix II-A.

The frontal stagnation pressure is almost independent of porosity at all Reynolds numbers. At low Reynolds numbers, it increases with increasing porosity.

TABLE C.5 STAGNATION PRESSURE AND DRAG COEFFICIENTS

N_{Re}	ε	P_o	P_{DP}	C_{DF}	C_D
0.1	0.408	45.483	1850.90	693.28	2544.18
	0.527	46.924	937.81	509.47	1447.28
	0.650	48.457	501.14	385.20	886.34
	0.741	49.611	321.91	316.05	637.96
	0.835	50.753	201.39	254.90	456.29
	0.909	51.363	133.75	208.39	342.14
1.0	0.408	5.415	185.10	69.328	254.428
	0.527	5.541	93.792	50.948	144.740
	0.650	5.670	50.130	38.522	88.652
	0.741	5.757	32.206	31.608	63.814
	0.835	5.829	20.161	25.495	45.656
	0.909	5.837	13.401	20.852	34.253
10.0	0.408	1.410	18.615	6.935	25.550
	0.527	1.406	9.494	5.100	14.594
	0.650	1.398	5.159	3.865	9.024
	0.741	1.385	3.381	3.184	6.565
	0.835	1.366	2.198	2.597	4.795
	0.909	1.344	1.546	2.177	3.723
100.0	0.417	1.022	2.327	0.689	3.016
	0.535	1.020	1.362	0.522	1.884
	0.645	1.018	0.876	0.421	1.297
	0.752	1.016	0.581	0.350	0.931
	0.835	1.015	0.419	0.307	0.726
	0.909	1.014	0.297	0.274	0.571
500.0	0.417	1.002	0.808	0.144	0.952
	0.535	1.002	0.460	0.111	0.571
	0.645	1.002	0.286	0.091	0.377
	0.752	1.002	0.183	0.077	0.260
	0.835	1.001	0.149	0.069	0.218
	0.909	1.001	0.107	0.062	0.169
1000.0	0.417	1.000	0.481	0.073	0.554
	0.535	1.000	0.280	0.057	0.337
	0.645	1.000	0.179	0.048	0.227
	0.752	1.000	0.118	0.039	0.157
	0.835	1.000	0.108	0.036	0.144
	0.909	1.000	0.080	0.033	0.113

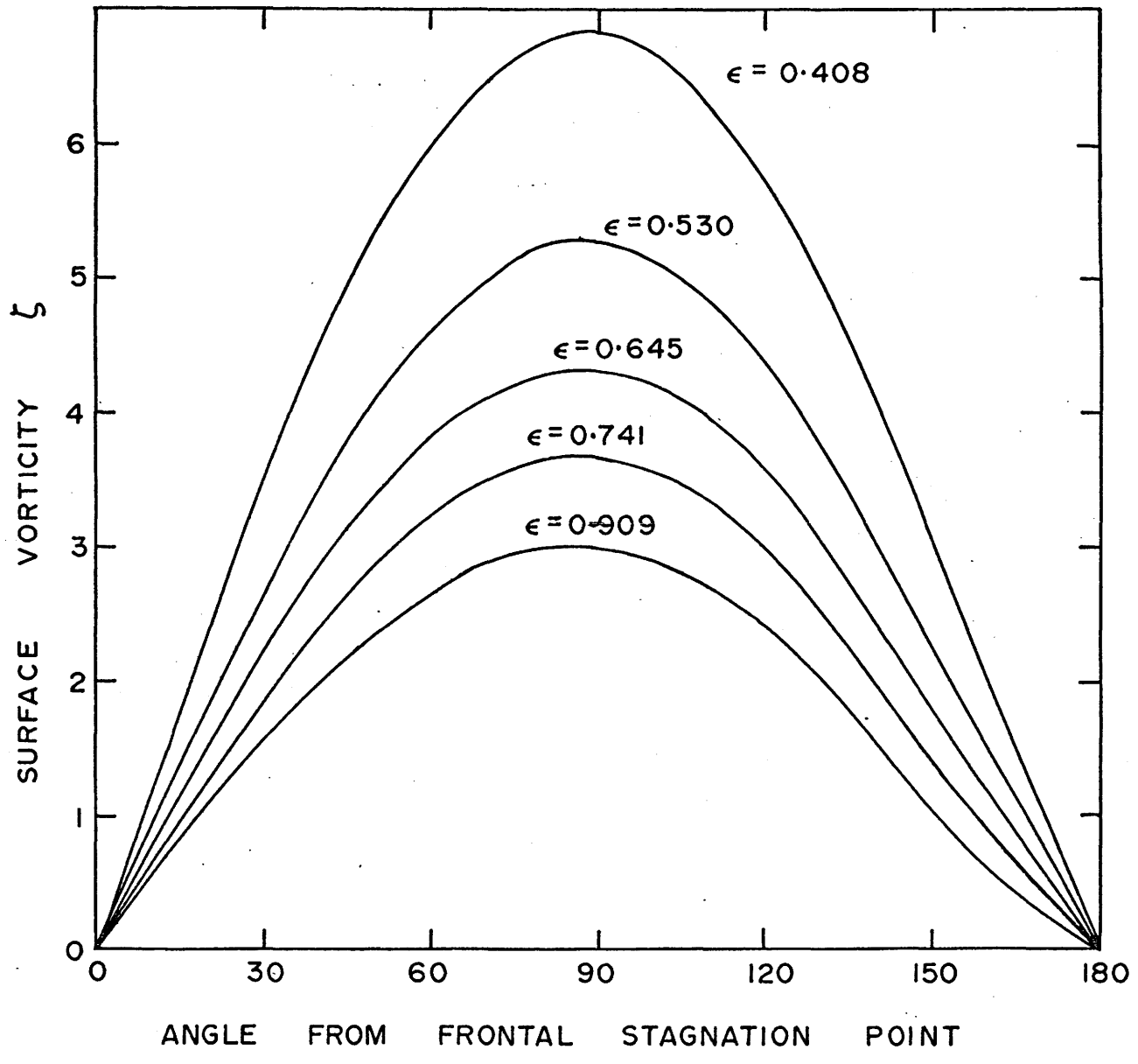

FIGURE C.11.A SURFACE VORTICITY DISTRIBUTION ABOUT A BUBBLE AT N_{Re} = 500

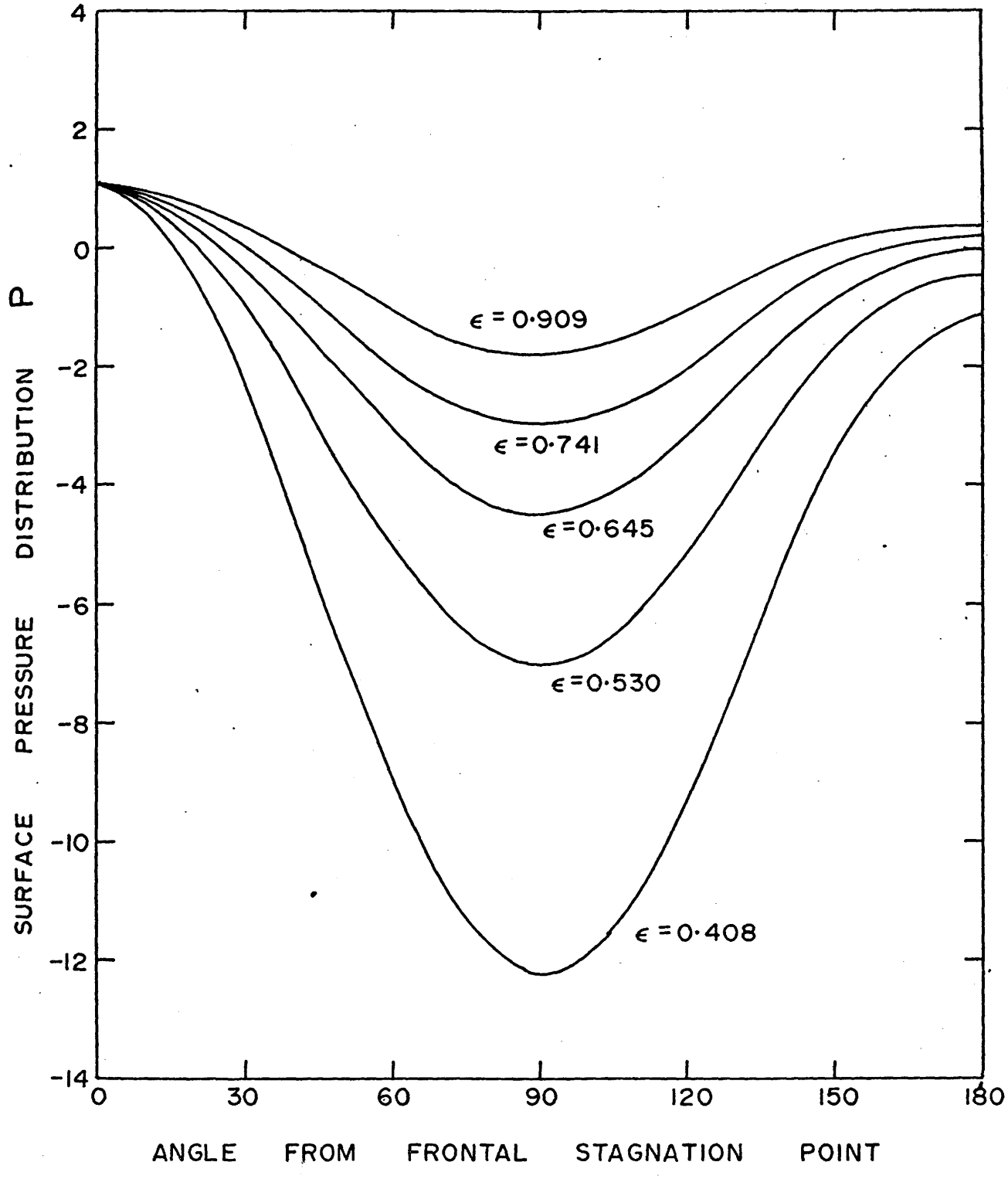

FIGURE C.11.B SURFACE PRESSURE DISTRIBUTION ABOUT A BUBBLE AT N_{Re} = 500

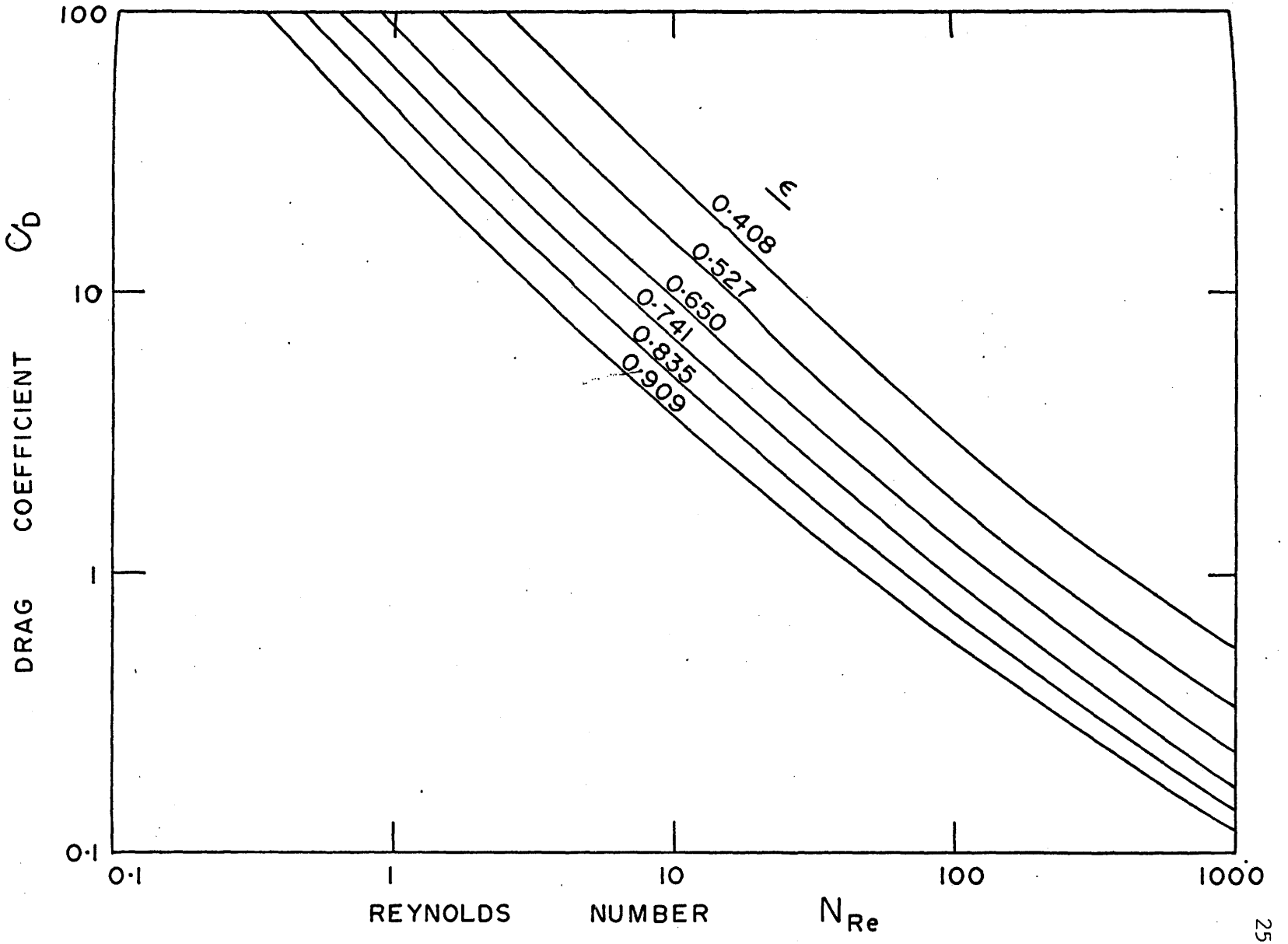

FIGURE C.12 TOTAL DRAG COEFFICIENT VARIATION WITH REYNOLDS NUMBER AND POROSITY

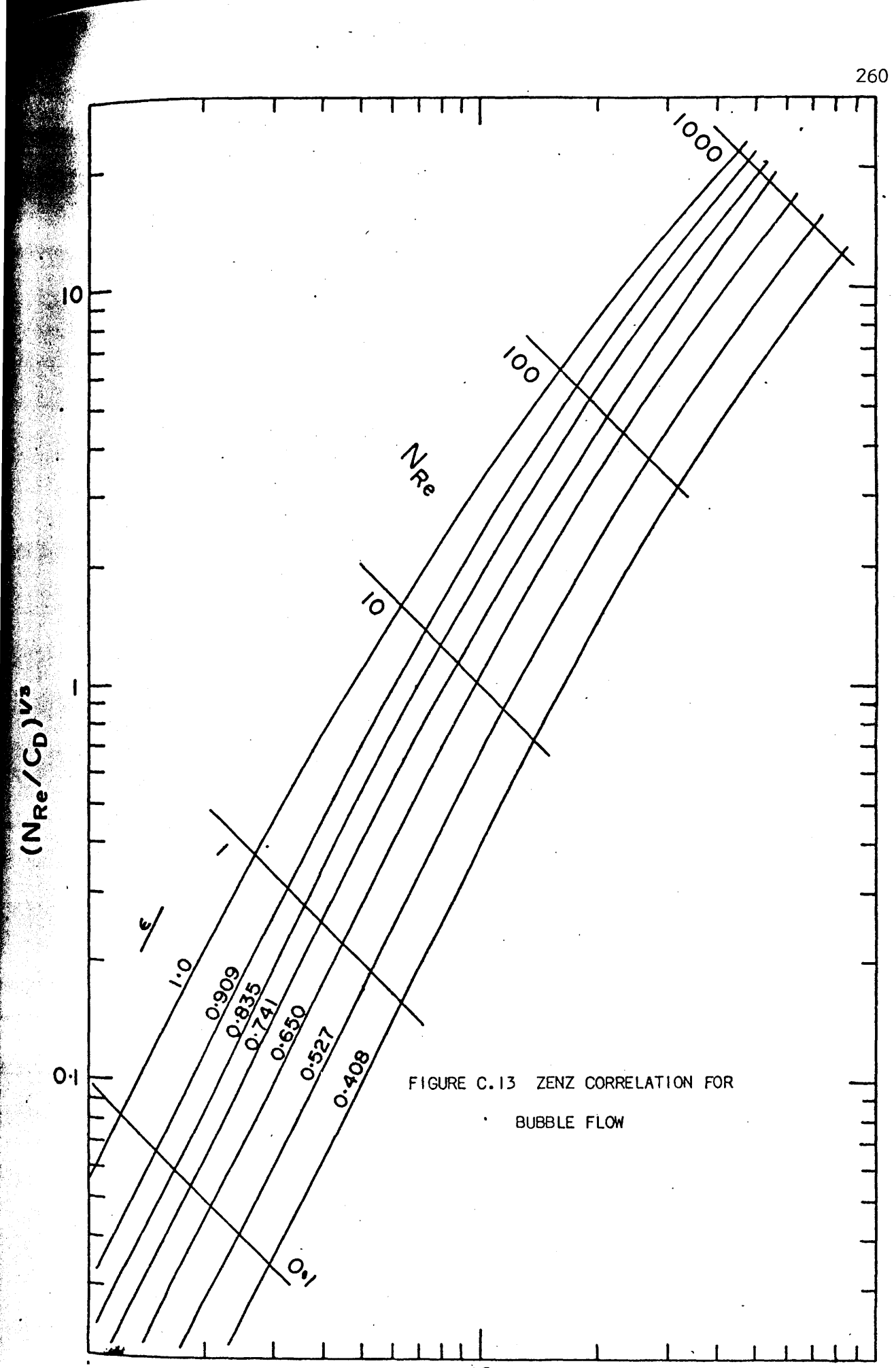

FIGURE C.13 ZENZ CORRELATION FOR BUBBLE FLOW

C.3.4 Pressure, Friction and Total Drag Coefficients

Total drag coefficients for a range of porosities (ε=0.4 to 1.0) and a range of Reynolds numbers are shown in Figure C.12. The values for a porosity of one were obtained from the literature (Hamielec, Johnson and Houghton, 1957) or calculated when no literature value could be found. Similar results have been obtained for the form and friction drag coefficients. These coefficients are presented in Table C.5. The drag results are also presented in Figure C.13 using the general correlating method after Zenz (1957).

C.3.5 Comparison with Experimental Data

When gas and liquid flow together in a vertical tube, several flow patterns are possible. In bubble swarms, the gas phase is dispersed throughout the liquid phase as bubbles of various sizes. The continuous liquid phase may move cocurrently or countercurrently with the bubble swarm.

The model developed in this work is based upon the average bubble diameter, the free stream velocity and the fluid properties. It predicts the reduction in the rise velocity of a bubble in a swarm. This relative rise velocity, U_R, is a function of the rise velocity at infinite dilution (ε=1) and the porosity. Figure C.14 presents a plot of the relative rise velocity-infinite dilution rise velocity ratio against bubble concentration 1-ε, with the infinite dilution Reynolds number as parameter. The plot is obtained from Figure C.13 by drawing lines at constant $(C_D N_{Re}^2)^{1/3}$ (constant bubble diameter), and picking the velocity off the $(N_{Re}/C_D)^{1/3}$ axis for

various porosity ratios. Also shown in Figure C.14 are the predictions of Marrucci (1965) and Bhatia (1969).

To compare the results with experiment the relationships derived by Nicklin (1962) are used. For gas-liquid bubble flow Nicklin has shown that the rise velocity of a bubble swarm, V_B, is related to the superficial gas, G/A, and liquid, L/A, rates by a relationship of the following form

$$V_B = \frac{G}{\varepsilon A} = V_R + \frac{G}{A} \pm \frac{L}{A} \tag{C.25}$$

If the equation is divided by the rise velocity at infinite dilution (ε=1)

$$\frac{G}{\varepsilon A U_\infty} = \frac{V_R}{U_\infty} + \frac{G}{A U_\infty} \pm \frac{L}{A U_\infty} \tag{C.26}$$

but $\frac{V_R}{U_\infty} = f(N_{Re_\infty}, \varepsilon)$ and is given graphically in Figure C.14.A. The above two relationships may be solved simultaneously to determine the porosity in a bubble swarm for any set of superficial gas and liquid rates. To solve the above set of equations a knowledge of the average bubble diameter and the physical properties of the liquid and gas are also necessary.

Figure C.14.B compares the theoretical predictions with the experimental results of Bridge, Lapidus and Elgin (1964). In Figure C.14.B(A), air is bubbling through a 58% glycerine-water mixture and in Figure C.14.B(B), air is bubbling through a continuous column of water. The two experimental curves in Figure C.14.B(A) are the results for two column locations, one high and one low. The model predicts the experimental results reasonably well.

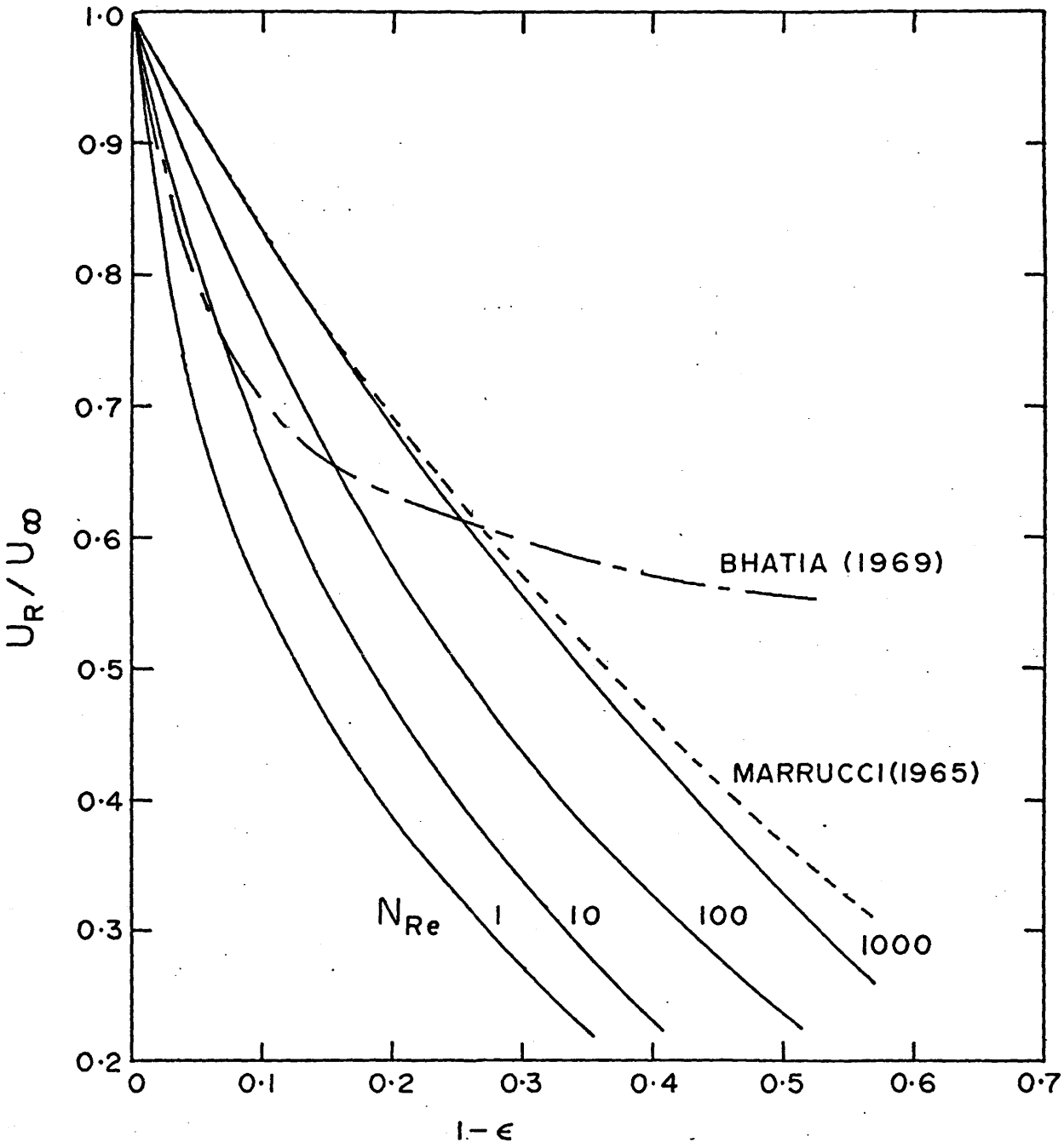

FIGURE C.14.A RELATIVE VELOCITY VARIATION WITH REYNOLDS NUMBER AND BUBBLE CONCENTRATION

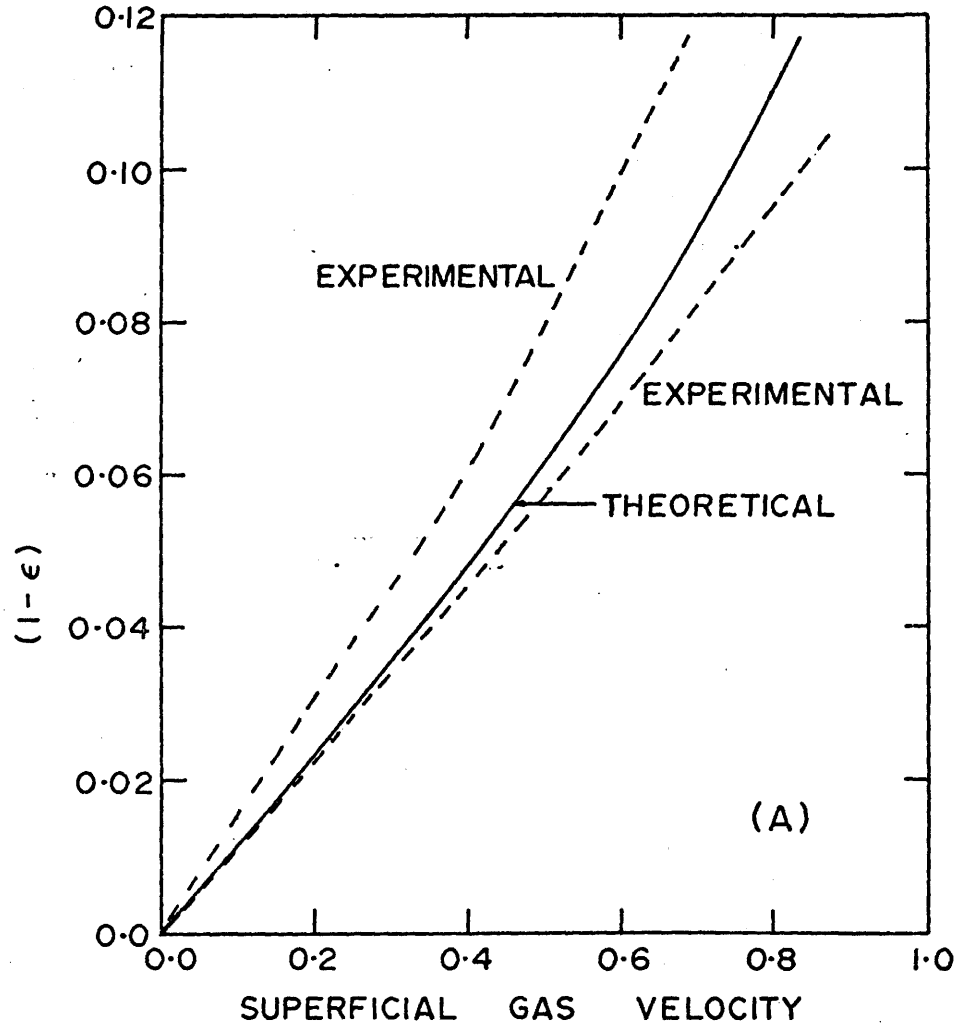

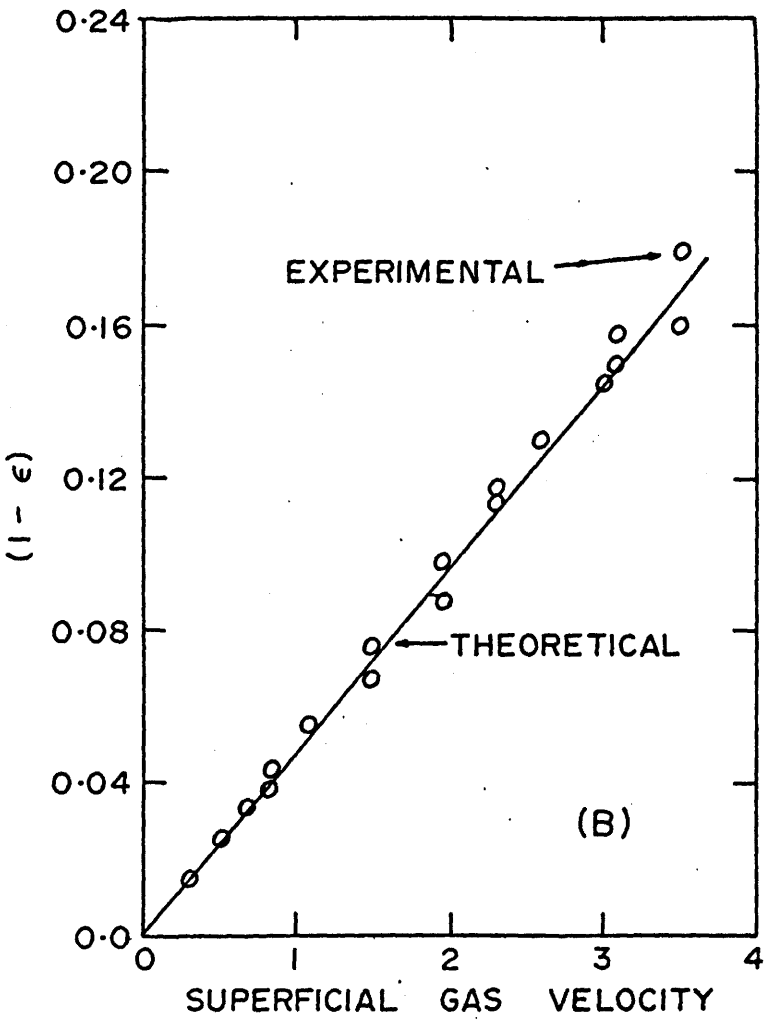

FIGURE C.14.B COMPARISON OF THEORETICALLY PREDICTED AND EXPERIMENTAL POROSITY

C.4 Mass or Heat Transport

C.4.1 Sphere Assemblages

C.4.1.1 Single Spheres

The mass transfer rate for single spheres depends on the Reynolds and Schmidt numbers. In multiparticle systems the dependency is altered by the modified flow regime caused by particle interaction. Although this work was primarily concerned with multiparticle systems, in all cases a single particle in an infinite fluid was also considered. The analyses on single particles were primarily carried out to test the mass transfer equations in an area where a large amount of experimental information existed and where the velocity profiles were essentially exact (Hamielec, Hoffman and Ross, 1967).

Typical local mass transfer profiles, plotted as local Sherwood Number vs angle (θ) from the forward stagnation point, with particle Reynolds number as parameter have been presented in Figure C.15.A. Also presented are several experimental profiles obtained by Peltzman and Pfeffer (1967). Their local mass transfer rates are greater than the theoretical results obtained in this work as free convection is also important in the intermediate Reynolds number range (Garner and Keey, 1958a, 1958b). However, beside the difference in magnitude the transfer rate profiles are almost identical. It should be noted that the Baird and Hamielec "fresh fluid" assumption was used to calculate the transfer rates in the trailing vortex.

Boundary layer theory and experimental results suggest that the mass transfer rate should be a maximum at the forward stagnation point. However the theoretical results had maximum mass transfer rates at 6-10° from the frontal stagnation point. Glen and Keey (1965) studied this effect experimentally and found that the rate at the frontal point is less than that predicted by boundary layer theory. They also suggest this effect should disappear when the Reynolds number is less than 50. The results obtained in this work show the effect is still present at a Reynolds numbers of 0.1. However this may not be entirely correct as the angular diffusion terms were neglected in the continuity equation.

Linton and Sutherland (1960) suggest that the local mass transfer data over the front of the sphere can be correlated using boundary layer theory. The following equation was derived by them from Aksel'rud's published graphs

$$T_R(\theta) = N_{Sh}(\theta) N_{Re}^{-\frac{1}{2}} N_{Sc}^{-1/3} = 1.523\ (1 - 0.1728\theta^2 - 0.0114\theta^4) \quad (C.27)$$

They show that the ratio $T_R(\theta)/T_R(0)$ (where $T_R(0)$ is the value at the frontal stagnation point) for experimental data agrees with the theoretical curve derived. The theoretical results presented in Figure C.15.B indicate that the $T_R(\theta)/T_R(0)$ ratio is a function of Reynolds number. Secondly, they also state that the transfer rate at the frontal stagnation point is independent of Reynolds number. The results of this work qualitatively agree with those of Garner and Suckling (1958) where the mass transfer rate at the frontal stagnation point depends on the Reynolds number. The following equation was

obtained for the transfer rate at the frontal stagnation point

$$N_{Sh} = 2 + 1.44\, N_{Re}^{0.394}\, N_{Sc}^{1/3} \qquad (C.28)$$

C.4.1.2 Multiparticle Systems

Mass or heat transfer in multiparticle systems is affected by particle interaction, and thus a relationship between bed porosity, fluid velocity and mass transfer coefficient is required before one can predict overall mass transfer rates. This problem has been attacked experimentally in a number of ways. Principally these methods are normal fluidized and packed bed analyses and extended bed (identical size spheres arranged in a regular geometric pattern at a fixed spacing) analyses.

The "surface interaction models" are essentially a mathematical extended bed containing one further simplication. This simplication is related to the shape of the cell boundary enclosing the particle. In this work a globular boundary was used to enclose the particle, which eliminates the mathematical complications arising when regions contain irregular boundaries. A parallelopiped boundary as suggested by Gunn and Malik (1966) probably best represents the cell of an extended bed and accounts for all the void volume. Theoretical considerations however suggest the shape of the cell should vary with Reynolds number. At low Reynolds numbers, where the momentum boundary layer is thick, the cell dimensions perpendicular to flow would be greater than those in the flow direction, with increasing Reynolds number and thus decreasing boundary layer thickness and downstream diffusion of vorticity the cell would

elongate in the flow direction and contract in the normal direction. This is undoubtedly why fixed boundary shape used in this work always predicts drag coefficients which are greater than experiment.

Results obtained from extended beds and packed or fluidized beds are essentially the same. Which, in fact, suggests the model is essentially correct. However, some doubt exists as to how the bed porosity affects mass or heat transfer. Two alternatives have been suggested by the literature: (1) J factor is a function of a modified Reynolds number

$$J_D = f\ (N_{RE}/(1-\varepsilon)) \tag{C.29}$$

and (2) porosity times J factor is a function of Reynolds number

$$\varepsilon\ J_D = f\ (N_{RE}) \tag{C.30}$$

This difference is undoubtedly related to the narrow 0.4-0.6 void fraction range used by most experimenters to develop the correlations. Rowe and Claxton (1965) and Gupta and Thodes (1963) have done extensive work with extended beds over a wide porosity range. The correlations of these authors are presented in Figure C.16.A along with the theoretical results obtained in this work. The agreement is satisfactory. The very pronounced Schmidt number effect at low Reynolds numbers further emphasizes the fact that "thin concentration boundary layer theory" applies only to high Peclet number situations.

In Figure C.16.B the effect of porosity on the local Sherwood number at a particle Reynolds number of 100 is presented. The suppression of flow separation is clearly indicated. There is also a pronounced increase in the average Sherwood number at the front of the sphere with decreasing porosity.

Most experimental heat and mass transfer data for multiparticle systems are correlated by plotting a dimensionless j factor against a dimensionless Reynolds number. A plot of the theoretical results for different values is given in Figure C.16.C. Using the method of least squares the following equation was found to best correlate the data.

$$J\,\varepsilon^{0.854} = 1.485\,N_{Re}^{-0.632} \qquad (C.31)$$

The modified Reynolds number ($N_{Re}/(1-\varepsilon)$) correlation produced good results as well, however the above equation was better.

Figure C.16.D compares the theoretical results obtained with recent extended bed data. In this figure the work of Williamson, Bazaire and Geankoplis (1963) and Wilson and Geankoplis (1966) which were taken using a packed bed having a void volume of approximately 0.400 is presented. Also included is the work of Rowe and Claxton (1965) and Gupta and Thodes (1963). Figure C.16.E compares the theoretical work with the fixed and fluidized bed data of Chu, Kalil and Wetteroth (1953), McCune and Wilhelm (1949) and Gaffney and Drew (1950). The results of this work predict mass transfer rates which are 15-20 percent higher than the experimental extended bed results, however they are bracketed by the experimental fixed and fluidized bed results.

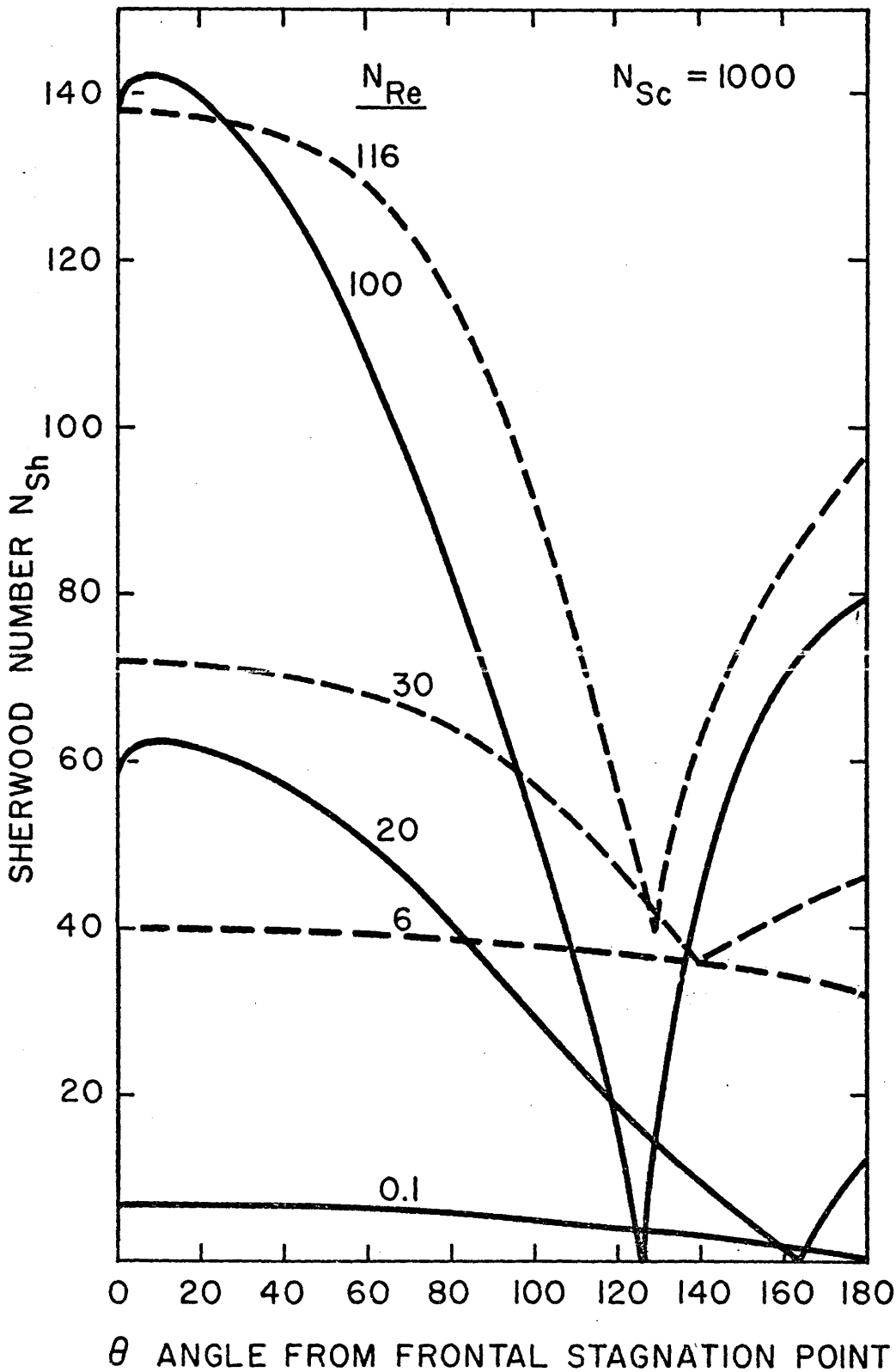

FIGURE C.15.A LOCAL MASS TRANSFER PROFILES FOR SINGLE RIGID SPHERES IN AN INFINITE FLUID

---- PELTZMAN AND PFEFFER (1967), EXPERIMENTAL
THEORETICAL

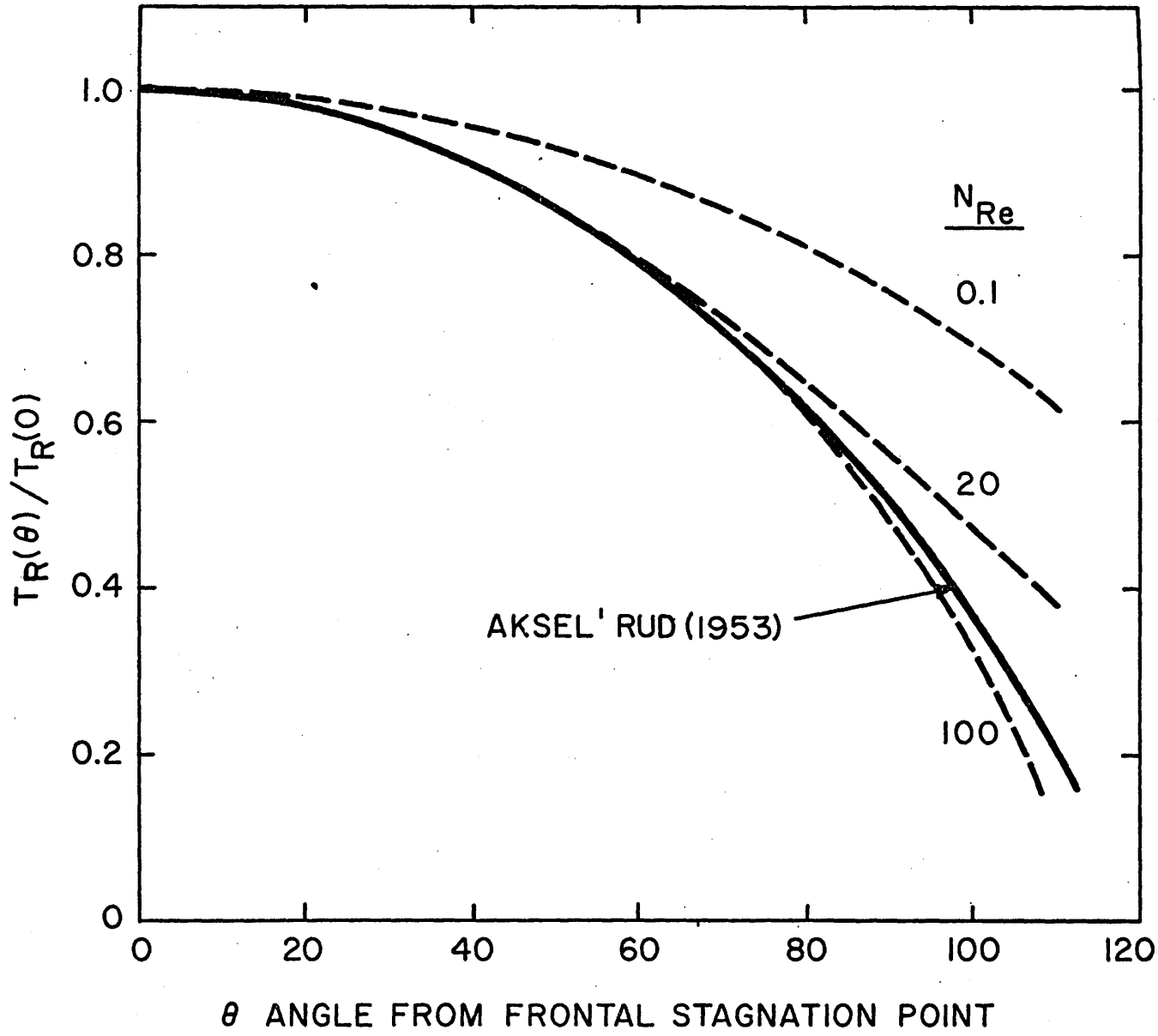

FIGURE C.15.B LOCAL UNIVERSAL TRANSFER NUMBER RATIO COMPARISON FOR INTERMEDIATE REYNOLDS NUMBERS

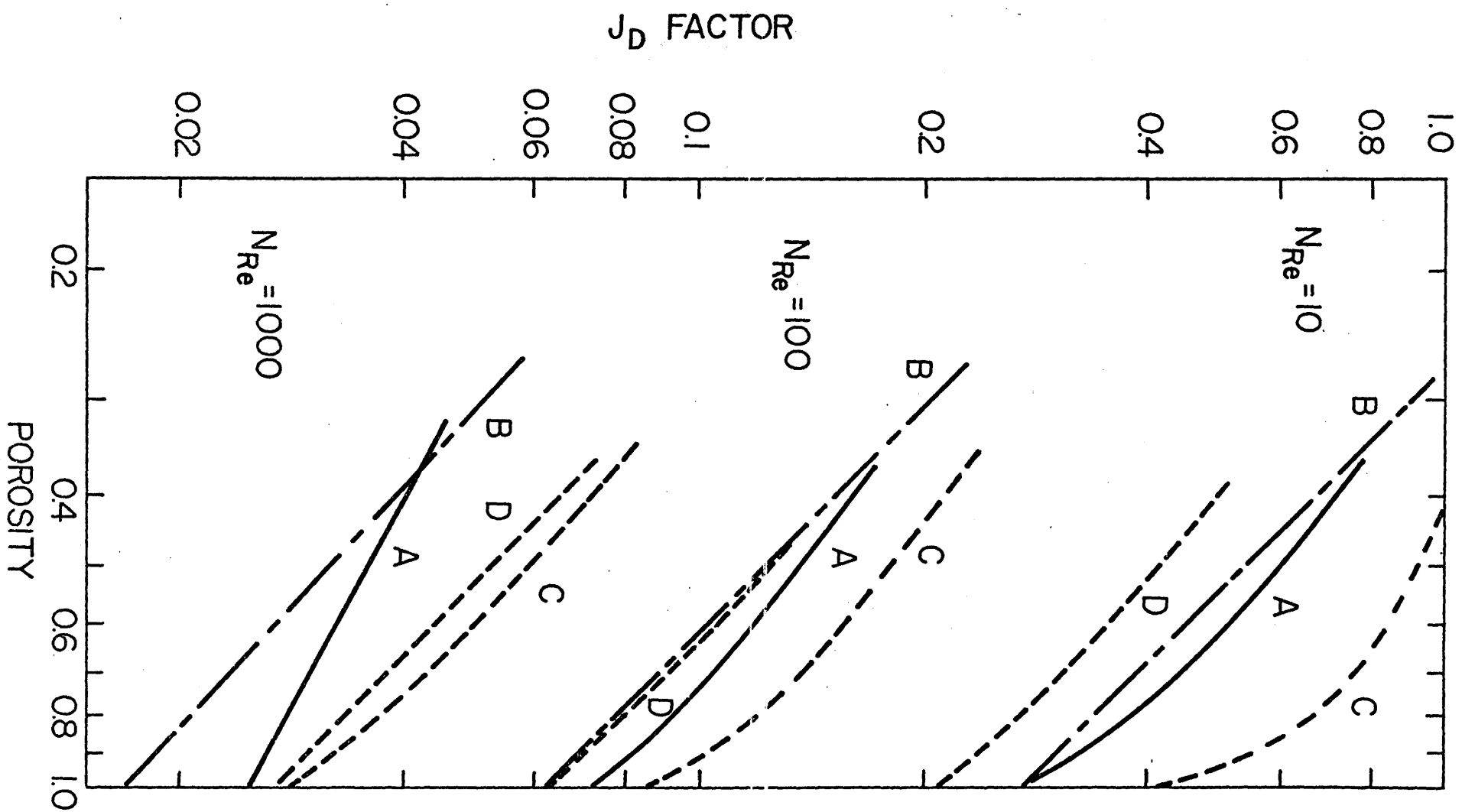

FIGURE C.16.A EFFECT OF POROSITY AND SCHMIDT NUMBER ON MASS TRANSFER RATE

A - THEORETICAL

B - GUPTA AND THODOS (1963)

C - ROWE AND CLAXTON (1965), N_{Sc} = 0.76

D - ROWE AND CLAXTON (1965), N_{Sc} = 1000.

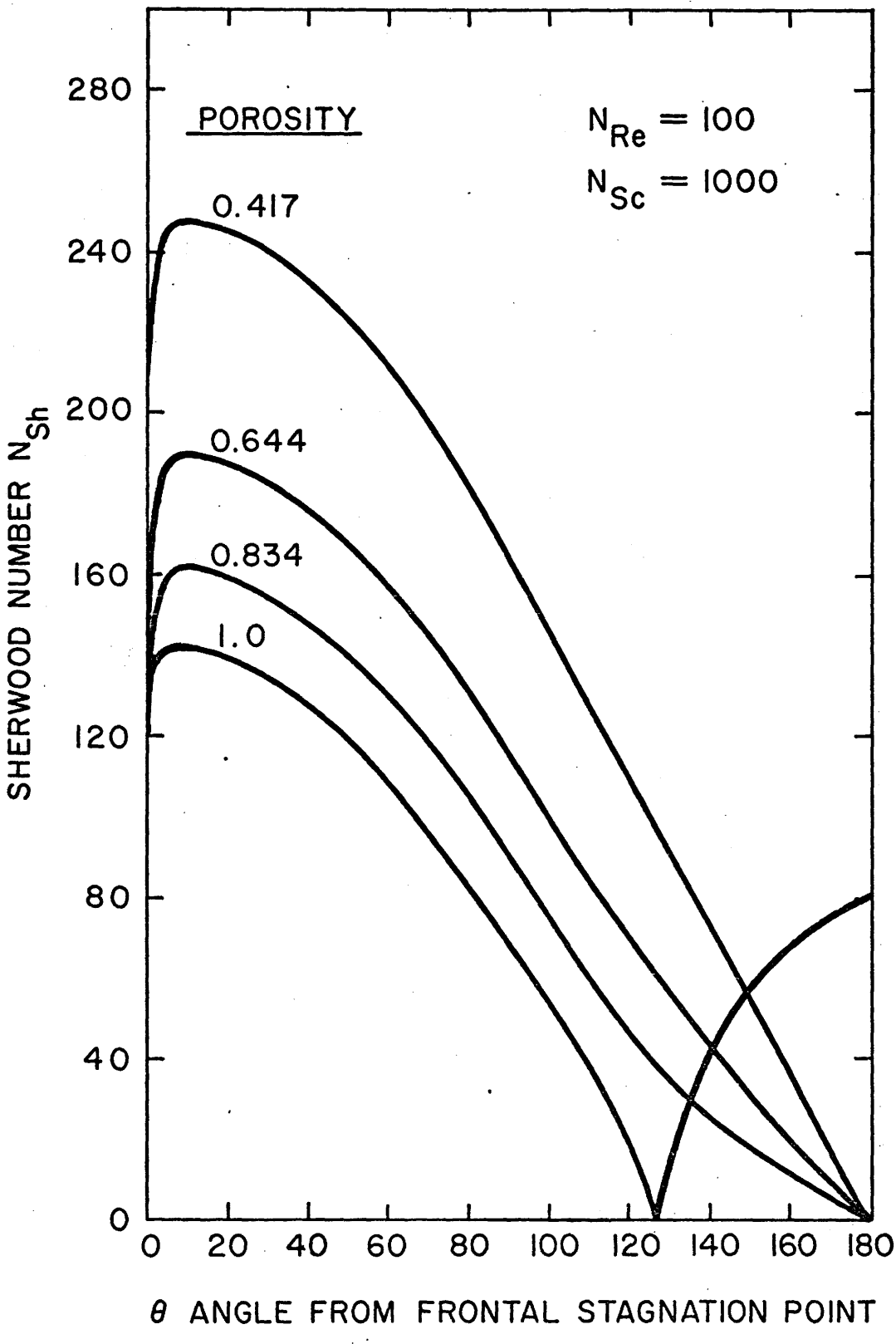

FIGURE C.16.B EFFECT OF POROSITY ON THE LOCAL MASS TRANSFER RATE FROM SPHERES AT N_{Re} = 100

FIGURE C.16.C COLBURN FACTOR VS REYNOLDS NUMBER WITH THE POROSITY OF THE SYSTEM AS PARAMETER

(THE DASHED LINES ARE EXPANSION CURVES FOR FLUIDIZED BEDS AT THE GIVEN FREE SETTLING REYNOLDS NUMBERS)

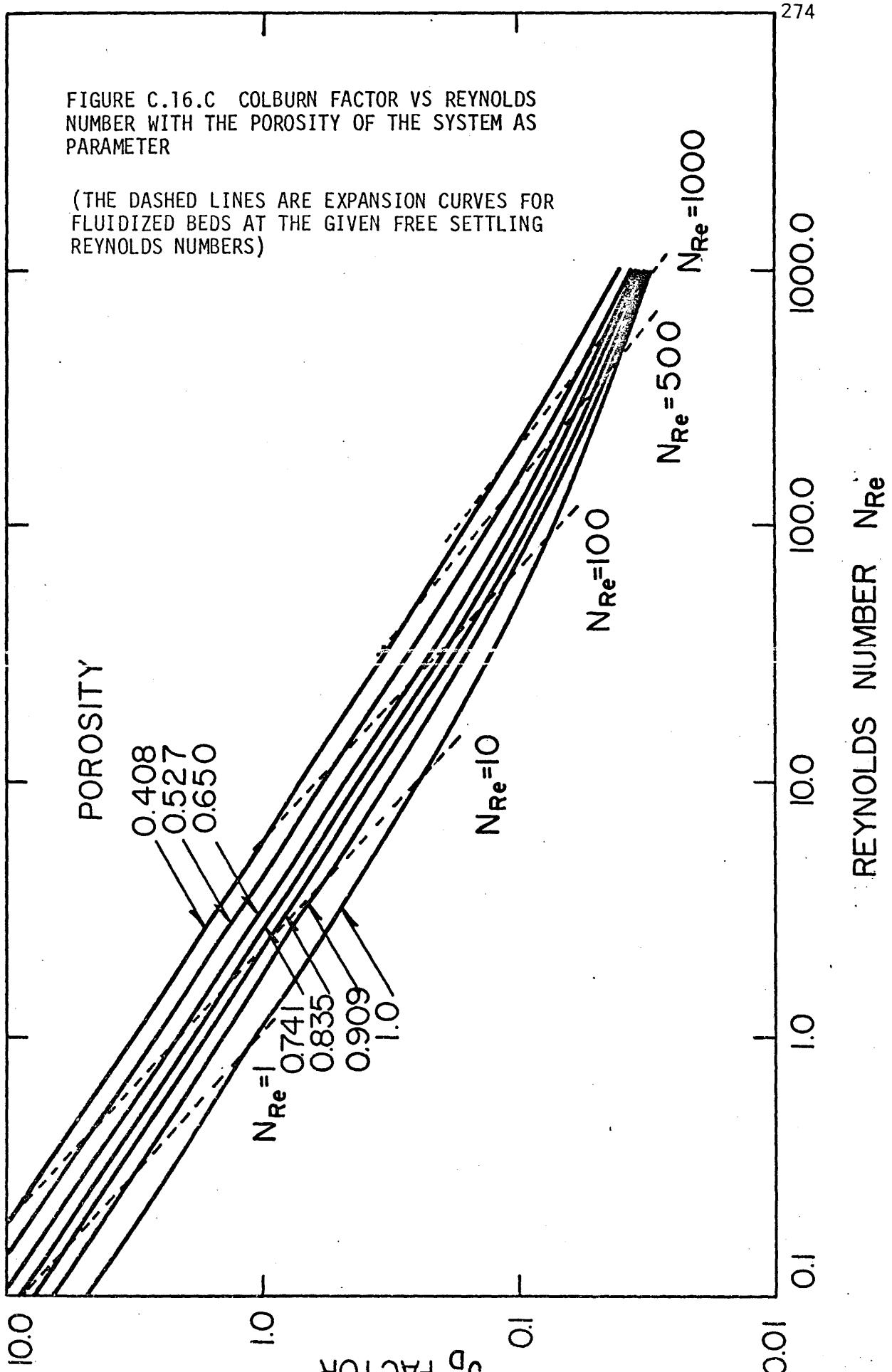

FIGURE C.16.D εJ_D VS REYNOLDS NUMBER FOR MULTI-PARTICLE SYSTEMS

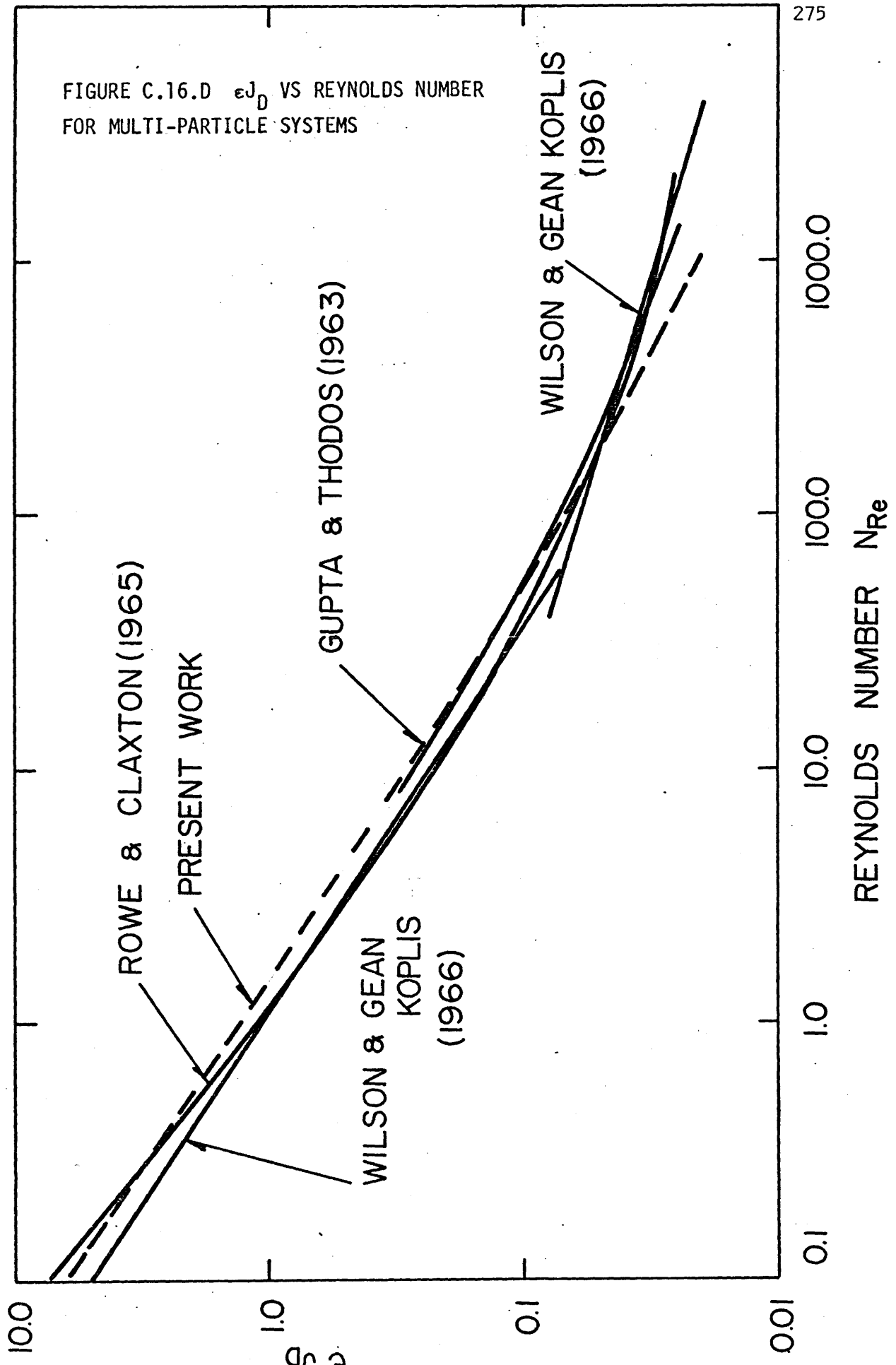

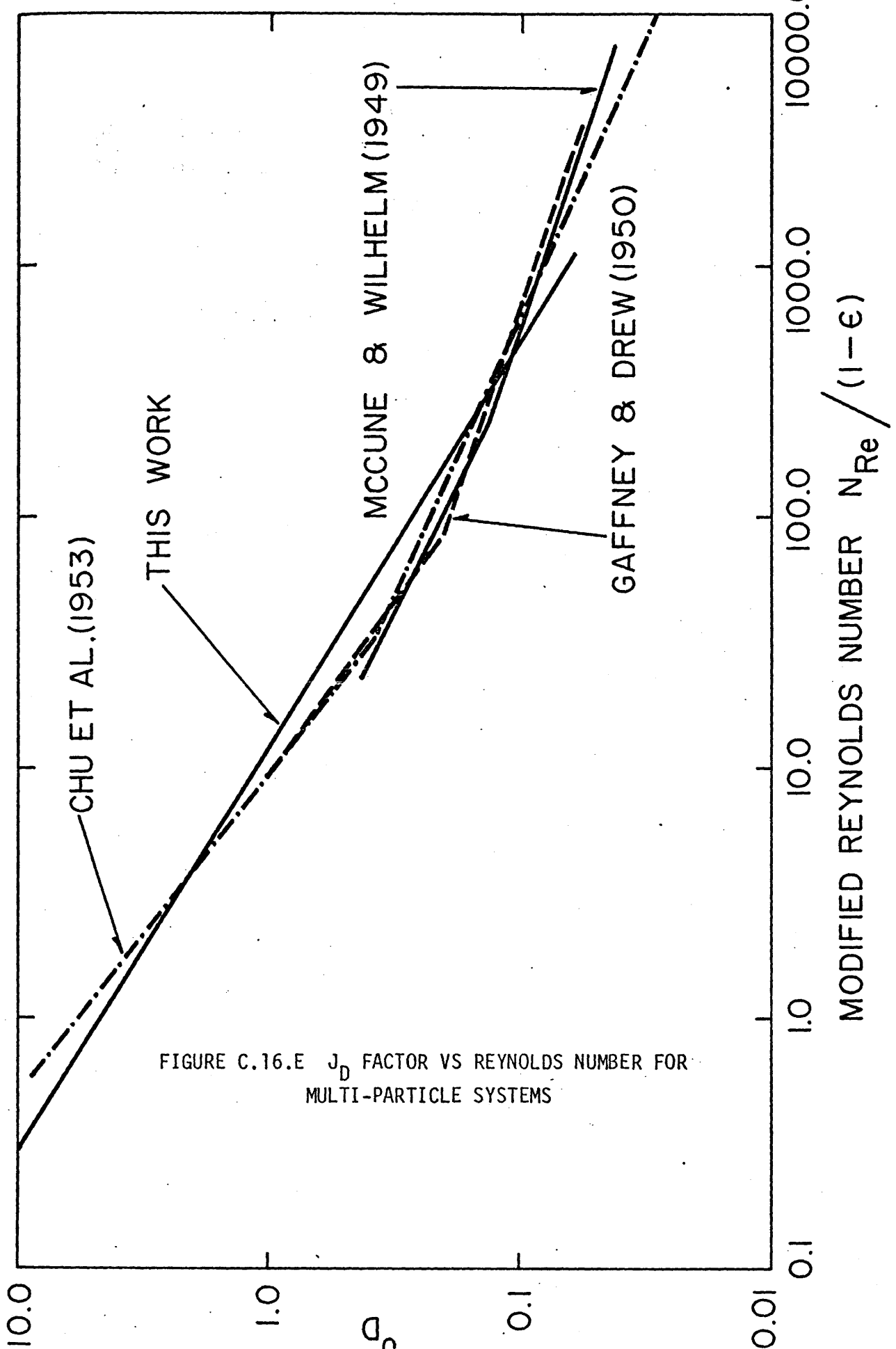

FIGURE C.16.E J_D FACTOR VS REYNOLDS NUMBER FOR MULTI-PARTICLE SYSTEMS

C.4.2 Cylinder Bundles and Bubble Swarms

C.4.2.1 Single Infinitely Long Cylinders in Cross Flow

There has been little experimental investigation of local coefficients of heat or mass transfer around cylinders in the intermediate Reynolds number range. The only work is that of Eckert and Soehngen (1952) who studied the flow of air past heated cylinders. In Figure C.17.A a comparison of the theoretical profiles obtained in this work is made with the experimental work of the above authors. Qualitative agreement was obtained between the two results. These curves demonstrate the variation of the local Nusselt number over the cylindrical surface. The local Nusselt number at the frontal stagnation point of a circular cylinder in cross flow to an air stream has been given by Goldstein (1938) as:

$$N_{Nu}(0) = 1.14\, N_{Pr}^{0.4}\, N_{Re}^{0.5} \qquad (C.32)$$

Goldstein's equation is presented in Figure C.17.B along with the experimental data of Eckert and Soehngen and the theoretical calculations of this work. The theoretical results, presented as a ratio of the transfer rate at an angle θ to that at the frontal stagnation point, are compared with boundary layer theory predictions in Figure C.17.C.

The difference between the local Sherwood number profiles for the cylinder and sphere is interesting. For the sphere, Figure C.15.A, there is a pronounced drop in the transfer rate at the frontal stagnation point, whereas for the cylinders in cross flow the transfer rate is a maximum at the frontal stagnation point.

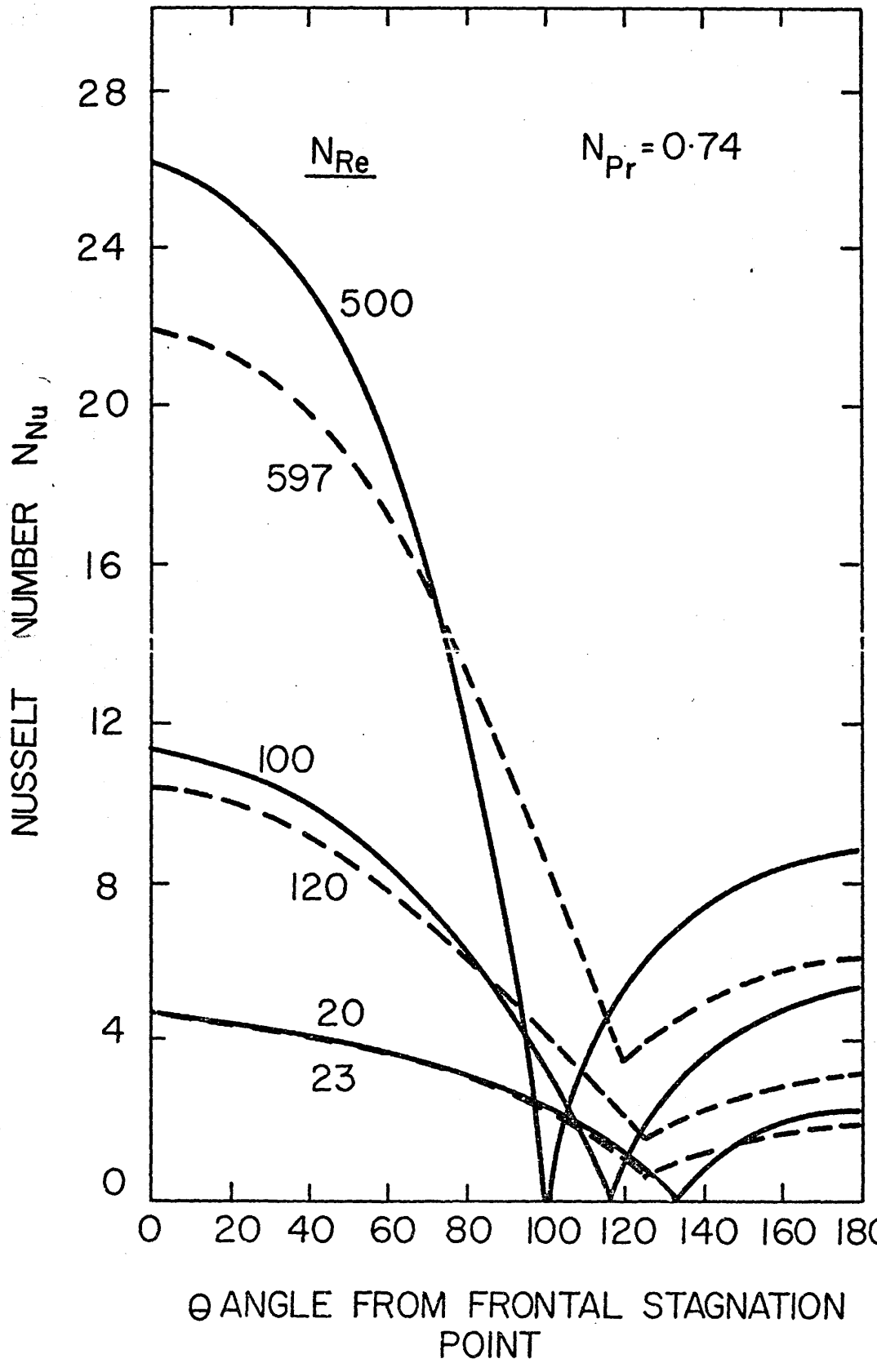

FIGURE C.17. A LOCAL HEAT TRANSFER PROFILES FOR SINGLE CYLINDER IN CROSS-FLOW

---- ECKERT AND SOEHUGEN (1952), EXPERIMENTAL

____ THEORETICAL

FIGURE C.17.B HEAT TRANSFER RATE AT THE FRONTAL STAGNATION POINT VS REYNOLDS NUMBER

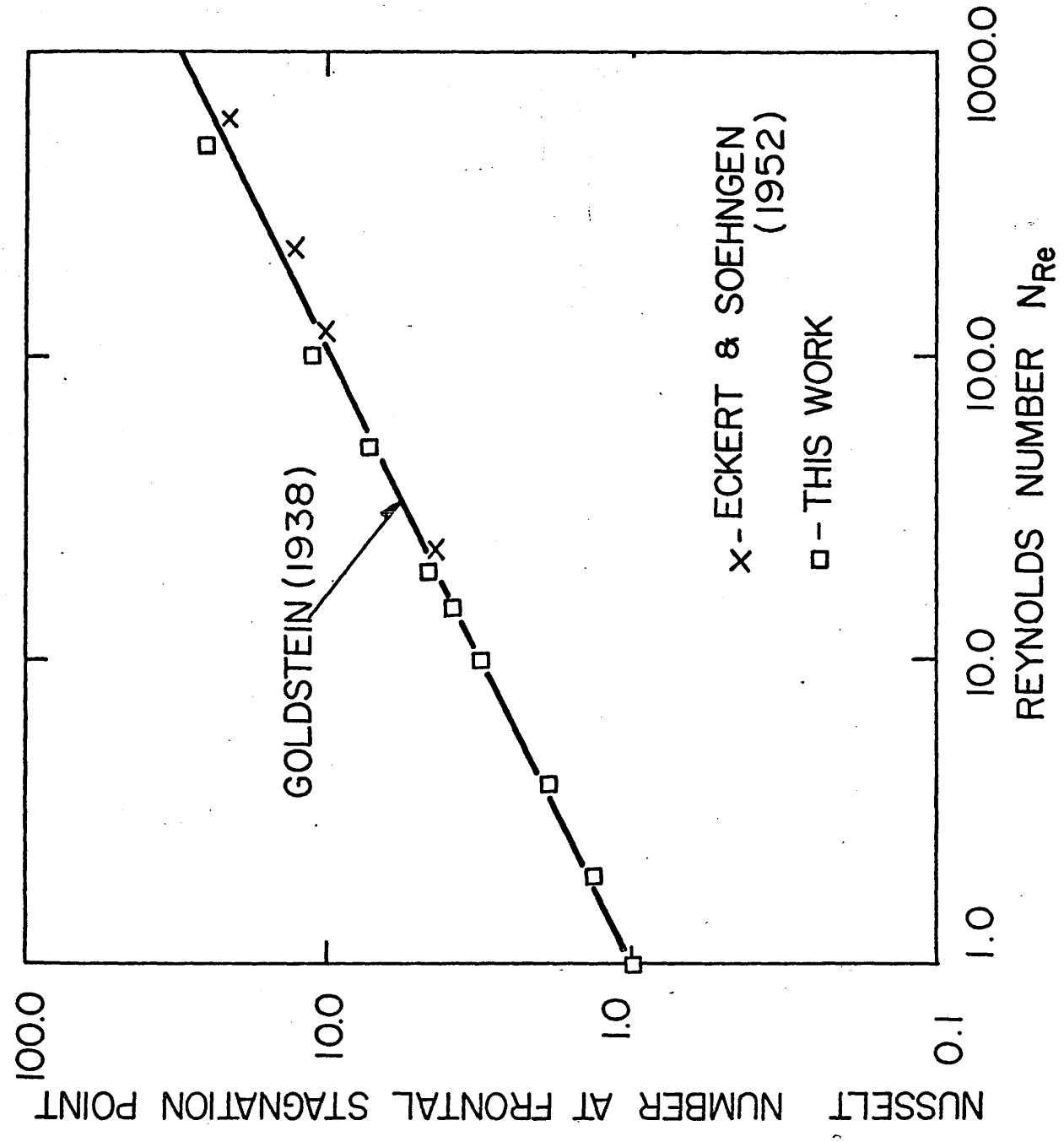

FIGURE C.17.C LOCAL UNIVERSAL TRANSFER RATIO COMPARISON FOR AN INFINITELY LONG CYLINDER IN CROSS-FLOW

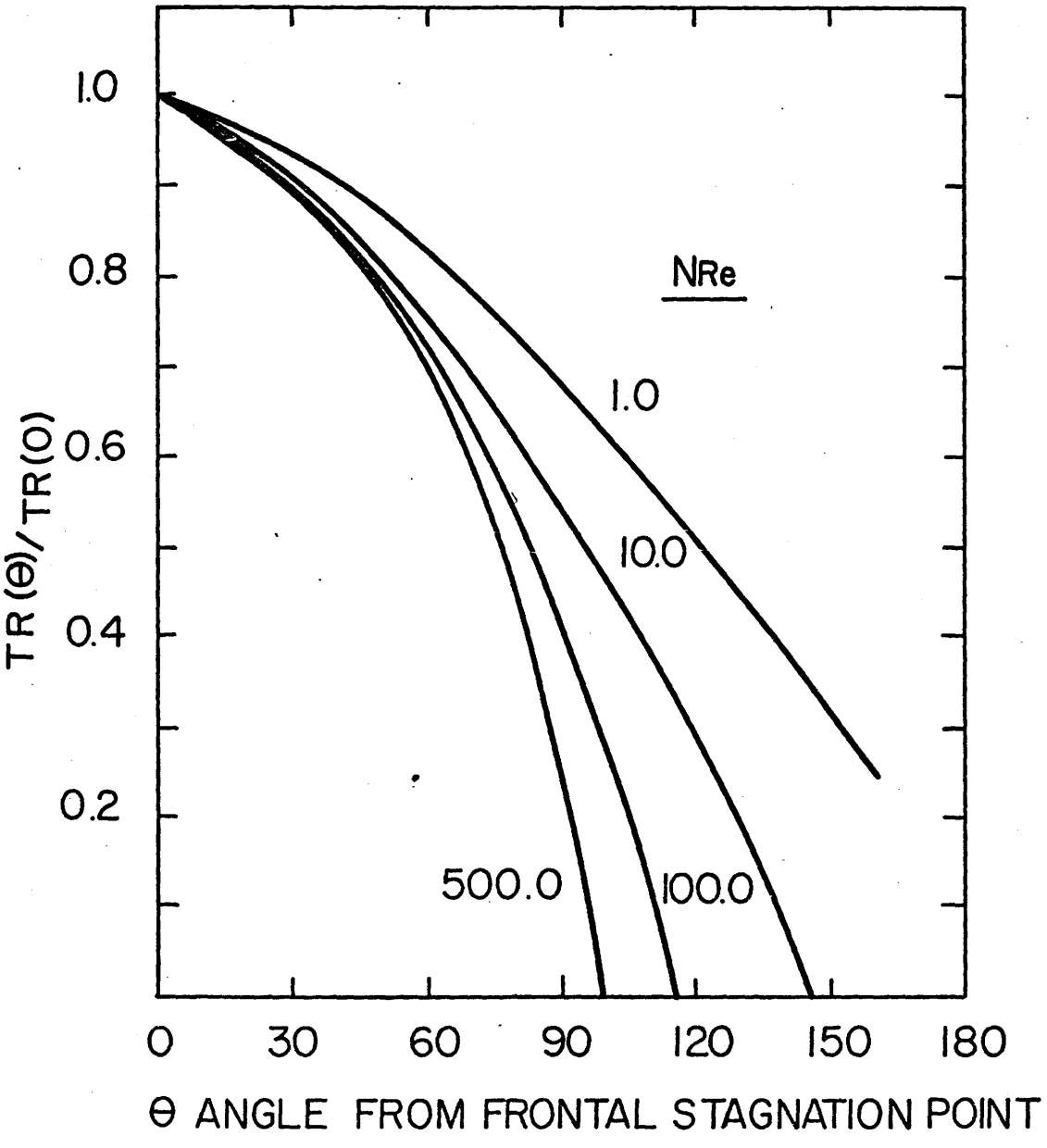

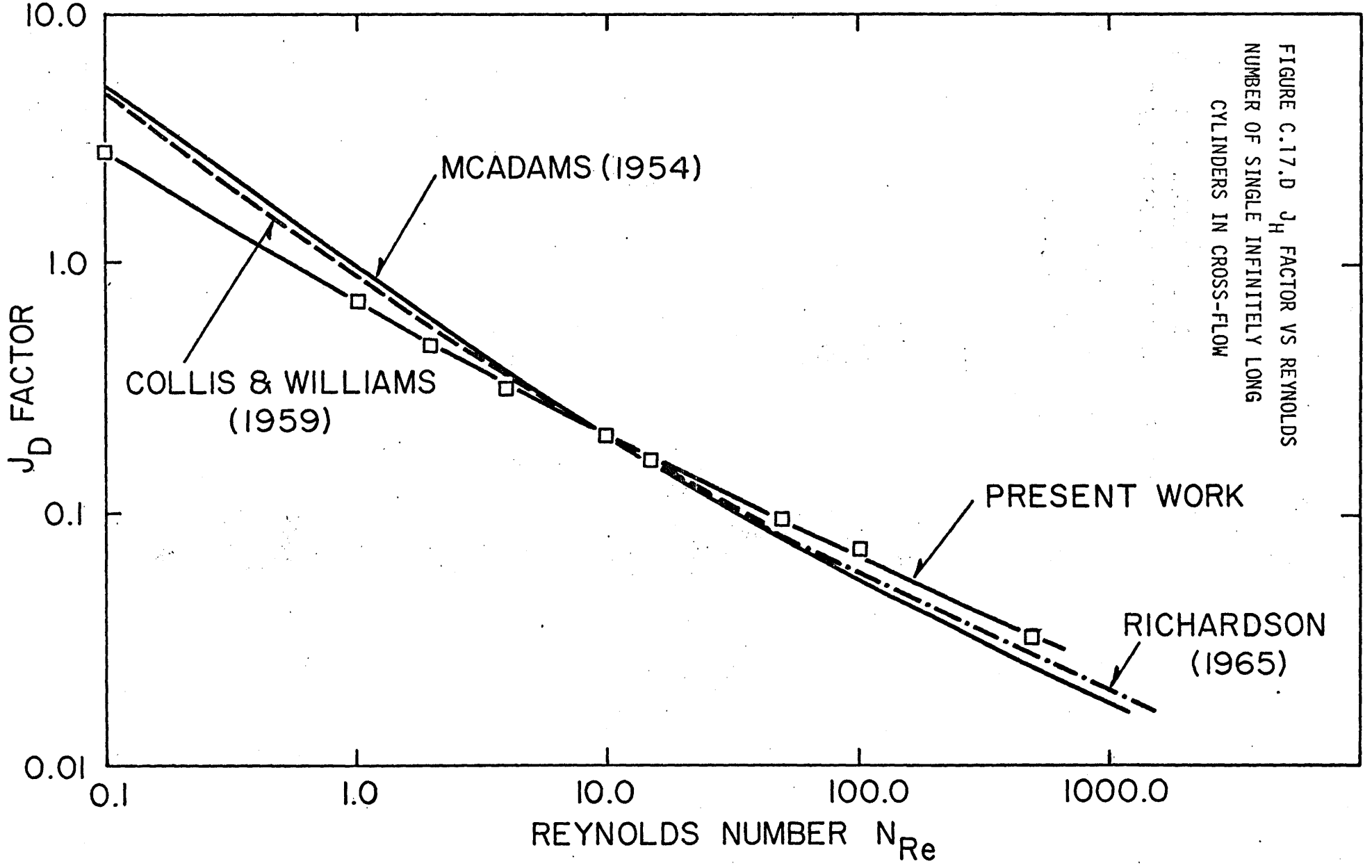

FIGURE C.17.D J_H FACTOR VS REYNOLDS NUMBER OF SINGLE INFINITELY LONG CYLINDERS IN CROSS-FLOW

Eckert and Soehngen have also presented an equation for the average transfer rate from a cylinder in cross flow. This equation is presented in Figure C.17.D along with the equation recommended by McAdams (1954) and the calculated theoretical results. Also plotted in this figure are the semi-theoretical line of Richardson (1965) and the least squares line of the data of Collis and Williams (1959). The theoretical equation predicts heat transfer rates which are low at low Reynolds numbers and high at high Reynolds numbers.

C.4.2.2 Multicylinder Systems

Multicylinder systems can be divided into two broad regions (1) cross flow to banks of circular tubes and (2) flow through packed fiber layers. Although some data is available for these systems it was almost impossible to reduce it to a form suitable for comparison with the theoretical results. Figure C.18.A presents the effect of porosity on the local Sherwood number at a Reynolds number of 100. Theoretical curves of Colburn mass transfer factor vs Reynolds number for various porosities are presented in Figure C.18.B. Least squares analysis of the results produced the following regression equation:

$$J\,\varepsilon^{0.833} = 1.05(N_{Re})^{-0.582} \qquad (C.33)$$

In Figure C.18.C the heat transfer factors predicted by the present model are replotted after the method of Bergelin, Brown and Doberstein (1952). In their method the interstitial Reynolds number is used. Thus

FIGURE C.18.A EFFECT OF POROSITY ON THE LOCAL MASS TRANSFER RATE FROM A CYLINDER IN CROSS-FLOW AT N_{Re} = 100

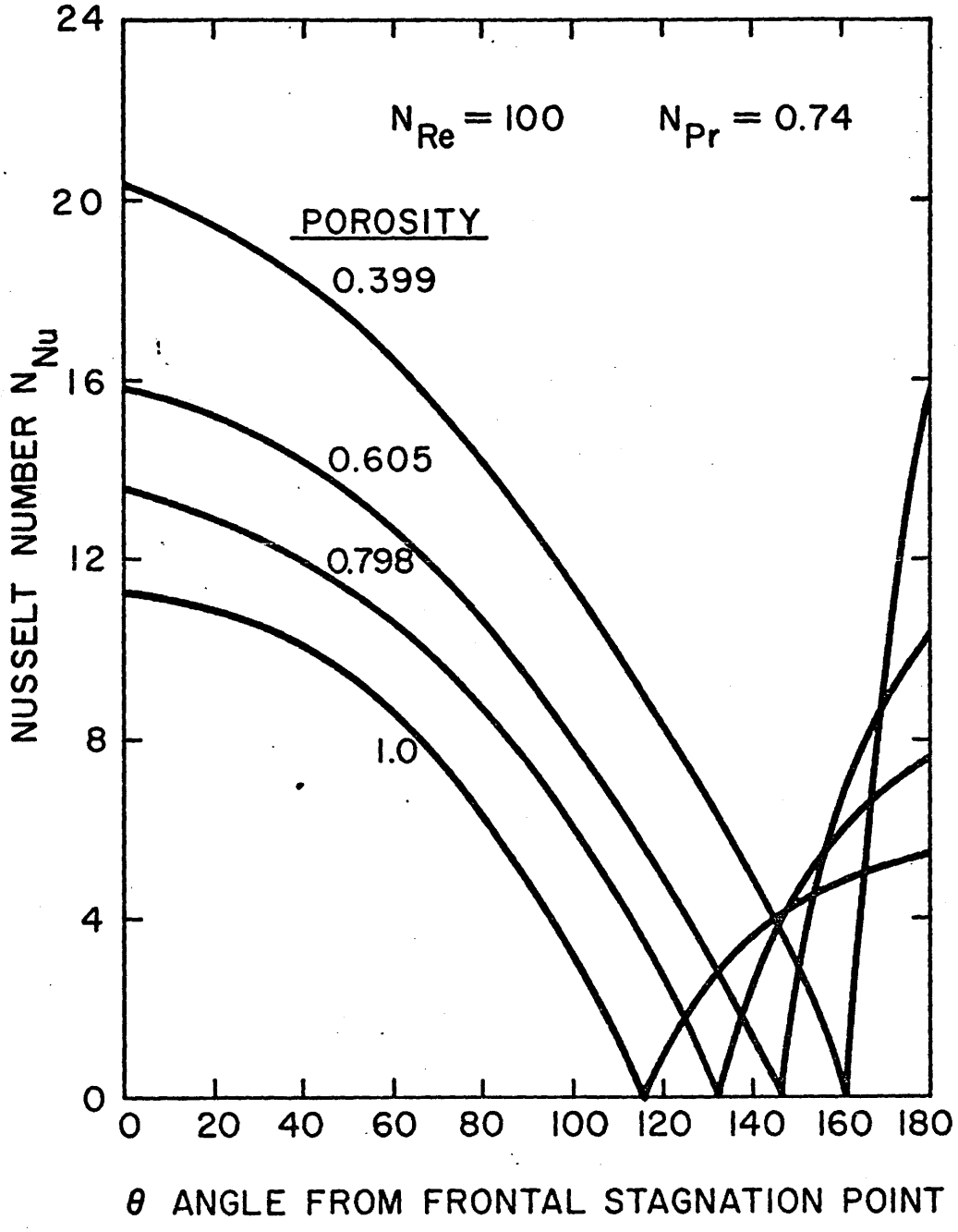

FIGURE C.18.B J_D FACTOR VS REYNOLDS NUMBER FOR A MULTI-CYLINDER SYSTEM IN CROSS-FLOW

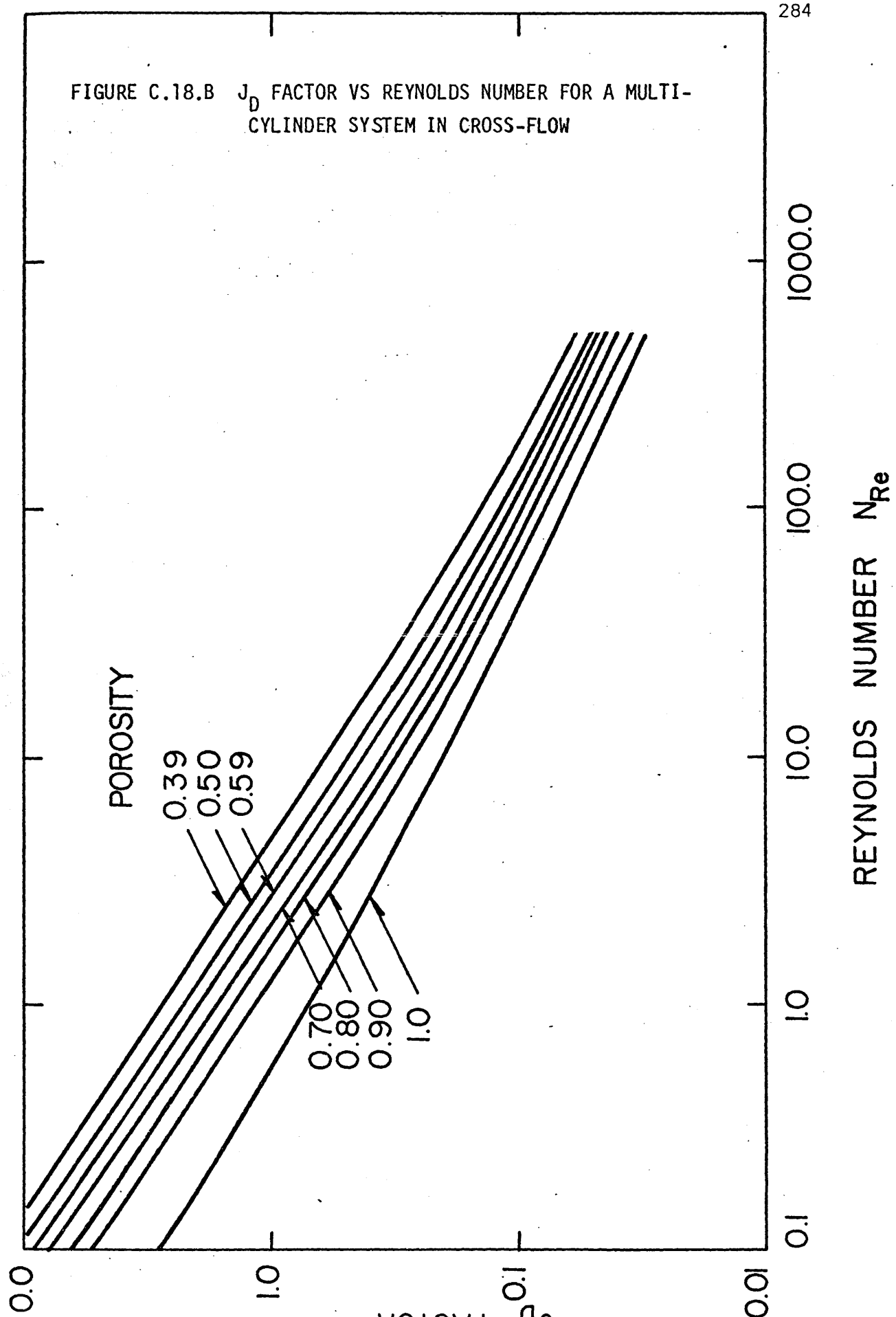

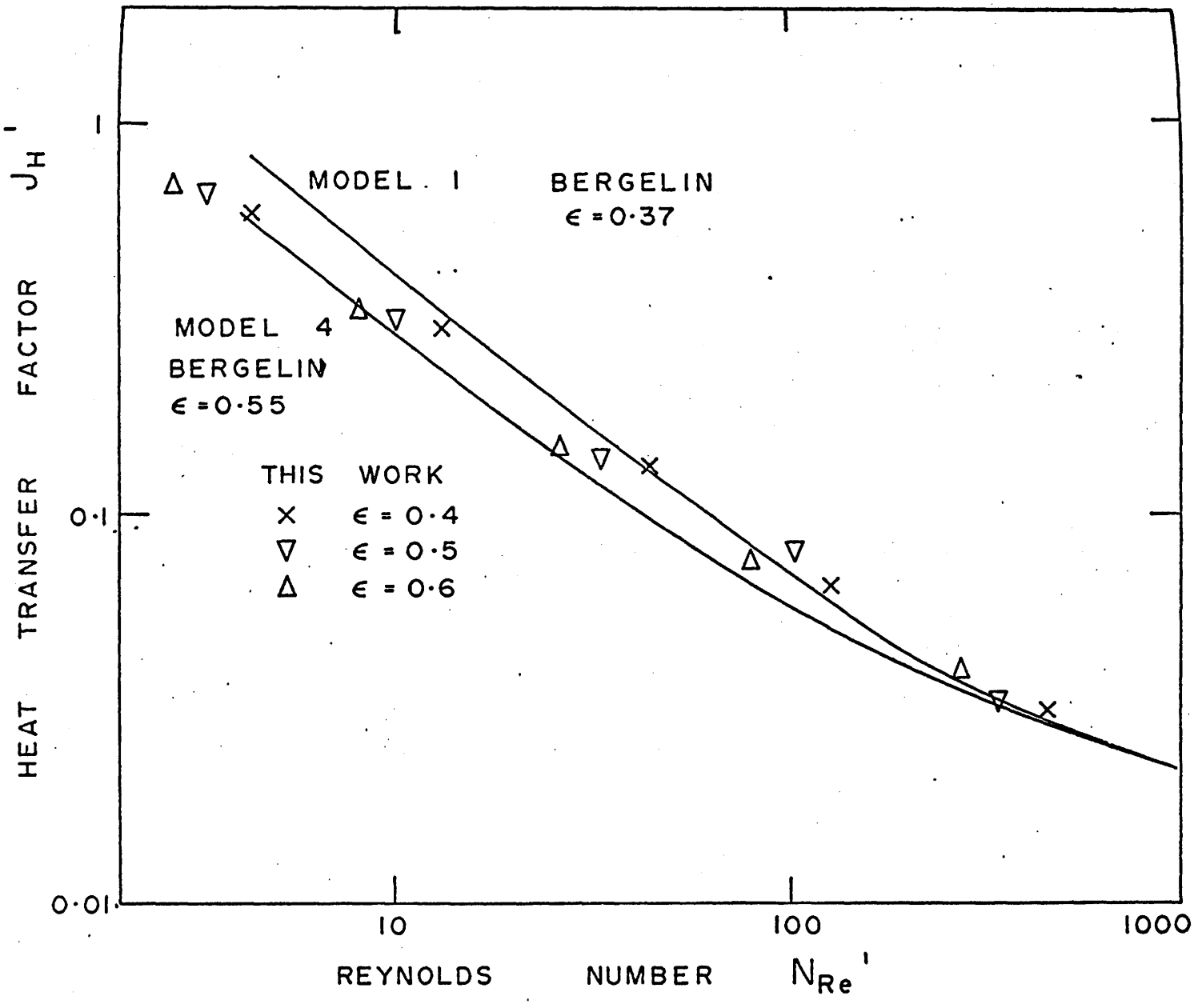

FIGURE C.18.C HEAT TRANSFER FACTOR VS REYNOLDS NUMBER FOR FLOW IN TUBE BUNDLES

$$J_H^I = \left(\frac{h}{C_p G_{max}}\right)\left(\frac{C_p \mu}{k}\right)^{2/3}\left(\frac{\mu_w}{\mu}\right)^{0.14}$$

$$= J_H \left[1-(1-\varepsilon)^{\frac{1}{2}}\right] \qquad (C.34)$$

The agreement between the theoretical prediction and the experimental data is good.

C.4.2.3 Single Fluid Spheres

Theoretical predictions of mass transfer rates from circulating spheres in the intermediate Reynolds number range have mainly been derived from approximations of the flow regime around a bubble. Hamielec and Johnson (1962) obtained approximate solutions using the Galerkin method. Baird and Hamielec (1962) used the approximate velocity profiles of Kawaguti (1948) and Hamielec (1961) to obtain heat and mass transfer rates. These results are not totally satisfactory as they are not asymptotic to the limiting values as $N_{Re} \to 0$ and $N_{Re} \to \infty$. The low Reynolds number limiting value of

$$N_{Sh} N_{Re}^{-\frac{1}{2}} = 0.65 \qquad (C.35)$$

was obtained by Levich (1962) and the limiting value at $N_{Re} = \infty$ of

$$N_{Sh} N_{Pe}^{-\frac{1}{2}} = 1.13 \qquad (C.36)$$

was obtained by Boussinesq (1905).

Numerous workers such as Chao (1962) and Wennikow (1967) have applied boundary layer theory to the flow around circulating spheres to extrapolate potential flow results into the intermediate Reynolds number

range. The most accurate of these is that of Wennikow who used the velocity data of Moore (1963). The equation he obtained is

$$N_{Sh}\, N_{Pe}^{-\frac{1}{2}} = \frac{2}{\sqrt{\pi}} (1 - 2.89\, N_{Re}^{-\frac{1}{2}})^{\frac{1}{2}} \qquad (C.37)$$

In this work, the velocity profiles developed by Hamielec, Johnson and Houghton (1967) were used to obtain mass transfer rates. The results, including those of earlier workers, are presented in Figure C.19.A.

C.4.2.4 Bubble Swarms

The "surface interaction" model was used to develop mass transfer correlations for bubbles as a function of Reynolds number and porosity. The results obtained using the model are presented in Figure C.19.B. The correlating equation obtained was

$$J'\, \varepsilon^{0.627} = 0.935\, N_{Re}^{-0.652} \qquad (C.38)$$

In Figure C.19.C the effect of porosity on the local mass transfer rate at a Reynolds number of 10 is presented.

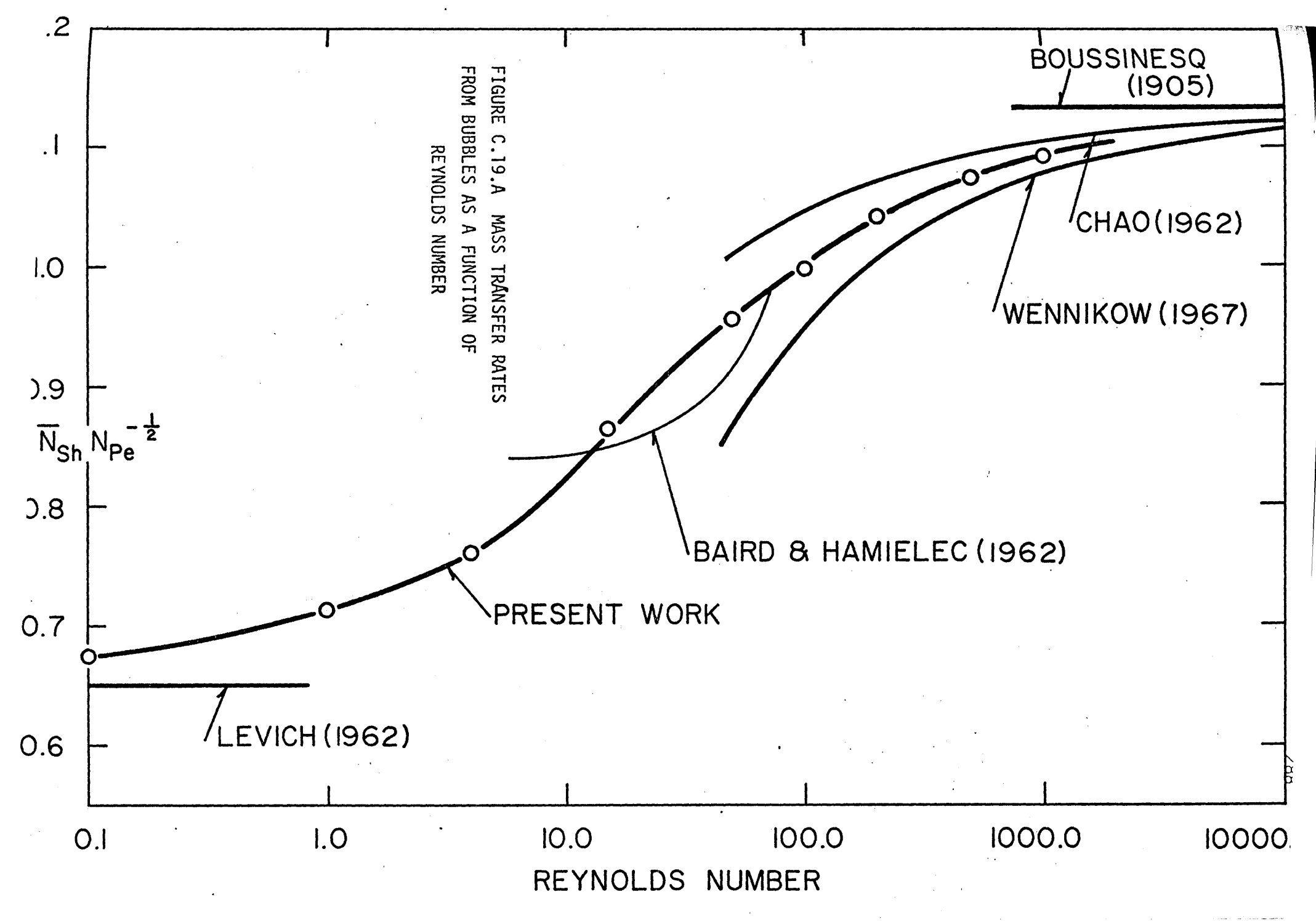

FIGURE C.19.A MASS TRANSFER RATES FROM BUBBLES AS A FUNCTION OF REYNOLDS NUMBER

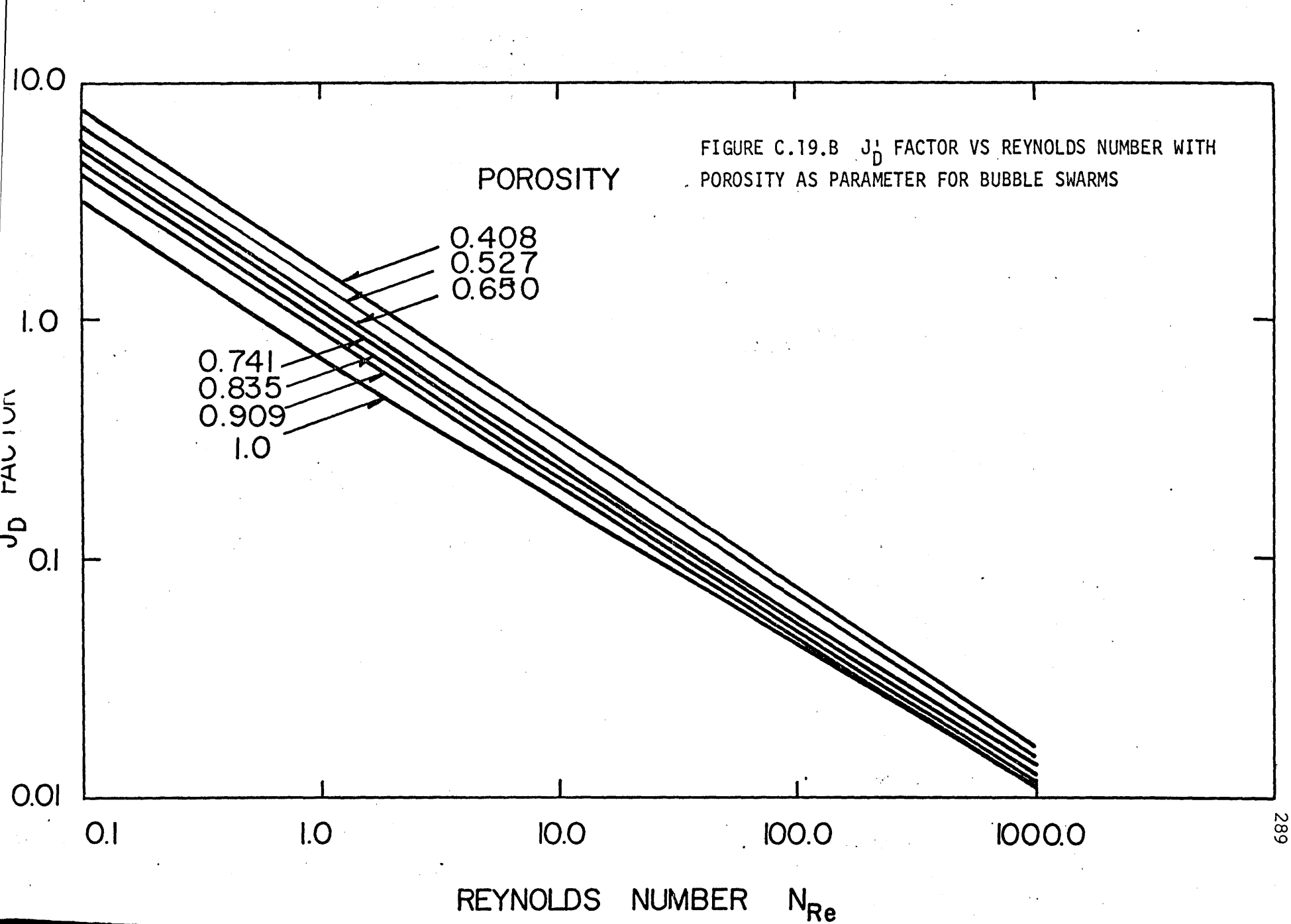

FIGURE C.19.B J_D' FACTOR VS REYNOLDS NUMBER WITH POROSITY AS PARAMETER FOR BUBBLE SWARMS

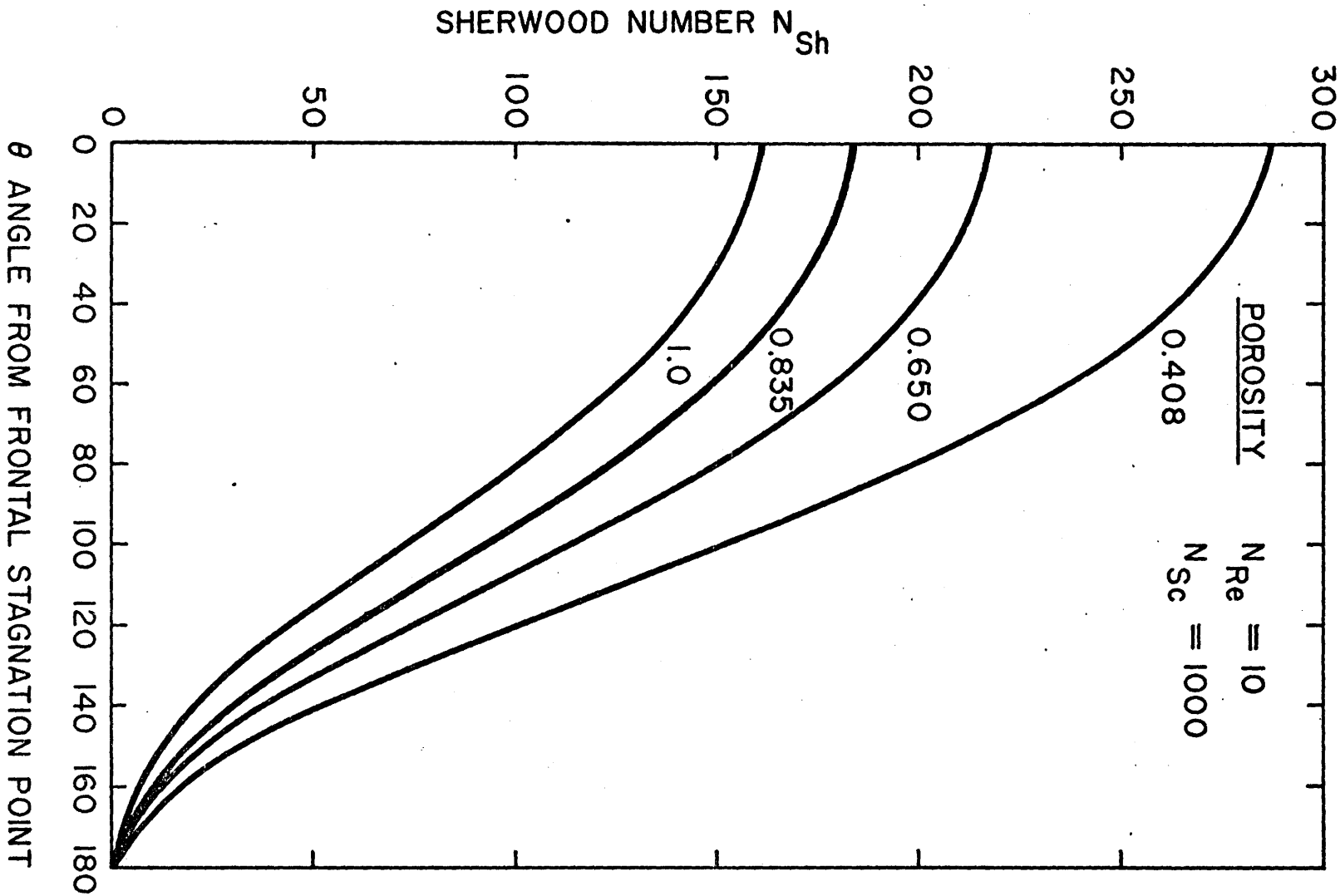

FIGURE C.19.C EFFECT OF POROSITY ON THE LOCAL MASS TRANSFER RATE FROM A GAS BUBBLE AT N_{Re} = 10

C.4.3 Discussion

The limitations of the thin concentration or temperature boundary layer should be emphasized. Its applicability is questionable for systems with low Prandtl and Schmidt numbers, for transfer in the vortex ring and situations which involve high mass transfer rates (when radial velocity at the particle surface is significant).

The condition of high Peclet numbers for the thin concentration boundary layer solution appears to be too restrictive. Reasonable results are obtained at relatively low Peclet numbers, as is shown in Figures C.20.A and C.20.B. In Figure C.20.A, results are presented for flow perpendicular to a cylinder where: 1, is the thin concentration boundary layer solution at N_{Re}=100; 2, the experimental results of Eckert and Soehngen (1952) at N_{Re}=120; and 3, the complete solution of the convection equation for N_{Re}=85. In Figure C.20.B results are presented for a packed bed of spheres at N_{Re}=100, the solid lines are the complete solution of the convection equation and the dashed lines are the thin concentration boundary layer solutions.

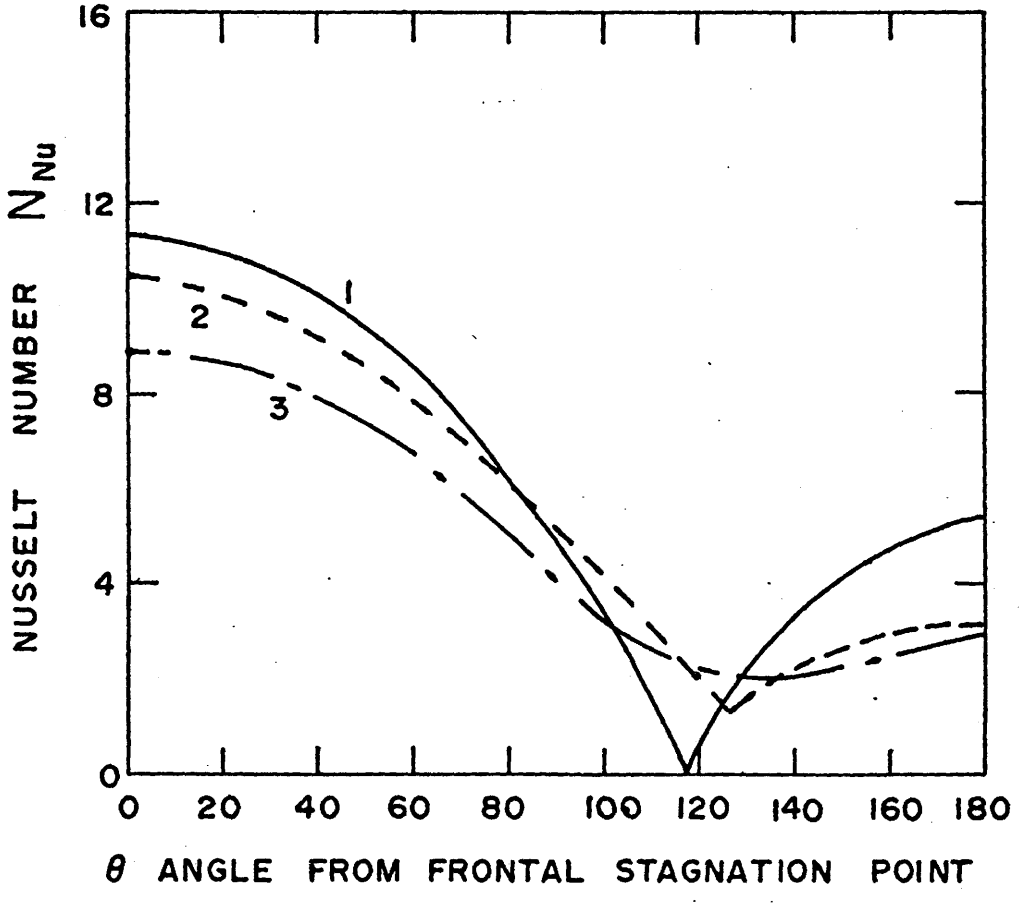

FIGURE C.20.A COMPARISON OF THIN CONCENTRATION BOUNDARY LAYER SOLUTION AND COMPLETE SOLUTION OF CONVECTION EQUATION FOR CYLINDER

FIGURE C.20.B COMPARISON OF THIN CONCENTRATION BOUNDARY LAYER SOLUTION AND COMPLETE SOLUTION OF CONVECTION EQUATION FOR SPHERE ASSEMBLAGE

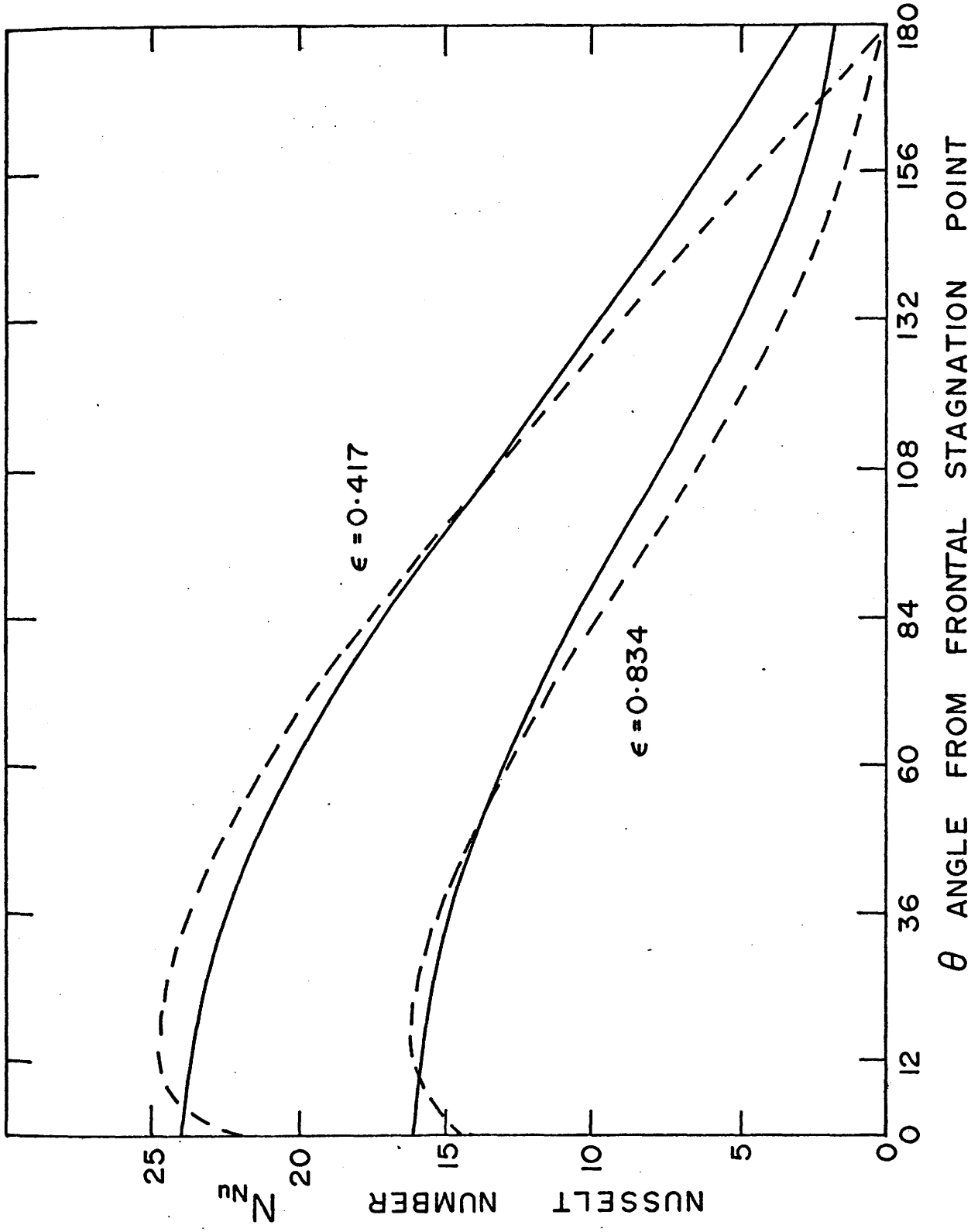

D. Summary and Conclusions

Several contributions were made. In the first, forced convection mass transfer rates were obtained for single particle systems. The agreement between the calculated local mass transfer rates for spheres and cylinders in cross flow and experimental correlations is excellent. A correlation was also obtained for mass transfer from circulating gas bubbles which bridges the gap from the region of low Reynolds number flow where the Levich equation is valid to the region of high Reynolds numbers where the Boussinesq equation applies.

In the second contribution the zero vorticity model developed by Kawabura was extended to the intermediate Reynolds number region to predict mass or heat transfer rates for multiparticle systems of either spheres, cylinders or circulating fluid drops of low viscosity. The models may also be used to predict voidage and drag in fluidized beds and bubble columns, and pressure drop through tube banks. Reasonable agreement was found between the model and experiment at intermediate and high porosities; on the other hand, agreement was poor at low porosities. The model does not adequately account for the blockage affect of the upstream particle.

It should be emphasized however, that this has been an initial attempt to use the transport approach for the solution of a practical industrial problem where the complexity has warranted empirical correlations in the past. This preliminary surface-interaction model was based upon

boundary conditions which were thought to be theoretically realistic. Secondly, results were required to determine the general suitability of these types of models. Comparison of the calculated results with experimental data has suggested laboratory experiments to obtain more realistic boundary conditions and conceptual modifications to the model which should yield more exact results. In essence it is believed that with microscopic transport equations and constitutive equations developed from experiments suggested by the model it will be possible to predict the macroscopic phenomena of multiparticle systems.

E. Recommendations for Future Work

The spherical cell model predicts relative velocity ratios which are lower than experimental data for all Reynolds Numbers. The cause is blockage at low Reynolds numbers where the boundary layer is thick and suppression of the downstream growth of the vortex ring at higher Reynolds numbers. To obtain reduced drag, these flow restrictions must be decreased. This may be accomplished by using oblate - to - prolate outer boundary shapes for the outer imaginary boundary or by incorporating a finite value of vorticity on the outer boundary rather than the present zero vorticity condition. A systematic study could be performed to determine the effect of incorporating these conditions into the model.

A much more profitable approach would involve experimental work within an extended bed similar to that of Gunn and Malik (1966) in conjunction with the theoretical work. Instead of measuring total pressure drop as Gunn and Malik did, point values of the parameters should be measured. Of particular interest are the pressure and vorticity distributions on the surface of the particles. These are extremely sensitive to bed porosity and Reynolds Number and can be easily measured. Relatively more difficult to measure would be point velocities as a function of position with respect to the particle. However with further laser development, these should be easily measured also. If this experimental data is obtained it will make the search for a boundary shape or boundary conditions much easier.

In the cell model concept, it is assumed that a multiparticle system has a uniform porosity. Thus one cell may be used to describe the system. Because of end effects and enclosing container walls multiparticle systems are generally heterogeneous. To develop a more realistic model, time average spatial distribution in bed porosity should be incorporated into the model. An experimental study should be carried out to determine the parameters affecting porosity variation. The parameters should then be used to develop a stochastic model of the porosity variation. Incorporation of the cell model, which would now be used in a local sense, with the stochastic model containing porosity variation should give realistic predictions for most multiparticle phenomena.

F. Contributions to Knowledge

In this dissertation the cell model approach which has been used in the creeping flow regime to model multiparticle systems, has been extended to the intermediate Reynolds number regime by including the inertia terms in the Navier Stokes equation. Three types of multiparticle systems were studied: beds of solid spheres, cylinder bundles in cross flow and gas bubble swarms. The convection equation for mass or heat transport has also been solved for these systems using the Levich thin concentration boundary layer approach, yielding a model which can predict both mass and momentum transport for most forms of multiparticle systems. Several learned papers which have been written on this work are listed below:

LeClair, B.P., and Hamielec, A.E.,
"Viscous Flow Through Particle Assemblages at Intermediate Reynolds Numbers -Steady-State Solutions for Flow Through Assemblages of Spheres",
I & EC Fundamentals, 7, 542 (1968).

LeClair, B.P., and Hamielec, A.E.,
"Viscous Flow Through Particle Assemblages at Intermediate Reynolds Numbers - Heat or Mass Transport",
in press, I. Chem. E. Symposium Series Fluidization, No. 30 (1968).

LeClair, B.P., and Hamielec, A.E.,
"Viscous Flow Through Particle Assemblages at Intermediate Reynolds Numbers - Steady-State Solutions for Flow Through Assemblages of Cylinders",
in press I & EC Fundamentals

LeClair, B.P. and Hamielec, A.E.,
"Viscous Flow Through Particle Assemblages at Intermediate Reynolds Numbers - Design Approach for Steady-State Flow of Bubble Swarms".

G. Nomenclature

a - radius of dispersed phase object

b - radius of imaginary outer boundary of cell

C - concentration of diffusing species

C_D - drag coefficient

C_{DF} - friction drag coefficient

C_{DP} - pressure drag coefficient

C_s - surface concentration of diffusing species

$A', B', C', D', E', F',$ - constants in analytical solution

D - mass diffusivity

D_v - volumetric hydraulic diameter

E^2 - differential operator

g - acceleration of gravity

g_c - gravitational conversion factor

G - mass velocity based upon minimum cross section

G/A - superficial gas velocity based upon column diameter

h - heat transfer coefficient

j_D - Colburn factor for mass transfer, $N_{Sh}\, N_{Re}^{-1}\, N_{Sc}^{-1/3}$

j_D' - modified Colburn factor, $N_{Sh}\, N_{Re}^{-7/6}\, N_{Sc}^{-1/2}$

J_H - Colburn factor for heat transfer, $N_{Nu}\, N_{Re}^{-1}\, N_{Pr}^{-1/3}$

J_H' - modified Colburn factor based on minimum cross section Reynolds number

k - thermal conductivity

k_D - mass transfer coefficient

k_H - heat transfer coefficient

(L/A) - liquid superficial velocity based on column diameter

N - number of tubes in bundle

N_{Nu} - Nusselt number, $2ah/kH$

N_{Pe} - Peclet number, $N_{Re}\ N_{Sc}$

N_{Pr} - Prandtl number, $C_p\mu/k$

N_{Re} - Reynolds number, $2aU\rho/\mu$

N_{Re}' - Reynolds number based upon mass velocity through the minimum cross-section

N_{Re_v} - Reynolds number based upon mass velocity through the minimum cross-section and volumetric hydraulic diameter

N_{Sc} - Schmidt number, $\mu/\rho D$

N_{Sh} - Sherwood number, $2ak_D/D$

$\bar{N}_{Sh}$ - mean Sherwood number

P - pressure

P_o - frontal stagnation pressure

r - radial position

r_e - effective bubble radius

r_∞ - radial position of outer boundary

S_T - transverse pitch

S_L - longitudinal pitch

T_R - transfer number, $N_{Sh}\ N_{Re}^{-\frac{1}{2}}\ N_{Sc}^{-1/3}$

U, V, U_∞, V_∞ - superficial liquid velocity

v - velocity

V_B - bubble velocity

v_p - dispersed phase velocity

y - radial position, r-a

ψ - stream function

ξ - vorticity

θ - angular coordinate

υ - kinematic viscosity

ε - porosity

ρ - density

ρ_p - dispersed phase density

μ - viscosity

μ_w - viscosity at tube wall

J - shear stress

∇^2 - differential operator

λ - relative radius ratio, a/b

ϕ - dispersed phase fraction, 1-ε

subscripts

r, x, y, z, θ $1, 2, 3,$ - coordinate directions

H. References

Acrivos, A., and Taylor, T.D.,
Phys. Fluids, 5, 387 (1962).

Adler, I.L., and Happel, J.,
Chem. Eng. Progr. Symp. Ser., 58, 98 (1962).

Aksel'rud, G.A.,
Zh. Fiz. Klim., 27, 1445 (1953).

Baird, M.H.I., and Hamielec, A.E.,
Can. J. Chem. Eng., 40, 119 (1962).

Bergelin, O.P., Brown, G.A., and Doberstein, S.C.,
Trans. ASME, 74, 953 (1952).

Bhatia, V.K.,
AIChEJ, 15, 446 (1969).

Boussinesq, J.J.,
J. Math. Pure Appl., 11, 285 (1905).

Brenner, H.,
Chem. Eng. Sci., 19, 599 (1964).

Bridge, A.G., Lapidus, L., and Elgin, J.C.,
AIChEJ, 10, 819 (1964).

Calderbank, P.H.,
The Chem. Engineer, 45, CE209 (1967).

Chao, B.F.,
Phys. Fluids, 5, 69 (1962).

Chen, W.C., and Pfeffer, R.,
IEC Fundamentals, 9, 101 (1970).

Chu, J.D., Kalil, J., and Wetteroth, W.A.,
Chem. Eng. Progr., 49, 141 (1953).

Collis, D.C., and Williams, M.J.,
J. Fluid Mech., 6, 357 (1959).

Eckert, E.R.G., and Soehngen, E.,
Trans ASME, 74, 343 (1952).

Ergun, S.,
Chem. Eng. Progr., 48, 89 (1952).

Fair, G.M., and Hatch, L.P.,
J. Am. Water Works Assoc., 25, 1551 (1933).

Friedlander, S.K.,
AIChEJ, 3, 43 (1957).

Friedlander, S.K.,
AIChEJ, 7, 347 (1961).

Gaffney, B.J., and Drew, T.B.,
Ind. Eng. Chem., 42, 1120 (1950).

Gal-Or, B., and Resnick, W.,
Chem. Eng. Sci., 19, 653 (1964).

Gal-Or, B., and Hoelscher, H.E.,
AIChEJ, 12, 499 (1966).

Gal-Or, B., and Waslo, S.,
Chem. Eng. Sci., 23, 1431 (1968).

Gal-Or, B., and Padmanabhan, L.,
AIChEJ, 14, 709 (1968).

Gal-Or, B.,
Int. J. Heat Mass Transfer, 11, 551 (1968).

Garner, F.H., and Keey, R.B.,
Chem. Eng. Sci., 9, 119 (1958a).

Garner, F.H., and Keey, R.B.,
Chem. Eng. Sci., 9, 208 (1958b).

Garner, F.H., and Suckling, R.D.,
AIChEJ, 4, 114 (1958).

Glen, J.B., and Keey, R.B.,
Chem. Eng. Sci., 20, 444 (1965).

Goldstein, S.,
"Modern Developments in Fluid Mechanics",
Vol. I, Oxford University Press, London, 1938.

Grosh, R.J., and Cess, R.D.,
Trans. ASME, 80, 667 (1958).

Gunn, D.J., and Malik, A.A.,
Trans. Inst. Chem. Engrs., 44, T371 (1966).

Gunter, A.Y., and Shaw, W.A.,
Trans. ASME, 67, 643 (1945).

Gupta, A.S., and Thodes, G.,
AIChEJ, 9, 751 (1963).

Hall, W.A.,
Trans. Amer. Geophys. Union, 3, 185 (1956).

Hamielec, A.E.,
Ph.D. Thesis, University of Toronto, Toronto, 1961.

Hamielec, A.E., and Johnson, A.I.,
Can. J. Chem. Eng., 40, 41 (1962).

Hamielec, A.E., Hoffman, T.W., and Ross, L.L.,
AIChEJ, 13, 212 (1967).

Hamielec, A.E., Johnson, A.I., and Houghton, W.T.,
AIChEJ, 13, 220 (1967).

Hamielec, A.E., and Raal, J.D.,
Phys. Fluids, 12, 11 (1969).

Hanratty, T.J., and Bandukuala, A.,
AIChEJ, 3, 293 (1959).

Happel, J., and Epstein, N.,
Ind. Eng. Chem., 46, 1187 (1954).

Happel, J.,
AIChEJ, 4, 197 (1958).

Happel, J.,
AIChEJ, 5, 174 (1959).

Happel, J., and Ast, P.A.,
Chem. Eng. Sci., 11, 286 (1960)

Happel, J., and Brenner, H.,
"Low Reynolds Number Hydrodynamics",
Prentice-Hall, Englewood Cliffs, 1965.

Hasimoto, H.J.,
Fluid Mech., 5, 317 (1959).

Hawksley, P.G.W.,
paper 7, "Some Aspects of Fluid Flow",
Edward Arnold, London, 1951.

Hiby, J.W.,
C70, Symp. on "The Interaction between Fluids and Particles",
Inst. Chem. Engrs. (London), 1962.

Howland, R.C.J., and McMullen, B.W.,
Cambridge Phil. Soc., 32, 402 (1936).

Hsu, C.,
Int. J. Heat Mass Transfer, 7, 431 (1966).

Johnson, A.I., and Akehata, T.,
Can. J. Chem. Eng., 43, 10 (1965).

Kawabura, S.,
J. Phys. Soc. Japan, 14, 527 (1959).

Kawaguti, M.,
Rept. Inst. Sci., Tokyo, 2, 66 (1948).

Kawaguti, M.,
J. Phys. Soc. Japan, 13, 209 (1958).

Kynch, G.J.,
J. Fluid Mech., 5, 193 (1959).

Lamb, H.,
"Hydrodynamics",
Dover, New York, 1945.

Lapple, C.E.,
"Fluid and Particle Mechanics",
University of Delaware Press, Newark, 1951.

LeClair, B.P.,
MASc Thesis, University of British Columbia, Vancouver, 1964.

Leva, M.,
"Fluidization",
McGraw-Hill, New York, 1959.

Leveque, J.,
Ann. Mines, 13, 201, 305, 381 (1928).

Levich, V.G.,
Zh. Eksperim., i Jeor. Fiz., 19, 8 (1949).

Levich, V.G.,
"Physicochemical Hydrodynamics",
Prentice-Hall, New York, 1962.

Lewis, W.K., Gilliland, E.R., and Bauer, W.C.,
Ind. Eng. Chem., 41, 1109 (1949).

Lighthill, M.J.,
Proc. Roy. Soc., A202, 359 (1950).

Linton, M., and Sutherland, K.L.,
Chem. Eng. Sci., 12, 214 (1960).

Maneri, C.C., and Mendelson, H.D.,
AIChEJ, 14, 295 (1968).

Marrucci, G.,
IEC Fundamentals, 4, 224 (1965).

McAdams, W.H.,
"Heat Transmission",
3rd Edition, McGraw-Hill, New York, 1954.

McCune, L.K., and Wilhelm, R.H.,
Ing. Eng. Chem., 41, 1124 (1949).

Mendelson, H.D.,
AIChEJ, 13, 250 (1967).

Mertes, T.S., and Rhodes, H.P.,
Chem. Eng. Progr., 51, 429 (1955).

Moore, D.W.,
J. Fluid Mech., 16, 161 (1963).

Natanson, G.L.,
Doklady Akad. Nauk., SSSR, 112, 100 (1957).

Nicklin, D.J.,
Chem. Eng. Sci., 17, 693 (1962).

Oliver, D.R.,
Chem. Eng. Sci., 15, 320 (1961).

Omohundro, G.A., Bergelin, O.P., and Colburn, A.P.,
Trans ASME, 71, 27 (1949).

Orr, C.,
"Particle Technology",
Macmillan, New York, 1966.

Peltzman, A., and Pfeffer, R.,
Chem. Eng. Symp. Series, 77, 63 (1967).

Pfeffer, R., and Happel, J.,
AIChEJ, 10, 605 (1964).

Pfeffer, R.,
IEC Fundamentals, 3, 380 (1964).

Redfield, J.A., and Houghton, G.,
Chem. Eng. Sci., 20, 131 (1965).

Richardson, P.D.,
AIAA J, 3, 537 (1965).

Richardson, J.F., and Zaki, W.N.,
Trans Inst. Chem. Engrs., 32, 35 (1954a).

Richardson, J.F., and Zaki, W.N.,
Chem. Eng. Sci., 3, 65 (1954b).

Rowe, P.N., and Claxton, K.T.,
Trans. Instn. Chem. Engrs., 43, T321 (1965).

Rowe, P.N., Claxton, K.T., and Lewis, J.B.,
Trans. Instn. Chem. Engrs., 43, T14 (1965).

Sieder, E.N., and Scott, N.A.,
ASME unpublished papers, No. 83, 1932.

Smoluchowski, M.A.,
Bull. Acad. Sci., Cracow, 1A, 28 (1911).

Stimson, M., and Jeffery, G.B.,
Proc. Roy. Soc., A111, 110 (1928).

Tavlarides, L.L., and Gal-Or, B.,
Israel J. Tech., 7, 1 (1969).

Tomotika, S., and Aoi, T.,
Quart. J. Mech. Appl. Math., 3, 140 (1950).

Wakiya, S.,
J. Phys. Soc. Japan, 8, 254 (1953).

Wennikow, S.,
Chem. Eng. Sci., 22, 477 (1967).

Williamson, J.E., Bazaire, K.E., and Geankoplis, C.J.,
IEC Fundamentals, 2, 126 (1963).

Wilson, E.J., and Geankoplis, C.J.,
IEC Fundamentals, 5, 9 (1966).

Yuge, T.,
Rept. Inst. High Speed Mech.,
Tokoku University, 57, 143 (1956).

Zenz, F.A.,
Petrol. Ref., 36, 147 (1957).

Zenz, F.A., and Othmer, D.F.,
"Fluidization and Fluid-Particle Systems",
Reinhold, New York, 1960.

APPENDIX II-A

SUPPLEMENTARY RESULTS

SOLID SPHERE SURFACE VORTICITY DISTRIBUTIONS FOR NRE = 0.1

POROSITY ANGLE	0.408	0.528	0.650	0.741	0.835	0.909
0	0.0	0.0	0.0	0.0	0.0	0.0
6	6.0738	3.1992	1.7912	1.1890	0.7663	0.5140
12	12.0741	6.3558	3.5559	2.3590	1.5195	1.0189
18	17.9437	9.4443	5.2825	3.5034	2.2559	1.5122
24	23.6169	12.4296	6.9516	4.6097	2.9675	1.9887
30	29.0313	15.2788	8.5445	5.6655	3.6465	2.4433
36	34.1272	17.9603	10.0437	6.6591	4.2856	2.8709
42	38.8488	20.4447	11.4326	7.5796	4.8774	3.2668
48	43.1443	22.7048	12.6959	8.4168	5.4156	3.6267
54	46.9668	24.7157	13.8198	9.1614	5.8942	3.9466
60	50.2742	26.4555	14.7920	9.8053	6.3078	4.2230
66	53.0304	27.9051	15.6018	10.3416	6.6521	4.4528
72	55.2053	29.0488	16.2404	10.7643	6.9233	4.6335
78	56.7751	29.8739	16.7009	11.0689	7.1184	4.7634
84	57.7227	30.3716	16.9783	11.2521	7.2355	4.8409
90	58.0378	30.5365	17.0696	11.3119	7.2731	4.8653
96	57.7170	30.3668	16.9738	11.2478	7.2311	4.8364
102	56.7640	29.8645	16.6922	11.0606	7.1100	4.7546
108	55.1892	29.0352	16.2279	10.7523	6.9111	4.6208
114	53.0100	27.8879	15.5860	10.3264	6.6367	4.4367
120	50.2503	26.4354	14.7735	9.7877	6.2898	4.2042
126	46.6937	24.6937	13.7996	9.1420	5.8743	3.9260
132	43.1169	22.6817	12.6747	8.3964	5.3948	3.6052
138	38.8213	20.4216	11.4114	7.5593	4.8567	3.2453
144	34.1009	17.9382	10.0233	6.6397	4.2657	2.8503
150	29.0073	15.2587	8.5259	5.6478	3.6284	2.4245
156	23.5963	12.4124	6.9355	4.5944	2.9518	1.9726
162	17.9272	9.4306	5.2699	3.4913	2.2434	1.4994
168	12.0624	6.3463	3.5473	2.3506	1.5106	1.0100
174	6.0675	3.1941	1.7867	1.1846	0.7618	0.5094
180	0.0	0.0	0.0	0.0	0.0	0.0

SOLID SPHERE SURFACE VORTICITY DISTRIBUTIONS FOR NRE = 1.0

POROSITY ANGLE	0.408	0.528	0.650	0.741	0.835	0.909
0	0.0	0.0	0.0	0.0	0.0	0.0
6	6.0996	3.2110	1.8111	1.2084	0.7860	0.5350
12	12.1243	6.3984	3.5947	2.3967	1.5578	1.0597
18	18.0163	9.5057	5.3384	3.5577	2.3110	1.5710
24	23.7088	12.5073	7.0223	4.6783	3.0371	2.0630
30	29.1382	15.3693	6.6270	5.7455	3.7276	2.5298
36	34.2447	18.0597	10.1343	6.7470	4.3747	2.9659
42	38.9717	20.5487	11.5273	7.6715	4.9707	3.3663
48	43.2673	22.8088	12.7907	8.5088	5.5090	3.7264
54	47.0844	24.8152	13.9105	9.2495	5.9837	4.0423
60	50.3814	26.5462	14.8747	9.8857	6.3896	4.3105
66	53.1225	27.9831	15.6729	10.4108	6.7227	4.5285
72	55.2783	29.1106	16.2969	10.8194	6.9796	4.6942
78	56.8258	29.9169	16.7403	11.1074	7.1581	4.8065
84	57.7489	30.3940	16.9989	11.2725	7.2568	4.8646
90	58.0384	30.5372	17.0706	11.3133	7.2754	4.8688
96	57.6920	30.3459	16.9552	11.2303	7.2142	4.8196

102	56.7145	29.8229	16.6549	11.0248	7.0747	4.7183
108	55.1174	28.9748	16.1734	10.7000	6.8590	4.5668
114	52.9191	27.8113	15.5168	10.2599	6.5702	4.3674
120	50.1443	26.3461	14.6927	9.7099	6.2120	4.1227
126	46.8240	24.5954	13.7107	9.0564	5.7885	3.8360
312	42.9950	22.5789	12.5817	8.3068	5.3049	3.5107
138	38.6994	20.3188	11.3183	7.4695	4.7665	3.1505
144	33.9842	17.8398	9.9343	6.5537	4.1793	2.7594
150	28.9010	15.1691	8.4447	5.5694	3.5497	2.3415
156	23.5051	12.3355	6.8659	4.5272	2.8842	1.9012
162	17.8551	9.3698	5.2147	3.4381	2.1898	1.4428
168	12.0125	6.3041	3.5091	2.3137	1.4736	0.9707
174	6.0419	3.1724	1.7671	1.1656	0.7426	0.4891
180	0.0	0.0	0.0	0.0	0.0	0.0

SOLID SPHERE SURFACE VORTICITY DISTRIBUTIONS FOR NRE = 10.0

POROSITY ANGLE	0.408	0.528	0.650	0.741	0.835	0.909
0	0.0	0.0	0.0	0.0	0.0	0.0
6	6.3650	3.4479	2.0234	1.4163	0.9985	0.7610
12	12.6415	6.8400	4.0074	2.8008	1.9710	1.4994
18	18.7638	10.1437	5.9343	4.1413	2.9081	2.2071
24	24.6544	13.3148	7.7763	5.4171	3.7940	2.8708
30	30.2413	16.3118	9.5073	6.6090	4.6139	3.4782
36	35.4577	19.0972	11.1040	7.6997	5.3549	4.0186
42	40.2427	21.6372	12.5458	8.6742	6.0059	4.4833
48	44.5419	23.9023	13.8154	9.5205	6.5583	4.8654
54	48.3083	25.8677	14.8992	10.2294	7.0060	5.1608
60	51.5028	27.5137	15.7869	10.7946	7.3456	5.3674
66	54.0942	28.8255	16.4720	11.2131	7.5763	5.4860
72	56.0598	29.7935	16.9514	11.4843	7.9696	5.5194
78	57.3851	30.4131	17.2255	11.6108	7.7195	5.4725
84	58.0640	30.6845	17.2976	11.5972	7.6420	5.3521
90	58.0978	30.6122	17.1738	11.4504	7.4745	5.1664
96	57.4955	30.2049	16.8628	11.1790	7.2258	4.9247
102	56.2731	29.4749	16.3750	10.7927	6.9054	4.6366
108	54.4527	28.4377	15.7224	10.3022	6.5234	4.3121
114	52.0624	27.1114	14.9183	9.7187	6.0896	3.9606
120	49.1350	25.5163	13.9764	9.0535	5.6138	3.5911
126	45.7081	23.6743	12.9110	8.3176	5.1049	3.2114
132	41.8229	21.6087	11.7365	7.5217	4.5710	2.8283
138	37.5237	19.3438	10.4670	6.6756	4.0191	2.4471
144	32.8575	16.9042	9.1161	5.7885	3.4551	2.0719
150	27.8735	14.3149	7.6971	4.8686	2.8837	1.7052
156	22.6225	11.6010	6.2225	3.9231	2.3083	1.3482
162	17.1565	8.7879	4.7045	2.9585	1.7314	1.0008
168	11.5290	5.9008	3.1547	1.9804	1.1543	0.6619
174	5.7938	2.9649	1.5844	0.9937	0.5776	0.3292
180	0.0	0.0	0.0	0.0	0.0	0.0

SOLID SPHERE SURFACE VORTICITY DISTRIBUTIONS FOR NRE = 100.0

POROSITY ANGLE	0.408	0.528	0.650	0.741	0.835	0.909
0	0.0	0.0	0.0	0.0	0.0	0.0

6	8.8984	5.6220	3.9771	2.9844	2.4776	2.0928
12	17.5894	11.0926	7.8345	5.8706	4.8676	4.1076
18	25.9342	16.3285	11.5157	8.6165	7.1331	6.0118
24	33.7630	21.2152	14.9366	11.1571	9.2179	7.7562
30	40.9247	25.6493	18.0204	13.4323	11.0703	9.2954
36	47.2884	29.5412	20.6996	15.3893	12.6446	10.5892
42	52.7461	32.8166	22.9184	16.9835	13.9027	11.6041
48	57.2160	35.4195	24.6339	18.1808	14.8153	12.3142
54	60.6448	37.3134	25.8184	18.9586	15.3639	12.7029
60	63.0095	38.4834	26.4600	19.3071	15.5411	12.7638
66	64.3174	38.9371	26.5646	19.2308	15.3523	12.5023
72	64.6059	38.7047	26.1559	18.7486	14.8165	11.9365
78	63.9396	37.8391	25.2759	17.8954	13.9668	11.0983
84	62.4076	36.4130	23.9848	16.7217	12.8509	10.0334
90	60.1172	34.5166	22.3584	15.2926	11.5298	8.8010
96	57.1887	32.2515	20.4851	13.6856	10.0760	7.4707
102	53.7474	29.7248	18.4602	11.9860	8.5681	6.1178
108	49.9173	27.0411	16.3784	10.2803	7.0853	4.8162
114	45.8139	24.2952	14.3258	8.6480	5.6988	3.6298
120	41.5395	21.5658	12.3718	7.1530	4.4644	2.6053
126	37.1796	18.9114	10.5636	5.8376	3.4171	1.7676
132	32.8015	16.3703	8.9247	4.7193	2.5687	1.1196
138	28.4541	13.9608	7.4569	3.7922	1.9105	0.6468
144	24.1696	11.6865	6.1452	3.0328	1.4180	0.3228
150	19.9645	9.5381	4.9641	2.4060	1.0576	0.1214
156	15.8454	7.5002	3.8832	1.8724	0.7910	0.0108
162	11.8030	5.5497	2.8711	1.3931	0.5803	-0.0350
168	7.8321	3.6669	1.9015	0.9349	0.3918	-0.0402
174	3.8978	1.8205	0.9498	0.4750	0.2026	-0.0242
180	0.0	0.0	0.0	0.0	0.0	0.0

SOLID SPHERE SURFACE VORTICITY DISTRIBUTIONS FOR NRE = 500.0

POROSITY ANGLE	0.408	0.528	0.650	0.741	0.835	0.909
0	0.0	0.0	0.0	0.0	0.0	0.0
6	17.7059	11.6115	8.4617	6.5242	5.8426	5.0092
12	34.8874	22.8535	16.6370	12.8164	11.4518	9.8134
18	51.1931	33.5171	24.3836	18.7698	16.7194	14.3183
24	66.1995	43.3224	31.4975	24.2267	21.4933	18.3944
30	79.5373	52.0208	37.7949	29.0453	25.6392	21.9178
36	90.8912	59.3992	43.1154	33.0957	29.0419	24.7932
42	100.0133	65.2824	47.3264	36.2754	31.6105	26.9331
48	106.7205	69.5429	50.3268	39.4964	33.2773	28.2753
54	110.9108	72.0965	52.0492	39.7039	34.0029	28.7771
60	112.5526	72.9146	52.4621	39.8628	33.7723	28.4195
66	111.7001	72.0146	51.5715	38.9721	32.5991	27.2060
72	108.4807	69.4737	49.4235	37.0577	30.5252	25.1700
78	103.1067	65.4198	46.1070	34.1849	27.6275	22.3809
84	95.6865	60.0448	47.7604	30.4613	24.0259	18.9601
90	87.1310	53.6014	36.5788	26.0532	19.8975	15.0974
96	77.3469	46.4125	30.8239	21.1966	15.4882	11.0668
102	67.0276	38.8659	24.8259	16.2051	11.1135	7.2156
108	56.7283	31.4000	18.9705	11.4493	7.1266	3.9092
114	46.9970	24.4628	13.6530	7.2997	3.8457	1.4229
120	38.3039	18.4475	9.2052	4.0298	1.4555	-0.1620
126	30.9595	13.6136	5.8134	1.7353	-0.0534	-0.9808

132	25.0623	10.0429	3.4818	0.3164	-0.8585	-1.2864
138	20.4922	7.6236	2.0675	-0.4387	-1.2027	-1.3189
144	16.9798	6.1239	1.3588	-0.7573	-1.2988	-1.1995
150	14.1673	5.2177	1.1282	-0.7989	-1.2969	-1.2031
156	11.7030	4.6139	1.1765	-0.6628	-1.2713	-1.5639
162	9.2237	3.9628	1.2799	-0.3857	-1.1932	-2.0517
168	6.4893	3.0505	1.2185	-0.1000	-0.9733	-2.1113
174	3.3387	1.6555	0.7893	0.0916	-0.5639	-1.4164
180	0.0	0.0	0.0	0.0	0.0	0.0

SOLID SPHERE SURFACE VORTICITY DISTRIBUTIONS FOR NRE = 1000.0

POROSITY ANGLE	0.408	0.528	0.650	0.741	0.835	0.909
0	0.0	0.0	0.0	0.0	0.0	0.0
6	23.9763	16.2670	12.2097	9.5109	9.3815	7.9567
12	47.2292	32.0123	24.0072	18.6650	18.3134	15.5363
18	69.2722	46.9360	35.1833	27.2924	26.5635	22.5331
24	89.5168	60.6408	45.4334	35.1441	33.8757	28.7906
30	107.4534	72.7660	54.5096	42.0267	39.9922	33.9638
36	122.6247	83.0156	62.1332	47.7109	44.7969	38.0786
42	134.7025	91.1201	68.1735	52.1022	48.1576	40.9169
48	143.3801	96.9036	72.3976	55.0247	50.0283	42.4633
54	148.5473	100.2268	74.7855	56.4586	50.4138	42.6771
60	150.0803	101.0356	75.1987	56.3235	49.3396	41.5825
66	148.0908	99.3424	73.7023	54.6510	46.8719	39.2053
72	142.6629	95.2193	70.2820	51.4572	43.1038	35.6168
78	134.1194	88.8405	65.0848	46.8391	38.1589	30.9224
84	122.7825	80.4219	58.2429	40.9214	32.2168	25.2968
90	109.1952	70.3309	50.0303	33.9352	25.5332	19.0451
96	93.9621	58.9928	40.8095	26.2340	18.5133	12.6392
102	77.8982	47.0557	31.1242	18.3690	11.7183	6.7769
108	61.9057	35.2457	21.6963	11.0783	5.8611	2.1899
114	47.0215	24.4799	13.3657	5.1561	1.5551	-0.6326
120	34.1481	15.5096	6.8397	1.1154	-0.9473	-1.8066
126	24.0137	8.8880	2.4606	-1.0691	-1.9641	-1.9810
132	16.7746	4.5629	-0.0412	-1.9477	-2.1293	-1.7778
138	12.2941	2.1702	-1.2035	-2.1343	-1.9591	-1.4043
144	9.9144	1.2822	-1.5618	-2.0565	-1.6724	-0.9305
150	8.8814	1.2112	-1.4534	-1.9657	-1.4788	-1.2599
156	8.4835	1.8490	-1.0515	-1.9845	-1.9590	-2.5700
162	7.8335	2.3719	-0.3354	-1.9984	-2.9993	-3.9262
168	6.4564	2.7221	0.3344	-1.7461	-3.4548	-4.1585
174	3.4017	1.7105	0.6190	-1.0308	-2.4444	-2.7871
180	0.0	0.0	0.0	0.0	0.0	0.0

GAS BUBBLE SURFACE VORTICITY DISTRIBUTIONS FOR NRE = 0.1

POROSITY ANGLE	0.408	0.528	0.650	0.741	0.835	0.909
0	0.0	0.0	0.0	0.0	0.0	0.0
6	0.6835	0.5029	0.3808	0.3129	0.2527	0.2070
12	1.3574	0.9982	0.7554	0.6204	0.5010	0.4103
18	2.0167	1.4826	1.1216	0.9209	0.7436	0.6088
24	2.6540	1.9508	1.4756	1.2114	0.9779	0.8006
30	3.2622	2.3978	1.8135	1.4886	1.2015	0.9835

36	3.8348	2.8185	2.1315	1.7495	1.4119	1.1555
42	4.3654	3.2084	2.4263	1.9912	1.6068	1.3149
48	4.8481	3.5631	2.6944	2.2112	1.7842	1.4597
54	5.2778	3.8788	2.9330	2.4069	1.9419	1.5886
60	5.6496	4.1520	3.1395	2.5763	2.0784	1.7000
66	5.9595	4.3797	3.3116	2.7174	2.1921	1.7928
72	6.2041	4.5594	3.4474	2.8287	2.2817	1.8659
78	6.3808	4.6891	3.5454	2.9090	2.3464	1.9185
84	6.4875	4.7675	3.6046	2.9575	2.3853	1.9502
90	6.5232	4.7937	3.6243	2.9736	2.3981	1.9604
96	6.4874	4.7673	3.6043	2.9571	2.3846	1.9492
102	6.3806	4.6887	3.5448	2.9082	2.3451	1.9167
108	6.2038	4.5588	3.4465	2.8275	2.2799	1.8632
114	5.9591	4.3789	3.3105	2.7158	2.1897	1.7894
120	5.6491	4.1511	3.1382	2.5744	2.0757	1.6961
126	5.2772	3.8778	2.9316	2.4049	1.9389	1.5843
132	4.8475	3.5621	2.6929	2.2091	1.7810	1.4552
138	4.3647	3.2074	2.4248	1.9891	1.6037	1.3103
144	3.8342	2.8175	2.1301	1.7474	1.4087	1.1511
150	3.2616	2.3969	1.8122	1.4867	1.1987	0.9794
156	2.6534	1.9500	1.4745	1.2097	0.9755	0.7971
162	2.0162	1.4819	1.1207	0.9196	0.7416	0.6061
168	1.3571	0.9977	0.7547	0.6194	0.4997	0.4084
174	0.6833	0.5026	0.3805	0.3124	0.2520	0.2060
180	0.0	0.0	0.0	0.0	0.0	0.0

GAS BUBBLE SURFACE VORTICITY DISTRIBUTIONS FOR NRE = 1.0

POROSITY ANGLE	0.408	0.528	0.650	0.741	0.835	0.909
0	0.0	0.0	0.0	0.0	0.0	0.0
6	0.6840	0.5037	0.3822	0.3147	0.2555	0.2111
12	1.3584	0.9997	0.7580	0.6240	0.5064	0.4182
18	2.0181	1.4848	1.1253	0.9261	0.7513	0.6202
24	2.6557	1.9536	1.4803	1.2180	0.9877	0.8150
30	3.2643	2.4010	1.8190	1.4963	1.2129	1.0003
36	3.8371	2.8221	2.1376	1.7580	1.4245	1.1741
42	4.3678	3.2121	2.4326	2.0001	1.6200	1.3344
48	4.8505	3.5668	2.7007	2.2201	1.7974	1.4794
54	5.2801	3.8824	2.9391	2.4155	1.9547	1.6076
60	5.6517	4.1552	3.1451	2.5841	2.0901	1.7175
66	5.9613	4.3825	3.3164	2.7242	2.2023	1.8081
72	6.2056	4.5616	3.4512	2.8342	2.2899	1.8784
78	6.3818	4.6907	3.5481	2.9130	2.3523	1.9277
84	6.4881	4.7684	3.6061	2.9597	2.3886	1.9555
90	6.5232	4.7937	3.6245	2.9739	2.3987	1.9619
96	6.4869	4.7666	3.6031	2.9556	2.3825	1.9467
102	6.3796	4.6873	3.5424	2.9049	2.3404	1.9103
108	6.2024	4.5566	3.4430	2.8226	2.2728	1.8533
114	5.9573	4.3762	3.3059	2.7095	2.1805	1.7764
120	5.6470	4.1469	3.1329	2.5670	2.0648	1.6806
126	5.2749	3.8743	2.9257	2.3967	1.9268	1.5670
132	4.8451	3.5584	2.6867	2.2004	1.7683	1.4369
138	4.3623	3.2036	2.4185	1.9804	1.5909	1.2918
144	3.8319	2.8139	2.1241	1.7391	1.3965	1.1333
150	3.2596	2.3936	1.8067	1.4791	1.1874	0.9631
156	2.6516	1.9472	1.4698	1.2032	0.9658	0.7830

162	2.0148	1.4797	1.1170	0.9144	0.7339	0.5949
168	1.3561	0.9961	0.7522	0.6758	0.4943	0.4006
174	0.6828	0.5019	0.3792	0.3105	0.2493	0.2020
180	0.0	0.0	0.0	0.0	0.0	0.0

GAS BUBBLE SURFACE VORTICITY DISTRIBUTIONS FOR NRE = 10.0

POROSITY ANGLE	0.408	0.528	0.650	0.741	0.835	0.909
0	0.0	0.0	0.0	0.0	0.0	0.0
6	0.6889	0.5113	0.3949	0.3322	0.2804	0.2458
12	1.3680	1.0146	0.7829	0.6581	0.5552	0.4862
18	2.0321	1.5063	1.1615	0.9757	0.8224	0.7196
24	2.6735	1.9811	1.5264	1.2813	1.0789	0.9429
30	3.2852	2.4333	1.8734	1.5713	1.3213	1.1531
36	3.8602	2.8580	2.1892	1.8420	1.5467	1.3474
42	4.3922	3.2502	2.4973	2.0903	1.7521	1.5232
48	4.8753	3.6057	2.7671	2.3133	1.9351	1.6781
54	5.3042	3.9204	3.0047	2.5083	2.0934	1.8103
60	5.6741	4.1910	3.2074	2.6732	2.2252	1.9180
66	5.9812	4.4145	3.3730	2.8064	2.3292	2.0001
72	6.2220	4.5886	3.5000	2.9064	2.4043	2.0558
78	6.3942	4.7116	3.5872	2.9725	2.4506	2.0850
84	6.4958	4.7822	3.6339	3.0044	2.4665	2.0878
90	6.5261	4.8001	3.6400	3.0022	2.4540	2.0649
96	6.4848	4.7652	3.6059	2.9664	2.4134	2.0177
102	6.3726	4.6782	3.5323	2.8981	2.3462	1.9477
108	6.1908	4.5403	3.4206	2.7987	2.2539	1.8569
114	5.9417	4.3534	3.2725	2.6699	2.1385	1.7478
120	5.6281	4.1197	3.0901	2.5138	2.0023	1.6228
126	5.2536	3.8421	2.8756	2.3327	1.8477	1.4846
132	4.8224	3.5236	2.6319	2.1291	1.6771	1.3358
138	4.3392	3.1681	2.3618	1.9056	1.4929	1.1790
144	3.8095	2.7793	2.0683	1.6647	1.2977	1.0164
150	3.2390	2.3616	1.7548	1.4093	1.0935	0.8499
156	2.6338	1.9194	1.4244	1.1419	0.8825	0.6812
162	2.0006	1.4575	1.0808	0.8650	0.6663	0.5114
168	1.3462	0.9806	0.7267	0.5811	0.4465	0.3412
174	0.6777	0.4938	0.3659	0.2924	0.2243	0.1708
180	0.0	0.0	0.0	0.0	0.0	0.0

GAS BUBBLE SURFACE VORTICITY DISTRIBUTIONS FOR NRE = 100.0

POROSITY ANGLE	0.408	0.528	0.650	0.741	0.835	0.909
0	0.0	0.0	0.0	0.0	0.0	0.0
6	0.7037	0.5422	0.4445	0.3764	0.3379	0.3073
12	1.3969	1.0755	0.8812	0.7458	0.6692	0.6085
18	2.0741	1.5963	1.3072	1.1060	0.9920	0.9018
24	2.7247	2.0983	1.7177	1.4527	1.3025	1.1836
30	3.3491	2.5757	2.1077	1.7819	1.5969	1.4506
36	3.9320	3.0226	2.4724	2.0893	1.8715	1.6993
42	4.4691	3.4338	2.8075	2.3713	2.1228	1.9265
48	4.9543	3.8044	3.1088	2.6243	2.3477	2.1293
54	5.3819	4.1298	3.3725	2.8449	2.5431	2.3050
60	5.7469	4.4062	3.5953	3.0304	2.7064	2.4509

66	6.0451	4.6300	3.7744	3.1783	2.8352	2.5649
72	6.2731	4.7987	3.9074	3.2863	2.9276	2.6451
78	6.4284	4.9102	3.9925	3.3529	2.9819	2.6901
84	6.5093	4.9621	4.0285	3.3770	2.9972	2.6985
90	6.5153	4.9569	4.0149	3.3579	2.9726	2.6698
96	6.4468	4.8920	3.9519	3.2958	2.9083	2.6039
102	6.3052	4.7698	3.8406	3.1914	2.8049	2.5013
108	6.0933	4.5925	3.6831	3.0466	2.6640	2.3636
114	5.8144	4.3636	3.4824	2.8642	2.4885	2.1938
120	5.4733	4.0874	3.2430	2.6485	2.2827	1.9961
126	5.0754	3.7695	2.9703	2.4050	2.0525	1.7767
132	4.6269	3.4158	2.6709	2.1407	1.8053	1.5436
138	4.1344	3.0330	2.3516	1.8632	1.5498	1.3058
144	3.6048	2.6277	2.0196	1.5803	1.2945	1.0726
150	3.0449	2.2060	1.6809	1.2988	1.0470	0.8518
156	2.4614	1.7733	1.3406	1.0236	0.8124	0.6487
162	1.8603	1.3340	1.0017	0.7570	0.5925	0.4649
168	1.2471	0.8912	0.6656	0.4989	0.3863	0.2984
174	0.6260	0.4464	0.3322	0.2475	0.1900	0.1450
180	0.0	0.0	0.0	0.0	0.0	0.0

GAS BUBBLE SURFACE VORTICITY DISTRIBUTIONS FOR NRE = 500.0

POROSITY ANGLE	0.408	0.528	0.650	0.741	0.835	0.909
0	0.0	0.0	0.0	0.0	0.0	0.0
6	0.7323	0.5684	0.4690	0.4000	0.3632	0.3319
12	1.4539	1.1277	0.9300	0.7928	0.7197	0.6575
18	2.1592	1.6741	1.3802	1.1762	1.0674	0.9751
24	2.8400	2.2015	1.8146	1.5460	1.4026	1.2809
30	3.4884	2.7037	2.2281	1.8980	1.7212	1.5717
36	4.0971	3.1750	2.6160	2.2279	2.0197	1.8439
42	4.6590	3.6098	2.9738	2.5321	2.2945	2.0943
48	5.1677	4.0031	3.2971	2.8068	2.5422	2.3199
54	5.6171	4.3502	3.5822	3.0488	2.7606	2.5181
60	6.0023	4.6471	3.8257	3.2551	2.9450	2.6862
66	6.3184	4.8902	4.0246	3.4232	3.0950	2.8222
72	6.5620	5.0766	4.1763	3.5508	3.2080	2.9241
78	6.7298	5.2038	4.2790	3.6363	3.2823	2.9905
84	6.8199	5.2702	4.3309	3.6782	3.3168	3.0202
90	6.8309	5.2745	4.3313	3.6757	3.3104	3.0123
96	6.7625	5.2164	4.2795	3.6281	3.2628	2.9662
102	6.6151	5.0961	4.1756	3.5354	3.1737	2.8817
108	6.3903	4.9145	4.0202	3.3978	3.0434	2.7589
114	6.0907	4.6735	3.8145	3.2161	2.8726	2.5983
120	5.7203	4.3757	3.5604	2.9919	2.6625	2.4012
126	5.2847	4.0253	3.2611	2.7276	2.4157	2.1699
132	4.7916	3.6285	2.9218	2.4279	2.1366	1.9089
138	4.2509	3.1443	2.5506	2.1002	1.8329	1.6259
144	3.6749	2.7349	2.1593	1.7562	1.5162	1.3328
150	3.0757	2.2640	1.7632	1.4116	1.2023	1.0452
156	2.4648	1.7943	1.3767	1.0822	0.9074	0.7789
162	1.8495	1.3338	1.0095	0.7793	0.6427	0.5444
168	1.2339	0.8840	0.6622	0.5034	0.4090	0.3421
174	0.6178	0.4414	0.3287	0.2473	0.1985	0.1643
180	0.0	0.0	0.0	0.0	0.0	0.0

GAS BUBBLE SURFACE VORTICITY DISTRIBUTIONS FOR NRE = 1000.0

POROSITY / ANGLE	0.408	0.528	0.650	0.741	0.835	0.909
0	0.0	0.0	0.0	0.0	0.0	0.0
6	0.7375	0.5810	0.4860	0.4066	0.3720	0.3412
12	1.4643	1.1528	0.9638	0.8060	0.7373	0.6760
18	2.1748	1.7117	1.4306	1.1960	1.0936	1.0026
24	2.8609	2.2514	1.8813	1.5720	1.4371	1.3173
30	3.5149	2.7656	2.3107	1.9306	1.7640	1.6167
36	4.1292	3.2486	2.7139	2.2668	2.0705	1.8972
42	4.6969	3.6948	3.0862	2.5772	2.3529	2.1557
48	5.2115	4.0991	3.4235	2.8579	2.6081	2.3891
54	5.6672	4.4568	3.7217	3.1059	2.8329	2.5946
60	6.0586	4.7638	3.9774	3.3180	3.0246	2.7697
66	6.3813	5.0164	4.1875	3.4919	3.1811	2.9124
72	6.6315	5.2117	4.3495	3.6253	3.3001	3.0208
78	6.8061	5.3472	4.4614	3.7165	3.3804	3.0934
84	6.9031	5.4213	4.5215	3.7641	3.4205	3.1291
90	6.9208	5.4326	4.5290	3.7674	3.4198	3.1272
96	6.8590	5.3807	4.4833	3.7258	3.3778	3.0872
102	6.7177	5.2658	4.3844	3.6394	3.2946	3.0091
108	6.4984	5.0886	4.2328	3.5082	3.1702	2.8929
114	6.2029	4.8505	4.0295	3.3331	3.0056	2.7393
120	5.8344	4.5536	3.7761	3.1151	2.8014	2.5489
126	5.3969	4.2008	3.4747	2.8558	2.5594	2.3232
132	4.8966	3.7966	3.1287	2.5577	2.2820	2.0647
138	4.3419	3.3474	2.7435	2.2257	1.9743	1.7784
144	3.7456	2.8641	2.3284	1.8683	1.6447	1.4729
150	3.1232	2.3626	1.8991	1.5007	1.3082	1.1629
156	2.4915	1.8614	1.4752	1.1424	0.9839	0.8670
162	1.8615	1.3745	1.0736	0.8131	0.6906	0.6030
168	1.2382	0.9065	0.6995	0.5189	0.4347	0.3762
174	0.6190	0.4515	0.3462	0.2533	0.2098	0.1802
180	0.0	0.0	0.0	0.0	0.0	0.0

CIRCULAR CYLINDER SURFACE VORTICITY DISTRIBUTIONS FOR NRE = 1.0

POROSITY / ANGLE	0.4	0.5	0.6	0.7	0.8	0.9
0	0.0	0.0	0.0	0.0	0.0	0.0
6	5.7338	3.0799	1.9635	1.1940	0.7443	0.4303
12	11.4019	6.1236	3.9035	2.3731	1.4788	0.8543
18	16.9394	9.0957	5.7966	3.5226	2.1936	1.2658
24	22.2831	11.9613	7.6202	4.6282	2.8796	1.6587
30	27.3724	14.6873	9.3530	5.6765	3.5279	2.0277
36	32.1496	17.2425	10.9745	6.6548	4.1303	2.3675
42	36.5614	19.5979	12.4662	7.5516	4.6795	2.6738
48	40.5587	21.7271	13.8112	8.3567	5.1691	2.9429
54	44.0976	23.6067	14.9948	9.0612	5.5937	3.1718
60	47.1400	25.2167	16.0044	9.6577	5.9489	3.3581
66	49.6538	26.5403	16.8297	10.1405	6.2315	3.5005
72	51.6130	27.5645	17.4629	10.5052	6.4393	3.5984
78	52.9983	28.2797	17.8987	10.7494	6.5714	3.6518
84	53.7971	28.6802	18.1340	10.8718	6.6278	3.6616
90	54.0034	28.7639	18.1684	10.8730	6.6095	3.6293

96	53.6179	28.5323	18.0034	10.7548	6.5186	3.5569
102	52.6478	27.9903	17.6432	10.5205	6.3578	3.4469
108	51.1064	27.1463	17.0937	10.1745	6.1305	3.3021
114	49.0133	26.0116	16.3629	9.7223	5.8410	3.1258
120	46.3936	24.6005	15.4603	9.1703	5.4937	2.9212
126	43.2779	22.9300	14.3973	8.5258	5.0937	2.6918
132	39.7014	21.0194	13.1863	7.7968	4.6461	2.4407
138	35.7041	18.8902	11.8413	6.9916	4.1564	2.1714
144	31.3298	16.5656	10.3769	6.1161	3.6299	1.8868
150	26.6257	14.0708	8.8088	5.1885	3.0721	1.5897
156	21.6423	11.4321	7.1532	4.2094	2.4884	1.2828
162	16.4325	8.6770	5.4271	3.1912	1.8841	0.9683
168	11.0510	5.8340	3.6477	2.1438	1.2646	0.6484
174	5.5544	2.9319	1.8327	1.0769	0.6348	0.3251
180	0.0	0.0	0.0	0.0	0.0	0.0

CIRCULAR CYLINDER SURFACE VORTICITY DISTRIBUTIONS FOR NRE = 10.0

POROSITY ANGLE	0.4	0.5	0.6	0.7	0.8	0.9
0	0.0	0.0	0.0	0.0	0.0	0.0
6	6.5302	3.7269	2.5296	1.6960	1.2049	0.8573
12	12.9620	7.3923	5.0140	3.3585	2.3833	1.6934
18	19.1995	10.9362	7.4091	4.9549	3.5097	2.4875
24	25.1507	14.3014	9.6731	6.4543	4.5598	3.2204
30	30.7299	17.4351	11.7675	7.8286	5.5119	3.8749
36	35.8593	20.2899	13.6584	9.0532	6.3470	4.4362
42	40.4707	22.8249	15.3165	10.1076	7.0496	4.8925
48	44.5065	25.0066	16.7189	10.9757	7.6082	5.2358
54	47.9208	26.8093	17.8484	11.6466	8.0155	5.4615
60	50.6801	28.2159	18.6947	12.1147	8.2687	5.5689
66	52.7634	29.2175	19.2539	12.3795	8.3692	5.5614
72	54.1620	29.8139	19.5288	12.4456	8.3230	5.4459
78	54.8795	30.0126	19.5280	12.3224	8.1399	5.2327
84	54.9307	29.8288	19.2662	12.0237	7.8332	4.9350
90	54.3408	29.2840	18.7627	11.5670	7.4190	4.5681
96	53.1440	28.4059	18.0411	10.9725	6.9157	4.1486
102	51.3823	27.2263	17.1283	10.2629	6.3429	3.6939
108	49.1035	25.7808	16.0533	9.4619	5.7207	3.2209
114	46.3598	24.1071	14.8465	8.5938	5.0689	2.7455
120	43.2062	22.2439	13.5387	7.6824	4.4063	2.2821
126	39.6984	20.2296	12.1600	6.7509	3.7506	1.8429
132	35.8913	18.1009	10.7387	5.8206	3.1173	1.4380
138	31.8377	15.8918	9.3009	4.9108	2.5206	1.0760
144	27.5864	13.6326	7.8691	4.0388	1.9727	0.7635
150	23.1815	11.3483	6.4616	3.2183	1.4843	0.5059
156	18.6616	9.0584	5.0913	2.4594	1.0633	0.3064
162	14.0590	6.7754	3.7647	1.7664	0.7132	0.1648
168	9.4007	4.5056	2.4808	1.1356	0.4300	0.0756
174	4.7082	2.2488	1.2310	0.5541	0.2001	0.0267
180	0.0	0.0	0.0	0.0	0.0	0.0

CIRCULAR CYLINDER SURFACE VORTICITY DISTRIBUTIONS FOR NRE = 50.0

POROSITY ANGLE	0.4	0.5	0.6	0.7	0.8	0.9

0	0.0	0.0	0.0	0.0	0.0	0.0
6	9.5886	6.0467	4.4398	3.3152	2.5489	1.9697
12	18.9773	11.9586	8.7759	6.5458	5.0291	3.8816
18	27.9716	17.6046	12.9074	9.6096	7.3738	5.6798
24	36.3877	22.8610	16.7388	12.4292	9.5204	7.3114
30	44.0578	27.6144	20.1830	14.9347	11.4116	8.7296
36	50.8342	31.7655	23.1634	17.0654	12.9981	9.8902
42	56.5936	35.2314	25.6161	18.7718	14.2395	10.7629
48	61.2406	37.9485	27.4920	20.0173	15.1061	11.3232
54	64.7100	39.8741	28.7589	20.7798	15.5802	11.5583
60	66.9685	40.9884	29.4020	21.0524	15.6575	11.4682
66	68.0158	41.2946	29.4257	20.8442	15.3477	11.0659
72	67.8838	40.8201	28.8537	20.1811	14.6754	10.3791
78	66.6354	39.6153	27.7294	19.1055	13.6804	9.4493
84	64.3620	37.7523	26.1145	17.6750	12.4166	8.3315
90	61.1769	35.3227	24.0880	15.9614	10.9508	7.0907
96	57.2245	32.4334	21.7424	14.0471	9.3591	5.7984
102	52.6472	29.2024	19.1801	12.0213	7.7222	4.5259
108	47.6065	25.7525	16.5072	9.9740	6.1191	3.3376
114	42.2630	22.2052	13.8272	7.9896	4.6205	2.2844
120	36.7725	18.6742	11.2339	6.1407	3.2821	1.3989
126	31.2817	15.2600	8.8054	4.4827	2.1399	0.6936
132	25.9234	12.0459	6.6005	3.0504	1.2093	0.1624
138	20.8151	9.0965	4.6568	1.8581	0.4857	-0.2163
144	16.0586	6.4588	2.9932	0.9020	-0.0516	-0.4726
150	11.7435	4.1660	1.6130	0.1636	-0.4328	-0.6339
156	7.9513	2.2430	0.5091	-0.3822	-0.6826	-0.7115
162	4.7687	0.7211	-0.3190	-0.7400	-0.7957	-0.6949
168	2.3013	-0.3141	-0.7980	-0.8462	-0.7289	-0.5646
174	0.7298	-0.5879	-0.7064	-0.5877	-0.4457	-0.3196
180	0.0	0.0	0.0	0.0	0.0	0.0

CIRCULAR CYLINDER SURFACE VORTICITY DISTRIBUTIONS FOR NRE = 100.0

POROSITY ANGLE	0.4	0.5	0.6	0.7	0.8	0.9
0	0.0	0.0	0.0	0.0	0.0	0.0
6	12.1072	8.2052	5.8198	4.5450	3.5624	2.8987
12	23.9412	16.2174	11.4970	8.9728	7.0286	5.7077
18	35.2357	23.8485	16.8928	13.1690	10.3047	8.3403
24	45.7392	30.9205	21.8753	17.0255	13.3014	10.7143
30	55.2203	37.2697	26.3234	20.4429	15.9365	12.7556
36	63.4764	42.7520	30.1296	23.3333	18.1368	14.3995
42	70.3354	47.2454	33.2034	25.6226	19.8403	15.5939
48	75.6660	50.6556	35.4732	27.2531	20.9979	16.3006
54	79.3751	52.9166	36.8894	28.1852	21.5763	16.4986
60	81.4193	53.9959	37.4264	28.3998	21.5595	16.1861
66	81.7976	53.8942	37.0848	27.9002	20.9524	15.3836
72	80.5636	52.6496	35.8931	26.7147	19.7853	14.1366
78	77.8142	50.3363	33.9105	24.8992	18.1077	12.5174
84	73.7007	47.0680	31.2283	22.5392	16.0108	10.6285
90	68.4120	42.9939	27.9706	19.7508	13.6086	8.5846
96	62.1847	38.2996	24.2938	16.6793	11.0436	6.5313
102	55.2762	33.1965	20.3805	13.4927	8.4756	4.6021
108	47.9731	27.9163	16.4295	10.3686	6.0634	2.9131
114	40.5497	22.6893	12.6381	7.4749	3.9428	1.5414
120	33.2809	17.7314	9.1806	4.9478	2.2045	0.5154

126	26.3838	13.2155	6.1862	2.8726	0.8826	-0.1836
132	20.0564	9.2656	3.7250	1.2746	-0.0436	-0.6072
138	14.3976	5.9370	1.8049	0.1249	-0.6335	-0.8248
144	9.5136	3.2402	0.3841	-0.6425	-0.9670	-0.9150
150	5.3753	1.1292	-0.6101	-1.1130	-1.1369	-0.9513
156	2.0702	-0.4368	-1.2629	-1.3876	-1.2341	-0.9680
162	-0.5457	-1.5499	-1.6806	-1.5578	-1.2825	-0.9345
168	-2.2204	-2.2518	-1.9028	-1.5670	-1.1742	-0.7784
174	-3.1641	-2.3408	-1.5443	-1.1011	-0.7425	-0.4527
180	0.0	0.0	0.0	0.0	0.0	0.0

CIRCULAR CYLINDER SURFACE VORTICITY DISTRIBUTIONS FOR NRE = 500.0

POROSITY ANGLE	0.4	0.5	0.6	0.7	0.8	0.9
0	0.0	0.0	0.0	0.0	0.0	0.0
6	25.5268	17.7098	12.8513	10.6577	8.4779	8.3165
12	50.4049	34.9616	25.3661	21.0107	16.6976	16.2365
18	73.8839	51.2584	37.1860	30.7240	24.4282	23.4411
24	95.5587	66.2513	48.0380	39.5619	31.4202	29.6144
30		79.4493	57.5875	47.2296	37.4711	34.5287
36		90.6083	65.6158	53.5287	42.3950	38.0440
42		96.3615	71.8813	58.2710	46.0309	40.0821
48			76.2293	61.3223	48.2552	40.6089
54			78.5226	62.5883	48.9702	39.6499
60			78.9601	62.0199	48.1162	37.2671
66			76.6976	59.6107	45.6722	33.5824
72			72.5696	55.4070	41.6674	28.7698
78		94.8768	66.3869	49.5143	36.2154	23.0995
84		84.9200	58.3148	42.1381	29.5493	16.9538
90		72.9324	48.6430	33.6201	22.1014	10.8724
96	93.5753	59.4231	37.8551	24.5163	14.5323	5.5123
102	74.5751	45.1264	26.6995	15.6100	7.7104	1.5018
108	55.3888	31.0230	16.1948	7.8505	2.4579	-0.9737
114	37.3725	18.2988	7.4530	2.0553	-0.7880	-2.0889
120	21.6972	8.0632	1.2763	-1.4371	-2.2388	-2.2711
126	9.4513	0.9546	-2.2378	-2.9639	-2.5467	-2.0238
132	0.9850	-3.1344	-3.6997	-3.2630	-2.3282	-1.6623
138	-4.2124	-4.9958	-3.9617	-2.9916	-1.9669	-1.1135
144	-6.5311	-5.4186	-3.6698	-2.5604	-1.4209	-0.6038
150	-7.9997	-5.3405	-3.2193	-1.9450	-1.2508	-0.7035
156	-7.1381	-4.6755	-2.5853	-1.3721	-1.0942	-1.4271
162	-8.2873	-4.3911	-2.2326	-0.9735	-0.9517	-2.5737
168	-4.8561	-3.6151	-1.5268	-0.9185	-0.8407	-3.3477
174	-1.3030	-2.3219	-1.0497	-0.5105	-0.6115	-2.5545
180	0.0	0.0	0.0	0.0	0.0	0.0

SOLID SPHERE SURFACE PRESSURE DISTRIBUTIONS FOR NRE = 0.1

POROSITY ANGLE	0.408	0.528	0.650	0.741	0.835	0.909
0	396.2581	293.2597	224.3258	185.9051	151.9724	126.0425
6	328.5600	268.7231	214.6075	180.8496	149.4330	124.6457
12	125.8718	195.2381	185.5230	165.7285	141.8486	120.4778
18	-209.9044	73.5557	137.3338	140.6908	129.3026	113.5909
24	-675.0363	-95.3277	70.5454	105.9917	111.9244	104.0593

30	-1264.3635	-309.2054	-14.1054	62.0089	89.9016	91.9873
36	-1971.3769	-565.8135	-115.6754	9.2309	63.4777	77.5091
42	-2788.2834	-862.3120	-233.0338	-51.7527	32.9484	60.7871
48	-3076.0880	-1195.4259	-364.8770	-210.2616	-1.3436	42.0101
54	-4714.6935	-1561.4801	-509.7437	-195.5326	-39.0138	21.3900
60	-5803.0095	-1956.4400	-666.0309	-276.7295	-79.6407	-0.8407
66	-6959.0757	-2375.9569	-832.0119	-362.9517	-122.7710	-24.4320
72	-8170.1943	-2815.4157	-1005.8559	-453.2452	-167.9247	-49.1195
78	-9423.0692	-3269.9859	-1185.6478	-546.6128	-214.6011	-74.6279
84	-10703.952	-3734.6747	-1369.4097	-642.0255	-262.2840	-100.6738
90	-11998.799	-4204.3831	-1555.1228	-738.4338	-310.4477	-126.9690
96	-13293.416	-4673.9610	-1740.7500	-834.7795	-358.5628	-153.2241
102	-14573.620	-5138.2640	-1924.2575	-930.0070	-406.1021	-179.1512
108	-15825.394	-5592.2103	-2103.6377	-1023.0751	-452.5461	-204.4674
114	-17035.039	-6030.8350	-2276.9307	-1112.9677	-497.3890	-228.8977
120	-18189.323	-6449.3442	-2442.2454	-1198.7056	-540.1434	-252.1777
126	-19275.624	-6843.1671	-2597.7799	-1279.3557	-580.3457	-274.0566
132	-20282.071	-7208.0053	-2741.8402	-1345.0417	-617.5612	-294.2997
138	-21197.667	-7539.8791	-2872.8573	-1421.9529	-651.3881	-312.6908
144	-22-12.410	-7835.1685	-2989.4044	-1482.3526	-681.4622	-329.0348
150	-22717.400	-8090.6521	-3090.2138	-1534.5864	-707.4607	-343.1592
156	-23304.932	-8303.5402	-3174.1920	-1578.0888	-729.1065	-354.9172
162	-23678.596	-8471.5006	-3240.4302	-1612.3914	-746.1722	-364.1882
168	-24103.212	-8592.6855	-3288.2163	-1637.1326	-758.4841	-370.8794
174	-24305.184	-8665.7872	-3317.0564	-1652.0682	-765.9230	-374.9255
180	-24372.634	-8690.1902	-3326.6928	-1657.0617	-768.4128	-376.2807

SOLID SPHERE SURFACE PRESSURE DISTRIBUTIONS FOR NRE = 1.0

POROSITY ANGLE	0.408	0.528	0.650	0.741	0.835	0.909
0	40.4712	30.1647	23.2733	19.4261	16.0294	13.4391
6	33.5976	27.6505	22.2625	18.8912	15.7531	13.2810
12	13.0227	20.1236	19.2394	17.2933	14.9288	12.8101
18	-21.0498	7.6562	14.2354	14.6509	13.5683	12.0343
24	-68.2253	-9.6067	7.3090	10.9958	11.6889	10.9649
30	-127.9588	-31.4608	-1.4552	6.3738	9.3156	9.6174
36	-199.5642	-57.6481	-11.9500	0.8434	6.4802	8.0112
42	-282.2229	-87.8616	-24.0474	-5.5253	2.2208	6.1696
48	-374.9930	-121.7493	-37.6014	-12.6525	-0.4195	4.1188
54	-476.8215	-158.9184	-52.4495	-20.4498	-4.3930	1.8875
60	-586.5573	-198.9410	-68.4158	-28.8218	-8.6486	-0.4938
66	-702.9648	-241.3593	-85.3130	-37.6675	-13.1326	-2.9932
72	-824.7395	-285.6914	-102.9449	-46.8819	-17.7898	-5.5784
78	-950.5229	-331.4377	-121.1095	-56.3573	-22.5639	-8.2168
84	-1078.9189	-378.0865	-139.6010	-65.9849	-27.3989	-10.8765
90	-1208.5095	-425.1201	-158.2127	-75.6561	-32.2395	-13.5265
96	-1337.8713	-472.0209	-176.7393	-85.2641	-37.0320	-16.1372
102	-1465.5905	-518.2773	-194.9793	-94.7046	-41.7246	-18.6806
108	-159.2787	-563.38888	-212.7369	-103.8772	-46.2683	-21.1309
114	-1710.5877	-606.8715	-229.8242	-112.6864	-50.6171	-23.4643
120	-1825.2231	-648.2629	-246.0628	-121.0424	-54.7284	-25.6593
126	-1932.9575	-687.1261	-261.2854	-128.8613	-58.5631	-27.6967
132	-2032.6432	-723.0540	-275.3373	-136.0664	-62.0859	-29.5599
138	-2123.2224	-755.6730	-288.0770	-142.5882	-65.2654	-31.2343
144	-2203.7378	-784.9460	-299.3777	-148.3649	-68.0741	-32.7075
150	-2273.3413	-809.6752	-309.1281	153.3423	-70.4884	-33.9694

156	-2331.3015	-830.5043	-317.2334	-157.4748	-72.4886	-35.0119
162	-2377.0094	-846.9202	-323.6153	-160.7251	-74.0593	-35.8286
168	-2409.9839	-858.7548	-328.2132	-163.0649	-75.1888	-36.4151
174	-2429.8779	-865.8891	-330.9862	-164.4752	-75.8696	-36.7684
180	-2436.5201	-868.2698	-331.9108	-164.9463	-76.0971	-36.8865

SOLID SPHERE SURFACE PRESSURE DISTRIBUTIONS FOR NRE = 10.0

POROSITY ANGLE	0.408	0.528	0.650	0.741	0.835	0.909
0	4.8934	3.8572	3.1717	2.7856	2.4520	2.2144
6	4.0975	3.5414	3.0276	2.6991	2.3984	2.1765
12	1.7200	2.5991	2.5985	2.4422	2.2394	2.0647
18	-2.2041	1.0464	1.8938	2.0216	1.9801	1.8831
24	-7.6131	-1.0892	0.9284	1.4473	1.6280	1.6375
30	-14.4220	-3.7691	-0.2772	0.7335	1.1927	1.3358
36	-22.5253	-6.9475	-1.6975	-0.1030	0.6864	0.9873
42	-31.7998	-10.5639	-3.3034	-1.0425	0.1226	0.6028
48	-42.1074	-14.5627	-5.0628	-2.0640	-0.4840	0.1934
54	-53.2983	-18.8764	-6.9422	-3.1452	-1.1183	-0.2294
60	-65.2139	-23.4369	-8.9073	-4.2642	-1.7654	-0.6543
66	-77.6906	-28.1750	-10.9342	-5.3993	-2.4113	-1.0709
72	-90.5632	-33.0220	-12.9601	-6.5303	-3.0429	-1.4699
78	-103.6670	-37.9115	-14.9846	-7.6387	-3.6489	-1.8436
84	-116.8419	-42.7805	-16.9686	-8.7085	-4.2197	-2.1856
90	-129.9336	-47.5699	-18.8911	-9.7259	-4.7481	-2.4917
96	-142.7964	-55.2266	-20.7274	-10.6801	-5.2287	-2.7592
102	-155.2948	-58.7029	-22.4615	-11.5630	-5.6583	-2.9872
108	-167.3042	-60.9571	-24.0795	-12.3691	-6.0358	-3.1764
114	-178.7119	-64.9539	-25.5715	-13.0954	-6.3615	-3.3287
120	-189.4177	-68.6641	-26.9306	-13.7411	-6.6377	-3.4470
126	-199.3334	-72.0638	-28.1528	-14.3075	-6.8673	-3.5353
132	-208.3829	-75.1347	-29.2367	-14.7970	-7.0546	-3.5976
138	-216.5013	-77.8629	-30.1827	-15.2134	-.2041	-3.6386
144	-223.6344	-80.2384	-30.9928	-15.5610	-7.3207	-3.6628
150	-229.7377	-82.2544	-31.6698	-15.8446	-7.4093	-3.6746
156	-234.7755	-83.9065	-32.2171	-16.0688	-7.4745	-3.6779
162	-238.7198	-85.1920	-32.6379	-16.2380	-7.5204	-3.6764
168	-241.5498	-86.1097	-32.9353	-16.3556	-7.5503	-3.6730
174	-243.2503	-86.6586	-33.1119	-16.4246	-7.5670	-3.6698
180	-243.8166	-86.8409	-33.1703	-16.4473	-7.5723	-3.6686

SOLID SPHERE SURFACE PRESSURE DISTRIBUTIONS FOR NRE = 100.0

POROSITY ANGLE	0.408	0.528	0.650	0.741	0.835	0.909
0	1.3395	1.2497	1.1975	1.1625	1.1428	1.1273
6	1.1324	1.1380	1.1273	1.1146	1.11052	1.0973
12	0.5188	0.8079	0.9200	0.9737	0.9946	1.0091
18	-0.4799	0.2718	0.5843	0.7459	0.8162	0.8673
24	-1.8302	-0.4508	0.1329	0.4404	0.5779	0.6782
30	-3.4865	-1.3336	-0.4167	0.0696	0.2900	0.4505
36	-5.3943	-2.3448	-1.0437	-0.3515	-0.0360	0.1946
42	-7.4920	-3.4490	-1.7244	-0.8062	-0.3833	-0.0782
48	-9.7147	-4.6083	-2.4338	-1.2768	-0.7403	-0.3556
54	-11.9965	-5.7848	-3.1469	-1.7453	-1.0914	-0.6258

60	-14.2739	-6.9418	-3.8396	-2.1947	-1.4230	-0.8775
66	-16.4884	-8.0461	-4.4898	-2.6094	-1.7227	-1.1007
72	-18.5888	-9.0692	-5.0793	-2.9767	-1.9809	-1.2867
78	-20.5336	-9.9886	-5.5938	-3.2869	-2.1904	-1.4330
84	-22.2917	-10.7891	-6.0234	-3.5342	-2.3478	-1.5345
90	-23.8433	-11.4625	-6.3670	-3.7170	-2.4530	-1.5932
96	-25.1794	-12.0082	-6.6236	-3.8378	-2.5094	-1.6129
102	-26.3011	-12.4320	-6.8006	-3.9029	-2.5236	-1.6000
108	-27.2178	-12.7448	-6.9082	-3.9215	-2.5042	-1.5626
114	-27.9456	-12.9613	-6.9592	-3.9043	-2.4607	-1.5094
120	-28.5051	-13.0980	-6.9672	-3.8629	-2.4028	-1.4483
126	-28.9196	-13.1719	-6.9455	-3.8077	-2.3390	-1.3862
132	-29.2135	-13.1990	-6.9058	-3.7475	-2.2757	-1.3277
138	-29.4105	-13.1936	-6.8574	-3.6890	-2.2177	-1.2758
144	-29.5329	-13.1678	-6.8074	-3.6366	-2.1676	-1.2318
150	-29.6010	-13.1316	-6.7609	-3.5927	-2.1268	-1.1958
156	-29.6322	-13.0927	-6.7208	-3.5583	-2.0956	-1.1676
162	-29.6411	-13.0570	-6.6888	-3.5334	-2.0733	-1.1467
168	-29.6392	-13.0288	-6.6658	-3.5170	-2.0590	-1.1325
174	-29.6345	-13.0107	-6.6521	-3.5080	-2.0513	-1.1244
180	-29.6321	-13.0044	-6.6475	-3.5052	-2.0489	-1.1218

SOLID SPHERE SURFACE PRESSURE DISTRIBUTIONS FOR NRE = 500.0

POROSITY ANGLE	0.408	0.528	0.650	0.741	0.835	0.909
0	1.0638	1.0482	1.0391	1.0328	1.0302	1.0273
6	0.8756	0.9431	0.9709	0.9850	0.9864	0.9920
12	0.3206	0.6334	0.7704	0.8444	0.8578	0.8884
18	-0.5750	0.1341	0.4472	0.6182	0.6521	0.7228
24	-1.7710	-0.5326	0.0162	0.3166	0.3801	0.5042
30	-3.2135	-1.3364	-0.5032	-0.0463	0.0562	0.2442
36	-4.8390	-2.2414	-1.0872	-0.4538	-0.3029	-0.0432
42	-6.5775	-3.2081	-1.7101	-0.8873	-0.6788	-0.3432
48	-8.3571	-4.1952	-2.3443	-1.3273	-1.0528	-0.6401
54	-10.1070	-5.1621	-2.9630	-1.7543	-1.4072	-0.9190
60	-11.7620	-6.0708	-3.5407	-2.1499	-1.7253	-1.1661
66	-13.2656	-6.8881	-4.0548	-2.4974	-1.9935	-1.3696
72	-14.5724	-7.5868	-4.4870	-2.7834	-2.2013	-1.5209
78	-15.6509	-8.1480	-4.8239	-2.9980	-2.3423	-1.6147
84	-16.4846	-8.5614	-5.0588	-3.1363	-2.4152	-1.6508
90	-17.0728	-8.8267	-5.1916	-3.1989	-2.4239	-1.6342
96	-17.4306	-8.9536	-5.2300	-3.1929	-2.3787	-1.5760
102	-17.5871	-8.9612	-5.1889	-3.1315	-2.2949	-1.4920
108	-17.5824	-8.8766	-5.0894	-3.0331	-2.1911	-1.3998
114	-17.4636	-8.7312	-4.9558	-2.9180	-2.0857	-1.3148
120	-17.2781	-8.5567	-4.8116	-2.8045	-1.9922	-1.2461
126	-17.0681	-8.3801	-4.6754	-2.7051	-1.9175	-1.1958
132	-16.8656	-8.2207	-4.5584	-2.6254	-1.8621	-1.1614
138	-16.6909	-8.0891	-4.4648	-2.5649	-1.8226	-1.1388
144	-16.5538	-7.9888	-4.3939	-2.5201	-1.7949	-1.1247
150	-16.4557	-7.9185	-4.3431	-2.4872	-1.7748	-1.1161
156	-16.3924	-7.8744	-4.3094	-2.4631	-1.7592	-1.1-85
162	-16.3564	-7.8509	-4.2902	-2.4464	-1.7458	-1.0966
168	-16.3384	-7.8412	-4.2828	-2.4366	-1.7343	-1.0794
174	-16.3303	-7.8381	-4.2797	-2.4326	-1.7261	-1.0622
180	-16.3276	-7.8372	-4.2995	-2.4319	-1.7230	-1.0546

SOLID SPHERE SURFACE PRESSURE DISTRIBUTIONS FOR NRE = 1000.0

POROSITY ANGLE	0.408	0.528	0.650	0.741	0.835	0.909
0	1.0312	1.0241	1.0199	1.0168	1.0163	1.0147
6	0.8551	0.9208	0.9501	0.9649	0.9580	0.9688
12	0.3360	0.6163	0.7444	0.8125	0.7880	0.8350
18	-0.5012	0.1255	0.4131	0.5680	0.5182	0.6228
24	-1.6183	-0.5294	-0.0289	0.2437	0.1661	0.3454
30	-2.9639	-1.3184	-0.5612	-0.1442	-0.2463	0.0205
36	-4.4774	-2.2057	-1.1595	-0.5763	-0.6945	-0.3325
42	-6.0917	-3.1518	-1.7970	-1.0317	-1.1534	-0.6936
48	-7.7376	-4.1153	-2.4452	-1.4886	-1.5984	-1.0427
54	-9.3468	-5.0553	-3.0760	-1.9257	-2.0075	-1.3616
60	-10.8559	-5.9333	-3.6628	-2.3231	-2.3622	-1.6345
66	-12.2092	-6.7151	-4.1814	-2.6638	-2.6481	-1.8492
72	-13.3620	-7.3729	-4.6121	-2.9338	-2.8554	-1.9970
78	-14.2825	-7.8862	-4.9402	-3.1235	-2.9797	-2.0743
84	-14.9538	-8.2439	-5.1572	-3.2286	-3.0223	-2.0827
90	-15.3751	-8.4449	-5.2623	-3.2509	-2.9910	-2.0310
96	-15.5621	-8.4994	-5.2633	-3.2003	-2.9010	-1.9360
102	-15.5469	-8.4290	-5.1777	-3.0949	-2.8754	-1.8219
108	-15.3756	-8.2662	-5.0321	-2.9604	-2.6418	-1.7144
114	-15.1035	-8.0503	-4.8590	-2.8244	-2.5247	-1.6311
120	-14.7872	-7.8212	-4.6892	-2.7085	-2.4374	-1.5761
126	-14.4756	-7.6106	-4.5446	-2.6223	-2.3798	-1.5434
132	-14.2021	-7.4361	-4.4336	-2.5639	-2.3445	-1.5246
138	-13.9834	-7.3019	-4.3531	-2.5260	-2.3231	-1.5140
144	-13.8226	-7.2040	-4.2861	-2.5012	-2.3103	-1.5098
150	-13.7150	-7.1356	-4.2550	-2.4839	-2.3032	-1.5097
156	-13.6528	-7.0920	-4.2250	-2.4699	-2.2981	-1.5080
162	-13.6253	-7.0691	-4.2047	-2.4567	-2.2890	-1.4977
168	-13.6191	-7.0622	-4.1943	-2.4438	-2.2718	-1.4766
174	-13.6188	-7.0625	-4.1914	-2.4337	-2.2516	-1.4529
180	-13.6181	-7.0627	-4.1914	-2.4299	-2.2421	-1.4421

GAS BUBBLE SURFACE PRESSURE DISTRIBUTIONS FOR NRE = 0.1

POROSITY ANGLE	0.408	0.528	0.650	0.741	0.835	0.909
0	45.4827	46.9240	48.4570	49.6113	50.7531	51.3626
6	37.7319	42.9869	46.3445	48.2491	49.8961	50.7898
12	14.5627	31.2225	40.0374	44.1838	47.3399	49.0820
18	-23.7644	11.7645	29.6116	37.4671	43.1189	46.2635
24	-76.8156	-15.1674	15.1842	28.1749	37.2820	42.3680
30	-143.9803	-49.2633	-3.0795	16.4139	29.8970	37.4415
36	-224.4878	-90.1298	-24.9684	2.3205	21.0500	31.5422
42	-317.4176	-137.2970	-50.2292	-13.9417	10.8443	24.7397
48	-421.7103	-190.2242	-78.5706	-32.1839	-0.6009	17.1138
54	-536.1814	-248.3075	-109.6669	-52.1955	-13.1526	8.7540
60	-659.5360	-310.8868	-143.1628	-78.7465	-26.6654	-0.2424
66	-790.3845	-377.2545	-178.6774	-96.5907	-40.9841	-9.7713
72	-927.2595	-446.6642	-215.8095	-120.4689	-55.9452	-19.7234
78	-1068.6335	-518.3392	-254.1422	-145.1121	-71.3795	-29.9856
84	-1212.9369	-592.4823	-293.2478	-170.2447	-87.1138	-40.4423

90	-1358.5755	-665.2847	-332.6932	-195.5879	-102.9730	-50.9768
96	-1503.9494	-738.9350	-372.0445	-220.8627	-118.7824	-61.4731
102	-1647.4698	-811.6287	-410.8719	-245.7931	-134.3695	-71.8166
108	-1787.5772	-882.5765	-448.7546	-270.1091	-149.5657	-81.8958
114	-1922.7569	-961.0129	-485.2846	-293.5496	-164.2083	-91.6029
120	-2051.5555	-1016.2037	-520.0714	-315.8647	-178.1418	-100.8357
126	-2172.5952	-1077.4535	-552.7456	-336.8183	-191.2198	-109.4978
132	-2284.5873	-1134.1129	-582.9625	-356.1906	-203.3061	-117.4996
138	-2386.3452	-1185.5838	-610.4051	-373.7794	-214.2756	-124.7596
144	-2476.7949	-1231.3258	-634.7872	-389.4027	-224.0162	-131.2042
150	-2554.9855	-1270.8604	-655.8559	-402.8998	-232.4290	-136.7693
156	-2620.0974	-1303.7757	-673.3937	-414.1329	-239.4294	-141.3996
162	-2671.4497	-1329.7301	-687.2211	-422.9886	-244.9482	-145.0500
168	-2708.5075	-1348.4565	-697.1984	-429.3790	-248.9312	-147.6851
174	-2730.8887	-1359.7670	-703.2279	-433.2421	-251.3400	-149.2761
180	-2738.3724	-1363.5499	-705.2640	-434.5356	-252.1468	-149.8132

GAS BUBBLE SURFACE PRESSURE DISTRIBUTIONS FOR NRE = 1.0

POROSITY ANGLE	0.408	0.528	0.650	0.741	0.835	0.909
0	5.4153	5.5409	5.6696	5.7571	5.8288	5.8375
6	4.5206	5.0785	5.4151	5.5892	5.7197	5.7619
12	1.8509	3.6994	4.6569	5.0893	5.3952	5.5374
18	2.5520	1.4264	3.4088	4.6272	4.8623	5.1690
24	-8.6201	-1.7044	1.6913	3.1370	4.1307	4.6641
30	-16.2588	-5.6430	-0.4670	1.7181	3.2136	4.0323
36	-25.3510	-10.3269	-3.0306	0.0349	2.1276	3.2857
42	-35.7588	-15.6830	-5.9577	-1.8842	0.8919	2.4382
48	-47.3277	-21.6291	-9.2015	-4.0076	-0.4722	1.5051
54	-59.8893	-28.0763	-12.7115	-6.3010	-1.9418	0.5028
60	-73.2655	-34.9308	-16.4349	-8.7288	-3.4929	-0.5516
66	-87.2719	-42.0956	-20.3170	-11.2543	-5.1013	-1.6410
72	-101.7213	-49.4731	-24.3035	-13.8412	-6.7421	-2.7487
78	-116.4280	-56.9667	-28.3408	-16.4539	-8.3950	-3.8586
84	-131.2100	-64.4823	-32.3773	-19.0687	-10.0353	-4.9556
90	-145.8927	-71.9305	-36.3644	-21.6236	-11.6436	-6.0262
96	-160.3110	-79.2273	-40.2569	-24.1197	-13.2107	-7.0581
102	-174.3113	-86.2952	-44.0136	-26.2509	-14.6936	-8.0410
108	-187.7532	-93.0643	-47.5988	-28.8043	-16.1054	-8.9661
114	-200.5100	-99.4722	-50.9800	-30.9505	-17.2456	-9.8267
120	-212.4698	-105.4648	-54.1303	-32.9431	-18.6459	-10.6173
126	-223.5350	-110.9945	-57.0282	-34.7692	-19.7583	-11.3342
132	-233.6222	-116.0253	-59.6525	-36.4184	-20.7582	-11.9752
138	-242.6613	-120.5223	-61.9918	-37.8832	-21.6422	-12.5389
144	-250.5947	-124.4609	-64.0341	-39.1581	-22.4082	-13.0250
150	-257.3756	-127.8208	-65.7714	-40.2397	-23.0555	-13.4339
156	-262.9676	-130.5868	-67.1981	-41.1256	-23.5839	-13.7664
162	-267.3427	-132.7476	-68.3103	-41.8149	-23.9938	-14.0236
168	-270.4804	-134.2955	-69.1058	-42.3072	-24.2860	-14.2064
174	-272.3671	-135.2254	-69.5834	-42.6026	-24.4610	-14.3158
180	-272.9963	-135.5355	-69.7427	-42.7010	-24.5193	-14.3522

GAS BUBBLE SURFACE PRESSURE DISTRIBUTIONS FOR NRE = 10.0

POROSITY ANGLE	0.408	0.528	0.650	0.741	0.835	0.909

0	1.4098	1.4059	1.3977	1.3854	1.3662	1.3447
6	1.1987	1.2887	1.3261	1.3337	1.3282	1.3145
12	0.5723	0.9419	1.1145	1.1810	1.2161	1.2257
18	-0.4463	0.3775	0.7708	0.9334	1.0347	1.0823
24	-1.8278	-0.3862	0.3070	0.6000	0.7911	0.8901
30	-3.5277	-1.3241	-0.2610	0.1927	0.4946	0.6570
36	-5.4929	-2.4058	-0.9173	-0.2738	0.1563	0.3922
42	-7.6632	-3.5969	-1.6291	-0.7833	-0.2113	0.1061
48	-9.9735	-4.8602	-2.3837	-1.3181	-0.5947	-0.1904
54	-12.3563	-6.1574	-3.1533	-1.8606	-0.9806	-0.4862
60	-14.7446	-7.4504	-3.9142	-2.3932	-1.3559	-0.7711
66	-17.0741	-8.7033	-4.6443	-2.8999	-1.7088	-1.0353
72	-19.2860	-9.8832	-5.3236	-3.3663	-2.0288	-1.2711
78	-21.3286	-10.9616	-5.9351	-3.7805	-2.3077	-1.4721
84	-23.1595	-11.9155	-6.4655	-4.1336	-2.5394	-1.6343
90	-24.7466	-12.7281	-6.9058	-4.4165	-2.7205	-1.7556
96	-26.0961	-13.3889	-7.2507	-4.6356	-2.8500	-1.8362
102	-27.1178	-13.8943	-7.4996	-4.7823	-2.9292	-1.8783
108	-27.8948	-14.2470	-7.6557	-4.8629	-2.9617	-1.8855
114	-28.4132	-14.4560	-7.7259	-4.8834	-2.9528	-1.8630
120	-28.6954	-14.5355	-7.7202	-4.8518	-2.9092	-1.8168
126	-28.7721	-14.5039	-7.6511	-4.7778	-2.8386	-1.7531
132	-28.6801	-14.3834	-7.5328	-4.6720	-2.7489	-1.6783
138	-28.4607	-14.1979	-7.3807	-4.5455	-2.6482	-1.5985
144	-28.1569	-13.9724	-7.2102	-4.4095	-2.5442	-1.5191
150	-27.8117	-13.7317	-7.0364	-4.2745	-2.4438	-1.4446
156	-27.4658	-13.4989	-6.8730	-4.1499	-2.3531	-1.3789
162	-27.1554	-13.2945	-6.7323	-4.0439	-2.2771	-1.3249
168	-26.9107	-13.1355	-6.6242	-3.9632	-2.2199	-1.2847
174	-26.7540	-13.0345	-6.5560	-3.9125	-2.1843	-1.2599
180	-26.6999	-12.9997	-6.5326	-3.8952	-2.1722	-1.2515

GAS BUBBLE SURFACE PRESSURE DISTRIBUTIONS FOR NRE = 100.0

POROSITY ANGLE	0.408	0.528	0.650	0.741	0.835	0.909
0	1.0224	1.0196	1.0177	1.0162	1.0152	1.0145
6	0.8773	0.9318	0.9577	0.9725	0.9795	0.9846
12	0.4492	0.6929	0.7810	0.8440	0.8743	0.8969
18	-0.2422	0.2546	0.4957	0.6366	0.7048	0.7555
24	-1.1706	-0.3053	0.1141	0.3595	0.4785	0.5669
30	-2.2934	-0.9829	-0.3474	0.0245	0.2052	0.3394
36	-3.5638	-1.7419	-0.8690	-0.3537	-0.1029	0.0821
42	-4.9278	-2.5710	-1.4280	-0.7587	-0.4324	-0.1906
48	-6.3278	-3.4137	-2.0004	-1.1729	-0.7687	-0.4694
54	-7.7052	-4.2413	-2.5618	-1.5783	-1.0970	-0.7409
60	-9.0027	-5.0191	-3.0882	-1.9575	-1.4030	-0.9931
66	-10.1675	-5.7149	-3.5574	-2.2942	-1.6732	-1.2146
72	-11.1531	-6.3004	-3.9501	-2.5742	-1.8960	-1.3957
78	-11.9218	-6.7528	-4.2506	-2.7860	-2.0620	-1.5284
84	-12.4463	-7.0558	-4.4476	-2.9214	-2.1645	-1.6071
90	-12.7113	-7.2004	-4.5352	-2.9761	-2.2001	-1.6291
96	-12.7137	-7.1853	-4.5128	-2.9498	-2.1688	-1.5946
102	-12.4628	-7.0177	-4.3858	-2.8467	-2.0746	-1.5073
108	-11.9799	-6.7120	-4.1651	-2.6756	-1.9252	-1.3742
114	-11.2970	-6.2897	-3.8668	-2.4491	-1.7319	-1.2058

120	-10.4545	-5.7778	-3.5112	-2.1833	-1.5092	-1.-148
126	-9.4992	-5.2069	-3.1211	-1.8966	-1.2731	-0.8161
132	-8.4811	-4.6090	-2.7202	-1.6077	-1.0403	-0.6239
138	-7.4507	-4.0151	-2.3305	-1.3338	-0.8251	-0.4506
144	-6.4563	-3.4531	-1.9708	-1.0883	-0.6383	-0.3046
150	-5.4516	-2.9465	-1.6550	-0.8799	-0.4857	-0.1894
156	-4.7439	-2.5134	-1.3923	-0.7128	-0.3682	-0.1043
162	-4.0937	-2.1666	-1.1871	-0.5868	-0.2834	-0.0455
168	-3.6138	-1.9144	-1.0410	-0.4999	-0.2271	-0.0081
174	-3.3195	-1.7612	-0.9536	-0.4491	-0.1953	0.0123
180	-3.2202	-1.7098	-0.9246	-0.4325	-0.1851	0.0187

GAS BUBBLE SURFACE PRESSURE DISTRIBUTIONS FOR NRE = 500.0

POROSITY ANGLE	0.408	0.528	0.650	0.741	0.835	0.909
0	1.0021	1.0018	1.0017	1.0015	1.0014	1.0014
6	0.8574	0.9140	0.9419	0.9574	0.9646	0.9705
12	0.4306	0.6550	0.7640	0.8277	0.8562	0.8796
18	-0.2592	0.2368	0.4777	0.6184	0.6815	0.7333
24	-1.1821	-0.3227	0.0949	0.3387	0.4482	0.5379
30	-2.2978	-0.9989	-0.3678	0.0008	0.1666	0.3022
36	-3.5577	-1.7624	-0.8901	-0.3805	-0.1510	0.0366
42	-4.9066	-2.5797	-1.4490	-0.7885	-0.4904	-0.2473
48	-6.2858	-3.4152	-2.0203	-1.2054	-0.8369	-0.5368
54	-7.6353	-4.2324	-2.5789	-1.6128	-1.1750	-0.8192
60	-8.8965	-4.9958	-3.1004	-1.9929	-1.4899	-1.0820
66	-10.0150	-5.6722	-3.5621	-2.3291	-1.7679	-1.3136
72	-10.9428	-6.2327	-3.9441	-2.6068	-1.9966	-1.5038
78	-11.6406	-6.6531	-4.2299	-2.8138	-2.1662	-1.6442
84	-12.0794	-6.9159	-4.4074	-2.9412	-2.2693	-1.7285
90	-12.2423	-7.0106	-4.4692	-2.9837	-2.3015	-1.7532
96	-12.1245	-6.9343	-4.4132	-2.9396	-2.2616	-1.7172
102	-11.7347	-6.6920	-4.2430	-2.7112	-2.1519	-1.6222
108	-11.0940	-6.2965	-3.9670	-2.6050	-1.9778	-1.4731
114	-10.2363	-5.7684	-3.5994	-2.3312	-1.7482	-1.2775
120	-9.2064	-5.1352	-3.1594	-2.0041	-1.4755	-1.0459
126	-8.0592	-4.4312	-2.6708	-1.6419	-1.1754	-0.7923
132	-6.8564	-3.6960	-2.1623	-1.2665	-0.8667	-0.5331
138	-5.6628	-2.9723	-1.6651	-0.9025	-0.5706	-0.2869
144	-4.5398	-2.3016	-1.2105	-0.5741	-0.3077	-0.0711
150	-3.5386	-1.7175	-0.8236	-0.3011	-0.0936	0.1013
156	-2.6957	-1.2407	-0.5184	-0.0931	0.0649	0.2260
162	-2.0316	-0.6777	-0.2955	0.0520	0.1715	0.3074
168	-1.5550	-0.6252	-0.1468	0.1440	0.2362	0.3553
174	-1.2682	-0.4766	-0.0621	0.1941	0.2701	0.3795
180	-1.1724	-0.4274	-0.0345	0.2100	0.2805	0.3868

GAS BUBBLE SURFACE PRESSURE DISTRIBUTIONS FOR NRE = 1000.0

POROSITY ANGLE	0.408	0.528	0.650	0.741	0.835	0.909
0	1.0007	1.0007	1.0006	1.0005	1.0005	1.0005
6	0.8576	0.9113	0.9378	0.9562	0.9629	0.9688
12	0.4352	0.6480	0.7529	0.8255	0.8524	0.8756
18	-0.2474	0.2227	0.4545	0.6149	0.6742	0.7254

24	-1.1608	-0.3462	0.0553	0.3333	0.4363	0.5250
30	-2.2650	-1.0339	-0.4271	-0.0068	0.1491	0.2831
36	-3.5117	-1.8103	-0.9717	-0.3905	-0.1747	0.0105
42	-4.8465	-2.6415	-1.5546	-0.8011	-0.5209	-0.2808
48	-6.2111	-3.4912	-2.1504	-1.2206	-0.8742	-0.5780
54	-7.5459	-4.3222	-2.7330	-1.6305	-1.2191	-0.8680
60	-8.7928	-5.0983	-3.2770	-2.0129	-1.5405	-1.3181
66	-9.8976	-5.7857	-3.7587	-2.3511	-1.8240	-1.3762
72	-10.8126	-6.3546	-4.1570	-2.6303	-2.0575	-1.5721
78	-11.4983	-6.7805	-4.4548	-2.8385	-2.2309	-1.7172
84	-11.9256	-7.0450	-4.6392	-2.9666	-2.6633	-1.8051
90	-12.0769	-7.1372	-4.7023	-3.0091	-2.3702	-1.8321
96	-11.9469	-7.0537	-4.6419	-2.9644	-2.3305	-1.7972
102	-11.5430	-6.7990	-4.4608	-2.8347	-2.2196	-1.7021
108	-10.8849	-6.3853	-4.1678	-2.6261	-2.0428	-1.5512
114	-10.0043	-5.8322	-3.7764	-2.3481	-1.8085	-1.3518
120	-8.9437	-5.1662	-3.3053	-2.0141	-1.5281	-1.1137
126	-7.7553	-4.4201	-2.7775	-1.6405	-1.2160	-0.8491
132	-6.4996	-3.6321	-2.2204	-1.2472	-0.8895	-0.5732
138	-5.2437	-2.8456	-1.6656	-0.8576	-0.5685	-0.3033
144	-4.0564	-2.1068	-1.1474	-0.4971	-0.2749	-0.0585
150	-2.9993	-1.4587	-0.6985	-0.1904	-0.0287	0.1442
156	-2.1169	-0.9314	-0.3417	0.0462	0.1572	0.2950
162	-1.4312	-0.5357	-0.0833	0.2099	0.2825	0.3945
168	-0.9460	-0.2665	0.0859	0.3111	0.3573	0.4526
174	-0.6570	-0.1090	0.1805	0.3645	0.3955	0.4815
180	-0.5609	-0.0576	0.2110	0.3811	0.4070	0.4902

CIRCULAR CYLINDER SURFACE PRESSURE DISTRIBUTIONS FOR NRE = 1.0

POROSITY ANGLE	0.4	0.5	0.6	0.7	0.8	0.9
0	27.8441	20.8975	17.0233	13.5898	10.9577	8.4446
6	22.7218	18.8524	15.9638	13.0686	10.6853	8.3093
12	7.4208	12.7452	12.8009	11.5133	9.8729	7.9064
18	-17.8627	2.6596	7.5803	8.9485	8.5348	7.2438
24	-52.8053	-11.2662	0.3777	5.4146	6.6941	6.3349
30	-96.9621	-28.8432	-8.7035	0.9666	4.3825	5.1977
36	-149.7747	-49.8346	-19.5341	-4.3269	1.6392	3.8544
42	-210.5796	-73.9605	-31.9617	-10.3857	-1.4901	2.3307
48	-278.6203	-100.9031	-45.8143	-17.1195	-4.9544	0.6548
54	-353.0587	-130.3126	-60.9034	-24.4301	-8.6985	-1.1427
60	-432.9884	-161.8135	-77.0277	-32.2137	-12.6648	-3.0307
66	-517.4490	-195.0109	-93.9770	-40.3626	-16.7942	-4.9775
72	-605.4403	-229.4970	-111.5359	-48.7680	-21.0277	-6.9523
78	-695.9362	-264.8573	-129.4875	-57.3215	-25.3076	-8.9255
84	-787.8987	-300.6774	-147.6168	-65.9173	-29.5784	-10.8696
90	-880.2914	-336.5479	-165.7138	-74.4536	-33.7880	-12.7597
96	-972.0924	-372.0702	-183.5765	-82.8344	-37.8887	-14.5738
102	-1062.3056	-406.8609	-201.0130	-90.9705	-41.8372	-16.2933
108	-1149.9709	-440.5556	-217.8436	-98.7802	-45.5957	-17.9030
114	-1234.1741	-472.8125	-233.9023	-106.1901	-49.1313	-19.3912
120	-1314.0549	-503.3147	-249.0377	-113.1353	-52.4168	-20.7495
126	-1388.8128	-531.7721	-263.1135	-119.5592	-55.4300	-21.9725
132	-1457.7135	-557.9229	-276.0091	-125.4140	-58.1534	-23.0577
138	-1520.0928	-581.5338	-287.6192	-130.6592	-60.5739	-24.0048
144	-1575.3601	-602.4005	-297.8535	-135.2616	-62.6820	-24.8154

150	-1623.0007	-620.3472	-306.6358	-139.1943	-64.4714	-25.4923
156	-1662.5771	-635.2273	-313.9030	-142.4367	-65.9381	-26.0390
162	-1693.7311	-646.9225	-319.6049	-144.9732	-67.0799	-26.4594
168	-1716.1837	-655.3416	-323.7034	-146.7927	-67.8957	-26.7568
174	-1729.7354	-660.4193	-326.1725	-147.8877	-68.3853	-26.9340
180	-1734.2660	-662.1163	-326.9972	-148.2532	-68.5485	-26.9929

CIRCULAR CYLINDER SURFACE PRESSURE DISTRIBUTIONS FOR NRE = 10.0

POROSITY ANGLE	0.4	0.5	0.6	0.7	0.8	0.9
0	3.6102	2.9113	2.5259	2.1937	1.9533	1.7517
6	2.8063	2.5415	2.3070	2.0646	1.8704	1.6977
12	0.4141	1.4421	1.6567	1.6818	1.6245	1.5379
18	-3.5093	-0.3572	0.5943	1.0577	1.2245	1.2785
24	-8.8706	-2.8084	-0.8493	0.2123	0.6845	0.9298
30	-15.5441	-5.8466	-2.6323	-0.8273	0.0232	0.5054
36	-23.3761	-9.3932	-4.7043	-2.0288	-0.7362	0.0215
42	-32.1900	-13.3582	-7.0078	-3.3552	-1.5686	-0.5041
48	-41.7927	-17.6439	-9.4810	-4.7674	-2.4470	-1.0523
54	-51.9807	-22.1486	-12.0596	-6.2250	-3.3439	-1.6044
60	-62.5471	-26.7697	-14.6800	-7.6885	-4.2328	-2.1424
66	-73.2877	-31.4078	-17.2807	-9.1208	-5.0892	-2.6503
72	-84.0076	-35.9693	-19.8052	-10.4871	-5.8915	-3.1146
78	-94.5258	-40.3697	-22.2033	-11.7594	-6.6218	-3.5245
84	-104.6805	-44.5358	-24.4327	-12.9139	-7.2665	-3.8731
90	-114.3327	-48.4070	-26.5469	-13.9331	-7.8166	-4.1563
96	-123.3684	-51.9372	-28.2611	-14.8060	-8.2685	-4.3736
102	-131.7002	-55.0946	-29.8216	-15.5278	-8.6189	-4.5274
108	-139.2678	-57.8620	-31.1366	-16.0993	-8.8744	-4.6225
114	-146.0370	-60.2358	-32.2096	-16.5268	-9.0406	-4.6654
120	-151.9980	-62.2253	-33.0522	-16.8208	-9.1269	-4.6638
126	-157.1629	-63.8509	-33.6825	-16.9956	-9.1441	-4.6260
132	-161.5622	-65.1422	-34.1243	-17.0683	-9.1044	-4.5601
138	-165.2412	-66.1358	-34.4056	-17.0579	-9.0204	-4.4740
144	-168.2550	-66.8732	-34.5570	-16.9846	-8.9048	-4.3753
150	-170.6645	-67.3983	-34.6016	-16.8697	-8.7708	-4.2714
156	-172.5315	-67.7546	-34.5985	-16.7346	-8.6320	-4.1699
162	-173.9141	-67.9827	-34.5511	-16.6006	-8.5025	-4.0787
168	-174.8623	-68.1179	-34.4954	-16.4874	-8.3966	-4.0060
174	-175.4149	-68.1873	-34.4527	-16.4120	-8.3270	-3.9589
180	-175.5963	-68.2085	-34.4369	-16.3854	-8.3027	-3.9425

CIRCULAR CYLINDER SURFACE PRESSURE DISTRIBUTIONS FOR NRE = 50.0

POROSITY ANGLE	0.4	0.5	0.6	0.7	0.8	0.9
0	1.4753	1.3492	1.2833	1.2338	1.1953	1.1637
6	1.0534	1.1217	1.1327	1.1279	1.1209	1.1110
12	-0.1972	0.4481	0.6868	0.8151	0.9011	0.9553
18	-2.2314	-0.6460	-0.0365	0.3091	0.5462	0.7045
24	-4.9767	-2.1189	-1.0085	-0.3679	0.0724	0.3712
30	-8.3361	-3.9153	-2.1911	-1.1864	-0.4984	-0.0281
36	-12.1926	-5.9681	-3.5382	-2.1115	-1.1404	-0.4736
42	-16.4150	-8.2035	-4.9983	-3.1038	-1.8247	-0.9437
48	-20.8632	-10.5410	-6.5169	-4.1226	-2.5215	-1.4159

54	-25.3948	-12.9006	-8.0387	-5.1273	-3.2011	-1.8685
60	-29.8714	-15.2046	-9.5111	-6.0797	-3.8361	-2.2816
66	-34.1641	-17.3819	-10.8858	-6.9463	-4.4028	-2.6398
72	-38.1592	-19.3707	-12.1217	-7.6997	-4.8824	-2.9285
78	-41.7625	-21.1214	-13.1869	-8.3206	-5.2628	-3.1438
84	-44.9021	-22.5988	-14.0597	-8.7981	-5.5385	-3.2840
90	-47.5303	-23.7825	-14.7297	-9.1306	-5.7112	-3.3537
96	-49.6243	-24.6675	-15.1979	-9.3251	-5.7892	-3.3623
102	-51.1850	-25.2631	-15.4753	-9.3960	-5.7862	-3.3223
108	-52.2346	-25.5909	-15.5820	-9.3632	-5.7194	-3.2479
114	-52.8137	-25.6826	-15.5444	-9.2501	-5.6074	-3.1532
120	-52.9771	-25.5764	-15.3927	-9.0810	-5.4684	-3.0503
126	-52.7896	-25.3142	-15.1581	-8.8785	-5.3181	-2.9486
132	-52.3219	-24.9380	-14.8703	-8.6622	-5.1690	-2.8547
138	-51.6469	-24.4882	-14.5557	-8.4476	-5.0295	-2.7719
144	-50.8371	-24.0011	-14.2363	-8.2454	-4.9046	-2.7010
150	-49.9623	-23.5085	-13.9290	-8.0624	-4.7957	-2.6405
156	-49.0889	-23.0370	-13.6457	-7.9008	-4.7011	-2.5881
162	-48.2808	-22.6077	-13.3927	-7.7594	-4.6187	-2.5421
168	-47.6016	-22.2388	-13.1739	-7.6386	-4.5490	-2.5040
174	-47.1277	-21.9654	-13.0090	-7.5498	-4.4996	-2.4779
180	-46.9530	-21.8592	-12.9443	-7.5159	-4.4812	-2.4685

CIRCULAR CYLINDER SURFACE PRESSURE DISTRIBUTIONS FOR NRE = 100.0

POROSITY ANGLE	0.4	0.5	0.6	0.7	0.8	0.9
0	1.2252	1.1712	1.1358	1.1152	1.0977	1.0857
6	0.8655	0.9591	1.0018	1.0170	1.0268	1.0296
12	-0.1916	0.3316	0.6053	0.7268	0.8175	0.8640
18	-1.9076	-0.6862	-0.0370	0.2575	0.4792	0.5979
24	-4.2162	-2.0533	-0.8984	-0.3700	0.0285	0.2455
30	-7.0289	-3.7151	-1.9430	-1.1280	-0.5146	-0.1745
36	-10.2389	-5.6060	-3.1279	-1.9832	-1.1247	-0.6395
42	-13.7265	-7.6522	-4.4048	-2.8983	-1.7737	-1.1250
48	-17.3643	-9.7754	-5.7223	-3.8340	-2.4319	-1.6056
54	-21.0233	-11.8963	-7.0285	-4.7509	-3.0696	-2.0566
60	-24.5786	-13.9368	-8.2736	-5.6112	-3.6590	-2.4559
66	-27.9158	-15.8323	-9.4123	-6.3820	-4.1755	-2.7856
72	-30.9355	-17.5177	-10.4060	-7.0357	-4.5996	-3.0336
78	-33.5585	-18.9480	-11.2257	-7.5526	-4.9184	-3.1948
84	-35.7290	-20.0917	-11.8528	-7.9227	-5.1270	-3.2719
90	-37.4168	-20.9346	-12.2814	-8.1457	-5.2290	-3.2748
96	-38.6178	-21.4799	-12.5184	-8.2320	-5.2364	-3.2195
102	-39.3529	-21.7476	-12.5815	-8.2011	-5.1681	-3.1254
108	-39.6649	-21.7724	-12.5005	-8.0795	-5.0471	-3.0119
114	-39.6138	-21.5996	-12.3108	-7.8973	-4.8974	-2.8956
120	-39.2708	-21.2804	-12.0503	-7.6839	-4.7403	-2.7881
126	-38.7112	-20.8665	-11.7551	-7.4647	-4.5918	-2.6960
132	-38.0092	-20.4053	-11.4551	-7.2583	-4.4614	-2.6215
138	-37.2315	-19.9356	-11.1721	-7.0758	-4.3535	-2.5638
144	-36.4354	-19.4869	-10.9193	-6.9221	-4.2679	-2.5207
150	-35.6663	-19.0787	-10.7030	-6.7971	-4.2018	-2.4881
156	-34.9599	-18.7228	-10.5239	-6.6976	-4.1499	-2.4614
162	-34.3404	-18.4241	-10.3778	-6.6157	-4.1089	-2.4368
168	-33.8261	-18.1780	-10.2537	-6.5425	-4.0626	-2.4140
174	-33.4096	-17.9712	-10.1484	-6.4808	-4.0279	-2.3966

180	-33.2210	-17.8755	-10.1015	-6.4545	-4.0139	-2.3899

CIRCULAR CYLINDER SURFACE PRESSURE DISTRIBUTIONS FOR NRE = 500.0

POROSITY ANGLE	0.4	0.5	0.6	0.7	0.8	0.9
0	1.0437	1.0341	1.0275	1.0245	1.0209	1.0213
6	0.6997	0.8248	0.8920	0.9149	0.9406	0.9410
12	-0.3170	0.2063	0.4917	0.5915	0.7038	0.7062
18	-1.9587	-0.7924	-0.0709	0.0709	0.3227	0.3328
24	-4.1515	-2.1255	-1.0164	-0.6209	-0.1829	-0.1540
30	-6.7950	-3.7318	-2.0542	-1.4491	-0.7869	-0.7221
36	-9.7706	-5.5380	-3.2198	-2.3724	-1.4580	-1.3358
42	-12.9462	-7.4628	-4.4596	-3.3449	-2.1612	-1.9578
48	-16.1830	-9.4205	-5.7171	-4.3187	-2.8600	-2.5524
54	-19.3435	-11.3257	-6.9356	-5.2463	-3.5176	-3.0858
60	-22.2969	-13.0971	-8.0608	-6.0828	-4.0991	-3.5292
66	-24.9278	-14.6622	-9.0436	-6.7885	-4.5740	-3.9602
72	-27.1402	-15.9605	-9.8429	-7.3313	-4.9180	-4.0643
78	-28.8645	-16.9477	-10.4281	-7.6899	-5.1166	-4.1382
84	-30.0607	-17.5985	-10.7823	-7.8562	-5.1690	-4.0917
90	-30.7230	-17.9101	-10.9062	-7.8403	-5.0917	-3.9507
96	-30.8817	-17.9057	-10.8214	-7.6732	-4.9205	-3.7574
102	-30.6047	-17.6366	-10.5734	-7.4071	-4.7057	-3.5637
108	-29.9945	-17.1808	-10.2283	-7.1066	-4.4978	-3.4110
114	-29.1797	-16.6338	-9.8606	-6.8311	-4.3308	-3.3111
120	-28.2952	-16.0899	-9.5323	-6.6156	-4.2142	-3.2519
126	-27.4581	-15.6188	-9.2772	-6.4659	-4.1400	-3.2171
132	-26.7438	-15.2523	-9.0981	-6.3695	-4.0950	-3.1960
138	-26.1794	-14.9878	-8.9800	-6.3097	-4.0676	-3.1841
144	-25.7575	-14.8054	-8.9042	-6.2723	-4.0516	-3.1807
150	-25.4473	-14.6805	-8.8551	-6.2498	-4.0462	-3.1826
156	-25.2271	-14.5954	-8.8244	-6.2407	-4.0470	-3.1839
162	-25.0618	-14.5368	-8.8087	-6.2377	-4.0443	-3.1772
168	-24.9578	-14.5011	-8.7922	-6.2203	-4.0233	-3.1544
174	-24.8274	-14.4197	-8.7322	-6.1664	-3.9805	-3.1217
180	-24.7235	-14.3492	-8.6841	-6.1280	-3.9551	-3.1052

APPENDIX II-B

COMPUTATIONAL DETAILS

COMPUTER PROGRAM FOR CALCULATING THE FLOW AROUND A CIRCULAR CYLINDER IN CROSSFLOW

```
      SOLUTION OF THE NAVIER STOKES EQUATION FOR INCOMPRESSIBLE FLOW
      PERPENDICULAR TO AN ASSEMBLAGE OF CYLINDERS
      DIMENSION PSI(62,120),G(62,120),THETA(62),Z(120),ANGLE(62),X1(120)
     1 ,X2(120),SI(62),DVORT(120),DSRVT(62),OMIKO(62)
      READ(5,100) N,M,RE,A,EPS,W,WW
      READ(5,101) JRD,JPT,NPT,NNPT
      WRITE(6,102) N,M,RE,A,EPS,W,WW
      JJJJ=0
      NN=N-1
      MM=M-1
      B=3.1416/(FLOAT(MM))
      Z(1)=0.
      THETA(1)=0.
      THETA(2)=B
      DO 90 I=2,MM
      THETA(I+1)=THETA(I)+B
      SI(I)=SIN(THETA(I))
      SI(1)=0.
      SI(M)=0.
      DO 91 J=1,NN
      Z(J+1)=Z(J)+A
      X1(J)=EXP(Z(J))
      X2(J)=EXP(2.*Z(J))
      X1(N)=EXP(Z(N))
      X2(N)=EXP(2.*Z(N))
      THTC=180./3.1416
      DO 27 I=2,MM
      ANGLE(I)=THETA(I)*THTC
      DO 92 J=1,N
      G(1,J)=0.
      PSI(1,J)=0.
      G(M,J)=0.
      PSI(M,J)=0.
      DO 93 I=1,M
      PSI(I,1)=0.
      DO 94 I=1,M
      G(I,N)=0.
      PSI(I,N)=X1(N)*SI(I)
      IF(JRD.EQ.0) GO TO 9
      READ(5)((PSI(I,J),I=1,M),J=1,N)
      READ(5)((G(I,J),I=1,M),J=1,N)
      GO TO 26
    9 REWIND 8
      READ(8)((PSI(I,J),I=1,M),J=1,N)
      READ(8)((G(I,J),I=1,M),J=1,N)
      GO TO 26
      CONTINUE
      DO 95 I=2,MM
      DO 95 J=2,NN
      G(I,J)=0.
      PSI(I,J)=(X1(J)-1./X1(J))*SI(I)
      CONTINUE
      DUMA=A*A*B*B/(2.*(A*A+B*B))
      DUMB=RE*1./(8.*A*B)
      DUMC=1./(B*B)
      DUMD=1./(A*A)
      DUME=1./(2.*A*A)
      JJJ=0
      JJ=0
```

```
      II=0                                                              0600
      DO 35 I=2,MM                                                335   0610
      G(I,1)=(8.*PSI(I,2)-PSI(I,3))*DUME                                0620
      DO 35 J=2,NN                                                      0630
      DUMF=PSI(I,J+1)+PSI(I,J-1)                                        0640
      DUMG=PSI(I+1,J)+PSI(I-1,J)                                        0650
      STRMF=DUMA*(-G(I,J)*X2(J)+DUMF*DUMD+DUMG*DUMC)                    0660
      STRMF=PSI(I,J)+WW*(STRMF-PSI(I,J))                                0670
      DUMH=G(I,J+1)+G(I,J-1)                                            0680
      DUMI=G(I+1,J)+G(I-1,J)                                            0690
      DUMJ=PSI(I,J+1)-PSI(I,J-1)                                        0700
      DUMK=G(I+1,J)-G(I-1,J)                                            0710
      DUML=PSI(I+1,J)-PSI(I-1,J)                                        0720
      DUMM=G(I,J+1)-G(I,J-1)                                            0730
      VORT=DUMA*(DUMH*DUMD+DUMI*DUMC-DUMB*(DUMJ*DUMK-DUML*DUMM))        0740
      VORT=G(I,J)+W*(VORT-G(I,J))                                       0750
      IF(ABS(STRMF-PSI(I,J)).GT.EPS) II=1                               0760
      IF(STRMF.GT.10000.) GO TO 75                                      0770
      PSI(I,J)=STRMF                                                    0780
      IF(ABS(VORT-G(I,J)).GT.EPS) II=1                                  0790
      G(I,J)=VORT                                                       0800
      CONTINUE                                                          0810
      IF(II.EQ.1) GO TO 65                                              0820
      GO TO 87                                                          0830
      JJ=JJ+1                                                           0840
      JJJ=JJJ+1                                                         0850
      JJJJ=JJJJ+1                                                       0860
      IF(JPT.EQ.1.AND.JJ.EQ.NPT) GO TO 87                               0870
      IF(JJJ.EQ.300) GO TO 7000                                         0890
      GO TO 1000                                                        0900
      PRINT 7001                                                        0910
      JJJ=0                                                             0920
      GO TO 1000                                                        0930
      WRITE(6,988) JJ                                                   0940
      REWIND 8                                                          0950
      WRITE(8)((PSI(I,J),I=1,M),J=1,N)                                  0960
      WRITE(8)((G(I,J),I=1,M),J=1,N)                                    0970
      WRITE(8) I                                                        0980
      GO TO 70                                                          0990
      WRITE(6,994) I,J                                                  1000
      CONTINUE                                                          1010
      LL1=1                                                             1020
      DO 8000 LLLL=1,10                                                 1030
      LL2=LL1+14                                                        1040
      IF(LL2.GE.M) LL2=M                                                1050
      WRITE(6,997)                                                      1060
      WRITE(6,999) (ANGLE(I),I=LL1,LL2).                                1070
      WRITE(6,997)                                                      1080
      WRITE(6,995) (Z(J),(PSI(I,J),I=LL1,LL2),J=1,N)                    1090
      WRITE(6,997)                                                      1100
      WRITE(6,995) (Z(J),(G(I,J),I=LL1,LL2),J=1,N)                      1110
      IF(LL2.EQ.M) GO TO 8001                                           1120
      LL1=LL1+15                                                        1130
      DO 200 J=1,N                                                      1140
      DVORT(J)=(4.*G(2,J)-G(3,J))/(2.*B)                                1150
      OK=0.                                                             1160
      DO 201 J=2,N                                                      1170
      OK=A*(DVORT(J-1)+DVORT(J))/2. + OK                                1180
```

```
      OK=1.+4.*OK/RE                                                    1190
      DO 202 I=2,M                                                      1200
202   DSRVT(I)=(4.*G(I,2)-3.*G(I,1)-G(I,3))/(2.*A)                      1210
      OMIKO(1)=0.                                                       1220
      DO 203 I=2,M                                                      1230
203   OMIKO(I)=B*(DSRVT(I-1)+DSRVT(I))*2./RE+OMIKO(I-1)                 1240
      DO 204 I=1,M                                                      1250
204   OMIKO(I)=OMIKO(I)+OK                                              1260
      CDP=0.                                                            1270
      DO 205 I=2,M                                                      1280
205   CDP =CDP+B*(OMIKO(I-1)*COS(THETA(I-1))+ OMIKO(I)*COS(THETA(I)))/2.  1290
      CDF=0.                                                            1300
      DO 206 I=2,M                                                      1310
206   CDF=CDF+B*(G(I,1)*SI(I)+G(I-1,1)*SI(I-1))/2.                      1320
      CDF=CDF*4./RE                                                     1330
      CD=CDF+CDP                                                        1340
      WRITE(6,997)                                                      1350
      WRITE(6,1013) CDP                                                 1360
      WRITE(6,997)                                                      1370
      WRITE(6,1014) CDF                                                 1380
      WRITE(6,997)                                                      1390
      WRITE(6,989) OK                                                   1400
      WRITE(6,997)                                                      1410
      WRITE(6,1010)                                                     1720
      WRITE(6,997)                                                      1430
      WRITE(6,996) (OMIKO(I),I=1,M)                                     1440
      IF(JJ.LT.NPT) GO TO 112                                           1450
      IF(JJJJ.EQ.NNPT) GO TO 112                                        1460
      GO TO 111                                                         1470
12    CONTINUE                                                          1480
      IF(STRMF.GT.10000.) GO TO 43                                      1490
      REWIND 8                                                          1500
      READ(8)((PSI(I,J),I=1,M),J=1,N)                                   1510
      READ(8)((G(I,J),I=1,M),J=1,N)                                     1520
      READ(8) I                                                         1530
      WRITE(7,321) RE,A,N,M                                             1540
      WRITE(7) ((PSI(I,J),I=1,M),J=1,N)                                 1550
      WRITE(7) ((G(I,J),I=1,M),J=1,N)                                   1560
3     STOP                                                              1570
97    FORMAT(//)                                                        1580
95    FORMAT(1X,F9.3,15F8.4)                                            1590
99    FORMAT(1H0,9X,15F8.2)                                             1600
00    FORMAT(2I5,5F10.0)                                                1610
01    FORMAT(4I5)                                                       1620
02    FORMAT( 10X 26H NO. RADIAL MESH POINTS = ,I5,10X  26H NO. ANGULAR 1630
     1MESH POINTS = ,I5,10X 6H RE = ,F10.4/ 10X 20H RADIAL STEP SIZE = , 1640
     2 F10.4,10X 7H EPS = ,F12.6, 10X 5H W = ,F10.4,10X 6H WW = ,F10.4) 1650
94    FORMAT(1H0, 25H DIVERGING AT MESH POINT  ,2I4)                    166
010   FORMAT(1X,30H SURFACE PRESSURE DISTRIBUTION  )                    167
96    FORMAT(1X,10F12.4)                                                1680
89    FORMAT(10X, 23H STAGNATION PRESSURE = ,F12.6)                     1690
013   FORMAT(10X, 17H PRESSURE DRAG = ,F12.6)                           1700
014   FORMAT(10X, 17H FRICTION DRAG = ,F12.6)                           1710
001   FORMAT(3X, 40HTHE SOLUTION IS CONVERGING ** CONTINUING )          1720
21    FORMAT(F10.4,10X,F10.6,10X,I5,10X,I5)                             1730
38    FORMAT(30X 19H LOOPS COMPLETED = ,I5)                             1740
      END                                                               1750
```

COMPUTER PROGRAM FOR CALCULATING THE FLOW AROUND A SPHERICAL GAS BUBBLE

```
      PROGRAM GAS  (INPUT,OUTPUT,TAPE5=INPUT,TAPE6=OUTPUT,TAPE8)      338
      SOLUTION OF THE NAVIER STOKES EQUATIONS FOR SPHERICAL GAS BUBBLES
      THIS PROGRAM IS CONTROLLED BY THE FOLLOWING PARAMETERS----
      JRD---CONTROL FOR BEGINNING A NEW CALCULATION OR CONTINUING OLD
      CALCULATION
      NPT---MAXIMUM NUMBER OF LOOPS ALLOWED FOR ANY CASE
      PARAMETERS IN SOLUTION
      N---NUMBER OF RADIAL MESH POINTS
      M---NUMBER OF ANGULAR MESH POINTS
      RE---REYNOLDS MUNBER
      A---RADIAL STEP SIZE
      W---VORTICITY RELAXATION FACTOR
      WW---STREAM FUNCTION RELAXATION FACTOR
      EPS---TOLERANCE
      DIMENSION PSI(31,61),G(31,61),          Z(61),COT(31),ANGLE(31),
     1 SURVT(31),CO(31),SI(31),XX(61),X2(61),DVORT(61),OMIKO(31),
     2 SCDP(31),SCDF(31),BETA(31),ALPHA(31),DSRVT(31),DK(31),CDP(31),
     3CDF(31),SRVEL(61),DSVEL(61),DUM3(61),DUM4(61),XXX2(61),SII(31)
      READ(5,1001) N,M,RE,A,W,WW,EPS
      READ(5,1002) JRD,JPT,NPT
      WRITE(6,1003)
      WRITE(6,1006) RE
      WRITE (6,1007) W,WW
      WRITE (6,1008) N,M
      WRITE (6,1015) A
      WRITE (6,1015) EPS
      WRITE(6,1016) JRD,JPT,NPT
      NN=N-1
      MM=M+1
      B=3.1416/(FLOAT(M))
      Z(1)=0.0
      THTC=57.2956
      THETA=B
      DO 90 I=2,M
      CO(I)=COS(THETA)
      SI(I)=SIN(THETA)
      SII(I)=1./(SI(I)**2)
      COT(I)=CO(I)/SI(I)
      ANGLE(I)=THETA*THTC
      THETA=THETA+B
      ANGLE(1)=0.0
      ANGLE(MM)=180.0
      SI(1)=0.0
      CO(1)=1.0
      SI(MM)=0.0
      CO(MM)=-1.0
      COT(1)=0.0
      COT(MM)=0.0
      DO 91 J=1,NN
      Z(J+1)=Z(J)+A
      XX(J)=EXP(Z(J))
      X2(J)=XX(J)**2
      XXX2(J)=1./X2(J)
      XX(N)=EXP(Z(N))
      X2(N)=XX(N)**2
      XXX2(N)=1./X2(N)
      DO 10 I=1,MM
      PSI(I,1)=0.0
      DO 15 J=1,N
```

```
      G(1,J)=0.0                                                        0600
      PSI(1,J)=0.0                                                      0610
      G(MM,J)=0.0                                                       0620
      PSI(MM,J)=0.0                                                     0630
      DO 20 I=1,MM                                                      0640
      PSI(I,N)=0.5*X2(N)*SI(I)**2                                       0650
   20 G(I,N)=0.0                                                        0660
      IF(JRD.EQ.0) GO TO 9                                              0670
      REWIND 8                                                          0680
      READ(8) ((PSI(I,J),I=1,MM),J=1,N)                                 0690
      READ (8) ((G(I,J),I=1,MM),J=1,N)                                  0700
      REWIND 8                                                          0710
      GO TO 26                                                          0720
    9 CONTINUE                                                          0730
      DO 30 I=2,M                                                       0740
      SIIJ2=SI(I)**2                                                    0750
      SIIJ=0.5*SIIJ2                                                    0760
      DO 30 J=2,NN                                                      0770
      PSI(I,J)=(X2(J)-XX(J))*SIIJ                                       0780
      G(I,J)=SIIJ2/XX(J)                                                0790
   26 CONTINUE                                                          0800
      DUM1=B*B*((2.-A)/2.)                                              0810
      DUM2=B*B*((2.+A)/2.)                                              0820
      DUM5=A*A*B*B                                                      0830
      DUM6=1./(2.*(A*A+B*B))                                            0840
      DUM7=1./A                                                         0850
      DUM8=RE*DUM5/4.                                                   0860
      DUM9=1./(2.*A)                                                    0870
      DUM10=1./(2.*B)                                                   0880
      DUM11=A*A/2.                                                      0890
      DUM12=DUM9/B                                                      0900
      DUM13=DUM10/A                                                     0910
      DUM14=0.5*DUM10                                                   0920
      DUM15=4.0/RE                                                      0930
      DUM16=DUM15                                                       0940
      DUM17=B/2.0                                                       0950
      DUM18=1./(4.*A**3)                                                0960
      DUM19=A/2.                                                        0970
      DUM20=8./RE                                                       0980
      DUM21=2./(B*SI(2))                                                0990
      DUM22=1./(2.*B*SI(3))                                             1000
      DO 41 I=2,M                                                       0101
      DUM3(I)=DUM11*(2.-B*COT(I))                                       1020
      DUM4(I)=DUM11*(2.+B*COT(I))                                       1030
      JJ=0                                                              1040
    0 II=0                                                              1050
      DO 35 I=2,M                                                       1060
      IP1=I+1                                                           1070
      IM1=I-1                                                           1080
      G(I,1)=(4.*PSI(I,2)-PSI(I,3))*DUM7                                1090
      DO 35 J=2,NN                                                      1100
      JP1=J+1                                                           1110
      JM1=J-1                                                           1120
      DUMA=G(I,JP1)*SII(I)*XXX2(JP1)                                    1130
      DUMC=G(I,JM1)*SII(I)*XXX2(JM1)                                    1140
      IF(I.EQ.2) GO TO 45                                               1150
      DUMD=G(IM1,J)*SII(IM1)*XXX2(J)                                    1160
      GO TO 50                                                          1170
```

```
      DUMD=G(2,J)/(X2(J)*B*SI(2))                                        1180
      IF(I.EQ.M) GO TO 55                                                1119
      DUMB=G(IP1,J)*SII(IP1)*XXX2(J)                                     1200
      GO TO 60                                                           1210
      DUMB=G(M,J)/(X2(J)*B*SI(M))                                        1220
      STRMF=DUM6*(PSI(I,JP1)*DUM1+PSI(I,JM1)*DUM2+PSI(IP1,J)*DUM3(I)     1230
     1  +PSI(IM1,J)*DUM4(I)-DUM5*G(I,J)*X2(J))                           1240
      STRMF=PSI(I,J)+WW*(STRMF-PSI(I,J))                                 1250
      DPSI=DUM12*(PSI(I,JP1)-PSI(I,JM1))*(DUMB-DUMD)-DUM13*(PSI(IP1,J)-  1260
     1  PSI(IM1,J))*(DUMA-DUMC)                                          1270
      VORT=DUM6*(G(I,JP1)*DUM1+G(I,JM1)*DUM2+G(IP1,J)*DUM3(I)+           1580
     1  G(IM1,J)*DUM4(I)-DUM8*SI(I)*XX(J)*DPSI)                          1290
      VORT=G(I,J)+W*(VORT-G(I,J))                                        1300
      IF (ABS(STRMF-PSI(I,J)).GT.EPS)  II=1                              1310
      PSI(I,J)=STRMF                                                     1320
      IF(ABS(VORT-G(I,J)).GT.EPS) II=1                                   1330
85    G(I,J)=VORT                                                        1340
35    CONTINUE                                                           1350
      IF(II.EQ.1) GO TO 65                                               1360
      GO TO 87                                                           1370
65    JJ=JJ+1                                                            1380
      IF(JJ.EQ.NPT) GO TO 87                                             1390
      GO TO 100                                                          1400
      REWIND 9                                                           1410
      WRITE(9)((PSI(I,J),I=1,MM),J=1,N)                                  1420
      WRITE(9)((G(I,J),I=1,MM),J=1,N)                                    1430
      ENDFILE 9                                                          1440
      REWIND 9                                                           1450
      LL1=1                                                              1460
      DO 8000 LLLL=1,10                                                  1470
      LL2=LL1+14                                                         1480
      IF(LL2.GE.MM) LL2=MM                                               1490
      WRITE(6,997)                                                       1500
      WRITE(6,999)(ANGLE(I),I=LL1,LL2)                                   1510
      WRITE(6,997)                                                       1520
      WRITE(6,998)(XX(J),(PSI(I,J),I=LL1,LL2),J=1,N)                     1530
      WRITE(6,997)                                                       1540
      WRITE(6,998)(XX(J),(G(I,J),I=LL1,LL2),J=1,N)                       1550
      IF(LL2.EQ.MM) GO TO 8001                                           1560
)     LL1=LL1+15                                                         1570
1     CONTINUE                                                           1580
      DO 71 I=2,M                                                        1590
71    SURVT(I)=G(I,1)/SI(I)                                              1600
      SURVT(1)=0.0                                                       1610
      SURVT(MM)=0.0                                                      1620
      DK(1)=0.0                                                          1630
      DK(MM)=0.0                                                         1640
      OMIKO(1)=0.0                                                       1650
      CDP(1)=0.0                                                         1660
      SCDP(1)=0.0                                                        1670
      CDF(1)=0.0                                                         1680
      CDF(MM)=0.0                                                        1690
      SCDF(1)=0.0                                                        1700
      DO 73 I=2,MM                                                       1710
      IP1=I+1                                                            1720
      IM1=I-1                                                            1730
      IF(I.EQ.MM) GO TO 72                                               1740
      DSRVT(I)=DUM9*(4.*G(I,2)/XX(2)-G(I,3)/XX(3)-3.*G(I,1))/SI(I)       1750
```

```
      DSVEL(I)=DUM14*(SURVT(IP1)-SURVT(IM1))                                1760
      SRVEL(I)=0.5*SURVT(I)                                                 1770
      DK(I)=DUM15*DSRVT(I)+DUM16*SURVT(I)-2.*SRVEL(I)*DSVEL(I)              1780
      OMIKO(I)=DUM17*(DK(IM1)+DK(I))+OMIKO(IM1)                             1790
      CDP(I)=OMIKO(I)*2.*SI(I)*CO(I)                                        1800
      SCDP(I)=DUM17*(CDP(IM1)+CDP(I))+SCDP(IM1)                             1810
      CDF(I)=DUM20*CO(I)*(SURVT(I)*CO(I)+2.*DSVEL(I)*SI(I))                 1820
      SCDF(I)=DUM17*(CDF(IM1)+CDF(I))+SCDF(IM1)                             1830
      DO 74 I=1,MM                                                          1840
      ALPHA(I)=0.5*G(I,1)                                                   1850
      BETA(I)=DUM18*(3.*PSI(I,1)-4.*PSI(I,2)+PSI(I,3))                      1860
      DO 31 J=1,N                                                           1870
      DVORT(J)=DUM21*G(2,J)/XX(J)-DUM22*G(3,J)/XX(J)                        1888
      OK=0.                                                                 1890
      DO 32 J=2,N                                                           1900
      OK=DUM19*(DVORT(J-1)+DVORT(J))+OK                                     1910
      OK=1.+8.*OK/RE                                                        1920
      DO 33 I=1,MM                                                          1930
   33 OMIKO(I)=OMIKO(I)+OK                                                  1940
      WRITE (6,1009)                                                        1950
      WRITE (6,996) (SURVT(I),I=1,MM)                                       1960
      WRITE(6,1010)                                                         1970
      WRITE(6,996)(OMIKO(I),I=1,MM)                                         1980
      WRITE(6,1011)                                                         1990
      WRITE(6,996)(ALPHA(I),I=1,MM)                                         2000
      WRITE(6,1012)                                                         2010
      WRITE(6,996)(BETA(I),I=1,MM)                                          2020
      WRITE(6,1014)SCDF(MM)                                                 2030
      WRITE(6,1013)SCDP(MM)                                                 2040
      WRITE(6,997)                                                          2050
      WRITE(6,1004)OK                                                       2060
      WRITE(6,1017)JJ                                                       2070
      STOP                                                                  2080
  993 FORMAT(3X,2I5,F20.6,2I5,F20.6)                                        2090
  992 FORMAT(3X,2F20.6)                                                     2100
  995 FORMAT (1X,F9.3,14F8.4)                                               2110
  996 FORMAT(1X,10F12.4)                                                    2120
  997 FORMAT(//)                                                            2130
  998 FORMAT(1X,F9.3,15F8.4)                                                2140
  999 FORMAT (1H0,9X,15F8.2)                                                2150
 1001 FORMAT(2I5,7F10.0)                                                    2160
 1002 FORMAT(5I5)                                                           2170
 1003 FORMAT(1H1)                                                           2180
 1004 FORMAT (F10.6)                                                        2190
 1005 FORMAT (3I5)                                                          2200
 1007 FORMAT (2F10.4)                                                       2210
 1006 FORMAT (3F10.5)                                                       2220
 1008 FORMAT (2I5)                                                          2230
 1009 FORMAT(1H0,1X,19HSURFACE VORTICITIES)                                 2240
 1010 FORMAT(1H0,1X,29HSURFACE PRESSURE DISTRIBUTION)                       2250
 1011 FORMAT(1H0,1X,18HALPHA DISTRIBUTION)                                  2260
 1012 FORMAT(1H0,1X,17HBETA DISTRIBUTION)                                   2270
 1013 FORMAT(1H0,22H  THE PRESSURE DRAG IS,E12.6)                           2280
 1014 FORMAT(1H0,22H  THE FRICTION DRAG IS,E12.6)                           2290
 1015 FORMAT (F12.7)                                                        2300
    6 FORMAT(3(2X,I5))                                                      2310
 1017 FORMAT(1I5)                                                           2320
      END                                                                   2330
```